AMERICAN ASSOCIATION FOR THE ADVANCEMENT OF SCIENCE

SCIENCE

10 MARCH 1995
VOL. 267 • PAGES 1393–1564

$7.00

#BXNCCNG ********** 5-DIGIT 99775
#000015986631#AS 10/27/95 M 1095 90
RICHARD JAY STOLZBERG
UNIV ALASKA
CHEMISTRY DEPT
UNIVERSITY ALASKA
FAIRBANKS AK 99775

ROBUST PCR

TaqPlus™ DNA Polymerase

Why on earth would you ever use anything else?

The answer is... *you wouldn't.*

Because Stratagene's new* TaqPlus™ *DNA polymerase† does it all!

TaqPlus™ DNA Polymerase is an optimized blend of Stratagene's highest quality *Taq* DNA polymerase† and *Taq* Extender™ PCR additive, the most powerful PCR-enhancement reagent available. [1,2]

***You'll never go back to* Taq.**

ROBUST PERFORMANCE

TaqPlus DNA polymerase boosts PCR yield. For long and short templates. For everyday PCR. Use it instead of *Taq*, and you'll understand the meaning of robust PCR!

LONG PCR

The robust nature of *TaqPlus* DNA polymerase makes it ideal for long PCR. It amplifies templates up to 35 kb long. So this potent polymerase is all you need.

TOUGH TEMPLATES

TaqPlus DNA polymerase reduces mismatch pausing. So more extension reactions reach completion in each cycle of PCR. Armed with this greater efficiency, *TaqPlus* DNA polymerase can even tame tough templates to bring out the bands.

REFERENCES
1. Nielson, K.B., Scott, B., Bauer, J.C., and Kretz, K. (1994) Strategies 7: 64-65.
2. Nielson, K.B., Schoettle, W., Bauer, J.C., and Mathur, E. (1994) Strategies 7: 27.

FOOTNOTES
† Purchase of this enzyme is accompanied by a license to use it in the polymerase chain reaction (PCR) process in conjunction with an authorized thermal cycler. This product is sold under licensing arrangements with Roche Molecular Systems, Inc., F. Hoffmann-La Roche Ltd. and The Perkin-Elmer Corporation.

***TaqPlus*™ polymerase**
100 U Catalog #600203
500 U Catalog #600204

INTERNET MAIL
tech_services@stratagene.com

USA
Corporate Headquarters
(800) 424-5444

GERMANY
Stratagene GmbH
Telephone: (06221) 400634

UNITED KINGDOM
Stratagene Ltd
Telephone: (0223) 420955

SWITZERLAND
Stratagene GmbH
Telephone: (01) 3641106

STRATAGENE®

Circle No. 73 on Readers' Service Card

Accelerated for Power Macintosh

Lasergene

PREMIER SOFTWARE FOR THE MACINTOSH

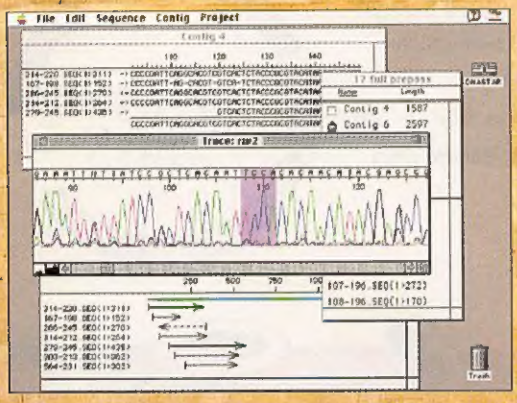

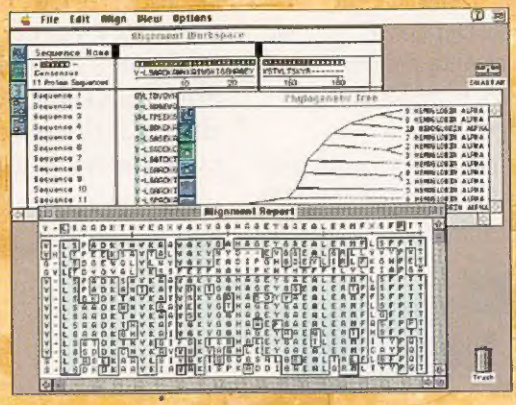

AVAILABLE NOW FOR WINDOWS!

Call **DNASTAR**
USA: (608) 258-7420
Fax (608) 258-7439
Europe: (44)-81-566 8282
Fax (44)-81-566 9555
Internet:
sales@dnastar.com
support@dnastar.com
for 30 days FREE software
on Macintosh or
WINDOWS

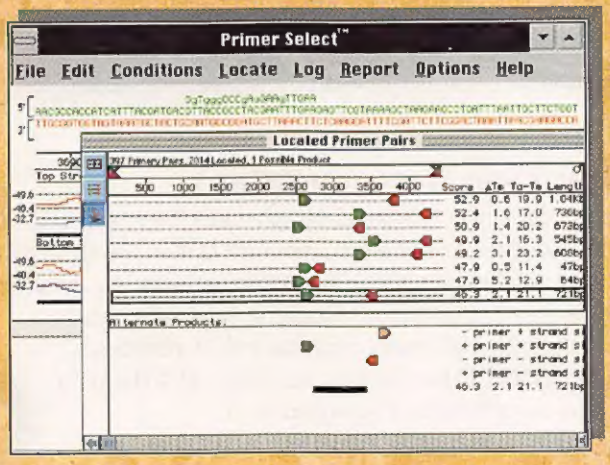

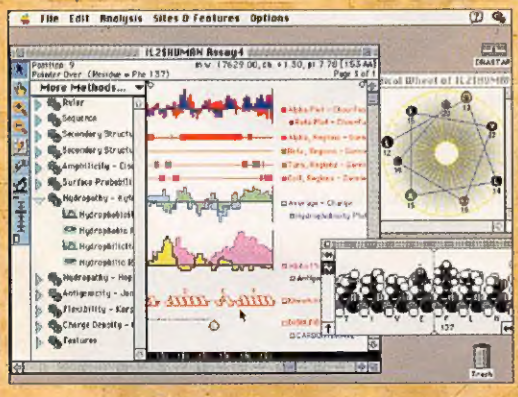

"This is a powerful, expandable and comprehensive molecular biology package for the Mac, with the best protein analysis and restriction mapping software available. I recommend DNASTAR to any lab requiring this level of power and expandability. DNASTAR is currently unique in its support for networking as well."

Peter Markiewicz, *UCLA*

BIOCOMPUTING

- SEQUENCING
- NETWORKS
- DATABASES
- PROTEINS
- PRIMERS
- RESTRICTION
- ALIGNMENT
- EVOLUTION

DNASTAR

DNASTAR Inc USA: 1228 South Park Street, Madison, Wisconsin 53715. Tel (608) 258 7420, Fax (608) 258 7439
European Sales & Support: Abacus House, West Ealing, London, W13 OAS, U.K. Tel (44) 81 566 8282, Fax (44) 81 566 9555.

Circle No. 87 on Readers' Service Card

High-Efficiency Cloning of PCR Products.

The most efficient method to clone PCR products? TA Cloning® Kits from Invitrogen. The Original TA Cloning® Kit achieves guaranteed cloning efficiencies of > 80%! There's no modification or purification of your PCR product necessary. And that's not all! Our new Eukaryotic TA Cloning® Kits now allow direct cloning and mammalian expression of PCR products. To learn more about these state-of-the-art kits, contact Invitrogen today.

Original TA Cloning® Kit	*Catalog no. K2000-01*	*$255*
Eukaryotic TA Cloning® Kit - Unidirectional	*Catalog no. K3001-01*	*$290*
Eukaryotic TA Cloning® Kit - Bidirectional	*Catalog no. K3000-01*	*$275*

Circle No. 79 on Readers' Service Card

High-Powered Mammalian Expression.

The pZeoSV vector is the most efficient, cost-effective tool for high-level recombinant protein expression in mammalian cells. pZeoSV carries only one selectable marker, the unique Zeocin™ resistance gene. This keeps the vector extremely small–only 3.45 kb–for maximum transfection efficiency. Check out this efficient, high-powered mammalian expression system today.

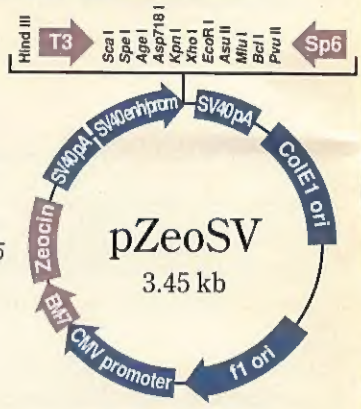

pZeoSV Vector Kit	*Catalog no. V850-01*	*$285*

Circle No. 80 on Readers' Service Card

Way Cool ST
Gene Expre

The Surprisingly Affordable Electroporator II.

The Electroporator II connects directly to existing electrophoresis power supplies. This means you'll save thousands of dollars compared to traditional units with built-in power supplies. The Electroporator II features variable capacitance and resistance controls, and accepts standard cuvettes for electroporation of bacteria, yeast, plant, and mammalian cells. Each unit comes complete with 10 cuvettes, a comprehensive manual, plus a one-year warranty. Call today for a demonstration of our affordable Electroporator II.

Electroporator II	*Catalog no. S1670-01*	*$975*

Circle No. 83 on Readers' Service Card

Cuvettes! We've Got Your Size!

Our electroporation cuvettes fit virtually all electroporation devices, and when you buy 3 bags of 50 cuvettes, you get one FREE! Our cuvettes are available with either 0.1, 0.2, or 0.4 cm gap sizes for efficient electroporation of bacteria, yeast, and mammalian cells. Each cuvette is sterilized by gamma irradiation and individually packaged to ensure sterility. Don't pay more! Order now and save!

Catalog no. P410-50	*0.1 cm*	*$130*
Catalog no. P450-50	*0.2 cm*	*$130*
Catalog no. P460-50	*0.4 cm*	*$130*

Circle No. 84 on Readers' Service Card

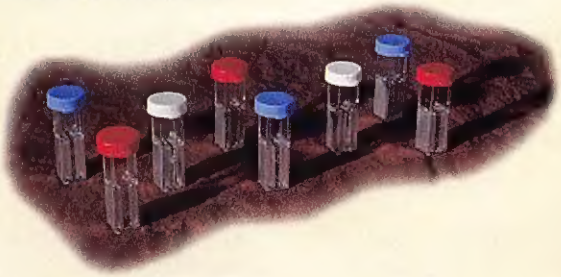

The Only Kit for Subtracted cDNA.

Only one product gives you a simple, easy-to-follow method for the enrichment of differentially expressed genes. It's the Invitrogen Subtractor® Kit. The procedure uses the technique of subtractive hybridization to remove common messages from differentially expressed pools of cDNA. You can use the subtracted cDNA as a probe, or amplify and clone it to produce "hard copies" of enriched genes. If you need to isolate differentially expressed genes, call Invitrogen today to get the facts on the Subtractor® Kit.

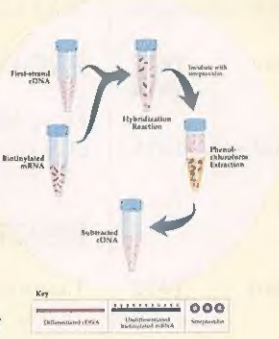

Subtractor® Kit *Catalog no. K4320-01* *$265*

Circle No. 81 on Readers' Service Card

Exceptional Yields of mRNA.

The FastTrack® mRNA Isolation Kit produces very high yields of mRNA directly from tissues, plants, or cells. The kit utilizes gentle lysis and efficient binding of mRNA to oligo dT cellulose powder to isolate large amounts of pure, intact mRNA. Yields of 40-70 µg of mRNA are routinely achieved from 1 x 10^8 cells. Call Invitrogen today and start increasing your yield and quality of mRNA.

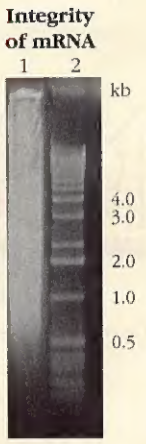

mRNA was isolated from 1 x 10^8 insect cells and resuspended in 30 µl of water. 10 µl was run on a 1% agarose gel (lane 1).

FastTrack® Kit *Catalog no. K1593-02* *$235*

Circle No. 82 on Readers' Service Card

utt From The ssion Folks.

Genomic DNA in a Jiffy.

What's the fastest, easiest, most efficient way to isolate genomic DNA? That's simple: the Easy-DNA™ Kit. It works quickly and efficiently in only four steps, minimizing DNA degradation and loss. In less than 90 minutes, this simple procedure yields high-quality genomic DNA from a wide variety of samples for use in any molecular biology application. Make your life a little easier, isolate genomic DNA with the Easy-DNA™ Kit from Invitrogen.

Easy-DNA™ Kit *Catalog no. K1800-01* *$165*

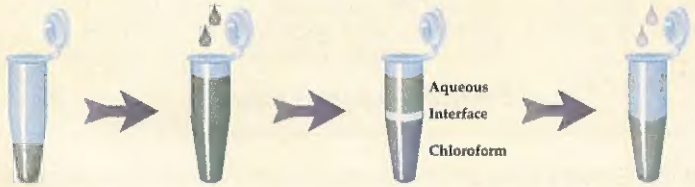

Add Lysis Solution. Incubate at 65°C for 10 minutes.

Add Precipitation Solution and vortex. Add chloroform and vortex. Centrifuge.

Transfer aqueous phase to a new tube.

Add ethanol and precipitate DNA.

Circle No. 85 on Readers' Service Card

Genuine High-Level Mammalian Expression.

Invitrogen's pcDNA3 is the most versatile mammalian vector for high-level expression. Either transient or stable expression is achieved using the powerful cytomegalovirus (CMV) promoter/enhancer. Call our Technical Services Department and ask for the extensive citation list demonstrating successful mammalian expression with pcDNA3. Find out how you can express high levels of your recombinant protein in mammalian cells. Contact Invitrogen today!

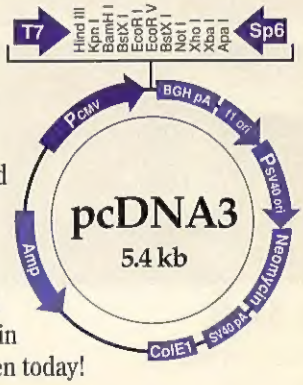

pcDNA3 *Catalog no. V790-20* *$195*

Circle No. 86 on Readers' Service Card

Invitrogen®

Easy ordering and *FAST* delivery.

1-800-955-6288

3985 B Sorrento Valley Boulevard
San Diego, California 92121
Fax orders to 619-597-6201
Prices/Offers valid in U.S. & Canada only.

ISSN 0036-8075
10 MARCH 1995
VOLUME 267
NUMBER 5203

SCIENCE

AMERICAN ASSOCIATION FOR THE ADVANCEMENT OF SCIENCE

NATIONAL CANCER INSTITUTE

1412
Varmus takes stock

1498
More on p53 structure

NEWS & COMMENT

A New Phase in the War on Cancer 1412
Reports From the Front 1414

Nobelists Make a Plea for NIH Budget 1415

Russian Chaos Breeds Diphtheria Outbreak 1416

Biotechnology: European Parliament Axes Patent Policy 1417

Canadian R&D: Science Budget Takes 15% Whack 1418

India Cracks Whip to End Addiction to State Funds 1419

Galvin, DOE Spar Over Reform Plan 1420

RESEARCH NEWS

Did Darwin Get It All Right? 1421

With Quark Discovery, Truth Comes Out on Top—Twice 1423

How Quixotic Is SLAC's Quest to Detect "Crazy Particle"? 1424

Plucking Images From the Digital Floods 1425

NASA Picks a Budget Lunar Trip 1425

PROFILE

Floyd Bloom: The Next Editor-in-Chief of *Science* 1441
R. A. Lerner and R. Guillemin

PERSPECTIVE

Targeting Retroviral Integration 1443
F. Bushman

ARTICLES

APOPTOSIS

Mechanisms and Genes of Cellular Suicide 1445
H. Steller

The Fas Death Factor 1449
S. Nagata and P. Golstein

Apoptosis in the Pathogenesis and Treatment of Disease 1456
C. B. Thompson

RESEARCH ARTICLE

Structure of a Hyperthermophilic Tungstopterin Enzyme, Aldehyde Ferredoxin Oxidoreductase 1463
M. K. Chan, S. Mukund, A. Kletzin, M. W. W. Adams, D. C. Rees

DEPARTMENTS

THIS WEEK IN *SCIENCE* 1401

EDITORIAL 1403
Letter to Floyd Bloom, Editor-in-Chief–Elect

LETTERS 1405
AIDS Research Policy: W. E. Paul; S. Cox; B. Goldberg and R. B. Stricker • Biosphere 2: J. Allen • Oncogenes and Cancer: P. H. Duesberg; D. Stéhelin • China's Internet Links: X. Hao • Zinc Selenide Lasers: B. J. Fitzpatrick

SCIENCESCOPE 1411

RANDOM SAMPLES 1426

BOOK REVIEWS 1529
Structures in the Stream, reviewed by P. L. Shiman • *HIV and the Pathogenesis of AIDS*, R. A. Weiss • *The History and Geography of Human Genes*, D. H. O'Rourke • Vignettes • Books Received

PRODUCTS & MATERIALS 1541

Board of Reviewing Editors

Frederick W. Alt
Don L. Anderson
Michael Ashburner
Stephen J. Benkovic
David E. Bloom
Floyd E. Bloom
Piet Borst
Henry R. Bourne
Michael S. Brown
James J. Bull
Kathryn Calame
C. Thomas Caskey
Dennis W. Choi
John M. Coffin
F. Fleming Crim
Paul J. Crutzen
James E. Dahlberg
Robert Desimone
Bruce F. Eldridge
Paul T. Englund
Richard G. Fairbanks
Douglas T. Fearon
Harry A. Fozzard
Klaus Friedrich
Theodore H. Geballe
John C. Gerhart
Roger I. M. Glass
Stephen P. Goff
Peter N. Goodfellow
Corey S. Goodman
Ira Herskowitz
Eric F. Johnson
Stephen M. Kosslyn
Michael LaBarbera
Nicole Le Douarin
Charles S. Levings III
Alexander Levitzki
Harvey F. Lodish
Richard Losick
Reinhard Lührmann
Diane Mathis
Anthony R. Means
Shigetada Nakanishi
Roger A. Nicoll
Stuart L. Pimm
Yeshayau Pocker
Dennis A. Powers
Ralph S. Quatrano
V. Ramanathan
Douglas C. Rees
T. M. Rice
David C. Rubie
Erkki Ruoslahti
Gottfried Schatz
Jozef Schell
Ronald H. Schwartz
Terrence J. Sejnowski
Ellen Solomon
Thomas A. Steitz
Michael P. Stryker
Robert T. N. Tjian
Emil R. Unanue
Geerat J. Vermeij
Bert Vogelstein
Harold Weintraub
Arthur Weiss
Zena Werb
George M. Whitesides
Owen N. Witte
William A. Wulf

COVER

Apoptosis (programmed cell death) in the nervous system of the *Drosophila* sine oculis mutant. A retina and brain exhibiting excessive cell death during development of the visual system were stained with acridine orange to identify cells undergoing apoptosis (orange dots). The mechanism of programmed cell death (see page 1445), along with the Fas system of triggering apoptosis (page 1449) and cell death in disease and therapy (page 1456), are examined in a trio of Articles focusing on apoptosis. [Photo: Hermann Steller, Howard Hughes Medical Institute, Massachusetts Institute of Technology]

REPORTS

The Elemental Composition of the Corona of Procyon: Evidence for the Absence of the FIP Effect 1470
J. J. Drake, J. M. Laming, K. G. Widing, J. H. M. M. Schmitt, B. Haisch, S. Bowyer

Conducting Layered Organic-Inorganic Halides Containing ⟨110⟩-Oriented Perovskite Sheets 1473
D. B. Mitzi, S. Wang, C. A. Feild, C. A. Chess, A. M. Guloy

A "Double-Diamond Superlattice" Built Up of $Cd_{17}S_4(SCH_2CH_2OH)_{26}$ Clusters 1476
T. Vossmeyer, G. Reck, L. Katsikas, E. T. K. Haupt, B. Schulz, H. Weller

Micrometer- and Nanometer-Sized Polymeric Light-Emitting Diodes 1479
M. Granström, M. Berggren, O. Inganäs

Influence of Lunar Phase on Daily Global Temperatures 1481
R. C. Balling Jr. and R. S. Cerveny

Conformation of Macromolecules in the Gas Phase: Use of Matrix-Assisted Laser Desorption Methods in Ion Chromatography 1483
G. von Helden, T. Wyttenbach, M. T. Bowers

Control of IκB-α Proteolysis by Site-Specific, Signal-Induced Phosphorylation 1485
K. Brown, S. Gerstberger, L. Carlson, G. Franzoso, U. Siebenlist

Requirement of RNA Polymerase III Transcription Factors for in Vitro Position-Specific Integration of a Retroviruslike Element 1488
J. Kirchner, C. M. Connolly, S. B. Sandmeyer

Glutamate Receptor RNA Editing in Vitro by Enzymatic Conversion of Adenosine to Inosine 1491
S. M. Rueter, C. M. Burns, S. A. Coode, P. Mookherjee, R. B. Emeson

Involvement of CRAF1, a Relative of TRAF, in CD40 Signaling 1494
G. Cheng, A. M. Cleary, Z.-s. Ye, D. I. Hong, S. Lederman, D. Baltimore

Crystal Structure of the Tetramerization Domain of the p53 Tumor Suppressor at 1.7 Angstoms 1498
P. D. Jeffrey, S. Gorina, N. P. Pavletich

Pineal Opsin: A Nonvisual Opsin Expressed in Chick Pineal 1502
M. Max, P. J. McKinnon, K. J. Seidenman, R. K. Barrett, M. L. Applebury, J. S. Takahashi, R. F. Margolskee

Massive Cell Death of Immature Hematopoietic Cells and Neurons in Bcl-x–Deficient Mice 1506
N. Motoyama, F. Wang, K. A. Roth, H. Sawa, K.-i. Nakayama, K. Nakayama, I. Negishi, S. Senju, Q. Zhang, S. Fujii, D. Y. Loh

Synaptic Desensitization of NMDA Receptors by Calcineurin 1510
G. Tong, D. Shepherd, C. E. Jahr

Storage of 7 ± 2 Short-Term Memories in Oscillatory Subcycles 1512
J. E. Lisman and M. A. P. Idiart

TECHNICAL COMMENTS

Interhelical Angles in the Solution Structure of the Oligomerization Domain of p53: Correction 1515
G. M. Clore, J. G. Omichinski, K. Sakaguchi, N. Zambrano, H. Sakamoto, E. Appella, A. M. Gronenborn

1473
On a different plane

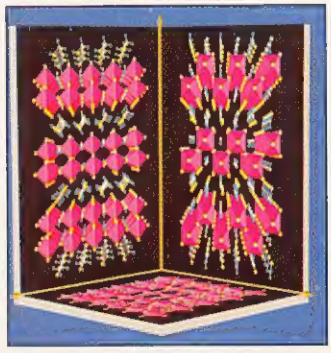

AAAS Board of Directors

Francisco J. Ayala
Retiring President, Chairman
Rita R. Colwell
President
Jane Lubchenco
President-elect
William A. Lester Jr.
Simon A. Levin
Michael J. Novacek
Anna C. Roosevelt
Alan Schriesheim
Jean E. Taylor
Chang-Lin Tien
Nancy S. Wexler
William T. Golden
Treasurer
Richard S. Nicholson
Executive Officer

◩ **Indicates accompanying feature**

■ **SCIENCE (ISSN 0036-8075) is published weekly on Friday, except the last week in December, by the American Association for the Advancement of Science, 1333 H Street, NW, Washington, DC 20005.** Second-class postage (publication No. 484460) paid at Washington, DC, and additional mailing offices.

Copyright © 1995 by the American Association for the Advancement of Science. The title SCIENCE is a registered trademark of the AAAS.

Domestic individual membership and subscription (51 issues): $97 ($50 allocated to subscription). Domestic institutional subscription (51 issues): $228. Foreign postage extra: Mexico, Caribbean (surface mail) $53; other countries (air assist delivery) $93. First class, airmail, student and emeritus rates on request. Canadian rates with GST available upon request, GST #1254 88122. **Printed in the U.S.A.**

Change of address: allow 6 weeks, giving old and new addresses and 11-digit account number. **Postmaster:** Send change of address to *Science*, P.O. Box 2033, Marion, OH 43305-2033. **Single copy sales:** $7.00 per issue prepaid includes surface postage; bulk rates on request.

Authorization to photocopy material for internal or personal use under circumstances not falling within the fair use provisions of the Copyright Act is granted by AAAS to libraries and other users registered with the Copyright Clearance Center (CCC) Transactional Reporting Service, provided that the base fee of $1 per copy plus $0.10 per page is paid directly to CCC, 27 Congress Street, Salem, MA 01970. The identification code for *Science* is 0036-8075/83 $1 + .10. *Science* is indexed in the *Reader's Guide to Periodical Literature* and in several specialized indexes.

Five New Products Every Day.

Sigma scientists work every day on requests for new products from researchers like you.

Over 50 years ago Sigma produced the first stable crystalline ATP for just one reason...researchers needed a reliable source. This tradition of "listening to our customers" is deeply ingrained in the Sigma philosophy. Our R&D scientists constantly review literature to keep abreast of refinements and revolutions in research.

But without input from our customers, we would never be able to offer such an extensive list of new products year after year.

We added over 2,000 new products to the 1995 Sigma Catalog. *That's more than five products every day!* In addition, our scientists have already manufactured and stocked many new items that will not appear in the catalog until 1996. So if you don't find what you need, give us a call. You may be surprised; a colleague may already have suggested the product you are looking for!

SIGMA

Where Science and Service Come Together.

Call collect: 314-771-5750,
800-325-3010,
or contact your local Sigma office.

AUSTRALIA AUSTRIA BELGIUM BRAZIL CZECH REPUBLIC FRANCE GERMANY HUNGARY INDIA ITALY JAPAN
KOREA MEXICO NETHERLANDS POLAND SPAIN SWEDEN SWITZERLAND UNITED KINGDOM UNITED STATES

A Sigma-Aldrich Company

Circle No. 19 on Readers' Service Card

edited by DAVID LINDLEY

Taking the heat

Hyperthermophilic organisms thrive at high temperatures: The archaebacterium *Pyrococcus furiosus* grows optimally at 100°C. How do enzymes maintain structure and activity at

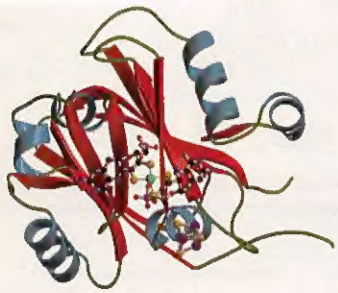

temperatures that normally denature proteins? Chan *et al.* (p. 1463) report the crystal structure of a *P. furiosus* metalloenzyme, aldehyde ferrodoxin oxidoreductase (AOR), which has two identical subunits containing an Fe_4S_4 cluster and a tungsten atom that is coordinated by four sulfur atoms from two molybopterin cofactors. The thermal stability of this enzyme does not appear to be directly attributable to the presence of metals; rather, AOR has a low surface area and a large number of ion pairs and buried atoms relative to other proteins.

Anomalous anomaly?

Spectroscopy in the extreme ultraviolet (EUV) reveals element abundance anomalies in the sun's corona relative to the photosphere. Until recently, similar measurements of other stars were technically impossible, but the launch of the Extreme Ultraviolet Explorer in 1992 allowed EUV observations of a few nearby stars. In EUV spectra of the sunlike star Procyon, Drake *et al.* (p. 1470) failed to find an abundance anomaly comparable to the sun's. The dissimilarity may be due to different heating mechanisms in the stars' outer layers, and bears on the rate at which certain elements are supplied into the galactic population of cosmic rays.

Knowing when to go

Programmed cell death, or apoptosis, is essential to organismal development and homeostasis. This week's special section summarizes what is known of the molecular mechanisms of apoptosis, and of its physiological functions in healthy and diseased organisms. Steller (p. 1445) describes the similarities of cell death genetics and pathways in *Calnorhabditis elegans*, *Drosophila*, and mammals, concluding that the machinery of cell death is highly conserved. Cell survival generally depends on the constant inhibition of apoptosis, but as Nagata and Golstein (p. 1449) explain, the immune system makes use of the apoptosis effector FasL, which triggers cell death when it binds to its cell-surface receptor. Thompson (p. 1456) reviews diseases, such as cancer, AIDS, and neurodegenerative diseases, that are related to insufficient or excessive apoptosis. Alteration of the apoptosis threshold could have therapeutic value in both cases. In a related report, Motoyama *et al.* (p. 1506) show that the *bcl-x* gene regulates apoptosis in immature neural and hematopoietic cells in developing mice.

Double diamond

Optical absorption in nanometer-scale clusters of semiconductors such as cadmium sulfide (CdS) can occur at dramatically different wavelengths than it does in CdS crystals. Vossmeyer *et al.* (p. 1476) found an aqueous reaction that produces $Cd_{17}S_4(SC_2H_4OH)_{26}$ clusters covalently linked in two interlaced diamond lattices. This is a crystal lattice of CdS clusters unlike the bulk material, and the difference may be at the root of the shifted optical properties.

Polymeric points of light

Light-emitting diodes (LEDs) are already widely used, but would find even more applications if they could be fabricated from cheap, durable polymers. Granström *et al.* (p. 1479) have made polymer LEDs of nanometer and micrometer dimensions, using the tiny pores in a commercially available filtration membrane to define the geometry of a doped conducting polymer. An electroluminescent polymer layer completes the LED sandwich. With more sophisticated pore fabrication methods, large-scale patterning of thousands or millions of LEDs is conceivable.

Warm out tonight

The influence of the moon's phase on the weather has been the subject of anecdote more than of science, but Balling and Cerveny (p. 1481) have used a globally averaged measurement of the temperature of the lower troposphere temperature, derived from satellite observations, to show that there is a tiny but significant warming at full moon. When 15 years of daily temperature measurements are correlated with the lunar period, a difference of 0.03 K between full moon and new moon appears. The authors speculate that the correlation may be due simply to the monthly variation in solar radiation reflected by the moon onto the Earth.

Hostile take-over

The mechanism by which retroviruses and retrotransposons integrate their replicated DNA into the host genome is clearly nonrandom, but the determinants of insertion sites are largely unknown. Kirchner *et al.* (p. 1488; see also perspective by Bushman, p. 1443) have devised an in vitro assay to study the site-specific insertion of the yeast retroviruslike element Ty3. Site-specific integration in vitro required Ty3 integrase, RNA polymerase III transcription factors TFIIIC and TFIIIB, and a tRNA gene, indicating that components of the host's polymerase III transcription machinery are commandeered to direct the integration event and the insertion site.

Moving recollections

Learning tests show that the human brain can store about seven distinct short-term memories. By simulating the phenomenon of afterdepolarization (ADP), in which neurons that fire in the presence of the neuromodulators acetylcholine and serotonin are rendered temporarily more excitable, Lisman and Idiart (p. 1512) have constructed a computer model which can store a similar number of memories as cycling patterns of repeatedly firing neurons. ADP allows a single stimulus to provoke and sustain a feedback cycle of repeated firings, and the observed time dependence of the ADP effect permits several such patterns to be stored at different phases of an oscillatory structure.

STATISTICA®

NEW release 5.0

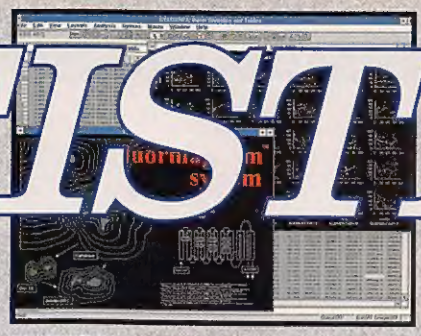

STATISTICA supports multitasking.
For example, now I am typing this text in MS Word, and in the background, STATISTICA is recalculating a large model (see the red progress bar).

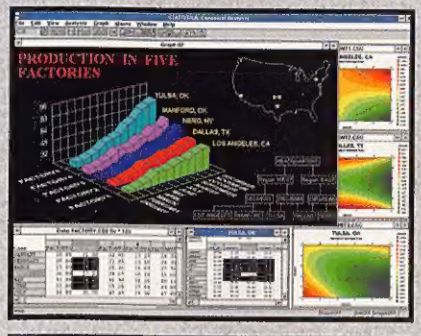

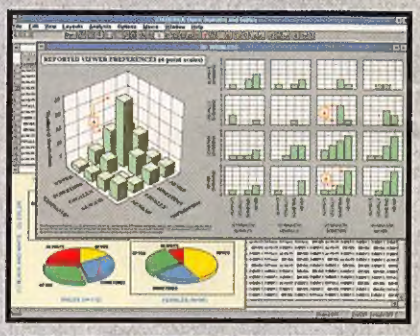

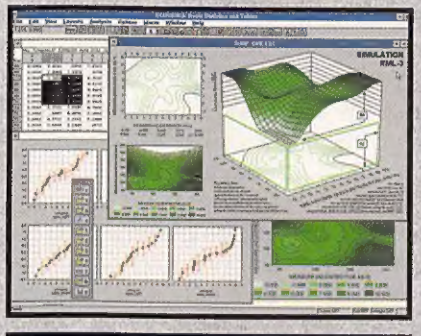

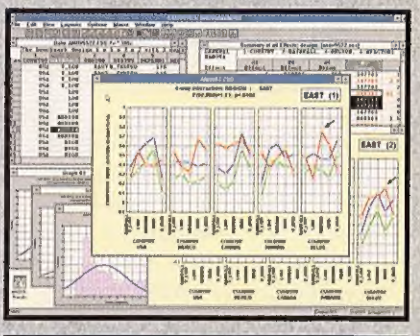

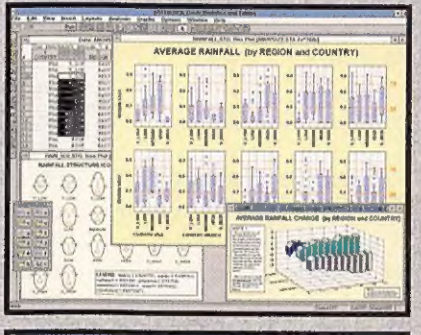

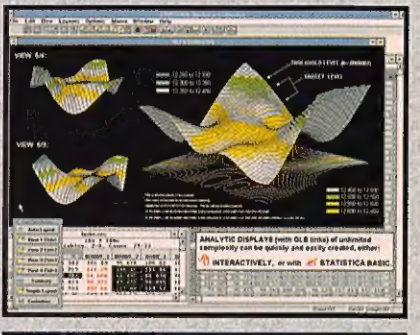
ANALYTIC DISPLAYS (with OLE links) of unlimited complexity can be quickly and easily created, either:
INTERACTIVELY, or with STATISTICA BASIC

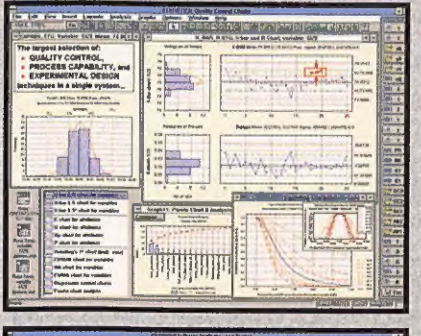

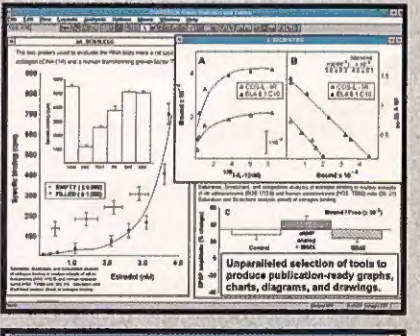

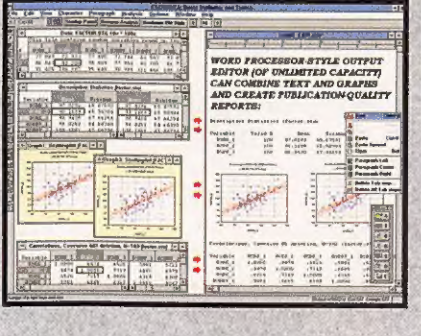
WORD PROCESSOR-STYLE OUTPUT EDITOR (OF UNLIMITED CAPACITY) CAN COMBINE TEXT AND GRAPHS AND CREATE PUBLICATION-QUALITY REPORTS!

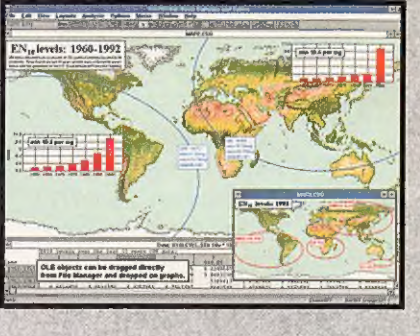

STATISTICA® (for Windows) ▪ A complete data analysis system with thousands of on-screen customizable, presentation-quality graphs fully integrated with all procedures ▪ Comprehensive *Windows*™ support, OLE (client and server), DDE, customizable *Auto Task* toolbars, pop-up menus ▪ Multiple data-, results-, and graph-windows with *data-graph* links ▪ The largest selection of statistics and graphs in a single system; comprehensive implementations of: Exploratory techniques with advanced brushing; multi-way tables with banners (presentation-quality reports); nonparametrics; distribution fitting; multiple regression; general nonlinear estimation; stepwise logit/probit; general ANCOVA/MANCOVA; stepwise discriminant analysis; log-linear analysis; confirmatory/exploratory factor analysis; cluster analysis; multidimensional scaling; canonical correlation; item analysis/reliability; survival analysis; a large selection of time series modeling/forecasting techniques; structural equation modeling with *Monte Carlo* simulations; and much more ▪ Online *Electronic Manual* with comprehensive introductions to each procedure and examples ▪ Hypertext-based Stats Advisor expert system ▪ Workbooks with multiple *AutoOpen* documents (e.g., graphs, reports) ▪ Extensive data management facilities (fast spreadsheet of unlimited capacity with long formulas, *Drag-and-Drop, AutoFill, Auto-Recalculate,* split-screen/variable-speed scrolling, advanced Clipboard support, DDE links, hot links to graphs, relational merge, data verification/cleaning) ▪ Powerful *STATISTICA BASIC* language with matrix operations, full graphics support, and interface to external programs (*DLLs*) ▪ Batch command language and editable macros, flexible "turn-key" and automation options, custom-designed procedures can be added to floating *Auto Task* toolbars ▪ All output displayed in Scrollsheets™ (dynamic, customizable, presentation-quality tables with instant 2D, 3D, and multiple graphs) or word processor-style report editor (of unlimited capacity) that combines text and graphs ▪ Extremely large analysis designs (e.g., correlation matrices up to 32,000x32,000, unlimited ANOVA designs) ▪ Megafile Manager with up to 32,000 variables (8 Mb) per record ▪ Unlimited size of files; extended ("quadruple") precision; unmatched speed ▪ Exchanges data and graphs with other applications via DDE, OLE, or an extensive selection of file import/export facilities (incl. *ODBC* access to virtually all data bases and mainframe files) ▪ Hundreds of types of graphs, incl. categorized multiple 2D and 3D graphs, ternary 2D/3D graphs, matrix plots, icons, and unique multivariate (e.g., 4D) graphs ▪ Facilities to custom-design new graph types and add them permanently to menus or toolbars ▪ On-screen graph customization with advanced drawing tools (e.g., scrolling and editing of complex objects in 32x real zoom mode), compound (nested) OLE documents, *Multiple-Graph AutoLayout Wizard,* templates, special effects, icons, page layout control for slides and printouts; unmatched speed of graph redraw ▪ Interactive rotation, perspective and cross-sections of 3D displays ▪ Large selection of tools for graphical exploration of data: extensive brushing tools with animation, fitting, smoothing, overlaying, spectral planes, projections, layered compressions, marked subsets ▪ Price **$995.**

Quick STATISTICA (for Windows) ▪ A subset of *STATISTICA*; comprehensive selection of basic statistics and the full analytic and presentation-quality graphics capabilities of *STATISTICA* ▪ Price **$495.**

STATISTICA/QC - *Industrial statistics add-on package* (requires *STATISTICA* or Quick *STATISTICA* for Windows) ▪ The largest selection of industrial statistics in a single package; quality control charts (compatible with real-time data acquisition systems), process capability analysis, R&R, sampling plans, and an extremely comprehensive selection of experimental design (DOE) methods ▪ Flexible tools to customize and automate all analyses and reports (incl. "turn-key" system options, and tools to add custom procedures) ▪ Price **$495.**

STATISTICA/Mac (for Macintosh) ▪ Price **$695** (Quick - **$395**).

Domestic sh/h $12 per product; 30-day money back guarantee.

Circle No. 13 on Readers' Service Card

StatSoft®

2325 E. 13th St. • Tulsa, OK 74104 • (918) 583-4149
Fax: (918) 583-4376

Overseas Offices: StatSoft of Europe (Hamburg, FRG), ph: 040/ 4200347, fax: 040/4911310; **StatSoft UK** (London), ph: 0462/482822, fax: 0462/482655; **StatSoft Pacific** (Melbourne, Australia), ph: (03) 663 6580, fax: (03) 663 6117; **StatSoft France** ph: (1) 45 66 97 00, fax: (1) 45 66 08 51; Available from other Authorized Representatives worldwide: Sweden: AkademiData Scientific ph: 018-210035, fax: 018-210039; Finland: Statcon Oy ph: 24-334678, fax: 24-333867; Belgium: Texma NewTech ph: 10 61 16 28, fax 10 61 69 57; South Africa: Osiris ph: 12-663-4500, fax 12-663-6114; Japan (Macintosh): Three's Company, Inc., ph: 03-3770-7600, fax 03-3770-7784; Japan (Windows): Design Technologies, Inc., ph: 03-3667-1110, fax: 03-3668-3110; Italy: Prompt SRL ph: 49-893-3227, fax: 49-893-2897; Poland: Companion Oprogramowanie ph: 12-369680, fax: 12-360791; Taiwan: Intelligent Integration Corp. ph: 2-759-1791, fax: 2-759-1790.

StatSoft, the StatSoft logo, STATISTICA, and Scrollsheet are trademarks of StatSoft, Inc.

SCIENCE

Publisher: Richard S. Nicholson
Editor-in-Chief: Daniel E. Koshland Jr.
Editor: Ellis Rubinstein
Managing Editor: Monica M. Bradford
Deputy Editors: Philip H. Abelson *(Engineering and Applied Sciences)*; John I. Brauman *(Physical Sciences)*; Thomas R. Cech *(Biological Sciences)*

Editorial Staff

Assistant Managing Editor: Dawn Bennett
Senior Editors: Eleanore Butz, R. Brooks Hanson, Pamela J. Hines, Barbara Jasny, Katrina L. Kelner, Paula A. Kiberstis, David Lindley, Linda J. Miller, L. Bryan Ray, Phillip D. Szuromi, David F. Voss
Associate Editors: Gilbert J. Chin, Suki Parks
Letters: Christine Gilbert, *Editor*; Steven S. Lapham
Book Reviews: Katherine Livingston, *Editor*
Contributing Editor: Lawrence I. Grossman
Editing: Valerie Jablow, *Supervisor*; Cara Tate, *Senior Copy Editor*; Jeffrey E. Cook, Harry Jach, Erik G. Morris, Christine M. Pearce
Copy Desk: Ellen E. Murphy, *Supervisor*; Joi S. Granger, Daniel T. Helgerman, Melissa Q. Rosen, Beverly Shields, Kameaka Williams, *Assistant*
Editorial Support: Sherryl Farmer, *Supervisor*; Brent Gendleman, Carolyn Kyle, Michele Listisard, Diane Long, Patricia M. Moore, Ted Smith
Administrative Support: Sylvia Kihara, Charlene King, Jeanette Prastein
Telephone: 202-326-6501; **FAX:** 202-289-7562; **TDD:** 202-408-7770

News Staff

News Editor: Colin Norman
Features Editor: John M. Benditt
Deputy News Editors: Tim Appenzeller, Joshua Fischman, Jean Marx, Jeffrey Mervis
News & Comment/Research News Writers: Linda B. Felaco (copy), Constance Holden, Richard A. Kerr, Andrew Lawler, Eliot Marshall, Rachel Nowak, Antonio Regalado (intern), Robert F. Service, Richard Stone, John Travis
U.S. Bureaus: Marcia Barinaga (Berkeley), Jon Cohen (San Diego), Anne Simon Moffat (Chicago), Wade Roush (Boston)
Contributing Correspondents: Barry A. Cipra, Robert Crease, Elizabeth Culotta, Ann Gibbons, Virginia Morell, Dennis Normile (Tokyo), Robert Pool, Gary Taubes
Administrative Support: Fannie Groom, Jennifer Hodgin
Telephone: 202-326-6500; **FAX:** 202-371-9227; **Internet Address:** science_news@aaas.org

Art & Production Staff

Production: James Landry, *Director*; Wendy K. Shank, *Manager*; Lizabeth A. Harman, *Assistant Manager*; Laura A. Creveling, Scherraine B. Mack, Stephen E. Taylor, *Associates*; Leslie Blizard, *Assistant*
Art: Amy Decker Henry, *Director*; C. Faber Smith, *Associate Director*; Katharine Sutliff, *Scientific Illustrator*; Holly Bishop, *Graphics Associate*; Elizabeth Carroll, Preston Morrighan, *Graphics Assistants*

Europe Office

Editorial: Richard B. Gallagher, *Office Head and Senior Editor*; Stella M. Hurtley, Julia Uppenbrink, *Associate Editors*; Belinda Holden, *Editorial Associate*
News: Daniel Clery, *Editor*; Michael Balter *(Paris)*, Patricia Kahn *(Heidelberg)*, *Contributing Correspondents*
Administrative Support: Janet Mumford; Anna Riches
Address: 14 George IV Street, Cambridge, UK CB2 1HH
Telephone: (44) 1223-302067; **FAX:** (44) 1223-302068
Internet address: science@science-int.co.uk

Science Editorial Board

Charles J. Arntzen
David Baltimore
J. Michael Bishop
William F. Brinkman
E. Margaret Burbidge
Pierre-Gilles de Gennes
Joseph L. Goldstein
Mary L. Good
Harry B. Gray
John J. Hopfield
F. Clark Howell
Paul A. Marks
Yasutomi Nishizuka
Helen M. Ranney
Bengt Samuelsson
Robert M. Solow
Edward C. Stone
James D. Watson
Richard N. Zare

EDITORIAL

Letter to Floyd Bloom, Editor-in-Chief–Elect

When I was offered the editorship of *Science*, I asked Phil Abelson, my predecessor, about the job. As you know, Phil is a man known for his understatement, so when he said, "It's the best job in the world," I was impressed. As usual, he was right and, as usual, he had understated.

It is difficult to analyze what makes the job so fascinating. Part certainly comes from the wide spectrum of the constituency—scientists from mathematics to social science, from Beijing to London, from student apprentice to institute director, from abstract academic to pragmatic production chief. Part certainly comes from the narrow focus of the constituency—intellectuals all, fragmented between authors and readers, with today's authors, tomorrow's readers, and vice versa, and a fragmentation between the specialized scientists advancing through the cutting edge and the nonspecialized scientist and highly intelligent layperson keeping up with the sweep of history.

Part is certainly the challenge of the mechanics of producing a weekly—from the editors who must choose between the best and the very best, to the art team that must bring colorful life to pages of dull numbers, to the production team that keeps prima donnas on the straight-and-narrow; from the news team that must make picoseconds sound leisurely and ice ages sound urgent, to the copy editors and proofreaders to whom perfection is beauty and misspelled words and misplaced commas are cardinal sins, to the manuscript trackers who are strong advocates of "timeliness is saintliness," to administrative staff members who discover infinite supplies of oil for squeaky wheels, to the advertising department that wants to sell more ads than we have pages. Part is the intimacy of the editor with the constituency—from the irate author who calls from Sydney to the equally irate senator who calls from Washington, D.C.

Part is the constant communication with pioneers in science—the Board of Reviewing Editors, the Editorial Board, the anonymous reviewers—who so altruistically give up time from busy schedules to lend a hand to a mutual enterprise. You have chosen, as I did, to keep your lab going—a wise move, because you remain part of the constituency, constantly reminded of what it means to have a paper rejected or a grant proposal accepted.

You will find that *Science* requires you to place one foot firmly in the world of science and timelessness, producing a penetrating, clear light that illuminates obscurity and makes clear concepts that must stand firm through the slings and arrows of the ages. It will also require you to put the other foot firmly in the world of journalism and timeliness, in which the goal is a Roman candle that flashes its brilliance across the darkened sky, revealing the newest in a fleeting moment of entertainment and awe. The combination in one slender journal makes unusual demands for insight and objectivity in the news and for timeliness and excitement in the science.

If this listing of the responsibilities seems daunting, you will be sustained by a superb staff who, far from being dismayed by the ambiguities of the frontier, are exhilarated and eager to confront the challenge. Indeed, that may be the ultimate reward—the joy of camaraderie with the dedicated fellow adventurers listed on the masthead, in the table of contents, and below the title of every manuscript, who sail forth each week through mountainous waves of information to make their way to the quiet harbor of a portable issue of the journal.

On page 1441, two of your colleagues, Richard A. Lerner and Roger Guillemin, have described your illustrious career to our readers. A career of scientific discovery and professional responsibilities will serve you well, and it pleases me that the torch is passed on to one so worthy. So enjoy your leisure between now and 1 May. Weeklies and roller coasters are designed for fun and excitement, not tranquility.

Daniel E. Koshland Jr.

NOW YOU HAVE THE GREEN LIGHT FOR...

GFP

GREEN FLUORESCENT PROTEIN

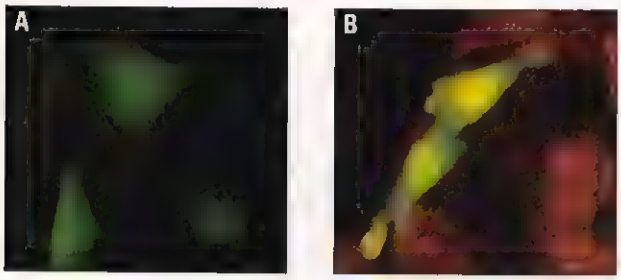

Transient expression of GFP in mammalian cells. Monolayer cultures of CHO-K1 cells were transfected using liposomes with a mammalian GFP expression construct. The transfection efficiency of this technique is typically 10–15% with CHO cells **Panel A.** Cells were prepared for fluorescence microscopy 24 hr post-transfection and photographed immediately to prevent loss of normal morphology **Panel B.** Cells were fixed 24 hr post-transfection in 3.7% formaldehyde/PBS, counterstained with 1.0 µg/ml propidium iodide, and photographed in 90% glycerol in 100 mM Tris-HCl (pH 7.5).

NOTE Graphic, "GFP" above is actually *E. coli* transformed with a bacterial GFP expression vector and photographed under illumination and a long wave UV lamp.

Vector	Size	Cat.#
pGFP-1	20 µg	6090-1
pGFP-N1	20 µg	6091-1
pGFP-N2	20 µg	6092-1
pGFP-N3	20 µg	6093-1
pGFP-C1	20 µg	6094-1
pGFP-C2	20 µg	6095-1
pGFP-C3	20 µg	6096-1

The Green Fluorescent Protein (GFP) is a revolutionary *in vivo* marker of gene expression and protein localization. CLONTECH has incorporated GFP in its new Living Color™ family of reporter vectors which can be used for real time, *in vivo* reporting of gene expression and protein localization, for separation of cells by FACS, as a convenient assay for cell transformation, and for many other applications. Now you have the Green Light. Only from CLONTECH. Call 1-800-662-CLON or contact your local distributor.

Come visit us at AACR Booth #301 & 303

DON'T EXPERIMENT WITH ANYTHING ELSE.

CLONTECH

4030 Fabian Way, Palo Alto, California 94303 USA
FAX: 800/424-1350 415/424-1064 • TEL: 800/662-CLON 415/424-8222
e-mail: tech@CLONTECH.com • orders@CLONTECH.com

©1995 CLONTECH Laboratories, Inc.

(AD51020)

Circle No. 35 on Readers' Service Card

SCIENCE

Published by the American Association for the Advancement of Science (AAAS), *Science* serves its readers as a forum for the presentation and discussion of important issues related to the advancement of science, including the presentation of minority or conflicting points of view, rather than by publishing only material on which a consensus has been reached. Accordingly, all articles published in *Science*—including editorials, news and comment, and book reviews—are signed and reflect the individual views of the authors and not official points of view adopted by the AAAS or the institutions with which the authors are affiliated.

The American Association for the Advancement of Science was founded in 1848 and incorporated in 1874. Its objectives are to further the work of scientists, to facilitate cooperation among them, to foster scientific freedom and responsibility, to improve the effectiveness of science in the promotion of human welfare, to advance education in science, and to increase public understanding and appreciation of the importance and promise of the methods of science in human progress.

Membership/Circulation
Director: Michael Spinella
Deputy Director: Marlene Zendell
Member Services: Rebecca Dickerson, *Manager*; Mary Curry, *Supervisor*; Pat Butler, Helen Williams, Laurie Baker, *Representatives*
Marketing: Dee Valencia, *Manager*; Jane Pennington, *Europe Manager*; Hilary Baar, *Associate*; Angela Mumeka, *Coordinator*
Research: Renuka Chander, *Manager*
Business and Finance: Jacquelyn Roberts, *Manager*; Robert Smariga, *Assistant Manager*
Administrative Assistant: Nina Araujo de Kobes
***Science* Member Services**
Marion, Ohio: 800-347-6969;
Washington, DC: 202-326-6417
Other AAAS Programs: 202-326-6400

Advertising and Finance
Associate Publisher: Beth Rosner
Advertising Sales Manager: Susan A. Meredith
Recruitment Advertising Manager: Janis Crowley
Business Manager: Deborah Rivera-Wienhold
Finance: Randy Yi, *Senior Analyst*; Shawn Williams, *Analyst*
Marketing: John Meyers, *Manager*; Allison Pritchard, *Associate*
Traffic Manager: Tina Turano
Recruitment: Terri Seiter, *Assistant Manager*; Pamela Sams, *Production Associate*; Debbie Cummings, Celeste Miller, Rachael Wilson, *Sales*; Charlotte Longhurst, *European Sales*
Reprints Manager: Corrine Harris
Permissions Manager: Lincoln Richman
Exhibits Coordinator: Arlene Ennis
Sales Associate: Carol Maddox

PRODUCT ADVERTISING SALES: East Coast/E. Canada: Richard Teeling, 201-904-9774, FAX 201-904-9701 • **Midwest/Southeast:** Elizabeth Mosko, 312-665-1150, FAX 312-665-2129 • **West Coast/W. Canada:** Neil Boylan, 415-673-9265, FAX 415-673-9267 • **UK, Scandinavia, France, Italy, Belgium, Netherlands:** Andrew Davies, (44) 1-457-838-519, FAX (44) 1-457-838-898 • **Germany/Switzerland/Austria:** Tracey Peers, (44) 1-270-760-108, FAX (44) 1-270-759-597 • **Japan:** Mashy Yoshikawa, (3) 3235-5961, FAX (3) 3235-5852
RECRUITMENT ADVERTISING SALES: US: 202-326-6555, FAX 202-682-0816 • **Europe:** Gordon Clark, (44) 1-81539-5211, FAX (44) 1223-302068 • **Australia/New Zealand:** Keith Sandell, (61) 02-922-2977, FAX (61) 02-922-1100
Send materials to *Science* Advertising, 1333 H Street, NW, Washington, DC 20005.

Information for Contributors appears on pages 112–114 of the 6 January 1995 issue. Editorial correspondence, including requests for permission to reprint and reprint orders, should be sent to 1333 H Street, NW, Washington, DC 20005.
Internet addresses: science_editors@aaas.org (for general editorial queries); science_letters@aaas.org (for letters to the editor); science_reviews@aaas.org (for returning manuscript reviews); membership@aaas.org (for member services); science_classifieds@aaas.org (for submitting classified advertisements)

LETTERS

AIDS Research Policy

Larry Kramer writes (Letters, 3 Mar., p. 1249) to criticize aspects of my recent policy forum ("Reexamining AIDS research priorities," 3 Feb., p. 633). Kramer has played an important role in the community response to human immunodeficiency virus (HIV) infection and acquired immune deficiency syndrome (AIDS). All of us engaged in the struggle to conquer AIDS must salute his efforts. Nonetheless, his criticisms represent an inaccurate description of the role and the actions of the National Institutes of Health (NIH) Office of AIDS Research (OAR).

Kramer states that the OAR has abdicated or postponed its responsibility for the preparation of a comprehensive plan to guide NIH-sponsored AIDS research. Quite the opposite is the case. Within 6 weeks of my appointment as director of OAR (in February 1994), such a plan was completed and formed the basis for the development of the fiscal year (FY) 1996 budget request, now being considered by Congress. This plan was prepared with extensive input from close to 200 government, university, and industrial scientists and from representatives of a wide array of community organizations, including some that Kramer founded. The process produced a consensus on the goals, objectives, and strategies that lie before us. The plan states the scientific priorities and opportunities for which precious resources should be allocated. Implementation of this plan has already led to substantial redirections of the AIDS research effort in response to these new priorities, with the goal of finding new molecular targets and, most important, filling the "pipeline" of new therapeutic agents and potential vaccine candidates. The plan has been forwarded to the President, as required by law. The OAR is already completing the update of that plan to reflect priorities for the FY 1997 budget.

This planning function is not the same as the responsibilities of the evaluation working group Kramer refers to in his letter. The evaluation group consists of distinguished scientists, chaired by Arnold Levine of Princeton University. The working group has been asked to conduct an evaluation of all NIH-sponsored AIDS research. Such an evaluation must be an essential part of any serious effort to plan for AIDS research and will make possible the enunciation of guiding principles for such research over the next 5 years.

Kramer appears to be unaware of the high priority we at the OAR have placed on primate research, although this was clearly stated in our policy forum. NIH currently sponsors much primate research, and the National Institute of Allergy and Infectious Diseases has under review a series of research grant proposals aimed at further expanding such efforts. Kramer's view that drug development would be markedly accelerated by the use of the simian immunodeficiency virus/ macaque model is not supported by advice we have received from a number of senior scientists in the pharmaceutical industry who do not place such work on the critical path for drug development. By contrast, macaque research can make central contributions to the understanding of the pathogenesis of AIDS, to the development of novel interventions, and to the clarification of the nature of protective immunity. It is precisely this type of research that we intend to enhance. In fact, the OAR has provided emergency support to the National Center for Research Resources to purchase *nemestrina* macaques and import them into the United States.

Kramer scoffs at the use of conventional grant applications and at the process of peer review by knowledgeable scientists to determine priorities for funding innovative research. What does he propose as a substitute—the central direction of such research by a science "commissar?" Such "command science" is likely to be as ineffective as "command economics" proved to be. It is precisely the view that a small group of administrators, scientists, or activists can foresee where key breakthroughs are likely to occur that is of such concern. Peer review as a guide to science funding has proven over and over to be the most effective way to gain new knowledge. By contrast, efforts to exploit promising leads have been and will continue to be vigorously pursued by the more directed funding mechanisms available at NIH.

Finally, Kramer's contention that the U.S. taxpayers "are getting rotten value for their money" in their "$14 billion" investment in NIH-sponsored medical research is untrue, unsupportable, and extremely unfortunate. First, the total NIH budget is somewhat over $11 billion (not $14 billion, as stated in Kramer's letter). The nation's commitment to the support of medical science, through NIH-sponsored research, has contributed immeasurably to the health of the American people. New treatments for heart

disease, cancer, and infectious diseases, among others, have emerged from NIH-conducted and supported work. The mapping and identification of genes controlling susceptibility to various diseases is opening new vistas for diagnostic and therapeutic advances. NIH support has advanced research on gene therapy and formed the knowledge base for the biotechnology industry. Within the last few months a series of exciting and potentially important advances in AIDS research, sponsored by NIH funding, have been reported.

I applaud Kramer's personal commitment to furthering our efforts against AIDS and, indeed, all diseases. Nonetheless, I must differ fundamentally with him regarding the quality and the urgency of the government's efforts to deal with the HIV epidemic. In the past year we have consulted with a wide range of experts within the scientific community and, in collaboration with community representatives, have prepared the first truly comprehensive plan for NIH AIDS research. We have set in place refocused scientific priorities and have shifted resources to meet these priorities. We are preparing the first frank appraisal of the overall AIDS research program. We are confident that a new and effective course is being charted for the future of NIH AIDS research.

William E. Paul
Director,
Office of AIDS Research,
National Institutes of Health,
Bethesda, MD 20892–2340, USA

Congratulations to William Paul for so clearly and boldly laying out the key questions that must be addressed if we are to make progress in the coming 5 years of AIDS research.

To many AIDS patients, myself included, the systematic process of the scientific method has often seemed brutally insensitive to the pressing realities of living with AIDS. For the first 15 years of the epidemic, scientists and activists alike sought fast answers, shortcuts, and ways to jimmy-rig the system, in hopes of avoiding the difficult step-by-step effort to answer basic questions. That we have made little progress in preventing the spread of HIV or treating AIDS suggests a need to abandon these failed policies and to methodically create a solid evidential basis for future behavioral and therapeutic research, as well as for vaccine research programs.

Paul has brought together our nation's leaders in the fields of immunology and virology in an effort to develop a comprehensive program to investigate the AIDS pandemic. Now we must ensure that policy-makers continue to provide the monetary and political support that will be needed to answer these questions. Without the kind of concerted effort proposed by Paul, it is unlikely that our clinical research effort will offer credible hope to those currently living with or at risk for acquiring HIV and AIDS.

Spencer Cox
Treatment Action Group,
200 East 10 Street, #601,
New York, NY 10003, USA

Paul clearly sets forth the mandate of the OAR to create a comprehensive blueprint for the study of HIV disease. A key prerequisite for this plan is that everyone needs to be speaking the same language.

With the focus of AIDS research shifting away from CD4 T cells and toward CD8 T cells, antigen-presenting cells, cytokines, and viral load, an obvious problem with both basic science and clinical trials is that important immunological data may not be examined or reported in these studies. Consequently, a fundamental task for the OAR should be to set standards for all NIH-funded research in terms of the immunological parameters to be monitored. As a guideline for these

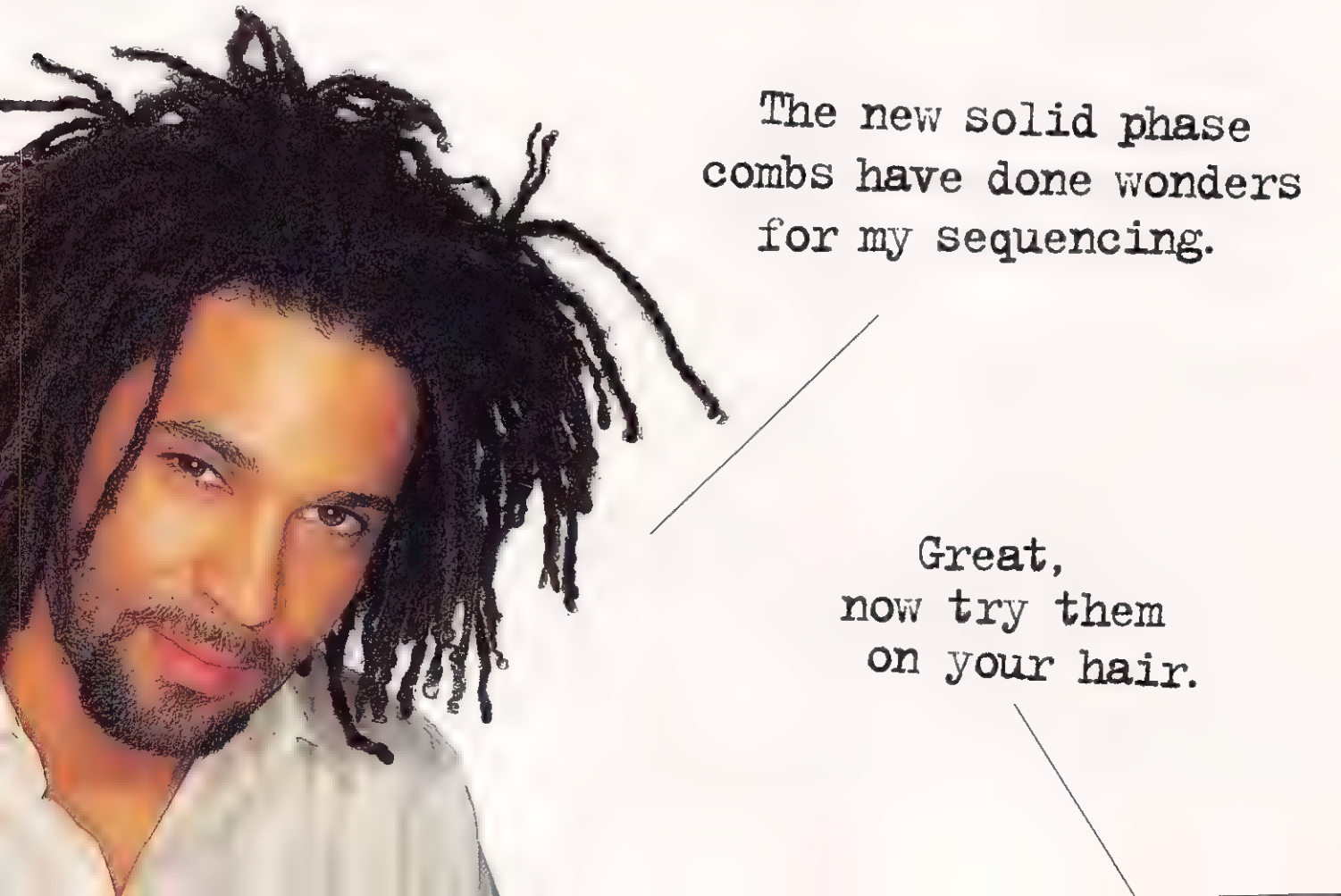

parameters, one could draw from the factors mentioned by Paul: Th1/Th2 cytokines; natural killer cells; markers that define cytotoxic, suppressor, activated, naïve/memory, or primed T cell subsets; and quantitative HIV polymerase chain reaction.

The language of AIDS immunology has changed over the years. It is imperative for the OAR to provide a much needed immunological thesaurus in order to give meaning to future AIDS trials.

Billi Goldberg
Dinitrochlorobenzene Study Group, San Francisco, CA 94114, USA
Raphael B. Stricker
HemaCare Corporation, 450 Sutter Street, Suite 1504, San Francisco, CA 94108, USA

■

Biosphere 2

Gary Taubes' article about Biosphere 2 (News & Comment, 13 Jan., p. 169) does not acknowledge that "the previous management" were, in fact, the creative team that beginning in 1984 partially owned, designed, built, and then experimentally tested Biosphere 2 until April 1994 (*1*). Taubes writes as if Biosphere 2 materialized by itself. I conceived and invented Biosphere 2 and directed its research and development division; Margret Augustine co-designed and built Biosphere 2; William Dempster devised and supervised engineering systems, making essential patented inventions; Abigail Alling created and brought to sustained life the extraordinary ocean and marsh systems; Mark Nelson worked with me on biospheric theory and in convening international scientific conferences on closed ecological life systems (biospheres)—at the Royal Society (1987), at Krasnoyarsk, Russian Republic (1989), and at Biosphere 2 (1992).

Taubes states that "Mission One" experienced "technical glitches and [was] criticized for producing little of scientific value." We lifted off a complexly engineered $150-million project and ran it for a 2-year experimental test, as scheduled. Our "glitches" should be compared with those of any new experimental project.

John Allen
Founder, Biosphere 2, Director, Biospheric Design, Inc., Director, Planetary Coral Reef Foundation, Director, Institute of Ecotechnics, Director, EcoFrontiers, Inc., 32038 Caminito Quieto, Bonsall, CA 92003, USA

References

1. J. Allen, *Biosphere 2: The Human Experiment* (Penguin, New York, 1991); *Space Biospheres* (Orbit/Synergetic, Malabar, FL/Tucson, AZ, 1987); *Biological Life Support Technologies* (National Aeronautics and Space Administration, Washington, DC, 1990); H. Odum, *Ecological Mesocosms* (Springer-Verlag, New York, 1994); M. Nelson *et al.*, *Bioscience* **43**, 225 (April 1993).

■

Oncogenes and Cancer

Most cellular oncogenes were discovered because they share their coding sequences with retroviral oncogenes. On that basis, it was postulated that cellular oncogenes could function like viral oncogenes, provided they have "somehow gone awry" (Jean Marx, Research News, 23 Dec., p. 1942). However, in the excitement about homology, nonhomology was overlooked, and cellular and viral oncogenes received the same names. But retroviral oncogenes have promoters that are 100 to 1000 times stronger than the promoters of the corresponding oncogenes from both normal and cancer cells (*1*). Therefore cloned viral oncogenes and artificial genes, in which the coding regions of unmutated cellular oncogenes (*ras*, *src*, and *myc*) are linked to retroviral

What do most people with threadlike cranial outgrowth reach for after a shower? What revolutionary new tool for automated DNA sequencing controls everything from capture of crude PCR® products to ensuring results are generated quickly and easily? The one answer to both these questions—combs.

In fact, new solid phase sequencing combs let you process samples with ease, reduce your pipetting by about 70% and speed up your sequencing. What's more, these combs give you control over it all at the prep stage. So where can you find these little wonders?

In the AutoLoad™ Solid Phase Sequencing Kit from Pharmacia Biotech—a product that quite literally puts the future of sample handling and DNA sequencing in the palm of your hand. With AutoLoad, your sequencing results will come faster as you simultaneously prepare 10 samples in the same time it now takes you to do one. The AutoLoad combs allow for easy elution into an ALF™ DNA Sequencer gel cassette without having to split samples or do centrifuging for sample clean-up—just stick them in and your sample handling is finished.

Since the eight streptavidin-coated comb teeth bind the biotinylated PCR products virtually forever, you won't have to pipette material from tube to tube. This patented technique is also partly a purifying step and is the most innovative way of preparing material for sequencing to date.

If permanently securing samples to the teeth of a comb sounds like a simple enough solution, that's only because it is. But who says a major step forward in sample handling has to be complicated? You'll certainly never hear that from Pharmacia Biotech.

Just call 1 (800) 526-3593 in North America, or +46 18 16 5011 from the rest of the world, and we'll send you a brochure that shows how combs make molecular biology research easier for you. But don't be surprised if you hear words like threadlike cranial outgrowth coming across your phone's ear piece.

After all, we're scientists.

Pharmacia Biotech

Uppsala, Sweden. (And the rest of the world)

* PCR is a patented process of Hoffman La Roche.

Circle No. 48 on Readers' Service Card

promoters (*2*, *3*), transform normal, euploid cells to cancer cells (*1*), but cloned cellular oncogenes do not (*4*).

The finding that point-mutated *ras* genes from some cancers transform aneuploid 3T3 mouse cells upon transfection appeared to be "making the link" between viral and cellular oncogene functions.

But the hypothesis that point mutation generates cancer genes is confirmed neither (i) experimentally nor (ii) numerically. All cells transformed by transfected *ras* genes proved to express *ras* genes 100 to 1000 times more than the cancer cells from which they were isolated—just as in cells transformed by retroviruses with *ras* genes (*1*, *2*). In other words, the transfection assay created an expression artifact in which some *ras* genes were rearranged and concatenated to allow high expression. In primary cancers, mutated *ras* genes are expressed no more than in normal proliferating cells (*1*). Indeed, point-mutated cellular *ras* genes, which transform 3T3 cells only upon transfection—are found in normal animals and in normal transgenic mice (*1*, *7*).

According to Daniel E. Koshland Jr. (Editorial, 23 Dec., p. 1925), 1 in 10^9 nucleotides is mutated every time a cell divides. As our cells contain 10^9 nucleotides and we are made up of 10^{14} cells, we contain 10^5 cells with a mutated *ras* gene. In addition, there are 70×10^5 cells with other mutated oncogenes in our bodies because there are 70 oncogenes in our cells. If these mutations were indeed oncogenic, we would all contain 70×10^5 cancer cells.

In view of this, it has been postulated that mutated cellular oncogenes play a role in multigene carcinogenesis. However, the autonomous viral oncogenes are not even models for multigene carcinogenesis (*5*). Moreover the oncogene mutation hypothesis predicts euploid cancers that are rarely found (*6*). Therefore I suggest that imbalance of chromosomes, carrying just normal genes—a perfect correlate with cancer (*6*)—be reconsidered for the understanding of oncogenesis (*1*).

Peter H. Duesberg
Department of Molecular and Cell Biology, University of California, Berkeley, CA 94720, USA

References

1. P. H. Duesberg and J. R. Schwartz, *Prog. Nucleic Acid Res. Mol. Biol.* **43**, 135 (1992).
2. A. K. Chakraborty, K. Cichutek, P. H. Duesberg, *Proc. Natl. Acad. Sci. U.S.A* **88**, 2217 (1991); M. Lang, I. Treines, P. H. Duesberg, R. Kurth, K. Cichutek, *ibid.* **91**, 654 (1994).
3. R.-P. Zhou and P. H. Duesberg, *ibid.* **85**, 2924 (1988); Y. Wu, H. Zhou, P. Duesberg, *ibid.* **89**, 6393 (1992).
4. E. J. Stanbridge, *Annu. Rev. Gen.* **24**, 615 (1990).
5. Y. Wu and P. H. Duesberg, *Proc. Natl. Acad. Sci. U.S.A.* **91**, 4039 (1994)
6. J. German, Ed., *Chromosomes and Cancer* (Wiley, New York, 1974).
7. Y. Haupt, W. S. Alexander, G. Barri, S. P. Klinken, J. M. Adams, *Cell* **65**, 753 (1991); A. Balmain, M. Ramsden, G. T. Bowden, J. Smith, *Nature* **307**, 658 (1984); S. H. Reynolds, S. J. Stowers, R. R. Maronpot, M. W. Anderson, S. A. Aaronson, *Proc. Natl. Acad. Sci. U.S.A.* **83**, 33 (1986); J. Leon, H. Kamino, J. J. Steinberg, A. Pellicer, *Mol. Cell. Biol.* **8**, 786 (1988); H. Hirai *et al.*, *Nature* **337**, 430 (1987); E Liu, B. Hjelle, R. Morgan, F. Hecht, J. M. Bishop, *ibid.* **330**, 186 (1987); E. Sinn *et al.*, *Cell* **49**, 465 (1987); R. E. Finney and J. M. Bishop, *Science* **260**, 1524 (1993)

I disagree with the wording in two places in the Research News article by Jean Marx "Oncogenes reach a milestone." I am described as a "then [1972–1975] postdoc of Bishop's." Yet when I joined Michael Bishop, I was not a postdoc. I was a visiting scientist from France, holding a long-term, faculty-like position at the Centre National de la Recherche Scientifique.

Reference is also made to "Bishop and Varmus's discovery," when the first experimental evidence of the "Cellular origin of retroviral oncogenes" (*1*) is mentioned. This is work of which I am the first author and for which I received the 1987 Louis Jeantet Prize for Medicine.

Sophisticated cyclic AMP and cyclic GMP Analogues Available!

- cyclic nucleotide – based inhibitors of cAMP-/cGMP-dependent protein kinases (cAK/cGK)
- hydrolysis-resistant activators of cAK/cGK for long-term activation experiments
- rapidly metabolizable structures for pulse – type activation
- potent activators of cyclic nucleotide dependent ion channels
- analogues with different cGK isozyme selectivity (Iα/β)
- pairs of analogues with opposite site selectivity for preferential activation of either type I or type II of the cAK isozymes
- pairs of synergistic analogues with high activation potential
- analogues with extremely high membrane-permeability
- affinity gels with PDE-stable ligands for cAK, cGK & PDE
- main metabolites of PDE-sensitive structures
- common cAMP/cGMP analogues
- fluorescent structures
- reactive intermediates

BIOLOG - LIFE SCIENCE INSTITUTE -

Forschungslabor und Biochemica – Vertrieb GmbH

Head office:
Flughafendamm 9a,
P.O. Box 107125
D-28071 Bremen, Germany
Phone: 49 (0) 421 59 13 55
Fax: 49 (0) 421 59 47 71

US/Canada distributor:
Ruth Langhorst Int'l. Marketing
7514 Girard Ave. Suite 1-411
La Jolla, CA 92037
Phone: (619) 457-1573
Fax: (619) 456 0810

In Japan contact:
Wako Pure Chemical Ind., Ltd
Phone
Tokyo 03-270-8571
Osaka 06 203-3741

Circle No. 33 on Readers' Service Card

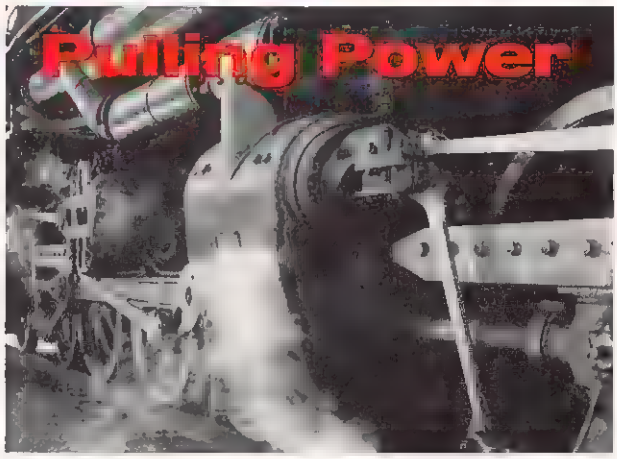

Model P-97

Sutter micropipette pullers are the finest available.
Built-in versatility and repeatability are based on 20 years of continuous research and development.
Call or write for a free catalog.

Sutter
Instrument Company
40 Leveroni Court
Novato CA 94949

phone 415-883-0128 fax 415-883-0572

Circle No. 18 on Readers' Service Card

The time has come to recognize the truth about this productive collaboration among scientists from France and the United States.

Dominique Stéhelin
Director,
Unite d'Oncologie Moleculaire, URA 1160,
Centre National de la Recherche Scientifique,
Institut Pasteur de Lille,
59019 Lille Cédex, France

References

1. D. Stéhelin, H. Varmus, M. Bisnop, P. Vogt, *Nature* **260**, 170 (1976).

■

China's Internet Links

As someone who has worked at both the Chinese Academy of Sciences' (CAS's) Computer Network Center and at the Institute of High Energy Physics (IHEP) in Beijing, I would like to correct an error in Ted Plafker's article "China to triple Internet links with commercial hookups" (News & Comment, 13 Jan., p. 168). The link between the CAS's Computer Network Center and Stockton, California, provided by Sprint is not "the single connection available since last spring," as the article states; nor is it "China's first direct link to a U.S. Internet gateway."

The first direct academic link from China to the United States was a link between IHEP to the Stanford Linear Accelerator Center. It was provided jointly by the Chinese Ministry of Post and Telecommunication and AT&T. It became operational in March 1993 and was used to connect IHEP with the DECnet portion of the U.S. Department of Energy's Energy Sciences network (ESnet). In March 1994, this link also became an Internet link through a gateway at ESnet. In August 1994, the far end of the link was moved from the Stanford Linear Accelerator Center to KEK, the high energy physics center of Japan, making way for a future transition from satellite to terrestrial communication using underwater fiber optic cables. Since 1993, IHEP has provided many Chinese scientists with access—first electronic mail only and, later, full access—to the Internet. Both Hu Daoyuan and Qian Hualin used IHEP's service before CAS's link to the United States was established.

Xin Hao
IHEP Computing Center,
Post Office Box 918-7,
Beijing 100039,
People's Republic of China
E-mail: haoxin@bepc2.ihep.ac.cn

Zinc Selenide Lasers

In the Meeting Briefs of 22 April 1994, in a section entitled "Happy to see the blues" (Research News, p. 510), the work of Shuji Nakamura on gallium nitride blue light–emitting diodes (LEDs) was described, and comments were made about the rapid breakdown of zinc selenide lasers, "obviously rendering them useless for commercial applications." Gallium nitride blue light–emitting diodes should not be compared with lasers, because the conditions under which lasing occurs are vastly more demanding. The applied power density is much higher. Zinc selenide devices, when operated in the LED mode, show comparable lifetimes; these are steadily improving, as is common in the early stages of electronic devices.

Zinc selenide, as a laser, does indeed have serious problems; however, it is fundamentally a very rugged material (melting point, 1520°C). Laser action in the usable diode form has been positively established, and research solving the lifetime problems of these lasers is making rapid progress.

Brian J. Fitzpatrick
Optical Semiconductors, Inc.,
8 John Walsh Boulevard, Suite 421,
Peekskill, NY 10566, USA

Get It FASTER

Get It BIGGER℠

Get It RIGHT

Get an 85–100kb, 120+kb, or 1,000kb Genomic Clone in a Matter of Days From Genome Systems

Our services include; P1 (85kb) genomic library screening service (human, ES mouse for knockouts, rat and drosophila).

New! Human PAC/BAC™ (120kb+ insert) genomic library screening service.

New! Human PAC/BAC™ high density filters.

New! Fluorescent in-situ hybridization (FISH).

New! YAC library screening service (human, mouse).

New! Go Germline℠ ES and MEF cells for making mouse knockouts.

New! Custom robotic colony picking and spotting services.

GenomeSystemsInc™

8620 Pennell Drive
St. Louis, Missouri 63114, USA

800 – 430 – 0030 or, 314 – 692 – 0033
Facsimile: 314 – 692 – 0044

France: Appel gratuit, 0590 – 2104

Germany: Rufen sie uns an zum ortstarif, 0130 – 81 – 9081

UK: Call us free on, 0800 – 89 - 3733

Circle No. 15 on Readers' Service Card

A Dynamite way to get your data:

Protein-Protein/DNA/RNA interactions

Cooperative Protein-DNA binding studies
van Dijk, M.A. and Murre, C. (1994) *Cell*, **78**, 1.

DNA-Protein complex formation, immunoprecipitation
Sif, S. and Gilmore, T.D. (1993) *J. Virol.* **67**, 7612.

Protein-RNA binding assays
Lutz, C.S. and Alwine, J.C. (1994) *Gen. Devel.* **8**, 576.

DNA binding
Loh, L.C. *et al.* (1994) *Virology* **200**, 413.

Protein-protein interaction, Mapping protein binding sites
Patrick, D.R. *et al.* (1994) *J. Biol. Chem.* **269**, 6842.

Fusion protein binding assays
Lukac, D.M. *et al.* (1994) *J. Virol.* **68**, 5184.

Analysis of truncation mutations in MDS
Screening for translation-terminating mutations in MDS
Roest, P.A. *et al.* (1993) *Human Mol. Gen.* **2**, 1719.

Mutational analysis

Easy, rapid method of screening large number of mutants. Safety assessment prior to large scale culture of toxins
Johnson, V.G. and Nicholls, P.J. (1994) *J. Biol. Chem.* **269**, 4349.

Confirmation of ligand-binding region, analysis of mutants
Kallio, P.K. *et al.* (1994) *Endocrinology* **134**, 998.

Gel shift analysis of deletion mutants
Palvimo, J.J. *et al.* (1993), *Mol. Endo.* **7**, 1399.

Verification of cloned genes

Verification that clone expressed a protein of the predicted size
Daigle, I. and Li, C. (1993) *Proc. Natl. Acad. Sci. USA*, **90**, 12045.

Verification of clone and immunoprecipitation
Greig, A. *et al.* (1994) *Carcinogenesis Research*, **74**, 41.

Protein translation studies
Joyce, G.F. (1993) *Nature* **366**, 1205.

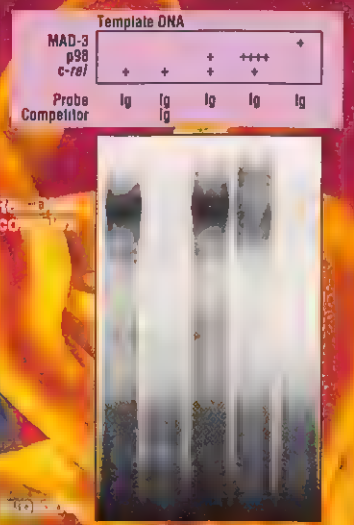

DNA to protein in a single tube... TNT® Coupled Transcription and Translation Systems*

The TNT® Coupled Transcription/Translation Systems are a fast, efficient and reliable method for *in vitro* production of proteins.

We would like to recognize some of the numerous innovative applications our customers have developed using *in vitro* translated proteins generated in the TNT® Systems. For a bibliography, please call Promega and request part #BL001.

Reagents and a detailed protocol provided for 40 x 50µl coupled reactions

Polymerase	Rabbit Reticulocyte Part #	Wheat Germ Extract Part #
T7	L4610	L4140
SP6	L4600	L4130
T3	L4950	L4120
T7/SP6	L5020	L5030
T7/T3	L5010	L5040

Send us a copy of a publication using a TNT® System, and we'll send you a TNT® System T-shirt free.

...only from Promega

Try the new trial size TNT® Coupled Reticulocyte System (Cat.# L4611). The system provides sufficient reagents for 8 x 50µl reactions or 16 x 25µl reactions.

*U.S. Patent No. 5,324,637 has been issued to Promega Corporation for coupled transcription/translation systems that use bacteriophage RNA polymerases and eukaryotic lysates.
TNT is a registered trademark of Promega Corporation.

For Direct Sales in USA: Promega Corporation • 2800 Woods Hollow Road • Madison Wisconsin • 53711-5399 • Toll Free 800-356-9526 • Fax 800-356-1970
Promega products may also be purchased from Fisher Scientific • Toll Free 800-766-7000 • Fax 800-926-1166

Branch Offices: Australia 1 800 225 123 • China 01 256 3159 • France 05 48 79 99 • Netherlands 071 324 244 • Switzerland 01 830 70 37 • United Kingdom 0800 378994

Worldwide Distribution:

Argentina	1 381 7962	Finland	90 708 0900	Indonesia	21 726 0567	New Zealand	9 570 3200	Sweden	0346 83050
Austria	1 60105 324	France	1 45 33 67 17	Ireland	01 8426644	Norway	035 541999	Taiwan	02 733 6877
Belgium	(see Netherlands)	Germany	06221 502122	Israel	8 406 530	Poland	(see Ger. Export)	Thailand	2 284 0950-51
Brazil	031 275 12 40	Ger. Export	49 6221 502 114	Italy	055 5001871	Portugal	1 458 1641	Trinidad & Tobago	809 673 1378
Canada	800 267 7424	Greece	01 643 6138	Japan	03 3270 0536	Russia	095 135 4206	Turkey	216 385 8321
Czech Republic	02 361 825	Hong Kong	2751 9488	Korea	2 548 5911 or 02 588 5961	Singapore	273 0898	Uruguay	(see Argentina)
Denmark	44 94 88 22	Hungary	01 251 0344	Luxembourg	(see Netherlands)	Slovakia	(see Czech Republic)	Venezuela	2 265 0891
Egypt	2 245 1785	Iceland	(see Sweden)	Malaysia	3 735 1559	South Africa	11 886 4710		
		India	11 684 6565	Mexico	5 525 8579	Spain	93 404 52 14		

©1995 Promega Corporation. All Rights Reserved. No part of this document may be reproduced, stored in a retrieval system, or transmitted in any form or by any means, electronic, mechanical, photocopying, recording or otherwise, without the prior written permission of Promega Corporation. Prices and specifications subject to change without prior notice. Revised 1/3/95

Promega
In USA Call
800-356-9526
Fax 800-356-1970

Circle No. 76 on Readers' Service Card

edited by RICHARD STONE

DAEMMRICH/UNIPHOTO

A bad smell. Critics dump on EPA for ignoring the cost of cleaning up environmental hazards.

EPA's Goals Lack A Price Tag

Few argue with the goals: Safe air, safe drinking water, and protection of endangered species are always popular. But an attempt by the Environmental Protection Agency (EPA) to spell out how it plans to achieve such goals through regulations is being criticized by other federal agencies for failing to specify how much they will cost or who will pay.

The exercise is a departure for EPA, which in its 25-year history has rarely tried to set an internal agenda for implementing regulations or achieving its goals. Two years ago, however, EPA policy experts began to sum up what the agency hoped to accomplish under existing regulations. This approach is now mandated by a law that requires every agency to set internal performance standards as part of its budget request (*Science*, 6 January, p. 20).

Last month, EPA completed a draft report that spells out both long-range goals and short-term benchmarks. For instance, one long-term goal is to ensure that "the air will be safe to breathe in every city and community"; the corresponding benchmark is to reduce the number of cities failing to meet air quality standards from 60 in 1995 to six in 2005.

Although EPA's Peter Truitt says "People have been extremely pleased we're doing this," a Department of Energy official who has seen the report says the absence of a cost-benefit analysis "is ludicrous." Truitt acknowledges the defect but says the final report, to be released next month, won't contain one. "I've been told we won't be able to do [such an analysis] in less than 2 years," Truitt says.

More Clout for Federal Health Research?

Big changes in the federal health bureaucracy may occur this spring as a result of the "Reinventing Government" campaign started in 1993 by Vice President Al Gore. Phase two of this process, or REGO-2 as it's known, looks like it could benefit agencies of the Public Health Service (PHS). The reason: One scheme under consideration would promote PHS to a higher status within the Department of Health and Human Services (HHS). In addition to reducing paperwork, sources say, it would give more autonomy to the National Institutes of Health.

According to an official who asked to remain anonymous, a change of this kind could come about if a REGO-2 plan drafted by HHS wins favor in the next few weeks. One idea reportedly discussed with Gore's staff recently would do away with redundancies cropping up in HHS now that the Social Security Administration has moved out of the department. Some regulatory review functions would be consolidated. And one plan would fold the Agency for Toxic Substances and Disease Registry into the Centers for Disease Control and Prevention, while at the same time combining the Agency for Health Care Policy and Research with the Health Resources and Services Administration. Each PHS supergroup would report directly to the HHS secretary, as would other large health divisions. The position of assistant secretary for health, now held by Philip Lee, might be merged into the secretary's office as deputy secretary, according to this scheme. Substantial changes of this kind would require legislation, however.

Officially, HHS and the vice president's office have no comment on these plans, although one White House official said decisions arising from the REGO-2 review are likely to be made public "by the end of March."

State Court Restores Tobacco Research Fund

In a victory for researchers studying the health effects of tobacco, a state judge has ordered California to stop spending $56 million in tax revenues diverted from a tobacco research fund. The decision paves the way for new grants from California's highly regarded Tobacco-Related Disease Research Program (TRDRP).

TRDRP has received $135 million from California's Proposition 99, a voter-mandated surtax on tobacco products. Run by the University of California, TRDRP has funded research in areas such as cardiovascular disease, cancer, nicotine addiction, and public policy.

Last July, the California legislature rerouted 80% of TRDRP's $22 million budget to pay for health care for the poor—cutting off 66 current grantees. The American Lung Association and the American Cancer Society sued (*Science*, 16 September 1994, p. 1647). California Superior Court judge Roger Warren agreed with the plaintiffs: At a 16 February hearing, he ordered the state to stop spending the money immediately. The court decision "was one of the highlights of my career," says TRDRP Director Charles Gruder.

Charles Gruder

Researchers left high and dry this year will have first dibs on the restored funds, says Gruder. The state has 60 days to appeal the ruling.

RAC Learns of Fourth Human Retrovirus

A Seattle cancer researcher may have found a new human retrovirus while screening patients in a gene marking experiment. Dusty Miller, a researcher at the Fred Hutchinson Cancer Center in Seattle, made the surprise discovery this year while running a sensitive test for viral contaminants in a clinical experiment he was monitoring, according to federal officials.

The organism, unlike most other viral fragments in the human genome, appears capable of replicating and migrating to other cells. If it proves "replication competent," in the jargon of the field, it would be the fourth human retrovirus isolated, after the three well-known pathogenic types HTLV-I, HTLV-II, and HIV.

Miller was unavailable at press time, but his name was included on the 7 March agenda of the Recombinant DNA Advisory Committee of the National Institutes of Health (RAC), on which he sits. Government officials say Miller found the new retrovirus, which is similar to a known cat virus called RD 114, at low concentrations in the bone marrow cells of four cancer patients. As far as has been determined, it is not pathogenic.

Pharmacia Offers $20,000 Thesis Prize

New molecular biologists the world over can now compete for a major award and publication in *Science* as part of the new Pharmacia Biotech and *Science* Prize for Young Scientists. Anyone who received a Ph.D. in 1994 is eligible for a $20,000 first prize and seven runners-up prizes of $5000. A *Science*-chosen panel headed by Nobelist Thomas E. Cech will pick the most outstanding essay based on a thesis. For more information, call 202-326-6501 in the U.S. or 44 1223 302-067 in Britain; or via Internet at science_editors@aaas.org or science@science-int.co.uk. The deadline is 5 July.

A New Phase in the War on Cancer

NIH Director Harold Varmus has launched a review of the National Cancer Institute, which is facing budget shortfalls and is losing several top officials, including its director

Samuel Broder has spent his entire professional life as a soldier in the war on cancer: "I started as a private, and now I'm a general," he said in an interview with *Science* a few days before celebrating his 50th birthday and ending a 23-year career at the National Cancer Institute (NCI). But even old soldiers finally fade away. On 1 March, Broder stepped down as NCI director, quitting public service to join a small drug company in Florida. "I'm doing my part to downsize government," he jokes—"downsizing myself out of it." Jokes aside, Broder's departure signals a dramatic change for NCI.

Broder's history is intertwined with that of the institute. He came to NCI from Stanford University in 1972, arriving just months after President Nixon launched the war on cancer and gave NCI special status within the National Institutes of Health (NIH). He's been NCI director for the past 6 years. But he is leaving just as some bloody battles are shaping up—over NCI's budget, organization, and priorities. After two decades of budget growth, economic changes are converging on NCI, compelling its leaders to find a new strategy. "I don't look forward to the level of extreme budget austerity which I think is coming," Broder said last fall. NCI intramural program chief Edward Tabor puts it succinctly: "The NCI you see 6 months from now is going to be very different from the one you see today."

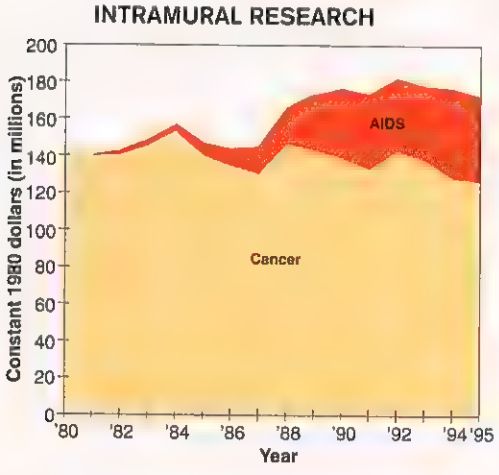

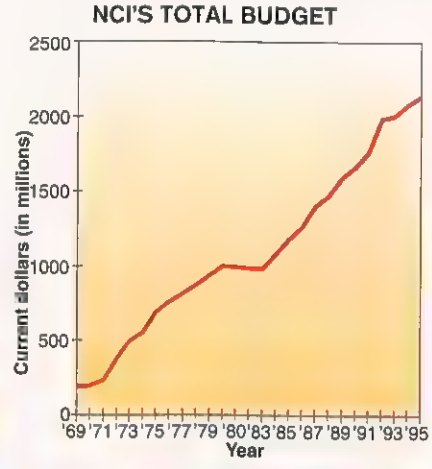

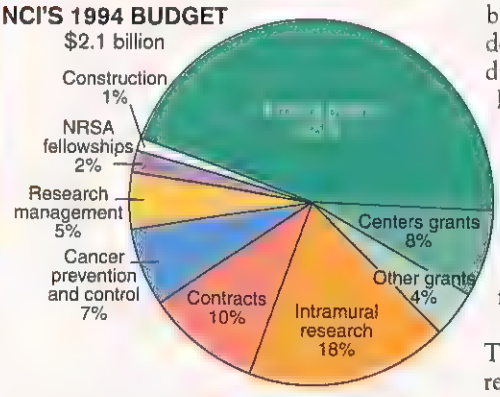

SOURCE FOR GRAPHS: NCI

Three views of the budget. NCI's budget has grown rapidly *(top)*, but the cost of biomedical research has grown almost as fast, and new priorities are claiming a growing share of intramural funds *(above, left)*. NCI spends 18% of its funds on intramural research, a larger proportion than other institutes *(above, right)*.

Even before Broder announced in December that he was leaving, NIH Director Harold Varmus had ordered a stem-to-stern review of NCI. Last October, in a move some NCI officials resented, Varmus persuaded Broder to create an "ad hoc working group" of outside reviewers under the National Cancer Advisory Board. Their assignment from Varmus: "To evaluate the intramural program in a more organic way" than is possible in individual reviews of labs or investigators. Varmus chose NCI to be the first NIH institute to undergo large-scale scrutiny because of its size and complexity, and because it seemed "opportune" in view of the impending departure of two division chiefs. With Broder's departure, the review could provide a blueprint for his successor.

This panel, whose final report is due in May, is widely respected within NCI: It is co-chaired by clinician Paul Calabresi, professor emeritus of Brown University, and by Michael Bishop, Varmus's friend and co-winner of the 1989 Nobel Prize, a virologist from the University of California, San Francisco.

Four issues are expected to dominate the panel's deliberations: the size and structure of NCI's intramural program, low morale and the problems of recruiting top scientists, peer review and priority-setting in the intramural program, and the growing inflexibility of NCI's budget as Congress singles out specific areas for funding.

Issue I: Dealing with duplication

The public expects a lot from NCI, and, until recently, Congress responded by giving more funds each year, creating the largest, richest, and most complex institute at NIH. After 57 years of growth, however, NCI is hitting the wall. Its budget, now $2.1 billion, is not keeping up with inflation, and its favored status is unlikely to provide complete protection from the icy fiscal winds now blowing in Washington. If NCI is to explore new projects in these austere times, it must prune programs and consolidate activities. Yet much of the staff, one harried NCI manager says, is in a "psychological state of denial."

Broder says he saw how the wind was blowing 2 years ago. In mid-1993, he endorsed a project led by Michael Friedman, director of the Clinical Trials Evaluation Program, to find ways to tighten up operations. A group of eight extramural program leaders delivered a 38-page memo in January 1994—now called the "Hard Times Report"—recommending "a comprehensive process of analysis and evaluation to define and prioritize the problems confronting NCI."

The basic problem at NCI, the Hard Times authors wrote, is that each of its four research divisions "exists as a separate administrative and scientific structure," like four "individual cancer institutes." Intramural research gets 18% of NCI's funds and 74% of its personnel, but unlike any other NIH institute, NCI mixes intramural and extramural research within each division. The report noted that divisional leaders are chiefly drawn from labs on campus, and that they "retain their deep interest and affection for intramural activities." This creates two problems, the panel found: redundancy between divisions and, in some areas, competition within divisions between intramural and extramural projects.

The Hard Times panel tagged several pro-

Acting Director: Edward J. Sondik
Deputy Director: vacant

Research Divisions

SOURCE: NCI

Division of Cancer Biology, Diagnosis, and Centers
Director: Alan S. Rabson
1994 budget: $307,373,000
13 labs, 7 branches
1 top position vacant
Biggest lab: Laboratory of Pathology; Lab chief: Lance Liotta; 1993 budget: $10,225,000

Division of Cancer Treatment
Director: Bruce Chabner (leaving)
1994 budget: $231,011,000
9 labs, 25 branches
6 top positions vacant
Biggest lab: Laboratory of Experimental Immunology; Lab chief: John R. Ortaldo; 1993 budget: $3,447,000

Division of Cancer Etiology
Director: Jerry Rice (acting)
1994 budget: $105,385,000
14 labs, 10 branches
10 top positions vacant
Biggest lab: Laboratory of Tumor Cell Biology; Lab chief: Robert Gallo; 1993 budget: $7,382,000

Division of Cancer Prevention and Control
Director: Peter Greenwald
1994 budget: $161,584,000
1 lab, 14 branches
6 top positions vacant
Lab: Laboratory of Nutritional and Molecular Regulation; Lab chief: James M. Phang; 1993 budget: $1,809,000

grams as duplicative and candidates for merging. For example, each division carries on its own preclinical evaluations of new anti-cancer agents. This work could be combined, the report said, streamlining management and creating a single point of contact for companies that want to develop commercial products. Other areas that might benefit from tighter coordination, according to the report, are clinical trials, tissue banking, animal model research, work on gene transfection vectors, and programs that deal with carcinogenesis and basic biology. "Too many activities remain separated artificially by divisional administrative structures," the authors concluded. They wondered, for example, why NCI supports intramural work on oncogenes in three divisions, when everyone is working on the same genes and the same concepts.

Broder did not act on the Hard Times report. Just after he received it, Congress began investigating fraud in an NCI-sponsored breast cancer clinical trial (*Science*, 25 March 1994, p. 1679). That furor and other controversies kept NCI busy putting out fires most of the year. "We've had one commission after another" looking over NCI's shoulder, and "you can OD on oversight reviews," explains Broder.

NCI division chiefs were not asked to respond formally to issues raised in the Hard Times report. If you ask them today, they disagree with many of its conclusions. For example, Peter Greenwald, director of the Division of Cancer Prevention and Control, would not want to merge traditional research on cancer drugs with his own division's search for "chemopreventative" agents, mostly nontoxic food derivatives, because the regulatory problems entailed by the two kinds of research are so different. Bruce Chabner, director of the Division of Cancer Treatment, who will soon leave after 26 years at NCI, spoke out on 27 February against the view that all intramural research should be merged into one office. Chabner told members of his advisory council that it would demand too much of any individual to oversee all of NCI's intramural projects, as NCI's clinical research alone is twice as large as any other institute's. He argued that NCI's extramural programs are better run because their chiefs work side-by-side with clinicians and bench scientists.

In spite of this apparent internal resistance, Broder says he is "proud" that NCI itself was the first to raise the question of program overlap, adding that the Hard Times report shows "we were ahead of the curve." And he's annoyed that Varmus plunged ahead with the Bishop-Calabresi panel before checking to see what NCI had done on its own. "It would be helpful sometimes if people in the chain of authority would ask us, rather than simply asking for another review," says Broder. One top NCI manager warns that the agency may begin to "fibrillate" from all the reviewing. For example, this official says, Bishop is running staffers ragged; last week he demanded data on a division's tenure decisions and lab allocations for a 6-year period, to be delivered in a few days.

Issue II: Room at the top

NCI's top priority in 1995 may be to rebuild and reorganize, but before it can do that, it must recruit several top officials and stem a hemorrhage of scientific talent to outside organizations. NCI needs both a director and a deputy director. The former deputy, Daniel Ihde, left in early 1994 for Washington University in St. Louis and hasn't been replaced. Two of four division heads, Richard Adamson of cancer etiology and Chabner of cancer treatment, are gone or about to go. Below them, 17 lab and branch chiefs and five associate directors have departed or announced plans to go. NCI is now being run by Edward Sondik, deputy director of the Division of Cancer Prevention and Control. James Watson of the Cold Spring Harbor Laboratory says, "Twenty-five years ago, when viruses were the center of attention, NCI was more than any other place the center of an enormous amount of talent. Most of that talent has moved out."

The exodus, Broder says, is part of a "natural cycle of renewal." He thinks NIH is an ideal place for young scientists because it offers lots of responsibility and lab support at an early age. But "if you're a superstar, this is a bad place, because you can't get ... the resources you would get at a university." Ironically, NCI's own efforts have contributed to its current straits. The main reason good academic jobs are available is that for two decades NCI has been pumping billions of dollars into a network of cancer centers. When the war on cancer began in 1972, there were only three independent cancer centers in the United States; NCI now funds 55. As the relative importance of cancer rises—it's likely to replace heart disease as the leading cause of death in the United States—hospitals are raiding NCI's top talent to build up oncology staffs.

But it's not just the pull of outside jobs that has caused the intramural program to slide. NCI's deteriorating environment may also be providing a push. The Hard Times authors complained a year ago about the agency's "exaggerated efforts to respond to political imperatives," the role of "powerful advocacy groups," hierarchy, and bureaucracy. These problems worsened last year when Congress zeroed in on allegations of fraud and mismanagement in NCI studies. Chabner spoke of the "extraordinary pressures" some staffers have experienced. A hiring freeze has hit NCI hard, and many staffers

were overworked before the big exodus began. He also noted that scientific directors have "lost authority and independence" under the new regime, which relieves them of control over tenure, lab space, and decisions on AIDS research. Clinicians feel particularly left out, Chabner said, because "they have the sense that their research is less important than laboratory-based investigations" in genetics and molecular biology (*Science*, 27 January, p. 448).

One final factor adding to clinicians' uncertainty is the future of the NIH clinical center. This 450-bed hospital on the NIH campus is overdue for repairs. But even if it is rebuilt at half the size, as has been proposed, it will be an expensive project, and Congress is hesitating. The cancer institute, with 40% of the inpatients, has a lot at stake: Without a new center, NCI could find it even more difficult to compete with academic medical centers for top clinical researchers.

Broder accepts some responsibility for the malaise on campus. But he feels morale would be better if NCI's staff—people of "character, depth, high integrity"—had been defended in recent months by those above him. "It is quite important for the chain of authority not simply to do political calculations but to stand up; that's the most important aspect of leadership," Broder says. "You need to have people [at the top] express faith, not silence or a vague undertone of bewilderment."

NCI staffers are hoping morale will improve when the institute gets a new chief and new marching orders. Donna Shalala, secretary of Health and Human Services, has named a 14-member search committee under Paul Marks of the Memorial Sloan Kettering Cancer Center to recruit a director. Shalala said: "We are looking for an individual ... who has vision to explore new directions in the field and leadership qualities to mobilize researchers ... in the basic and clinical areas." The committee's choices will be submitted to the president, who will make the final selection, as provided for in the 1971 National Cancer Act.

Reports From the Front

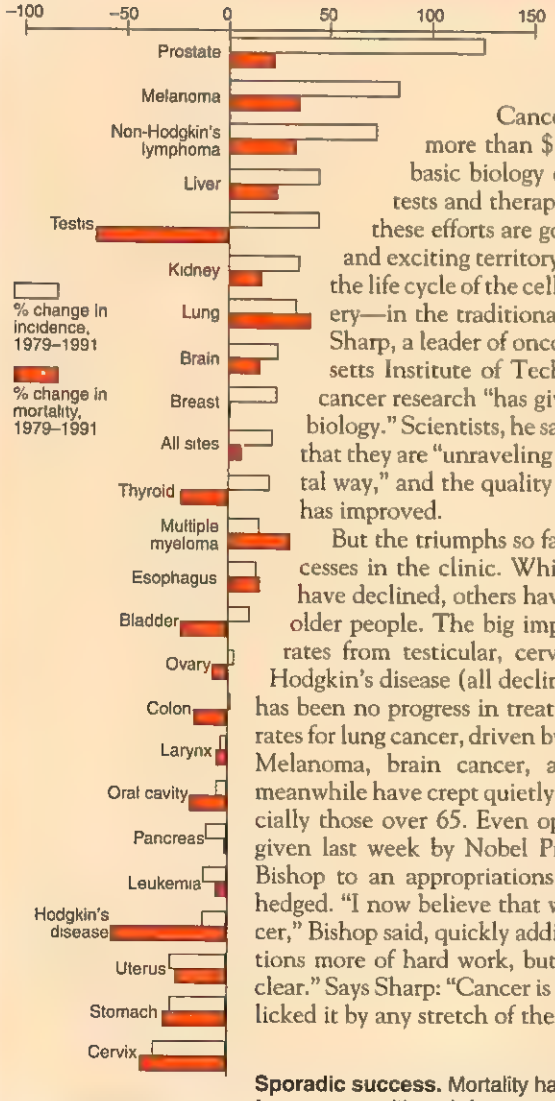

Sporadic success. Mortality has declined dramatically for only a few cancers, although for most, incidence is increasing faster.

Since President Richard Nixon signed the National Cancer Act in 1971, the National Cancer Institute has spent a total of more than $27 billion trying to unravel the basic biology of the disease and develop new tests and therapies. Ask cancer researchers how these efforts are going, and they will point to new and exciting territory opening up for cancer genetics, the life cycle of the cell, and even—with taxol's discovery—in the traditional field of chemotherapy. Phillip Sharp, a leader of oncogene research at the Massachusetts Institute of Technology, notes that support for cancer research "has given rise to much of modern cell biology." Scientists, he says, are more confident than ever that they are "unraveling a disease process in a fundamental way," and the quality of life for many cancer patients has improved.

But the triumphs so far have led only to sporadic successes in the clinic. While death rates for some cancers have declined, others have increased, particularly among older people. The big improvements have been in death rates from testicular, cervical, and stomach cancer and Hodgkin's disease (all declining by 30% to 70%). But there has been no progress in treating pancreatic cancer. And the rates for lung cancer, driven by tobacco use, have skyrocketed. Melanoma, brain cancer, and non-Hodgkin's lymphoma meanwhile have crept quietly up the charts, threatening especially those over 65. Even optimistic forecasts, like the one given last week by Nobel Prize–winning biologist Michael Bishop to an appropriations committee (see p. 1415), are hedged. "I now believe that we will eventually conquer cancer," Bishop said, quickly adding, "It may take several generations more of hard work, but the strategies for conquest are clear." Says Sharp: "Cancer is still a major disease. We haven't licked it by any stretch of the imagination."

–E.M.

Issue III: Setting research priorities

The Bishop-Calabresi panel has spent a lot of time so far focusing on one question: How does NCI plan and review its intramural program? Intramural studies are getting attention for several reasons. For one, panel members find NCI's method of setting in-house priorities obscure. Each NCI division steers an independent course, guided by its scientific advisers. While all the divisions use the same method of evaluating research—site visits at 4-year intervals—the peer comments are private, not binding, and, according to Bishop, mild. This disconnection between reviews and intramural funding decisions is pervasive at NIH, some say (*Science*, 27 August 1993, p. 1120).

Another reason for focusing on the intramural budget is its size. In 1994, NCI spent more than $374 million on in-house research, 18% of the total NCI budget, a fraction far higher than the NIH-wide average of 11%. In addition, according to NCI's budget chief John Hartinger, the agency spends about 10% of its total budget, $205 million, on R&D contracts. Much of this work is done in support of intramural objectives, and about half the sum supports a dedicated laboratory at the Fort Detrick Army base in Frederick, Maryland, where NCI and contract staff screen anti-cancer agents and design new drugs.

At Varmus's request, the Bishop-Calabresi panel is trying to learn how NCI evaluates its internal projects and how it decides which should be expanded or shrunk. This line of inquiry follows the lead of a blue-ribbon committee, co-chaired by Marks and Gail Cassell of the University of Alabama, that made a strong plea last year for rigorous peer review and priority-setting throughout NIH's intramural programs (*Science*, 13 May 1994, p. 896). A few institutes, the Cassell-Marks report said, plan aggressively, but others allow historical patterns to become "a rationale for current decisions."

Is NCI's intramural program one of those run by inertia? Broder says it is not. "We have tried to develop a system where young people are given very substantial opportunities, ahead of schedule if you will," he says. Acting NCI Director Sondik told the Bishop-Calabresi panel at its 16 February meeting that recent "scientific advances" have the "biggest influence" on setting the intramural agenda. Sondik then described a complex process used by NCI to incorporate new sci-

ence into its budget plan. Staffers talk with lab chiefs; lab chiefs negotiate with division chiefs; and division chiefs huddle with administrative officers in retreats to discuss a document called the bypass budget. This annual statement of NCI's scientific goals, and the funds it needs to meet them, is drawn up by the NCI director and his executive committee. As stipulated by the 1971 Cancer Act, it goes directly to the White House, offering the executive branch scientists' judgment on what must be done to fight cancer. Later, the Health and Human Services Department and NIH submit a "real" budget request to the White House, which is revised and sent to Congress.

The bypass budget—some refer to it as NCI's "wish list"—bears little relation to the budget that is finally submitted to Congress. The 1996 bypass budget, for example, called for a total of $3.6 billion for NCI—a whopping $1.4 billion more than the Clinton Administration requested. Clearly, NCI has to do a lot of squeezing to shape its wish list to fiscal realities, but how that shaping is achieved isn't clear even to many on the inside. The Bishop-Calabresi panel seems ready to recommend that the next NCI director create a more comprehensive and transparent system for setting priorities.

Issue IV: Loss of flexibility

NCI's priorities are not all set from within. Patient advocacy groups, professional societies, and disease lobbies all have a hand in shaping the agenda, mainly by asking Congress to earmark certain tasks for funding. One example: research on cancer prevention and control. The 1993 bill authorizing NIH specified that NCI must devote a fixed percentage of funds to this area, reaching 10% this year. NCI is having trouble hitting that target, however, and is asking Congress to drop the requirement.

Perhaps the most striking earmark is for breast cancer research, for which funding at NCI has increased 236% since 1991, when cancer patients began lobbying hard. Broder says he agrees that breast cancer and prostate cancer research were due for an increase. But he warns that "we have to be cautious that we don't overcompartmentalize the process" by creating "scientific entitlements."

Broder doesn't think earmarking has unbalanced cancer research—at least not yet. But he worries that the process could become unbalanced if a set-aside for AIDS research (also part of the 1993 NIH authorization bill) isn't handled carefully. AIDS-related research already consumes 26% of the NCI intramural budget, and Chabner told the Bishop-Calabresi panel that all intramural growth in his division since 1992 has gone into AIDS, while funding for cancer "headed south." The result: "We shift research," and people change what they do.

But when it comes to predicting what the NCI itself will look like a year from now, nobody is ready to make a guess. Varmus is waiting for the Bishop-Calabresi report, and he says he wants to hear the views of the new NCI director—whoever that may be. "I would be surprised if there weren't some changes," says Varmus, but beyond that, "I don't know enough to say what they should be." But Varmus is certain of one thing: The Bishop-Calabresi review won't be the last of its kind. He says he will soon order up a similar review of the National Institute of Mental Health, which is also looking for a new director, and other institutes will get their turn.

–Eliot Marshall

With reporting by Antonio Regalado.

BIOMEDICAL FUNDING

Nobelists Make a Plea for NIH Budget

Six Nobel Prize winners who went to Capitol Hill last week to make a pitch for biomedical research themselves came away with an unsettling message: Prospects for funding this year are more uncertain than at any time in recent memory.

The Nobelists had been invited to testify before a key panel—the House appropriations subcommittee for Labor and Health and Human Services, author of the appropriation bill for the National Institutes of Health (NIH). But before they even began, the panel's most senior Democrat, David Obey of Wisconsin, rattled them with a warning that a fiscal "train wreck" lies ahead for basic research if a federal tax cut—promised by the Republican leadership in Congress and by the White House—is enacted. He predicted such a tax cut would lead to a 30% reduction in all domestic spending, including funds for NIH. Another panel member, Louis Stokes (D–OH), agreed that a tax cut would be devastating, but doubted it would be approved.

It fell to the subcommittee's Republican chair, John Porter (R–IL), to provide some reassurance. Torn between his party's plan to cut spending and his own support for NIH, he reiterated his own opposition to the tax cut: "I believe in the end we will not cut taxes," Porter said, suggesting that his colleagues are "wise enough" to avoid the governmental crisis it would create. And Porter said he would do his best to support biomedical research in what will be a tough budget year, with or without a tax cut. Another Republican member, Dan Miller (FL), also noted that House Speaker Newt Gingrich (R–GA) is "a very strong supporter of basic research" and not one to abandon biomedicine. However, the most junior Republicans on the subcommittee—members who favor stringent spending cuts—didn't show up for the hearing and have not yet indicated how they will vote on research funding.

SAM MITTNER

Show and tell. Phillip Sharp demonstrates for House appropriations committee members how cancer genes are spliced and expressed.

Only then did the scientists get to talk about their own experiences and the importance of federal support for research. Michael Bishop, friend of NIH Director Harold Varmus and co-winner with Varmus of a Nobel in 1989, orchestrated this part of the hearing. Bishop described his own work on retroviruses and the progress since 1970 in understanding the causes of cancer, declaring that a strategy for conquering the disease is now in hand. Other speakers included Michael Brown of the Southwestern Medical Center at the University of Texas, Dallas, on heart disease; David Hubel and Joseph Murray of the Harvard Medical School, on brain research and organ transplantation, respectively; Phillip Sharp of the Massachusetts Institute of Technology on oncogenes and biotechnology; and James Watson of the Cold Spring Harbor Laboratory on the Genome Project.

Murray's presentation, illustrated with a photo of the "oldest living organ transplant recipient"—one of his patients, now living in Oklahoma, not far from the home town of one of the House panel members—was especially powerful, in the opinion of one longtime observer of these hearings. But some of the other discussions, he said, verged on "whining" about the hardships associated with applying for federal grants, which is unlikely to evoke sympathy from the subcommittee. The "real question" facing biomedical funding, this observer says, is: What if funding decisions get entirely "out of Porter's control?" In this topsy-turvy year, it could happen.

–Eliot Marshall

Russian Chaos Breeds Diphtheria Outbreak

GENEVA—Since the fall of the Communist regime 4 years ago, the former Soviet Union has become a land of opportunity—for better or worse—for many of its inhabitants. One opportunist is *Corynebacterium diphtheriae*, the micro-organism responsible for diphtheria. Slipping through rents in Russia's tattered health system and gaps in its population's immunity against the disease, this bug has taken advantage of a newly mobile population to kindle an epidemic that so far has affected about 80,000 people and killed more than 2000 throughout the former Soviet Union.

The epidemic has swept swiftly westward across Russia and moved into Ukraine, Belarus, and the Baltic states. By last December it had spread to all 15 states of the ex-Soviet empire. "It's one vast epidemic and it's escalating off the graph paper," says Nick Ward, acting head of the World Health Organization's (WHO's) Expanded Program on Immunization (EPI). Vadim Ivanov, who was head of the diphtheria department at Moscow's Tushinskaya Pediatric Hospital in the early days of the epidemic, recalls how "people reacted with shock and disbelief—this was a disease most people in the street thought had been wiped out."

Last week a group of specialists including an epidemiologist from the Centers for Disease Control and Prevention (CDC) in Atlanta visited Ukraine to help plan the containment of its epidemic. Western health agencies have every reason to get involved: The outbreak has begun to leak cases to a few Western countries—including the United States—via infected travelers, and populations in several countries may be vulnerable because levels of immunity in adults have decined in recent decades. Says Ward: "We're worried and believe me, the Russians and their new neighbors are worried."

Breeding ground. In many ways, Western health experts say, Russia's diphtheria outbreak was an accident waiting to happen. Too few Russian children were getting a full three-dose series of anti-diphtheria shots—only 68% in 1990 compared with more than 80% in 1980—and WHO says that at least 95% coverage is needed to prevent an epidemic. In some places, like St. Petersburg, only 45% of children had been fully vaccinated, according to WHO figures.

In addition, too few Russian adults had protective immunity against the disease—only about 20% of those between 30 and 50 years old, according to surveys carried out by researchers at Moscow's Gabrichevsky Institute. The reason is that in most countries widespread vaccination of children in the 1970s virtually wiped out *C. diphtheriae*, so that by the 1980s there was not enough around to boost adults' immunity naturally. "In Russia, with such a large pool of susceptible people—both in children and in adults—there was a real potential for an epidemic," says Artur Galazka, the EPI's diphtheria expert.

All it took to spark the epidemic was the arrival in Moscow in 1990 of a few infected paramilitary recruits from southern Russia, where *C. diphtheriae* is commonplace but only causes a mild skin disease. (The more serious throat diphtheria of the current epidemic begins with flulike symptoms which can eventually cause fatal damage to the heart and central nervous system.) In Moscow—and later in St. Petersburg—the infection quickly took hold in a large, immunologically weakened population of homeless, ill-nourished people, many of them alcoholics or drug users.

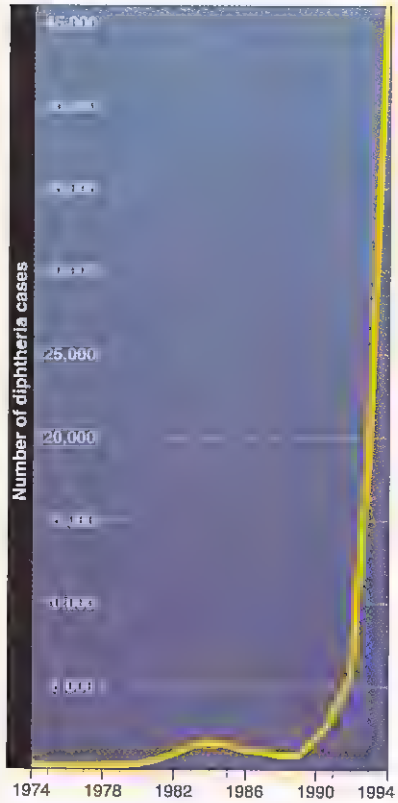

Off the chart. There have been over 80,000 cases since the epidemic began.

Galazka says the Russians could have stamped out the epidemic in its infancy, but did little or nothing at first. He was part of a WHO team that went to Moscow in February 1991 to warn government officials about the coming epidemic and to recommend urgent action. "In the early months of the epidemic most cases were confined to Moscow and St. Petersburg. The outbreak could have been snuffed out without too much trouble if they had acted quickly. But they denied there was a real problem."

Part of the reason for the delay, many health officials believe, is the fact that in the changeover from a Soviet to a federal system, Russia emerged with two health authorities in charge of infectious diseases—one in the health ministry, the other in one of the President's state committees. "The two just don't speak the same language," one official told *Science*. Arkady Yashinsky, chief of program development in the State Committee for Sanitary and Epidemiological Surveillance, says some protective measures were put into effect as soon as the epidemic started, but he admits that "really strong action was only taken in 1993."

Sieghart Dittmann, head of immunization at the Robert Koch Institute in Berlin, who is coordinating efforts by WHO's European office in Copenhagen, Denmark, to battle the epidemic, believes the Russians perceived the danger, but "this problem got buried under the huge pile of other problems the country was facing." Over the past 18 months, however, the Russians have finally begun to take effective action. Last year more than 30 million of the country's 150 million inhabitants were immunized with at least one dose of vaccine, according to Mikhail Narkevich, chief of the health ministry's infectious diseases department. "We hope to vaccinate another 40 or 50 million people this year," he says. If things go according to plan, he believes, "we could wipe out this epidemic in 2 years."

Other Russian scientists are skeptical. Maya Gasparyan, former professor of infectious diseases at Moscow's No. 1 Infectious Disease Hospital, says "We've got too many people on the move in Russia," spreading the disease and not easily brought into a vaccination program. "Our economic and ecologic problems have increased the numbers of our immunosuppressed children. I'm really pessimistic."

One hurdle most Russian officials recognize is the difficulty of convincing Russian pediatricians, especially in remote rural areas, to immunize their patients. In the 1980s, unconfirmed but widely publicized reports of brain damage and other side effects of childhood vaccines created resistance to immunization among the general public. Pediatricians were also reluctant to immunize because the health ministry had issued a very long list of conditions when vaccines should not be administered (WHO lists only five). Today, these barriers have been overcome, at least officially and in the big cities. But, Dittmann fears, "the message has still to get to the rest of the country."

Other newly independent states of the former Soviet bloc are also struggling to contain diphtheria epidemics that were not caught in time. In Ukraine, the next hardest-hit country, with over 8000 cases over the past 4 years, the epidemic seems to have

peaked. At last week's meeting in Kiev, Ukrainian health officials presented to experts and aid organizations a plan to vaccinate or complete the vaccination of the entire population of 52 million by the end of this year. Earlier this year, the other ex-Soviet republics approved an outbreak containment plan drawn up by WHO and UNICEF, involving rapid diagnosis and treatment of cases and their contacts, and mass vaccination campaigns.

But for most of these countries, the plan could be sunk by a desperate shortage of vaccine, particularly of the adult variety known as Td. There is also a dearth of antitoxin, a horse serum containing anti-C. *diphtheriae* antibodies that can prevent the cardiac and neural damage that kills between 3% and 10% of patients. The only production plants in the region are on Russian soil. Narkevich and Yashinsky say that because these plants can only supply Russia's own needs, the Russian government banned export of the vaccine and antitoxin after the breakup of the Soviet Union, leaving its neighbors to rely on international donors. Dittmann reckons that about 500 million doses of vaccine will be needed over the next 2 years at a cost of more than $50 million and at least 200,000 vials of antitoxin costing about $1 million—although prices are rising rapidly as world demand outstrips supply. Colette Roure, EPI adviser to WHO's European office, says funds are desperately needed.*

Heading west. Before the lifting of the Iron Curtain, such an outbreak would almost certainly have been contained within the Soviet Union. No longer. A few cases have cropped up in close neighbors such as Poland, Finland, and Norway. Further west, Germany has reported six cases, and in the last few months two Russian-born American citizens returned home to give the United States its first taste of the Russian epidemic.

WHO's Galazka believes some industrialized countries may have the ingredients for an epidemic. Some have certainly let childhood immunization slip in recent years: In the United States, for example, only 44% of children were fully vaccinated in 1991–92, according to CDC estimates. More disturbing, says the CDC's Iain Hardy, is the large proportion of adults—between 30% and 60%, he reckons—whose immunity has fallen to low levels in many countries, including the United States, Canada, and Australia. In Europe, the proportion of unprotected adults ranges from as low as 20% in Finland and Denmark to 53% in Poland.

WHO has advised all European countries to ensure that at least 95% of children are immunized by 2 years of age and that they receive a booster on starting and another on leaving school. Most countries have begun implementing these measures, says Roure. States close to the Russian epidemic are taking special measures: Finland, for example, has already vaccinated 80% of its adult population, and Poland has immunized all adolescents aged 19 and all officials policing its eastern border.

In the United States, Hardy believes the risk of infection spreading from a few isolated cases "is real but not worrying: We have a fairly aggressive management approach to contact tracing, surveillance, diagnosis ... and rapid hospitalization of cases." But state public health authorities and physicians throughout the country "should be made more aware of this disease. Most American doctors have not seen a single case of diphtheria and could easily fail to diagnose it or could misdiagnose it."

Meanwhile, back in Russia, officials are understandably anxious to get the diphtheria epidemic out of the way so they can get on with the other problems of daily life, such as cholera, dysentery, tuberculosis, AIDS, and even malaria.

–John Maurice

John Maurice is a science writer in Challex, France.

*For more information, contact Roure at WHO Europe, 8 Scherfigsvej, Copenhagen 2100, Denmark. Fax: +45 391 71 1851

BIOTECHNOLOGY

European Parliament Axes Patent Policy

After 6 years in the drafting, a European Union (EU) directive seeking to set common standards of patent protection for biotechnological inventions was thrown out last week by the European Parliament in Brussels. The directive would have set ground rules for the patentability of genes, cells, and other biological material derived from humans, animals, and plants. Its demise means that the biotech industry will have to stick with existing legislation—which was not designed to deal with the complex issues of living inventions—and build up precedents on a case-by-case basis. It could also result in a patchwork of different regulations in different European countries.

The ethics of patenting biological organisms has long been controversial in Europe, and the Directive on the Legal Protection of Biotechnological Inventions had a stormy ride through Europe's legislative corridors. Indeed, at one point last year, the Parliament and the Council of Ministers were so deeply divided over the text and subsequent amendments that a conciliation procedure established by the 1992 Maastricht Treaty had to be invoked for the first time. But even that wasn't enough: Unexpected opposition from many new members of the European Parliament (MEPs) elected last year killed the directive by 240 votes to 188, with 23 abstentions.

The vote was hailed as a victory by environmentalists and animal-rights groups, who opposed the basic premise of the directive, that life is patentable. But genetics researchers are disappointed. They fear that without guidelines specifically designed to address genetic engineering inventions, the existing practice of patent offices may give commercial companies too much control over genetic data, thereby restricting research. The biotech industry, surprisingly, isn't hitting the panic button: It feels that in its final form the directive was too ambiguous and would have achieved few of its original aims.

"We'll see what comes out of EPO case law, and I think industry's happy to abide by that."

—Nick Scott-Ram

The biotech industry provided the initial impetus for the directive. It wanted to ensure that European patent regulations were generally in line with those of the United States and Japan, which have tended to be less restrictive in deciding what kinds of living inventions can be patented. Currently, applications in Europe can be filed with a national patent office for protection in that country only, or with the European Patent Office (EPO) in Munich, Germany, for protection in the 17 countries that signed the 1973 European Patent Convention (EPC). Each nation has been treating biotech patents slightly differently, and the EPO has been interpreting the EPC on a case-by-case basis. If the directive had been passed, all EU member states would have had to write its provisions into their patent laws.

It took more than 5 years of negotiations before the European Parliament and the Council of Ministers agreed on a draft text in December 1993. This was modified in February 1994 to address the biotech community's concern that the directive would have been more restrictive than the EPC. Then last May, MEPs requested several amendments, one of which—aiming to clarify exactly the instances in which a human body part can be patented—required conciliation proceed-

ings that were only concluded on 23 January.

By the time the directive was put to the vote last week, however, a clutch of new MEPs were in place following elections last year. They hadn't been exposed to years of lobbying from the biotech industry, and homed in on issues that hadn't been sticking points in earlier drafts of the directive. In particular, some of the new parliamentarians opposed the directive because it would not have explicitly banned human germline gene therapy, which introduces permanent, inheritable traits into genes. And, in a surprise move, the European socialist group resolved to vote against the directive, one of their members saying that patents on living things would inhibit research in the field.

Biotech industrialists seem untroubled by the defeat. Ron James, managing director of PPL Therapeutics in Edinburgh, U.K., which has patent applications pending in the United States and Europe on transgenic sheep that produce drugs in their milk, believes the final directive would have been little improvement on the EPC. "Clarity wouldn't have occurred. ... Many of the clauses were open to different interpretations." And industry leaders are now adopting a wait-and-see attitude. "We'll see what comes out of EPO case law, and I think industry's happy to abide by that," says Nick Scott-Ram, chair of the intellectual-property advisory committee of the U.K. BioIndustry Association.

Biotech companies are encouraged because since they first began pushing for the directive, the EPO has granted one patent for a transgenic animal: Harvard University's "oncomouse." And Christian Gugerell, a director of the EPO, predicts further applications on transgenic animals "in the pipeline ... will be granted," including James' sheep, because they satisfy the necessary criteria of novelty, inventiveness, and utility.

Researchers are more worried. The directive made a clear distinction in the case of DNA between a "discovery," which is not patentable, and an "invention," which is. Thus a strand of complementary DNA, for example, with no other defined use than "expected" applications such as a probe or primer, would have been declared unpatentable. Without the directive, that distinction remains untested. Cells, complete genes, or proteins would not have been patentable under the directive unless they were part of an invention—which corresponds to the situation that exists under the EPC.

Green Party MEPs and various lobby groups such as Greenpeace and animal-rights organizations will continue to try to stop the patenting of animals by challenging individual cases. The British Union for the Abolition of Vivisection, for example, is challenging the oncomouse patent in a case to be heard at the EPO in November. In the absence of the directive, the outcome of such cases will provide the basis for European biotech patent law.

–Claire O'Brien

Claire O'Brien is a science writer in Cambridge, U.K.

CANADIAN R&D

Science Budget Takes 15% Whack

TORONTO—The Canadian government last week unveiled a draconian budget that will slash research spending by roughly 15% in the next 3 years. The cuts—the first significant across-the-board reductions to Canadian science in more than a decade—are part of a campaign to shrink government and reduce a budget deficit that, in proportion to its economy, exceeds that of the United States. The government also made it clear that it will step up pressure on research agencies and institutions to show the economic value of the work they are funding.

"We will be putting government activities on a commercial basis wherever that is practical and productive," said Finance Minister Paul Martin last week in presenting the government's budget to the House of Commons. "In the future, our science and technology efforts will be concentrated more strategically on activities that foster innovation, rapid commercialization, and value-added production."

Approval of the government's budget for the 1995–96 fiscal year starting 1 April is a foregone conclusion, given the ruling Liberal Party's parliamentary majority. It will wipe out a scheduled 1.5% increase in the budgets of all three university granting councils—the Natural Sciences and Engineering Research Council, the Social Sciences and Humanities Research Council, and the Medical Research Council. Instead, they will see their funding drop by 12% to 13% over the next 3 years (see table).

Even harder hit is the Canadian Space Agency (CSA). Its base budget will drop by 15% in the next 3 years, with spending increasingly directed toward private-sector partnerships and joint ventures in Earth observation, space science, and technology. One third of the cut will come out of work on the sophisticated robotic arm that is Canada's main contribution to the international space station; the remainder will come from reductions in the agency's infrastructure. Daniel Goldin, head of the U.S. National Aeronautics and Space Administration, told *Science* that CSA chief Mac Evans last week assured him the reductions should not affect Canada's participation in the space station effort.

RESEARCH CUTS IN SELECTED R&D AGENCIES
(millions of Canadian dollars)

Organization	Current budget	Proposed for '97–98	% change
Canadian Space Agency	174*	148	–15%
Nat'l Research Council	449	372	–17%
Natural Sci. & Engin. Res. Coun.	494	428	–13%
Soc. Sci. & Humanities Res. Coun.	101	89	–12%
Medical Research Council	266	235	–12%
Agriculture Ministry	269	239	–11%

*Base programs, excludes Radarsat SOURCE: CANADIAN GOVERNMENT MINISTRIES
One Canadian dollar = $0.71 U.S.

The National Research Council (NRC), a network of government laboratories, will have to trim spending by 17% by 1997–98, including a $30 million cut in the coming year. "I'm disappointed. We've certainly taken a hit," says NRC President Arthur Carty. "With limited resources you just can't afford to spread yourself too thin."

While the impact of the new budget on specific programs remains unclear, the cuts have focused attention on the way Canada funds science. Current total R&D expenditures of $4.1 billion are spread across 18 departments, and a recent report by the auditor-general called the distribution "more incidental than the result of a well-formulated strategy." In response, the government launched a review of federal spending on science and technology that is expected to be finished in June, and Bill Milliken, a spokesperson for Industry Canada, says the exercise has benefited from the fact that "a shortage of funds tends to focus things."

As bad as the cuts are for science, the government's new budget is even worse news for other sectors. The $116 billion budget includes spending cuts of $9.2 billion over 2 years, as well as the elimination of 45,000 civil service jobs, about 15% of the government payroll.

–Douglas Powell

Douglas Powell is a graduate student at the University of Guelph.

JOINT RESEARCH

India Cracks Whip to End Addiction to State Funds

NEW DELHI—Basic researchers in the United States who have been grumbling in recent years about efforts to encourage scientists to become more involved in "strategic" research might take a look at what is happening to their colleagues in India. The Indian government is using strong medicine to try to cure academic and government scientists of their near-total dependence on government funding and encourage them to work with industry.

Part of the prescription is a set of powerful inducements: bonuses and a share of royalties from products created in their labs, changes in a 25-year-old patent law allowing product patents of new technologies, and greater protection for intellectual property that should come with membership in the World Trade Organization. But the government is also prescribing an unpalatable remedy: flat or declining research budgets, which should push institutions to find private sources for a growing share of their activities.

PHOTOS BY PALLAVA BAGLA

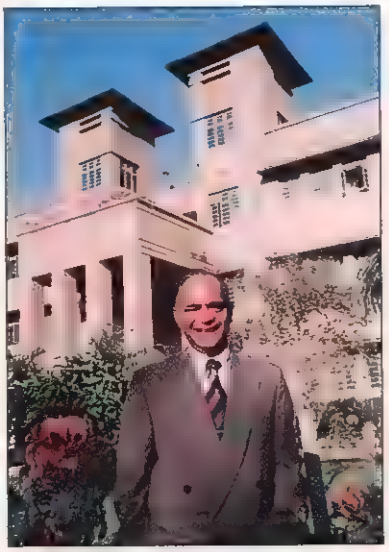

Industrial strength. Bombay University's department of chemical technology, led by Man Mohan Sharma, benefits from corporate ties.

The idea of greater cooperation is not new: "We have been advising universities to reach out to industry through their research since 1990," says G. Ram Reddy, who has just retired as chair of the University Grants Commission (UGC), the government agency that oversees higher education. And science policy-makers now believe it is needed to promote high-tech development in India. For example, the theme of last month's 82nd annual meeting of the Indian Science Congress Association in Calcutta was "Science, Technology, and Industrial Development in India," and several speakers reminded the 6000 scientists and government officials that greater cooperation between industry and academia is long overdue.

But strong words are not enough to bring about change. Industry increased its share of national R&D expenditures from 24.3% in 1990–91 to 26.4% in 1992–93, but the change amounted to less than $35 million in a $1.6 billion R&D budget. Clearly, more is needed to keep academic research alive and well. "The initiative has to come from the particular university," says Reddy, who points out that the great majority of R&D institutions rely on government funds to keep their research programs going. The prestigious Jawaharlal Nehru University in New Delhi, for example, "gets 95% of its funds from the government," he says. Indeed, most academic administrators tend to lump together a range of possible collaborations—from courses that deal with practical questions to research collaborations—and view them all with contempt. "We should not be expected to do product development," says Y. K. Alagh, the university's vice chancellor.

Dependence on the government runs deep. Last summer at the University of Delhi, for instance, a projected shortfall of $5 million from the UGC triggered a financial crisis that led to the resignation of its vice chancellor, Upendra Baxi. Baxi said the university "would lose its soul" if the government did not increase its support of faculty salaries and the research supplies and equipment they needed.

Not every university scientist and administrator regards the situation in such dire terms, however. J. B. Joshi is a chemical engineer and faculty member at the University Department of Chemical Technology at Bombay University who designed a novel gas-liquid reactor for catalytic hydrogenation, a process used to produce industrial chemicals. The reactor is selling briskly, in large part because the savings from the catalyst it uses cover the cost of the entire system in only 3 months. And Joshi collects $15,000 a year in consulting fees, thanks in part to a 200% increase in 1993 in the rates that faculty members can charge for their time working with industry.

Joshi and his fellow consultants aren't the only ones who benefit from stronger links to industry. The department receives one third of their consulting fees, which last year totaled $133,000. Industry has also given the department $600,000 over the past 5 years for research, most of it from Reliance Industries, a manufacturing conglomerate, which has provided the funding with no strings attached. This outside income has helped the state-owned Bombay University thrive in the face of a stagnant public subsidy for general operating expenses.

A few government institutions are also learning how to flourish in the new environment. The National Environmental Engineering Research Institute (NEERI) in Nagpur is part of the Council of Scientific and Industrial Research (CSIR), which receives $99 million a year from the Indian government to operate a network of 40 laboratories. NEERI is earning 65% of its $1.7-million-a-year budget from selling its wares, says its director, environmental engineer Purushottam Khanna, who oversees 146 externally funded projects ranging from making biosurfactants from industrial wastes to making lead-resistant catalytic converters.

One way CSIR hopes to get closer to industry is through participation in its governing boards. The powerful Research Advisory Councils (RACs), which oversee each laboratory, are now required to draw two thirds of their members from industry, says CSIR's director-general, Shri Krishna Joshi. This added representation—the old councils were comprised mostly of eminent scientists with the occasional industrialist—is causing labs to incorporate research objectives that are relevant to the problems facing local industry, he says.

Patent pending. None of CSIR's 470 patents has generated revenue, laments Director-General S. K. Joshi.

But CSIR has a long way to go. It has promised the government that each CSIR lab will earn half its budget from external sources by 2000; at present, only 11% of CSIR's earnings now come from private industry. With recent budget increases lagging behind inflation, the money would certainly come in handy. But Joshi confesses that "CSIR has yet to earn anything at all from its 470 patents."

That pitiable performance doesn't surprise C. N. R. Rao, former adviser to the prime minister on science and technology and now president of the Jawaharlal Nehru Center for Advanced Scientific Research in Bangalore. "The patent scene in India is rotten," he says, referring to his country's traditional disregard for intellectual-property rights. "China has managed

to train 500 [legal] specialists in patents in the past few years, while India has just half a dozen," he notes.

One reason for the scarcity of patent examiners is the lack of interest among academics in the needs of industry, says Nagaraj Vittal, chief of administration for the government's Department of Electronics. Vittal, who dismisses most Indian research as "metooism," feels that little will change until Indian scientists begin carrying out "innovative rather than imitative research."

That philosophy has already taken hold among the faculty of India's premier research and teaching institution, the Indian Institute of Science (IISc) in Bangalore. Govindaranjan Padmanabhan, IISc's soft-spoken chief, points to several cases where industrial partnerships have led to significant economic gains. "Research at the institute helped the nation become self-sufficient in silicon manufacture through cooperation with Metur Chemicals in southern India," he says. And Padmanabhan notes that the institute has also made important—but harder to measure—contributions to the country's space and defense programs.

The new emphasis on industrial ties, he says, has also been a catalyst for such changes as a new course on patenting and a promotion system that relies more heavily on the impact of publications than sheer numbers. But he says there is still room for improvement. Private sponsors provide half of the institute's funding, he notes, but only 10% of that total comes from industry. Padmanabhan would like to triple the size of that industrial slice. "While the institute can never give up on its primary mandate of basic research," he says, "we have no intention of resisting change."

Even with the backing of such important institutions, however, it's not yet certain that the government's effort to make Indian science more financially independent will permanently alter the country's research enterprises. Rao says the answer lies in increasing export of technology-related products, adding, "but that can happen only with an increasing outlay for targeted and product-identified R&D." Before that can occur, though, university scientists and their industrial counterparts need to learn how to work together.

–Pallava Bagla

Pallava Bagla is a science writer based in New Delhi.

NATIONAL LABORATORIES

Galvin, DOE Spar Over Reform Plan

The chairs of most blue-ribbon panels dutifully release their reports and then return quietly to their regular jobs. But not Robert Galvin, the chairman of Motorola and head of a Department of Energy (DOE) task force that in February suggested radical changes in how DOE's national laboratories are managed. At a Senate hearing last week, Galvin went a step further, describing in detail how Congress could create a private company that would receive federal funding to operate the labs but function largely free of government oversight.

The idea to "corporatize" the labs is not popular with DOE or lab officials, as Energy Secretary Hazel O'Leary made clear to the committee during the same hearing. But Galvin hopes to strike a chord with those in Congress who are eager to reduce the size of government. He offered the senators a seven-page paper, prepared after his panel was disbanded, outlining how a quasi-government corporation could be established and the precedents for doing so. Under Galvin's plan, DOE would either lease or transfer its property to the organization. The bottom line, Galvin forecast, would be a 20% to 30% reduction in operating costs.

Galvin's presentation won some plaudits from Senator Pete Domenici (R–NM), who chairs the appropriations panel that controls DOE's budget and whose state includes two weapons laboratories. Domenici said he favored "a bold initiative," and warned O'Leary that "we don't intend to let the Galvin report gather dust. ... We want results." However, he and other Republicans stopped short of endorsing Galvin's proposal.

"We don't intend to let the Galvin report gather dust. We want results."
—Sen. Pete Domenici (R–NM)

Galvin's plan held little appeal for the panel's senior Democrat and former chair. "I'm really highly skeptical," Senator Bennett Johnston (D–LA) told Galvin. "This is a formula for abolishing the labs." O'Leary, who sat next to Galvin at the witness table, believes the proposal goes too far. The labs "are an investment on behalf of U.S. taxpayers of over $100 billion," she said. "I am very loath to submit them to some experiment."

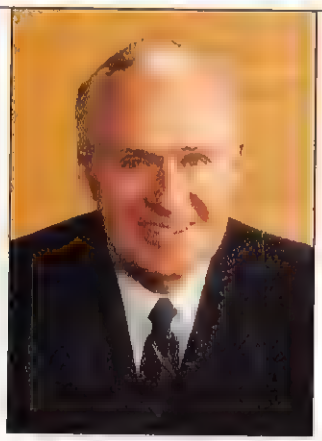

Working overtime. Robert Galvin's "visionary" plan would corporatize DOE's labs.

O'Leary has already embarked on a major shake-up of the department to streamline operations and save $10.6 billion over 5 years. (This effort helped her shoot down a White House trial balloon lofted shortly after the election, to abolish DOE, although a group of freshmen Republicans has since revived the idea.) Last week she announced plans to create a Laboratory Operating Board of Directors within 1 month. This, she says, is in keeping with a less radical proposal contained in Appendix B of the Galvin report that calls for DOE to streamline the current system. The board, a panel of DOE managers and outside experts chaired by Energy Undersecretary Charles Curtis, would help the labs set strategic goals and monitor DOE efforts to cut costs. One lab director said he and his colleagues endorsed the moves at a meeting last month.

But Galvin told the senators that such an approach amounts to "rearranging the deck chairs [on the *Titanic*]." The corporation approach, he said, "is a no-risk test" and "a sure bet" to save money and make the labs more efficient. He praised the labs and damned DOE and congressional micromanagement of the system.

The plan Galvin presented to the senators calls for Congress to set up a not-for-profit organization through the Government Corporations Control Act, which has created entities like the Resolution Trust Corp., the Federal Land Banks, and the Federal Deposit Insurance Corp. A presidentially selected board of trustees would oversee the lab system and select its officers. "DOE, as the government sponsor and customer, should not serve as auditor or manager of the laboratories," Galvin's paper states. DOE would ask Congress for a budget, however, and the Comptroller General of the General Accounting Office could audit the new corporation.

Although O'Leary has not publicly rejected Galvin's plan, she does not believe it is politically realistic. "Bob Galvin is a visionary; I am focused on what I can do—and what I can do is Appendix B," the secretary told *Science*. For his part, Galvin insists he is not sparring with the secretary and that his goal is to "clarify" the task force report. He doesn't deny, however, that his efforts have created tension between him and O'Leary. "I don't think she is thrilled," he says.

–Andrew Lawler

Did Darwin Get It All Right?

The most thorough study yet of species formation in the fossil record confirms that new species appear with a most un-Darwinian abruptness after long periods of stability

In a 20-year debate about the pace of evolution, paleontologist Alan Cheetham had always known exactly where he stood. Since 1972, when Niles Eldredge of the American Museum of Natural History and Stephen Gould of Harvard University first proposed their theory of punctuated equilibrium, some paleontologists have argued that new species appear suddenly in the geologic record, after millions of years of evolutionary stasis. But Cheetham, like many of his colleagues, thought differently. As a student of the renowned evolutionary paleontologist George Gaylord Simpson, Cheetham had learned that a species changes gradually, through millions of years of natural selection—Darwin's survival of the fittest—until it is so different that it constitutes a new species.

That's the pattern he expected to confirm when he began an exhaustive study of the filigreed remains of corallike animals known as bryozoa, hoping to determine the pace at which new species had appeared during the past 15 million years. But Cheetham, who works at the Smithsonian Institution's National Museum of Natural History, was in for a surprise. "I came reluctantly to the conclusion," he says, "that I wasn't finding evidence for gradualism." What Cheetham did see, again and again, was individual species persisting virtually unchanged for millions of years and then, in a geologic moment lasting only 100,000 years or so, giving rise to a new species.

This just-completed study isn't the first to confirm punctuated equilibrium in the fossil record. But it is the strongest yet, other researchers agree. "Theirs is by far the most complete," says Dana Geary of the University of Wisconsin. Recognizing new species based only on their fossils can be problematic, as critics of earlier studies have emphasized. Cheetham and his collaborator Jeremy Jackson of the Smithsonian Tropical Research Institute in Panama seem to have defused that criticism, at least for the bryozoa, by testing their methods for distinguishing fossil species on living bryozoa. With their study, some paleontologists are now leaning toward punctuated equilibrium as the dominant mode of speciation. "Those who have looked hard, and that's not a large number, have tended to find punctuation," says Geerat Vermeij of the University of California, Davis.

Eldredge and Gould made their original proposal as graduate students, after they had been sent off in search of fossils—Eldredge to upstate New York for trilobites and Gould to Bermuda for land snails—to document the gradual, pervasive evolution that the textbooks said was there. Neither could find it. Instead they saw species that had gone unchanged for millions of years suddenly give rise to new ones.

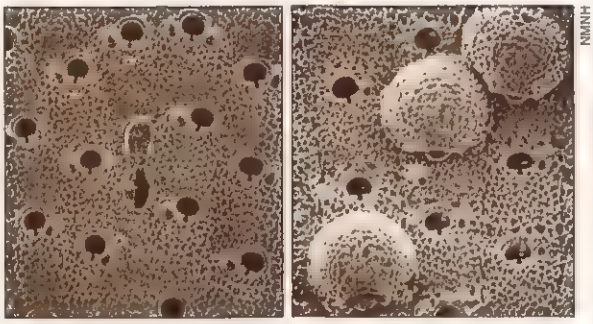

NMNH

Marks of distinction. Submillimeter skeletal features identify this bryozoan as *Stylopoma spongites*.

Since Darwin, paleontologists have attributed such findings to flaws in the geologic record: The stratum recording the gradual change that led to speciation must simply be missing. But Gould and Eldredge decided to take the fossil record at face value. They proposed that a long-standing mechanism for generating new species—the geographic isolation of a small population of one species for tens of thousands of years—could produce geologically abrupt speciation when the isolation broke down and the new species spread into the rest of the world.

Cheetham, though, regarded punctuated equilibrium as an unnecessary complication, and in 1986 he set out to demonstrate gradualism among the fossil bryozoa he had already spent decades studying. It was awkward for his views that the bryozoan species he was acquainted with did seem to have appeared abruptly. But he was confident that when he made a detailed study of their skeletal features to identify as many different species as he could, gradual speciation would prove to be the norm.

First, with the help of colleagues, Cheetham amassed a large sample of bryozoan fossils of the genus *Metrarabdotos* from the Caribbean and adjacent regions. He meticulously classified them into 17 species using 46 microscopic characteristics of their skeletons such as the length of the individual zooids (the animals that make up bryozoan colonies) and the detailed dimensions of the pores and larger orifices that dot the zooids. Then he arranged them in a *Metrarabdotos* family tree. Yet even though Cheetham's analysis often allowed him to split what had seemed to be a single species into several, the abruptness was stronger than ever. Through 15 million years of the geologic record, these species would persist unchanged for 2 to 6 million years, then, in less than 160,000 years, split off a new species that would continue to coexist with its ancestor species. Cheetham the gradualist "was amazed when he saw the punctuated result that he got," says Jackson.

A biological test

Jackson too was impressed, but he wasn't convinced. What if the subtle morphological differences Cheetham was using to split his fossil species really didn't mark separate species at all but rather, say, variants within a species? "Clearly, the strength of any discovery of punctuated equilibrium—a model of speciation—depends on our ability to recognize species," says Jackson. "So I challenged him to submit his methods to biological examination."

As test material, Jackson gathered many different modern bryozoa that are native to the Caribbean. He and Cheetham then tried to distinguish among modern species by applying the same kinds of morphological measurements Cheetham had used for the fossils. The first part of the exam tested consistency: Would the classification depend on how many morphological features they applied? No, the morphological differences that defined 22 species in three distantly related genera of modern bryozoa held up whether Cheetham and Jackson used 20 or 40 morphological characters.

KJELL B. SANDVED / VISUALS UNLIMITED

Living descendant. Genes from living bryozoa—corallike colonial animals a few millimeters long—helped sort out their family tree.

Then came reliability: Do the skeletal details accurately distinguish species? One worry was that the immediate environment might affect skeletal morphology, making populations of the same species living in different environments look like separate species. But when the researchers transplanted bryozoan colonies from different reefs to a single spot, the skeletons of the descendant colonies still closely resembled those of their parents in spite of the changed environment.

Another concern was that morphology might not be a fine enough scalpel: It might lump several different real species into a single apparent "species." So Jackson resorted to genetics. Using protein electrophoresis, he analyzed enzymes extracted from specimens of each of eight morphologically defined species. In each case, all the specimens from each morphological species had much the same enzymes, indicating that they belonged to the same genetically defined species. Cheetham's fossil species had passed the biological test with flying colors.

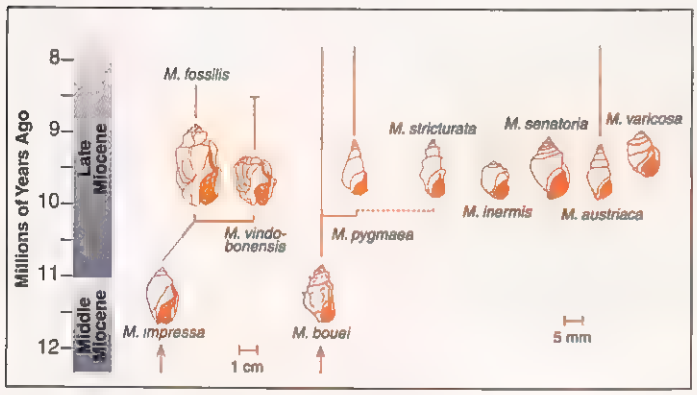

A favored tempo? The snail *M. bouei (right)* spun off new species in a geologic moment, while *M. impressa* took 2 million years of gradual change.

"Morphology still seems to be a way to say something about the way evolution occurred," says Cheetham. With this confirmation of Cheetham's method of identifying species, Jackson says he "became a believer." He and Cheetham have now extended the earlier work with *Metrarabdotos* to the genus *Stylopoma*. And once again, the 19 different fossil species they traced revealed textbook cases of punctuated equilibrium.

Because of their fastidious identification of species, Cheetham and Jackson's work is widely regarded as the strongest such evidence so far, but it has some competition. Timothy Collins of the University of Michigan and his colleagues, for example, recently took the same biologically based approach as Cheetham and Jackson when they studied a genus of coastal snails called *Nucella*. Although *Nucella* has fewer distinctive characteristics than the bryozoa, Collins and his colleagues also found punctuated equilibrium in the evolution of these snails in California over the past 20 million years.

Those who doubt the importance of punctuated equilibrium, however, can still take heart from earlier studies of fossil freshwater snails by Geary, who documented gradual change within two snail species over periods as long as 2 million years, along with six cases of punctuated speciation. Another verdict of gradual change came from Peter Sheldon of the Open University in Milton Keynes, United Kingdom, who studied morphological change among trilobites from Wales.

Faced with a welter of evidence, some paleontologists are sticking to a middle ground. In *New Approaches to Speciation in the Fossil Record*, the soon-to-be-published proceedings of a 1992 symposium, editors Douglas Erwin of the National Museum of Natural History and Robert Anstey of Michigan State University survey 58 studies published since 1972. They concede that many of these studies have their weaknesses, but they still conclude that "paleontological evidence overwhelmingly supports a view that speciation is sometimes gradual and sometimes punctuated, and that no one mode characterizes this very complicated process in the history of life."

But Jackson, for one, thinks most of the studies supporting gradualism are flawed—for example, because the researchers relied on only a single characteristic to monitor evolutionary change and couldn't be sure they had identified all the species. "I'm imposing pretty strict criteria," says Jackson, "but in the few cases I know [that meet those criteria], it's perhaps 10-to-1 punctuated." Geary, whose work has been used to buttress both sides of the argument, tends to agree. "Gould was my adviser," she says, "but I don't think I have a stake in it. I think that a whole host of patterns is possible, but it does seem to me punctuated patterns predominate."

How to punctuate evolution

If so, evolutionary biologists will feel new pressure to explain how punctuated equilibrium could actually work, a topic about which "there are a lot of hypotheses and not many facts," says evolutionary theorist Mark Ridley of Emory University in Atlanta. One mystery is what would maintain the equilibrium in punctuated equilibrium, keeping new species from evolving in spite of environmental vagaries.

One much-discussed possibility is that species become caught in what Vermeij calls "an adaptive gridlock." Called stabilizing selection, this gridlock results because "there's so much [natural] selection pushing at a species from different directions," Vermeij explains. "It can't go anywhere because moving in one direction has implications for its other competing functions." If a shellfish could reduce the weight of its shell, for example, it might have a better chance of escaping from some fast-moving predators. But that evolutionary route could be closed because a lighter, thinner shell would also decrease its resistance to other predators that bore into their victims. So the species remains unchanged for millions of years until a small population, isolated in a new environment, quickly evolves into a new species.

Stabilizing selection gets some new support in Cheetham and Jackson's chapter in *New Approaches to Speciation in the Fossil Record*. Over millions of years, they point out, any species would be expected to change slightly because of random genetic drift, but their analysis of the *Metrarabdotos* and *Stylopoma* bryozoa suggests something more like evolutionary paralysis. "Our tests strongly favor stabilizing selection" as an explanation of long-term species stasis, says Cheetham.

But that explanation only deepens another mystery: "If stability is the rule, how do you get large-scale shifts in morphology" over many successive species? asks paleontologist David Jablonski of the University of Chicago. "How do you get from funny little Mesozoic mammals to horses and whales? From *Archaeopteryx* to hummingbirds?" One possibility is species selection, a process analogous to Darwin's natural selection but acting at a higher level. A species might be especially likely to spawn new species because of some characteristic of that species that could never appear in an individual, such as having a broad geographic range. As a species wins out in this higher level evolutionary game, Jablonski explains, "all sorts of things get swept along." Body characteristics of individual members of the species, which might have nothing to do with the success of the species as a whole, would turn up in an increasing number of descendant species.

To finally resolve how common such processes are, and how many of his teacher's lessons Cheetham will eventually have to reject, researchers will have to apply a paleontological scalpel as sharp as Cheetham and Jackson's to a variety of organisms, living in many different environments. As Eldredge and Gould have written, "Only the punctuational and unpredictable future can tell."

–Richard A. Kerr

Additional Reading

D. H. Erwin and R. L. Anstey, Eds., *New Approaches to Speciation in the Fossil Record* (Columbia University Press, New York, in press).

J. B. C. Jackson and A. H. Cheetham, "Phylogeny reconstruction and the tempo of speciation in Cheilostome bryozoa," *Paleobiology* **20**, 407 (1994).

PHYSICS

With Quark Discovery, Truth Comes Out on Top—Twice

Last week's announcement by physicists at the Fermi National Accelerator Laboratory that they had finally discovered the top quark marked the end of one quest and the start of another. The 18-year search to find the sixth and final quark, a relative of the quarks that make up most of ordinary matter, was over after a last-minute sprint to the finish by groups working independently on Fermilab's mammoth accelerator, the Tevatron. In what might be called the moon shot of particle physics, two 450-person collaborations staffing detectors costing $100 million each had collided trillions of particles and sifted tens of millions of collisions to corner the elusive particle.

But the 2 March announcement, which Energy Secretary Hazel O'Leary called a "crowning moment of success," doesn't close the book on the understanding of matter. Instead it marks the start of a new era in which, like naturalists poking and prodding an exotic new specimen, experimenters will be scrutinizing the top quark for clues to new physics. "Finding the top is much more than just filling in the blank in the table of quarks," says Fermilab collaborator John Huth of Harvard University. The top, after all, stands out from the crowd: With roughly the same mass as an entire gold atom, it is far and away the heaviest elementary particle and may hold clues to a major unsolved puzzle in physics—the origin of mass.

The top had been at large since the 1977 discovery of what turned out to be the fifth quark: the bottom, or beauty, quark. Physicists' standard picture of matter demanded a sixth: Beauty must have a mate. Fittingly, it was named truth, or top, and the search to find it was on. The top, like all but two of the other quarks, does not exist as part of ordinary, observable, matter and must be created by colliding high-energy streams of particles in an accelerator. In a tiny fraction of the collisions, physicists hoped, a top quark would materialize and live for 10^{-25} seconds before decaying into a characteristic shower of particles. But for 18 years, experiments designed to create the quark failed to muster enough energy.

Indeed, even the Tevatron—the world's most powerful accelerator at 1.8 trillion electron volts—was just barely able to probe the energy range where the top was thought to hide. The first hints that the search might be ending came last April, when the CDF (Collider Detector at Fermilab) collaboration announced that their massive detector had recorded residue from 12 events that looked like top quark decays. It was "evidence" for the quark, but not enough to rule out the possibility that the events were due to background "noise" (*Science*, 29 April 1994, p. 658). Adding to the doubts, physicists at the other Tevatron detector, D0 (D-Zero), had seen no clear evidence. Since then, however, both groups continued to amass new data and reanalyze their earlier runs.

As rumors of strong results flew back and forth between the two groups in January and February, each began to fear that the other would be the first to submit a report of the discovery, and the pace of the analysis sped up. Anxiety gripped the CDF group, for example, after an early February rumor that D0 had scheduled a seminar. At this "wine and cheese" event, some at CDF feared, D0 might announce top quark results. "It was only human to imagine that," says Huth, a CDF member.

The meeting never took place, and in the end the announcement followed a protocol established 2 years ago by Fermilab Director John Peoples: If either group was ready to report significant results, it had to let the director know first and give the other collaboration a week to prepare and respond. In the end it was CDF that approached Peoples first, but at that point D0 was ready. Both groups submitted papers claiming "observation of the top quark" to *Physical Review Letters* on 24 February and agreed to preview their results in a joint seminar.

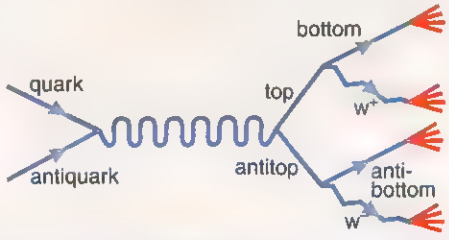

SOURCE: FERMILAB

	CDF	D0
Top events	43	17
Significance	4.8σ	4.6σ
Mass (billion electron volts)	176 ±13	199 ±30
Cross section (picobarns)	$6.8^{+3.6}_{-2.4}$	6.4 ± 2.2

Two views of the top quark. In a rare high-energy collision *(top)* ordinary quarks interact to produce top quarks, which decay into lighter particles.

At the 2 March Fermilab seminar both collaborations reported detecting enough possible top quark events (see table) to reduce the odds that the signal arose by chance to around one in a million. The collaborations also presented data on what physicists call the "production cross section"—a measure of how, and how often, the top quark is produced—and on the quark's mass, determined from the energies of the decay products. "Everybody gets confidence from the fact that two collaborations that are pretty competitive with each other see the same result," says CDF physicist Richard Hughes.

Now experimenters are looking ahead to the work to come. As Hughes puts it, "In a couple of months no one will be asking you how sure you are the top exists; they will be asking you 'What is the mass?' " A precise mass should provide insight into a theoretical mass-giving entity called the Higgs boson. "Particles are endowed with mass in proportion to their coupling with the Higgs field," explains William Bardeen, the acting head of Fermilab's theory group. "In that sense the more massive the particle, the closer you are to a place where the Higgs might reveal itself." Right now, he adds, you can't get any closer than the top quark.

Besides its mass, physicists would like to test the new quark's spin, charge, and decay modes to see how well they match the predictions of standard theory. Serious gaps could serve as a window onto some new physics. Bardeen and his colleagues at Fermilab have theorized, for example, that certain energy states of the top quark may actually be the Higgs, or at least a part of it.

Pursuing these questions, however, will mean creating top quarks in droves, says Bardeen. "You need a lot of events of all kinds to find the few events that will tell you the hint of the new physics." Fermilab's current schedule gives CDF and D0 another year to collect top quarks. That should be enough to improve measurements of the top's mass and cross section, but it won't satisfy physicists' craving for the particles.

After that, top quark enthusiasts will have to wait for two new machines. At Fermilab, the Tevatron is scheduled for a major upgrade, known as the main injector, slated to come on line in early 1999. "We are shooting for a factor of 10 and maybe 20 in total observable top quarks," says Peoples. Then the torch will pass to Europe's Large Hadron Collider, which will take the place of the Tevatron as the world's highest energy accelerator sometime after the turn of the century.

–Antonio Regalado

How Quixotic Is SLAC's Quest To Detect "Crazy Particle"?

On the cult television hit *The X-Files*, FBI Agent Fox Mulder investigates reports of everything from attacks by vampires to visits from UFOs. Living by the motto "The truth is out there," Mulder will not accept offhand dismissals; he carefully attempts to disprove or corroborate each report, no matter how bizarre or improbable. And—at least in the fictional world of a TV series—such persistence sometimes has a dramatic payoff.

Physicist John Jaros thinks that spirit has a place in the real world. He and colleagues at the Stanford Linear Accelerator Center (SLAC) are now conducting a search for what Jaros jokingly calls a "crazy particle": a subatomic morsel carrying only the merest wisp of electric charge. For the last few months, Jaros, Willy Langeveld, Allen Odian, Alyssa Prinz, and their team have been watching for these so-called millicharged particles in subatomic debris produced as high-energy electrons slam into an inch-thick slab of tungsten. Jaros admits that the team has only the slimmest chance of finding anything, but he notes that millicharged particles aren't ruled out by established theories in physics. And he and others believe the implications of millicharged particles, should they exist, are noteworthy enough to justify the search.

"If you found one of these things, it would be as exciting as a massive neutrino," says physicist Sacha Davidson of the University of California, Berkeley, Center for Particle Astrophysics, referring to the recent announcement that the elusive subatomic particle known as the neutrino might have mass (*Science*, 10 February, p. 789). Like massive neutrinos, millicharged particles might be a clue to the universe's "dark matter"—the invisible matter that seems to exert a gravitational pull on the rest of the universe but has eluded vigorous efforts to track it down.

If the search does pay off, it would not be the first time physicists have had to revise their views on electric charge. The charges of an individual electron or proton were once seen as indivisible, but that mindset changed in the 1960s when theorists began arguing that protons and neutrons consist of quarks, particles carrying charge—either positive or negative—in quantities one-third or two-thirds that of the electron. And there's no clear reason why charges can't come in still smaller packages, say some physicists. "Electrical charge is quantized, but we don't know why it's quantized. Who says new particles would have familiar charges?" asks David Bailey, a University of Toronto experimental physicist.

What is more, theory has provided physicists with a few threads of hope that millicharged particles exist. The most discussed one is the idea—seemingly outlandish but proposed by a number of theorists over the years—that our universe is mirrored by another. Consisting of particles completely different from our own, this so-called shadow universe would be "another universe coincident with ours that we don't interact with except gravitationally," explains dark matter researcher David Caldwell of the University of California, Santa Barbara. This shadow realm would provide the dark matter whose gravity helps shape our own universe.

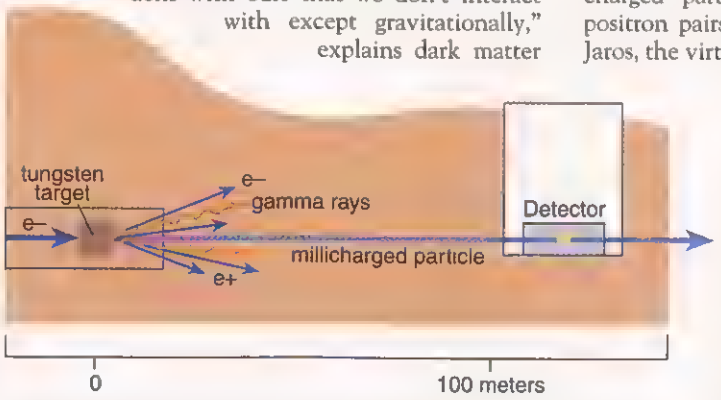

SOURCE: JAROS *ET AL.*

Vigil for a phantom. Any millicharged particle generated when electrons slam into a tungsten target should pass effortlessly through 100 meters of rock to a detector, where it might spark a single proton.

On rare occasions these two universes might intersect in another way, according to a theory devised by University of Toronto physicist Bob Holdom in 1986. Through a complex chain of events, some of our own universe's electric charge could rub off onto shadow particles, giving them a tiny fraction of a normal electron charge. In principle, this tiny borrowed charge would open the shadow particles to detection.

Fanciful as this sounds, says Jaros, Holdom's notion does not violate any known law of physics. In 1990, however, Russian physicists M. I. Dobroliubov and Alex Ignatiev and, a bit later, Davidson, Bailey, and Bruce Campbell of the University of Alberta in Canada pointed out that existing data rule out new particles with a charge greater than a thousandth of the electron's. Working independently, the two groups calculated that such particles would have revealed themselves in previous accelerator experiments or dark matter searches.

Particles with charges smaller than a millionth of an electron's could also be ruled out, the two groups concluded, because they would have had noticeable astrophysical and cosmological consequences. For instance, says Davidson, the core of a white dwarf star would probably create millicharged particles. If their charge was much smaller than a millionth of an electron's, she explains, the particles would escape the star so readily that they would rob it of energy and end its life more quickly than observations suggest.

Between a thousandth and a millionth of the charge of the electron, however, lies unexplored territory. To probe it, the Russian physicists suggested the scheme Jaros and his colleagues are now exploiting at SLAC. As energetic electrons bombard the tungsten target, they radiate short-lived "virtual" photons, which immediately convert into charged particles—most often, electron-positron pairs. But on rare occasions, says Jaros, the virtual photons should spawn particles with smaller charges, if any exist.

In the SLAC setup, magnets siphon off the positrons and other strongly charged particles for use in other experiments, but any millicharged particles should continue undeterred in a straight line. Last year, the SLAC researchers installed a detector to watch for them, positioned behind hundreds of feet of sandstone that would filter out other subatomic debris. Consisting of a cooled block of plastic scintillator, the detector might register the arrival of a millicharged particle by generating a single detectable photon.

Jaros and his colleagues were able to sell the unusual project to SLAC management because its cost—some $250,000—is modest (for high-energy physics), and the project can be carried out without interfering with SLAC's normal production of positrons. They started the search last fall and plan to continue until the end of March. So far, the SLAC team has seen no light flashes they can attribute to millicharged particles, although Jaros cautions that the group has only completed preliminary analyses of the data.

Nevertheless, they and some of their colleagues think this quest for improbable particles has been time and money well spent. "I've had more fun on this than I've had in years," comments Odian. Adds Bailey, "You should always do a crazy experiment every so often; otherwise you might miss important things." Fox Mulder would approve.

–John Travis

INFORMATION TECHNOLOGY

Plucking Images From the Digital Floods

Consider this apparently simple request: Find a picture of yellow flowers on the Internet. The simplicity is deceiving, for at present this can't be done—unless you're rescued by serendipity. Existing software can only sift through words, blind to the deluge of images, sounds, and video that increasingly swamps computer networks.

Building tools to filter drops of visual information from the digital flood is one goal of the ambitious National Science Foundation "digital library" program (*Science*, 7 October 1994, p. 20). Six university-led groups are trying to learn how best to sort, file, and retrieve information, creating pockets of digital order amid informational chaos. Two weeks ago in Atlanta, at the annual meeting of the American Association for the Advancement of Science (the publisher of *Science*), one of these groups showed that, when it comes to image searches, a picture can be worth a thousand descriptive key words.

Typically, image collections in libraries use such key words as tags for searches. But what a botanist sees as "yellow" might be "golden" to a cataloger writing the tags. As a result, the flower-gathering botanist will come up empty-handed. So when scientists at the University of California, Berkeley, began collecting images as part of their library of California environmental information, they decided to develop software that searched the images themselves.

By computing and storing the distribution of colors in an image, the prototype system allows a user to combine a key word search for "flower" with a further condition that the picture "contains some yellow." The computer delves through the archives for pictures of flowers, then examines each for splotches of yellow. Small versions of images matching these criteria pop onto the screen, and the user can click on them to retrieve full-size pictures. In contrast, says Robert Wilensky, principal investigator of the Berkeley group, a search for the key words "yellow" and "flower" with a text search program missed many of these images entirely. The original cataloger had not even entered the key word "yellow" for many of the images.

While not the first to design a system that searches through colors, "the Berkeley group is the first to apply these techniques to such a large, unified corpus of material and to hook it into a database system," says James Frew, one of the principal investigators on another digital library project, at the University of California, Santa Barbara. It's even possible for a user to scan in a picture of yellow flowers and then tell the computer to find "pictures that look like that." In the future the Berkeley system, written by grad student Ginger Ogle, may know that a "blob" is some irregularly shaped object; the user could then query for pictures with "blobs of yellow."

None of this experimentation means digital librarians have given up on words entirely. In fact, they also want to improve the way software uses text. In the hit-or-miss search through ordinary text, for example, hits can be as frustrating as misses. "Ninety percent of what you get back is garbage," Wilensky complains. "And you look at it and say, 'Hmm, this is garbage. Throw it out.' So why couldn't the computer do that?" If you use the word "film" to find information on movies, you'll also get back hits on color print film, thin-film chromatography, and maybe even soap film. What's more, the 10% that isn't garbage doesn't contain everything you need. For example, searching for the word "education" will miss most of the documents about education, as "the word 'education' doesn't occur in most of the articles about education," Wilensky says. "What occurs is 'school' and 'teacher.' "

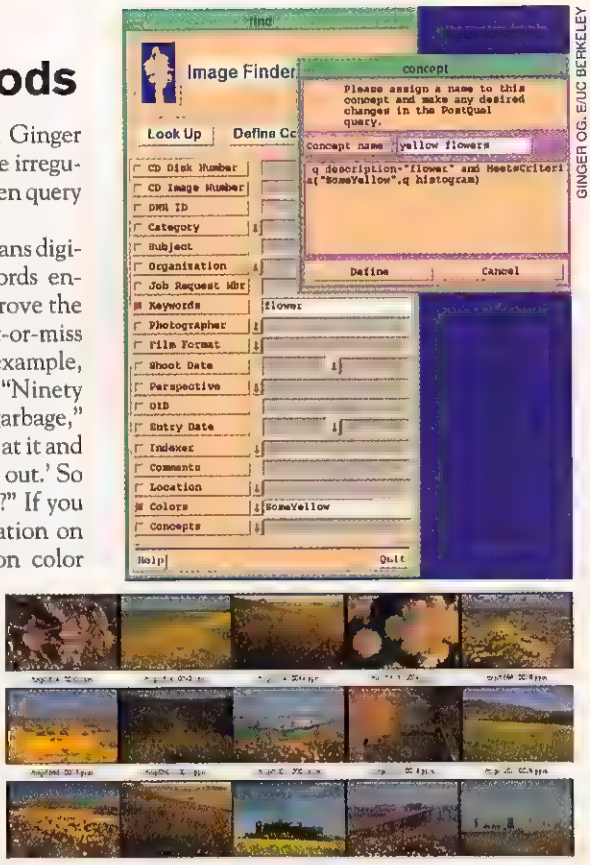

GINGER OG. E/UC BERKELEY

Picking flowers. Digital library software, called Chabot, searches for yellow pixels in images rather than the word "yellow," and pictures of yellow flowers pop onto the screen.

The potential solution to both problems lies in semantics. A smarter system would understand relationships between words, recognizing that "education" includes "school" and "teacher." The search for "film" would include the notion of movies. The Berkeley system currently works with 4000 semantic concepts, and they hope to increase that number by an order of magnitude. There are unsolved problems—how, for instance, would a user sift through 40,000 concepts to find the desired one? But the hope is that one day picking yellow flowers on the Internet will be as easy as going outside on a summer day and picking them by hand.

–Kenneth Chang

Kenneth Chang is a science writer based in Santa Cruz, California.

PLANETARY SCIENCE

NASA Picks a Budget Lunar Trip

In the National Aeronautics and Space Administration's (NASA's) push for smaller, faster, and cheaper space missions, cheaper turns out to be a big winner. Last week NASA picked the least costly of 28 candidates for the next launch in Discovery, the agency's low-cost planetary exploration program. The $59 million spacecraft, known as the Lunar Prospector, is an orbiter for Earth's moon, and came in well below the mission budget cap of about $330 million.

"We got some dynamite proposals—very innovative and clever," says NASA Associate Administrator for Space Science Wesley Huntress. But NASA was most impressed with the return on the dollar promised by Lunar Prospector. Proposed by Alan Binder of the Lockheed Electronics and Science Corp., Prospector's price tag includes development, launch, and operations. The spacecraft will survey the composition of the moon's crust and its magnetic and gravitational fields to elucidate the crust's complex history. The craft will also search for surface ice and gas releases; ice deposits might be useful water sources during crewed exploration.

The probe, scheduled for launch in June 1997, will need to be impressive to match the cost-effectiveness of last year's Clementine lunar mission. That Department of Defense (DOD) project focused on testing Star Wars instrumentation, but provided a nearly free bonus of new scientific data from its lunar orbit. Congress will be watching to see if NASA can approach DOD's economy.

–Richard A. Kerr

edited by CONSTANCE HOLDEN

Overdrawn at the Brain Bank

The Canadian Brain Tissue Bank in Toronto is suffering from insufficient funds. One of three such repositories in North America, the bank lost its government funding last year in a Canadian science budget crunch. Now its hopes for survival rest on its utility for studying environmental toxicants.

The bank, founded in 1981, includes samples from people with degenerative neurological disorders and psychiatric ailments, as well as reference samples from normal brains. Tissue is made available to any researcher doing a peer-reviewed project. Schizophrenia researcher Philip Seeman of the University of Toronto points out that human brain tissues are in growing demand by researchers, as no animal model can replicate a human behavioral disorder.

The bank was funded, at something less than a quarter of a million Canadian dollars a year, by two government sources—the Medical Research Council and the Ontario Mental Health Foundation—as well as a charitable group, the Canadian Neurological Diseases Coalition. With two thirds of its support gone, it now has only two full-time employees overseeing its collection of tissue from some 1340 brains.

Annette Dukszta, the bank's administrator, says she hopes the Great Lakes Health Effects Program—established in 1989 to assess the effects of industrial pollutants—will provide an "escape route." Budget allocations won't be decided before the end of March, but "they have us as a priority," she says. According to toxicologist Moe Hussain of the health effects program, studies up to now have focused on gauging peoples' intake of poisons, mainly through fish consumption. But researchers also want to examine a variety of human tissues to gauge toxic exposure, and many of the brains in the bank are from people who lived in the Great Lakes basin.

Brain tissue is valuable in the study of cumulative poisons such as heavy metals, says Seeman, because there is no cell turnover. He says the Great Lakes project could also help fill out the picture of how environmental toxicants conspire with genes to bring about Parkinson's and other degenerative diseases.

LONG ISLAND UNIVERSITY

Crossing the bar in style. Egyptologist Bob Brier *(right)* and Webb Institute senior Stu Greene with replica of pharaoh's boat.

The Boat in the Tomb

In 1954 the pieces of a 170-foot-long cedar boat were discovered in the Great Pyramid of Giza, tomb of King Cheops. Could the 4000-year-old boat serve as a practical vessel in this world, or was it built only for use in the next? Long Island University Egyptologist Bob Brier wanted to find out. On 23 February, researchers put a 7-foot model of the boat to the test and found it seaworthy. The boat, says Brier, is an "elegant, beautifully designed craft."

Brier relates that he and colleagues from the university's C. W. Post Campus in Brookville, New York, drew a blueprint from the original vessel, which is housed in a museum at Giza. Professional model carvers based the pine-and-glue model—including 12 little oars—on these plans. Then the scientists tested the craft in a 93-foot-long tank at the Webb Institute, a marine engineering college in Glen Cove, New York. "We pulled it through the water several hundred times under different conditions," says Brier. They concluded that the low-riding craft was a river boat because in the ocean it would have been swamped. And it was not designed for cargo because there is no hold. "It may have only gone on one voyage, crossing a river to take the pharaoh's body for burial," says Brier. Nonetheless, he says, it has "wonderful properties in the water" and left no wake, causing observing naval architects to gape with wonder.

Marsha Hill of New York's Metropolitan Museum of Art says that there has long been speculation about whether such funerary vessels were navigable. Brier's experiment confirms the current prevailing belief that the craft was navigable, she says—"but not for very far" because the lashings (it was bound together by ropes) were not secure enough for serious boating.

Portrait of a Killing

Two years ago Venezuelan biologist Aldomero Romero, campaigning against commercial fishing practices that were destroying dolphins, filmed a dolphin being slaughtered. Now his government, embarrassed by the furor Romero's film has provoked, has accused him of orchestrating the killing and has moved to extradite him from the United States, where he has sought refuge. Romero, an adjunct professor at the University of Miami, says in a complaint filed with the Federal Bureau of Investigation (FBI) last week that Venezuelan authorities have threatened to kidnap him.

The strange saga began in February 1993 when Romero and another biologist shot a video allegedly showing Venezuelan fishermen butchering a dolphin for use as shark bait. Romero, then director of the Venezuelan Foundation for the Conservation of Biological Diversity, says he gave a copy of the video and a report to Venezuela's Attorney General in May 1993, but it failed to elicit action. After Romero gave the footage to CNN, however, the cable network broadcast an edited version in November 1993 that spurred thousands of viewers to send angry letters to Venezuelan diplomats in the United States.

That outpouring apparently irked certain Venezuelans, who Romero says began calling his house in Caracas with death threats. Romero fled to Miami with his family in February 1994. A few months later, a provincial prosecutor in Venezuela charged him with killing the dolphin in the film. Romero denies the charge and says he filmed the slaughter to expose the illegal killing. But last month, Venezuela's Supreme Court approved an extradition request from the province.

Few observers believe the U.S. State Department will honor it. "I think it's most unlikely that State would act on a request from a province rather than the government," says Bruce Winick, a University of Miami law professor. But Romero still expects more trouble. "The Venezuelan authorities will take illegal forceful action to take me back to Venezuela," his FBI complaint states. The Venezuelan embassy failed to return calls from *Science*. As for Romero, he says, "I feel like I'm in a Hitchcock movie. I'm afraid for my life."

Public Health Threats

For emerging health threats, 1993 appears to have been a vintage year, with the surge to prominence of three new diseases: cryptosporidiosis, in which a parasite in Milwaukee's drinking water sickened thousands of people; hantavirus disease, a mouse-borne respiratory illness that killed a dozen people; and hemolytic uremic syndrome, caused by foodborne bacteria that, among other things, made a score of people ill from Jack-in-the-Box hamburgers.

These scourges, along with four others, have been added to the list of some 50 communicable diseases that are reported by states to the U.S. Centers for Disease Control and Prevention in Atlanta, Georgia. During the past 2 decades, such new illnesses as Legionnaires disease, Lyme disease, and AIDS have joined the list. But last month the Atlanta-based Council of State and Territorial Epidemiologists voted on additional changes following a meeting in November—the first major reassessment of the list since the 1950s.

"What we're seeing is the constant evolution" of the list, matching the changes in diseases and the conditions that nourish them, says epidemiologist Ed Thompson, Mississippi's state health officer. A strain of *Escherichia coli*, for example, which causes hemolytic uremic syndrome, appears to have mutated from an innocuous bacterium to a killer bug in the '80s. The hantavirus multiplied as damp weather provided food conditions favorable for the disease-carrying mice.

The additions may not be welcomed by state and local health officials who are coping with a growing caseload of infections—AIDS and drug-resistant tuberculosis in particular—despite stagnant budgets and staffing. On the upside, several diseases, such as rheumatic fever, which has been dramatically reduced, are expected to be removed from the list. And officials are trying to streamline surveillance for some diseases such as influenza by sampling the caseloads of "sentinal" physicians rather than trying to tally every case.

Attacking Corruption In Academe

The campaign to clean up the *concorsi*, Italy's system for picking professors, is gaining speed, pushed along by a new research minister who replaced an avowedly reluctant reformer, the unpopular Stefano Podestà, in January.

The *concorsi*, national competitions that should be held every 2 years, have been criticized for furthering the careers of weak candidates, many of whom are collaborators or even relatives of members of the judging panels (*Science*, 11 November 1994, p. 965). Frustration is high, too: The last round for associate professors was held in 1990 and for professors in 1992. This latter round is still not closed, as investigations into corruption are in progress.

Now the new minister, Giorgio Salvini, a physicist and technocrat, wants to change the way business is done. He and many academics favor drawing up national lists of selected *concorsi* candidates from which universities could choose. Other proposals may be forthcoming from a newly formed academic research and culture association whose aim is to raise standards throughout Italian academia.

Given the widespread criticism of the old system, new legislation must pass parliament before any new *concorsi* are held. Salvini wants his proposals approved before he opens new rounds of *concorsi* this spring and summer.

There are already signs of change. Medical faculty at Padua have just approved more stringent requirements for scientists serving on panels that define criteria for university positions. The courts are also getting involved. A medical panel chair recently received a 1-year suspended sentence for abuse of power in assigning university chairs, and the Roman public prosecutor has initiated criminal investigations of a dozen professors for similar offenses.

Discovering Women in Science

Human face of physics. Harvard's Melissa Franklin.

Six U.S. women scientists will be featured in a six-part documentary series to be aired by the Public Broadcasting System starting on 29 March. The series, produced by WGBH in Boston, is designed to attract more women, who now make up 16% of the scientific work force, says spokesperson Judy Matthews. And, she says, it wants to demonstrate that you don't have to be an eccentric genius but can become a scientist with "human-level" intelligence.

Harvard University high-energy physicist Melissa Franklin says she thinks this series will indeed help make science seem like an option for more people. She recently gave a talk to some high school students in Worcester, Massachusetts, who seemed gratified that she appeared normal. "A lot of students said they always thought scientists were more nerdy and weirder," she says. The other five scientists are biochemist Lynda Jordan of North Carolina A&T State University; geophysicist Marcia McNutt of the Massachusetts Institute of Technology; Washington University archaeologist Patty Jo Watson; computational neuroscientist Misha Mahowald, a postdoc at Oxford University; and Harvard molecular biologist Lydia Villa-Komaroff.

Producer Judith Vecchione says an accompanying outreach program called "Seek Out Science" for middle-schoolers encourages them to create research projects around women scientists which will then be displayed in several museums around the country. The project, "Discovering Women," is being sponsored by the Intel Foundation with support from the Sloan Foundation and the National Science Foundation.

Message in a Bottle

The Republicans may want their Contract with America, but what America really needs is "a contract with nature." So spoke Cornell biologist Thomas Eisner at a gathering in Washington, D.C., held to announce the formation of the "medicine bottle crusade." The crusade is a campaign to salvage the Endangered Species Act by flooding legislators with old prescription containers.

The message is that plants hold a wealth of beneficial yet undiscovered chemicals, and extinction will rob humanity of these treasures. Eisner passed around one of the most recent examples, a type of mint, discovered on the grounds of the Archbold Biological Station in Florida in 1962, that has been found to harbor both a new kind of insect repellent and a new anti-fungal compound.

The campaign, sponsored by a group of organizations calling themselves the Endangered Species Coalition, is designed to influence legislators as they contemplate some major changes to the Endangered Species Act, which comes up for reauthorization in September (*Science*, 3 March, p. 1256). The House has already, on 23 February, voted to suspend further listings of critical habitats until after the law is reauthorized. Coalition chair Randall Snodgrass said the Republicans are also keen to cut the National Institutes of Health's Office of Alternative Medicine, which funds research on botanical drugs.

EXPLORE APOPTOSIS

With Monoclonal Antibodies to Mouse and Human FAS

PanVera presents powerful NEW tools to study programmed cell death. These new antibodies react specifically with mouse or human cells expressing the FAS antigen.

Applications Include:

- Induction/Inhibition of Apoptosis
- Flow Cytometry
- Immunohistochemistry
- Immunoprecipitation
- Western Blotting

Also Available

Non-Radioisotopic Protein Kinase Assay (NRPK)
Measures the activity of protein kinase A and C in a 96 well format.

(800) 791-1400

PanVera Corporation
565 Science Drive
Madison, WI 53711 USA
(608) 233-5050
FAX (608) 233-3007
e-mail: info@panvera.com

Products manufactured by Medical & Biological Laboratories Co., Ltd

Circle No. 40 on Readers' Service Card

Call For FREE T-Shirt Offer!

If you're paying too much for antibodies, check out these numbers:

1-800-242-0607

The right call for the largest selection and best value!

Use our 800# to learn about our other large numbers - antibodies, over 400 of them. Custom antibody production is offered, too.

Goat anti mouse F(ab')$_2$
Goat anti human IgD
Goat anti human IgM
Goat anti rat IgG
Mouse anti human CD-4

820 Flynn Road
Camarillo, CA 93012
1-800-242-0607
Fax: (805) 987-3385

TAGO IMMUNOLOGICALS
IMMUNODIAGNOSTIC REAGENTS
BIOSOURCE INTERNATIONAL

Circle No. 72 on Readers' Service Card

Get to the Point

F A S T !

Data Desk is fast, visual data analysis software that takes you straight to the heart of your data. Its dynamically linked graphics show you key patterns and relationships—even the first time you use the program. The fastest calculations of *any* Macintosh statistics package let you spend less time computing—even for the largest datasets.

Start Fast — **"The program teams ease of use with advanced features, making it a good choice for novices as well as experienced statisticians."** —*MacUser, 9/93* ♣♣♣♣½

Compute Fast — **"The fastest statistics package for the Macintosh, and it is also the easiest statistics program to use on any platform."** —*Walter T. Linde-Zwirble, Clinical Outcomes, Summer 93*

Analyze Fast — **"Its user interface and recalculation speed actively encourage users to examine data sets using many different tools."** —*MacWeek, 7/5/93* ◆◆◆◆

Get to the Point Fast — **"For getting to the heart of the matter, which is finding patterns in data, Data Desk 4.0 has no peer."** —*MacWorld, 5/93* ★★★★

Data Desk
The Fast, Visual Tool for Data Analysis
Data Description, Inc., PO Box 4555, Ithaca, NY 14852

CALL FOR A FREE MAC DEMO! 800-573-5121

Circle No. 22 on Readers' Service Card

Reaching for the Top with Quality Products

- Methylcellulose-based media for colony assays of hematopoietic progenitors
- Long-term culture media for assays of the most primitive progenitors
- Pre-selected Sera and Serum Substitutes
- Pre-tested Tissue Culture Supplies

NEW

ClonaCell™-HY

Monoclonal Antibody Production Made Easy
Faster and more efficient than conventional methods for generating hybridomas
Complete Kit with Instructions

MethoCult™-GF & MethoCult™-SF^{BIT}

New formulations of methylcellulose-based media for hematopoietic progenitor cell assays prepared with recombinant growth factors(GF) or FBS-Free (SF^{BIT})

For more information on our expanding line of products and services please contact:

StemCell TECHNOLOGIES

StemCell Technologies Inc
808-777 West Broadway
Vancouver, BC
Canada V5Z 4J7
Phone: (604) 877-0713
Fax: (604) 877-0704

Toll free phone: 1-800-667-0322
fax: 1-800-567-2899

For your convenience international distributors are available in Europe and Asia. Call or fax for more information.

Circle No. 63 on Readers' Service Card

On The Leading Edge...

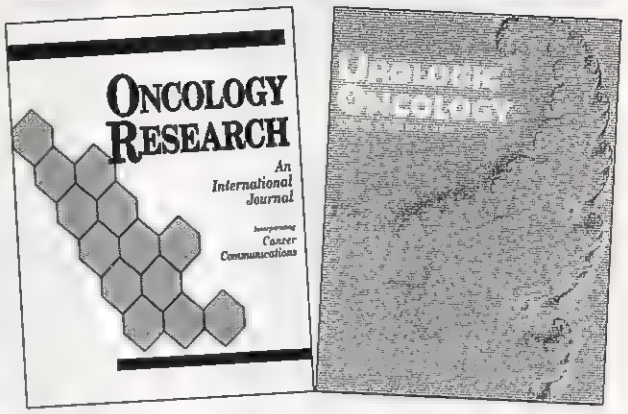

Cancer Journals from Elsevier Science

New Editor in Japan!

ONCOLOGY RESEARCH

An International Journal
Incorporating Cancer Communications

EDITORS:
Takashi Tsuruo
University of Tokyo, Tokyo, Japan
Alan Sartorelli
Yale University, New Haven, CT, USA

Publishing in just 7 weeks full length research and commentary papers of the highest quality.

ISSN: 0965-0407 Volume 7, 1995 12 issues

Announcing a New Journal!

UROLOGIC ONCOLOGY

EDITOR-IN-CHIEF:
George R. Prout, Jr.
Maryland Medical Research Institute, Baltimore, MD, USA

Dedicated to advances in the biology and management of urologic cancer.

ISSN: 1078-1439 Volume 1, 1995 6 issues

Stop By Booth #333 At AACR

for free sample copies of these and other cancer titles from:

ELSEVIER SCIENCE
660 White Plains Road, Tarrytown, NY 10591
655 Avenue of the Americas, New York, NY 10010

Circle No. 32 on Readers' Service Card

Genset

SERVES
GENOME
RESEARCH
WORLDWIDE
WITH
GUARANTEED
OLIGOS

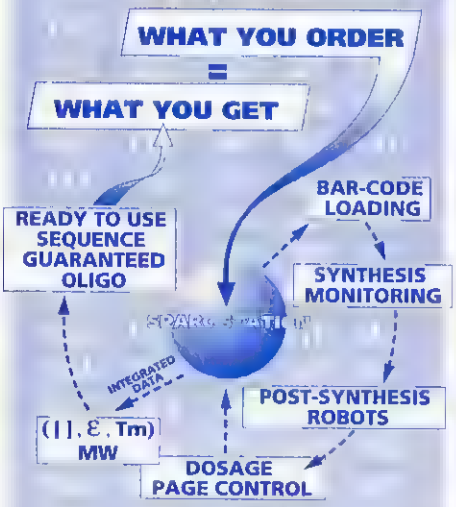

ORDERS & INFORMATION

USA - GENSET Corp.
FAX : (1) - 800 551 5291

EUROPE - GENSET SA
FAX : (33) - 1 43 56 68 18

JAPAN - GENSET KK
FAX : (81) - 3 3585 5351

GENSET

GUARANTEED OLIGOS ™

Circle No. 45 on Readers' Service Card

At Ericomp, temperature cyclers are all we make.

Before you decide on the best cyclers for your DNA amplification lab, check with Ericomp, the pioneer in single and multi-block thermal cyclers. We offer the widest selection of air, water, or Peltier cooled units to labs needing throughput, reliability, reproducibility *and* economy.

NEW for '95:

- **DeltaCyclers:** High throughput Peltier-based
- **PowerBlock I:** Peltier-based MiniSingle™
- **SingleStar and TwinStar:** High throughput with economy–The lowest cost per sample on the market

In the US, call 800-541-8471.
Outside the US, 619-457-1888.

ERICOMP

6044 Cornerstone Court West
San Diego, CA 92121
Circle No. 68 on Readers' Service Card

Boehringer Mannheim Worldwide Representatives

Australia
Tel.: (02) 899 7999

Austria
Tel.: (0222) 277 87
DW 420 to 423

Belgium
Tel.: (02) 247 4930

Canada
Tel.: (514) 686 7050

Central/Eastern Europe
Tel.: (0222) 277 87

Chile
Tel.: 00 56 (2) 22 33 737

China
Tel.: (852) 2485 7596

Denmark
Tel.: 49 13 83 42

Finland
Tel.: (90) 429 2342

France
Tel.: 76 76 30 86

Germany
Tel.: 0621 759 8568

Greece
Tel.: (01) 64 96 683-6

Hong Kong
see China

India
Tel.: (22) 837 0794

Indonesia
see Singapore

Italy
Tel.: (02) 270 96209

Japan
Tel.: (03) 3432 3155

Malaysia
see Singapore

Mexico
Tel.: (5) 227 8967

Netherlands
Tel.: (036) 539 4911

New Zealand
Tel.: (09) 276 4157

Norway
Tel.: 22 07 65 00

Philippines
see Singapore

Portugal
Tel.: (01) 417 1717

Singapore
Tel.: 65 479 4111

South Korea
Tel.: 02 569 6902

Spain
Tel.: (93) 201 4411

Sweden
Tel.: 08 98 8150

Switzerland
Tel.: 042 65 4242

Taiwan
Tel.: (02) 736 7125

Thailand
see Singapore

Turkey
Tel.: 1 349 8176, -77, -78, -79

United Kingdom
Tel.: Lewes 0273 480 444

USA
Tel.: 800 262 1640

Peace of Mind

At the watering hole, even rhinos and lions defer to the African elephant — secure in its extended family group. Unparalleled loyalty and powerful communal defense provide this gentle creature with a peace of mind shared by few inhabitants of the African savannah.

Boehringer Mannheim has been scanning the forefront of PCR research to make better PCR a reality. Our newest innovation combines recent research findings with 42 years of enzyme purification experience. The result is the Expand™ PCR System* — with powerful proofreading, and unparalleled yield — you'll enjoy PCR peace of mind shared only by other Expand users.

Simply better PCR

The graph says it all. The Expand PCR System delivers greater fidelity and higher yields, amplifying genomic DNA fragments of up to 27 kb – up to 40 kb for λDNA. This unique enzyme blend combines the high processivity of our *Taq* DNA polymerase* with the proofreading accuracy of our exclusive *Pwo* DNA polymerase*.

Expand now

Achieve peace of mind by relying on Boehringer Mannheim for all your PCR needs. Contact your local representative for more information.

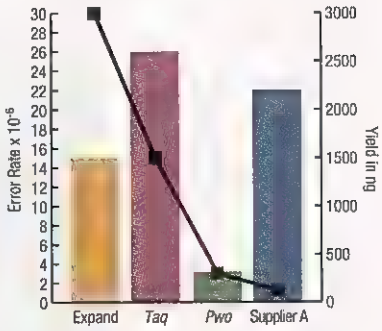

Comparison of error rates (bar graph) and yields (line graph) obtained with the Expand Long Template PCR System and three thermostable polymerases. Expand Long Template PCR System, *Taq* DNA polymerase, *Pwo* DNA polymerase, and a well-known "proofreading" enzyme from Supplier A were each used to amplify a 3.5 kb pUC18Q17 fragment. A lacI-based PCR fidelity assay was utilized to determine error rates. Briefly, the resulting PCR products were cloned and plated. The colonies were then screened, and the error rate per base pair determined according to methodology described by Barnes, W.M., P.N.A.S. 91:2216-2220 (1994). Amount of template DNA: 5 ng for Expand and *Taq*, and 10 ng for *Pwo* and the "proofreading" enzyme from Supplier A.

Expand™ is a trademark of Boehringer Mannheim.

*These products are sold under licensing arrangements with Roche Molecular Systems and The Perkin-Elmer Corporation. Purchase of these products is accompanied by a license to use them in the Polymerase Chain Reaction (PCR) process in conjunction with an Authorized Thermal Cycler.

© 1995 Boehringer Mannheim. All Rights Reserved.

mannheim boehringer *Biochemicals*

Twenty Years After Molecular Biologists Invented Haystacks, Someone's Finally Figured Out How To Find The Needles.

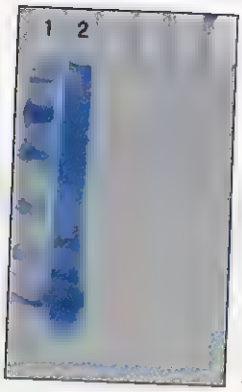

Crude cytokine prep.
Lane 1: MW markers.
Lane 2: Crude.

You know it's in there.
Somewhere in that liter of crude extract, there's a few µg of your recombinant protein, if you're lucky.

It took you a year and a half to get this far. The important research won't happen until you purify the active protein. You've made several attempts with conventional chromatography columns and instruments and still don't have a clean molecule to work with.

Is it the pH? the gradient? the loading? the surface chemistry? the...
You're in uncharted territory. There's no way to know which variable holds the key, and you don't have the luxury to test them all. Time is running out.

There has to be a more rational approach to purification.
There is. It starts by using POROS® Perfusion Chromatography® media and one of our automated systems, like the BioCAD™ Workstation.

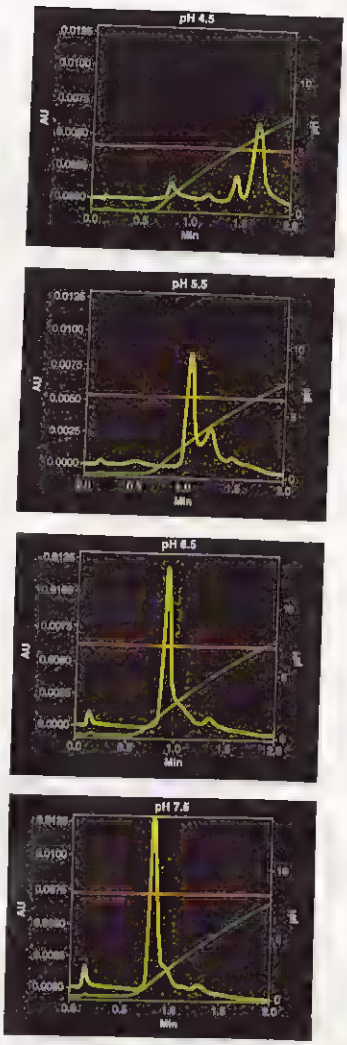

Initial pH mapping experiment of crude cytokine prep on POROS 20 HS cation exchange. Optimization of key separation variables including pH, gradient, loading, and flow rate can be completed in minutes.

At one to three minutes per run, you are able to explore more variables (pH, buffers, column chemistries...) than you've ever considered possible. By the end of the day you've generated all the data you need for an optimal method. Then you run a final gel.

There it is!
A nice, clean, biologically active protein. You're back on track, and ready to pursue the true objectives of your work.

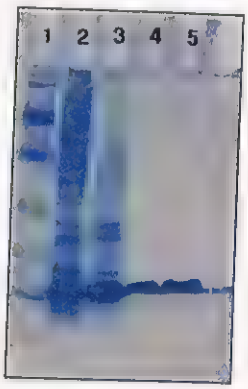

Lane 1: MW markers.
Lane 2: Crude
Lane 3: Pooled fractions after initial cation exchange step.
Lanes 4 & 5: Purified cytokine after second purification step with POROS 20 PH hydrophobic interaction column.

Accelerate your research with PerSeptive.
Complete your purification projects in days, not weeks or months. Join the thousands of researchers who have discovered PerSeptive Biosystems' broad selection of enabling tools, for every molecule and budget. Call PerSeptive Biosystems today toll-free: **1-800-899-5858.**

BioCAD/SPRINT™

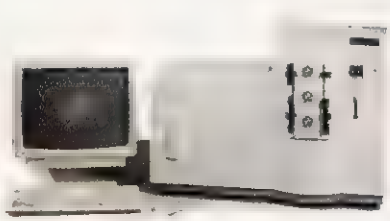

BioCAD™ Workstation

ConSep™

POROS® Columns and Media

PerSeptive Biosystems
Bioseparations Products

38 Sidney Street, Cambridge, MA 02139 (617) 621-1787
Germany Tel: +49 761 452 240 • Japan Tel: +81 353 89 7371
France Tel: +33 1 42 05 40 81 • U.K. Tel: +44 0895 810 289

Perfusion Chromatography and POROS are registered trademarks of PerSeptive Biosystems. BioCAD, BioCAD/SPRINT, Self Pack and ConSep are trademarks of PerSeptive Biosystems
Perfusion Chromatography and POROS perfusive media are protected by US patents 5,019,270 5,228,989 and 5,030,352
Molecular image courtesy of J. Taner G. Borgstahl and H. Parge, Metallocorrhizin Structure and Design Group, the Scripps Research Institute
© 1994 PerSeptive Biosystems

Circle No. 47 on Readers' Service Card

NEW OLIGO 1000 MULTI: A SYNTHESIS OF SPEED, CONVENIENCE AND ECONOMY

Now you can acquire high-quality oligonucleotides quickly, conveniently and affordably, with the new Oligo 1000M DNA Synthesizer from Beckman. The 1000M is ideal for groups of scientists with individual needs, as well as for individuals with high-volume requirements.

FASTER

Produce a research-ready primer in about one hour. Two-minute cycles and ten-minute cleavage and deprotection make it possible.

MORE CONVENIENT

Make oligonucleotides easily available to anyone in your lab, with no dedicated operator required. Eight independent column positions and automatic synthesis monitors allow continuous operation.

MORE AFFORDABLE

Acquire DNA at a cost-per-base at least half that advertised by commercial suppliers. The 1000M gives you a broad range of capabilities on an eight-column synthesizer — at the cost of a conventional two-column system.

THE BECKMAN PLUS

With the Oligo 1000M you get the science, support and solutions from Beckman that you need to help you in your DNA research. Call your local Beckman representative today for *free* information about how you can get a synthesis of speed, convenience and economy for your laboratory.

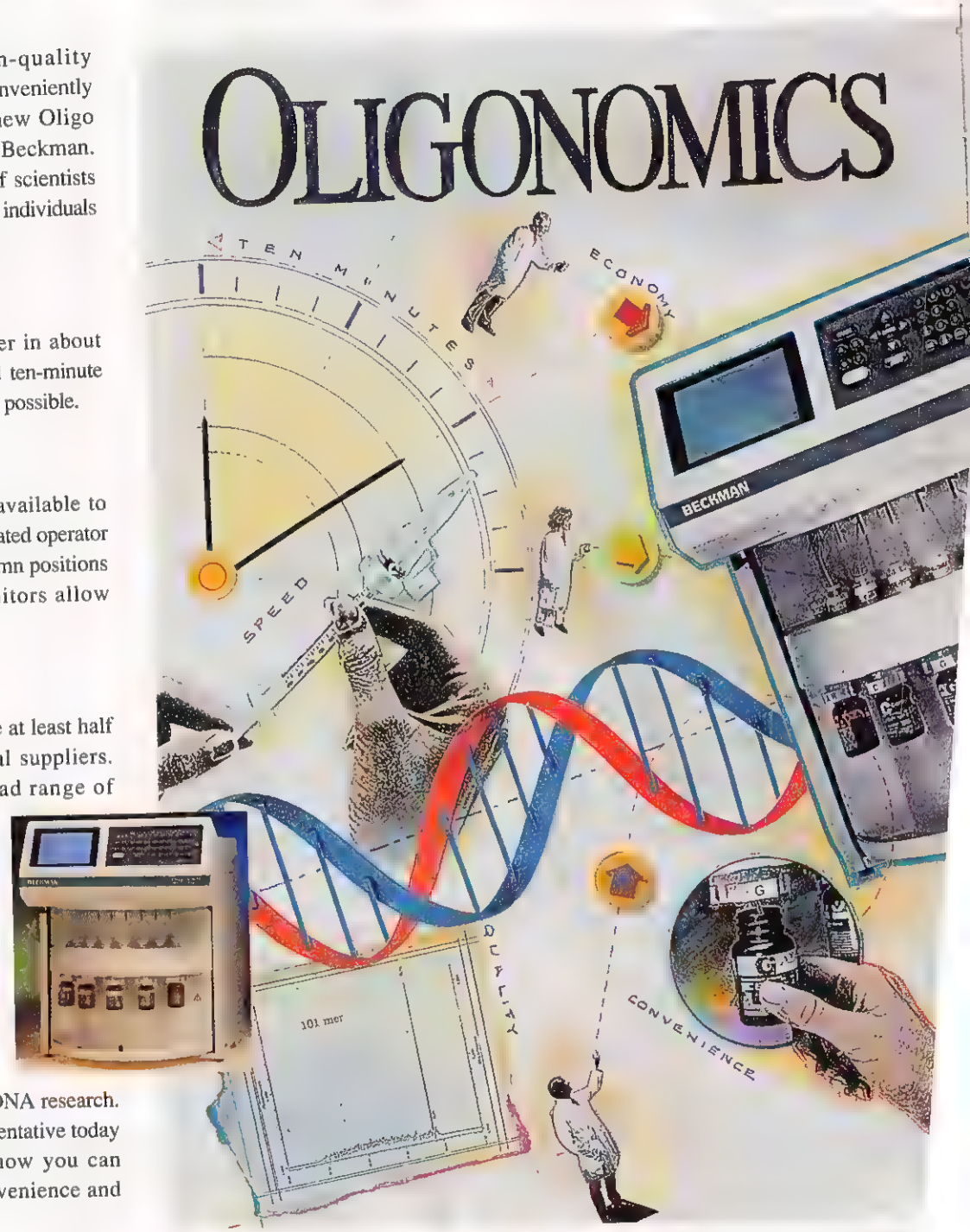

BECKMAN

Worldwide Offices: Africa, Middle East, Eastern Europe (Switzerland) (22) 994 07 07. **Australia** (61) 02 816-5288. **Austria** (2243) 7292164. **Canada** (800) 387-6799. **China** (861) 5051241-2. **France** (33) 1 43 01 70 00. **Germany** (49) 89-38871. **Hong Kong** (852) 814 7431. **Italy** (39) 2-953921. **Japan** 3-3221-5831. **Mexico** 525 575 5200, 525 575 3511. **Netherlands** 02979-85651. **Poland** 40882, 408833. **Singapore** (65) 339 3633. **South Africa** (27) 11-805-2014/5. **Spain** (1) 358-0051. **Sweden** (8) 98-5320. **Switzerland** (22) 994 07 07. **Taiwan** (886) 02 378-3456. **U.K.** (01494) **U.S.A.** 1-800-742-2345.

©1995 Beckman Instruments, Inc.

Circle No. 29 on Readers' Service Card

New E-Z Hold™ Plastic Bottle for Gibco BRL Media, Sera, & Reagents

E-Z to Hold, Hard to Break.

Specially Designed for Cell Culture
E-Z Hold Bottles are **easy** to use with no-drip spout, wide mouth design, and visible graduations. Overall round shape allows **easy** swirling. Patented* cap is **easy** to hold while performing aseptic procedures.

Room for Supplementation
Extra headspace for **easy** supplementation of at least 20% over normal fill volumes.

No-Slip Grip
Flat sides make these bottles **easy** to hold, even when handling wet bottles while wearing gloves.

Gibco BRL Quality
It's **easy** to see that the best thing about the E-Z Hold Bottles is what comes in them: time-tested Gibco BRL media, sera, and reagents. Extensive testing has proven that you can count on E-Z Hold Bottles to protect these quality products.

For more information, please call our Tech-Line℠ at (800) 828-6686, ext. 6890.

Virtually Unbreakable
It's **easy** to be safe with E-Z Hold Bottles made from tough, yet lightweight, polyethylene terephthalate (PET) plastic. And, PET plastic is the most recycled plastic in the world.

LIFE TECHNOLOGIES™

Producer of Gibco BRL Products

U.S.A. Orders
Facsimile: (800) 331-2286
To Order/Tech-Line: (800) 828-6686

Latin America Orders
To Order/Tech-Line: (301) 840-4027
Facsimile: (301) 258-8238

Canada Orders
To Order: (905) 335-2255
Tech-Line: (800) 757-8257
Facsimile: (800) 387-1007

E-Z Hold™, Tech-Line℠, and the Life Technologies logo are marks of Life Technologies, Inc.

94-110

* Patent No. 5,246,127

Circle No. 69 on Readers' Service Card

POWER PCR

TaKaRa LA PCR Kit *for The Ultimate Exploration of the Human Genome*

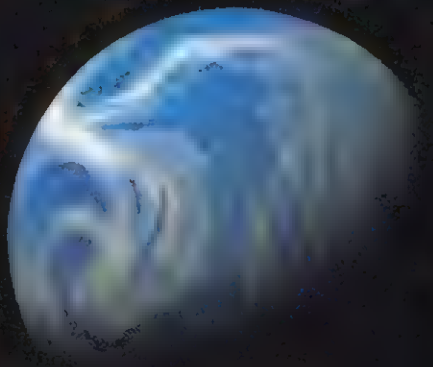

TaKaRa LA PCR Kit (Code No. RR011) is proven for premium performance: Long and Accurate PCR with greater fidelity and higher yields.

Amplification of Genomic DNA Fragments

Human genomic DNA fragments in various lengths were efficiently amplified with this LA PCR Kit.

Lane 1	λDNA/*Hind* III marker	
Lane 2	Mitochondria	16.3 kb
Lane 3	β-globin cluster	16.5 kb
Lane 4	β-globin cluster	17.5 kb
Lane 5	β-globin cluster	21.5 kb
Lane 6	β-globin cluster	22.5 kb
Lane 7	High MW marker	

Available Soon: LA PCR *in vitro* Cloning Kit and LA PCR *in vitro* Mutagenesis Kit

TaKaRa BIOMEDICALS

TAKARA SHUZO CO., LTD.
Biomedical Group
Otsu, Shiga, Japan
Tel: +81 775-43-7247
Fax: +81 775-43-9254

DISTRIBUTORS *for More Information and Orders:*

PanVera Corporation (USA and South America)
Tel: 608-233-5050 Fax: 608-233-3007
Toll Free: 1-(800) 791-1400

ITC Biotechnology GmbH (Germany)
Tel (06221) 303907 Fax (06221) 303511

Cheng Chin Trading Co., Ltd (Taiwan)
Tel: (02) 331-3111 Fax. (02) 382-2197

Protech Technology Enterprise Co., Ltd. (Taiwan)
Tel: (02) 381-0844 Fax: (02) 311-8524

POWER PCR products from **TaKaRa** are sold under licensing arrangements with Roche Molecular Systems and F. Hoffman -La Roche Ltd. and The Perkin-Elmer Corporation Purchase of these products is accompanied by a licence to use them in the Polymerase Chain Reaction (PCR) process in conjunction with an Authorized Thermal Cycler.

Circle No. 11 on Readers' Service Card

Substantial journals...

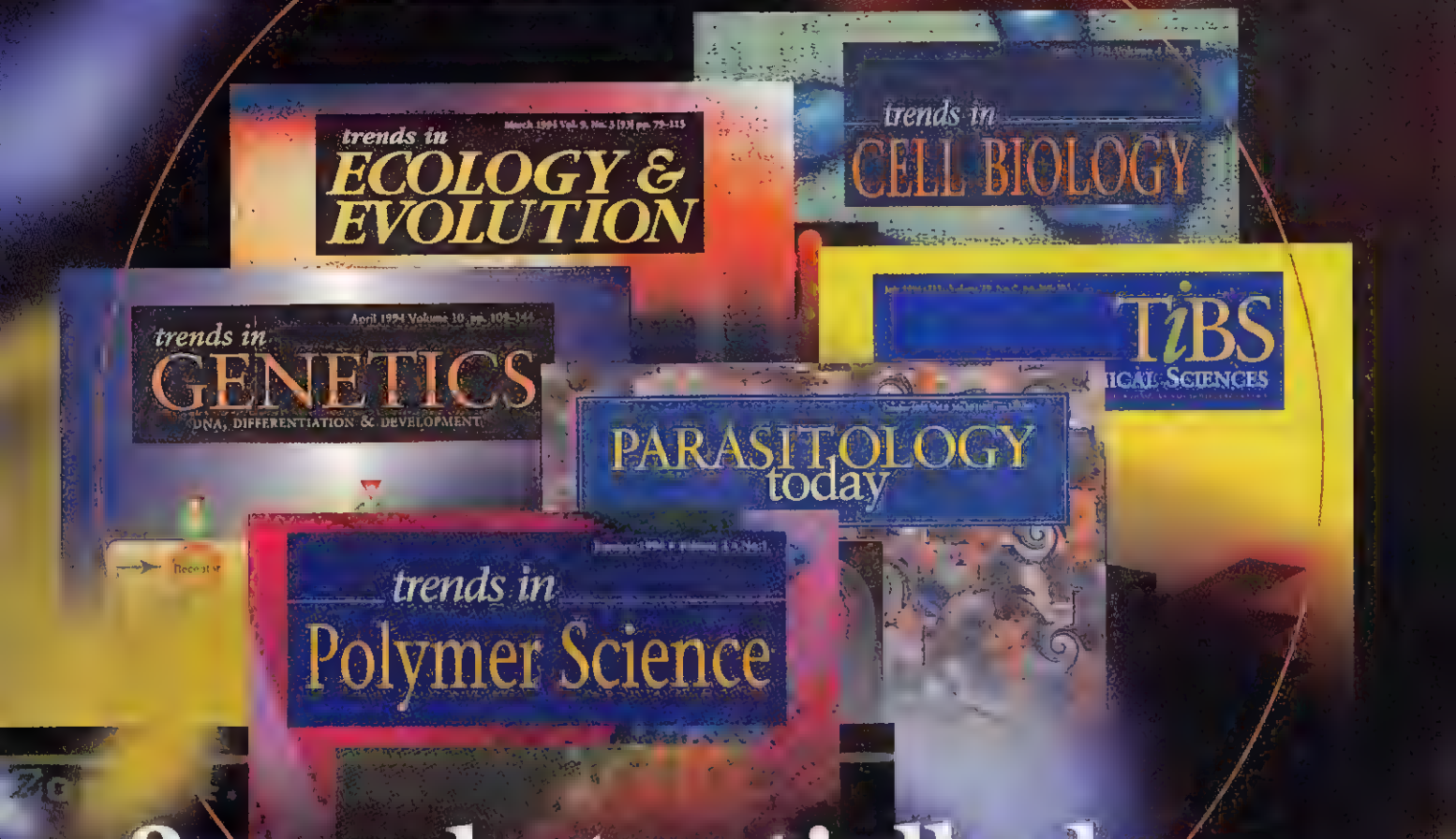

for substantially less.

For a limited period only, Elsevier Trends Journals is offering a substantial saving on the cost of one year's subscription to some of our most respected titles. We've reduced the price from $115 to $99 a year. Make the most of it, fill in the coupon right away.

Offer ends 31 July '95

One year's subscription to any one journal for only

$99

Orders must be postmarked by 31 July 1995

TA5A13

YES I must subscribe at the special personal subscription price of $99 to:

☐ Parasitology Today ☐ Trends in Biochemical Sciences ☐ Trends in Cell Biology
☐ Trends in Ecology & Evolution ☐ Trends in Genetics ☐ Trends in Polymer Science

12 monthly issues beginning _____ (enter month in 1995)

Payment Details

☐ CHEQUE made payable to 'ELSEVIER'

☐ CREDIT CARD ☐ Visa ☐ Mastercard ☐ Am Exp

Card No. _____

Exp Date _____ Total Payment _____

Signature _____

☐ Please send a sample copy of _____

Address Details

Name _____

Position _____

Address _____

_____

_____ Zip Code _____

Country _____

Tel _____ Fax _____

☐ Please do not send me information from other organisations

Please return this form to: Elsevier Trends Journals, 660 White Plains Road, Tarrytown, NY 10591-5153, US
Tel: +1 (914) 524 9200 Fax: +1 (914) 333 2444

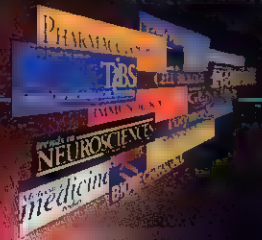

ELSEVIER TRENDS JOURNALS

Rapid access to the cutting edge of science

ELSEVIER TRENDS JOURNALS

Circle No. 65 on Readers' Service Card

INTRODUCING

Green-Pak®

NEW!

environmentally-friendly pipette tip-rack refills

At last, a practical way to reload tip racks!

Now you can refill Rainin's 96-place tip racks quickly and easily in your own laboratory, and dramatically reduce plastic waste... all with one convenient new product. Rainin's Green-Pak refills are available with a wide range of tips for 2 µL to 250 µL pipettes including standard, presterilized, and presterilized filter tips. Using Green-Pak is as easy as 1–2–3...

1 **Turn refill upside down. Peel away paper lid. Hands never touch tips.**

2 **Place over empty racks. Refills align perfectly each and every time.**

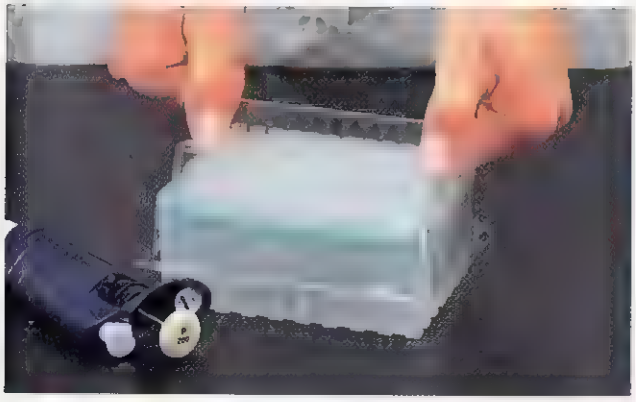

3 **Press down firmly with thumbs to release tips. Tips snap into place.**

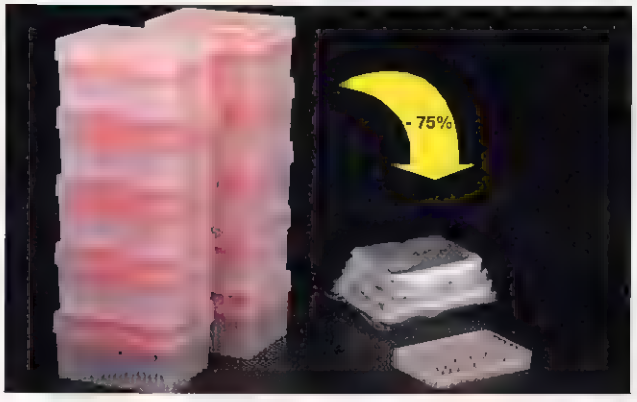

Look at the reduction in plastic waste! Reuse the racks. Recycle the shells.

GP-10	Green-Pak Standard, for volumes to 10 µL. Ten sealed refills containing 960 tips.	$45.50
GP-10S	Same as above, Presterilized.	55.50
GP-96	Green-Pak Standard, for volumes to 250 µL. Ten sealed refills containing 960 tips.	39.50
GP-96S	Same as above, Presterilized.	49.50
GP-10F3	Green-Pak FilterPro™ for volumes to 8 µL. Ten sealed refills containing 960 presterilized tips.	$79.50
GP-96F1	Green-Pak FilterPro for volumes to 30 µL. Ten sealed refills containing 960 presterilized tips.	79.50
GP-96F4	Green-Pak FilterPro for volumes to 200 µL. Ten sealed refills containing 960 presterilized tips.	79.50

RAININ INSTRUMENT CO., INC.

To order, call 800-4-RAININ

Patents Pending. Prices and specifications subject to change without notice. © 1995 Green-Pak and FilterPro are trademarks of Rainin Instrument Co.

Mack Road · Box 4026, Woburn, MA 01888-4026 · 617-935-3050
5400 Hollis Street, Emeryville, CA 94608-2508 · 510-654-9142

Circle No. 50 on Readers' Service Card

PulseTrac

With PulseTrac Delivery the Gene Pulser® II System offers Unprecedented Electroporation Performance

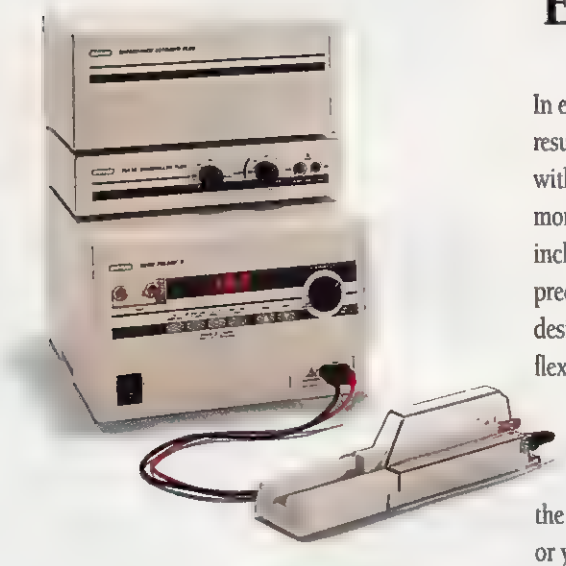

In electroporation, precise pulse delivery is essential for reproducible results. The Gene Pulser II system provides maximum reproducibility with PulseTrac, an exclusive pulse delivery feature. PulseTrac monitors and compensates for subtle variations in the pulse circuit, including minute sample-to-sample differences, for unparalleled precision. The Gene Pulser II system retains the proven modular design of the original Gene Pulser system. This ensures maximum flexibility and accommodates future upgrades. Each module provides the greatest power and range of appropriate settings for optimizing a specific application. The result is unprecedented electroporation performance. To find out how PulseTrac and the Gene Pulser II system can deliver for you, call 1-800-4BIORAD or your local Bio-Rad representative today.

BIO-RAD **Bio-Rad Laboratories**

Life Science Group

(US) (800) 4BIORAD • (AU) 02-805-5000 • (AT) (1)-877 89 01 • (BE) 09-385 55 11 • (CA) (905) 712-2771 • (CN) (01) 2051873 • (FR) (1) 49 60 68 34 • (DE) 089 31884 0 • (IT) 02-21609 1 • (JP) 03-3534-7665 • (HK) 7893300 • (NL) 08385-40666 • (NZ) 09-443 3099 • (SG) (65) 443 2529 • (ES) (91) 661 70 85 • (SE) 46 (0) 8 735 83 00 • (CH) 01-810 16 77 • (GB) 0800 181134

SIG 071494

Circle No. 34 on Readers' Service Card

Advanced Ergonomy and Accessibility

DAS Mikroskop LEICA DM IRB/E is an inverted research microscope that will impress even the perfectionist. Accessibility is excellent, even when several different peripherals are adapted simultaneously. **So you can fully use all the accessories you need without sacrificing operational convenience.**

As you'd expect, the thoroughly modular system design ensures easy upgrading for individual contrast requirements such as phase/interference contrast or fluorescence. It also allows extensive image documentation solutions and features an integrated interface for the ***LEICA TCS 4D*** Confocal Module.

There are two models to choose from:

- ***conventional focus and objective change or***
- ***electronic focus and motorized objective change***

As you'll see, the age of comfort for inverted microscope users has arrived at last!

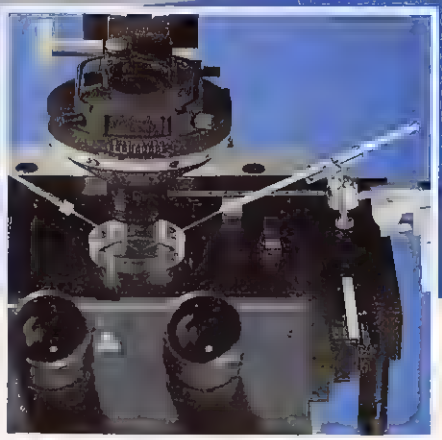

Leica Mikroskopie und Systeme GmbH
P.O. Box 2040
D-35530 Wetzlar
Tel.: 0 64 41/29-0
Fax: 0 64 41/29 33 99

Leica

Circle No. 70 on Readers' Service Card

Floyd Bloom: The Next Editor-in-Chief of *Science*

Richard A. Lerner and Roger Guillemin

On 1 May 1995, Floyd Bloom will replace Dan Koshland as the editor-in-chief of *Science*. This is a bittersweet event. We lose a man who has guided the journal through what has been a very successful and visionary decade. However, we are fortunate now to have as the new editor another scientist and administrator of extraordinary abilities.

The main credential that Floyd Bloom brings to the editorship is his quality as a scientist. Bloom's entry into science had a rather inauspicious beginning in that it did not begin with the usual chemistry set in the basement. His aptitude test in high school revealed that he should be in journalism, publishing, or advertising, and that he should definitely stay away from the hard sciences. So he went home and told this to his father, who basically said that was all well and good but that the first thing Floyd had to do was to graduate from medical school and after that he could do anything he wanted to. This parental guidance was not altogether unexpected by the young Bloom because he grew up working in his father's drug store in Minneapolis and thus was already oriented toward doctors and medications. In reality he had no great desire to become a doctor, but he did desire to fulfill his father's wishes. So, in 1954 he was off to pre-med studies at Southern Methodist University, where his teachers soon found that he was talented in both inorganic and organic chemistry.

Accordingly, the professor of organic chemistry, Harold Jesky, became Floyd's champion and was able to introduce him to the traveling registrar who interviewed prospective students for Washington University Medical School in St. Louis. Because of his success in chemistry, Floyd obtained interviews and was accepted into medical school. However, he still showed no flair for research and wanted to be an obstetrician. Given the Floyd Bloom that we know today, we would expect him to do well in all his courses, but that was not quite the case. At that time Washington University did not give grades; performance was ranked as upper, middle, or lower. Floyd received uppers in everything except physiology, where his curiosity may have interfered with his class achievement because he had become wrapped up in what was going on at that time concerning ions and the transmission of nerve impulses. Nevertheless, his teacher in physiology, Gordon Schoepfle, sensing that there was much to the young Bloom, invited him to come to his laboratory for the summer on a National Institutes of Health student fellowship. In the process of working with his own hands, Floyd began to get an appreciation for science and eventually was to produce a thesis under the direction of Oliver Lowry on the kinetics of the procaine effect on single frog axons, a study combining physiology and pharmacology. After graduation, he did an internship and a year of residency in medicine at Barnes Hospital in St. Louis and then, on the basis of his student research, was accepted as a research associate at the National Institute of Mental Health (NIMH) St. Elizabeth's Hospital Clinical Neuropharmacology Research Center. This research project was his first encounter with brain research, which soon became his passion and remains so even now.

It was an exciting time at NIMH in the early 1960s, and Bloom was carrying out ground-breaking studies on the mechanism of the antihypertensive effects of the then important drug reserpine. Although it may seem obvious today, 30 years ago it was quite puzzling as to how a drug that works in the brain could have effects on peripheral vascular resistance. It turned out that the effects of reserpine were mediated through brain norepinephrine and serotonin, but there was little knowledge of the way that these and other small molecules controlled brain functions. These studies led to Bloom's first article under the modest title, "The Pharmacology of Individual Neurons" (*1*). After 2 years at NIMH, Bloom received a fellowship to work with Russell Barrnett in the Department of Anatomy at Yale University, where they devised cytochemical methods to localize acetylcholinesterase, at the electron microscopic level, in the electroplaque of the electric eel (*2*). These early studies were the first in which structural techniques were used to obtain quantitative information about neurotransmitters in the brain. Already at this time, it was possible to pick up the lifelong theme of Bloom's research, which was aimed at understanding the chemical basis by which the anatomical connections in the brain function.

After 4 years at Yale, Floyd returned to NIMH in 1968, where he was appointed chief of the laboratory of neuropharmacology at St. Elizabeth's Hospital. Together with George Siggins, who was his first postdoc

R. A. Lerner is in the Departments of Chemistry and Molecular Biology, Scripps Research Institute, 10666 North Torrey Pines Road, La Jolla, CA 92037, USA. R. Guillemin is Distinguished Scientist, Whittier Institute for Diabetes and Endocrinology, La Jolla, CA 92037, USA and an adjunct professor in the Department of Reproductive Medicine at the University of California, San Diego, La Jolla, CA 92037, USA.

toral fellow (and is still with him), and Barry Hoffer, who had done his thesis at Rochester on the developing cerebellum, he carried out the now classical studies on the locus ceruleus and the norepinephrine-containing afferents to the rat cerebellum (3). These studies, which began in the late 1960s and continued through the early 1970s, represent a milestone in mapping out chemical pathways in the brain.

In 1975 Bloom and his group moved to the Salk Institute in La Jolla, where he became the director of the Arthur V. Davis Center for Behavioral Neurobiology. While waiting for his laboratory to be completed, Floyd and his senior staff were offered a share of the very limited laboratory space in the Guillemin laboratory. These were the days of the exploding discoveries of the small polypeptides isolated and characterized throughout the central nervous system. Floyd's expertise in immunocytochemistry was immediately of great use and led to the observation that the distribution of the enkephalins and that of the endorphins were so different throughout the brain that the peptides, even though they shared common amino acid sequences, had to come from different precursors (4). Neurons containing β-endorphin in rat brain exist separately from those containing enkephalins. These studies were amply confirmed and proved by the subsequent cloning studies of Numa and Nakanishi and Goldstein and their colleagues (5). Floyd's work also demonstrated in vivo that stress stimulates concomitant secretion of adrenocorticotropic hormone and β-endorphin. While at Salk, Floyd initiated several ambitious research programs in neuropsychopharmacology, investigating with George Koob (who also is still with him) the behavioral effects of these novel neuropeptides and the mechanisms of addictive behavior to alcohol.

At the Scripps Research Institute since 1983, where he is now the chairman of the Department of Neuropharmacology, Floyd began, with Greg Sutcliffe, to use the techniques of molecular biology to study brain proteins and processes (6). Making more and more use of all tools of molecular biology, Bloom has increasingly turned his attention to the present-day complex problems of human neurophysiology and neuropathology, including drug addiction, the chemical basis of alcoholism, and the dementia associated with HIV infection (7). He and his group have recently made the proposal that the nucleus accumbens seems to be the only locus associated with critical reinforcement, as well as adaptation to continuous exposure to any addictive drug, each of these making use of different neuromediators or receptors on the same population of neurons (8).

Bloom brings many personal qualities and attitudes to the journal and these will ensure his success as an editor. He is a man of extraordinary goodwill, with a passion to support all that is good about the scientific enterprise. Those who know him well often remark about the energy that he is willing to expend in the service of science, whether it be on a committee of the National Academy of Sciences or in a speech to a group of young students who are contemplating a career in science. He is a compelling speaker with a remarkable ability to communicate scientific results to experts and layman alike. He is fair. This is not to say that he is a pushover but, rather, that he bases his decisions on evidence rather than prejudice. He is not only encyclopedic in his own field but also current on a wide range of concepts and results in areas quite distant from neuroscience. Perhaps this stems from his belief in an interdisciplinary approach to scientific issues. There is, therefore, no need to worry that this or that field will not fare well in the journal because Bloom does not appreciate the area. His tastes are varied. He is interested in ideas and not the stature of the individual or the discipline whence they come. Bloom's people skills are legendary. Once into the Bloom orbit, one remains there whether as a friend, colleague, or collaborator. The main reason for this is that he gives at least as much as he gets to any scientific relationship and one remains secure because of his overriding sense of fairness. Finally, he has the all too rare trait that he honors his commitments and more than keeps his part of the bargain. The contributors to *Science* can be sure that if he says he is going to look into a matter or think about their paper it will be done. The outcome may not be what was wished for but the judgment will be reasoned.

The younger members of the scientific community should rejoice in the Bloom appointment. He has often remarked that he feels obligated to ensure their well being. But his interest in the young goes beyond the obvious issue that they will inherit the enterprise. They have hope and energy and reflect his own boundless enthusiasm.

As befits a scientist of Bloom's stature, he has received many honors and awards. He was elected to the National Academy of Sciences in 1977, served as chairman of the Neurobiology Section of the Academy from 1979–1983 and 1985–86, and was Secretary of Class II from 1986–1989. He received the degree of Doctor of Science, honoris causae, from Hahnemann University, Philadelphia, in 1985 and the University of Rochester, New York, in 1985. He served on the Board of Directors of the American Association for the Advancement of Science, from 1985–1989, the Science Advisory Board of the MacArthur Foundation from 1982–1992, the Science Advisory Board of the DuPont Corporation from 1983–1990, and the Science Advisory Board of the Massachusetts General Hospital from 1984– 1988. In 1989 he was elected a foreign Member of the Royal Swedish Academy of Sciences. He received both the Janssen Award in the Basic Sciences and the Pasarow Award in Neuropsychiatry in 1989. He is also a member of the National Academy of Medicine.

Bloom has been married since 1980 to Jody P. Corey, whom he had met 2 years earlier at a meeting of the Society for General Physiology at Woods Hole, Massachusetts. Already with a Ph.D. in neuroanatomy at that time, Jody went to medical school at the University of California, Irvine, and then to the University of California, San Diego (UCSD) and graduated from UCSD in 1986. She is now an assistant professor of neurosciences at UCSD and is chief of Outpatient Neurology of the UCSD Perlman Clinic. Floyd has two children, a daughter, Fl'nell, 33, and a son, Evan, 31. Fl'nell is a schoolteacher in Hawaii and has two sons. Evan is a photographer in San Diego.

At the Scripps Research Institute, Bloom now leads a department of 30 faculty members and more than 100 postdoctoral fellows and graduate students in 50,000 square feet of laboratory space devoted to that new type of neuropharmacology that started when he and his colleagues began to characterize genes specifically expressed in the brain. This has led to a multicenter international effort at brain mapping for all known brain-specific messages, or gene products; it is currently funded by NIH, the National Aeronautics and Space Administration, the U.S. Navy, and the European Community Human Science Frontier Program.

Like all successful scientists, Floyd Bloom is able to identify the basic principles at issue and to design and pursue experiments with the aim of using the knowledge to solve critical problems.

REFERENCES

1. G. C. Salmoiraghi and F. E. Bloom, *Science* **144**, 493 (1964).
2. F. E. Bloom and R. J. Barrnett, *J. Cell Biol.* **29**, 475 (1966).
3. G. R. Siggins, B. J. Hoffer, F. E. Bloom, *Science* **165**, 1018 (1969).
4. F. E. Bloom, E. Battenberg, J. Rossier, N. Ling, R. Guillemin, *Proc. Natl. Acad. Sci. U.S.A.* **75**, 1591 (1978).
5. S. Nakanishi, A. Inoue, T. Kita, M. Nakamura, A. C. Chang, S. N. Cohen, S. Numa, *Nature* **278**, 423 (1979); O. Civelli, J. Douglass, A. Goldstein, E. Herbert, *Proc. Natl. Acad. Sci. U.S.A.* **82**, 4291 (1985).
6. J. G. Sutcliffe, R. J. Milner, T. M. Schinnick, F. E. Bloom, *Cell* **33**, 671 (1983); F. H. Burton, K. W. Hasel, F. E. Bloom, J. G. Sutcliffe, *Nature* **350**, 74 (1991).
7. A. V. Moses, F. E. Bloom, C. D. Pauza, J. A. Nelson, *Proc. Natl. Acad. U.S.A.* **90**, 10474 (1993); P. P. Sanna, D. P. Folsom, M. J. Banzo, K. R. Milia, D. Maciejewski-Lenoir, F. E. Bloom, *Mol. Brain Res.* **19**, 241 (1993); F. Weiss, M. T. Lorang, F. E Bloom, G. F. Koob, *J. Pharmacol. Exp. Therap* **267**, 250 (1993); T. T. Yang *et al.*, *Nature* **368**, 3 (1994).
8. G. F. Koob and F. E. Bloom, *Science* **242**, 715 (1989).

Targeting Retroviral Integration

Frederic Bushman

Retroviral vectors are currently the most widely used method of gene transfer in gene therapy, in part because the retroviral integration system precisely links the therapeutic sequences to the host chromosome with neat covalent bonds. DNA integration, however, comes with a price. Retroviral integration systems show little target site specificity, and haphazard insertions into a patient's chromosomes can create problems. Integration near cellular proto-oncogenes may lead to ectopic gene activation and cancer, not a desirable outcome of gene therapy (*1*). Retroviral integration can also inactivate genes (*2*). Recent findings on site-specific DNA integration by retroviruses and retrotransposons suggest a strategy for retrovirus-based gene therapy that avoids such insertional mutagenesis: Tethering the integration machinery to a specific target sequence can control the location of DNA integration, potentially making it possible to direct integration of therapeutic sequences to innocuous chromosomal sites.

In a report on page 1488 of this week's *Science*, Kirchner and co-workers begin to define the molecular elements necessary for integration of the retrovirus-like Ty retrotransposons of yeast cells which, unlike the retroviruses, are highly selective in their choice of integration sites. The Ty genome is transcribed, reverse transcribed, and integrated all within a single cell by reverse transcriptase and integrase enzymes homologous to their retroviral counterparts. This mode of growth imposes unique constraints. Because yeast cells are often haploid, a retrotransposition event that disrupts a required cellular gene can mean suicide for both the Ty element and the host. Probably for this reason, the Ty elements display extreme biases in target site selection. Ty3 tends to integrate strictly into the five base pairs at the start site of transcription of polymerase (Pol) III–transcribed genes (*3*). Ty1 also usually integrates upstream of Pol III–transcription units, but over a region of several hundred base pairs (*4*). At first this may seem like an odd choice of integration sites, but the Ty insertions have very little effect on transcription, probably because the recognition sites for the sequence-specific Pol III factors TFIIIB and TFIIIC lie within the transcribed region.

How do the Ty elements select these innocuous target sites from the background of total genomic DNA? Previously, Sandmeyer and co-workers have shown in vivo that intact DNA sites for the transcription factors TFIIIB and TFIIIC were necessary for selective integration of Ty3 (*3*). In the new work, this group has established an in vitro system that recapitulates selective Ty3 integration (*5*). Ty3 viruslike particles from yeast cells induced to express Ty3 can direct selective integration in vitro when presented with integration targets containing assembled Pol III transcription units. Only those fractions containing TFIIIB and TFIIIC, but not RNA Pol III, are necessary for selective integration, indicating that bound factors and not transcription itself are required.

The current models for the mechanism of integration invoke tethering of the Ty3 integration machinery to the target DNA by protein-protein contacts with the Pol III transcription apparatus (see figure). Such a model fits neatly with ideas from the site-specific recombination field. Many site-specific recombination enzymes are composed of two domains, one that directs sequence-specific DNA binding at the recombination site and a second domain that catalyzes DNA breaking and joining. In Ty3, the two functions are apparently contributed by different proteins, a point that may soon be confirmed with the new in vitro system.

The mechanism of integration in yeast cells may be quite similar to that in retroviruses, and tethering may also be involved in normal integration of human immunodeficiency virus (HIV) DNA. In a recent report published in *Science*, Kalpana and co-workers used the popular yeast two-hybrid system to identify a protein that binds to the HIV-1 integrase protein (*6*), the viral-encoded enzyme responsible for forming the initial covalent connection between viral DNA and target DNA. Binding of this protein, Ini1 (integrase interacting protein), to integrase was specific both in vivo and in vitro. The Ini1 protein also bound DNA, and in integration reactions in vitro containing purified integrase, Ini1 stimulated integration under certain conditions. This latter result must be interpreted with some caution, because nonspecific DNA-binding proteins can stimulate integration in vitro (*7*) and the new results do not yet confirm that Ini1 stimulates integration by tethering integrase to the target.

Nevertheless, the sequence of the Ini1 protein is consistent with an important role in vivo. Portions of Ini1 are up to 55% identical to yeast SNF5, a component of a multi-protein complex proposed to be involved in activation of gene expression (*8*). That the SNF5 complex can remodel chromatin so as to promote transcription factor

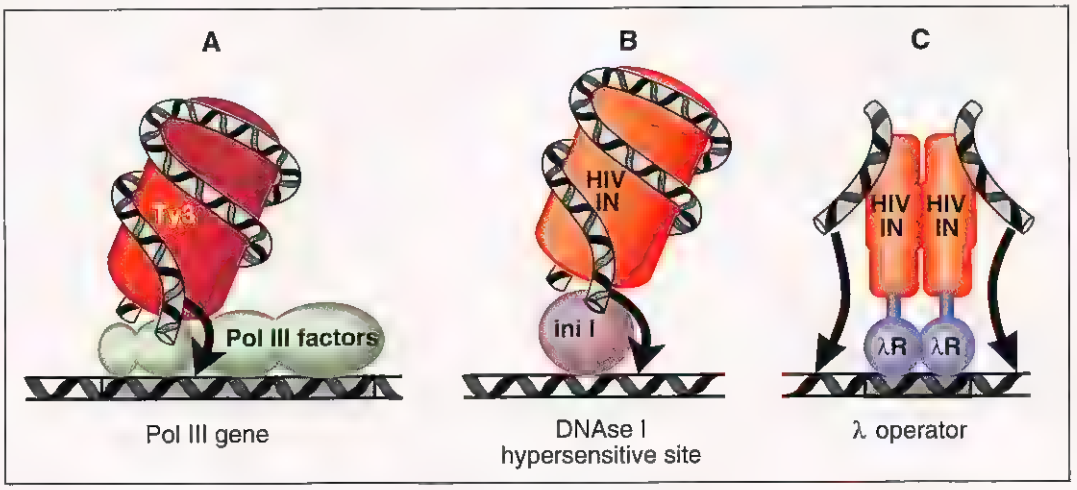

Models for selective integration by tethering. (**A**) An interaction between Pol III transcription factors and the Ty3 viruslike particle results in selective integration at the start site of transcription of Pol III genes. (**B**) An interaction between HIV-1 integrase and Ini1 may promote integration into DNA at DNAse I–hypersensitive sites. (**C**) A fusion of HIV-1 integrase to the DNA-binding domain of λ repressor promotes integration near λ operators in vitro. In the reactions in (C), the viral DNA end is modeled by a short oligonucleotide matching the sequence of one end of the unintegrated retroviral DNA. Heavy arrows indicate the covalent attachment of retrovirus or retroelement DNA to target DNA.

The author is in the Infectious Disease Laboratory, Salk Institute, 10010 North Torrey Pines Road, La Jolla, CA 92037, USA.

binding (9) fits with previous work indicating that retroviral integration acceptor sites tend to be enriched near deoxyribonuclease (DNAse) I–hypersensitive sites in chromatin. These findings support a model in which tethering of the HIV integration machinery to host DNA via a protein-protein interaction with Ini1 promotes integration in open chromatin.

Tethering can be exploited to control integration; tethering an integrase enzyme to a chosen target DNA can suffice to direct localized integration (*10*). HIV integrase was modified by fusion to a sequence-specific DNA-binding domain, that of phage λ repressor. The modified protein (λR-IN) was tested for integration site selection in reactions in vitro containing target DNAs with or without λ repressor binding sites. Integration by λR-IN was strongly favored in those target DNAs containing repressor binding sites, whereas wild-type integrase showed no such bias. Prebinding of λ repressor blocked selective integration, indicating that binding to the λ repressor sites was required. The λR-IN protein directed integration primarily to the same face of the B-DNA helix as the operators, as expected if the λR-IN protein bound to repressor sites captures target DNA by looping out the intervening sequences. These findings bolster the idea that tethering can be sufficient to direct selective integration and establish that specific binding can be engineered into an integrase without disruption of its function (at least under the conditions examined).

Can integration site selection by retroviruses be controlled in vivo by fusion of a sequence-specific DNA-binding domain to integrase? If so, then not only might therapeutic genes be integrated at innocuous chromosomal sites, but retroviral integration might be used to deliberately disrupt harmful sequences such as activated oncogenes or integrated viral genomes. It might even be possible to modify retroviruses to serve as attenuated retroviral vaccines by using integrase fusions to allay fears of insertional mutagenesis upon vaccination.

Whether fusions of integrase to sequence-specific DNA-binding domains can be used to meet these goals in practice remains to be seen. For this idea to work, high-titer stocks of these modified viruses or vector derivatives must be readily obtainable, discrimination between specific and nonspecific sites in vivo must be adequate, and useful binding specificities must be identified and built into integrase fusions. Although some of these hurdles may be difficult to leap, the fact that the Ty elements somehow manage to target integration encourages optimism for modified retroviruses.

References

1. B. Shiramizu, B. G. Herndier, M S. McGrath *Cancer Res* **54**, 2069 (1994)
2. J. M. Coffin, in *Virology*, B N. Fields and D M. Knipe, Eds (Raven, New York, 1990), vol. 2, pp. 1437–1500
3. D. L. Chalker and S B Sandmeyer, *Genes Dev.* **6**, 117 (1992).
4. H. Ji *et al.*, *Cell* **73**, 1 (1993)
5. J Kirchner, C. M. Connolly, S. B. Sandmeyer, *Science* **267**, 1488 (1995)
6. G. V. Kalpana, S. Marmon, W. Wang, G R Crabtree, S. P Goff, *ibid* **266**, 2002 (1994)
7. F. D. Bushman, T. Fujiwara, R Craigie, *ibid.* **249**, 1555 (1990)
8. M. Carlson and B. C. Laurent, *Curr Opin. Cell Biol* **6**, 396 (1994)
9. J. Côté, J. Quinn, J. L. Workman, C. L. Peterson, *Science* **265**, 53 (1994).
10. F. D. Bushman, *Proc. Natl Acad Sci. U.S.A.* **91**, 9233 (1994)

Mechanisms and Genes of Cellular Suicide

Hermann Steller

Apoptosis is a morphologically distinct form of programmed cell death that plays a major role during development, homeostasis, and in many diseases including cancer, acquired immunodeficiency syndrome, and neurodegenerative disorders. Apoptosis occurs through the activation of a cell-intrinsic suicide program. The basic machinery to carry out apoptosis appears to be present in essentially all mammalian cells at all times, but the activation of the suicide program is regulated by many different signals that originate from both the intracellular and the extracellular milieu. Genetic studies in the nematode *Caenorhabditis elegans* and in the fruit fly *Drosophila melanogaster* have led to the isolation of genes that are specifically required for the induction of programmed cell death. At least some components of the apoptotic program have been conserved among worms, insects, and vertebrates.

Most, if not all animal cells have the ability to self-destruct by activation of an intrinsic cell suicide program when they are no longer needed or have become seriously damaged. The execution of this death program is often associated with characteristic morphological and biochemical changes, and this form of cell death has been termed apoptosis (*1*). During apoptosis, the nucleus and the cytoplasm condense, and the dying cell often fragments into membrane-bound apoptotic bodies that are rapidly phagocytosed and digested by macrophages or by neighboring cells. In this way, dead cells are rapidly removed, and any leakage of their noxious and possibly dangerous contents is avoided. In contrast, during necrosis, a pathological form of cell death that results from overwhelming cellular injury, cells swell and lyse, thereby releasing cytoplasmic material which often triggers an inflammatory response. Apoptosis is usually associated with the activation of nucleases that degrade the chromosomal DNA first into large (50 to 300 kilobases) and subsequently into very small oligonucleosomal fragments (*2*).

It is now widely accepted that apoptosis is of central importance for the development and homeostasis of metazoan animals. For example, apoptosis serves as a prominent force in sculpting the developing organism (*3*), as a major mechanism for the precise regulation of cell numbers (*4*, *5*), and as a defense mechanism to remove unwanted and potentially dangerous cells, such as self-reactive lymphocytes (*6*), cells that have been infected by viruses (*7*, *8*), and tumor cells (*9*). Not surprisingly, the initiation of apoptosis is carefully regulated. Many different signals that may originate either from within or outside a cell have been shown to influence the decision between life and death. These include lineage information, cellular damage inflicted by ionizing radiation or viral infection, extracellular survival factors, cell interactions, and hormones (*4*, *5*, *10*). These diverse signals may act to either suppress or promote the activation of the death program, and the same signal may actually have opposing effects on different cell types (*11*).

In addition to the beneficial effects of programmed cell death, the inappropriate activation of apoptosis may cause or contribute to a variety of diseases, including acquired immunodeficiency syndrome (AIDS) (*12*), neurodegenerative diseases, and ischemic stroke (*5*, *13*). The realization that apoptosis represents an active, gene-directed mechanism has fostered optimism that it may be possible to control apoptosis with the development of drugs that act against the molecular components of the death machinery. However, despite considerable progress, it has proven difficult to identify the molecules responsible for apoptosis by conventional biochemical and molecular approaches in mammalian systems. Fortunately, there is increasing evidence that apoptosis occurs by a mechanism that has been at least partially conserved throughout animal evolution. Therefore, results obtained from the study of experimentally more accessible invertebrate model systems may be directly relevant for understanding the mechanism of apoptosis in vertebrates. Indeed, much of our current knowledge about specific cell death genes has been derived from genetic studies in the nematode *Caenorhabditis elegans* (*14*). A large number of mutations that affect specific stages of programmed cell death have been isolated in this organism, and the corresponding genes have been ordered into a genetic pathway (Fig. 1).

Programmed cell death in C. *elegans* can be divided into four distinct stages. These include the decision of whether a given cell will die or adopt another fate, the death of the cell, the engulfment of the dead cell by phagocytes, and the degradation of the engulfed corpse. Mutations that affect each of these stages have been isolated, and these mutations define 14 genes that function in programmed cell death in the nematode. Mutations that interfere with the execution of death, engulfment, or degradation affect all somatic cell deaths, whereas genes implicated in the decision step influence only very few cells. Three genes have been shown to affect the execution of all somatic cell deaths, *ced-3*, *ced-4*, and *ced-9* (*ced* stands for cell death defective). The activity of two of these genes, *ced-3* and *ced-4*, is

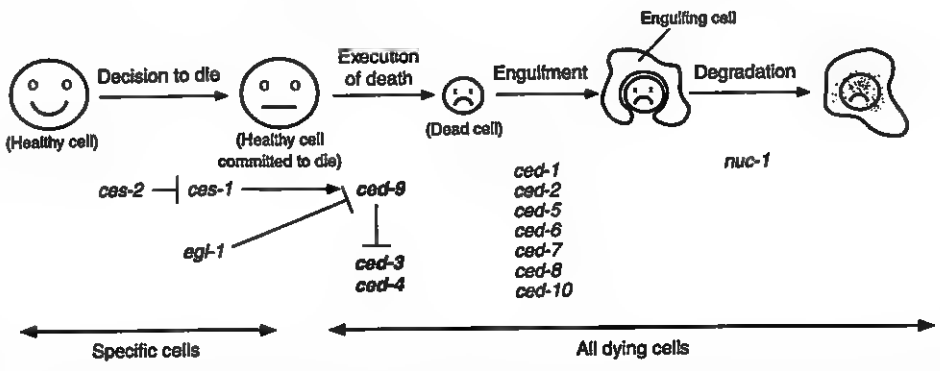

Fig. 1. Genetic pathway for programmed cell death in *C. elegans*. Mutations in 14 different genes have been isolated that affect specific stages of programmed cell death in *C. elegans*. Mutations that influence the decision to die affect only a small number of cells. In contrast, genes involved in all subsequent stages of cell death are common to all somatic cell deaths in this organism. Three genes, *ced-3*, *ced-4*, and *ced-9*, affect the execution of the death program. The activity of *ced-3* and *ced-4* promotes cell death, and *ced-9* activity prevents this process. The epistatic relationship among these genes has been deduced from double-mutant combinations. Symbols: → (positive regulation); ——| (negative regulation). [Adapted from (*14*)]

The author is at the Howard Hughes Medical Institute, Department of Brain and Cognitive Sciences and Department of Biology, Massachusetts Institute of Technology, Cambridge, MA 02139, USA.

required in dying cells for cell death to occur, and the properties of these genes are summarized below. The third gene, *ced-9*, is required to protect cells that should survive from undergoing programmed cell death (*15*). This gene encodes a protein that is homologous to the Bcl-2 family of cell death regulators (*16*, *17*). Furthermore, expression of human Bcl-2 can inhibit cell death in nematodes and can even partially substitute for the loss of *ced-9* function (*16*, *18*). These results indicate that at least some components of the apoptotic program have been conserved throughout most of animal evolution. This notion has received further support from reports that expression of the anti-apoptotic p35 protein from baculovirus can protect against programmed cell death in insects, nematodes, and mammalian neurons (*19*). The relevant proteins that interact with Bcl-2 and p35 have not yet been identified, but it is likely that they have an important and conserved function in the execution of the cell death program.

Here I focus on recent advances in characterizing the properties of the cell death program and of the genes implicated in the process of apoptosis. Although the exact mechanism of death is unknown, progress has been made in identifying key components of the apoptotic machinery. First, I will summarize work indicating that the cell death effector molecules, that is, the components that are directly responsible for the morphological changes during apoptosis, are always present but are inhibited in most mammalian cells. Then I will discuss various biochemical mechanisms that have been proposed as the possible cause of apoptotic death. Next, I will review the evidence that implicates proteases of the *ced-3*/interleukin-1β–converting enzyme (ICE) family in causing the onset of apoptosis. Finally, I will present a model for how distinct signaling pathways may converge in order to activate a common apoptotic program.

Properties of the Cell Death Program

Some of the initial evidence for the idea that apoptosis is caused by an active cell suicide program was derived from experiments in which cell death could be suppressed by inhibitors of RNA or protein synthesis (*20*). However, it was subsequently shown that these inhibitors fail to block and may even induce apoptosis in many other situations, which suggests that the apoptotic effector molecules are always present in most mammalian cells (*5*). The most compelling evidence for the idea that all the proteins required for apoptosis are constitutively expressed in mammalian cells has come from experiments with cells whose nuclei have been removed (*21*). If such cytoplasts are deprived of survival factors or are treated with high concentrations of the protein kinase inhibitor staurosporine, they will undergo all of the cytoplasmic changes that are characteristic of apoptosis. Cytoplasts prepared from cells that express high levels of the Bcl-2 protein are protected against these apoptotic changes. Thus, major aspects of apoptosis do not require the transcription of new genes, and Bcl-2 can protect against this process in the absence of a cell nucleus. As discussed below, the requirement of RNA and protein synthesis for the induction of cell death in certain situations may reflect the need to synthesize molecules that activate or derepress the existing cell death machinery, rather than making any components required for the basic cell death program itself.

If the apoptotic effector proteins are present in living cells, their potentially lethal activities must be suppressed in cells that normally survive. Raff and colleagues (*4*, *5*) have proposed that cells are programmed to commit suicide and require signals from other cells continuously in order to survive. This model is an extension of the well-accepted neurotrophic theory (*22*), and there is indeed growing support for this view. Many different cells in mammals (*4*, *5*) and also in *Drosophila* (*10*) require extracellular factors that are produced by other cells in order to stay alive. This social control of cell survival appears to guarantee that appropriately matching numbers of different cell types in a particular tissue are maintained. Several survival factors and their receptors have been molecularly characterized (*23*), but it is unclear how the activated receptors regulate the apoptotic program. Survival factors might prevent the induction of apoptosis by reducing the amount or activity of crucial cell death effector proteins to harmless levels. Alternatively, they may inhibit cell death by boosting the activity of protective, anti-apoptotic proteins, such as Bcl-2 family members. In the absence of *ced-9* activity, nematodes display widespread ectopic cell death. Therefore, at least in this organism, cell death occurs by default in the absence of protective functions (*16*).

The actual cause and mechanism of apoptotic death is still unknown. Owing to the prominence of nuclear changes at an early stage of apoptosis, it has been suggested that cells are killed by the endonucleolytic cleavage of their DNA (*2*, *24*). However, cells without a nucleus are physiologically active for a considerable time and can be induced to undergo the characteristic cytoplasmic changes of apoptosis. In contrast, isolated nuclei can exhibit condensation and oligonucleosomal DNA degradation in a cell-free system (*25*). These observations imply that multiple factors may contribute to death, and that different cellular compartments have considerable autonomy in undergoing structural changes during apoptosis. It has been suggested that apoptosis may be caused by the accumulation of reactive oxygen species in a process that might be controlled by levels of Bcl-2 (*26*). This idea resulted from experiments showing that Bcl-2 protects against peroxide-induced death, and that certain antioxidants protect against death in response to cytokine deprivation. However, it is questionable whether reactive oxygen species are widely used by cells to commit suicide. Apoptosis and Bcl-2 protection have been observed in the absence of mitochondrial respiration and in cells grown essentially without oxygen, conditions that should greatly reduce the amount of free radicals (*27*).

Finally, numerous overall similarities between apoptosis and the cell cycle have been noted, and it has been suggested that apoptosis and mitosis may be mechanistically related or even coupled. An extreme view of this idea is that apoptosis may be an aberrant mitosis (*28*). Some support for a connection between apoptosis and mitosis has come from implicating genes that play a role in the regulation of cell proliferation, such as p53, c-myc, Rb-1, E1A, cyclin D1, c-fos, and $p34^{cdc2}$ kinase in the control of apoptosis (*8*, *29*, *30*). Some of these genes affect apoptosis in specific situations. For example, p53 appears to be predominantly required for mediating the apoptotic response to chromosomal damage (*31*). In contrast, developmental cell death is not significantly affected in p53 null mice, which develop normally into adult animals. These results place p53 in an activation pathway that is upstream of the basic cell death program. Similar conclusions apply to several other genes on this list. Other genes associated with cell proliferation, such as c-*myc*, are capable of inducing apoptosis when they are aberrantly expressed (*30*), and it has been suggested that *myc* functions normally to induce both proliferation and apoptosis. However, it has been difficult to rule out the alternative interpretation that apoptosis under these conditions is simply the result of a conflict of incompatible growth signals (*32*). The observation that p53 is required for *myc*-induced death (*33*) also suggests that *myc* does not regulate developmental cell death, which can occur in the absence of p53 function (*31*). Likewise, a clear demonstration that any of the other growth control or cell cycle genes function in apoptosis in vivo is still outstanding. In any event, it is likely that some components of the apoptotic program are shared with other cellular processes, including mitosis. However, it appears that the terminal nature and specialized features of apoptosis require at least some components that are specifically devoted to this process.

Role of Cysteine Proteases in Apoptosis

Systematic genetic studies in the nematode *C. elegans* have led to the identification of two genes, *ced-3* and *ced-4*, that are required for all somatic cell deaths (*14*). If either gene is inactivated, all the cells that normally die during development survive. Genetic mosaic studies indicate that these genes act autonomously in dying cells, consistent with a function of *ced-3* and *ced-4* in mediating cellular suicide (*34*). Furthermore, mutations in these genes suppress the ectopic cell deaths otherwise seen in animals that have lost *ced-9* function (*15*). Double mutants between *ced-3* and *ced-9* or *ced-4* and *ced-9* lack all programmed cell death and have phenotypes equivalent to either *ced-3* or *ced-4* single mutants. The simplest interpretation of these results is that *ced-9* inhibits the activities of *ced-3* and *ced-4*. If these genes operate in a linear pathway, *ced-9* would be expected to act upstream of *ced-3* and *ced-4* (Fig. 2). Because it is unlikely that Ced-9/Bcl-2 proteins regulate gene expression, these results also indicate that *ced-3*, *ced-4*, and *ced-9* are expressed in many more cells than in those that actually die. There appears to be a delicate balance between the opposing activities of proteins that promote and those that inhibit cell death.

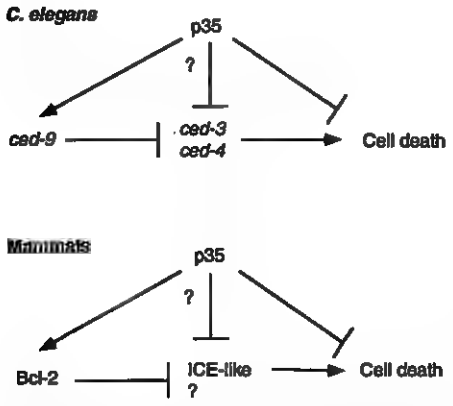

Fig. 2. At least some components of the cell death pathway have been conserved throughout animal evolution. Two of the three genes that control the initiation of programmed cell death in *C. elegans* are homologous to mammalian genes that are thought to play a similar role during apoptosis. In addition, the baculovirus p35 protein has been shown to suppress cell death in insects, nematodes, and mammals, indicating that it interacts with a component of the cell death program that has been conserved in evolution. The identity of this component has not yet been determined. The p35 protein could act by either increasing the activity of protective functions or by blocking the activity of ICE-like proteases or other cell death effector proteins. This regulation could occur by direct protein-protein interactions or could involve other intermediate components. Symbols are as in Fig. 1.

The genes for both Ced-3 and Ced-4 have been cloned and molecularly characterized. The *ced-4* gene encodes a 63-kD protein with no significant similarity to other known polypeptides (*35*). In contrast, the *ced-3* gene encodes a protein that is similar to the family of cysteine proteases, which includes interleukin-1β–converting enzyme (ICE) (*36–38*), *nedd-2/Ich-1* (*39, 40*), and CPP32 (*41*). Furthermore, overexpression of either *ced-3*, ICE, or Nedd-2/Ich-1 in mammalian cells causes apoptosis (*40, 42*). These observations suggest that ICE or a related cysteine protease may function in mammalian cell death. Additional support for this idea comes from the observation that expression of the cowpox virus *crmA* gene, a very potent and specific inhibitor of ICE-like proteases (*43*), can protect cells against apoptosis in response to growth factor withdrawal (*44*). However, it remains to be shown—by targeted gene knockout, for example—whether ICE itself or a similar protease encoded by another gene has a physiological role during apoptosis in vivo that is comparable to that of *ced-3*. Recently, three nuclear proteins, poly(A)DP ribose polymerase, lamins, and U1-70kD have been identified as substrates for proteolytic cleavage by an activity that is very similar to but distinct from that of ICE (*45*). Therefore, although several genes encoding proteins homologous to ICE have already been isolated (*39–41*), it is possible that additional family members, including the true functional homolog or homologs of *ced-3*, remain to be discovered.

ICE has a rather unusual substrate specificity, cleavage at Asp-X bonds (where X is any amino acid), that is shared with only one other known eukaryotic protease, granzyme B (also known as cytotoxic cell proteinase–1, fragmentin 2, and RNKP-1) (*46, 47*). In addition, ICE and granzyme B can be inhibited by similar types of reagents (*37*). These observations are intriguing, because granzyme B is a serine protease that is responsible for apoptosis caused by cytotoxic T lymphocytes (CTLs) (*46, 48*). CTLs can kill cells by delivering the contents of enzyme-bearing granules to the target. Even though CTL-mediated cell killing was originally viewed as a "murder," it has become clear that this process involves the induction of apoptosis in the target cells (*46, 49*). The delivery of granzyme B appears to be both necessary and sufficient for the induction of apoptosis (*46, 48*). Thus, granzyme B may induce apoptosis either by mimicking the action of a *ced-3*/ICE-like cell death gene or by converting such an enzyme, through proteolytic processing of its inactive precursor, to its active state (*7*). The appeal of this hypothesis is that it provides a unified view of the mechanisms underlying programmed cell death and CTL-mediated cytotoxicity. Although it has been reported that ICE itself is not a substrate for granzyme B cleavage (*50*), other ICE-family members may be processed by granzyme B. The identification and biochemical characterization of additional *ced-3*/ICE homologs and their substrates will clearly be an important goal for the near future. Despite these uncertainties, there are good reasons to believe that a *ced-3*/ICE-like cysteine protease initiates the irreversible stage of apoptosis in both nematodes and mammals, by acting at or very close to the cell death effector level (Fig. 2). Two of the three genes that are known to control the onset of programmed cell death in nematodes, *ced-3* and *ced-9*, are similar to mammalian genes that are thought to play a similar role in apoptosis (Fig. 2). Because nematodes and vertebrates have origins that date back to very early stages of animal evolution, predating the separation of chordates and arthropods, it is likely that similar genes operate during programmed cell death in all animals. Furthermore, because these genes can at least partially function in heterologous systems, additional components of the cell death pathway must have been conserved as well.

Universal Regulators of Apoptosis

A fundamental unresolved question is how the apoptotic program is regulated so that only certain cells are selected to die. Apoptosis is controlled by many different, distinct signals, and this work has been extensively reviewed in the recent past (*4, 5, 10, 32, 51*). Yet, it appears that different signaling pathways ultimately converge to activate a common apoptotic program. The expression of anti-apoptotic proteins, such as Bcl-2 and baculovirus p35, can inhibit apoptosis in response to many different death-inducing signals (*17, 19*). This indicates that these proteins interact with components that are either shared among different signaling pathways or act downstream from the convergence point of these pathways.

A step toward understanding how different signals may converge to activate a common cell death program has come from genetic studies on the control of apoptosis in the fruit fly, *Drosophila melanogaster*. In *Drosophila*, as in mammals, the onset of apoptosis is influenced by many different intra- and extracellular signals that may either promote or suppress cell death (*10*). Nevertheless, it appears that most, if not all programmed cell deaths in this organism, are mediated by one common mechanism. Genetic analyses have led to the isolation of a gene, *reaper*, that is capable of integrating information from different signaling pathways to activate the apoptotic program (*52*). Deletions that include *reaper* suppress

apoptosis in response to every apoptotic stimulus tested to date. In the *Drosophila* embryo, *reaper* messenger RNA is specifically found in cells that are doomed to die, and the onset of expression precedes the first morphological signs of apoptosis by 1 to 2 hours. This gene is also rapidly induced upon irradiation with x-rays (*53*), and deletions that include *reaper* offer substantial protection against radiation-induced apoptosis. These observations show that multiple signaling pathways for the activation of apoptosis converge onto the *reaper* gene. Furthermore, expression of *reaper* is sufficient to induce apoptosis in cells that would normally survive (*52*, *54*). Taken together, these results implicate *reaper* as a universal activator of apoptosis in *Drosophila*.

The mechanism by which *reaper* induces apoptosis is not yet clear. The *reaper* gene encodes a small polypeptide of 65 amino acids with no significant similarity to other known proteins, so the sequence provides no information about its biochemical function. However, it appears that *reaper* is not part of the actual death program. This conclusion is based on the observation that some apoptosis can be induced in embryos deficient for *reaper* by irradiation with very high doses of x-rays. Even though the induction of radiation-provoked cell death is much more efficient in the presence of *reaper*, the morphology of those cells that do die is unaffected by its absence. This suggests that *reaper* encodes a regulatory molecule, rather than an apoptotic effector. The selective expression of *reaper* in cells that are doomed to die is consistent with this model, because cell death effectors, at least in mammalian cells, are expected to be constitutively expressed. A highly speculative model for the role of *reaper* in apoptosis with respect to other cell death genes is shown in Fig. 3. One prediction of this model is that *reaper* acts upstream of cell death effectors—for example, by activating a *ced-3*/ICE-like protease. Alternatively, *reaper* may inhibit negative regulators of cell death, such as *ced-9*/Bcl-2 family members. In either case, *reaper* would serve as an integrator that links different signaling pathways with the basic cell death program. In the future, it will be important to identify downstream targets for *reaper* and also to investigate whether this gene and its function have been conserved during evolution. Another interesting question is how *reaper* mRNA expression is regulated in response to different death-inducing signals. It is possible that the convergence of different signaling pathways occurs at the level of the *reaper* promoter. In this case, pathway-specific transcription factors may bind to distinct control elements of the *reaper* gene. Alternatively, the convergence of signaling pathways may occur upstream of *reaper*. In this case, a death-specific transcription factor may be activated and induce *reaper* transcription by binding to a single regulatory site. In principle, it should be possible to distinguish between both models by standard promotor analyses.

The universal requirement of *reaper* for the activation of programmed cell death in *Drosophila* poses an apparent paradox in light of the finding that apoptosis can be induced in mammalian tissue culture cells in the absence of de novo protein synthesis. One possible interpretation is that there are fundamental differences in the expression of cell death genes between *Drosophila* and mammals. Yet one does not have to invoke such differences at this point. As discussed above, the inhibition of apoptosis by protective, anti-apoptotic proteins is of fundamental importance for cell survival, and it appears that many cells require the constant production of these proteins in order to survive. The absence of protein synthesis (or a cell nucleus) should lead to a steady decrease in the levels of both protective and death-promoting proteins. Therefore, a block of RNA or protein synthesis will set up a "race" between proteins with opposing functions in cell death. The outcome of this competition will depend on the relative amounts, activities, and stabilities of these proteins. Because different cell types are known to express distinct levels and types of protective functions, it is expected that different results will be obtained for different cell types. According to this model, cells that start out with a relative excess of protective proteins should continue to be protected against apoptosis upon blocking protein synthesis. However, other cells may lose their protection more rapidly than the proteins that mediate apoptosis, and such cells will die upon treatment with inhibitors of RNA or protein synthesis. It is easy to envision that the outcome of this competition can also be affected by a variety of drugs and manipulations that may influence the activity and stability of the relevant components, perhaps often in ways that differ from the mechanisms normally used by cells to control apoptosis. Consequently, whereas *reaper* and related molecules may be used to initiate apoptosis in vivo, it may be possible to bypass the requirement for such positive regulators of cell death in less physiological situations.

Future Prospects

During the past few years, substantial progress has been made in understanding the control and mechanisms of apoptosis. Nevertheless, major aspects of the apoptotic pathway remain undefined, and it is not even clear what exactly causes cells to die. However, the availability of several important cell death genes should facilitate the isolation of interacting proteins and additional components of the cell death pathway. The development of cell-free model systems for apoptosis (*25*) should help to elucidate the biochemical basis of this process. Finally, one should expect many more contributions to understanding the mechanism of apoptosis from studies of cell death in highly accessible genetic model systems, such as *C. elegans* and *Drosophila*. It appears that *Drosophila* has been underutilized in the past for this purpose. In this organism, apoptosis is under epigenetic control, providing the opportunity to apply an extremely powerful combination of genetics and molecular and cell biology to studying both the signaling pathways and the mechanism of apoptosis. Because the basic cell death program appears to have been remarkably well conserved during evolution, knowledge gained from further studies of programmed cell death in worms and flies should contribute to a better understanding of mammalian apoptosis.

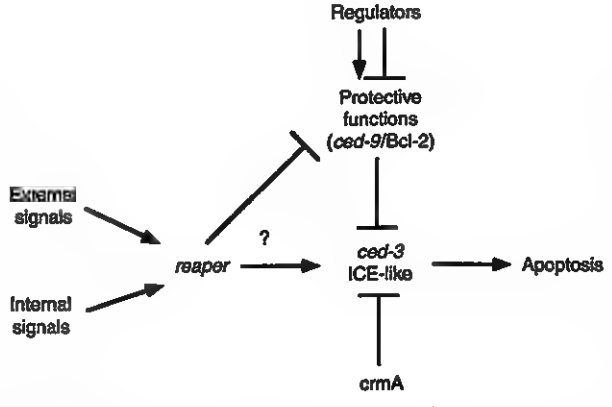

Fig. 3. Model for the convergence of death signals on the apoptotic program. The *Drosophila reaper* gene may serve as a universal activator of apoptosis in response to different death-inducing signals. Expression of *reaper* gene is induced by many different death signals, and deletions that include *reaper* suppress cell death in response to these signals. The *reaper* gene appears to function as a regulator, and not part of the basic cell death effector machinery. Therefore, it should act upstream of cell death effectors, either by activating death-promoting genes, such as *ced-3*/ICE-like proteases, or by inhibiting negative regulators, such as *ced-9*/Bcl-2. This model is highly speculative, because *reaper* homologs have not yet been reported in other systems and interactions between *reaper* and other cell death genes have not yet been experimentally tested. Symbols are as in Fig. 1.

REFERENCES AND NOTES

1. A. H. Wyllie, J. F. R. Kerr, A. R. Currie, *Int. Rev. Cytol.* **68**, 251 (1980); M. J. Arends and A. H. Wyllie, *Int. Rev. Exp. Pathol.* **32**, 223 (1991).
2. C. Roy *et al.*, *Exp. Cell Res.* **200**, 416 (1992); A. H. Wyllie, *Nature* **284**, 555 (1980).
3. A. Glucksman, *Biol. Rev. Camb. Philos. Soc.* **26**, 59 (1951); J. W. Saunders, *Science* **154**, 604 (1966); S. P. Hammar and N. K. Mottet, *J. Cell Sci.* **8**, 229 (1971).
4. M. C. Raff, *Nature* **356**, 397 (1992).
5. M. C. Raff *et al.*, *Science* **262**, 695 (1993).
6. J. J. Cohen, *Adv. Immunol.* **50**, 55 (1991); P. Golstein, D. M. Ojcius, J. D. E. Young, *Immunol. Rev.* **121**, 29 (1991); T. Tsubata *et al.*, *Philos. Trans. R. Soc. London Ser. B* **345**, 297 (1994).
7. D. L. Vaux, G. Haecker, A. Strasser, *Cell* **76**, 777 (1994).
8. M. Debbas and E. White, *Genes Dev.* **7**, 546 (1993).
9. G. T. Williams, *Cell* **65**, 1097 (1991); D. P. Lane *et al.*, *Philos. Trans. R. Soc. London Ser. B* **345**, 277 (1994).
10. H. Steller and M. E. Grether, *Neuron* **13**, 1269 (1994).
11. For example, changes in the level of the steroid hormone ecdysone have different effects on cell death at different stages of insect development [J. W. Truman and L. M. Schwartz, *J. Neurosci.* **4**, 274 (1984); S. Robinow *et al.*, *Development* **119**, 1251 (1993)].
12. A. G. Laurent-Crawford *et al.*, *Virology* **185**, 829 (1991); N. K. Banda *et al.*, *J. Exp. Med.* **176**, 1099 (1992).
13. J. C. Martinou *et al.*, *Neuron* **13**, 1017 (1994).
14. R. E. Ellis, J. Yuan, R. H. Horvitz, *Annu. Rev. Cell Biol.* **7**, 663 (1991); M. O. Hengartner and R. H. Horvitz, *Philos. Trans. R. Soc. London Ser. B* **345**, 243 (1994).
15. M. O. Hengartner, R. E. Ellis, H. R. Horvitz, *Nature* **356**, 494 (1992).
16. M. O. Hengartner and R. H. Horvitz, *Cell* **76**, 665 (1994).
17. C. B. Thompson, *Science* **267**, 1456 (1995).
18. D. L. Vaux, I. L. Weissman, S. K. Kim, *ibid.* **258**, 1955 (1992).
19. R. J. Clem, M. Fechheimer, L. K. Miller, *ibid.* **254**, 1388 (1991); A. Sugimoto, P. D. Friesen, J. H. Rothman, *EMBO J.* **13**, 2023 (1994); B. A. Hay, T. Wolff, G. M. Rubin, *Development* **210**, 2121 (1994); S. Rabizadeh *et al.*, *J. Neurochem.* **61**, 2318 (1993).
20. J. R. Tata, *Dev. Biol.* **13**, 77 (1966); R. A. Lockshin, *J. Insect Physiol.* **15**, 1505 (1969); D. P. Martin *et al.*, *J. Cell Biol.* **106**, 829 (1988); R. W. Oppenheim, D. Prevette, M. Tytell, S. Homma, *Dev. Biol.* **138**, 104 (1990); L. M. Schwartz, L. Kosz, B. K. Kay, *Proc. Natl. Acad. Sci. U.S.A.* **87**, 6594 (1990).
21. M. D. Jacobson, J. F. Burne, M. C. Raff, *EMBO J.* **13**, 1899 (1994).
22. D. Purves, *Body and Brain: A Trophic Theory of Neural Connections* (Harvard Univ. Press, Cambridge, MA, 1988); R. W. Oppenheim, *Annu. Rev. Neurosci.* **14**, 453 (1991).
23. R. M. Lindsay *et al.*, *Trends Neurosci.* **17**, 182 (1994); W. D. Snider, *Cell* **77**, 627 (1994).
24. S. R. Umansky, *J. Theor. Biol.* **97**, 591 (1982); J. J. Cohen and R. C. Duke, *J. Immunol.* **132**, 38 (1984).
25. Y. A. Lazebnik *et al.*, *J. Cell Biol.* **123**, 7 (1993); D. D. Newmeyer, D. M. Farschon, J. C. Reed, *Cell* **79**, 353 (1994).
26. D. M. Hockenbery *et al.*, *ibid.* **75**, 241 (1993).
27. M. D. Jacobson *et al.*, *Nature* **361**, 365 (1993).
28. D. S. Ucker, *New Biol.* **3**, 103 (1991); L. L. Rubin, K. L. Philpott, S. F. Brooks, *Curr. Biol.* **3**, 391 (1993).
29. E. Yonish-Rouach *et al.*, *Nature* **352**, 345 (1991); R. S. Freeman, S. Estus, E. M. Johnson Jr., *Neuron* **12**, 343 (1994); R. J. Smeyne *et al.*, *Nature* **363**, 166 (1993); L. Shi *et al.*, *Science* **263**, 1143 (1994); W. Meikrantz, S. Gisselbrecht, S. W. Tam, R. Schlegel, *Proc. Natl. Acad. Sci. U.S.A.* **91**, 3754 (1994).
30. D. Askew, R. Ashmun, B. Simmons, J. Cleveland, *Oncogene* **6**, 1915 (1991); G. Evan *et al.*, *Cell* **63**, 119 (1992); R. P. Bissonnette, F. Echeverri, A. Mahboubi, D. R. Green, *Nature* **359**, 552 (1992).
31. S. W. Lowe, E. M. Schmitt, S. W. Smith, B. A. Osborne, T. Jacks, *Nature* **362**, 847 (1993); A. R. Clarke *et al.*, *ibid.*, p. 849.
32. E. White, *Genes Dev.* **7**, 2277 (1993).
33. H. Hermeking and D. Eick, *Science* **265**, 2091 (1994).
34. J. Yuan and H. R. Horvitz, *Dev. Biol.* **138**, 33 (1990).
35. ———, *Development* **116**, 309 (1992).
36. D. P. Cerretti *et al.*, *Science* **256**, 97 (1992).
37. N. A. Thornberry *et al.*, *Nature* **356**, 768 (1992).
38. J. Yuan, S. Shaham, S. Ledoux, H. M. Ellis, H. R. Horvitz, *Cell* **75**, 641 (1993).
39. S. Kumar, Y. Tomooka, M. Noda, *Biochem. Biophys. Res. Commun.* **185**, 1155 (1992).
40. L. Wang, M. Miura, L. Bergeron, H. Zhu, J. Yuan, *Cell* **78**, 739 (1994).
41. T. Fernandez-Alnemri, G. Litwack, E. S. Alnemri, *J. Biol. Chem.* **269**, 30761 (1994).
42. M. Miura, H. Zhu, R. Rotello, E. A. Hartwieg, J. Yuan, *Cell* **75**, 653 (1993); S. Kumar *et al.*, *Genes Dev.* **8**, 1613 (1994).
43. C. A. Ray *et al.*, *Cell* **69**, 597 (1992).
44. V. Gagliardini *et al.*, *Science* **263**, 826 (1994); L. Wang, M. Miura, L. Bergeron, H. Zhu, J. Yuan, *Cell* **78**, 739 (1994).
45. S. H. Kaufmann *et al.*, *Cancer Res.* **53**, 3976 (1993); Y. A. Lazebnik *et al.*, *Nature* **371**, 346 (1994); L. A. Casciola-Rosen, D. K. Miller, G. J. Anhalt, A. Rosen, *J. Biol. Chem.* **269**, 30757 (1994).
46. L. Shi *et al.*, *J. Exp. Med.* **176**, 1521 (1992).
47. S. Odake *et al.*, *Biochemistry* **30**, 2217 (1991); A. Caputo *et al.*, *Nat. Struct. Biol.* **1**, 364 (1994); A. D. Howard *et al.*, *J. Immunol.* **147**, 2964 (1991); P. R. Sleath *et al.*, *J. Biol. Chem.* **265**, 14526 (1990).
48. J. W. Heusel *et al.*, *Cell* **76**, 977 (1994).
49. G. Berke, *Annu. Rev. Immunol.* **12**, 735 (1994); L. Shi, R. P. Kraut, R. Aebersold, A. H. Greenberg, *J. Exp. Med.* **175**, 553 (1992).
50. A. J. Darmon, N. Ehrman, A. Caputo, J. Fujinaga, R. C. Bleackley, *J. Biol. Chem.* **269**, 32043 (1994).
51. S. Nagata, *Science* **267**, 1449 (1995).
52. K. White *et al.*, *ibid.* **264**, 677 (1994).
53. J. M. Abrams, A. F. Lamblin, H. Steller, unpublished results.
54. K. White and H. Steller, unpublished results.
55. H.S. is an Associate Investigator of the Howard Hughes Medical Institute.

The Fas Death Factor

Shigekazu Nagata* and Pierre Golstein

Fas ligand (FasL), a cell surface molecule belonging to the tumor necrosis factor family, binds to its receptor Fas, thus inducing apoptosis of Fas-bearing cells. Various cells express Fas, whereas FasL is expressed predominantly in activated T cells. In the immune system, Fas and FasL are involved in down-regulation of immune reactions as well as in T cell–mediated cytotoxicity. Malfunction of the Fas system causes lymphoproliferative disorders and accelerates autoimmune diseases, whereas its exacerbation may cause tissue destruction.

Homeostasis of multicellular organisms is controlled not only by the proliferation and differentiation of cells but also by cell death (*1*). The death of cells during embryogenesis, metamorphosis, endocrine-dependent tissue atrophy, and normal tissue turnover is called programmed cell death. Most of programmed cell death proceeds by apoptosis, a process that includes condensation and segmentation of nuclei, condensation and fragmentation of the cytoplasm, and often extensive fragmentation of chromosomal DNA into nucleosome units.

Apoptosis in vertebrate development often occurs by default when cells fail to receive the extracellular survival signals needed to suppress an intrinsic cell suicide program (*2*); the survival factors can be produced by neighboring cells of a different type (a paracrine mechanism), or of the same type (an autocrine mechanism). In contrast, in the immune system there are situations where cells actively kill other cells; for example, cytotoxic T lymphocytes (CTLs) or natural killer (NK) cells induce apoptosis in their targets such as virus-infected cells or tumor cells (*3*). In these cases, an effector molecule expressed at the surface of CTLs or NK cells or a soluble cytokine produced by these effector cells is thought to be responsible for target cell death.

Molecular and cellular characterization of Fas, a cell surface protein recognized by cytotoxic monoclonal antibodies, revealed its role as a receptor for a Fas ligand (FasL) (*4*). When FasL binds to Fas, the target cell undergoes apoptosis. Spontaneous mutations for Fas and FasL have been identified in mice, and from the phenotypes of these mutants and from studies on mechanisms of cytotoxicity, it was concluded that the Fas-FasL system is involved not only in CTL-mediated cytotoxicity but also is down-regulation of immune responses. In this article, we summarize current knowledge on Fas and FasL and discuss their physiological and pathological roles in the immune system.

Fas and Fas Ligand

In 1989 two groups independently isolated mouse-derived antibodies that were cytolytic for various human cell lines (*5*, *6*). The cell surface proteins recognized by the antibodies were designated Fas and APO-1, respectively. The antibody to Fas (anti-Fas) was an immunoglobulin M (IgM) antibody, whereas the antibody to APO-1 was classified as IgG3. The Fas complementary DNA

S. Nagata is with the Osaka Bioscience Institute, 6-2-4 Furuedai, Suita, Osaka 565, Japan. P. Golstein is with the Centre d'Immunologie INSERM-CNRS de Marseille-Luminy, Case 906, 13288 Marseille Cedex 9, France.

*To whom correspondence should be addressed.

(cDNA) was isolated by expression cloning from a cDNA library of human KT-3 lymphoma cells which abundantly express Fas (*7*). Human Fas consists of 325 amino acids with a signal sequence at the NH_2-terminus and a membrane-spanning region in the middle of the molecule, indicating that Fas is a type I membrane protein.

The function of Fas was assessed by the establishment of mouse cell transformants that constitutively expressed human Fas. When the transformed cells were treated with the antibody to human Fas, the cells died by apoptosis within 5 hours, which indicated that Fas can transduce an apoptotic signal and that anti-Fas works as an agonist. The subsequent purification of human APO-1 antigen and molecular cloning of its cDNA established the identity of APO-1 and Fas (*8*).

The structure of Fas indicated that it belongs to the tumor necrosis factor (TNF) and nerve growth factor (NGF) receptor family (Fig. 1A) (*7–9*). This family includes two TNF receptors (TNF-R1 and TNF-R2), the low-affinity NGF receptor, CD40, OX40, CD27, 4-1BB, and CD30 (*10*). The extracellular regions of members of this family consist of three to six cysteine-rich domains. The amino acid sequence of the extracellular region is relatively conserved, whereas the cytoplasmic region is not, except for some similarity between Fas and TNF-R1 (*7, 8*). Subsequent mutational analyses of Fas and TNF-R1 indicated that the cytoplasmic domain (about 70 amino acids) conserved between Fas and TNF-R1 is necessary and sufficient for transduction of the apoptotic signal (*11*). This domain was therefore designated a death domain.

In humans the single Fas gene per haploid genome is located on the long arm of chromosome 10 (*12*), whereas in the mouse, the gene is on chromosome 19 (*9*). The human and mouse genes span 12 kb and more than 70 kb, respectively, and both genes comprise nine exons (*13*). As for the expression patterns of Fas in various tissues and cell lines, there is considerable variability. Many tissues and cell lines weakly express Fas, but abundant expression was found in mouse thymus, liver, heart, lung, kidney, and ovary (*9*). Unlike mouse thymocytes human thymocytes only weakly express Fas. In mouse thymocytes, Fas is expressed in almost all populations except for double-negative ($CD4^-CD8^-$) thymocytes (*14*). Fas is highly expressed in activated mature lymphocytes (*5*) or lymphocytes transformed with human T cell leukemia virus (HTLV-I), human immunodeficiency virus (HIV), or Epstein-Barr virus (EBV) (*15, 16*). Some other tumor cells also express Fas, although the expression level is low compared with that of lymphoblastoid cells. The expression of Fas is up-regulated by interferon-γ (IFN-γ) in various cell lines (*6, 7, 9*), or by a combination of IFN-γ and TNF-α in human B cells (*17*), which may explain the enhancement of the cytotoxic activity of anti-Fas by these cytokines (*6*). The induction mechanism of Fas expression or the promoter elements of the Fas gene have not been intensively studied.

The structure of Fas suggested that Fas was a receptor for an unknown cytokine. In 1993, Rouvier *et al.* (*18*) reported on a subline from a cytotoxic T cell hybridoma (PC60) between a mouse CTL cell line and a rat lymphoma. The subline (PC60-d10S, d10S for short) could kill target cells expressing Fas but not target cells which did not express Fas. Soluble forms of Fas (Fas-Fc) and TNF receptor (TNFR-Fc) were constructed by fusing their extracellular regions to human IgG (*19*). The Fas-Fc but not TNFR-Fc inhibited the CTL activity of d10S cells, indicating that the d10S cells expressed a FasL and that this FasL played a major role in d10S-mediated cytotoxicity. The FasL on d10S cells could be stained by biotinylated Fas-Fc, and a subline of the d10S cells (d10S16), which expressed ~100 times more FasL than did the original d10S cells, was then established by repeated fluorescence-activated cell sorting. The d10S16 cells showed about 100 times more CTL activity against the Fas-expressing cells than did the d10S cells.

FasL was purified to homogeneity from the solubilized membrane fraction of d10S16 cells by means of affinity-chromatography with Fas-Fc (*19*). The purified FasL was a protein with a molecular weight ratio of ~40,000, and it showed strong cytotoxic activity against Fas-expressing cells. Rat FasL cDNA was then cloned by expression cloning from the d10S subline with Fas-Fc (*20*), and mouse and human FasL cDNAs were subsequently cloned by cross-hybridization (*21, 22*). FasL has no signal sequence at the NH_2-terminus, but it has a domain of hydrophobic amino acids in the middle of the molecule, indicating that it is a type II membrane protein with the COOH-terminal region outside the cell. Mouse and human

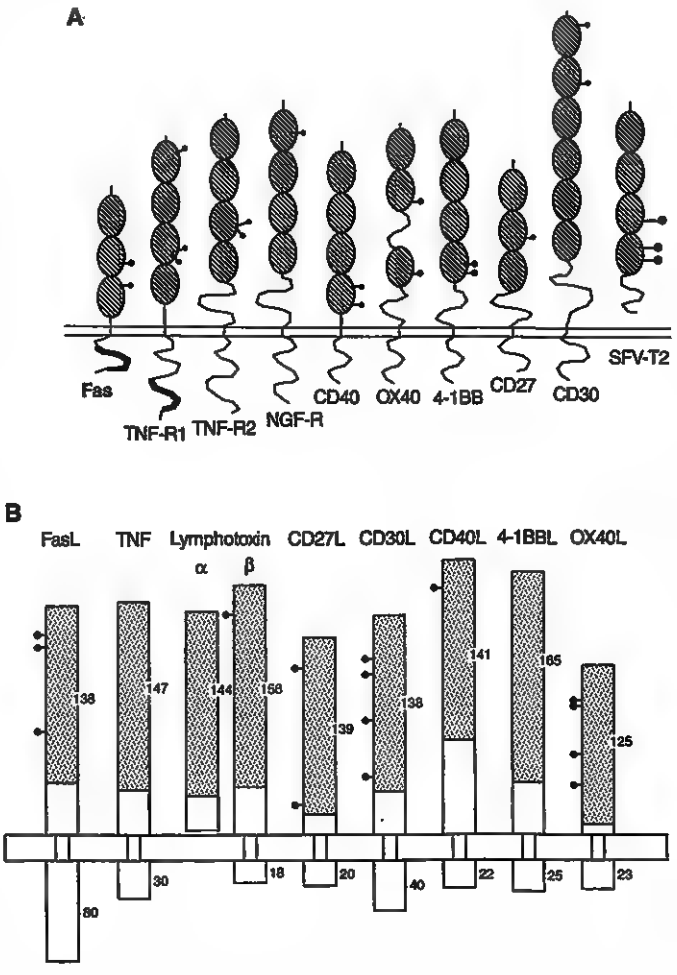

Fig. 1. TNF and its receptor family. **(A)** The TNF and NGF receptor family. Members of the TNF-NGF receptor family are schematically shown. These include Fas, TNF-R1, TNF-R2, NGF receptor, B cell antigen CD40, T cell antigens OX40, 4-1BB, and CD27, Hodgkin's lymphoma antigen CD30, and the soluble protein coded by Shope fibroma virus (SFV-T2). The striped regions represent cysteine-rich subdomains; each member of the family contains three to six of them. The death domains (about 80 amino acids) in the cytoplasmic regions of Fas and TNF-RI, which have some similarity, are shown as bold lines. The symbol —● indicates an N-glycosylation site. [Reproduced from (*4*), S. Nagata, with permission from Academic Press.] **(B)** The TNF family. Members of the TNF family are schematically shown. These include Fas ligand, TNF, the α and β subunits of lymphotoxin, CD27 ligand, CD30 ligand, CD40 ligand, 4-1BB ligand, and OX40 ligand. These members are type II membrane proteins, except for the α subunit of lymphotoxin which is a secretory protein. The shaded portion of each member is the extracellular region which shows significant similarity (25 to 30% identity) among the members. The number of the amino acids in the homologous region and the cytoplasmic region are indicated. The symbol —● indicates an N-glycosylation site.

FasLs are 76.9% identical at the amino acid sequence level, and they are functionally interchangeable. A stretch of about 150 amino acids in the extracellular region of the FasL has significant homology to the corresponding region of other members of the TNF family which includes TNF, lymphotoxin (LT), CD40 ligand, CD27 ligand, CD30 ligand, and OX40 ligand (Fig. 1B). Expression of recombinant FasL on the cell surface of fibroblast-like COS cells was sufficient to induce apoptosis in Fas-expressing target cells within a few hours (*20*), indicating that FasL is a death factor and Fas is its receptor (*4*).

A single FasL gene is located on human and mouse chromosome 1 (*21*, *22*) in the neighborhood of the OX40 ligand gene, another member of the TNF family (*23*). The FasL gene comprises five exons, and its organization is similar to those of TNF-α and LT-β. Among the various cell lines examined, only activated T cell lines expressed FasL (*24*). FasL messenger RNA (mRNA) was not detected in B cells or macrophage, fibroblast, endothelial, or thymic stroma cell lines. The exception was the testis, where abundant FasL expression was found in mouse and rat (*20*), but interestingly, not in human (*25*). The expression of FasL in T cells could be rapidly induced by activation with phorbol 12-myristate 13-acetate (PMA) and ionomycin or T cell receptor engagement (*24*). Herbimycin A and genistein (protein tyrosine kinase inhibitors) as well as cyclosporin A (an inhibitor of the calmodulin-dependent protein phosphatase calcineurin) inhibited the induction of FasL expression. It is likely that some tyrosine kinases and calcineurin are involved in the activation of the FasL gene through the T cell receptor, as has been found for the induction of other lymphokine genes. The nuclear factor–κB (NF-κB) or interferon regulatory factor–1 (IRF-1) element found in the promoter region of the FasL gene may be responsible for this induction (*21*).

A Death Signal from Fas

Signaling by means of Fas leads to apoptotic cell death, with characteristic cytoplasmic and nuclear condensation and DNA fragmentation (*5*, *7*, *20*, *26*, *27*). Triggering this pathway requires the cross-linking of Fas either with antibodies to Fas (*28*), with cells expressing FasL, or with purified FasL (*19*). Similar to TNF, the soluble form of FasL has a trimeric structure in solution (*29*). Therefore, it is likely that the cross-linking of Fas molecules, rather than just their engagement, leads to further signaling within the cell.

Cell death via Fas does not require the presence of a nucleus or DNA fragmentation. Cells enucleated with cytochalasin B undergo apoptosis (that is, the characteristic cytoplasmic lesions appear) when triggered by the Fas-based mechanism with anti-Fas or with cytotoxic T cells (*27*). This is in line with the fact that a nucleus is not required in other apoptotic death systems, such as staurosporin-induced apoptosis (*30*). These results, as well as others showing the death-inducing ability of cytoplasmic extracts on isolated nuclei (*31*), indicate that "nuclear death" is only secondary to essential cytoplasmic death events. What are these cytoplasmic death events and how are they related to the first irreversible step of cell death? The answers are not better known in the case of death via Fas than in the case of death induced by other means. Answers to these questions may provide a biochemical definition of cell death and be of considerable practical importance.

Additional results showed that the Fas-triggered pathway to death is independent of extracellular Ca^{2+} (*18*, *32*) and does not require macromolecular synthesis (*6*, *7*, *33*–*35*). As for many other death pathways, the cellular background plays an essential role in the interpretation and modulation of the Fas-originating signal. Thus, cell sensitivity or resistance involves factors other than just the level of expression of Fas (*26*, *33*, *36*, *37*). The molecular basis underlying this variability in response may depend on which intracellular molecules are available to bind given segments of the Fas intracytoplasmic region, or depend on other molecules such as Bcl-2 and related proteins that modulate cell death (*38*). In fact, the Fas-transduced cell death is partially inhibited by overexpression of Bcl-2 (*39*), but it is completely inhibited by coexpression of

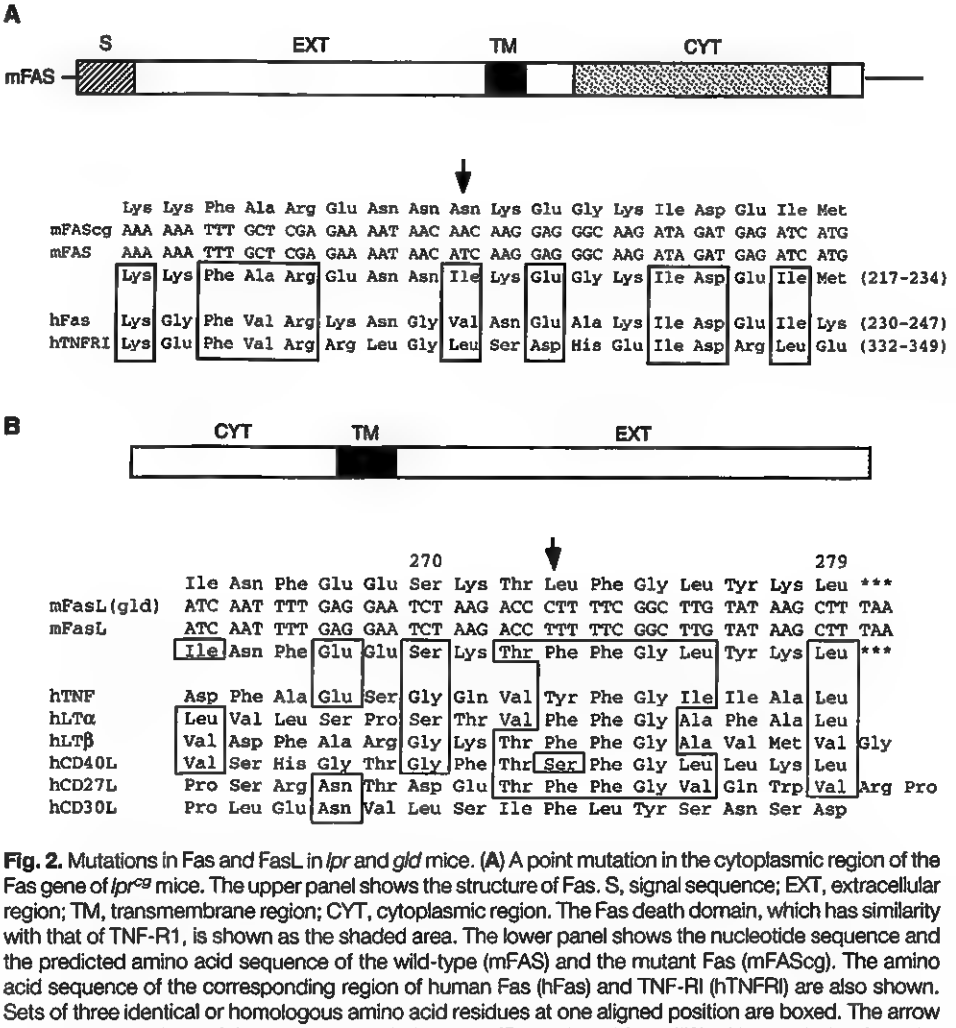
A
S
EXT
TM
CYT
mFAS
Lys Lys Phe Ala Arg Glu Asn Asn Asn Lys Glu Gly Lys Ile Asp Glu Ile Met
mFAScg AAA AAA TTT GCT CGA GAA AAT AAC AAC AAG GAG GGC AAG ATA GAT GAG ATC ATG
mFAS AAA AAA TTT GCT CGA GAA AAT AAC ATC AAG GAG GGC AAG ATA GAT GAG ATC ATG
Lys Lys Phe Ala Arg Glu Asn Asn Ile Lys Glu Gly Lys Ile Asp Glu Ile Met (217-234)
hFas Lys Gly Phe Val Arg Lys Asn Gly Val Asn Glu Ala Lys Ile Asp Glu Ile Lys (230-247)
hTNFRI Lys Glu Phe Val Arg Arg Leu Gly Leu Ser Asp His Glu Ile Asp Arg Leu Glu (332-349)
B
CYT
TM
EXT
270
279
Ile Asn Phe Glu Glu Ser Lys Thr Leu Phe Gly Leu Tyr Lys Leu ***
mFasL(gld) ATC AAT TTT GAG GAA TCT AAG ACC CTT TTC GGC TTG TAT AAG CTT TAA
mFasL ATC AAT TTT GAG GAA TCT AAG ACC TTT TTC GGC TTG TAT AAG CTT TAA
Ile Asn Phe Glu Glu Ser Lys Thr Phe Phe Gly Leu Tyr Lys Leu ***
hTNF Asp Phe Ala Glu Ser Gly Gln Val Tyr Phe Gly Ile Ile Ala Leu
hLTα Leu Val Leu Ser Pro Ser Thr Val Phe Phe Gly Ala Phe Ala Leu
hLTβ Val Asp Phe Ala Arg Gly Lys Thr Phe Phe Gly Ala Val Met Val Gly
hCD40L Val Ser His Gly Thr Gly Phe Thr Ser Phe Gly Leu Leu Lys Leu
hCD27L Pro Ser Arg Asn Thr Asp Glu Thr Phe Phe Gly Val Gln Trp Val Arg Pro
hCD30L Pro Leu Glu Asn Val Leu Ser Ile Phe Leu Tyr Ser Asn Ser Asp

Fig. 2. Mutations in Fas and FasL in *lpr* and *gld* mice. **(A)** A point mutation in the cytoplasmic region of the Fas gene of lpr^{cg} mice. The upper panel shows the structure of Fas. S, signal sequence; EXT, extracellular region; TM, transmembrane region; CYT, cytoplasmic region. The Fas death domain, which has similarity with that of TNF-R1, is shown as the shaded area. The lower panel shows the nucleotide sequence and the predicted amino acid sequence of the wild-type (mFAS) and the mutant Fas (mFAScg). The amino acid sequence of the corresponding region of human Fas (hFas) and TNF-RI (hTNFRI) are also shown. Sets of three identical or homologous amino acid residues at one aligned position are boxed. The arrow indicates the position of the Fas mutation in *lpr* mice. [Reproduced from (*57*) with permission from the author and *Nature*, copyright Macmillan Magazines.] **(B)** A point mutation in the extracellular region of FasL of *gld* mice. The upper panel shows the structure of FasL. The lower panel shows the nucleotide and amino acid sequences of the mutant FasL [mFasL(gld)] and wild type (mFasL). The arrow indicates the position of the mutation in FasL of *gld* mice. Amino acid sequences of the corresponding region of the other members of the TNF family (TNF, LT-α, LT-β, CD40L, CD27L, and CD30L) are also shown. The amino acids of favored substitutions in more than four members are boxed. [Reproduced from (*22*), T. Takahashi *et al.*, with permission from the author and *Cell*, copyright Cell Press.]

Bcl-2 and its binding protein BAG-1 (*40*). It is not yet known whether molecules such as interleukin-1 converting enzyme (ICE) protease and Cdc2 kinase, which have been implicated in some cell death systems (*41*), play a role in Fas-induced cell death.

Because Fas and TNF-R1 have homologous cytoplasmic death domains, one might expect that death transduced by means of one or the other of these surface receptors would have similar characteristics. This may not be the case. Unlike TNF-R1–transduced death in the same type of cells, Fas-transduced death is not blocked by manganese superoxide dismutase (MnSOD), metallothionein, plasminogen activator type 2, A20, or mitochondrial inhibitors (*37, 42*), and it does not activate the transcription factor NF-κB. The latter observation in particular is not completely consistent with indications that it is the death domain of TNF-R1, homologous to that of Fas, which triggers the acidic sphingomyelinase that leads to activation of NF-κB (*43*). Moreover, the Fas-induced cell death is quicker than that induced by TNF-R1 (*44*).

Why do these similar receptors transduce death pathways with such different characteristic? One possibility, still unsubstantiated, is that other parts of the cytoplasmic domains of these receptors generate other signals that modulate the main cell death signal. Indeed, distinct signals can originate from distinct parts of the TNF-R1 cytoplasmic region (*43*). Recently, cytosolic molecules have been identified that can associate with TNF-R2 and CD40, which are other members of the TNF-NGF receptor family (*45*). It would be interesting to examine whether these cytosolic molecules or related molecules can associate with Fas or TNF-R1.

A fast-developing field of research deals with the possibility that Fas signals by means of the complex lipid ceramide. Ceramide is one of the products that results from the breakdown by sphingomyelinases of sphingomyelin, a sphingosine–fatty acid–phosphorylcholine molecule found in the plasma membrane and cytoplasm. The involvement of ceramide in the Fas death pathway has been suggested by the following experiments. When various Fas-bearing cells were incubated with anti-Fas for 5 min, acidic sphingomyelinase activity was detected, there was partial hydrolysis of sphingomyelin, and the amount of ceramide increased. Cell-permeable synthetic C2-ceramide itself, when added to the culture medium, was able to induce apoptosis in less than 3 hours (*46*). The addition of sphingomyelinase or ceramide extracellularly led to the induction of cell death with DNA fragmentation and apoptotic morphology (*47*). Downstream signaling by ceramide might take place by means of a ceramide-activated protein kinase (*48*), which could account in part for the phosphorylations observed within 1 min after antibody-mediated Fas ligation on Jurkat cells; protein kinase inhibitors block the resulting DNA fragmentation and cell death (*49*).

The *lpr* and *gld* Mutations

The mouse spontaneous mutants *lpr* (lymphoproliferation) and *gld* (generalized lymphoproliferative disease) carry autosomal recessive mutations (*50*) on mouse chromosome 19 and 1, respectively (*51*). MRL *lpr/lpr* and MRL *gld/gld* mice develop lymphadenopathy and splenomegaly and produce large quantities of IgG and IgM antibodies including anti-DNA and rheumatoid factor (*52*). They develop nephritis or arthritis and die at around 5 months of age. The allelic mutation (lpr^{cg}) in the *lpr* locus (*53*), distinct from the original *lpr* mutant, causes a weak *lpr* phenotype in double heterozygotes with *gld* ($lpr^{cg}/+$, $gld/+$), in addition to the *lpr* phenotype of its homozygous mutation. The other strains of mice carrying *lpr* or *gld* mutations develop lymphadenopathy and splenomegaly, but not nephritis or arthritis (*54*). Because the wild-type MRL mice develop weak and delayed autoimmune disease, it is likely that *lpr* and *gld* mutations accelerate or worsen the autoimmune disease rather than induce it.

The lymphocytes that accumulate in the lymph nodes and spleen in *lpr* or *gld* mice are arrested at the G_0-G_1 stage of the cell cycle and express the T cell marker Thy-1 and the B cell marker B-220 (*52*). These cells express a rearranged T cell receptor but not a rearranged IgG gene. Because neonatal thymectomy prevents the accumulation of lymphocytes, it seems that it is T cells that accumulate in the mutants. However, the CD4 and CD8 antigens, which are usually expressed on mature T cells, are not expressed on the lymphocytes that accumulate in *lpr* or *gld* mice. The CD4 and CD8 gene loci are demethylated in these lymphocytes, and the administration of anti–Thy-1, anti-CD4, or anti-CD8 inhibits development of the lymphadenopathy (*52*). When mature $CD4^+$ T cells from *lpr* mice were transplanted into wild-type mice, these T cells became double-negative T cells (*55*), suggesting that the cells accumulating in *lpr* mice are derived from mature, single-positive ($CD4^+CD8^-$ or $CD4^-CD8^+$) T cells.

Although *lpr* and *gld* mutations are nonallelic mutations, they show a similar phenotype. In 1991, Allen *et al.* (*56*) carried out a series of bone marrow transplantation experiments among *lpr*, *gld*, and wild-type mice. From these experiments they concluded that *lpr* and *gld* are mutations in genes encoding a pair of interacting proteins: *gld* may affect a soluble or membrane-bound cytokine, whereas *lpr* may affect its receptor. The Fas gene was mapped to a location near the *lpr* locus on mouse chromosome 19 (*9*). Northern (RNA) hybridization analysis indicated that, in contrast to wild-type mice, *lpr* mice express very little Fas mRNA in the liver and thymus (*57*). Characterization of the Fas gene in *lpr* mice indicated that an early transposable element (ETn), a variety of mouse endogenous retrovirus, is inserted into intron 2 (*58*). The ETn carries a polyadenylate signal (AATAAA) on the long terminal repeat (LTR) sequence, which causes premature termination of the Fas RNA transcript.

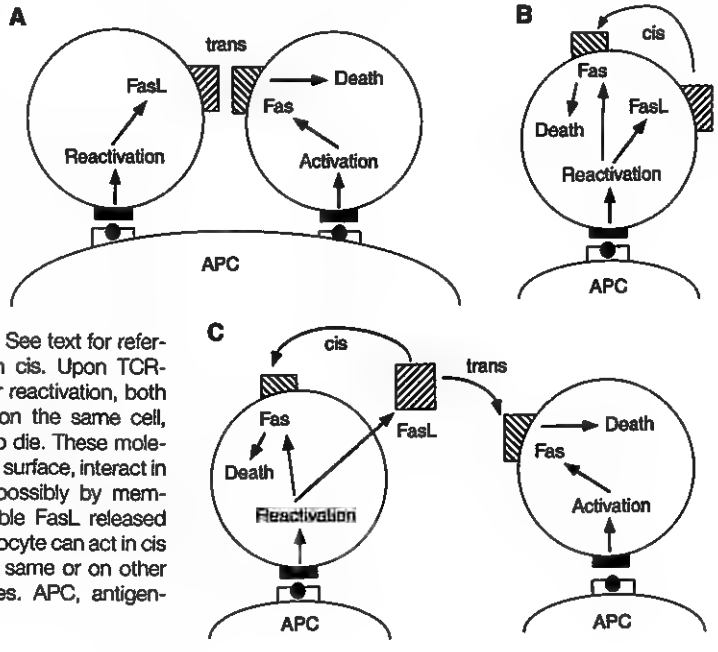

Fig. 3. A schematic representation of three mechanisms that may be involved in Fas-based immune down-regulation at the lymphocyte level. (**A**) Fas and its ligand, FasL, may be expressed on different cells, leading to Fas-based death in trans through a cytotoxicity-like mechanism. See text for references. (**B**) "Suicide" in cis. Upon TCR-transduced activation or reactivation, both Fas and FasL appear on the same cell, which is then induced to die. These molecules, situated at the cell surface, interact in an unknown manner, possibly by membrane folding. (**C**) Soluble FasL released from an activated lymphocyte can act in cis or trans, that is, on the same or on other Fas-bearing lymphocytes. APC, antigen-presenting cell.

Small mRNAs coding for exons 1 and 2 were found in the thymus and liver of *lpr* mice. When the ETn in the Fas gene of *lpr* mice was inserted into the corresponding intron in a mammalian expression vector, the expression efficiency of the vector was reduced to a few percent of that of the original vector.

These results demonstrated that transcription of the Fas gene is impaired in *lpr* mice by an insertion of a transposable element in an intron of the gene. However, this mutation is leaky. Intact Fas mRNA could be found in the thymus and liver of the *lpr* mice at the level of several percent that of the wild-type mouse. The lpr^{cg} mice express normal size Fas mRNA at a level similar to that of wild-type mice (*57*). However, the mRNA carries a T→A point mutation in the Fas cytoplasmic region (Fig. 2A). This mutation changes an isoleucine to an asparagine in the death domain, abolishing the ability of Fas to transduce the apoptotic signal. Together, these results indicate that *lpr* mutations are loss-of-function mutations of the Fas gene. Recent results with transgenic mice, in which the expression of the Fas gene in T cells of *lpr* mice corrected the phenotype (*59*), confirm this conclusion.

The FasL gene was similarly mapped on mouse chromosome 1 where the *gld* mutation is localized (*22*). There is no rearrangement of the FasL gene in the *gld* mice, but there is a point mutation near the COOH-terminus of the coding region (Fig. 2B). This mutation changes a phenylalanine to a leucine in the extracellular region and abolishes the ability of FasL to bind to Fas.

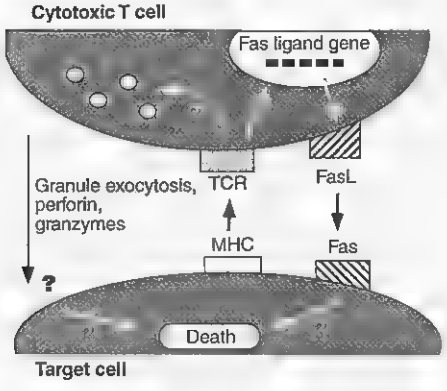

Fig. 4. A schematic representation of two major pathways of T cell–mediated cytotoxicity. The sensitizing antigen, presented by the MHC at the target cell surface, is recognized by the T cell receptor (TCR) at the effector cell surface. The engaged TCR-CD3 complex then transduces within the effector cell a signal toward the granule exocytosis mechanism, and a signal toward the effector cell nucleus that leads to transcription of, in particular, the FasL gene. Swift expression of the FasL protein then leads to engagement of Fas at the target cell surface, signaling target cell death. Interactions of molecules other than TCR-MHC and the Fas-FasL pairs may further modulate the outcome of the effector–target cell encounter. The question marks indicate some of the steps in these processes for which information is particularly incomplete. TCR engagement leads to increased amounts of FasL mRNA, assumed here to be due to increased transcription, although an increase in message stability is not ruled out.

Fas-Mediated Death of Lymphocytes

As described above, the mouse spontaneous mutations *lpr* and *gld* are loss-of-function mutations of Fas and FasL, respectively. The abnormal accumulation of lymphocytes in *lpr* and *gld* mice suggested that Fas and FasL may be involved in normal lymphocyte death. In the life of lymphocytes, both T cells and B cells normally die at various stages of their development. Precursor T cells originate in the bone marrow and migrate into the thymus, where they mature into single-positive ($CD4^+CD8^-$ or $CD4^-CD8^+$) T lymphocytes. The T cells that can interact with self–major histocompatibility complex (MHC) expressed in the thymus are positively selected (positive selection), whereas those that cannot die by apoptosis. On the other hand, T cells that strongly react with self antigen complexed with self-MHC are induced to undergo apoptosis (negative selection) (*60*). More than 95% of the T cells that immigrate into the thymus die there; the remaining 5% migrate to the peripheral lymphoid organs as mature T lymphocytes (*61*). In the periphery, the mature T cells again undergo an additional selection process. Those that interacted with the self antigens expressed only in peripheral tissues would die (peripheral clonal deletion) (*62*). Furthermore, there must be some mechanism in the periphery to eliminate lymphocytes after they have been activated by antigen to ensure that the organism does not fill up with activated lymphocytes (*63*).

The positive and negative selections in the thymus are apparently normal in *lpr* mice (*64*), indicating that a Fas-mediated mechanism is unlikely to be involved. On the other hand, several groups showed that peripheral clonal deletion and the elimination of activated T cells are impaired in *lpr* and *gld* mice (*65*, *66*). Apparently, antigenic stimulation first triggers the proliferation of mature T cells, which are later eliminated by apoptosis. In *lpr* or *gld* mice, an antigen can stimulate the proliferation of mature T cells, but the subsequent death process is severely retarded, both in vitro and in vivo. These results indicate that the Fas system is normally involved in both the clonal deletion of autoreactive T cells in peripheral lymphoid organs and the elimination of activated T cells after they have responded to foreign antigens.

As described below, the Fas system is one of the mechanisms that cytotoxic T cells use to kill infected target cells. A similar cytotoxic mechanism may operate to delete activated T cells. Although mature T cells constitutively express Fas, activation by antigens up-regulates this expression and makes the T cells sensitive to Fas-mediated apoptosis (*26*, *33*). At the same time, activation by antigens induces FasL expression on cytotoxic T cells (*24*, *67*), which are now able to kill Fas-expressing activated lymphocytes by a Fas-based mechanism. The Fas and FasL may interact on the same cell (*66*) (Fig. 3B) or on different cells (*67*) (Fig. 3A). In addition, FasL may be released from the activated cytotoxic cells and then activate Fas from solution (*29*, *68*) (Fig. 3C). In each case, the cytotoxicity is not directed against nonself or modified self, but against activated self.

In the absence of a properly functioning Fas-FasL system, such as in *lpr* or *gld* mutants, activated lymphocytes accumulate (*69*), and because these cells are not efficiently eliminated, autoimmune disease is enhanced. However, other mechanisms may also contribute to the elimination of activated lymphocytes, and there is evidence that these other mechanisms may predominate in young mice, whereas the Fas-based mechanism may be essential in older mice (*70*, *71*).

B cells are also thought to die by apoptosis at several steps of their development (*72*). During development in the bone marrow, the B cells that are strongly reactive to self components are deleted, apparently by a Fas-independent mechanism (*71*). The surviving B cells then migrate to peripheral lymphoid organs where they can be activated by antigen. As with T cells, Fas may be involved in the deletion of B cells activated by the self or foreign antigens in the periphery. Activation of mature B cells causes the expression of Fas (*5*) and renders the cells sensitive to Fas-mediated killing by anti-Fas (*73*). It is possible that the FasL on activated T cells binds to Fas on activated autoaggressive B cells and kills them by apoptosis. This process would be blocked in *lpr* or *gld* mice, and the B cells that escape deletion may be responsible for the production of a large quantity of immunoglobulins, including autoantibodies, in these mutant mice.

Fas-Based T Cell–Mediated Cytotoxicity

Cytotoxic T lymphocytes (CTLs) are the main effector arm of the immune system responsible for eliminating virus-infected cells. The CTLs can both specifically recognize and lyse their targets. What mechanism or mechanisms are involved in lysis? A well-

known perforin-granzyme–based mechanism (*74*) does not account for all examples of CTL killing, so a search has begun for alternative mechanisms.

A clue was provided by the demonstration that a CTL hybridoma subline (d10S) (*35*), upon activation with phorbol 12-myristate 13-acetate (PMA) and ionomycin, lysed Fas-positive but not Fas-negative cells (*18*). Additional evidence for the existence of Fas-based cytotoxicity came from blocking experiments with the soluble form of Fas (Fas-Fc) or anti-Fas under nonlytic conditions. With these reagents, many T cell lines were found to exert Fas-based cytotoxicity (*32*, *34*, *75*, *76*).

It has long been known that part of T cell–mediated cytotoxicity was Ca^{2+}-independent (*77*), whereas the perforin-granzyme–based mechanism was Ca^{2+}-dependent at several levels (*78*). The cytotoxicity by preactivated d10S cells was Ca^{2+}-independent (*35*). The presence of EGTA-Mg^{2+} in cytotoxicity assays suppresses the perforin-based mechanism and allows one to study the Fas-based mechanism (*18*), even in situations where both mechanisms would normally operate simultaneously. In the presence of EGTA-Mg^{2+}, the antigen-specific cytotoxicity expressed by in vitro–raised and in vivo–raised cytotoxic T cells was shown to be Fas-based (*18*, *79*).

The Fas-based cytotoxicity by CTLs can be divided into two processes. First, on recognition of the target cell by the cytotoxic cell, FasL expression is induced in the cytotoxic cell. Second, engagement of FasL on the cytotoxic cells and Fas on the target cell leads to activation of an intrinsic suicide program in the target cell. Interestingly, transfection of FasL cDNA into fibroblast-like recipient cells is enough to render these cells cytotoxic (*20*), showing that expression of the FasL may be sufficient to make even a nonlymphoid cell cytotoxic.

Which T cells are able to exert Fas-based cytotoxicity? Among the classical $CD4^+$ T helper (T_H) subpopulations (*80*), T_H1 cells can express the FasL and lyse in a Fas-based manner much more readily than T_H2 cells (*32*, *75*). Neither helper T cell population usually expresses the perforin-based mechanism of lysis. In contrast, $CD8^+$ cells, which are the professional cytotoxic T cells, usually express both the Fas-based and the perforin-based mechanisms (*18*, *24*, *32*, *34*).

Thus, two mechanisms of cytotoxicity, perforin-based and Fas-based, have been molecularly defined (Fig. 4). There seems to be little cross-talk between these mechanisms, because cytotoxic cells from perforin knock-out mice (*79*), as well as cytotoxic cell lines that do not express perforin (*81*), can lyse by means of the Fas pathway, whereas *gld* cytotoxic cells and *lpr* target cells can lyse or be lysed, respectively, by means of the perforin pathway (*18*, *67*, *79*, *82*). No other mechanism of cytotoxicity has been found, at least in short-term in vitro cytotoxicity tests (*79*, *81*), suggesting that there are only two main mechanisms of T cell–mediated cytotoxicity, Fas-based and perforin-based mechanisms.

Fas and FasL in Pathology

As described above, the Fas system is involved in eliminating normal activated lymphocytes as well as probably some virus-infected cells. The loss-of-function mutations of Fas or FasL causes activated lymphocytes to accumulate, and in mice this produces autoimmune disease. An injection of antibodies to Fas kills adult mice within a few hours (*83*). These results suggest that the Fas system may have a role in human pathology in two different ways.

First, diseases may be caused by a malfunction of the Fas system. The *lpr* and *gld* mutations in mice are in this category, and several patients have been described with phenotypes similar to that of *lpr* mice (*84*). It is possible that these patients have defects in Fas or FasL. Indeed, patients with altered Fas were recently reported (*85*). The *lpr* and *gld* mice produce large amounts of immunoglobulin, including autoantibodies, and develop an autoimmune disease that resembles human systemic lupus erythematosus (SLE) (*52*). Cheng *et al.* (*86*) detected an elevated level of the soluble form of Fas in the serum of some human SLE patients. This soluble form of Fas seemed to be produced by a Fas mRNA that was generated by alternative splicing and that encoded a soluble form of Fas protein lacking a transmembrane domain. Because this form of Fas could induce lymphadenopathy and splenomegaly, Cheng *et al.* (*86*) suggested that it inhibits Fas-mediated elimination of activated lymphocytes and thereby causes the SLE phenotype. Although this is an interesting possibility, it will be necessary to examine more patients to test this hypothesis.

The *lpr* phenotype is dependent on background genes in the mouse (*54*). MRL mice carrying the *lpr* mutation develop nephritis or arthritis, whereas C3H mice carrying the *lpr* mutation do not, indicating that genes other than Fas, such as those regulating autoimmunity, are involved in Fas-related pathology (*87*). It may be noteworthy that nitric oxide (NO) synthase expression and NO production are increased in MRL *lpr*/*lpr* mice, and spontaneous glomerulonephritis and arthritis can be reduced by orally administered N^G-monomethyl-L-arginine which inhibits NO production (*88*). Active transforming growth factor–β (TGF-β) is overproduced in *lpr* mice, possibly as a homeostatic mechanism for suppressing exaggerated and inappropriate immunostimulation. This apparently leads to a failure of polymorphonuclear leukocytes to migrate to the site of bacterial infection, diminishing the host defense against bacterial infection and thus increasing the bacterial burden (*89*). This situation is reminiscent of the increased risk of bacterial infection observed in patients with autoimmune disease.

A second category of Fas-related diseases may be caused by excessive activity of the Fas system. There is growing circumstantial evidence that Fas might be involved in the death of $CD4^+$ T cells during the course of an HIV infection. Fas is abundantly expressed on T lymphocytes of HIV-infected children (*15*) and in retrovirus-induced immunodeficiency syndrome in mice (*90*). In unfractionated human peripheral blood lymphocytes (PBLs), cross-linking of CD4 molecules, either by an antibody or by the HIV envelope protein gp160, up-regulated the expression of Fas on the PBLs, which closely correlated with the occurrence of apoptotic cell death (*91*). Injection of mice with antibody to CD4 led to rapid Fas-based apoptosis of T cells (*92*). Human T cell lines transformed with HIV were more sensitive to Fas-mediated apoptosis than the parental cells (*15*). These data are consistent with the involvement of Fas in the pathology of acquired immunodeficiency syndrome (AIDS), and this potentially important line of research is now being actively pursued in several laboratories.

An injection of monoclonal anti-Fas into adult mice caused rapid hepatic failure and death (*83*), suggesting that acute fulminant hepatitis in humans may be Fas-mediated. Accumulating data such as the involvement of specific CTLs in fulminant hepatitis (*93*), the sensitivity of primary hepatocytes to Fas-mediated apoptosis in vitro (*94*), and the overexpression of Fas in hepatocytes transformed with human hepatitis C virus (HCV) (*95*) are consistent with this hypothesis. In this model, virus antigens of hepatitis B virus or HCV expressed on hepatocytes would activate CTLs to express FasL, which then would bind to Fas on hepatocytes, inducing them to undergo apoptosis. This process may normally occur to remove virus-infected cells but, if exaggerated, may lead to fulminant hepatitis.

Fas is abundantly expressed not only in the liver but also in the heart and lungs (*9*). The primary cells from these tissues are sensitive to Fas-mediated apoptosis (*96*), suggesting that the Fas system may also be involved in CTL-mediated diseases in these tissues. The lymphocytes in *lpr* mice constitutively express FasL (*69*), which may be responsible for the graft-versus-host disease (GVHD) observed when *lpr* bone marrow is transferred to wild-type mice (*97*). These

results suggest that the Fas system may also be involved in GVHD induced by allogenic bone marrow transplantations in humans. Furthermore, a functional soluble form of the FasL was recently identified in the culture medium of activated human T cells (*29*). If such a molecule is produced in vivo, it may work as a pathological agent to cause systemic tissue injury.

Therapeutic uses of the Fas system might include blocking the exacerbated Fas-based pathological manifestations with either soluble forms of Fas, neutralizing antibodies to Fas or FasL, or inhibitors of FasL induction or Fas-mediated apoptosis. Some groups considered using Fas-based reagents (such as activating anti-Fas or FasL) for human cancer patients (*15*, *98*). To avoid the potential risks of these reagents for normal tissues (*83*), it would be necessary to find a way to accurately target the reagents to the tumor cells.

Conclusions

Cell proliferation, differentiation, and survival are often regulated by growth, differentiation, and survival factors, respectively, which are collectively called cytokines. Cytokines bind to their complementary receptors, which transduce the extracellular signal into an intracellular signaling cascade. As described above, characterization of Fas and FasL revealed that, in some cases, cytokines can induce cell death. FasL binds to its receptor and kills the cell within hours by inducing apoptosis. Whereas dozens of factors are known to promote growth, differentiation, or survival, only a few cytokines, including FasL and tumor necrosis factor (TNF), have been found to induce apoptosis. The Fas and TNF systems seem to be mainly restricted to the immune system. It is possible that there are other death-inducing molecules functionally related to FasL that may help remove unwanted cells in nonlymphoid tissues and organs.

Binding of a growth factor to its receptor usually induces dimerization of the receptor (homodimerization or heterodimerization). The dimerized receptor then activates a cascade of intracellular reactions, which eventually induce the gene expression necessary for cell proliferation or differentiation. On the other hand, binding of FasL to its receptor probably induces trimerization of the receptor, which can then transduce the death signal. The fact that Fas-mediated apoptosis can occur without a nucleus indicates that no specific gene induction is required for this death process. The cells seem to have an intrinsic death program in the cytoplasm, which Fas may activate. This death program may be identical to that involved in apoptosis induced in other ways, for example, by the deprivation of survival factors. Some cells are resistant to Fas-mediated apoptosis, suggesting that they either lack this death program or express molecules that inhibit the signals induced by Fas or the death program itself. Biochemical characterization of this death program and its eventual inhibitor proteins in the cytoplasm may reveal other signaling intermediates.

The identification of FasL as a cell death–inducing molecule suggested that the Fas-FasL system has a pathological role in humans. It is known that TNF works as a cachectin and mediates septic shock. Like TNF, FasL may work as an agent that causes tissue damage. The gain-of-function mutation of the growth factor system causes cellular transformation, whereas the loss-of-function mutation of the Fas system (*lpr* or *gld* mutation) causes lymphadenopathy. In this regard, Fas and FasL may be considered as tumor suppressor genes. It is possible that one or more mutations in oncogenes or tumor suppressor genes in addition to the Fas-FasL mutation causes cellular transformation. Further elucidation of the mechanism of Fas-mediated apoptosis and of its role in physiology or pathology should contribute to a better understanding of not only the life and death of cells but also of the basic mechanism of some human diseases.

REFERENCES AND NOTES

1. M. C. Raff, *Nature* **356**, 397 (1992); N. I. Walker, B. V. Harmon, G. C. Gobe, J. F. R. Kerr, *Methods Achiev. Exp. Pathol.* **13**, 18 (1988); A. H. Wyllie, J. F. R. Kerr, A. R. Currie, *Int. Rev. Cytol.* **68**, 251 (1980).
2. M. C. Raff *et al.*, *Science* **262**, 695 (1993).
3. J. J. Cohen, R. C. Duke, V. A. Fadok, K. S. Sellins, *Annu. Rev. Immunol.* **10**, 267 (1992).
4. S. Nagata, *Adv. Immunol.* **57**, 129 (1994); S. Nagata and T. Suda, *Immunol. Today* **16**, 39 (1995).
5. B. C. Trauth *et al.*, *Science* **245**, 301 (1989).
6. S. Yonehara, A. Ishii, M. Yonehara, *J. Exp. Med.* **169**, 1747 (1989).
7. N. Itoh *et al.*, *Cell* **66**, 233 (1991).
8. A. Oehm *et al.*, *J. Biol. Chem.* **267**, 10709 (1992).
9. R. Watanabe-Fukunaga *et al.*, *J. Immunol.* **148**, 1274 (1992).
10. S. Nagata, in *Apoptosis II, The Molecular Basis of Cell Death*, L. D. Tomei and F. C. Cope, Eds. (Cold Spring Harbor Laboratory Press, Cold Spring Harbor, NY, 1993), pp. 313–326; C. A. Smith, T. Farrah, R. G. Goodwin, *Cell* **76**, 959 (1994); B. Beutler and C. van Huffel, *Science* **264**, 667 (1994).
11. N. Itoh and S. Nagata, *J. Biol. Chem.* **268**, 10932 (1993); L. A. Tartaglia, T. M. Ayres, G. H. W. Wong, D. V. Goeddel, *Cell* **74**, 845 (1993).
12. J. Inazawa, N. Itoh, T. Abe, S. Nagata, *Genomics* **14**, 821 (1992); P. Lichter, H. Walczak, S. Weitz, I. Behrmann, P. H. Krammer, *ibid.*, p. 179.
13. I. Behrmann, H. Walczak, P. H. Krammer, *Eur. J. Immunol.* **24**, 3057 (1994); R. Watanabe-Fukunaga and S. Nagata, unpublished observations.
14. S. Andjelic, J. Drappa, E. Lacy, K. B. Elkon, J. Nikolic-Zugic, *Int. Immunol.* **6**, 73 (1994); J. Ogasawara, T. Suda, S. Nagata, *J. Exp. Med.*, **181**, 485 (1995).
15. K.-M. Debatin *et al.*, *Blood* **83**, 3101 (1994); N. Kobayashi *et al.*, *Proc. Natl. Acad. Sci. U.S.A.* **87**, 9620 (1990).
16. M. H. Falk *et al.*, *Blood* **79**, 3300 (1992).
17. P. Möller *et al.*, *ibid.* **81**, 2067 (1993).
18. E. Rouvier, M.-F. Luciani, P. Golstein, *J. Exp. Med.* **177**, 195 (1993).
19. T. Suda and S. Nagata, *ibid.* **179**, 873 (1994).
20. T. Suda, T. Takahashi, P. Golstein, S. Nagata, *Cell* **75**, 1169 (1993).
21. T. Takahashi *et al.*, *Int. Immunol.* **6**, 1567 (1994).
22. T. Takahashi *et al.*, *Cell* **76**, 969 (1994); D. H. Lynch *et al.*, *Immunity* **1**, 131 (1994).
23. P. R. Baum *et al.*, *EMBO J.* **13**, 3992 (1994).
24. A. Anel, M. Buferne, C. Boyer, A.-M. Schmitt-Verhulst, P. Golstein, *Eur. J. Immunol.* **24**, 2469 (1994); F. Vignaux *et al.*, *J. Exp. Med.* **181**, 781 (1995); T. Suda *et al.*, *J. Immunol.*, in press.
25. T. Suda and S. Nagata, unpublished results.
26. L. B. Owen-Schaub, S. Yonehara, W. L. Crump III, E. A. Grimm, *Cell. Immunol.* **140**, 197 (1992).
27. K. Schulze-Osthoff, H. Walczak, W. Dröge, P. H. Krammer, *J. Cell Biol.* **127**, 15 (1994); H. Nakajima, P. Golstein, P. A. Henkart, *J. Exp. Med.*, in press.
28. J. Dhein *et al.*, *J. Immunol.* **149**, 3166 (1992).
29. M. Tanaka, T. Suda, T. Takahashi, S. Nagata, *EMBO J.*, in press.
30. M. D. Jacobosn, J. F. Burne, M. C. Raff, *ibid.* **13**, 1899 (1994).
31. Y. A. Lazebnik, S. Cole, C. A. Cooke, W. G. Nelson, W. C. Earnshaw, *J. Cell Biol.* **123**, 7 (1993); D. D. Newmeyer, D. M. Farschon, J. C. Reed, *Cell* **79**, 353 (1994).
32. S. T. Ju, H. Cui, D. J. Panka, R. Ettinger, A. Marshak-Rothstein, *Proc. Natl. Acad. Sci. U.S.A.* **91**, 4185 (1994).
33. C. Klas, K.-M. Debatin, R. R. Jonker, P. H. Krammer, *Int. Immunol.* **5**, 625 (1993).
34. T. Stalder, S. Hahn, P. Erb, *J. Immunol.* **152**, 1127 (1994).
35. P. Golstein, M.-G. Mattéi, C. Foa, M.-F. Luciani, in *Apoptosis and the Immune Response*, C. D. Gregory, Eds. (Wiley, New York, 1994), pp. 143–163.
36. T. Miyawaki *et al.*, *J. Immunol.* **149**, 3753 (1992); S. Takahashi *et al.*, *Eur. J. Immunol.* **23**, 1935 (1993).
37. G. H. W. Wong and D. V. Goeddel, *J. Immunol.* **152**, 1751 (1994).
38. Z. N. Oltvai and S. J. Korsmeyer, *Cell* **79**, 189 (1994).
39. N. Itoh, Y. Tsujimoto, S. Nagata, *J. Immunol.* **151**, 621 (1993).
40. S. Takayama *et al.*, *Cell* **80**, 279 (1995).
41. L. Shi, R. P. Kraut, R. Aebersold, A. H. Greenberg, *J. Exp. Med.* **175**, 553 (1992); M. Miura, H. Zhu, R. Rotello, E. A. Hartwieg, J. Yuan, *Cell* **75**, 653 (1993).
42. H. Hug, M. Enari, S. Nagata, *FEBS Lett.* **351**, 311 (1994); K. Schulze-Osthoff, P. Krammer, W. Dröge, *EMBO J.* **13**, 4587 (1994).
43. K. Wiegmann, S. Schütze, T. Machleidt, D. Witte, M. Krönke, *Cell* **78**, 1005 (1994).
44. M.-V. Clement and I. Stamenkovic, *J. Exp. Med.* **180**, 557 (1994).
45. M. Rothe, S. C. Wong, W. J. Henzel, D. V. Goeddel, *Cell* **78**, 681 (1994); H. M. Hu, K. O'Rourke, M. S. Boguski, V. M. Dixit, *J. Biol. Chem.* **269**, 30069 (1994).
46. M. G. Cifone *et al.*, *J. Exp. Med.* **180**, 1547 (1994).
47. W. D. Jarvis *et al.*, *Proc. Natl. Acad. Sci. U.S.A.* **91**, 73 (1994).
48. R. Kolesnick and D. W. Golde, *Cell* **77**, 325 (1994).
49. C. M. Eischen, C. J. Dick, P. J. Leibson, *J. Immunol.* **153**, 1947 (1994).
50. B. S. Andrews *et al.*, *J. Exp. Med.* **148**, 1198 (1978); J. B. Roths, E. D. Murphy, E. M. Eicher, *ibid.* **159**, 1 (1984).
51. T. Watanabe *et al.*, *Biochem. Genet.* **29**, 325 (1991); M. L. Watson *et al.*, *Mamm. Genome* **2**, 158 (1992).
52. P. L. Cohen and R. A. Eisenberg, *Annu. Rev. Immunol.* **9**, 243 (1991).
53. A. Matsuzawa *et al.*, *J. Exp. Med.* **171**, 519 (1990).
54. S. Izui *et al.*, *J. Immunol.* **133**, 227 (1984).
55. Y. Laouar and S. Ezine, *ibid.* **153**, 3948 (1994).
56. R. D. Allen, J. D. Marshall, J. B. Roths, C. L. Sidman, *J. Exp. Med.* **172**, 1367 (1990).
57. R. Watanabe-Fukunaga, C. I. Brannan, N. G. Copeland, N. A. Jenkins, S. Nagata, *Nature* **356**, 314 (1992).
58. M. Adachi, R. Watanabe-Fukunaga, S. Nagata, *Proc. Natl. Acad. Sci. U.S.A.* **90**, 1756 (1993); S. Kobayashi, T. Hirano, M. Kakinuma, T. Uede, *Biochem. Biophys. Res. Commun.* **191**, 617 (1993); J. Wu, T. Zhou, J. He, J. D. Mountz, *J. Exp. Med.* **178**, 461 (1993); B. J.-L. Chu, J. Drappa, A. Parnassa, K. B. Elkon, *ibid.*, p. 723.

59. J. Wu *et al.*, *Proc. Natl. Acad. Sci. U.S.A.* **91**, 2344 (1994).
60. H. von Boehmer, *Cell* **76**, 219 (1994); G. J. V. Nossal, *ibid.*, p. 229.
61. R. G. Scollay, E. C. Butcher, I. L. Weissman, *Eur. J. Immunol.* **10**, 210 (1980); M. Egerton, R. Scollay, K. Shortman, *Proc. Natl. Acad. Sci. U.S.A.* **87**, 2579 (1990).
62. S. R. Webb, J. Hutchinson, K. Hayden, J. Sprent, *J. Immunol.* **152**, 586 (1994); B. Rocha and H. von Boehmer, *Science* **251**, 1225 (1991); S. Webb, C. Morris, J. Sprent, *Cell* **63**, 1249 (1990); J. E. McCormack, J. E. Callahan, J. Kappler, P. C. Marrack, *J. Immunol.* **150**, 3785 (1993); H. R. MacDonald, S. Baschieri, R. K. Lees, *Eur. J. Immunol.* **21**, 1963 (1991).
63. D. Kabelitz, T. Pohl, K. Pechhold, *Immunol. Today* **14**, 338 (1993).
64. C. L. Sidman, J. D. Marshall, H. von Boehmer, *Eur. J. Immunol.* **22**, 499 (1992); L. R. Herron *et al.*, *J. Immunol.* **151**, 3450 (1993).
65. I. N. Crispe, *Immunity* **1**, 347 (1994); P. Musette, C. Pannetier, G. Gachelin, P. Kourilsky, *Eur. J. Immunol.* **24**, 2761 (1994); G. G. Singer and A. K. Abbas, *Immunity* **1**, 365 (1994); M. R. Alderson *et al.*, *J. Exp. Med.* **181**, 71 (1995).
66. J. H. Russell, B. Rush, C. Weaver, R. Wang, *Proc. Natl. Acad. Sci. U.S.A.* **90**, 4409 (1993); J. H. Russell and R. Wang, *Eur. J. Immunol.* **23**, 2379 (1993).
67. F. Vignaux and P. Golstein, *Eur. J. Immunol.* **24**, 923 (1994); I. Gillette-Ferguson and C. L. Sidman, *ibid.*, p. 1181.
68. J. Dhein, H. Walczak, C. Bäumler, K.-M. Debatin, P. H. Krammer, *Nature* **373**, 438 (1995).
69. D. Watanabe, T. Suda, H. Hashimoto, S. Nagata, *EMBO J.* **14**, 12 (1995); J. L. Chu *et al.*, *J. Exp. Med.* **181**, 393 (1995).
70. M. Papiernik, C. Pontoux, P. Golstein, in preparation.
71. J. C. Rathmell and C. C. Goodnow, *J. Immunol.* **153**, 2831 (1994).
72. K. Rajewsky, *Curr. Opin. Immunol.* **4**, 171 (1992).
73. P. T. Daniel and P. H. Krammer, *J. Immunol.* **152**, 5624 (1994).
74. P. A. Henkart, *Annu. Rev. Immunol.* **3**, 31 (1985); E. R. Podack, *Immunol. Today* **6**, 21 (1985); J. W. Shiver, L. Su, P. A. Henkart, *Cell* **71**, 315 (1992); J. W. Heusel, R. L. Wesselschmidt, S. Shresta, J. H. Russell, *Cell* **76**, 977 (1994); D. Kägi *et al.*, *Nature* **369**, 31 (1994).
75. F. Ramsdell *et al.*, *Int. Immunol.* **6**, 1545 (1994).
76. S. Hanabuchi *et al.*, *Proc. Natl. Acad. Sci. U.S.A.* **91**, 4930 (1994).
77. I. C. M. MacLennan, F. M. Gotch, P. Golstein, *Immunology* **39**, 109 (1980); R. Tirosh and G. Berke, *Cell. Immunol.* **95**, 113 (1985); H. L. Ostergaard, K. P. Kane, M. F. Mescher, W. R. Clark, *Nature* **330**, 71 (1987); G. Trenn, H. Takayama, M. V. Sitko, *ibid.*, p. 72; J. D.-E. Young, W. R. Clark, C.-C. Liu, Z. A. Cohn, *J. Exp. Med.* **166**, 1894 (1987).
78. E. R. Podack, J. D.-E. Young, Z. A. Cohn, *Proc. Natl. Acad. Sci. U.S.A.* **82**, 8629 (1985); J. D.-E. Young, A. Damiano, M. A. DiNome, L. G. Leong, Z. A. Cohn, *J. Exp. Med.* **165**, 1371 (1987); S. Ishiura *et al.*, *Mol. Immunol.* **27**, 803 (1990).
79. D. Kägi *et al.*, *Science* **265**, 528 (1994); B. Lowin, M. Hahne, C. Mattmann, J. Tschopp, *Nature* **370**, 650 (1994).
80. T. R. Mosmann *et al.*, *Immunol. Rev.* **123**, 209 (1991).
81. C. M. Walsh, A. A. Glass, V. Chiu, W. R. Clark, *J. Immunol.* **153**, 2506 (1994); H. Kojima *et al.*, *Immunity* **1**, 357 (1994).
82. F. Ramsdell *et al.*, *Eur. J. Immunol.* **24**, 928 (1994).
83. J. Ogasawara *et al.*, *Nature* **364**, 806 (1993).
84. M. C. Sneller *et al.*, *J. Clin. Invest.* **90**, 334 (1992).
85. F. Rieux-Laucat, F. Le Deist, K. M. Debatin, A. Fischer, J. P. De Villartay, *Abstracts of the 12th European Immunology Meeting*, Barcelona, Spain, June 1994 (European Federation of Immunological Societies, 1994).
86. J. Cheng *et al.*, *Science* **263**, 1759 (1994).
87. M. L. Watson *et al.*, *J. Exp. Med.* **176**, 1645 (1992).
88. J. B. Weinberg *et al.*, *ibid.* **179**, 651 (1994).
89. J. H. Lowrance, F. X. O'Sullivan, T. E. Caver, W. Waegell, H. D. Gresham, *ibid.* **180**, 1693 (1994).
90. K. Hiromatsu *et al.*, *Eur J. Immunol.* **24**, 2446 (1994).
91. N. Oyaizu *et al.*, *Blood* **84**, 2622 (1994).
92. Z.-Q. Wang *et al.*, *Eur. J. Immunol.* **24**, 1549 (1994).
93. K. Ando *et al.*, *J. Exp. Med.* **178**, 1541 (1993).
94. R. Ni *et al.*, *Exp. Cell Res.* **215**, 332 (1995).
95. N. Hiramatsu *et al.*, *Hepatology* **19**, 1354 (1994).
96. D. Watanabe and S. Nagata, unpublished observations.
97. A. N. Theofilopoulos *et al.*, *J. Exp. Med.* **162**, 1 (1985).
98. K.-M. Debatin, C. K. Goldmann, R. Bamford, T. A. Waldmann, P. H. Krammer, *Lancet* **335**, 497 (1990).
99. We thank the members of our laboratories in Osaka and in Marseille, and collaborators from other laboratories, for dedicated participation to the work quoted in this article. We thank M. Raff for critical reading of the manuscript. S.N. is grateful to O. Hayaishi and C. Weissmann for encouragement and discussion. Supported in part by Grants-in-Aid from the Ministry of Education, Science and Culture of Japan (to S.N.), and the Centre National de la Recherche Scientifique, the Institut National de la Santé et de la Recherche Médicale and l'Association pour la Recherche contre le Cancer (to P.G.).

Apoptosis in the Pathogenesis and Treatment of Disease

Craig B. Thompson

In multicellular organisms, homeostasis is maintained through a balance between cell proliferation and cell death. Although much is known about the control of cell proliferation, less is known about the control of cell death. Physiologic cell death occurs primarily through an evolutionarily conserved form of cell suicide termed apoptosis. The decision of a cell to undergo apoptosis can be influenced by a wide variety of regulatory stimuli. Recent evidence suggests that alterations in cell survival contribute to the pathogenesis of a number of human diseases, including cancer, viral infections, autoimmune diseases, neurodegenerative disorders, and AIDS (acquired immunodeficiency syndrome). Treatments designed to specifically alter the apoptotic threshold may have the potential to change the natural progression of some of these diseases.

The survival of multicellular organisms depends on the function of a diverse set of differentiated cell types. Once development is complete, the viability of the organism depends on the maintenance and renewal of these diverse lineages. Within vertebrates, different cell types vary widely in the mechanisms by which they maintain themselves over the life of the organism. Blood cells, for instance, undergo constant renewal from hematopoietic progenitor cells. In addition, lymphocytes and cells within the reproductive organs undergo cyclical expansions and contractions as they participate in host defense and reproduction, respectively. In contrast, neural cells have at best a limited capacity for self-renewal, and most neurons survive for the life of the organism.

Within each lineage, the control of cell number is determined by a balance between cell proliferation and cell death (Fig. 1). Cell proliferation is a highly regulated process with numerous checks and balances. For example, growth factors and proto-oncogenes are positive regulators of cell cycle progression (*1*). In contrast, tumor suppressor genes act to oppose uncontrolled cell proliferation (*1*, *2*). Tumor suppressors can prevent cell cycle progression by inhibiting the activity of proto-oncogenes. In the last 15 years there has been a rapid increase in our understanding of the mechanisms that control cell proliferation.

Biologists are now beginning to appreciate that the regulation of cell death is just as complex as the regulation of cell proliferation (*3*). The differentiated cells of multicellular organisms all appear to share the ability to carry out their own death through activation of an internally encoded suicide program (*4*). When activated, this suicide program initiates a characteristic form of cell death called apoptosis (*5*, *6*). Apoptosis can be triggered by a variety of extrinsic and intrinsic signals (*7*) (Fig. 2). This type of regulation allows for the elimination of cells that have been produced in excess, that have developed improperly, or that have sustained genetic damage. Although diverse signals can induce apoptosis in a wide variety of cell types, a number of evolutionarily conserved genes regulate a final common cell death pathway that is conserved from worms to humans (*8*) (Fig. 3).

Apoptotic cell death can be distinguished from necrotic cell death (*4*–*6*). Necrotic cell death is a pathologic form of cell death resulting from acute cellular injury, which is typified by rapid cell swelling and lysis. In contrast, apoptotic cell death is

The author is in the Howard Hughes Medical Institute, Departments of Medicine and Molecular Genetics and Cell Biology, Gwen Knapp Center for Lupus and Immunology Research, University of Chicago, Chicago, IL 60637, USA.

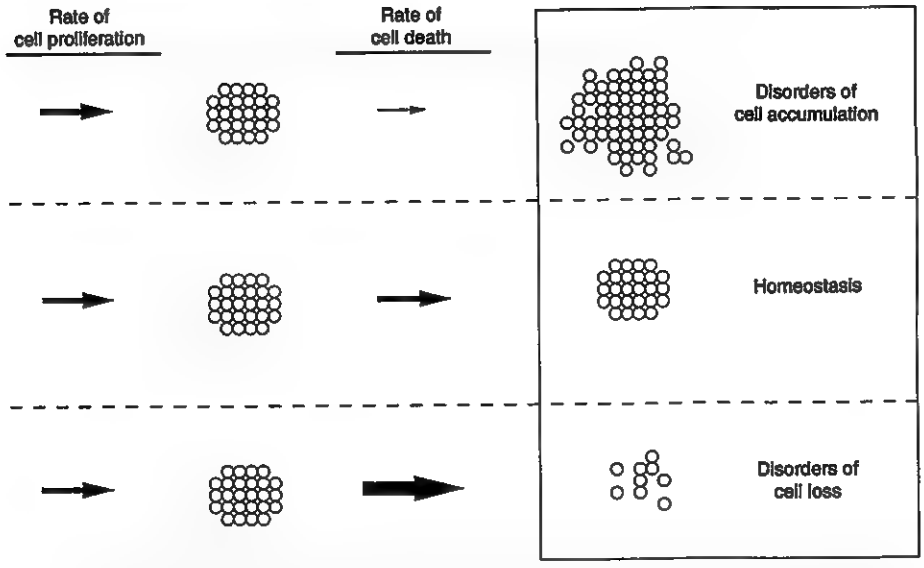

Fig. 1. The effect of different rates of cell death on homeostasis. In mature organisms, cell number is controlled as a result of the net effects of cell proliferation and cell death. Here, the rates of cell proliferation and cell death are indicated by the size of the arrows. In the absence of compensatory changes in the rate of cell proliferation, changes in the rate of cell death can result in either cell accumulation or cell loss.

Inhibitors of Apoptosis

Physiologic inhibitors
1. Growth factors
2. Extracellular matrix
3. CD40 ligand
4. Neutral amino acids
5. Zinc
6. Estrogen
7. Androgens

Viral genes
1. Adenovirus *E1B*
2. Baculovirus *p35*
3. Baculovirus *IAP*
4. Cowpox virus *crmA*
5. Epstein-Barr virus *BHRF1, LMP-1*
6. African swine fever virus *LMW5-HL*
7. Herpesvirus γ1 34.5

Pharmacological agents
1. Calpain inhibitors
2. Cysteine protease inhibitors
3. Tumor promoters
   PMA
   Phenobarbital
   α-Hexachlorocyclohexane

Inducers of Apoptosis

Physiologic activators
1. TNF family
   Fas ligand
   TNF
2. Transforming growth factor β
3. Neurotransmitters
   Glutamate
   Dopamine
   N-methyl-D-aspartate
4. Growth factor withdrawal
5. Loss of matrix attachment
6. Calcium
7. Glucocorticoids

Damage-related inducers
1. Heat shock
2. Viral infection
3. Bacterial toxins
4. Oncogenes
   myc, rel, E1A
5. Tumor suppressors
   p53
6. Cytolytic T cells
7. Oxidants
8. Free radicals
9. Nutrient deprivation—antimetabolites

Therapy-associated agents
1. Chemotherapeutic drugs
   Cisplatin, doxorubicin, bleomycin, cytosine arabinoside, nitrogen mustard, methotrexate, vincristine
2. Gamma radiation
3. UV radiation

Toxins
1. Ethanol
2. β-amyloid peptide

Fig. 2. A partial list of the agents that have been reported to induce or inhibit apoptosis.

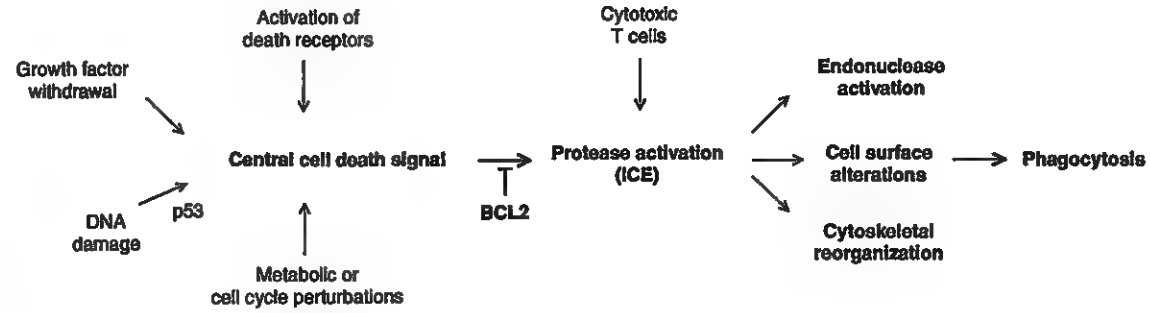

Fig. 3. A hypothetical model for the regulation of apoptotic cell death. As diagrammed, the major end point of apoptotic cell death is the removal of the dying cell by phagocytosis. One of the difficulties in determining the contribution of apoptosis to the pathogenesis of disease is the rapidity with which the phagocytosis of apoptotic cells occurs in vivo. Both the death repressor *BCL2* and ICE are members of larger gene families.

characterized by controlled autodigestion of the cell. Cells appear to initiate their own apoptotic death through the activation of endogenous proteases. This results in cytoskeletal disruption, cell shrinkage, and membrane blebbing. Apoptosis also involves characteristic changes within the nucleus. The nucleus undergoes condensation as endonucleases are activated and begin to degrade nuclear DNA. In many cell types, DNA is degraded into DNA fragments the size of oligonucleosomes, whereas in others larger DNA fragments are produced. Apoptosis is also characterized by a loss of mitochondrial function. This has led to speculation that mitochondria may have an important function in regulating apoptosis; however, data to support this hypothesis are currently unavailable. The dying cell maintains its plasma membrane integrity. However, alterations in the plasma membrane of apoptotic cells signal neighboring phagocytic cells to engulf them and thus to complete the degradation process (*9*). Cells not immediately phagocytosed break down into smaller membrane-bound fragments called apoptotic bodies. An important feature of apoptosis is that it results in the elimination of the dying cell without induction of an inflammatory response. In contrast, necrotic cell death is associated with an early loss of cell membrane integrity, resulting in leakage of cytoplasmic contents and the induction of an inflammatory response.

In most tissues, cell survival appears to depend on the constant supply of survival signals provided by neighboring cells and the extracellular matrix (*10*). Cells from most organs will undergo apoptosis if cultured individually in the absence of exogenous survival factors. Death in these cases appears to occur even in the absence of new protein synthesis, which suggests that the proteins that mediate apoptosis are constitutively expressed in many cell types (*4*). One interpretation of these results is that most cells are programmed to commit suicide if survival signals are not received from the environment, either constantly or at regular intervals (*4*). Viewed in this way, apoptotic cell death can be thought of as a

default pathway. However, some types of physiologic cell death involve the induction of apoptosis through mechanisms that require new protein synthesis.

Recent evidence suggests that the failure of cells to undergo apoptotic cell death might be involved in the pathogenesis of a variety of human diseases, including cancer, autoimmune diseases, and viral infections (6). In addition, a wide number of diseases characterized by cell loss, such as neurodegenerative disorders, AIDS (acquired immunodeficiency syndrome), and osteoporosis, may result from accelerated rates of physiologic cell death (Fig. 4). Specific therapies designed to enhance or decrease the susceptibility of individual cell types to undergo apoptosis could form the basis for treatment of a variety of human diseases.

Disorders Associated with Increased Cell Survival

Diseases characterized by the accumulation of cells include cancer, autoimmune diseases, and certain viral illnesses. Cell accumulation can result from either increased proliferation or the failure of cells to undergo apoptosis in response to appropriate stimuli (Fig. 1). Although much attention has focused on the potential role of cell proliferation in these disorders, increasing evidence suggests that alterations in the control of cell survival are important in the pathogenesis of these so-called proliferative disorders.

Cell death in cancer. Cells from a wide variety of human malignancies have a decreased ability to undergo apoptosis in response to at least some physiologic stimuli (*11*). This is most apparent in metastatic tumors. Most normal cells depend on environment-specific factors to maintain their viability (*10*). This dependence may serve to prevent normal cells from surviving in nonphysiologic sites. Metastatic tumor cells have circumvented this homeostatic mechanism and can survive at sites distinct from the tissue in which they arose. To do this, tumor cells must develop some degree of independence from the survival factors that restrict the distribution of their nontransformed counterparts. Recent advances are beginning to shed some light on the molecular bases for the increased resistance of tumor cells to undergo apoptosis, and several genes that are critical in the regulation of apoptosis have been defined.

The gene *BCL2* was first discovered as a result of its location at the site of a translocation between chromosomes 14 and 18 and is present in most human follicular lymphomas (*12*). Initially viewed as an oncogene, *BCL2* was found to have little or no ability to promote cell cycle progression or cell proliferation. Instead, overexpression of *BCL2* specifically prevents cells from initiating apoptosis in response to a number of stimuli (*13*). Furthermore, the introduction of genes that inhibit *BCL2* can induce apoptosis in a wide variety of tumor types, which suggests that many tumors continually rely on *BCL2* or related gene products to prevent cell death (*14*). Consistent with this hypothesis, *BCL2* expression has been associated with a poor prognosis in prostatic cancer, colon cancer, and neuroblastoma (*15*).

Recently, it has been demonstrated that *BCL2* is only one member of a family of genes that can control the apoptotic threshold of a cell (*16*). The roles of these other *BCL2* family members in the pathogenesis of human malignancies are just beginning to be examined. In tumor cell lines, overexpression of *BCL2* or of the related gene *BCLx* has been found to confer resistance to cell death in response to chemotherapeutic agents such as cytosine arabinoside, methotrexate, vincristine, and cisplatin (*17*). These results are surprising because chemotherapy was previously thought to kill cells by inducing irreversible metabolic damage that results in target cell necrosis. It now appears that the primary mechanism by which most chemotherapeutic agents induce cell death is through creating aberrations in cellular physiology that result in the induction of apoptosis. Consistent with this hypothesis, overexpression of *BCL2* or related genes can result in a multidrug resistance phenotype in vitro. The role of the *BCL2* family in the development of multidrug resistance in vivo has not yet been evaluated.

A wide variety of chemotherapeutic agents work by initiating DNA damage. Cell death in response to DNA damage in most instances has been shown to result from apoptosis. The p53 gene product is required for cells to initiate apoptosis in response to genotoxic damage (*18*). It is also fundamental in the pathway that leads from the sensing of DNA damage to the initiation of apoptosis. The inability of cells to undergo apoptosis in response to DNA damage may underlie the enhanced resistance to chemotherapeutic agents and radiation observed in tumors that are deficient in p53 (*19*). The failure of cells to die in response to DNA damage may also underlie the high rate of gene amplification observed in p53-deficient cells (*20*). Cells unable to undergo apoptosis in response to DNA damage may be more prone to acquire genetic alterations than normal cells. Errors in the repair of DNA damage that might otherwise induce apoptosis could contribute to the high mutation rate observed in many human cancers.

For years investigators have used chemicals referred to as tumor promoters to induce experimental malignancies. The exact role of tumor promoters in the pathogenesis of cancer is not clear. Most tumor promoters cannot induce cell proliferation on their own. Recently, it has been shown that tumor promoters such as phorbol myristate acetate (PMA) and α-hexachlorocyclohexane can act as specific survival factors for the cells in which they promote tumor development (*21*). These data suggest that inhibition of apoptosis is more important in the development of malignancy than previously believed.

A critical question in cancer biology is why two or more cooperative transforming events are usually required to induce a full neoplastic lesion. One potential explanation is that oncogene transformation leads to a dysregulation of genes that control cell division, such as cyclins and cyclin-dependent kinases (*22*). Cells normally appear to be able to detect such an imbalance and respond by undergoing apoptosis. Apoptosis may represent a mechanism for protecting the organism from cells that have acquired genetic alterations that predispose them to cell proliferation. For example, in the absence of other transforming events, dysregulation of the *myc* oncogene leads to the induction of apoptosis in serum-starved fibroblasts (*23*). However, simultaneous overexpression of *BCL2* prevents this apoptotic

Diseases Associated with the Inhibition of Apoptosis

1. Cancer
   - Follicular lymphomas
   - Carcinomas with *p53* mutations
   - Hormone-dependent tumors
     - Breast cancer
     - Prostate cancer
     - Ovarian cancer
2. Autoimmune disorders
   - Systemic lupus erythematosus
   - Immune-mediated glomerulonephritis
3. Viral infections
   - Herpesviruses
   - Poxviruses
   - Adenoviruses

Diseases Associated with Increased Apoptosis

1. AIDS
2. Neurodegenerative disorders
   - Alzheimer's disease
   - Parkinson's disease
   - Amyotrophic lateral sclerosis
   - Retinitis pigmentosa
   - Cerebellar degeneration
3. Myelodysplastic syndromes
   - Aplastic anemia
4. Ischemic injury
   - Myocardial infarction
   - Stroke
   - Reperfusion injury
5. Toxin-induced liver disease
   - Alcohol

Fig. 4. Diseases associated with the induction or inhibition of apoptotic cell death.

response. Cooperation between *myc* and *BCL2* in the pathogenesis of experimental tumors has also been demonstrated (*24*).

Cell death and autoimmunity. Physiologic regulation of cell death is essential for the removal of potentially autoreactive lymphocytes during development and for the removal of excess cells after the completion of an immune response. Failure to remove autoimmune cells that arise during development or that develop as a result of somatic mutation during an immune response can result in autoimmune disease. Recent work in animal model systems has clearly demonstrated the importance of dysregulated apoptosis in the etiology of autoimmune diseases. For example, one molecule critical in regulating cell death in lymphocytes is the cell surface receptor Fas, a member of the tumor necrosis factor (TNF) receptor family (*25*). Stimulation of Fas on activated lymphocytes can induce apoptosis. Two forms of hereditary autoimmune disease have been attributed to alterations in Fas-mediated apoptosis (*25*, *26*). MRL-lpr mice, which develop fatal systemic lupus erythematosus by 6 months of age, have a mutation in the Fas receptor. In contrast, the GLD mouse, which develops a similar illness, has a mutation in the Fas ligand (*26*). In humans, a secreted form of Fas has been identified (*27*). Patients with systemic lupus erythematosus have elevated levels of soluble Fas, which may competitively inhibit Fas ligand–Fas interactions. The resulting decrease in Fas-mediated apoptosis may contribute to the accumulation of autoimmune cells in this disorder. A lupuslike autoimmune disease has also been reported in transgenic mice constitutively overexpressing *BCL2* in their B cells (*28*). Finally, linkage analysis has established an association between the *BCL2* locus and autoimmune diabetes in nonobese diabetic (NOD) mice (*29*).

To date, no autoimmune diseases in humans have been directly linked to genes involved in the control of apoptosis. However, investigations into the role of apoptosis in the development of autoimmune diseases such as systemic lupus erythematosus, rheumatoid arthritis, psoriasis, inflammatory bowel disease, and autoimmune diabetes mellitus are just beginning. Alterations in the susceptibility of lymphocytes to die by apoptosis in vitro have been reported in several of these diseases (*30*).

Cell death in viral infection. The disruption of cell physiology as a result of viral infection can cause an infected cell to undergo apoptosis (*31*). The suicide of an infected cell may be viewed as a cellular defense mechanism to prevent viral propagation. Cytotoxic T cells also act to prevent viral spread (*32*) by recognizing and killing cells that present viral peptides in association with cell surface major histocompatibility complex (MHC) class I molecules. Recent evidence has demonstrated that T cells can induce cell death by activating the target cell's endogenous cell death program. Cytotoxic T cells induce apoptosis either by activation of the Fas receptor on the surface of the target cell or by introduction of proteases, such as granzyme B, which activate the cell death program from within the cytoplasm (*33*).

To circumvent these host defenses, a number of viruses have developed mechanisms to disrupt the normal regulation of apoptosis within the infected cell. For example, establishment of an effective adenoviral infection depends on the function of the E1B 19-kD protein (*34*). The E1B 19-kD protein has been shown to block apoptosis directly, and its function can be replaced in adenovirus by *BCL2*. Primary sequence and mutational analyses suggest that there may also be structural similarity between these two genes (*35*). The *BHRF1* gene of Epstein-Barr virus and the *LMW5-HL* gene of African swine fever virus both have sequence and functional similarity to *BCL2* (*36*).

Other viral genes that can inhibit apoptosis have been reported that show no similarity to *BCL2*. For example, both the p35 gene and the inhibitor of apoptosis gene (*IAP*) found in baculoviruses can inhibit apoptosis in response to a wide variety of stimuli (*37*). The ability of p35 to inhibit apoptosis is not dependent on the expression of any other viral proteins. Poxviruses appear to inhibit apoptosis by producing an inhibitor of the death effector molecule interleukin-1β (IL-1β)–converting enzyme (ICE). ICE is a cysteine protease closely related to the protein encoded by the *Caenorhabditis elegans* cell death gene, *ced-3*. The *ced-3* product is required for cells to undergo programmed cell death during development in *C. elegans* (*38*). The cowpox gene *crmA* is a member of the serpin family of protease inhibitors and acts as a specific inhibitor of ICE (*39*). The *crmA* gene can inhibit apoptosis in response to a number of stimuli and has also been shown to be required to inhibit the development of an inflammatory response to virally infected cells (*39*, *40*).

The prevention of apoptosis is also important for the establishment of viral latency. Epstein-Barr virus establishes a latent infection in B cells. The viral gene *LMP-1*, which is produced during latency, specifically up-regulates the expression of *BCL2*, potentially providing a survival advantage to latently infected cells (*41*). Chronic Sindbis virus infection has also been reported to be dependent on the host cell's expression of *BCL2* (*31*).

Disorders Associated with Excess Cell Death

Excessive cell death can result from acquired or genetic conditions that enhance the accumulation of signals that induce apoptosis or that decrease the threshold at which such events induce apoptosis. Although increased apoptotic cell death has been observed in many of the diseases discussed below, in most degenerative disorders an underlying defect in cell death control has not been defined.

Virus-induced lymphocyte depletion: AIDS. Perhaps the most dramatic example of virus-associated cell depletion is AIDS, which is induced by the human immunodeficiency virus (HIV) (*42*). The development of AIDS has been directly correlated with the depletion of $CD4^+$ T cells, the cellular targets of viral infection. It has been shown that CD4 acts as a receptor for viral attachment, thus facilitating HIV infection of $CD4^+$ T cells. Surprisingly, most T cells that die during HIV infections do not appear to be infected with HIV. Although a number of explanations have been proposed, recent evidence suggests that stimulation of the CD4 receptor, by its binding to the soluble viral product gp120, results in the enhanced susceptibility of uninfected T cells to undergo apoptosis (*43*). In several models of cell death, it has been suggested that disordered signal transduction can result in the induction of apoptosis, perhaps by inducing an abortive cell cycle. $CD4^+$ T cells are normally activated by simultaneous engagement of the T cell receptor and CD4 by antigen–MHC class II complexes on the surface of an antigen-presenting cell. Both $CD4^+$ T cells from normal individuals as well as from individuals with HIV undergo apoptosis in vitro if cell-surface CD4 is crosslinked before engagement of T cell receptors (*44*). Thus, it is possible that gp120 promotes apoptotic cell death by its interaction with CD4.

One important question concerning this model is why the virus would develop a mechanism to selectively deplete its host cell. The answer perhaps reflects the fact that $CD4^+$ T cells have an important function in establishing protective immunity against a wide variety of viral infections. The establishment of a chronic HIV infection may therefore depend on virally mediated depletion of $CD4^+$ T cells and the concomitant loss of a protective cell-mediated immune response. Viral replication itself may not be limited by this form of CD4-dependent cell death because the viral protein Nef specifically down-regulates the CD4 receptor on infected T cells (*45*). This down-regulation has been thought to be involved in preventing viral reinfections. However, it may also help to prevent apop-

tosis in response to dysregulated CD4 stimulation. Immunodepletion as a result of viral infection is not restricted to HIV. Viruses in birds, cats, and mice have all been reported to induce immune cell depletion during systemic infection (*46*).

Cell death in neurodegenerative disorders. A wide variety of neurological diseases are characterized by the gradual loss of specific sets of neurons (*47*). Such disorders include Alzheimer's disease, Parkinson's disease, amyotrophic lateral sclerosis (ALS), retinitis pigmentosa, spinal muscular atrophy, and various forms of cerebellar degeneration. In these diseases, cell death results in specific disorders of movement and central nervous system function. The cell loss in these diseases does not induce an inflammatory response, and apoptosis appears to be the mechanism of cell death. Oxidative stress, calcium toxicity, mitochondrial defects, excitatory toxicity, and deficiency of survival factors have all been postulated to contribute to the pathogenesis of these disorders (*48*). Each of these pathways predisposes neurons to apoptosis, either in vitro or in vivo. Overexpression of *BCL2* decreases the neurotoxicity of each of these potential inducers of cell death (*49*). Neurotrophic growth factors and the extracellular matrix also alter the apoptotic threshold of neural cells (*50*). Together, these data suggest a model in which the threshold for cell death is dynamically regulated. The apoptotic threshold of a cell is thus determined by the combined effects of external and internal survival factors.

One form of hereditary ALS results from mutations in the gene encoding copper-zinc superoxide dismutase (*51*). Patients with this form of ALS have a mutation that results in a decrease in the ability of a cell to detoxify free radicals. The cell injury caused by free radicals has been shown to induce cells to undergo apoptosis in vitro. Superoxide-induced death can be specifically inhibited by treatment with survival growth factors or antioxidants (*52*).

Retinal degeneration associated with retinitis pigmentosa occurs as a result of mutations in any one of three photoreceptor-specific genes: rhodopsin, the β subunit of cyclic guanosine monophosphate phosphodiesterase, and the peripherin gene. All three mutations lead to photoreceptor apoptosis (*53*). Apoptosis may be initiated in response to the accumulation of mutant proteins or as a result of the altered functional properties of the mutant proteins (*54*). In a hereditary rat model of light-induced retinal degeneration, intraocular injections of eight distinct neurotrophic and growth factors enhanced photoreceptor survival, whereas seven others displayed no beneficial effects (*55*). These data suggest that treatment of such disorders may be possible with specific neurotrophic factors either alone or in combination.

Alzheimer's disease is associated with the progressive accumulation of β-amyloid peptide in plaques. Mutations in the β-amyloid precursor protein are associated with some forms of familial Alzheimer's disease. Recently, several groups have shown that β-amyloid peptide induces neurons to undergo apoptosis (*56*). This effect can be reversed by antioxidants (*57*).

The spinal muscular atrophies are a group of recessive neurodegenerative disorders of childhood. These disorders are characterized by progressive spinal cord motor neuron depletion. One of the genes recently linked to these disorders, neuronal apoptosis inhibitory protein (*NAIP*), is homologous to the baculovirus inhibitor of apoptosis protein (IAP) (*58*). Baculovirus *IAP* genes have been shown to inhibit apoptosis in insect cells independent of other viral proteins. These data suggest that mutations in the *NAIP* gene may result in motor neurons being more susceptible to apoptosis in patients with spinal muscular atrophy.

Cell death in blood cell disorders. Mature blood cells are constantly being produced from hematopoietic stem cells located in the bone marrow. The regulation of hematopoiesis is influenced by a number of growth factors, including stem cell factor, erythropoietin, colony-stimulating factors, and thrombopoietin (*59*). In addition to stimulating the proliferation of hematopoietic progenitors, hematopoietic growth factors are required to support the survival of their target cells (*60*). Hematopoietic progenitors rapidly undergo apoptosis in vitro if deprived of growth factors. In fact, hematopoietic growth factors are also important in regulating the survival of postmitotic blood cells such as neutrophils.

It has been suggested that hematopoietic differentiation is primarily determined intrinsically within the precursor cell rather than as a result of the inductive effects of hematopoietic growth factors (*61*). Consistent with this view, hematopoietic stem cells in which apoptosis is suppressed by overproduction of *BCL2* can differentiate in the absence of extracellular growth factors or cell division. Together, these data suggest that hematopoietic growth factors control blood cell production at least in part by inhibiting apoptosis during the expansion and differentiation of intrinsically committed progenitors.

A number of hematologic diseases are associated with a decreased production of blood cells. Such disorders include anemia associated with chronic disease, aplastic anemia, chronic neutropenia, and the myelodysplastic syndromes. Disorders of blood cell production, such as myelodysplastic syndrome and some forms of aplastic anemia, are associated with increased apoptotic cell death within the bone marrow (*62*). These disorders could result from the activation of genes that promote apoptosis, acquired deficiencies in stromal cells or hematopoietic survival factors, or the direct effects of toxins and mediators of immune responses.

Several hematopoietic growth factors are now in widespread clinical use because of their ability to increase the net production of individual types of blood cells (*59*). For example, erythropoietin can be used to augment red blood cell production in patients with anemia secondary to renal failure and other chronic illnesses. Granulocyte-macrophage colony-stimulating factor (GM-CSF), macrophage CSF, and granulocyte CSF have all been used to promote the recovery of granulocytes and macrophages after systemic chemotherapy for cancer.

Additional Disorders in Which Apoptosis May Function

Two common disorders associated with cell death are myocardial infarctions and stroke. These diseases arise primarily as a result of an acute loss of blood flow (ischemia). In both disorders, cells within the central area of ischemia appear to die rapidly as a result of necrosis. However, outside the central ischemic zone, cells die over a more protracted time period and morphologically appear to die by apoptosis (*63*). Ischemia of both neurons and cardiac myocytes in culture results in the induction of apoptosis (*64*). Agents known to be inhibitors of apoptosis in vitro have been shown to limit infarct size in these disorders (*65*). However, the most effective method of limiting infarct size is restoration of blood flow. Advances in medicine have allowed for the development of a number of techniques to restore blood flow rapidly in acutely occluded blood vessels. Unfortunately, further tissue injury frequently occurs during establishment of reperfusion. Reperfusion is associated with acute increases in free radical production and increases in intracellular calcium, both potent inducers of apoptosis. The death of cardiomyocytes that occurs during reperfusion bears all the hallmarks of apoptosis (*66*). Whether agents that alter the apoptotic threshold can prevent reperfusion injury remains to be determined.

Relatively little is known about the mechanisms underlying the two major degenerative disorders of the musculoskeletal system: osteoporosis and degenerative arthritis. To date, no evidence exists that the genes involved in the control of apoptosis are involved in the pathogenesis of these disorders. Nevertheless, the progressive cell death of chondrocytes in osteoarthritis and osteocyte cell death in osteoporosis have morphological features suggestive of apoptosis (*67*).

Liver cells also undergo programmed cell death. In fact, the term apoptosis was originally used to describe the cell death that occurred outside the zone of central necrosis resulting from ligation of the portal vein (5). Since that time, various toxins (including alcohol) that are associated with acute fatty degeneration of the liver have been shown to induce apoptosis in hepatocytes (68).

Regulation of Cell Death: Therapeutic Potential

A number of effective methods that induce target cells to undergo apoptosis already exist. Both chemotherapeutic agents and radiation induce tumor cell death primarily by causing damage that induces the cell to commit suicide (17, 69). In addition, many tumors retain some of the same physiologic controls for cell death as the cells from which they arise. For example, tumors arising in reproductive organs are responsive to hormonal manipulation that results in apoptosis (6, 70). Prostate cancers can be treated with androgen-ablation therapy. Moreover, breast cancers often undergo regression when treated with estrogen receptor antagonists. Treatments that restore the ability to properly regulate apoptosis could also be of considerable benefit in some malignancies. For example, it has recently been shown that the growth of human B cell lymphomas bearing *BCL2* translocations can be specifically inhibited in vitro by antisense oligonucleotides targeted against the *BCL2* gene (71).

Autoimmune diseases are characterized by the proliferative expansion of lymphocytes reactive to self-antigens. Several groups have been exploring methods to induce selective apoptosis in the autoreactive cells that cause disease. Recently, it has been shown that repetitive treatment with antigen can result in the selective death of antigen-reactive lymphocytes in vivo. Although the exact mechanisms by which such treatments induce apoptosis are unclear, the treatments may prime cells for Fas-mediated death (72). Specific deletion of lymphocytes by repetitive treatment with a disease-associated autoantigen has been shown to be effective in the treatment of experimental autoimmune encephalitis in mice (73). Similar treatment strategies may prove effective in human autoimmune disease if the specific antigens involved in the autoimmune reaction can be identified.

Conversely, treatments that increase a cell's resistance to undergo apoptosis may be of benefit in degenerative disorders. These treatments may be of benefit even in the absence of specific alterations in the genes involved in cell death regulation. Current evidence suggests that the susceptibility of cells to undergo apoptosis is regulated continuously. For example, enhancing the expression of *BCL2* can increase the resistance of cells to almost all apoptotic stimuli (13, 17). Thus, treatments that can increase the apoptotic thresholds of specific cells may be beneficial in the treatment of disorders associated with cell loss. Such treatments include the use of growth factors to promote hematopoietic cell recovery after cancer chemotherapy (56), trials of neurotrophic survival factors to enhance the survival of neurons in neurodegenerative disorders or trauma (50, 55), and treatments with antioxidants such as *n*-acetyl cysteine to prevent the death of $CD4^+$ T cells in response to HIV infection (74). Agents that alter calcium metabolism are currently being tested for the treatment of ischemic injuries (75).

It may also be possible to alter the apoptotic threshold by inhibiting the action of cell surface death effectors. For example, treatment with soluble Fas receptor or TNF antibodies may limit cell death in vivo by preventing deaths induced by Fas ligand and TNF, respectively (27, 76). Although the use of cell surface receptors and second messenger systems to regulate cell death responses in vivo has much appeal, it should be reemphasized that these agents can have pleiotropic effects. Under some circumstances Fas activation has been reported to stimulate lymphocyte proliferation instead of cell death (77). IL-12 treatment in vivo has recently been shown to protect bone marrow cells from gamma irradiation; however, it also potentiates cell death within the gastrointestinal tract in response to the same stimulus (78).

In principle, the genes involved in central cell death control, such as members of the *BCL2* and ICE families, could provide ideal targets for therapeutic intervention. However, most diseases are not characterized by a generalized increase in the susceptibility or resistance to apoptosis. There may be relatively little benefit in a therapy that enhances the survival of all neural cells at the expense of an increase in autoimmune disease or the enhancement of tumor progression through the prevention of apoptotic cell death.

Several observations suggest that the central mediators of apoptosis may still be pharmacologically manipulated in a cell-specific fashion. Individual tissues in the body can vary significantly in the expression of individual members of the *BCL2* and *ICE* gene families (79). Furthermore, specific inhibitors of individual members of the ICE family exist. The gene *crmA* inhibits ICE but not the related Ich-1 cysteine protease (80). This suggests that cysteine protease inhibitors may be developed that are specific for individual members of the ICE family. There is also evidence that alternatively spliced forms of members of both the *BCL2* family and cysteine protease family of death effectors can act as dominant inhibitors, perhaps by forming multimers that inhibit the function of active family members (80, 81). Pharmacologic agents that mimic the inhibitors or prevent specific protein-protein interactions within the *BCL2* or ICE families may have relative specificity for individual family members or heteromers formed from them. Finally, there is evidence that both the expression and function of individual members of the *BCL2* and ICE families are themselves regulated by lineage-specific signal transduction events. *BCL2* has been shown to undergo specific modulation in response to cytokines, cell-cell contact, or cell contact with the extracellular matrix (82). In addition, certain growth factors may function by inducing posttranslational modification of *BCL2* (83). Recent data analyzing mice deficient in *BCL2* expression suggest that the function of *BCL2* is absolutely necessary only in a limited number of normal cell types or, alternatively, that there is significant redundancy within the *BCL2* family such that specific loss of *BCL2* is relatively well tolerated outside of the immune and renal systems (84). Therefore, systemic inhibition of *BCL2* may not be as toxic as might have been expected initially.

One future application of our knowledge concerning cell death may be in designing safer, more effective vectors for gene therapy or vaccination. That many DNA viruses require survival genes to establish persistent viral infection may allow for the generation of vaccines consisting of attenuated viruses that do not have the ability to establish latent infections. Similarly, engineering gene therapy vectors to incorporate specifically regulated cell survival genes may help facilitate the establishment and removal of genetically altered cells in vivo.

REFERENCES AND NOTES

1. T. Hunter, *Curr. Opin. Gen. Dev.* **3**, 1 (1993); E. Rozengurt, *Curr. Opin. Cell Biol.* **4**, 161 (1992).
2. A. J. Levine, *Annu. Rev. Biochem.* **62**, 623 (1993).
3. R. E. Ellis, J. Yuan, H. R. Horvitz, *Annu. Rev. Cell Biol.* **7**, 663 (1991).
4. M. C. Raff, *Nature* **356**, 397 (1992); M. D. Jacobson, J. F. Burne, M. C. Raff, *EMBO J.* **13**, 1899 (1994).
5. A. H. Wyllie, J. F. R. Kerr, A. R. Currie, *Int. Rev. Cytol.* **68**, 251 (1980); J. F. R. Kerr, A. H. Wyllie, A. R. Currie, *Br. J. Cancer* **26**, 18 (1972).
6. D. L. Vaux, G. Haecker, A. Strasser, *Cell* **76**, 777 (1994); W. Bursch, F. Oberhammer, R. Schulte-Hermann, *Trends Pharmacol. Sci.* **13**, 245 (1992).
7. L. Sachs and J. Lotem, *Blood* **82**, 15 (1993); T. M. Buttke and P. A. Sandstrom, *Immunol. Today* **15**, 7 (1994); J. C. Reed, *J. Cell Biol.* **124**, 1 (1994); D. L. Vaux, I. L. Weissman, S. K. Kim, *Science* **258**, 1955 (1992).
8. M. O. Hengartner and H. R. Horvitz, *Cell* **76**, 665 (1994); J. Yuan, S. Shaham, S. Ledoux, H. M. Ellis, H. R. Horvitz, *ibid.* **75**, 641 (1993).
9. R. E. Ellis, D. M. Jacobson, H. R. Horvitz, *Genetics* **129**, 79 (1991); V. A. Fadok *et al.*, *J. Immunol.* **148**, 2207 (1992); V. A. Fadok *et al.*, *ibid.* **149**, 4029 (1992); S. E. Hall, J. S. Savill, P. M. Henson, C.

Haslett, *ibid.* **153**, 3218 (1994).
10. M. C. Raff *et al.*, *Science* **262**, 695 (1993); G. T. Williams, C. A. Smith, E. Spooncer, T. M. Dexter, D. R. Taylor, *Nature* **343**, 76 (1990); P. E. Neiman, S. J. Thomas, G Loring, *Proc. Natl Acad. Sci. U S.A.* **88**, 5857 (1991); N. Boudreau, C. J. Sympson, Z. Werb, M. J. Bissel, *Science* **267**, 891 (1995); J. G. Cyster, S. B. Hartley, C. C. Goodnow, *Nature* **371**, 389 (1994); S. Cohen, *Proc. Natl. Acad. Sci. U.S.A.* **46**, 302 (1960)
11. B. Hoffman and D. A. Liebermann, *Oncogene* **9**, 1807 (1994).
12. Y. Tsujimoto, J. Gorham, J. Cossman, E. Jaffe, C. M. Croce, *Science* **229**, 1390 (1985); A. Bakhshi *et al.*, *Cell* **41**, 899 (1985); M. L. Cleary and J. Sklar, *Proc. Natl. Acad. Sci. U.S.A.* **82**, 7439 (1985).
13. D. M. Hockenbery, G. Nuñez, C. Milliman, R D. Schreiber, S. J. Korsmeyer, *Nature* **348**, 334 (1990); G. Nuñez *et al*, *J. Immunol.* **144**, 3602 (1990); D. L. Vaux, S. Cory, J. M. Adams, *Nature* **335**, 440 (1988); D. M. Hockenbery, Z. N. Oltvai, X.-M. Yin, C. L. Milliman, S. J. Korsmeyer, *Cell* **75**, 241 (1993).
14. M. F. Clarke *et al.*, unpublished results.
15. T. J. McDonnell *et al.*, *Cancer Res.* **52**, 6940 (1992); A. Hague, M. Moorghen, D. Hicks, M Chapman, C. Paraskeva, *Oncogene* **9**, 3367 (1994); V. P. Castle *et al.*, *Am. J. Pathol.* **143**, 1543 (1993).
16. L. H. Boise *et al.*, *Cell* **74**, 597 (1993); E. Y. Lin, A. Orlofsky, M. S. Berger, M. B. Prystowsky, *J. Immunol.* **151**, 1979 (1993); K. M. Kozopas, T. Yang, H. L Buchan, P. Zhou, R W. Craig, *Proc. Natl. Acad. Sci U.S A.* **90**, 3516 (1993); Z. N. Oltvai, C. L. Milliman, S J. Korsmeyer, *Cell* **74**, 609 (1993).
17. T. Ohmori *et al*, *Biochem. Biophys. Res. Commun.* **192**, 30 (1993); J. Lotem and L. Sachs, *Cell Growth. Differ.* **4**, 41 (1993); T. Miyashita and J. C. Reed, *Blood* **81**, 151 (1993), A. Minn, C. Rudin, C. B. Thompson, unpublished observations.
18. S. W. Lowe, E. M. Schmitt, S. W Smith, B. A. Osborne, T. Jacks, *Nature* **362**, 847 (1993), A R Clarke *et al.*, *ibid.*, p. 849; J. M. Lee and A Bernstein, *Proc. Natl. Acad. Sci. U.S.A.* **90**, 5742 (1993).
19. S. W. Lowe *et al.*, *Science* **266**, 807 (1994)
20. X. Lu and D. P. Lane, *Cell* **75**, 765 (1993).
21. W. Bursch *et al.*, *Carcinogenesis* **11**, 847 (1990), D McConkey *et al.*, *J. Biol. Chem.* **264**, 13399 (1989)
22. L. Shi *et al.*, *Science* **263**, 1143 (1994), R. S. Freeman, S. Estus, E. M. Johnson Jr., *Neuron* **12**, 343 (1994); L. L. Rubin, K. L. Philpott, S. F. Brooks, *Curr. Opin Cell. Biol.* **3**, 391 (1993).
23. G. I. Evan *et al.*, *Cell* **69**, 119 (1992).
24. A. Strasser, A. W. Harris, M. L. Bath, S. Cory, *Nature* **348**, 331 (1990).
25. R. Watanabe-Fukunaga, C. I. Brannan, N. G. Copeland, N. A. Jenkins, S. Nagata, *ibid.* **356**, 314 (1992).
26. T. Suda, T. Takahashi, P. Golstein, S. Nagata, *Cell* **75**, 1169 (1993).
27. J Cheng *et al.*, *Science* **263**, 1759 (1994).
28. A. Strasser *et al.*, *Proc. Natl Acad. Sci. U.S.A.* **88**, 8661 (1991).
29. H. J Garchon, J. J. Luan, L. Eloy, P. Bedossa, J. F. Bach, *Eur. J. Immunol.* **24**, 380 (1994)
30. J. D. Mountz, J. Wu, J. Cheng, T. Zhou, *Arthritis Rheum.* **37**, 1415 (1994); W. Emlen, J. Niebur, R. Kadera, *J. Immunol.* **152**, 3685 (1994).
31. B. Levine *et al.*, *Nature* **361**, 739 (1993).
32. P. A. Henkart, *Immunity* **1**, 343 (1994)
33. D Kägi *et al.*, *Science* **265**, 528 (1994); D. Kägi *et al.*, *Nature* **369**, 31 (1994); J. W. Heusel, R. L. Wesselschmidt, S. Shresta, J. H. Russell, T. J. Ley, *Cell* **76**, 977 (1994).
34. L. Rao *et al.*, *Proc. Natl. Acad. Sci. U.S.A.* **89**, 7742 (1992).
35. J. M. Boyd *et al.*, *Cell* **79**, 341 (1994).
36. J. G. Neilan *et al.*, *J. Virol.* **67**, 4391 (1993); S. Henderson *et al.*, *Proc. Natl. Acad. Sci. U.S.A.* **90**, 8479 (1993)
37. R. J. Clem, M. Fechheimer, L. K. Miller, *Science* **254**, 1388 (1991), A. Sugimoto, P. D. Friesen, J. H. Rothman, *EMBO J.* **13**, 2023 (1994), S. Rabizadeh, D. J. LaCount, P. D. Friesen, D. E. Bredesen, *J. Neurochem.* **61**, 2318 (1993); R. J. Clem and L. K. Miller, *Mol. Cell. Biol* **14**, 5212 (1994).
38. M. Miura, H. Zhu, R. Rotello, E. A. Hartwieg, J. Yuan, *Cell* **75**, 653 (1993).
39. C. A. Ray *et al.*, *ibid.* **69**, 597 (1992).
40. V. Gagliardini *et al.*, *Science* **263**, 826 (1994).
41. S. Henderson *et al.*, *Cell* **65**, 1107 (1991).
42. L. Meyaard *et al.*, *Science* **257**, 217 (1992).
43. J. C. Ameisen and A. Capron, *Immunol. Today* **12**, 102 (1991); H. Groux *et al.*, *J. Exp. Med* **175**, 331 (1992); M.-L. Gougeon and L. Montagnier, *Science* **260**, 1269 (1993).
44. M. K. Newell, L. J. Haughn, C. R. Maroun, M. H. Julius, *Nature* **347**, 286 (1990); N. K. Banda *et al.*, *J. Exp. Med.* **176**, 1099 (1992)
45. D. R. Littman, *Curr. Biol.* **4**, 618 (1994)
46. A. L. Guiot *et al.*, *C. R. Acad Sci. Ser. III* **316**, 1297 (1993); A. C. Vasconcelos and K. M Lam, *J. Gen. Virol.* **75**, 1803 (1994); D. A. Cohen *et al.*, *Cell Immunol.* **151**, 392 (1993).
47. O. Isacson, *Trends Neurosci.* **16**, 306 (1993), N. Heintz, *Trends Biochem. Sci.* **18**, 157 (1993).
48. D. W. Choi, *J. Neurobiol.* **23**, 1261 (1992); I Ziv *et al.*, *Neurosci Lett* **170**, 136 (1994).
49. L.-T. Zhong *et al.*, *Proc. Natl. Acad. Sci. U.S.A* **90**, 4533 (1993).
50. M. T. Herrero *et al.*, *Neuroscience* **56**, 965 (1993); M. Okamoto, S. Mori, H. Endo, *Brain Res.* **637**, 57 (1994); E. Arenas and H. Persson, *Nature* **367**, 368 (1994).
51. D. R. Rosen *et al.*, *Nature* **362**, 59 (1993), H.-X. Deng *et al.*, *Science* **261**, 1047 (1993).
52. C. M. Troy and M L. Shelanski, *Proc Natl. Acad. Sci. U.S A.* **91**, 6384 (1994).
53. G.-Q. Chang, Y. Hao, F. Wong, *Neuron* **11**, 595 (1993)
54. V. R. Rao, G. B. Cohen, D. D. Oprian, *Nature* **367**, 639 (1994)
55. M. M. LaVail *et al.*, *Proc Natl. Acad. Sci. U.S.A* **89**, 11249 (1992).
56. D. T. Loo *et al*, *ibid* **90**, 7951 (1993); A Takashima, K. Noguchi, K. Sato, T Hoshino, K. Imahori, *ibid.*, p. 7789
57. C. Behl, J. Davis, G M Cole, D. Schubert, *Biochem. Biophys Res Commun.* **186**, 944 (1992).
58. N. Roy *et al.*, *Cell* **80**, 167 (1995).
59. R. A. Fleischman, *Am. J. Med. Sci* **305**, 248 (1993), S. Blackwell and J. Crawford, *Pharmacotherapy* **12**, 20S (1992), D. Haase and C. Fonatsch, *Blut* **60**, 192 (1990).
60. K. Muta and S. B. Krantz, *J. Cell. Physiol.* **156**, 264 (1993); L. L. Kelley *et al.*, *Blood* **82**, 2340 (1993)
61. L. J. Fairbairn, G. J. Cowling, B M Reipert, T. M. Dexter, *Cell* **74**, 823 (1993).
62. Y. Yoshida, *Leukemia* **7**, 144 (1993).
63. J. J. Cohen, *Hosp. Pract.* **28**, 35 (1993).
64. M. Tanaka *et al.*, *Circ. Res.* **75**, 426 (1994); D. M Rosenbaum, J. Kalberg, J. A. Kessler, *Stroke* **25**, 857 (1994).
65. O. Uyama, T. Matsuyama, H. Michishita, H. Nakamura, M. Sugita, *Stroke* **23**, 75 (1992).
66. R. A. Gottlieb, K. O. Burleson, R A. Kloner, B. M. Babior, R. L. Engler, *J Clin. Invest* **94**, 1621 (1994).
67. C. R. Dunstan, N. M Somers, R. A. Evans, *Calcif. Tissue Int.* **53**, S113 (1993); A. M. Parfitt, *ibid.*, p. S82; W. Mohr and H. Lehmann, *Z. Rheumatol.* **51**, 35 (1992); Y. Ishizaki, J F Burne, M C Raff, *J. Cell Biol.* **126**, 1069 (1994).
68. R. D Goldin, N. C. Hunt, J. Clark, S. N. Wickramasinghe, *J. Pathol.* **171**, 73 (1993).
69. D. E. Fischer, *Cell* **78**, 539 (1994)
70. M. Colombel, C. A. Olsson, P.-Y. Ng, R. Buttyan, *Cancer Res.* **52**, 4313 (1992).
71. J. C. Reed *et al.*, *ibid* **50**, 6565 (1990).
72. G. G. Singer and A. K. Abbas, *Immunity* **1**, 365 (1994).
73. J. M. Critchfield *et al.*, *Science* **263**, 1139 (1994)
74. M. Roederer, F J. T. Staal, S. W Ela, L. A. Herzenberg, L. A. Herzenberg, *Pharmacology* **46**, 121 (1993).
75. J. Sharkey and S. P Butcher, *Nature* **371**, 336 (1994); M. P. Mattson, R. E. Rydel, I. Lieberburg, V. L. Smith-Swintosky, *Ann. N.Y. Acad. Sci.* **679**, 1 (1993).
76. M.-V Clement and I. Stamenkovic, *J Exp. Med.* **180**, 557 (1994).
77. M. R. Alderson *et al.*, *ibid.* **178**, 2231 (1993).
78. R Neta, S. M. Stiefel, F. Finkelman, S Herrmann, N Ali, *J. Immunol.* **153**, 4230 (1994).
79. M. González García *et al.*, *Development* **120**, 3033 (1994); D. M. Hockenbery, M. Zutter, W. Hickey, M. Nahm, S. J. Korsmeyer, *Proc. Natl. Acad. Sci. U S.A.* **88**, 6961 (1991).
80. L. Wang, M. Miura, L. Bergeron, H. Zhu, J. Yuan, *Cell* **78**, 739 (1994); S. Kumar, M Kinoshita, M. Noda, N. G. Copeland, N. A. Jenkins, *Genes Dev.* **8**, 1613 (1994)
81. X.-M. Yin, Z. N. Oltvai, S. J. Korsmeyer, *Nature* **369**, 321 (1994).
82. A. M. Genaro, J. A. Gonzalo, L. Bosea, C Martinez-A., *Eur. J. Immunol.* **24**, 2515 (1994); Y. Levy and J.-C Brouet, *J. Clin. Invest.* **93**, 424 (1994); M. Dancescu *et al.*, *J. Exp Med.* **176**, 1319 (1992).
83. W. S. May *et al.*, *J. Biol. Chem.* **269**, 26865 (1994).
84. D. J. Veis, C M. Sorenson, J. R Shutter, S. J. Korsmeyer, *Cell* **75**, 229 (1993).
85. I wish to thank J. Leiden, S. Reiner, C.-R. Wang, T. Lindsten, and the members of my laboratory for their thoughtful discussions and careful review of the manuscript, and T. Conway for her editorial assistance

Structure of a Hyperthermophilic Tungstopterin Enzyme, Aldehyde Ferredoxin Oxidoreductase

Michael K. Chan, Swarnalatha Mukund, Arnulf Kletzin, Michael W. W. Adams, Douglas C. Rees*

The crystal structure of the tungsten-containing aldehyde ferredoxin oxidoreductase (AOR) from *Pyrococcus furiosus*, a hyperthermophilic archaeon (formerly archaebacterium) that grows optimally at 100°C, has been determined at 2.3 angstrom resolution by means of multiple isomorphous replacement and multiple crystal form averaging. AOR consists of two identical subunits, each containing an Fe_4S_4 cluster and a molybdopterin-based tungsten cofactor that is analogous to the molybdenum cofactor found in a large class of oxotransferases. Whereas the general features of the tungsten coordination in this cofactor were consistent with a previously proposed structure, each AOR subunit unexpectedly contained two molybdopterin molecules that coordinate a tungsten by a total of four sulfur ligands, and the pterin system was modified by an intramolecular cyclization that generated a three-ringed structure. In comparison to other proteins, the hyperthermophilic enzyme AOR has a relatively small solvent-exposed surface area, and a relatively large number of both ion pairs and buried atoms. These properties may contribute to the extreme thermostability of this enzyme.

The recent discovery of life at temperatures of 100°C or higher is having increasing ramifications in biology and biotechnology (*1–4*). One of the fundamental questions arising from the study of these hyperthermophilic organisms concerns the structural and energetic basis of protein stability at extremely high temperatures, under conditions where many proteins from mesophilic organisms would be denatured. As part of a coordinated effort to establish the structural and functional properties of these intriguing macromolecules, we have initiated the structure determination of several proteins from hyperthermophilic organisms (*5*). We now describe the structure of one of the more unusual of these proteins, the aldehyde ferredoxin oxidoreductase (AOR) from the hyperthermophilic archaeon *Pyrococcus furiosus* (T_{opt} = 100°C); this protein catalyzes the reversible oxidation of aldehydes to their corresponding carboxylic acids with the accompanying reduction of the redox protein ferredoxin.

AOR was discovered because of the unusual growth requirement of *P. furiosus* for the third-row transition element tungsten (*6, 7*). Many enzymes utilize first-row transition elements at their active sites, but only two second- or third-row transition metals, tungsten and molybdenum, have such a biological role (*8*). Hence, one of the critical questions in studying proteins containing tungsten or molybdenum focuses on understanding the intrinsic properties that contribute to the incorporation of these metals compared to more traditional first row transition elements. The versatile redox chemistry of molybdenum and tungsten enables enzymes containing these elements to catalyze fundamental steps in the biological utilization of carbon, nitrogen, and sulfur. All tungsten and molybdenum enzymes, with the notable exception of the FeMo-cofactor of nitrogenase, belong to a family known as oxotransferases, which catalyze the transfer of an oxo group to or from substrate in a two-electron redox reaction (*9–11*). Although most members of this family are molybdoenzymes, including xanthine oxidases that convert xanthine to uric acid, sulfite oxidases involved in the metabolism of sulfur, and nitrate reductases that form nitrite from nitrate, several tungsten-containing enzymes have been isolated (*12*). To date, these tungstoenzymes have been found mainly in thermophilic anaerobes, and function either in CO_2 activation or, as in the case of *P. furiosus* AOR, in the conversion of aldehydes to carboxylic acids.

The catalytic site in these oxotransferase enzymes is a labile, oxygen-sensitive, metal cofactor consisting of a tungsten or molybdenum ion bound to an organic component. This ligand, termed molybdopterin (MPT), was first identified by Rajagopalan and coworkers (*13*), who isolated and characterized its di(carboxamidomethyl) derivative by fluorescence and mass spectroscopy. While additional studies have demonstrated that all eukaryotic molybdoenzymes contain this unmodified form of MPT, prokaryotic forms usually contain an alternative version with either a GMP (*14–17*), CMP (*18, 19*), AMP (*17*), or IMP (*17*) nucleotide appended to the molybdopterin via a pyrophosphate linkage. The role of the additional nucleotide in the chemistry of this system is unknown. As with molybdenum enzymes, all tungsten oxotransferases contain either the MPT or modified MPT ligand (*20*). The model for the molybdenum cofactor proposed by Rajagopalan *et al.* (*11, 21*) based on biochemical and spectroscopic analyses, consists of a single MPT ligand bound to molybdenum via two dithiolene sulfurs, as shown in Fig. 1A. Direct confirmation of this model, however, has been hindered by the lack of a three-dimensional structure for any molybdenum or tungsten oxotransferase. To establish the structural features of tungsten and MPT cofactors, and to gain insight into the structural origins of thermal stability in hyperthermophilic proteins, we determined the structure of *P. furiosus* AOR with x-ray diffraction methods.

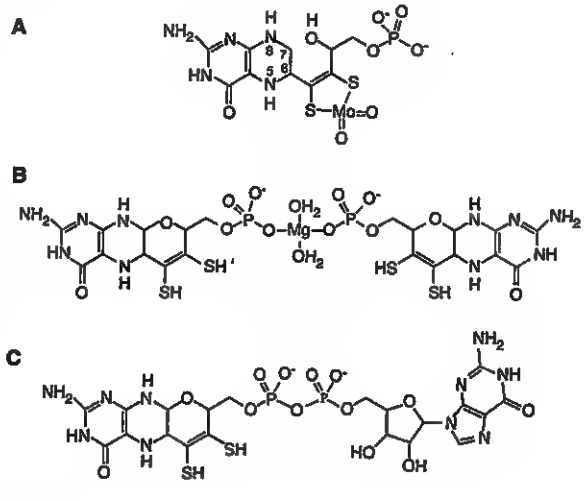

Fig. 1. Comparison of molybdopterin structures. **(A)** Rajagopalan's model of the molybdenum cofactor consisting of a single molybdopterin (MPT) ligand bound to molybdenum (*11, 21*); **(B)** the structure of the bis(MPT) ligand determined from x-ray analysis of the *P. furiosus* AOR protein; **(C)** proposed structure of molybdopterin guanine dinucleotide (MGD) based on the revised MPT structure. A single molecule of MGD and related ligands could possibly coordinate metals in a similar fashion to the bis(MPT) ligand by utilizing the sugar hydroxyl oxygens in place of the second dithiolene group.

M. K. Chan and D. C. Rees are in the Division of Chemistry and Chemical Engineering 147-75CH, California Institute of Technology, Pasadena, CA 91125, USA. S. Mukund, A. Kletzin, and M. W. W. Adams are in the Department of Biochemistry and Molecular Biology, and Center for Metalloenzyme Studies, University of Georgia, Athens, GA 30602, USA.

*To whom correspondence should be addressed.

The growth of *P. furiosus* and purification of AOR under anaerobic reducing conditions have been described (*7*). Details of the crystallization and structure determination are provided in Table 1. The AOR model contains 9888 total atoms (123 atoms in five cofactor sites, 9386 protein atoms and 379 water molecules) and has been refined to an *R* factor of 0.155 for 55520 observed reflections in the resolution range between 10 and 2.3 Å (no σ cutoff, 89 percent complete), with root-mean-square deviations from ideal bond distances and angles of 0.009 Å and 2.58°, respectively. The AOR molecule (Fig. 2, A and B), consists of two identical 605 residue (66 kD) subunits of known sequence (*22*). Three different types of metal sites are found in the AOR protein dimer; an Fe_4S_4 cluster and a tungsten cofactor that are contained within each subunit, and a single tetrahedral metal atom located at the dimer interface. The Fe_4S_4 cluster and tungsten cofactor within one subunit are in close proximity, but the mononuclear center is positioned ~25 Å from these groups. The Fe_4S_4 clusters and tungsten cofactors in different subunits of the dimer are separated by ~50 Å.

Structure of the metal sites. The mononuclear site is symmetrically coordinated by Glu^{332} and His^{383} from each subunit in a tetrahedral fashion. The metal site is tentatively identified as iron on the basis of anomalous scattering of the atom and a metal analysis of the AOR protein although direct confirmation of this assignment by Mössbauer spectroscopy is needed. Because of the ~25 Å distance between this site and the other metal centers, this mononuclear metal is not likely to play a redox role; rather it may be involved in stabilizing the protein dimer at high temperatures.

The tungsten cofactor fits into a pocket located at the center of each subunit (Fig. 2). The structure of this site (Fig. 3) reveals that the molybdopterin does bind to the metal via the dithiolene sulfurs, as proposed by Rajagopalan *et al.* (*21*). Surprisingly, however, two molybdopterin molecules, instead of the expected one molecule, are coordinated to the tungsten. The arrangement of the tungsten and the two pairs of dithiolene sulfurs may be described as a distorted square pyramid, with an angle between the planes of the molybdopterin ligands of ~97°. No protein ligands are coordinated to the tungsten atom, although our analysis of the electron density around the tungsten suggests that two additional coordination sites may be occupied by glycerol or oxo ligands (or both) to yield an overall distorted trigonal prismatic arrangement at the tungsten site. The glycerol presumably comes from the protein storage buffer and may represent a substrate analog. Unless substantial rearrangements in the tungsten coordination sphere occur during substrate oxidation, the presence of two MPT ligands in AOR enforces cis coordination for the substrate and oxo groups,

Table 1. Summary of AOR structure determination. Native and derivative data sets for each of the three crystal forms (*42*) were collected from single crystals at room temperature on either a RAXIS imaging plate system or a Siemens area detector mounted on rotating anode generators producing CuKα (λ = 1.54 Å) radiation. Diffraction data sets were processed with either RAXIS (provided by Rigaku), XENGEN (*43*), or XDS (*44*) software, as appropriate, and then locally scaled to the native data set for that crystal form with the use of the program package ROCKS (*45*). An additional native data set for crystal form 1 was collected at λ = 1.08 Å at the Stanford Synchrotron Radiation Laboratory, with a MAR imaging plate detector, and processed with MOSFLM (*46*). Data collection statistics from native and derivative crystals are summarized below. The positions of five anomalous scattering sites in crystal form 1 were determined from inspection of the anomalous difference Patterson maps, calculated from a native data set collected on the RAXIS system. Because of changes in the scattering factors for Fe and W between 1.54 Å and 1.08 Å, the Fe_4S_4 clusters and W sites were initially differentiated on the basis of anomalous Fourier maps calculated from data sets collected at these two wavelengths. In addition to anomalous scattering phasing information for crystal form 1, different Pt derivatives could be obtained by varying the time (12 hours to 2 weeks) of soaking crystals of each form in 10 mM K_2PtCl_4. The locations of the heavy atom sites were determined by difference Fourier analysis and refined in PHARE (*47*) to generate initial experimental phases for each crystal form. The figure of merits for crystal forms 1, 2, and 3 to 3.0 Å resolution were 0.60, 0.50, and 0.41, respectively. The multiple isomorphous replacement phases were refined by noncrystallographic symmetry averaging within and between the different crystal forms (*48*). The initial polyalanine model was built with TOM/FRODO (*50*), and the final model was constructed with the program O (*51*) as the sequence became available. The TNT program (*52*) was used for the initial stages of the model refinement, and positional and B factor refinements at the latter stages were calculated with X-PLOR (*53*). Model phases calculated at each stage were combined with the experimental phases to generate improved maps. All heavy atom derivative Pt sites were located near histidine or methionine side chains. The model quality was also assessed with the programs PROCHECK (*54*), VERIFY-3D (*55*), and ERRAT (*56*), which were consistent with a correct structure. More than 90 percent of the (ϕ, ψ) angles of the AOR model are in the most favored regions of the Ramachandran plot (*54*), and the secondary structure regions are listed in (*57*).

Crystal	Space group	Crystal parameters						
		a (Å)	*b* (Å)	*c* (Å)	α (°)	β (°)	γ (°)	*Z*
Native 1	$P2_12_12_1$	80.9	108.3	159.8	90.0	90.0	90.0	8
Native 2	P1	85.5	54.1	85.4	105.3	93.5	93.4	2
Native 3	P1	55.7	67.0	85.2	95.4	86.6	92.9	2

Data collection and processing statistics

Data set	Resolution (Å)	Reflections		Complete (%)	R_{sym}*	Isomorphous *R* factor†	Sites (No.)	Phasing power‡
		Measured	Unique					
Native 1	2.32	237,105	56,373	92.4	0.049		5§	1.33
SSRL	3.0	86,751	22,541	79.0	0.086			
$PtCl_4$ 1	2.37	114,240	35,556	62.1	0.095	0.096	2	0.68
$PtCl_4$ 2	2.67	242,839	37,676	92.5	0.120	0.149	8	1.37
Native 2	2.95	56,398	26,114	74.8	0.090		4§	0.67
$PtCl_4$ 3	2.05	227,138	81,661	84.5	0.124	0.154	8	1.43
Native 3	2.30	106,070	48,579	82.7	0.074		4§	0.97
$PtCl_4$ 4	2.31	103,475	48,981	82.8	0.078	0.206	10	1.4

*R_{sym} describes the agreement between multiple observations of symmetry related reflections, based on the absolute value of the intensity differences. †Mean fractional change between native and derivative structure factor amplitudes. ‡Ratio of the heavy atom scattering amplitude to estimated phasing model error, calculated to 3 Å resolution. §Native anomalous scattering sites.

which would have stereochemical consequences for the mechanism of the oxotransfer reaction. The side chains of residues Glu^{313} and His^{448} are in the vicinity of the substrate binding site on the tungsten and could participate in proton transfers associated with oxidation-reduction reactions.

In addition to interactions between the dithiolene sulfurs and tungsten, the two MPT ligands are also linked through their phosphate groups, which coordinate axial sites of the same magnesium ion. The two MPT ligands are approximately related by a twofold rotation about an axis that passes through both the tungsten and magnesium sites. The magnesium ion exhibits octahedral geometry. In addition to the two coordination sites filled by phosphate oxygens, two waters bind at cis sites on the side facing the tungsten atom, and the two backbone carbonyl oxygens from residues Asn^{93} and Ala^{183} bind at cis sites on the Mg directed away from the tungsten. The two waters form part of an intricate, asymmetric hydrogen bonding network within the tungsten cofactor (Fig. 3B). Each water is hydrogen-bonded to at least one phosphate oxygen and an N-5 nitrogen of the pterin ring, with one of the two waters also within hydrogen bond distance of the ether oxygen of one of the MPT ligands. The origin of this slight asymmetry is due to the hydrogen bonding of the side chain of Arg^{76} to the ether oxygen of the other MPT group.

The refined AOR structure also indicates that the MPT ligand itself is slightly different from that previously postulated (Figs. 1 and 3). The crystallographic analysis, as illustrated by the electron density map shown in Fig. 3A, reveals that the MPT groups in AOR contain a third ring formed by closure of the side-chain hydroxyl with the pterin ring at C-7. Such a cyclization would not be unprecedented in that related compounds have been synthesized (*23*). A plausible mechanism for formation of the third ring would be by attack of the side-chain hydroxyl on the C-7 carbon of a 5,6 dihydropterin (Fig. 1). Provided that this ring closure is reversible, there is no inconsistency between the three-ringed structure seen in the protein, and the two-ringed form observed for the isolated pterin (*11*, *21*). The nonplanar structure of the pterin ring system seen in AOR is consistent with a reduced form for the protein-bound pterin, which would likely be equivalent to a dihydropterin (possibly the 5,6-dihydropterin) in the ring-opened form. This revised MPT structure may be a common feature in all molybdopterin-containing enzymes.

The revised MPT structure may also be relevant to the structure of the various dinucleotide derivatives found in other molybdenum-cofactor systems (Fig. 1). Comparison of the dimolybdopterin to the modified molybdopterin dinucleotides reveals an overall similarity. In each case, two aromatic base systems attached to potential bidentate liganding groups are connected via a phosphate backbone. It is possible that molybdenum or tungsten cofactors containing these modified MPT dinucleotides do have a structure similar to that observed in AOR, with the only difference being replacement of the second pterin in AOR by a nucleotide, and consequent metal ligation by the sugar hydroxyl oxygens. There is precedent for metal coordination by sugar hydroxyl groups in this fashion (*24*). Such binding may help to explain why the sugar ring is the only common feature among the modified molybdopterin dinucleotides, and why differences appear to exist in the ligation of the Mo sites in different molybdoenzymes. An alternative possibility is that the nucleotide-containing end of the modified MPT cofactor could adopt a somewhat different conformation, that would permit metal coordination by groups on the nucleotide ring or, perhaps by protein side chains.

Electron paramagnetic resonance, magnetic circular dichroism, and resonance Raman studies indicate that AOR contains an Fe_4S_4 cluster located near a paramagnetic center (*7*). Indeed, the x-ray structure reveals that the Fe_4S_4 cluster is positioned approximately 10 Å from the tungsten atom. The Fe_4S_4 cluster is buried ~6 Å below the van der Waals surface of the protein. This arrangement is consistent with the postulated role of the Fe_4S_4 cluster as an intermediary for electron transfer between the tungsten cofactor and ferredoxin, the physiological electron acceptor of AOR. Four cysteine ligands, provided by the Sγ of Cys^{288}, Cys^{291}, Cys^{295}, and Cys^{494}, coordinate the Fe_4S_4 cluster. Whereas the first three Cys residues are part of a characteristic iron-sulfur cluster binding sequence (*22*), the polypeptide conformation of this region is distinct from that adopted by the Fe_4S_4 binding site found in ferredoxins. The Fe_4S_4 cluster is linked to one of the two molybdopterins of the tungsten cofactor by two distinct sets of interactions. The side

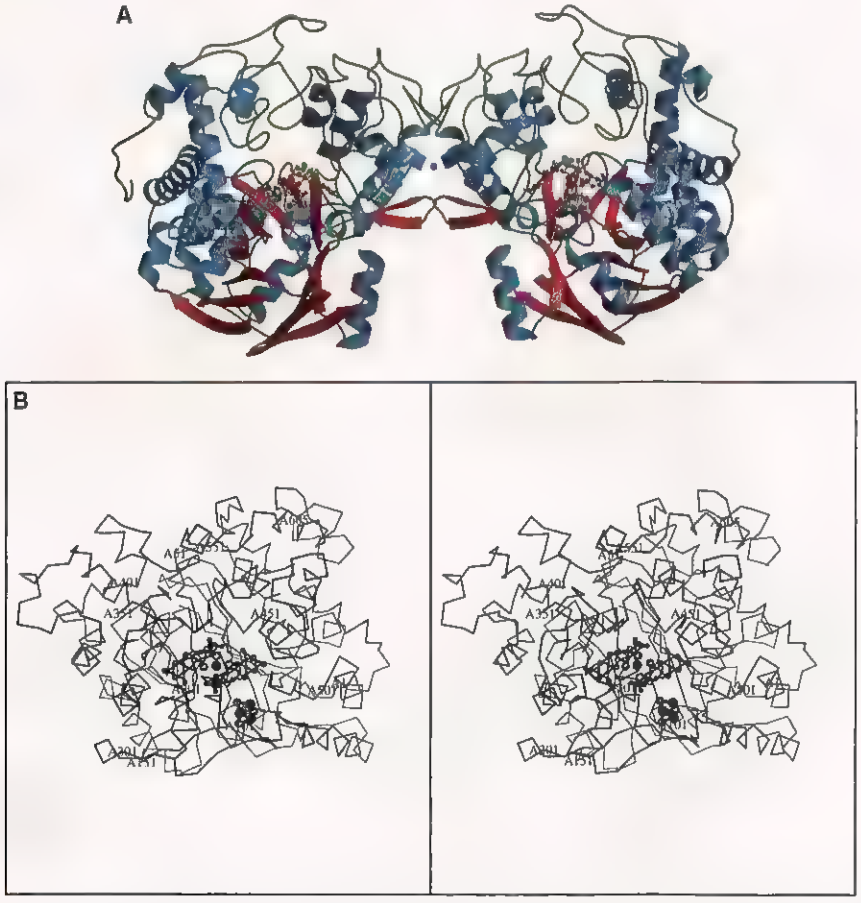

Fig. 2. Structure of the AOR protein. (**A**) Ribbons diagram of the AOR dimer viewed perpendicular to the dimer twofold axis. The secondary structures are color-coded with α helical regions as light blue, β sheet regions as red, and the remainder as green. Atoms in the cofactors are colored by elements, with carbon as black, nitrogen as blue, oxygen as red, sulfur as yellow, phosphate as magenta, magnesium as orange, iron as purple, and tungsten as cyan. (**B**) Stereodiagram of the polypeptide chain of a single AOR subunit. This figure was prepared with the programs MOLSCRIPT and Raster 3D (*58*).

chain of Arg^{76} bridges these two groups by forming hydrogen bonds to an inorganic sulfur of the Fe_4S_4 cluster, and to two sites on the molybdopterin, the ether oxygen and a phosphate oxygen. In addition, the Sγ of Cys^{494}, an Fe_4S_4 cluster ligand, is positioned to accept a hydrogen bond from the pterin ring nitrogen N-8, which is nearest the ether linkage of the molybdopterin. These interactions could provide electron transfer pathways between the two centers. Furthermore, this arrangement suggests that the pterin ligand does not merely play a passive structural role, but may be an active participant in the redox chemistry of AOR.

Protein structure. The binding sites for the tungsten cofactor and Fe_4S_4 cluster are located at the interfaces of the three domains that are formed by each AOR subunit. The location of redox centers at domain or subunit interfaces appears to be a general property of multicentered redox proteins (*25*). Domain 1 (residues 1 to 210) forms a base on which the saddle-like tungsten pterin cofactor sits, while domains 2 (residues 210 to 417) and 3 (residues 418 to 605) surround the opposite surface of the tungsten cofactor, and provide residues that form specific polar and ionic interactions with the different metal centers. Each subunit exhibits a pseudo twofold axis that coincides approximately with the twofold axis of the tungsten cofactor. This rotation axes passes through the center of domain 1, and approximately relates domains 2 and 3. The twofold symmetric arrangement of the polypeptide chain in domain 1 is particularly striking (Fig. 4A). The similarity of domains 2 and 3 is less apparent, which may result from the involvement of domain 2 in both generating the dimer interface, and in providing most of the Fe_4S_4 cluster binding site.

Domain 1 consists primarily of 12 β strands arranged in two six-stranded, predominantly antiparallel β sheets that are related approximately by the twofold rotation axis described above (Fig. 4A). The two sheets are joined by antiparallel β sheet interactions between the β strands containing residues 89 to 95 and 182 to 186. Residues Asn^{93} and Ala^{183}, which coordinate the magnesium ion through their carbonyl oxygens, are located within these two β strands. Within domain 1 is residue Arg^{182}, which forms a salt bridge to the phosphate group of the molybdopterin nearer the Fe_4S_4 cluster, whereas additional hydrogen bonding interactions to the phosphates are formed by the hydrogens on the main chain amide nitrogens of residues 93, 95, 183, 185, and 186. Residue Arg^{76}, which hydrogen bonds both a molybdopterin ether oxygen and an Fe_4S_4 inorganic sulfur, is also located within this domain.

The regular secondary structure of domains 2 and 3 consists primarily of α helices, with few β sheet regions. Although these two domains are related approximately by the twofold axis described above, this structural relationship is less apparent than for domain 1 and the tungsten cofactor. Consistent with an underlying structural similarity between the two domains, residues 338 to 344 and 489 to 495 in domains 2 and 3, respectively, contain Asp-X-X-Gly-Leu-(Cys or Asp)-X sequences, where the Asp carboxylate group and Leu main chain carbonyl oxygen are arranged to bind the primary amine group of their respective MPT ligand (Fig. 4, B and C). Asp^{343} and Cys^{494} interact with the secondary ring nitrogen, N-8, near the ether linkage, while the amide nitrogens from the carboxy terminal end of each motif, Thr^{344} and Leu^{495}, form a hydrogen bond with a secondary ring nitrogen on the pterin. This sequence motif occurs in both domains at the end of α helices (Fig. 4C), with the Gly residue adopting the left-handed helical (Lα) conformation characteristic of a helical capping interaction (*26*). An additional polar interaction to one of the two MPT rings is generated by a hydrogen bond between the side chain of Lys^{450} and a pterin carbonyl oxygen.

In addition to maintaining specific binding interactions with the pterin, another role for domains 2 and 3 may be to regulate substrate access to AOR. With the use of a 1.4 Å radius probe, a long hydrophobic channel leading from the tungsten site to the surface of the protein may be defined (*27*) between these two domains. The nonpterin coordination sites on the tungsten atom occupy one end of this cavity, consistent with the role of these coordination sites in substrate binding and catalysis. A 3_{10} helix formed by residues 495 to 500 runs parallel to the length of the cavity. Within this helix, the side chains of Phe^{496} and Phe^{499} are directed in a parallel fashion toward the central axis of the cavity. The channel seems large enough to accommodate a variety of substrates, which may help to explain the ability of AOR to oxidize both aliphatic and aromatic aldehydes. In contrast to AOR, the tungsten-containing enzyme, formaldehyde ferredoxin oxidoreductase (FOR), which is also found in hyperthermophiles such as *P. furiosus* and *Thermococcus litoralis* (*22*, *28*), is specific for small (one to three carbon) aldehydes. *Pyrococcus furiosus* AOR and *T. litoralis* FOR appear to be structurally related as their sequences are very similar [59 percent with 38 percent identity (*22*)]. Hence, different channel sizes in these two enzymes might account for the differences in their substrate specificities.

Although all molybdenum-tungsten oxotransferase enzymes that have been characterized contain similar pterin cofactors, it is not yet known whether any of the protein structural motifs found in AOR exist in the other enzymes. For example, with

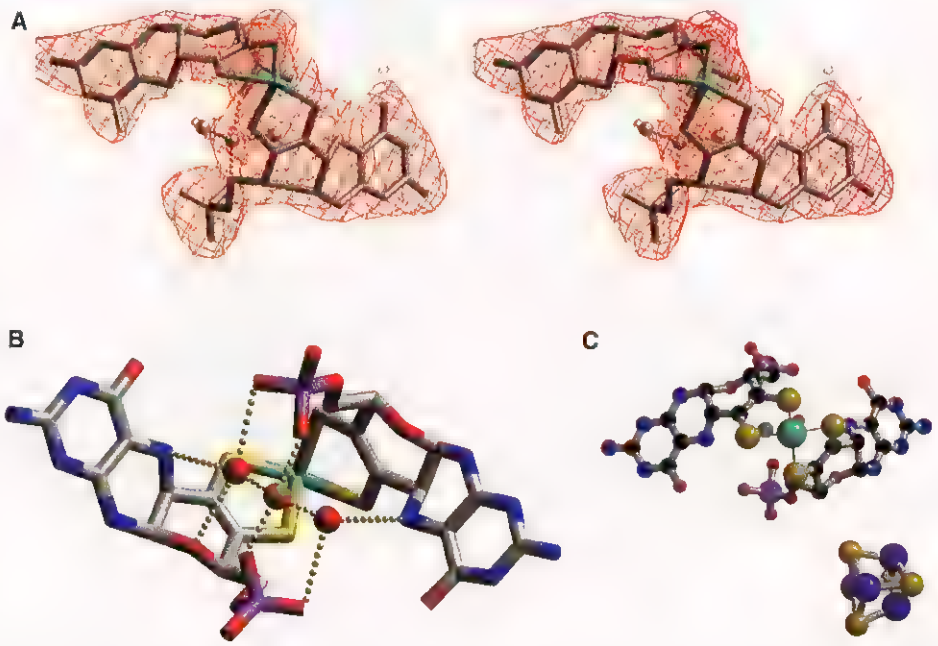

Fig. 3. Structure of the tungsten cofactor. (**A**) $F_o - F_c$ omit-refined electron density map of the tungsten-dimolybdopterin cofactor as viewed along the pseudo twofold axis. The contour level is three times the standard deviation of the electron density map. (**B**) Stick diagram of the internal hydrogen bonding network within the tungsten cofactor itself. The atom coloring scheme is the same as in Fig. 2, except that carbon atoms are gray. (**C**) Ball-and-stick figure of the tungsten cofactor and Fe_4S_4 cluster of AOR. (A) and (B) were prepared with the program SETOR (*59*) and (C) was prepared with the programs MOLSCRIPT and Raster 3D (*58*).

the exception of *T. litoralis* FOR, only NH_2-terminal sequences are available for the three other types of tungstoenzymes known: carboxylic acid reductases (CAR) from acetogens, formylmethanofuran dehydrogenases from methanogens, and glyceraldehyde-3-phosphate ferredoxin oxidoreductase from *P. furiosus* (*12*, *22*, *28*). Of these, only CAR shows similarity to the NH_2-terminal sequences of AOR and FOR (*22*). In contrast, the complete sequences are available for several molybdenum-containing oxotransferases, including various xanthine oxidases and nitrate reductases. However, these show no similarity to the AOR or FOR sequences (*22*). Thus, it is important to establish the structures of other oxotransferases to see whether these have truly different structures or whether the underlying structural similarity to AOR is obscured by sequence divergence.

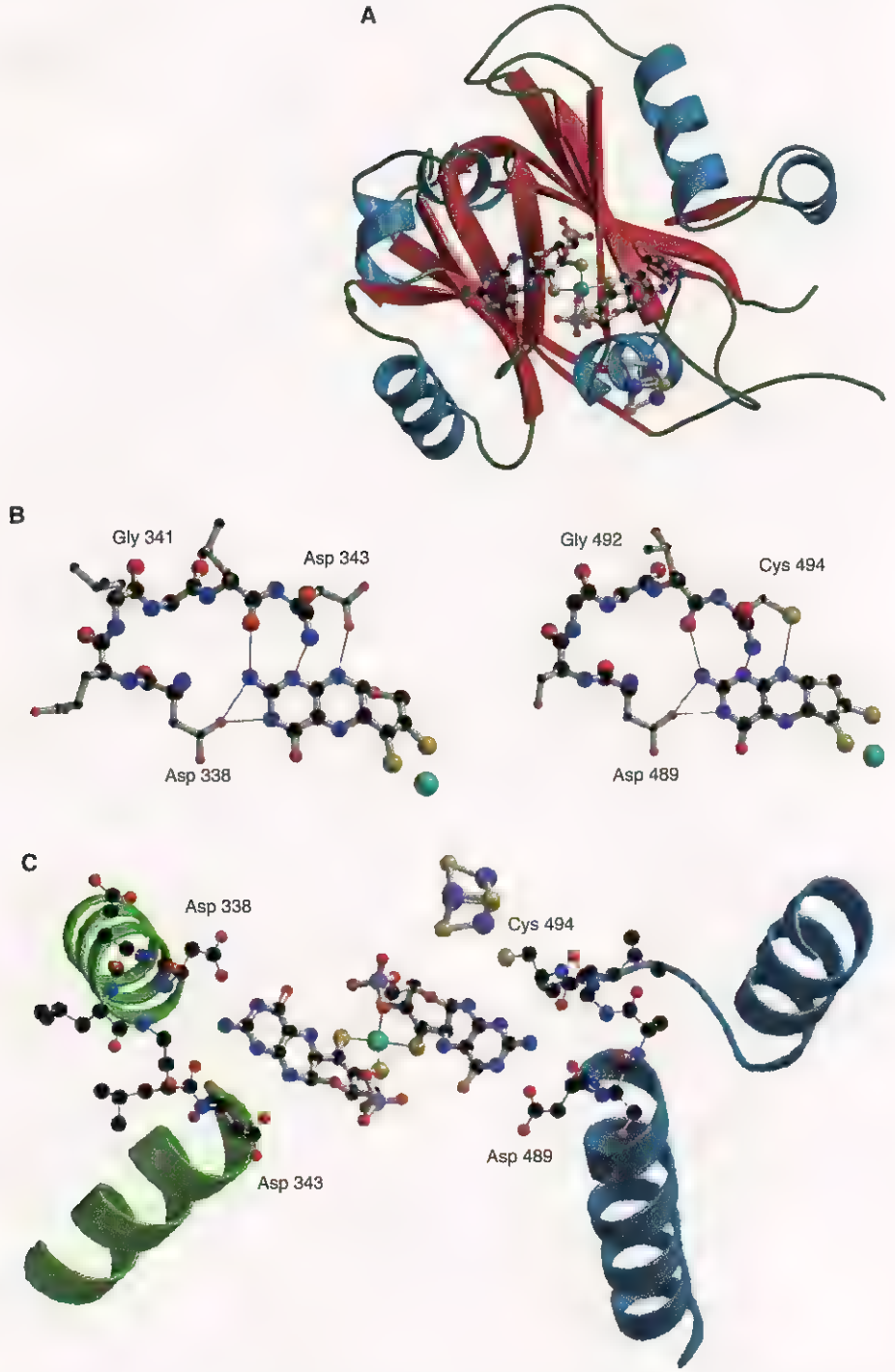

Fig. 4. Protein-molybdopterin interactions. (**A**) Ribbons diagram of the interaction of the tungsten cofactor and domain 1, illustrating the β sheet arrangement and the overall twofold symmetry of both the domain and the pterin cofactor. (**B**) Hydrogen bonding of the tungsten cofactor to domains 2 and 3. The DXXGL(D,C)X motifs in both domains 2 and 3, which are approximately related by the twofold axis passing through the cofactor, form multiple hydrogen bonds to each pterin ligand. (**C**) Ribbons diagram illustrating the interaction of the pterin ligands of the tungsten cofactor with α-helical regions of domains 2 and 3 that contain the sequence motif detailed in (B). This figure was prepared with the programs MOLSCRIPT and Raster 3D (*58*).

Protein thermostability. One of the striking properties of AOR is the extreme thermal stability of the protein structure. Although calorimetric studies of AOR stability have not yet been performed, the temperature for optimum aldehyde oxidation activity is more than 95°C, which sets a lower limit on the temperature range for AOR stability. Since AOR is the first hyperthermophilic enzyme to be structurally characterized, and in the absence of a mesophilic counterpart for direct comparison, an assessment of the origins of the thermal stability of AOR must necessarily be based on analysis of rather general features of protein structure and stability established primarily from mesophilic structures. The primary, secondary and tertiary structures of AOR are unexceptional for water-soluble, globular proteins. The amino acid composition of AOR (*22*) is close to the average observed for prokaryotic proteins, with the exception of glutamine, which occurs at a reduced frequency. The secondary structure composition of AOR (45 percent helix and 14 percent β sheet) is also within the range seen for water-soluble, globular proteins, and the tertiary packing interactions between the α helices and β strands are also standard. No disulfides exist in AOR and although metal complexation will contribute to protein stability, the number of metal binding sites is not exceptionally high.

The importance of ion pairing to stability has been suggested from both structural and genetic comparisons of mesophilic and thermophilic proteins (*29*–*31*), although some recent studies have questioned the significance of the contributions of these interactions to protein stability (*32*). To evaluate the possible significance of electrostatic interactions for the thermostability of AOR, we tabulated the numbers of ionic interactions per residue for a sampling of 30 monomeric and oligomeric proteins [from the Brookhaven Protein Data Base (*33*)] that contained ~300 to ~2400 residues (about half the size of the AOR monomer to twice the size of the AOR dimer), for comparison to the value determined for AOR (Fig. 5A). The number of ionic interactions per residue was defined as the difference between the number of interactions between oppositely charged side chains and the number of interactions between side chains of like charge, divided by the total number of residues in the protein. Interac-

tions were defined as occurring between polar (oxygen or nitrogen) atoms of potentially ionizable side chains (Arg, Asp, Glu, His, and Lys) that are positioned ≤4 Å apart (*34*). The average number of ion-pairs per residue indicated in Fig. 5A, ~0.04, is close to that observed in Barlow and Thornton's earlier study (*34*). The data in this comparison indicate that AOR does contain a relatively high number of salt bridges per residue, although other proteins also have a similar percentage of stabilizing ionic interactions. Thus, while ion pairs may contribute to the stability of AOR, they cannot represent the sole determinant of thermostability.

Richards pioneered the application of the concepts of molecular surface area and volume to the analysis of macromolecular structures (*35*). From this work, a general picture of water-soluble globular proteins has emerged emphasizing (i) the relatively smooth, polar surface that minimizes the surface energy in an aqueous environment, and (ii) the efficiently packed, relatively nonpolar interior. The solvent accessible surface of AOR can be defined by means of the ACCESS algorithm of Richmond and Richards (*36*), the group radii of Chothia (*37*), and a probe radius of 1.4 Å. The surface area for the AOR dimer and one subunit are 35,740 Å^2 and 19,050 Å^2, respectively, which indicates that about 1200 Å^2 per subunit are buried in the dimer interface. A dimeric protein the size of AOR (134 kD) is expected to have about a 17 percent larger accessible surface area (41,800 Å^2) on the basis of a survey of water-soluble oligomeric proteins (*38*). The accessible surface area of AOR was found to be 56 percent apolar, 27 percent polar, and 17 percent charged, values which are comparable to the values 57 percent, 24 percent, and 19 percent, respectively, observed in a survey of water-soluble proteins (*39*). Hence, the surface of AOR appears to have reduced area, but comparable polarity, when compared to other globular protein structures.

In general, minimization of the ratio of surface area to volume increases the stability of an object by simultaneously reducing the unfavorable surface energy and increasing the attractive interior packing interactions. Although the effects of surface area variation on protein stability have not been systematically explored, the influence of variations in packing interactions on protein stability, especially through the formation or removal of cavities, has been more extensively documented (*40*). Not surprisingly, the introduction of cavities into a protein is often associated with decreased protein stability. The possibility that minimization of the surface area to volume ratio might contribute to the stability of AOR was computationally assessed by evaluating the relative surface area and the number of buried atoms for the same set of proteins used in the ion-pair calculation. The relative surface area was obtained by first calculating the accessible surface area, A_0, for a particular protein, and then dividing by the expected surface area for a protein of that size. From a least squares fit of log (A_0) as a function of log (N), where N is the total number of atoms in the protein model, the expected area, A_c, of a generic protein as a function of N can be fit to the equation:

$$A_c = 15.0\, N^{0.866}$$

which reproduces the observed areas to within ±15 percent, comparable to the results of other studies (*38*, *39*). An estimate of the extent of surface area minimization for a given protein is provided by the ratio A_0/A_c. Variations in the ratio from the average value 1 reflect changes in the molecular shape or surface roughness (or both) that alter the accessible surface area of a particular protein. Evaluation of the efficiency of packing is more complex, but a relatively simple indicator is given by the fraction of atoms in a protein with no (zero) accessible surface area, n_B, because atoms are only buried if completely surrounded by other atoms. The larger the value of n_B, the greater the fraction of interior atoms that are present in the structure, which provides an estimate of the extent of atom sequestration from solvent exposure. The value n_B may be obtained directly from the surface area calculation.

In terms of these parameters, low values of A_0/A_c and high values of n_B correspond to minimization of the ratio of surface area to volume of a protein. Values of A_0/A_c and n_B calculated for the set of proteins used to establish A_c are illustrated in Fig. 5, A and B. The more detailed examination of these factors presented in Fig. 5B indicates that the relative surface area and the fraction of buried atoms in proteins are negatively correlated. Qualitatively, this observation seems reasonable, since in general the greater the surface area of a protein, the more atoms that will be on the surface and the fewer atoms that will be buried, and vice versa. The AOR structure simultaneously exhibits both the minimum value for the relative surface area ratio and the maximum fraction of buried atoms, indicating that AOR has a reduced ratio of surface area to volume relative to other proteins. A plausible inference from this result is that these effects may be related to the enhanced thermal stability of AOR. Consistent with this inference, the same general trends (especially in the surface area) are seen for three pairs of structures for which both mesophilic and thermophilic structures are available (PDB identifiers for the mesophilic and thermophilic structures, respectively, are indicated in parentheses): glyceraldehyde phosphate dehydrogenase (1GPD and 1GD1), phosphofructokinase (1PFK and 3PFK), and phosphoglycerate kinase (PGK and 1PHP), although this pattern is not exhibited by lactate dehydrogenase (9LDT and 1LDB). A role for improved packing in

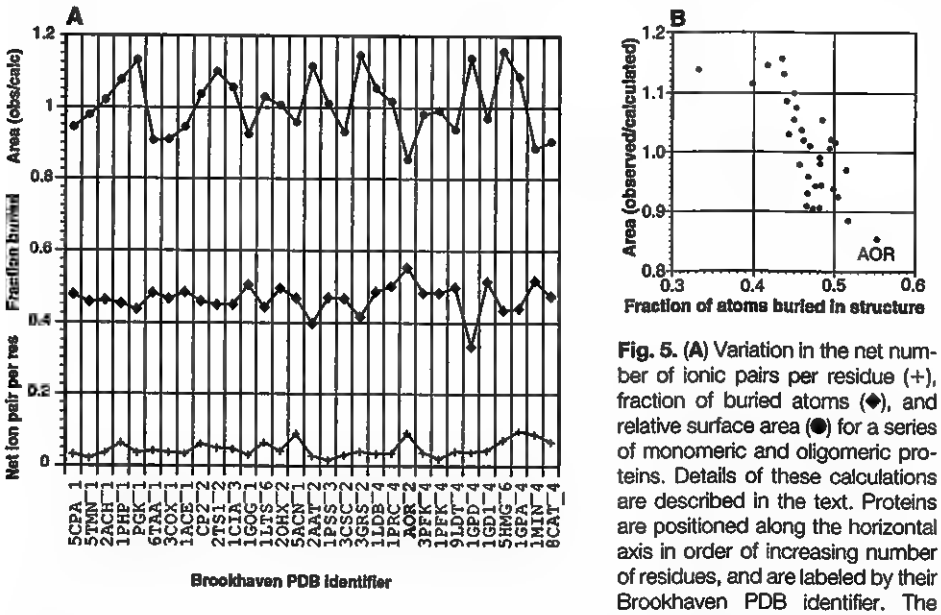

Fig. 5. (**A**) Variation in the net number of ionic pairs per residue (+), fraction of buried atoms (◆), and relative surface area (●) for a series of monomeric and oligomeric proteins. Details of these calculations are described in the text. Proteins are positioned along the horizontal axis in order of increasing number of residues, and are labeled by their Brookhaven PDB identifier. The number of subunits in each protein is indicated by the suffix to the PDB identifier. Two proteins, yeast phosphoglycerate kinase (PGK) and the *Clostridium pasteurianum* nitrogenase iron protein (CP2), have been refined but not yet deposited (*60*). (**B**) Relationship between the fraction of buried atoms and the relative surface area, calculated for the proteins used in (A), demonstrating the anti-correlation between these two parameters. The position of AOR is indicated.

the enhanced stability of hyperthermophilic enzymes has been previously discussed on the basis of biochemical and biophysical comparisons of homologous enzymes from mesophilic and thermophilic sources (*41*). The structural basis by which the surface area is reduced and the fraction of buried atoms is increased in AOR relative to other proteins remains an open question, as is the energetic basis for the possible correlation of these parameters with thermal stability.

The AOR structure demonstrates that hyperthermostability can be achieved without requiring any new types of interactions to stabilize the folded conformation. Rather than being the consequence of one dominant type of interaction, it appears that the stability of AOR may reflect a number of subtle interactions that both minimize the surface energy while maximizing packing and electrostatic interactions. It remains to be determined, however, if this is a general feature of hyperthermophilic enzymes. Similarly, to what extent the AOR structure is representative of other molybdenum or tungsten containing enzymes is also not clear. Surprisingly, the family of proteins represented by AOR shows no sequence similarity to any other molybdoenzyme, yet, the oxotransferase function of all of these proteins is achieved with similar cofactors, namely molybdopterin and typically one or more iron-sulfur clusters. The structure of the pterin site and an adjacent iron-sulfur cluster determined in AOR may therefore reflect a common motif in an apparently diverse group of enzymes, whose unifying feature is the use of a second or third row transition metal in catalysis.

REFERENCES AND NOTES

1. K. O. Stetter, G. Fiala, G. Huber, R. Huber, G. Segerer, *FEMS Microbiol. Rev.* **75**, 117 (1990).
2. M. W. W. Adams and R. M. Kelley, Eds., *Biocatalysis at Extreme Temperatures: Enzyme Systems Near and Above 100°C, ACS Sym. Ser.* **498**, pp. 1–215 (1992).
3. M. W. W. Adams, *Annu. Rev. Microbiol.* **47**, 627 (1993).
4. ———, *FEMS Microbiol. Rev.* **15**, 261 (1994).
5. M. W. Day *et al.*, *Protein Sci.* **1**, 1494 (1992).
6. S. Mukund and M. W. W. Adams, *J. Biol. Chem.* **265**, 11508 (1990).
7. ———, *ibid.* **266**, 14208 (1991).
8. M. J. Kendrick, M. T. May, M. J. Plishka, K. D. Robinson, *Metals in Biological Systems* (Horwood, New York, NY, 1992).
9. R. C. Bray, *Q. Rev. Biophys.* **21**, 299 (1988); J. C. Wootton *et al.*, *Biochim. Biophys. Acta* **1057**, 157 (1991); R. S. Pilato and E. I. Stiefel, in *Bioinorganic Catalysis*, J. Reedijk, Ed. (Dekker, New York, 1993), pp. 131–188; E. I. Steifel, D. Coucouvanis, W. E. Newton, Eds., *Molybdenum Enzymes, Cofactors, and Model Systems, ACS Symp. Ser.* **535**, pp. 1–387 (1993).
10. R. H. Holm, *Coord. Chem. Rev.* **100**, 183 (1990); J. H. Enemark, C. G. Young, *Adv. Inorg. Chem.* **40**, 1 (1994).
11. K. V. Rajagopalan, *Adv. Enzymol. Rel. Areas Mol. Biol.* **64**, 215 (1991); ——— and J. L. Johnson, *J. Biol. Chem.* **267**, 10199 (1992).
12. M. W. W. Adams, in *Encyclopedia of Inorganic Chemistry*, R. B. King, Ed. (Wiley, New York, 1994), pp. 4284–4291.
13. J. L. Johnson and K. V. Rajagopalan, *Proc. Natl. Acad. Sci. U.S.A.* **79**, 6856 (1982).
14. J. L. Johnson, N. R. Bastian, K. V. Rajagopalan, *ibid.* **87**, 3190 (1990).
15. M. Karrasch, G. Boerner, R. K. Thauer, *FEBS Lett.* **274**, 48 (1990).
16. J. L. Johnson, N. R. Bastian, N. L. Schauer, J. G. Ferry, K. V. Rajagopalan, *FEMS Microbiol. Lett.* **77**, 213 (1991).
17. G. Börner, M. Karrasch, R. K. Thauer, *FEBS Lett.* **290**, 31 (1991).
18. J. L. Johnson, K. V. Rajagopalan, O. Meyer, *Arch. Biochem. Biophys.* **283**, 542 (1990).
19. D. Hettrick, B. Peschke, B. Tschisuaka, F. Lingens, *Biol. Chem. Hoppe-Seyler* **372**, 513 (1991).
20. J. L. Johnson, K. V. Rajagopalan, S. Mukund, M. W. W. Adams, *J. Biol. Chem.* **268**, 4848 (1993).
21. S. P. Kramer, J. L. Johnson, A. A. Ribeiro, D. S. Millington, K. V. Rajagopalan, *J. Biol. Chem.* **262**, 16370 (1987).
22. A. Kletzin *et al.*, in preparation.
23. R. Soyka and W. Pfleiderer, *Helv. Chim. Acta* **73**, 808 (1990).
24. J. F. Conn, J. J. Kim, F. L. Suddath, P. Blattmann, A. Rich, *J. Am. Chem. Soc.* **96**, 7152 (1974); N. S. Begum and H. Manohar, *Tetrahedron* **11**, 2823 (1992).
25. J. Kim and D. C. Rees, *Nature* **360**, 553 (1992).
26. J. S. Richardson and D. C. Richardson, *Science* **240**, 1648 (1988); R. Aurora, R. Srinivasan, G. D. Rose, *ibid.* **264**, 1126 (1994).
27. G. J. Kleywegt and T. A. Jones, *Acta Crystallogr.* **D50**, 178 (1994).
28. S. Mukund and M. W. W. Adams, *J. Biol. Chem.* **268**, 13592 (1993); in preparation.
29. M. F. Perutz and H. Raidt, *Nature* **255**, 256 (1975); M. F. Perutz, *Science* **201**, 1187 (1978).
30. J. E. Walker, A. J. Wonacott, J. I. Harris, *Eur. J. Biochem.* **108**, 581 (1980).
31. G. J. Davies *et al.*, *Proteins* **15**, 283 (1993).
32. S. Dao-pin, U. Sauer, H. Nicholson, B. W. Matthews, *Biochemistry* **30**, 7142 (1991); Z. S. Hendsch and B. Tidor, *Protein Sci.* **3**, 211 (1994).
33. F. C. Bernstein *et al.*, *J. Mol. Biol.* **112**, 535 (1977).
34. D. J. Barlow and J. M. Thornton, *ibid.* **168**, 867 (1983).
35. F. M. Richards, *Annu. Rev. Biophys. Bioeng.* **6**, 151 (1977).
36. T. J. Richmond and F. M. Richards, *J. Mol. Biol.* **119**, 537 (1978).
37. C. Chothia, *Nature* **254**, 304 (1975).
38. S. Miller, A. M. Lesk, J. Janin, C. Chothia, *ibid.* **328**, 834 (1987).
39. S. Miller, J. Janin, A. M. Lesk, C. Chothia, *J. Mol. Biol.* **196**, 641 (1987).
40. W. A. Lim and R. T. Sauer, *Nature* **339**, 31 (1989); A. E. Eriksson *et al.*, *Science* **255**, 178 (1992); W. A. Lim, A. Hodel, R. T. Sauer, F. M. Richards, *Proc. Natl. Acad. Sci. U.S.A.* **91**, 423 (1994); F. M. Richards and W. A. Lim, *Q. Rev. Biophys.* **26**, 423 (1994); Y. Harpaz, M. Gerstein, C. Chothia, *Structure* **2**, 641 (1994).
41. A. Wrba, A. Schweiger, V. Schultes, R. Jaenicke, P. Závodszky, *Biochemistry* **29**, 7584 (1990).
42. Because of the oxygen-sensitivity of AOR, crystals were grown by the capillary method [M. M. Georgiadis *et al.*, *Science* **257**, 1653 (1992)] with 20 μl of protein (30 mg/ml in 50 mM tris, pH 8.0, containing 10 percent glycerol, 2 mM dithionite, 2 mM dithiothreitol) and 30 μl of precipitant, in an inert atmosphere glove box. Three different conditions yielded diffraction quality crystals: (native 1) 0.18 M Na_2MoO_4, 0.1 M tris, pH 8.0, and 30 percent 4K PEG; (native 2) 0.2 M sodium acetate, 0.1 M sodium cacodylate, pH 6.5, 30 percent 8K PEG; and (native 3) 0.2 M $MgCl_2$, 0.1 M tris, pH 8.0, 30 percent 4K PEG, and 10 percent glycerol. Cell constants and space groups for these three forms are summarized in Table 1. Each crystal form contains one AOR dimer in the asymmetric unit.
43. A. J. Howard *et al.*, *J. Appl. Crystallogr.* **20**, 383 (1987).
44. W. Kabsch, *ibid.* **21**, 916 (1988).
45. G. N. Reeke Jr. *ibid.* **17**, 125 (1984); P. Bethge, *ibid.*, p. 215.
46. A. G. W. Leslie, in *Joint CCP4 and ESF-EACMB Newsletter on Protein Crystallography*, no. 26, (Daresbury Laboratory, Warrington, United Kingdom, 1992).
47. PHARE was originally distributed by G. Bricogne (MRC, Cambridge, England) and subsequently modified for the VAX by J. L. Crawford and J. E. Ladner.
48. The location of the non-crystallagraphic NCS twofold between the AOR subunits in the $P2_12_12_1$ crystal form was established from an analysis of the heavy atom and anomalous scattering sites. The NCS twofold within each *P1* crystal form was located using the Crowther fast rotation function [R. A. Crowther, in *The Molecular Replacement Method*, M. G. Rossman, Ed. (Gordon and Breach, New York, 1972), pp. 173–178], as were the cross rotation angles between each crystal form. After determination of the NCS relationships, the initial experimental maps were averaged within and between the three crystal forms, which is effectively equivalent to sixfold averaging. For the averaging, a dimer mask was generated with a modification of the Wang algorithm (*49*). Several iterations of averaging produced electron density maps of sufficient quality to trace the chain and to build a polyalanine model. At the end of averaging, the final *R* factors between the observed structure factors and structures factors calculated from the averaged maps were 23.5, 20.2, and 22.0 percent to 3 Å resolution, for crystal forms 1, 2, and 3, respectively.
49. B. C. Wang, *Methods Enzymol.* **115**, 90 (1985).
50. T. A. Jones, *ibid.*, p. 151.
51. ———, J. Y. Zou, S. W. Cowan, M. Kjeldgaard, *Acta Crystallogr.* **A47**, 110 (1991).
52. D. E. Tronrud, L. F. Ten Eyck, B. W. Matthews, *ibid.* **A43**, 489 (1987).
53. A. T. Brünger, *J. Mol. Biol.* **203**, 803 (1968).
54. R. A. Laskowski, R. W. MacArthur, D. S. Moss, J. M. Thornton, *J. Appl. Crystallogr.* **26**, 283 (1993).
55. R. Lüthy, J. U. Bowie, D. Eisenberg, *Nature* **356**, 83 (1992).
56. C. Colovos and T. O. Yeates, *Protein Sci.* **2**, 1511 (1993).
57. The α helical and β sheet regions have been identified as (*54*): α-helical residues: 25-31, 34-45, 98-105, 135-137, 142-153, 165-169, 189-196, 214-230, 232-241, 237-241, 246-252, 269-272, 274-280, 312-317, 327-340, 344-360, 365-368, 380-390, 396-400, 403-410, 413-416, 433-441, 454-457, 472-491, 495-497, 503-514, 520-541, 545-548, 553-557, 573-583, 593-599; β sheet residues: 7-13, 17-24, 54-67, 76-82, 89-95, 109-113, 119-125, 128-133, 158-164, 174-178, 182-186, 198-206, 282-286, 296-301, 305-308.
58. P. J. Kraulis, *J. Appl. Cryst.* **24**, 946 (1991); E. A. Merritt and M. E. P. Murphy, *Acta. Crystallogr.* **D50**, 869 (1994).
59. S. V. Evans, *J. Mol. Graphics* **11**, 134 (1993).
60. D. C. Rees, in preparation.

61. We thank B. T. Hsu, J. Schlessman, J. Kim, S. Faham, M. Stowell, and T. McPhillips for advice and assistance, and A. G. Myers, M. K. Johnson, P. J. Bjorkman, and J. E. Bercaw for discussions. Supported by USPHS grant GM50775 (D.C.R.); ONR grant N00014-90-J-1894 (M.W.W.A.), DOE grant FG09-88ER13901 (M.W.W.A.) and NSF grant BCS-9320069 (M.W.W.A.); the Beckman Institute, the Joseph Irvine Equipment Fund, and the Howard Hughes Medical Institute (to P. J. Bjorkman) for part of the diffraction instrumentation; NIH fellowship 1F32 GM15006 (M.K.C.); and by the rotation camera facility at the Stanford Synchrotron Radiation Laboratory, which in turn is supported by the Department of Energy, Office of Basic Energy Sciences, and the National Institutes of Health Biomedical Resource Technology Program, Division of Research Resources. Coordinates have been deposited in the Brookhaven Protein Data base, not yet available.

30 September 1994; accepted 20 January 1995

The Elemental Composition of the Corona of Procyon: Evidence for the Absence of the FIP Effect

Jeremy J. Drake,* J. Martin Laming, Kenneth G. Widing, Jürgen H. M. M. Schmitt, Bernhard Haisch, Stuart Bowyer

The chemical composition of the solar corona is not the same as that of the underlying photosphere. In the corona, elements with a first ionization potential (FIP) of ≤10 electron volts (for example, iron, magnesium, silicon, and calcium) are overabundant relative to those with an FIP of ≥10 electron volts (for example, oxygen, neon, and sulfur) by factors of 3 to 10 with respect to the photosphere. The origin of this FIP effect is unknown. The launch of the Extreme Ultraviolet Explorer Satellite (EUVE) opened up the spectroscopic capability required to determine elemental abundances in the coronae of other stars. Spectroscopic observations of the corona of the nearby F5 IV star Procyon obtained with EUVE have yielded estimates of the relative abundances of high- and low-FIP species. The results provide evidence that Procyon, unlike the sun, does not exhibit the FIP effect. Whether the sun or Procyon is more typical of the general late-type stellar population is of fundamental interest to the physics of stellar outer atmospheres and has a bearing on the origin of cosmic rays.

The suggestion that the abundances of elements in the diffuse hot (temperature $T \sim 10^5$ to 10^7 K) plasma that makes up the solar corona differ from the corresponding values in the cooler ($T \sim 6 \times 10^3$ K), more dense photosphere dates back to pioneering extreme ultraviolet (EUV) spectroscopic studies of the corona in the 1960s (*1*). Subsequent work on solar energetic particles (*2*), which originate in the solar corona, and direct x-ray and EUV spectroscopic observations of the corona (*3–5*) confirmed, upon reexamination (*6*), that the abundances of elements such as Fe, Mg, and Si are enhanced in the corona by factors of up to 10. An additional surprise was that this abundance pattern bore notable similarity to that observed in cosmic rays (*2*). A systematic underlying trend was discovered in the abundance enhancements when the elements were ordered according to their FIPs (*7*): Elements with low FIP (≤10 eV) show a clear enhancement when compared to elements with high FIP (≥10 eV), a phenomenon now commonly known as the FIP effect (*6*, *8*). The highest FIP for which abundance enhancements are observed, ~10 eV, implies temperatures of ~10,000 K or so at the site of fractionation. Such temperatures occur in the solar chromosphere. However, as yet, there are no widely accepted models to explain the process responsible for the fractionation.

Do other stellar coronae share a solar-like abundance enhancement of low-FIP species, or by some rare coincidence of stellar parameters and evolutionary circumstance, are the enhancements in the solar corona unique? The only way to investigate the compositions of the coronae of other stars directly is through EUV and x-ray spectroscopy. The capability of resolving the individual spectral lines that can provide coronal abundance diagnostics at these short wavelengths has only been realized since the launch of the Extreme Ultraviolet Explorer (EUVE) satellite in 1992. The EUVE spectrometers provide moderate-resolution (wavelength $\lambda/\Delta\lambda \sim 200$) spectroscopy from 75 to 760 Å in three band passes (*9*), commonly designated short wavelength (SW), medium wavelength (MW), and long wavelength (LW). In this report, we present an analysis of the abundances of elements in the corona of a star other than the sun. Our analysis is based on EUVE spectroscopic observations of Ne and S (both high-FIP elements) and Fe, Mg, Si, and Ca (all low-FIP elements) features seen in the EUVE MW and LW spectra of the corona of the F5 IV star Procyon.

The photospheric abundances in Procyon are very well known from optical spectroscopy (*10–14*) and are, to within small experimental uncertainties (≤25%), solar. Unfortunately, although Ne lines appear prominently in coronal spectra, Ne abundances cannot be measured in late-type stellar photospheres because of a lack of suitable optical lines. On the basis of the fact that Procyon's composition in the other elements is the same as that of the sun and in view of the lack of any recognized Ne abundance anomaly effect in stellar atmospheres (in the manner of the abundances anomalies observed in, for example, Li), we assume with reasonable confidence that Procyon will have a solar abundance of this element.

Procyon was selected for observation by EUVE as a cornerstone wavelength calibration source and as a guest observer (GO) target. Its proximity (3.48 pc) and relatively energetic corona (approximately equal to the sun in its active state, x-ray luminosity $L_x = 10^{28}$ erg/s) make it the brightest effectively nonbinary EUV coronal source available for study; the 11th magnitude companion is too distant to produce any significant interaction effects and as a DF white dwarf would not be the source of any significant EUV or x-ray flux, as confirmed by high-resolution Einstein observations (*15*).

As one of the first observations of late-type stars during the GO phase of the mission, a continuous pointing began on 11 January 1993 UT (universal time) 22:19 and ended on 15 January 1993 UT 00:28; the nominal exposure time was about 100,000 s. The reduction of the raw data into the final flux-calibrated SW, MW, and LW spectra followed standard procedures and is detailed elsewhere (*16*).

The flux, F_{ji}, emitted through a spectral line $j \rightarrow i$ by an optically thin stellar corona can be closely approximated by the integral over the temperature interval, ΔT_{ji}, over which the line flux is nonnegligible (usually, $\log \Delta T_{ji} \sim 0.3$) (in ergs per square centimeter per second):

$$F_{ji} = AK_{ji} \int_{\Delta T_{ji}} G_{ji}(T)\, \overline{n_e^2}\,(T)\, \frac{dV(T)}{dT}\, dT \qquad (1)$$

where A is the abundance of the element in question, K_{ji} is a known constant that includes the frequency of the transition and the stellar distance, $n_e(T)$ is the number density of electrons at characteristic temperature T within the volume of the emitting plasma $V(T)$, and $G_{ji}(T)$ is the "contribution" function of the line. This last parameter defines the temperature interval, ΔT_{ji}, over which the line is formed and is dependent on the atomic physics of the particular transition. For most transitions of interest, $G_{ji}(T)$ can be theoretically estimated with fair reliability.

Extracting an elemental abundance from an observed F_{ji} cannot generally be accomplished without detailed knowledge of the

J. J. Drake and S. Bowyer, Center for Extreme Ultraviolet Astrophysics, University of California, 2150 Kittredge Street, Berkeley, CA 94720, USA.
J. M. Laming, Sachs Freeman Associates, Landover, MD 20785, USA, and E. O. Hulburt Center for Space Research, Naval Research Laboratory, Code 7674L, Washington, DC 20375, USA.
K. G. Widing, E. O. Hulburt Center for Space Research, Naval Research Laboratory, Code 7674W, Washington, DC 20375, USA.
J. H. M. M. Schmitt, Max-Planck-Institut für Extraterrestrische Physik, 85740 Garching, Germany.
B. Haisch, Lockheed Solar and Astrophysics Laboratory, Department 91-30, Building 252, 3251 Hanover Street, Palo Alto, CA 94304, USA, and Center for Extreme Ultraviolet Astrophysics, University of California, 2150 Kittredge Street, Berkeley, CA 94720, USA.
*To whom correspondence should be addressed.

integrand $\overline{n_e^2}(T)[dV(T)/dT]$. This quantity is known, historically, as the "differential emission measure." However, if two lines due to different elements can be found whose contribution functions, $G_{ji}(T)$, have the same temperature dependence, then in the expression for the ratio of the line fluxes all terms will cancel except for the elemental abundances and the relevant atomic physics parameters. The ratio of their abundances is obtained directly from the ratio of observed line fluxes. Furthermore, if the two lines are near the same wavelength, then any uncertainties that might arise from the spectrometer calibration and the absorption of radiation in the interstellar medium are removed.

A thorough search of our Procyon spectra revealed the best set of closely spaced features due to low- and high-FIP species with similar temperature dependence to be the closely spaced group of lines Fe XV 243.78 Å, Fe XIII 246.21 Å, and S XI 246.90, 247.13 Å. The S XI line is formed at log $T = 6.25$ and is bracketed by Fe XIII (log $T = 6.2$) and Fe XV (log $T = 6.3$); the Fe/S abundance ratio then lies between the ratios yielded by the Fe XIII and Fe XV lines. Also useful are the regions between 280 and 290 Å, which contain the Fe XV 284.15 Å, S XI 281.42, 285.60, 285.83 Å, and S XII 288.41 Å transitions, and the Si X and S X multiplets near 260 Å. Two other promising candidates whose utility has been pointed out (*8*, *17*) are the Mg VI and Ne VI multiplets at ~400 Å and the Ca IX and Ne VII lines near 465 Å. Unfortunately, in our Procyon spectra the 400 Å feature is dominated by stronger Fe XII and Fe XIII lines near 200 Å appearing in second order, rendering it unreliable; we have not pursued this feature further. The moderate resolution and signal-to-noise ratio of the Procyon LW spectrum also renders the Ne VII and Ca IX blend near 465 Å somewhat less useful: The blend is dominated by Ne, making the Ca contribution very difficult to measure. However, a nearby Mg VII line at 434.92 Å provides a reliable comparison for the Ne VII feature.

We measured the individual line intensities by fitting them with Gaussian profiles. All of the above features are partially blended, but because the corona of Procyon is likely to be optically thin, Gaussian fitting allows us to deconvolve readily the relative intensities of the blended lines. We verified that the instrument response of the spectrograph is very close to Gaussian by careful examination of strong, unblended lines such as He II 303.79 Å and Fe XV 284.17 Å. Our analytical fits to the Fe and S lines near 245 Å and between 280 and 290 Å and the Ne-Ca blend at 465 Å, together with residuals, are illustrated in Figs. 1, 2, and 3. The individual line intensity ratios

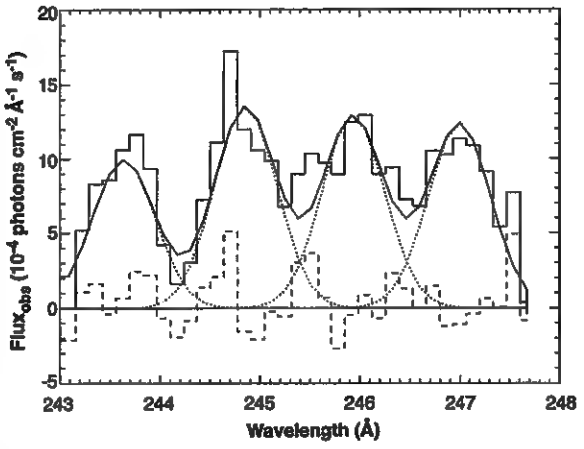

Fig. 1. Observations (solid histogram), fit (solid line), and residuals (dashed histogram) for the Fe XV 243.78 Å, Fe IX 244.91 Å, Fe XIII 246.21 Å, and S XI 246.90, 247.13 Å lines. The individual line components are indicated by the dotted lines. The small wavelength offsets for the Fe XV and Fe XIII lines are caused by known imperfections in the instrument calibration and small detector distortions. Several other strong lines from these ions are visible in the EUVE spectra, making these particular identifications unambiguous. S XI bracketed by Fe XIII and Fe XV (see text). We neglect the likely very small contribution of the Si VI 246.00 Å line to the intensity of Fe XIII 246.21 Å. We based the Gaussian fits and line intensity errors on a χ^2 minimization, using a Levenberg-Marquardt algorithm with single-value decomposition. The errors are estimated from the shape of the χ^2 minimum coming from the singular-value decomposition in the fitting program; this gives essentially the statistical error for clean unblended lines. The fit residuals and intensity errors are consistent with the noise level, which originates from photon noise and background counts. The measured line intensities are listed in Table 1. The Fe/S abundance ratio, based on the average between Fe XV and Fe XIII, and S XI and on the treatment of the atomic physics in (*19*) is Fe/S = 2.4 ± 1.2. This ratio is consistent with the solar photospheric abundance ratio of 2.1 but not with the solar coronal value of 6.8.

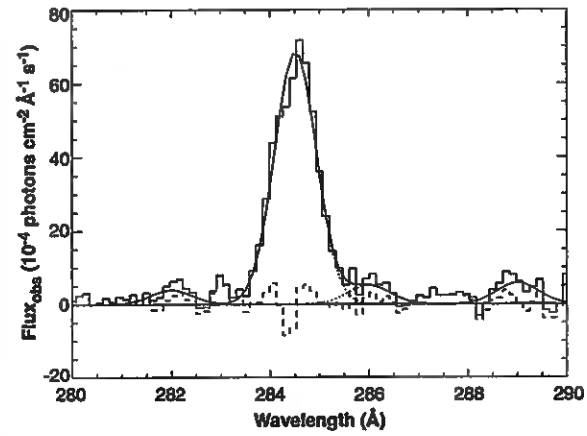

Fig. 2. Observations (solid histogram), fit (solid line), and residuals (dashed histogram) for the Fe XV 284.15 Å, S XI 281.42, 285.60/285.83 Å, and S XII 288.41 Å lines. Fits and intensity errors are as described for Fig. 1, except that the error associated with the S XII 288.42 intensity has been expanded to account for the possible blend with Fe XIV 289.16 Å. A constant wavelength offset of ~0.5 Å is caused by known errors in the spectrometer wavelength calibration. The individual line components in the 284 to 287 Å blend are indicated by the dotted lines. Several other strong lines from these ions are visible in the EUVE spectra, and these identifications are unambiguous: S XII is formed at log $T = 6.3$, like Fe XV, and so a direct comparison between these two is largely independent of the shape of the differential emission measure curve. Abundance ratios are based on the treatment of atomic physics in (*19*).

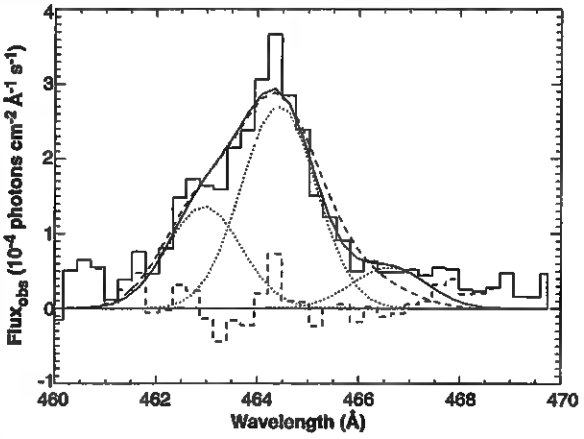

Fig. 3. Observations (solid histogram), fit (solid line), and residuals (dashed histogram) for the Ne VII 465.22 Å, Ca IX 466.23 Å, and unidentified lines at 463.75 and 467.40 Å [the only ones of the unidentified lines appearing in the Skylab atlas (*27*) we find to be statistically significant]. The peaks are displaced from the positions corresponding to the wavelength calibration by a constant offset of −0.8 Å. The dashed curve illustrates the profile resulting from a Ca abundance appropriate to the solar corona. Although this latter curve does not fit the observed data as well as that corresponding to a photospheric Ca abundance, the difference between the two cases is of low significance. We use only the Ne VII line for our abundance analysis.

measured from the fits to the S and Fe lines are also listed in Table 1, together with the derived abundance ratios, for an assumed electron density of 10^{10} cm^{-3}. The S XI lines are slightly sensitive to electron density in this region, in that lower electron densities would give higher emission measures for this ion, and hence a slightly higher Fe/S abundance ratio. The electron density in Procyon's corona has very recently been estimated as $n_e = (5.5 \pm 1.5) \times 10^9$ cm^{-3} (*18*) on the basis of a set of Fe XIV lines; however, if this electron density were used, our results would not be significantly affected.

The abundance ratios determined in this way are consistent with Procyon's photospheric abundances (which are equivalent to the solar photospheric abundances) rather than with solar coronal abundances. From the intensities of the S and Fe lines, using the treatment of the atomic physics in (*19*), we obtain an abundance ratio based on the average between Fe XV and Fe XIII, and S XI of Fe/S = 2.4 ± 1.2. The solar photospheric abundance ratio is 2.0, whereas the coronal value is 6.8 (*8*). Intensities for this same group of lines have also been measured recently from the spectrum of a solar-active region obtained with the Solar EUV Rocket Telescope and Spectrograph (*20*), and also in a full-disk, quiet-sun spectrum (*21*). The abundance ratios obtained in the same way from these spectra are 8 ± 4 and ~5, respectively [no measurement errors are given in (*21*)], essentially the same as the average solar coronal value (*8*). Thus, on the basis of these Fe and S lines, we have a clear indication that the FIP effect in the corona of Procyon is substantially smaller than that in the sun. This result is supported by the Si X 258.39/S X 264.24 ratio and the various intensities ratios available in the region from 280 to 290 Å, as reported in Table 1. These same ratios observed in solar EUV spectra (*20*, *21*) are significantly higher, indicating coronal abundances. These ratios do not include systematic errors arising from the atomic physics, because these cancel in the differential comparison with the sun.

We obtain a similar result from the Ne VII, Ca IX, and Mg VII lines. Because the Ca contribution to the Ne VII and Ca IX blend near 465 Å is rather weak, an accurate Ca/Ne abundance ratio cannot be extracted from this feature. The best fit we obtained for the observed feature, illustrated in Fig. 3, finds essentially no Ca in the blend. The profile corresponding to a coronal Ca abundance ratio is illustrated by the dashed curve. This result is not statistically significant, and instead, we rely on a comparison between Ne VII and a nearby line of Mg VII at 434.92 Å. Because these lines have a small wavelength separation, the relative strengths of the Ne VII and Mg VII lines are weakly dependent on the absorption of EUV flux by neutral hydrogen in the interstellar medium. We accounted for this by using the hydrogen column density from (*22*). The uncertainty in this measurement leads to a further small uncertainty in the Ne VII and Mg VII line intensity ratio of about 10%. The Mg VII 434.92 Å transition is blended with Ne VI 433.18 and 435.65 Å; we have accounted for this by using an emission measure estimated for Ne VI (the mean of those derived for the lines Ne V 416.20 Å and Ne VII 465.22 Å), inasmuch as all other strong lines from this ion (the mutiplets near 400 and 560 Å) are contaminated with higher order features.

The contribution due to the Ne lines amounts to approximately 50% of the total feature flux. The resulting Ne VII and Mg VII line flux ratio and corresponding abundance ratio are listed in Table 1; the uncertainty in the Mg VII line flux due to the subtraction of the Ne VI blend is included in the final result. We obtain an abundance ratio for Mg/Ne of 0.35 ± 0.35. This value is in concordance with Procyon's (and the solar) photospheric ratio rather than with the solar coronal value.

Why would the FIP effect occur in the sun's corona but not in Procyon's? Because the ionization potential separating the low and high FIP is indicative of chromospheric temperatures (~10,000 K), perhaps the answer lies in Procyon's chromosphere. Procyon's chromospheric emission is at, or very near, the "basal" level: The basal-flux stars are the slowest rotators, whose central dynamos are probably not significantly active. However, these stars still exhibit chromospheric emission at levels well above the detection thresholds of instruments such as the International Ultraviolet Explorer (*23*). In the solar chromosphere, the surface flux in regions away from the chromospheric network and plages is close to the basal limit.

It has often been suggested that the basal chromospheric activity level could be due to acoustic heating, in which convective energy is dissipated into the thermal energy of the chromosphere (*23*). According to this scenario, magnetic heating of the basal stars would not be significant. One requirement of potential FIP fractionation models is that the fractionation must occur in relatively short time scales (seconds to minutes) and consequently over small spatial scales (one to tens of kilometers). Otherwise, neutral species would have sufficient time to become ionized during the separation process (*24*). Such small spatial scales can occur quite naturally with magnetic fields but not with acoustic waves. If, then, Procyon's chromosphere is heated predominantly by acoustic means—significantly more so than that of the sun—its corona might not be expected to show any FIP effect. In contrast, the coronal regions of the sun, fed with low-FIP enhanced material from the magnetically active regions in the solar chromosphere, would be expected to show an FIP effect.

The coronal FIP effect is also potentially of central importance to the origin of cosmic rays. It was noticed that the FIP effect observed in the solar corona and wind is very similar to that observed in cosmic rays of medium to low energy ($\lesssim$100 GeV) (*7*). Suggestions followed that galactic cosmic rays could originate from late-type stellar coronal loss of mass (*6*). These seed particles, enhanced in low-FIP species, are then accelerated to relativistic energies by diffusive shock acceleration (*25*) provided by, for example, supernova remnants in interstellar space.

Table 1. Summary of lines used in the analysis, their observed intensity ratios in Procyon, and corresponding abundance ratios.

Abundance diagnostic	log *T*	Intensity ratio	Abundance ratio (by number)		
			Solar photosphere*	Solar coronat	Procyon corona
Fe XV 284.15 Å : S XII 288.41 Å	6.3	12 ± 6	Fe/S = 2.0	6.8	1.9 ± 1.0
Fe XIII 246.21 Å : S XI 246.90, 247.13 Å	6.2–6.25	1.2 ± 0.6	Fe/S = 2.0	6.8	1.7 ± 0.9
Fe XV 243.78 Å : S XI 246.90, 247.13 Å	6.25–6.3	0.96 ± 0.5	Fe/S = 2.0	6.8	3.1 ± 1.5
Fe XV 284.15 Å : S XI 281.42 Å	6.25–6.3	17 ± 6	Fe/S = 2.0	6.8	0.95 ± 0.3
Fe XV 284.15 Å : S XI 285.60, 285.83 Å	6.25–6.3	13 ± 5	Fe/S = 2.0	6.8	2.7 ± 1.0
Si X 258.39 Å : S X 264.24 Å	6.1–6.15	0.94 ± 0.5	Si/S = 2.1	6.8	1.4 ± 0.7
Mg VII 434.92 Å : Ne VII 465.22 Å	5.7	0.077 ± 0.07	Mg/Ne = 0.31	1.2	0.35 ± 0.35

*From (*28*). †From (*8*).

It has been pointed out (*26*) that this scenario is particularly appealing, because other nonstellar injection models suffer the disadvantage of both having to account for the fractionation through other means and facing the prospect that the remarkable similarity between the cosmic-ray source composition and the composition of solar energetic particles is purely accidental. However, this hypothesis is based entirely on extrapolation of the solar case, because before now it has not been possible to determine the abundances of elements in the coronae of other stars. Our failure to detect a similar FIP effect in the corona of Procyon provides evidence that the FIP effect is not a ubiquitous signature of late-type stellar coronae.

REFERENCES AND NOTES

1. S. R. Pottasch, *Astrophys J.* **137**, 945 (1963).
2. A. Mogro-Campero and J. A. Simpson, *ibid.* **171**, L5 (1972).
3. A. B. C. Walker, H. R. Rugge, K. Weiss, *ibid.* **194**, 471 (1974).
4. H. R. Rugge and A. B. C. Walker, *ibid.* **203**, L139 (1976).
5. J. H. Parkinson, *Astron. Astrophys.* **57**, 185 (1977).
6. J.-P. Meyer, *Astrophys. J. Suppl. Ser.* **57**, 172 (1985).
7. M. Cassé and P. Goret, *Astrophys. J.* **221**, 703 (1978).
8. U. Feldman, *Phys. Scr.* **46**, 202 (1992).
9. S. Bowyer and R. F. Malina, in *Extreme Ultraviolet Astronomy*, R. F. Malina and S. Bowyer, Eds. (Pergamon, New York, 1991), p. 94.
10. R. Griffin, *Mon. Not. R. Astron. Soc.* **155**, 139 (1971).
11. J. Tomkin and D. L. Lambert, *Astrophys. J.* **223**, 937 (1978).
12. K. Kato and K. Sadakane, *Astron. Astrophys.* **167**, 111 (1986).
13. M. Steffen, *Astron. Astrophys. Suppl. Ser.* **59**, 403 (1985).
14. B. Edvardsson *et al.*, *Astron. Astrophys.* **275**, 101 (1993).
15. J. H. M. M. Schmitt *et al.*, *Astrophys. J.* **290**, 307 (1985).
16. B. Haisch, J. J. Drake, J. H. M. M. Schmitt, *ibid.* **421**, L39 (1994).
17. K. G. Widing and U. Feldman, *ibid.* **334**, 1046 (1989).
18. J. H. M. M. Schmitt, B. M. Haisch, J. J. Drake, *Science* **265**, 1420 (1994).
19. P. L. Dufton, personal communication; D. R. Flower and H. Nussbaumer, *Astron. Astrophys.* **31**, 353 (1974); B. C. Fawcett and H. E. Mason, *At. Data Nucl. Data Tables* **43**, 245 (1989); H. E. Mason and A. K. Bhatia, *Mon. Not. R. Astron. Soc.* **184**, 423 (1978); D. F. Flower and H. Nussbaumer, *Astron. Astrophys.* **42**, 265 (1975).
20. R. J. Thomas and W. M. Neupert, *Astrophys. J. Suppl. Ser.* **91**, 461 (1994).
21. M. Malinovsky and L. Heroux, *Astrophys. J.* **181**, 1009 (1973).
22. J. Murthy *et al.*, *ibid.* **315**, 675 (1987).
23. C. J. Schrijver, *Astron. Astrophys.* **180**, 241 (1987).
24. R. von Steiger and J. Geiss, *ibid.* **225**, 222 (1989).
25. W. I. Axford, E. Leer, K. G. Skandron, *Proc. 15th Int. Cosmic Ray Conf.* **11**, 32 (1977).
26. H. Bloemen, in *Interstellar Processes*, D. J. Hollenbach and H. A. Thronson Jr., Eds. (Reidel, Dordrecht, Netherlands, 1987), p. 143.
27. U. Feldman, J. D. Purcell, B. C. Dohne, *NRL Rep. 90-4100* and *NRL Rep. 91-4100* (Naval Research Laboratory, Washington, DC, 1987).
28. E. Anders and N. Grevesse, *Geochim. Cosmochim. Acta* **53**, 197 (1989).

29. We thank G. Doschek, U. Feldman, K. Strong, and J. Saba for useful discussions and the EUVE Science Team for advice and support. We thank the referees for pertinent comments, which improved the manuscript. J.J.D. was supported by National Aeronautics and Space Administration grant AST91-15090 administered by the Center for Extreme Ultraviolet Astrophysics, University of California.

18 August 1994; accepted 28 December 1994

Conducting Layered Organic-Inorganic Halides Containing ⟨110⟩-Oriented Perovskite Sheets

D. B. Mitzi,* S. Wang, C. A. Feild, C. A. Chess, A. M. Guloy

Single crystals of the layered organic-inorganic perovskites, $[NH_2C(I)=NH_2]_2(CH_3NH_3)_mSn_mI_{3m+2}$, were prepared by an aqueous solution growth technique. In contrast to the recently discovered family, $(C_4H_9NH_3)_2(CH_3NH_3)_{n-1}Sn_nI_{3n+1}$, which consists of ⟨100⟩-terminated perovskite layers, structure determination reveals an unusual structural class with sets of m ⟨110⟩-oriented $CH_3NH_3SnI_3$ perovskite sheets separated by iodoformamidinium cations. Whereas the $m = 2$ compound is semiconducting with a band gap of 0.33 ± 0.05 electron volt, increasing m leads to more metallic character. The ability to control perovskite sheet orientation through the choice of organic cation demonstrates the flexibility provided by organic-inorganic perovskites and adds an important handle for tailoring and understanding lower dimensional transport in layered perovskites.

Recent interest in organic-inorganic multilayer perovskites stems from the flexibility to use organic layers to tailor magnetic (*1*, *2*), optical (*3*, *4*), thermochromic (*5*), or structural (*6*) properties of adjacent nonconducting metal halide perovskite sheets. Typically, these self-assembling structures consist of single ⟨100⟩-terminated perovskite sheets alternating with alkylammonium bilayers, with the alkyl chains extending into the space between layers and van der Waals interactions between chains holding the layers together. More complicated organic cations have also been incorporated, including those with benzene rings and unsaturated hydrocarbon tails (*4*, *7*). The ability to polymerize the organic layer (*7*, *8*) or to study conformational changes within long-chain alkylammonium bilayers (*9*) provides further flexibility and interest.

Recently, a family of conducting layered organic-inorganic perovskites, $(C_4H_9NH_3)_2(CH_3NH_3)_{n-1}Sn_nI_{3n+1}$ (n = 1 to 5), was found (*10*) in which n ⟨100⟩-terminated $CH_3NH_3SnI_3$ perovskite sheets alternate with butylammonium bilayers. These conducting non–oxide-layered perovskites share many of the structural features of the cuprate superconductors and other conducting layered-oxide perovskites (which also consist of ⟨100⟩ perovskite sheets). In addition, these systems are natural (self-assembling) analogs to semiconductor quantum-well multilayers, with the perovskite layers acting as wells and the longer-chain alkyl layers forming barrier layers. Observation of enhanced exciton binding energies in both the lead(II) and tin(II) analogs of these layered perovskites highlight the two-dimensional nature and the effect of dielectric modulation (*3*, *11*).

In this report, we discuss the synthesis, structure, and transport properties of a class of conducting layered halides, $[NH_2C(I)=NH_2]_2(CH_3NH_3)_mSn_mI_{3m+2}$ (m = 2 to 4), that consists of m $CH_3NH_3SnI_3$ perovskite layers terminating on a ⟨110⟩ crystallographic plane, rather than on the usual ⟨100⟩ plane. This structure appears to be stabilized by the interposed layers of iodoformamidinium cations, which orient along the channels provided by the ⟨110⟩ perovskite surfaces. The ability to form either ⟨100⟩- or ⟨110⟩-terminated perovskite sheets through the choice of organic cation in the initial crystal growth solution (in this case, butylammonium versus iodoformamidinium) demonstrates an additional degree of flexibility within the family of organic-inorganic perovskites. Many of the related ⟨100⟩-terminated conducting layered perovskites—including the oxides $(La_{1-x}Sr_x)_{n+1}Mn_nO_{3n+1}$ (*12*), $La_{n+1}Ni_nO_{3n+1}$ (*13*), and $Ba_{n+1}Pb_nO_{3n+1}$ (*14*) as well as the halide $(C_4H_9NH_3)_2(CH_3NH_3)_{n-1}Sn_nI_{3n+1}$ (*10*)—undergo a semiconductor-metal transition with increasing n. We find a similar trend in the ⟨110⟩-terminated layered perovskites.

Crystals of each tin(II)-based layered perovskite were grown in an argon atmosphere by slow cooling from concentrated aqueous hydriodic acid solutions of $CH_3NH_2{\cdot}HI$, NH_2CN, and SnI_2 (*15*). The chemistry of cyanamide in this synthesis is in itself unusual. Although anhydrous reaction between nitriles (RCN) and hydrogen halides (HX) generally results in the nucleophilic attack of X^- on the nitrile triple bond (resulting in an

D. B. Mitzi, C. A. Feild, C. A. Chess, IBM T. J. Watson Research Center, Post Office Box 218, Yorktown Heights, NY 10598, USA.
S. Wang and A. M. Guloy, Department of Chemistry and Texas Center for Superconductivity, University of Houston, Houston, TX 77204–5641, USA.

*To whom correspondence should be addressed.

imidyl halide), in aqueous acid solutions, cyanamide generally hydrolyzes to give urea (*16*). Kilpatrick (*17*) has demonstrated that the rate of hydrolysis in aqueous hydrochloric and hydrobromic acids increases to a maximum with increasing acid concentration and thereafter drops off as a result of the formation of competing less-hydrolyzable species. It is likely that our use of the stronger concentrated aqueous hydriodic acid effectively avoids the hydrolysis of cyanamide through a similar process, with the formation of the iodoformamidinium cation, which has greater hydrolysis resistance.

Infrared (IR) transmission spectroscopy of cleaved $m = 2$ single crystals confirms that these solid-state structures contain the iodoformamidinium cation. A strong band at 1652 cm^{-1} is characteristic of the amidine (N–C=N) stretching vibration (*18*). A second strong band is observed at 1712 cm^{-1}. Sumarokova *et al.* (*19*) assign bands at 1710 and 1665 cm^{-1} in diacetonitrile hydrogen chloride tin(IV) chloride to C=N stretching modes. A strong band at 604 cm^{-1} corresponds to the C–I stretch, and bands at 3327, 3263, and 3180 cm^{-1} correspond to the N–H_2 asymmetric and the N–H and N–H_2 symmetric stretches, respectively. In addition, two bands are observed at 1473 cm^{-1} (C–NH_2 deformation mode) and 1389 cm^{-1} (C–N stretch). Bands characteristic of hydrogen iodide and nitrile (C≡N) moieties, from the starting material, would be expected from 2100 to 2400 cm^{-1} and are not observed, and absorptions attributed to urea, especially the carbonyl expected between 1650 and 1500 cm^{-1} (*20*), are also not observed.

The organic-inorganic multilayer structure (Fig. 1 and Table 1) of $[NH_2C(I)=NH_2]_2(CH_3NH_3)_2Sn_2I_8$ ($m = 2$), as derived from a single-crystal structure refinement, has a monoclinic unit cell with a = 6.2649(4) Å, b = 8.6624(5) Å, c = 14.787(2) Å, and β = 92.960(8)° (numbers in parentheses are standard errors in the last digit). The perovskite sheets are derived from the three-dimensional perovskite structure of $CH_3NH_3SnI_3$, which consists of an infinite network of corner-sharing SnI_6 octahedra, by cutting two-layer-thick perovskite slabs terminating on ⟨110⟩ planes. Similar ⟨110⟩-terminated perovskite sheets also appear in a series of nonconducting inorganic oxides with general formula $A_mM_mO_{3m+2}$ (where A = Ca, Na/Ca or La, La/Ca; and M = Nb or Ti) (*21*) and in the fluorides $BaMF_4$ (where M = Ni, Co, Mn, or Fe) (*22*).

The tin(II) halide perovskites are unusual in that the tin(II) lone pair is stereochemically inactive, enabling tin(II) to achieve an uncharacteristic regular octahedral coordination (trigonal or square pyramidal coordination is more typical), presumably because the tin 5*s* nonbonding states are delocalized into a conduction band (*23*). Within the perovskite slabs (Fig. 2) of $[NH_2C(I)=NH_2]_2(CH_3NH_3)_2Sn_2I_8$, the tin(II) atoms sit in a slightly distorted octahedral coordination with I–Sn–I angles ranging from 85.67(5)° to 92.82(6)° and Sn–I bond distances ranging from 3.094(2) to 3.185(1) Å, where the shortest bonds are to the outer terminal iodines, I(3), and the longest are to the central layer of iodines, I(1). These values can be compared with the 90° I–Sn–I bond angles and six equal 3.12 Å Sn–I bonds in cubic (at room temperature) $CH_3NH_3SnI_3$. The Sn–I(2)–Sn angle of 173.3(1)° indicates a slight corrugation of the tin(II) iodide perovskite sheets along the a axis. The $CH_3NH_3^+$ cations are located on the A sites of the ABX_3 perovskite slabs, coordinated by 11 iodines from within the perovskite slabs and one iodine from the nearest iodoformamidinium cation, thereby yielding the same overall coordination as in the cubic perovskite.

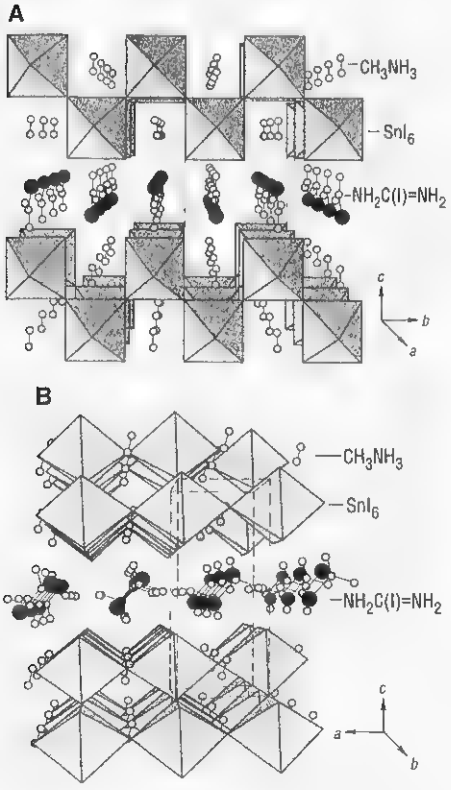

Fig. 1. Two schematic views of the $[NH_2C(I)=NH_2]_2(CH_3NH_3)_2Sn_2I_8$ ($m = 2$) crystal structure, along the (**A**) ⟨100⟩ and (**B**) ⟨010⟩ directions, highlighting the ⟨110⟩ orientation of the $CH_3NH_3SnI_3$ perovskite sheets. The SnI_6 octahedra are shown in a polyhedral representation with the iodine atoms removed for clarity.

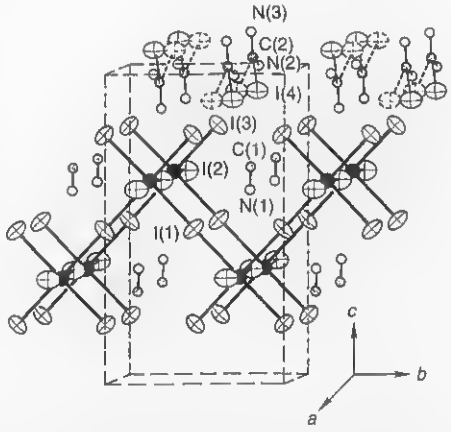

Fig. 2. Detailed structure of the Sn–I perovskite layer showing atom labeling and anisotropic thermal ellipsoids. A split position for I(4) with ½ occupancy indicates disordering of the iodoformamidinium cation.

Table 1. Crystallographic data for $[NH_2C(I)=NH_2]_2(CH_3NH_3)_2Sn_2I_8$. The space group $P2_1/m$ was selected in agreement with systematic absences and intensity distribution. Data were collected at room temperature in the ω-2θ scan mode up to 2θ = 48°, using an Enraf-Nonius CAD4 single-crystal diffractometer and graphite monochromatized MoKα radiation. The θ-dependent absorption correction, based on multiple psi-scans, was applied to all intensity data. Direct methods were used to determine the Sn and I heavy-atom positions, and subsequent refinement and Fourier synthesis steps located the lighter elements (C and N). Numbers in parentheses are statistical errors of the last significant digit (when absent, the parameter was held fixed). Final least squares refinement resulted in refinement parameters R_f/R_w = 0.047/0.051 [10 atoms, 52 parameters, 899 independent reflections with intensities $I \geq 3\sigma(I)$]. a = 6.2649(4) Å, b = 8.6624(5) Å, c = 14.787(2) Å; β = 92.960(8)°; and $Z = 1$.

Atom	Position*	x	y	z	B_{iso} (Å²)†
Sn	2e	0.0156(3)	¼	0.6582(1)	3.5(1)
I1	2c	0	½	½	7.0(1)
I2	2e	0.5207(3)	¼	0.6457(2)	6.7(1)
I3	4f	0.0299(2)	0.4997(2)	0.8080(1)	5.7(1)
I4‡	4f	0.6330(4)	0.6918(4)	0.9379(2)	5.6(2)
N1	2e	0.44(1)	¼	0.378(5)	20 (3)
N2	2e	0.203(5)	¾	0.009(2)	7.7(8)
N3	2e	0.473(6)	¾	0.115(2)	8.5(9)
C1	2e	0.55(1)	¼	0.330(6)	16 (3)
C2	2e	0.416(5)	¾	0.029(2)	5.2(7)

*Multiplicity and Wyckoff letter. †B_{iso} is the mean of the principal axes of the thermal ellipsoid. ‡Occupancy = ½ as a result of orientational disorder.

The $m = 2$ structure is distinct from the insulating $BaZnF_4$ (or equivalently $Ba_2Zn_2F_8$) structure in that the divalent Ba^{2+} cation is replaced by the monovalent $CH_3NH_3^+$ cation. To maintain charge neutrality, an additional monovalent cation needs to be incorporated into the structure, thereby forming the distinct organic layer of this unusual multilayer structure. The organic iodoformamidinium cations are therefore an integral part of the crystal structure and are not simply an intercalated species. The refined bond angles around the iodoformamidinium carbon range from 115° to 123°, consistent with sp^2 hybridization. The refined C(2)–I(4), C(2)–N(2), and C(2)–N(3) distances [2.02(3), 1.35(5), and 1.31(5) Å] are also typical for bonding in this hybridization. Within the solid-state structure, iodoformamidinium cations form nominal "chains" of $NH_2C(I)=NH_2^+$ along the a axis with the I(4) atoms of this cation directed toward and coordinating the nearest $CH_3NH_3^+$ cations in the perovskite sheet. The N(3) atoms orient toward the nearest I(3) atom of the perovskite slabs, whereas N(2) atoms are directed at the I(4) of the neighboring colinear organic cation. Hence, adjacent chains within the layer are oriented anti to each other.

More generally, a family of compounds, $[NH_2C(I)=NH_2]_2(CH_3NH_3)_mSn_mI_{3m+2}$, for $m \geq 1$, are expected. Isolation of the $m = 3$ and 4 members (Fig. 3) confirms this expectation. Lattice parameters for the observed members of $[NH_2C(I)=NH_2]_2(CH_3NH_3)_mSn_mI_{3m+2}$ approximately follow the rule $a = a_p$, $b = \sqrt{2}a_p$, and $c = K + ma_p/\sqrt{2}$, where a_p is defined as the lattice parameter for the cubic perovskite (for $CH_3NH_3SnI_3$, $a_p = 6.240$ Å) and $K \approx 5.98(5)$ Å. The monoclinic angle β is found to decrease with increasing m from 92.96(1)° ($m = 2$) to 91.83(1)° ($m = 4$). Evidence for other m members of this family have also been observed in both single-crystal and powder x-ray data.

Electrical resistivity measurements (Fig. 4) were performed in a displex (closed-cycle refrigeration) system with an airtight cell containing a calibrated four-point probe and a pressed-pellet sample. Given the rather severe chemical reactivity of these materials, ohmic electrical contacts were made with spring-activated pins directly contacting the sample. The $m = 2$ sample is semiconducting with a room-temperature resistivity of ~700 ohm·cm. Fitting the resistivity data to $\rho = A\exp(E_g/2k_BT)$ (Fig. 4, inset), where A is a constant, k_B is Boltzmann's constant, and T is temperature, yields a band gap of $E_g = 0.33(5)$ eV. Increasing the thickness of the perovskite sheets (larger m) dramatically reduces the resistivity and results in a transition to more metal-like transport properties, as has also been observed in the ⟨100⟩-oriented perovskites $(C_4H_9NH_3)_2(CH_3NH_3)_{n-1}Sn_nI_{3n+1}$, which undergo a semiconductor-metal transition with increasing n (*10*). In fact, comparing the resistivity data of the ⟨110⟩ and ⟨100⟩ layered perovskites reveals a consistent exponential drop in low-temperature resistivity with increasing perovskite layer thickness, approximately independent of layer orientation. A semiconductor-metal transition occurs for a perovskite layer thickness on the order of 20 Å, with a corresponding room-temperature resistivity of order 1 ohm·cm at the transition. The resistivity of $CH_3NH_3SnI_3$, which is the end-member compound of both the ⟨110⟩ and ⟨100⟩ families as m (or n) approaches infinity, is also shown for comparison. This cubic (at room temperature) perovskite has recently been shown to be a low–carrier density p-type metal with a well-defined plasma edge in the IR spectrum (*24*).

To better understand the nature of the semiconductor-metal transition in these unusual conducting halides, extended Hückel band structure calculations were performed on the $m = 2$ and $m \rightarrow \infty$ (cubic perovskite) systems, with a basis set consisting of Sn 5s and 5p and I 5s and 5p valence orbitals. The metallic character of $CH_3NH_3SnI_3$ results from the large dispersion of the Sn 5s band (hybridized with I 5p) along the ⟨111⟩ direction of the cubic Brillouin zone, leading to a marginal crossing of the Sn 5s and Sn 5p bands near the R point ($[\frac{1}{2}, \frac{1}{2}, \frac{1}{2}]2\pi/a$), with the Fermi energy falling roughly between the two bands. Low concentrations of defects or vacancies in the structure are

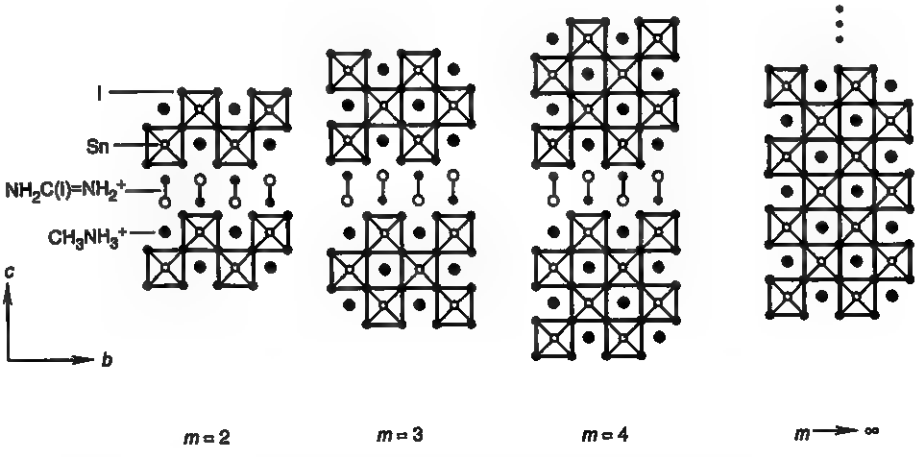

Fig. 3. Schematic representation of the $m = 2$ to 4 and ∞ (cubic perovskite) compounds. The monoclinic lattice constants for $m = 2$, 3, and 4 are $a = 6.2649(4)$ Å, $b = 8.6624(5)$ Å, $c = 14.787(2)$ Å, and $\beta = 92.960(8)°$; $a = 6.2671(3)$ Å, $b = 8.7183(4)$ Å, $c = 38.434(2)$ Å (2 × 19.217), and $\beta = 92.34(2)°$; and $a = 6.2485(7)$ Å, $b = 8.7162(10)$ Å, $c = 23.653(4)$ Å, and $\beta = 91.83(1)°$, respectively. In some crystals examined, weak superstructure reflections indicate a doubling or quadrupling of the basic unit cell along the c axis, perhaps as a result of partial ordering of the iodoformamidinium cations.

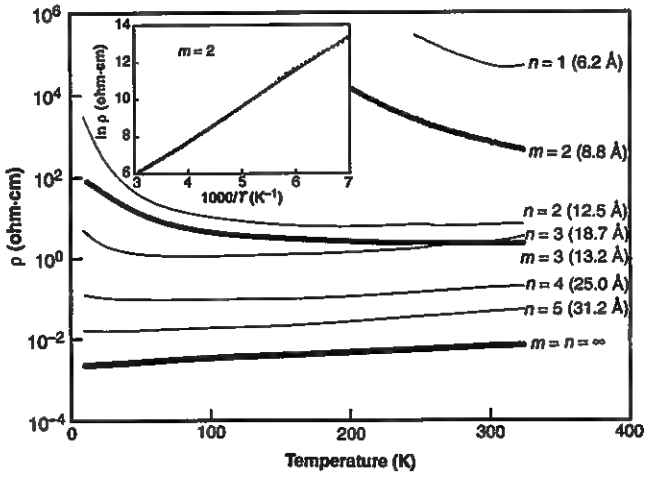

Fig. 4. Resistivity ρ as a function of temperature for pressed-pellet $m = 2$ and 3 samples of $[NH_2C(I)=NH_2]_2(CH_3NH_3)_mSn_mI_{3m+2}$ and the cubic (at room temperature) perovskite $CH_3NH_3SnI_3$ ($m \rightarrow \infty$). For comparison, resistivity data for $(C_4H_9NH_3)_2(CH_3NH_3)_{n-1}Sn_nI_{3n+1}$ are also shown. Distances in parentheses indicate the approximate thicknesses t of the perovskite sheets as calculated from either $t = 6.24m/\sqrt{2}$ or $t = 6.24n$ for the ⟨110⟩ and ⟨100⟩ families, respectively. The inset displays the natural logarithm of resistivity as a function of inverse temperature for $m = 2$. The line drawn through the data points is a least squares fit of the data. Analysis of the slope yields a band gap $E_g = 0.33(5)$ eV.

expected to influence the observed carrier densities (*24*). In going to the $m = 2$ structure, the layering of the perovskite structure results in the formation of terminal Sn–I interactions, which raise the Sn 5*p* antibonding (Sn–I) orbitals to higher energy, as well as reduce the band widths, resulting in a significant band gap (of order 0.5 eV). Increasing m leads to a progressive stabilization of the Sn 5*p* antibonding orbitals and a broadening of the Sn 5*s* and Sn 5*p* band widths, thereby effectively decreasing the band gap and leading to more metallic character. Notably, even for the metallic end-member of the series, $CH_3NH_3SnI_3$, the carrier density, measured by Hall effect (*24*), is only 2×10^{19} holes per cubic centimeter, which is two orders of magnitude smaller than in the superconducting bismuthate or cuprate perovskites. This, combined with the small effective mass ($m^* \approx 0.2$ for $CH_3NH_3SnI_3$), leads to a very small density of states at the Fermi energy, which (at least without doping) is not conducive to superconductivity.

Organic-inorganic multilayer materials, both self-assembling and artificially prepared, are particularly interesting because of the potential for tunability with respect to a given desired property. Artificially prepared organic-inorganic multilayers with interesting optoelectronic properties have, for example, been synthesized with the use of an ionized cluster beam apparatus with multiple ion sources (*25*). Self-assembling organic-inorganic perovskites offer the potential for tunability with, however, much simpler synthetic conditions than for the artificial structures.

Within the family of conducting tin iodide–based layered organic-inorganic perovskites, we have modified the orientation of the conducting perovskite layers through choice of organic cation. As with the ⟨100⟩ family of layered organic-inorganic perovskites, it is expected that the ⟨110⟩ structural family can accommodate a variety of different divalent metal halides, including the first-row transition-metal halides, and lead and cadmium halides, thereby providing additional interesting opportunities for the study of self-assembling multilayer quantum wells, two-dimensional magnetism, and optical, thermochromic, as well as transport properties. A preliminary demonstration of this is our recent synthesis, by the same technique described for the tin(II) compounds, of the lead(II) analog, which has monoclinic lattice parameters similar to those of the $m = 2$ tin compound but with a doubling of the basic unit cell along the *b* axis: $a = 6.315(3)$ Å, $b = 29.498(6)$ Å, $c = 8.713(1)$ Å, and $\beta = 90.96(3)°$ (*26*).

REFERENCES AND NOTES

1. G. V. Rubenacker, D. N. Haines, J. E. Drumheller, K. Emerson, *J. Magn. Magn. Mater.* **43**, 238 (1984).
2. L. J. de Jongh and A. R. Miedema, *Adv. Phys.* **23**, 1 (1974).
3. T. Ishihara, J. Takahashi, T. Goto, *Phys. Rev. B* **42**, 11099 (1990).
4. J. Calabrese *et al.*, *J. Am. Chem. Soc.* **113**, 2328 (1991).
5. M. F. Mostafa, M. M. Abdel-Kader, S. S. Arafat, E. M. Kandeel, *Phys. Scr.* **43**, 627 (1991).
6. H. Arend, K. Tichy, K. Baberschke, F. Rys, *Solid State Commun.* **18**, 999 (1976).
7. P. Day and R. D. Ledsham, *Mol. Cryst. Liq. Cryst.* **86**, 163 (1982).
8. B. Tieke and G. Chapuis, *ibid.* **137**, 101 (1986).
9. G. F. Needham, R. D. Willett, H. F. Franzen, *J. Phys. Chem.* **88**, 674 (1984).
10. D. B. Mitzi, C. A. Feild, W. T. A. Harrison, A. M. Guloy, *Nature* **369**, 467 (1994).
11. G. C. Papavassiliou, I. B. Koutselas, A. Terzis, M.-H. Whangbo, *Solid State Commun.* **91**, 695 (1994).
12. R. A. Mohan Ram, P. Ganguly, C. N. R. Rao, *J. Solid State Chem.* **70**, 82 (1987).
13. R. A. Mohan Ram, L. Ganapathi, P. Ganguly, C. N. R. Rao, *ibid.* **63**, 139 (1986).
14. R. J. Cava *et al.*, *Phys. Rev. B* **46**, 14101 (1992).
15. For $m = 2$, CH_3NH_2·HI (2.772 g, 17.44 mmol), NH_2CN (0.733 g, 17.44 mmol), and SnI_2 (6.495 g, 17.44 mmol) were dissolved in 70 ml of 57 weight % aqueous HI solution at 80°C. After soaking at 80°C for 12 hours, the solution was cooled to −10°C at 2°C/hour. The product was filtered under nitrogen, dried in flowing argon at 80°C for several hours, and then removed to an argon-filled dry box with oxygen and water levels maintained at <1 part per million. Powder x-ray diffraction indicated that the product was free of secondary phases such as starting materials, $CH_3NH_3SnI_3$, and higher m members of the homologous series. Crystals of the $m = 3$ compound were grown with a similar technique but with a 2:5:5 molar ratio of NH_2CN, CH_3NH_2·HI, and SnI_2. The product contained a mixture of $m = 3$ and $CH_3NH_3SnI_3$. The sheet-like $m = 3$ crystals could be mechanically separated from the rod-like or rhombic dodecahedral cubic perovskite crystals because of the very different crystalline habit for these two materials. Isolated single crystals of $m = 4$ were similarly extracted from samples prepared in a solution containing a large excess of CH_3NH_2·HI and SnI_2.
16. E. N. Zil'berman, *Russ. Chem. Rev.* **31**, 615 (1962).
17. M. L. Kilpatrick, *J. Am. Chem. Soc.* **69**, 40 (1947).
18. D. Lin-Vien, N. B. Colthup, W. G. Fateley, J. G. Grasselli, Eds., *Handbook of Infrared and Raman Characteristic Frequencies of Organic Molecules* (Academic Press, New York, 1991).
19. T. N. Sumarokova, R. A. Slavinskaya, I. G. Litvyak, Z. F. Orlova, *Russ. J. Inorg. Chem.* **13**, 561 (1968).
20. L. J. Bellamy, *Infrared Spectra of Complex Molecules*, vol. 1 (Chapman and Hall, New York, 1986).
21. M. Nanot, F. Queyroux, J.-C. Gilles, A. Carpy, J. Galy, *J. Solid State Chem.* **11**, 272 (1974).
22. E. T. Keve, S. C. Abrahams, J. L. Bernstein, *J. Chem. Phys.* **53**, 3279 (1970).
23. J. D. Donaldson and S. M. Grimes, *Rev. Silicon Germanium Tin Lead Compd.* **8**, 1 (1984).
24. D. B. Mitzi, C. A. Feild, Z. Schlesinger, R. B. Laibowitz, *J. Solid State Chem.* **114**, 159 (1995).
25. J. Takada, H. Awaji, M. Koshioka, A. Nakajima, W. A. Nevin, *Appl. Phys. Lett.* **61**, 2184 (1992).
26. D. B. Mitzi, unpublished material.

27. We thank T. Jackman, B. A. Scott, and A. Jacobson for stimulating discussions, and M. Ritter for use of a displex system for measuring the resistivity of these samples.

28 October 1994; accepted 9 January 1995

A "Double-Diamond Superlattice" Built Up of $Cd_{17}S_4(SCH_2CH_2OH)_{26}$ Clusters

T. Vossmeyer, G. Reck, L. Katsikas, E. T. K. Haupt, B. Schulz, H. Weller*

A simple preparation of $Cd_{17}S_4(SCH_2CH_2OH)_{26}$ clusters in aqueous solution leads to the formation of colorless blocky crystals. X-ray structure determinations revealed a superlattice framework built up of covalently linked clusters. This superlattice is best described as two enlarged and interlaced diamond or zinc blende lattices. Because both the superlattice and the clusters display the same structural features, the crystal structure resembles the self-similarities known from fractal geometry. The optical spectrum of the cluster solution displays a sharp transition around 290 nanometers with a large absorption coefficient (~84,000 per molar per centimeter).

In the nanometer-size regime, the optical and transport properties of semiconductor clusters are controlled by the cluster size, whereas their chemical composition remains almost unchanged (*1*–*6*). For example, the optical properties of CdS nanoclusters change enormously with decreasing cluster size: The onset of absorption is shifted to higher energies, and the volume-normalized oscillator strength of the lowest electronic (excitonic) transition increases dramatically (*7*). These size effects result from the spatial confinement of the photogenerated charge carriers to the dimensions of the cluster, which can be represented by the quantum mechanical model of a "particle in a box" (*8*). One of the most exciting questions is how solid-state properties develop when regular macroscopic structures are built up by the packing of clusters into a three-dimensional framework, as is fulfilled in crystallized cluster samples.

Because of cluster-cluster interactions, interesting collective phenomena are to be expected, and such well-structured systems should be useful for learning how quantum-size effects can be used for electronic devices. So far, only van der Waals or ionic crystals built up of CdS clusters, such as $Cd_{32}S_{14}(SC_6H_5)_{36} \cdot 4$ DMF (*1*)

(9) (DMF is *N*,*N*-dimethylformamide), $[Cd_{17}S_4(SC_6H_5)_{28}][N(CH_3)_4]_2$ (2) (*10*), and $[Cd_{10}(SCH_2CH_2OH)_{16}][SO_4]_2 \cdot 4H_2O$ (3) (*11*), have been prepared. In this report, we present a single-crystal structure in which semiconductor clusters of CdS are linked covalently to build up a superlattice that is best described as consisting of two enlarged and interlaced diamond or zinc blende lattices. These lattices are identical and unlinked to each other. The same connective patterns are realized in both the macrostructure and the microstructure (superlattice and cluster, respectively), in a manner reminiscent of the self-similarities of fractal geometries. As we will show by ^{113}Cd nuclear magnetic resonance (NMR) and ultraviolet-visible (UVVIS) absorption measurements, the clusters remain intact after the crystals are dissolved in dimethyl sulfoxide (DMSO), DMF, or water.

The procedure of preparation has been described in principle (*7*). Briefly, cadmium perchlorate and 2-mercaptoethanol were dissolved in water, and H_2S was injected under vigorous stirring in alkaline solution (molar ratios of Cd:RS:S approximately 1.0:2.4:0.2) (R = alkyl). After it was stirred for several hours at room temperature, the solution was dialyzed exhaustively against water; then crystals began to grow in the dialysis tubes as small colorless needles while the solution reached a pH of 9. After dialysis, the crystals were stored in their mother liquor under reduced light because prolonged exposure to UV radiation leads to decomposition of the clusters. Upon standing for several weeks, blocky crystals grew on the bundles of needles, which themselves slowly decayed.

These crystals, which decompose above 160°C and are poorly soluble in water but readily soluble in DMF or DMSO, were used for x-ray structure analysis (*12*). Because the crystals cracked on drying, we found it necessary to carry out these measurements with a crystal enclosed in a thin glass tube containing a few microliters of mother liquor. The optical absorption properties (see below) of solutions of both crystal types (needles and blocks) were found to be the same, as were the solubilities. X-ray diffraction of the powdered needles revealed a strong amorphous background. Both crystal types are obviously built up of the same CdS clusters and differ from each other only in their crystal shape and in the degree of crystallinity. The total yield obtained (including both crystal types) was 31%, and the elemental analysis was in good agreement with the results of the structure analysis (*13*).

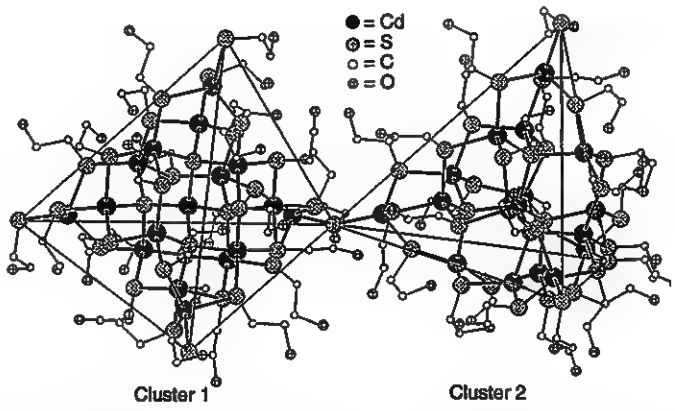

Fig. 1. The structures of the two $Cd_{17}S_4(SCH_2CH_2OH)_{26}$ clusters that form the basic units of the superlattice. Both clusters 1 and 2 are chemically equivalent but crystallographically independent (see text). As can be seen, four capping thiolate ligands at the vertices of each cluster form a tetrahedron (edge lengths, 14.4 to 15.5 Å). These ligands act as intermolecular μ-SR bridges and thus build up the superlattice framework. The Cd–(μ-SR) bonds have lengths between 2.48(1) and 2.60(1) Å (error in the last digit in parentheses). The intramolecular Cd–(μ-SR) bond lengths are similar and vary between 2.45(1) and 2.61(1) Å. The bond lengths between the central Cd atom and the four coordinating S atoms are also in the same range [2.48(1) to 2.53(1) Å].

The basic unit that builds up the two interlaced superlattices is a cluster with the stoichiometry of $Cd_{17}S_4(SCH_2CH_2OH)_{26}$ (4) (Fig. 1). This structure is similar to that of 2, which has been described by Dance and co-workers (*10*). If the cluster is considered as a part of the superlattice framework, it has the same approximate tetrahedral geometry (with exact D_2 symmetry) with open clefts running along each of the tetrahedral edges. These edges have a length between 14.4 and 15.5 Å. The CdS structure of the core is built up of four adamantanoid cages, sharing edges and one vertex, and may be regarded as a distorted fragment of the cubic CdS phase (zinc blende structure). However, the capping cages at each vertex are barrelanoid rather than adamantanoid and thus are more similar to the hexagonal (wurzite) phase than to the CdS (zinc blende) phase. The Cd–S bond lengths in the core are in the same range as for bulk CdS (2.519 Å) and vary between 2.45 and 2.61 Å.

Despite all of these similarities between 2 and 4, there is one decisive difference. Whereas 2 consists of negatively charged clusters with all vertices capped by terminating thiolate ligands to form an ionic cluster crystal, there are two ligands less in compound 4. Consequently, each cluster of the superlattice framework remains uncharged and is connected with four neighboring clusters by sharing each of its vertices. In other words, the four terminating thiolate ligands of 2 have been replaced in 4 by intermolecular μ-SR bridges between the clusters that build up the superlattice framework.

The superlattice shown in Fig. 2 is best described chemically as two interlaced and enlarged diamond lattices. A more detailed description, however, shows that, within each diamond lattice, two chemically identical but crystallographically independent cluster species can be identified. Thus, the superlattice should be regarded crystallographically as two interlaced and enlarged zinc blende lattices. This feature is depicted in Fig. 3, which shows a comparison between a fraction of one of the interlacing superlattices (Fig. 3A) and an analogous portion of the zinc blende structure (Fig. 3B). The connectivity pattern is almost exactly the same for both structures. The angles differ only

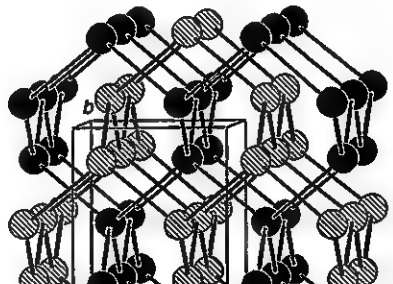

Fig. 2. The superlattice built up of the Cd_{17} clusters. This is best described as two enlarged and interlaced diamond (or zinc blende) lattices. Both lattices are identical and symmetry-related by the inversion center of the space group *I2/a* with the fractional coordinates 0.25, 0.25, and 0.75. Only the central Cd atom of each cluster is depicted and connected with the other Cd atom. The monoclinic cell parameters are given in (*12*).

T. Vossmeyer, Hahn-Meitner-Institut, Abteilung Kleinteilchenforschung, Glienicker Strasse 100, 14109 Berlin, Germany.
G. Reck and B. Schulz, Bundesanstalt für Materialforschung und-prüfung, Rudower Chaussee 5, 12489 Berlin, Germany.
L. Katsikas, University of Belgrade, Faculty of Technology and Metallurgy, Karnegijeva 4, 11000 Belgrade, Yugoslavia.
E. T. K. Haupt, Universität Hamburg, Institut für Anorganische und Angewandte Chemie, Martin-Luther-King-Platz 6, 20146 Hamburg, Germany.
H. Weller, Universität Hamburg, Institut für Physikalische Chemie, Bundesstrasse 45, 20146 Hamburg, Germany.
*To whom correspondence should be addressed.

slightly (<8.6°), whereas the "bond lengths" differ by a factor of ~6.9. Moreover, the structure of the cluster core (Fig. 3C) is similar to that of the superlattice framework, and it can be described as a fragment of the cubic CdS phase (zinc blende).

If the clusters remain intact upon dissolution (the prepared crystals dissolve poorly in water but readily in DMF or DMSO), only the intermolecular μ-SR bonds between the clusters are cleaved. This probably happens in such a manner that, on average, two vertices of each cluster are capped by a terminating thiolate ligand, whereas the other two vertices remain uncapped. For NMR considerations the Cd atoms at the latter sites are expected to display a significant high field shift compared with the other Cd atoms, because they are coordinated by only three S atoms (*14*). Thus, the signal at 440 ppm, seen in the ^{113}Cd NMR spectrum of Fig. 4, is attributed to the two coordinatively unsaturated Cd atoms of these sites. At lower field, two other peaks are recognized: a strong signal at 630 ppm and a very weak one at 650 ppm. Because the chemical environment of the 12 Cd atoms at the cluster surfaces is similar to that of the two Cd atoms at the vertices, which are capped by a terminating thiolate ligand, the signals of these sites are probably superimposed around 630 ppm. The weak peak at 650 ppm is attributed to the central Cd, which is coordinated by the four inner S atoms.

Because of the relative abundance of surface Cd atoms and the low signal-to-noise ratio of the weak peaks, the relative intensities of the three signals are hard to compare. However, taking into account this limitation, the relative intensities given in Fig. 4 are in reasonable agreement with our interpretation. The Cd atoms that are coordinatively not saturated by S will be coordinated by solvent molecules (*15*) or in alkaline water by OH^- ions. This explains the increasing solubility of **4** in water with increasing pH, as well as the reverse process of crystal formation in the dialysis tubings. As the pH value of an alkaline cluster solution decreases during dialysis, the thiolate S atoms of the two terminating ligands compete more successfully with OH^- ions for the two unsaturated coordination sites and finally form intermolecular μ-SR bridges between the clusters. This kind of polymerization leads to the crystal formation described above.

Because the thiolate ligand of **4** absorbs light only below 250 nm, the UVVIS spectrum of the cluster core could be investigated. Figure 5A shows spectra of solutions of the clusters in water, DMSO, and DMF. The well-pronounced absorption maximum around 290 nm is ascribed to the 1*s*1*s* excitonic transition. The molar absorption coefficient ($\varepsilon_{290} \sim 84{,}000\ M^{-1}\ cm^{-1}$), as well as the spectral position of the maximum, is almost independent of the solvent polarity. This result has also been observed in the case of cluster 1 by Herron *et al.* (9) and was taken as an indication that the clusters have a small dipole moment in the ground state or the corresponding excited state. Their cluster is actually a larger homolog of **4**. The optical absorption spectra of

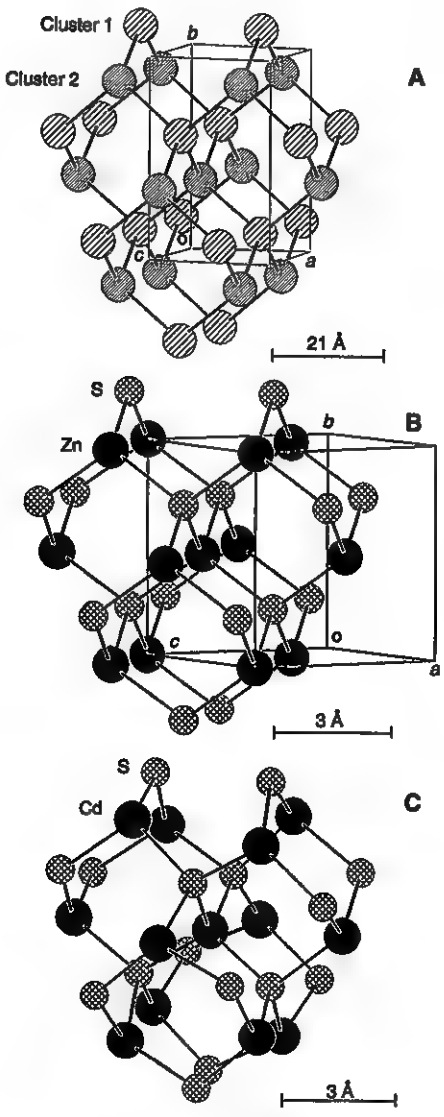

Fig. 3. Similarity between (**A**) the superlattice, (**B**) the zinc blende structure, and (**C**) the cluster core structure. In (A), the structure of one of the interlaced superlattices is depicted. In contrast to Fig. 2, in this figure the crystallographically different but chemically equal clusters are marked by different shadings (clusters 1 and 2). The unit cell refers to the whole structure and not only to the superlattice. Thus, the unit cells shown in (A) and (B) have different geometries. In (C), the capping vertices of the cluster are omitted. Note the scale bars of each part.

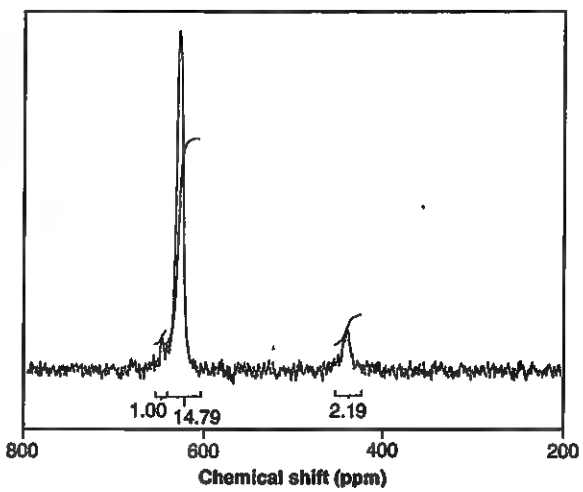

Fig. 4. A ^{113}Cd NMR spectrum recorded with a 0.06 M solution of **4** in DMSO-d_6. The relative intensities of the three signals at 650, 630, and 440 ppm are approximately 1:14.8:2.2. The spectrum was recorded with a Varian Gemini-200 BB-Spectrometer (4.7 T) at 44.4 MHz. We collected 53,200 pulses within 16 hours at room temperature (pulse width 45°, 1-s recycle delay). As a reference, $\delta_{CdCl_2} = 98$ ppm (1.0 M aqueous solution) was taken, which corresponds to $\delta_{Cd\text{-}(ClO_4)2} = 0$ ppm (0.1 M aqueous solution) (*16*).

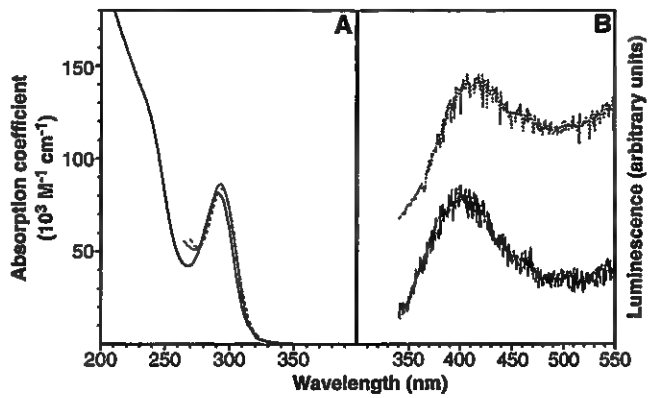

Fig. 5. (**A**) UVVIS spectra of **4** dissolved in different solvents (heavy line, water; light line, DMSO; dashed line, DMF). The transition near 290 nm has a large absorption coefficient ($\varepsilon_{290} \sim 84{,}000\ M^{-1}\ cm^{-1}$) and is almost independent of the solvent polarity. (**B**) Luminescence spectra of the crystalline solid (dotted line) and an aqueous solution (solid line) at 4 K. The excitation wavelength was 300 nm. The spectrum of the crystalline solid is slightly shifted to the red (~12 nm).

films, which were prepared on quartz plates by spin coating from concentrated cluster solutions, are similar to the spectrum of an aqueous solution. The position of the maximum is, however, shifted to the red by approximately 5 nm. The luminescence spectrum of the crystalline solid is also similar to the solution spectrum (Fig. 5B) and is also shifted slightly to the red (~12 nm). Thus, small optical changes that might reflect cluster-cluster interactions in the solid samples could be observed.

In (*7*) we described the synthesis and characterization of differently sized 1-thioglycerol–stabilized CdS clusters. One of the prepared species displayed exactly the same optical behavior as **4**. At that time, we speculated, on the basis of elemental analysis, small-angle x-ray scattering, and UV-VIS spectroscopy, that this sample might consist of Cd_{17} clusters. However, attempts to crystallize this compound, which is readily water-soluble, have not been successful. Nevertheless, it should be possible to crystallize clusters of the type $Cd_{17}S_4(RS)_{26}$ with various thiolate ligands RS. This should lead to a set of different superlattices consisting of almost identical CdS cluster cores, which can be regarded as ideal systems for the study of collective phenomena based on cluster-cluster interactions.

REFERENCES AND NOTES

1. A. Henglein, *Top. Curr. Chem.* **143**, 113 (1988).
2. ———, *Chem. Rev.* **89**, 1861 (1989).
3. L. E. Brus, *Appl. Phys. A* **53**, 465 (1991).
4. Y. Wang and N. Herron, *J. Phys. Chem.* **95**, 525 (1991).
5. H. Weller, *Angew. Chem. Int. Ed. Engl.* **32**, 41 (1993).
6. ———, *Adv. Mater.* **5**, 88 (1993).
7. T. Vossmeyer *et al.*, *J. Phys. Chem.* **98**, 7665 (1994).
8. L. E. Brus, *ibid.* **80**, 4403 (1984).
9. N. Herron, J. C. Calabrese, W. E. Farneth, Y. Wang, *Science* **259**, 1426 (1993).
10. G. S. H. Lee *et al.*, *J. Am. Chem. Soc.* **110**, 4863 (1988).
11. P. Strickler, *J. Chem. Soc. Chem. Commun.* **1969**, 655 (1969).
12. Diffraction data for the x-ray structure analysis were collected on an Enraf-Nonius (Delft, Netherlands) CAD4 diffractometer (graphite monochromatized MoKα radiation, wavelength of 0.7107 Å). The monoclinic cell parameters were determined from the Bragg angles of 25 computer-centered reflections as a = 25.147(4) Å, b = 40.096(5) Å, c = 25.358(5) Å, and β = 94.0(1)° (error in the last digit in parentheses). The space group was assigned as *I2/a* (no. 15), and the structure confirmed this assignment. The colorless, irregularly shaped crystals were very unstable, as indicated by the drastic loss in intensities during x-ray exposure. Therefore, three crystals (100 to 180 μm) sealed in capillaries were used for the data collection. Because of the instability and the weak diffraction power of the nonperfect crystals, only 5414 unique reflections with $I \geq 2\sigma(I)$ (where I is intensity) were measured in the range of $1.5° \leq 2\theta \leq 38°$ (θ is the dispersion angle). We solved the structure by direct methods and refined it by blocked full-matrix least squares techniques by using weighted restraints for the bond lengths and angles of the organic residues. Despite the poor quality of the available reflections, all C and O atoms could be located by difference Fourier synthesis. The final refinement of 587 parameters (data-to-parameter ratio = 9.2) in which only Cd was anisotropic converged at R = 0.115 (unit weights). This relatively high value may be attributable to the instability of the crystals, probably small structural changes during x-ray exposure, and rotational disorder of most of the organic residues indicated by the extreme high thermal parameters of some C and all O atoms. Additional data on this material can be ordered by referring to no. CSD-401359, names of the authors, and citation of the paper at the Fachinformationszentrum Karlsruhe, Gesellschaft für wissenschaftlich-technische Information mbH, D-76344 Eggenstein-Leopoldshafen, Germany.
13. Analysis calculated for $C_{52}H_{130}O_{26}S_{30}Cd_{17}$: C, 15.44%; H, 3.25%; O, 10.28%; S, 23.79%; and Cd, 47.24%. Found: C, 15.50%; H, 3.32%; O, 10.8%; S, 23.2%; and Cd, 46.5%.
14. R. A. Haberkorn *et al.*, *Inorg. Chem.* **15**, 2408 (1976).
15. The observed signals of the ^{113}Cd NMR spectrum, which are due to Cd atoms of the cluster surfaces and vertices (440 and 630 ppm) are most probably broadened by exchange phenomena involving coordination by solvent molecules and OH groups of the organic residues. The involvement of OH groups is also indicated by ^1H NMR measurements; three temperature-dependent signals of hydroxyl protons were detected in DMF solution. The fact that the signal at 440 ppm could not be detected in DMF solution also indicates extensive exchange processes. However, because of the decreasing solubility of **4** in DMF with decreasing temperature, and decomposition at higher temperatures, no information could be obtained by temperature-dependent ^{113}Cd NMR measurements.
16. A. D. Cardin, P. D. Ellis, J. D. Odom, J. W. Howard, *J. Am. Chem. Soc.* **97**, 1672 (1975).

17. We thank A. Mews for recording the luminescence spectra and A. Eychmüller for useful discussions.

30 August 1994; accepted 21 December 1994

Micrometer- and Nanometer-Sized Polymeric Light-Emitting Diodes

Magnus Granström,* Magnus Berggren, Olle Inganäs

A method for the fabrication of micrometer- and submicrometer-sized polymeric light-emitting diodes is presented. Such diodes have a variety of applications. Light sources of dimensions around 100 nanometers are required for subwavelength, near-field optical microscopy. Another possible application is patterning on the micrometer and nanometer scale. The diodes have been made in the form of a sandwich structure, with the conductive polymer poly(3,4-ethylene-dioxythiophene) polymerized in the pores of commercially available microfiltration membranes defining the hole-injecting contacts, poly[3-(4-octylphenyl)-2,2′-bithiophene] as the light-emitting layer, and a thin film of calcium-aluminum as the electron injector.

Since the first discoveries of electroluminescence in semiconducting conjugated polymers, interest has grown rapidly and many polymers have been used in light-emitting diodes (LEDs). The great interest is explained by the significant advantages that these systems have in processing, mechanical properties, and geometry possibilities as compared to conventional semiconductors (*1*–*4*). Another favorable aspect of the polymer LEDs is that today it is possible to cover the spectral range from blue to near-infrared, even within a single family of conductive polymers such as the polythiophenes (*5*). The recent demonstration of voltage-controlled electroluminescence colors from polymer blends in LEDs (*5*) as well as the possibility of obtaining polarized light from oriented polymers in LED devices (*6*) extend the possibilities of the polymer devices by comparison with inorganic devices. The mechanism for electroluminescence is also somewhat different from that found in conventional devices, because the emission takes place when charged polaron excitons recombine. When holes and electrons are injected into the polymer, they form positively and negatively charged polarons that can migrate under an applied field and radiatively recombine when they meet (*7*).

One of the advantages with polymer LEDs is the possibility to choose size and geometry freely. So far, this has mainly been exploited in making large (several square centimeters) LEDs. However, here we show that it is also possible to go in the other direction and make the light sources very small. Such LEDs could be used as light sources in scanning near-field optical microscopes (SNOMs), where the size of the emitting area is crucial (*8*, *9*).

Two different conjugated polymers have been used in making these small LEDs. The first one, poly(3,4-ethylene-dioxythiophene) (*10*–*13*) (PEDOT) (**1**), was used as the hole-injecting contact; the other, poly[3-(4-octylphenyl)-2,2′-bithiophene] (*14*) (PTOPT) (**2**), was used as the electroluminescent layer (Fig. 1). To define the size of the light sources, we polymerized the doped and conducting polymer PEDOT electrochemically in the randomly distributed pores of commercially available microfiltration membranes (*15*, *16*). The pore sizes in such mem-

Laboratory of Applied Physics, Department of Physics and Measurement Technology, Linköping University, S-581 83 Linköping, Sweden.

*To whom correspondence should be addressed.

branes span from 10 nm to 14 μm. Electrosynthesis of conjugated polymers inside these pores leads to high-conductivity materials, probably the result of increased ordering of the material (*17*, *18*). It also leads to electrodes of the same size as the pores, if care is taken to stop the polymerization before the growing polymer extends beyond the narrow pore and starts to spread out on the upper surface of the membrane. This is therefore a convenient way to prepare small electrodes.

The electrode size is also expected to define the size of the light sources. Because the electron and hole mobilities are low in undoped conjugated polymers, the charges will not travel far from the injecting electrode. The upper limit of the exciton diffusion length in conjugated polymers has been estimated to be 5 nm (*19*), which also supports the idea that the light will be emitted only at or very close to the injecting contact.

Polycarbonate membranes (Poretics and Nuclepore) with pore diameters of 10 μm (thickness, 10 μm) and 100 nm (thickness, 6 μm) were attached to Au contacts on top of a glass substrate (*16*). We polymerized PEDOT from a water solution of 0.1 M monomer and 0.1 M sodium polystyrene sulfonate, using an electrochemical analyzer (Bioanalytical Systems BAS100A). A standard three-electrode setup was used with Ag-AgCl and Pt as reference and counter electrodes, respectively, and the polymerization potential was 1.3 V versus Ag-AgCl. The polymerization was interrupted when the conductive polymer fibers reached the upper surface of the membrane (*16*). This procedure produces a membrane surface with electrical contacts defined by the doped polymer fibers that have grown in the pores. All these fibers can then be electrically contacted through the Au layer between the glass substrate and the membrane.

The electroluminescent polymer PTOPT was spin-coated in its undoped form from a warm xylene solution (5 mg/ml, 50°C) on top of the membrane-contact structure. The thickness of this layer was estimated from optical spectra to be 350 to 450 Å. To obtain a suitable electron-injecting contact, we evaporated a thin layer of the low-work-function metal Ca (*7*) on the PTOPT surface. The Ca layer was then covered with a thin layer of Al to protect the Ca from the ambient atmosphere. The total thickness of the Al-Ca metal layer was 180 to 250 Å. The resulting structure is shown in Fig. 2. The light is observed through the metal layer, resulting in a considerable decrease in light intensity.

We evaluated the diode structures using a computerized setup with an electrometer (Keithley 617), a picoamperemeter (Keithley 485), and a Si photodiode (Hamamatsu 1010BR). This setup makes it possible to measure the current-voltage (*I-V*) characteristics and light emission simultaneously. In addition to these measurements, an optical microscope (Olympus BHSP) equipped with a 35-mm camera was used to identify the individual light sources. In Fig. 3 a typical result from a 10-μm sample is shown. Comparing the current and light curves, it can be seen that one of the charge carriers starts to flow first, but no light is seen until both types are available and can recombine to give excitons (*20*). In Fig. 4 current and light curves for 100-nm diodes are shown. A similar behavior is found here, although with a lower light intensity because a smaller fraction of the surface is acting as a contact compared to the 10-μm samples (2.4% and 7.8%, respectively).

A photograph of the 100-nm LEDs is shown in Fig. 5. It is impossible to determine the exact size and shape of the light sources, because the optical microscope limits the resolution to 0.27 μm (magnification, ×1000; numerical aperture, 1.25). However, it is still possible to detect the light and to establish an upper limit to the size of the LEDs of not more than 300 nm. This is then within the region of a subwavelength light source [the emission peak from "normal" PTOPT LEDs is at about 600 nm (*14*)].

From Figs. 3 and 4 the number of photons emitted per second from an individual diode can be estimated; this can be calculated from the current produced in the photodiode and knowledge of the emitting area. Two important factors need to be taken into account when such a calculation is performed. First, there is a statistical length distribution of the PEDOT fibers, because all pores in the membrane are not oriented perfectly perpendicular to the surface. Second, the diodes have different lifetimes, and a limiting factor for the lifetime of a diode is the heat expansion of the PEDOT contacts, which is attributable to the high current densities. An expanding PEDOT fiber can then break through the thin electroluminescent PTOPT layer and cause local "burnouts." The number of working diodes is therefore always smaller than the number of pores in the membrane.

From pictures taken in the microscope, the fraction of working diodes is found to be in the range of 20 to 25% for both types. Taking this into account, a calculation of the photon emission gives 10^4 photons per second for the 10-μm diodes and 10 photons

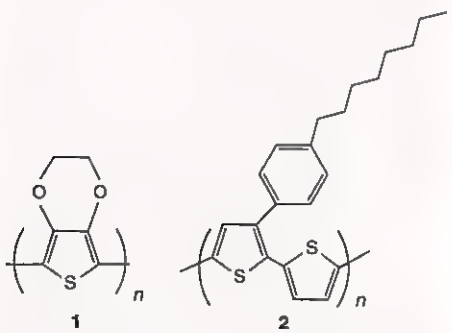

1 2

Fig. 1. Structures of compounds **1** and **2**.

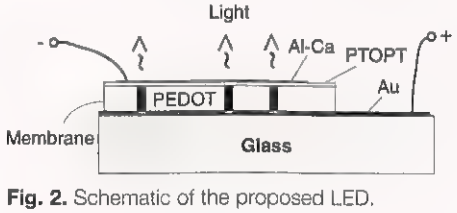

Fig. 2. Schematic of the proposed LED.

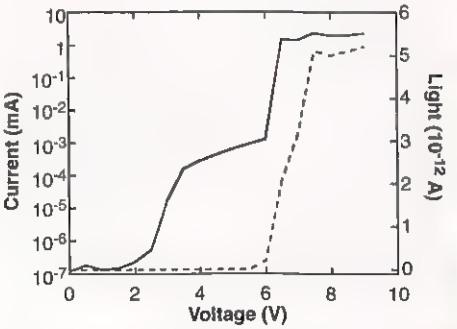

Fig. 3. Current (solid line) and light (dashed line) as functions of applied voltage for 10-μm diodes. The light is measured as the current from the photodiode.

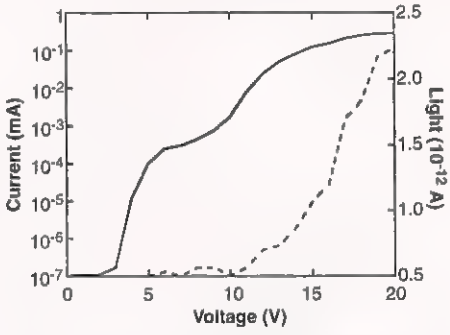

Fig. 4. Current (solid line) and light (dashed line) as a function of applied voltage for 100-nm diodes.

Fig. 5. Photo of nano-LEDs (100 nm) (magnification, ×1000; exposure time, 15 min).

per second for the 100-nm diodes. The value for the 100-nm diodes is calculated directly from the optical image, where the diodes appear as 300-nm spots. If the diameter is assumed to be 100 nm, the number of photons per second increases by one order of magnitude to 10^2. Looking at the quantum efficiencies established for large polymer LEDs in the family of polythiophenes, 0.1 to 1% external efficiencies, and current densities of 10 mA/cm^2, we could expect 10^8 to 10^9 photons per second from the 10-μm LEDs and 10^4 to 10^5 photons per second from the 100-nm LEDs. Transmission losses in the metal electrode account for a part of this discrepancy and are measured by optical spectroscopy to be on the order of 60 to 80%. For our combination of materials, the quantum efficiency is most probably less than 0.1%, which, together with the transmission losses, brings the theoretical and experimental values into agreement with each other.

The numbers of emitted photons per second are calculated for the currents and voltages shown in the figures. It should be possible to increase these numbers by at least two orders of magnitude by increasing the current and using pulse techniques (*21*). As a comparison, it could be mentioned that one of the standard probes for SNOM, a tapered Al-coated optical fiber with a small aperture, suppresses the incoming light typically by a factor of 10^5 (*8*). Different techniques have been used with light intensities between 10^3 and 10^{11} photons per second for subwavelength light sources (*22–24*). We can then compare these results with projections of the best results for polymer nano-LEDs, where we may assume that we could increase efficiency to somewhere in the range of 1 to 10% and also that we might be able to operate the devices at current densities 10 times higher than those used presently. These developments would bring the photon emission up to the range of 10^7 to 10^8 photons per second, which puts the polymer nano-LEDs somewhere in the mid-range of the available techniques with respect to light intensity. Therefore, it should not be expected that polymer nano-LEDs would offer drastically better performance as subwavelength light sources than alternative devices. Rather, an advantage for the use of nano-LEDs may be in the ability to manufacture not one but thousands of light sources at the same time. This accomplishment might then be used to create efficient photopatterning processes that could be used to produce a large number of identical patterns simultaneously.

It may be possible in the future to improve a number of aspects of these structures—for instance, increasing the efficiency by using transport layers (*20*) or finding an appropriate transparent electron injector that could be used in this type of geometry. The problem with heat expansion in the contacting polymer fibers could be reduced by using a much thinner insulating layer than the microfiltration membrane, in which small holes for polymerization could be made. The possibility of preparing thousands or millions of light sources at the same time, which is essential for some applications, may require methods such as ion-beam etching to control the distribution of light sources on the surface.

REFERENCES AND NOTES

1. J. H. Burroughes *et al.*, *Nature* **347**, 539 (1990).
2. D. Braun and A. J. Heeger, *Appl. Phys. Lett.* **58**, 1982 (1991).
3. G. Gustafsson *et al.*, *Nature* **357**, 477 (1992).
4. R. Friend, D. Bradley, A. Holmes, *Physics World* **1992**, 42 (1992).
5. M. Berggren *et al.*, *Nature* **372**, 444 (1994).
6. P. Dyreklev *et al.*, *Adv. Mater.*, in press.
7. I. D. Parker, *J. Appl. Phys.* **75**, 1656 (1994).
8. N. F. v. Hulst, M. H. P. Moers, B. Bölger, *J. Microsc.* **171**, 95 (1993).
9. N. F. v. Hulst *et al.*, *Appl. Phys. Lett.* **62**, 461 (1993).
10. Q. Pei, G. Zuccarello, M. Ahlskog, O. Inganäs, *Polymer* **35**, 1347 (1994).
11. G. Heywang and F. Jonas, *Adv. Mater.* **4**, 116 (1992).
12. J. C. Gustafsson, B. Liedberg, O. Inganäs, *Solid State Ionics* **69**, 145 (1994).
13. M. Dietrich, J. Heinze, G. Heywang, F. Jonas, *J. Electrochem. Soc.* **369**, 87 (1994).
14. M. Berggren *et al.*, *J. Appl. Phys.*, in press.
15. Z. Cai and C. R. Martin, *J. Am. Chem. Soc.* **111**, 4138 (1989).
16. M. Granström and O. Inganäs, *Synth. Metals* **55–57**, 460 (1993).
17. Z. Cai, J. Lei, W. Liang, V. Menon, C. R. Martin, *Chem. Mater.* **3**, 960 (1991).
18. M. Granström and O. Inganäs, in preparation.
19. A. R. Brown *et al.*, *Chem. Phys. Lett.* **200**, 1 (1992).
20. A. R. Brown *et al.*, *Appl. Phys. Lett.* **61**, 2793 (1992).
21. D. Braun, D. Moses, C. Zhang, A. J. Heeger, *ibid.*, p. 3092.
22. N. Kuck, K. Lieberman, A. Lewis, A. Vecht, *ibid.*, p. 139.
23. A. Lewis and K. Lieberman, *Nature* **354**, 214 (1991).
24. E. Betzig, J. K. Trautman, T. D. Harris, J. S. Weiner, R. L. Kostelak, *Science* **251**, 1468 (1991).

25. We thank N. F. van Hulst and M. H. P. Moers for fruitful discussions. This work was supported by the Micronics program of the Swedish National Board for Industrial and Technical Development.

20 September 1994; accepted 19 December 1994

Influence of Lunar Phase on Daily Global Temperatures

Robert C. Balling Jr.* and Randall S. Cerveny

A newly available data set of daily satellite-derived, lower-tropospheric global temperature anomalies provides an opportunity to assess the influence of lunar phase on planetary temperature. These results reveal a statistically significant 0.02 K modulation between new moon and full moon, with the warmest daily global temperatures over a synodic month coincident with the occurrence of the full moon. Spectral analysis of the daily temperature record confirms the presence of a periodicity that matches the lunar synodic (29.53-day) cycle. The precision of the satellite-based daily temperature record allows verification that the moon exerts a discernible influence on the short-term, global temperature record.

Throughout history, many societies and individuals have believed that the moon exerts an influence on weather and climate. Indeed, scientists have been able to identify lunar-phase impacts on precipitation variations (*1–4*), thunderstorm frequency (*5*), ice nuclei concentrations (*6*), diurnal pressure changes (*7*), hurricanes (*8*), cloudiness as measured by sunshine recorders (*9*), and possibly global surface-temperature estimates (*10*). Adderley and Bowen (*2*, p. 749) claimed that "the appearance of a lunar component in daily temperature in certain parts of the world [is] comparatively well known" but is "extremely small and difficult to detect." Until recently, the clear identification of a lunar influence on planetary temperature was complicated by the lack of an accurate measure of global temperature on a daily basis.

A data set of significant reliability and sensitivity is now available that is potentially capable of being used to detect a lunar influence on global temperature. Spencer and Christy (*11*) have developed a lower-tropospheric (lowest 6 km) measure of global temperature based on microwave emissions of molecular oxygen. These microwave measurements are made by polar-orbiting satellites, thereby providing for coverage of the entire planet. The details of the measurement procedures are well documented, and this global data set is now widely used in climatic research (*12–20*). Although most scientists have used the monthly averaged, satellite-based temperature measurements, daily, globally averaged lower-tropospheric temperatures are now available (*21*,

Office of Climatology, Arizona State University, Tempe, AZ 85287, USA.

*To whom correspondence should be addressed.

22). In this investigation, we use these daily global temperatures to identify the lunar influence on planetary temperature.

The daily temperature record used in this study extends from 3 January 1979 to 31 August 1994. These daily data are expressed as global temperature anomalies calculated from a 1982–1991 base period when the lower-tropospheric temperature averaged ≈269 K; only 1.8% of the data are missing over the entire length of record. The daily temperature anomalies have a mean of −0.01 K (reflecting the global cooling after the 1991 eruption of Mount Pinatubo), have a standard deviation of 0.21 K, and range from −0.61 K on 2 August 1992 to 0.61 K on 29 December 1987.

We computed the lunar phase for each day coinciding with the planetary temperature record by determining the average angular difference between the apparent longitudes of the moon and sun for that day. The cycle of lunar-phase magnitudes varies from 0.0 for the new moon to 1.0 for the full moon; lunar phase variations define the lunar synodic cycle of 29.53 days.

Four different analytical procedures reveal the existence of a lunar influence on the daily lower-tropospheric global temperatures:

1) The global temperature anomalies were averaged within 14 lunar categories of approximately equal n size similar in nature to the categories used in earlier studies (*1–4*). A plot of the results (Fig. 1) reveals a strong linear relation between lunar phase and mean planetary temperature. The warmest daily temperatures over a synodic month are coincident with the occurrence of the full moon when temperature anomalies are generally 0.02 K higher than during new moon periods.

2) We further divided the temperature data into two lunar phase classes characterizing the extremes of the synodic month. A near–new moon class was defined as having lunar phase values <0.10, whereas a near–full moon class was confined to lunar phase values >0.90. The mean global temperature anomaly was −0.02 K (n = 1129 days) in the new moon class and 0.00 K (n = 1066 days) in the full moon class. A t test comparing the group means determined that the global average temperatures were significantly different (t = 1.63; P = 0.05).

3) Similarly, we divided the lunar phase data into two classes based on the planetary temperature anomalies. One class with temperature anomalies <−0.3 K had a mean lunar phase of 0.49 (n = 518), whereas the other class with anomalies >0.3 K had a mean lunar phase of 0.55 (n = 415). A t test comparing the lunar phase averages showed that the means were significantly different (t = 2.43; P = 0.01).

4) The dominant cycles present in the daily global temperature data set may be identified with the spectral analysis program used by Ruddiman and McIntyre (*23*). The spectral analysis of the entire data set shows an identifiable periodicity corresponding to the lunar synodic (29.53-day) cycle (Fig. 2). A weaker cycle near 14.77 days, corresponding to a lunar half-synodic cycle, is also evident in the daily global temperature record.

The existence of an identifiable relation between lunar phase and global temperature begs the question as to its fundamental cause. Presumably the causal factor is lunar, but, as pointed out by researchers examining the relation between precipitation and lunar phase (*3, 4*), this cannot be demonstrated by statistical analyses alone. Other scientists who have examined the lunar influence on various climatic variables have suggested several causative linkages. For example, increased thunderstorm activity near the time of the full moon may be related to lunar distortions of Earth's magnetic tail (*5*). Another hypothesis advanced to explain the precipitation–lunar phase relation involves the lunar modulation of meteoritic dust (*2*). Others have speculated that lunar tidal changes could influence Earth's basic atmospheric circulation patterns, in particular, the position of the subtropical high-pressure belts (*24*).

Also, with respect to global temperature variations, a full moon results in an increased solar load due to the moon's reflection as well as to an increase in infrared emission from the moon's surface. The infrared flux to Earth is five orders of magnitude less than the direct flux from the sun, whereas the shortwave flux is six orders of magnitude less than the direct flux from the sun (*10, 25*); the 0.02 K modulation in temperature identified in this study is correspondingly five orders of magnitude less than the mean lower-tropospheric temperature. Feedback responses of global temperature to potentially lunar-related variations in other climatic parameters, such as precipitation, cloudiness, and thunderstorm activity, may also account for the lunar effect on global temperatures.

Our analyses show a significant empirical relation between lunar phase and daily planetary temperature over the past 15 years. The lunar phase appears to produce a modulation of approximately 0.03 K in the lower troposphere, with the warmest daily temperatures over a synodic month coincident with the occurrence of the full moon. The results not only confirm the suspicions of many past scientists but also suggest that the daily global temperature measurements are quite accurate. Most important, lunar influence is identified as another potential forcing mechanism to consider in the analysis of variability in the short-term, global temperature record.

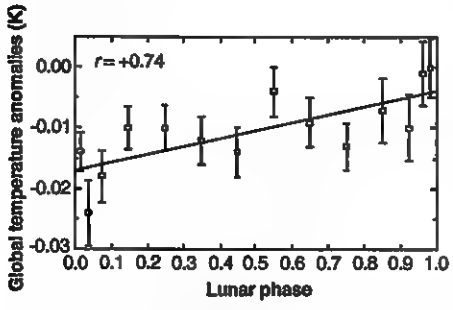

Fig. 1. Plot of averaged global temperature anomalies versus lunar phase category along with 0.95 confidence intervals for the means. The cycle of lunar phase magnitudes varies from 0.0 (new moon) to 1.0 (full moon).

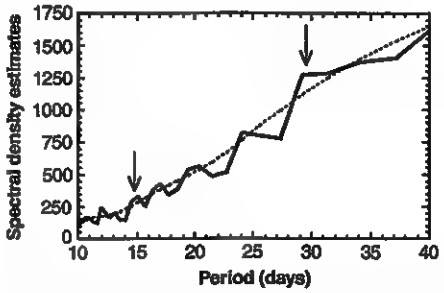

Fig. 2. Partial plot of the spectral density estimates (thick solid line) of the daily global temperature record from 3 January 1979 to 31 August 1994 at a bandwidth of 0.0281 (thin dotted line is for P = 0.10). Arrows indicate spectral peaks for the lunar period (29.53 days) and the synodic half-period (14.77 days).

REFERENCES AND NOTES

1. D. A. Bradley, M. A. Woodbury, G. W. Brier, *Science* **137**, 748 (1962).
2. E. E. Adderley and E. G. Bowen, *ibid.*, p. 749.
3. G. Brier and D. A. Bradley, *J. Atmos. Sci.* **21**, 386 (1964).
4. K. Hanson, G. A. Maul, W. McLeish, *J. Climate Appl. Meteorol.* **26**, 1358 (1987).
5. M. D. Lethbridge, *J. Geophys. Res.* **75**, 5149 (1970).
6. E. K. Bigg, *Nature* **197**, 172 (1963).
7. G. W. Brier and J. Simpson, *Q. J. R. Meteorol. Soc.* **95**, 120 (1969).
8. T. H. Carpenter, R. L. Holle, J. J. Fernadez-Partagas, *Mon. Weather Rev.* **100**, 451 (1972).
9. I. A. Lund, *J. Atmos. Sci.* **22**, 24 (1965).
10. C. H. Best, *Geophys. Res. Lett.* **21**, 2369 (1994).
11. R. W. Spencer and J. R. Christy, *Science* **247**, 1558 (1990).
12. ———, *J. Climate* **5**, 858 (1992).
13. M. R. Allen *et al.*, *Nature* **370**, 24 (1994).
14. J. R. Christy, in *Global Climate Change: Implications, Challenges, and Mitigation Measures*, S. K. Majumdar, L. S. Kalkstein, B. M. Yarnal, E. W. Miller, L. M. Rosenfeld, Eds. (Pennsylvania Academy of Science, Easton, 1992), pp. 165–178.
15. J. R. Christy and R. T. McNider, *Nature* **367**, 325 (1994).
16. J. W. Hurrell and K. E. Trenberth, *J. Climate* **5**, 1424 (1992).

17. P. D. Jones, *Geophys. Res. Lett.* **21**, 1149 (1994).
18. T. R. Karl, R. W. Knight, J. R. Christy, *J. Climate* **7**, 1144 (1994).
19. K. E. Trenberth, J. R. Christy, J. W. Hurrell, *ibid.* **5**, 1405 (1992).
20. P. D. Jones and T. M. L. Wigley, *Nature* **344**, 711 (1990).
21. J. R. Christy, R. W. Spencer, R. T. McNider, *J. Climate*, in press.
22. A. H. Gordon, *Nature* **367**, 325 (1994).
23. W. F. Ruddiman and A. McIntyre, *Science* **212**, 617 (1981).
24. R. A. Bryson, *Trans. Am. Geophys. Union* **29**, 473 (1948).
25. W. D. Sellers, *Physical Climatology* (Univ. of Chicago Press, Chicago, 1965).
26. Portions of this research were supported by NSF grant SES 9121398.

8 November 1994; accepted 11 January 1995

Conformation of Macromolecules in the Gas Phase: Use of Matrix-Assisted Laser Desorption Methods in Ion Chromatography

Gert von Helden, Thomas Wyttenbach, Michael T. Bowers*

Conformational data for macromolecules in the gas phase have been obtained by the coupling of a matrix-assisted laser desorption ion source to an ion chromatograph. A series of polyethylene glycol (PEG) polymers "cationized" (converted to a cation) by sodium ions (Na^+PEG9 to Na^+PEG19) and a protonated neurotransmitter protein, bradykinin, were studied. Mobilities of Na^+PEG9 to Na^+PEG19 are reported. Detailed modeling of Na^+PEG9 with molecular mechanics methods indicates that the lowest energy structure has the Na^+ ion "solvated" by the polymer chain with seven oxygen atoms as nearest neighbors. The agreement between the model and experiment is within 1 percent for Na^+PEG9, Na^+PEG13, and Na^+PEG17, giving strong support to both the method and the deduced structures. Similar agreement was obtained in initial studies that modeled experimental data for arginine-protonated bradykinin.

Determination of the preferred conformations of large molecules traditionally has been restricted to the condensed phase, both as a means of inhibiting intramolecular motion and as a way of increasing the number density of the target molecule. For biomolecules such as proteins, the relation between conformation and activity has long been an active area of research, especially the relation between protein folding and genetic expression (*1*). With the advent of matrix-assisted laser desorption ionization (MALDI) (*2*) and electrospray ionization (ESI) (*3*), it has become routine to desorb molecules of nearly any size into the gas phase, where they can be examined by mass spectrometry (*4*). A primary focus of this work has been the determination of structural features of these molecules. For example, considerable progress has been made in determining amino acid sequences of proteins (*5*) and, as an adjunct to this work, the importance of metal ions as cationizing agents both for sequence studies and for investigations of their influence on peptide chemistry (*6*, *7*).

More recently, attention has turned to conformational studies of macromolecules. For example, ESI charge distributions of select, multiply charged ions can change with solution properties such as pH or solvent. These results were interpreted in terms of conformational changes in the biomolecules of interest (*8*). Another approach involves counting the labile peptide protons by isotopic exchange, because the extent of exchange is believed to correlate with the degree of folding of the protein (*9*). Finally, the different collision cross sections that different conformers might exhibit have been used to distinguish "larger" conformers from "smaller" conformers of multiply charged ions in triple quadrupole instruments (*10*).

Each of the above conformational studies used ESI and hence dealt with multiply charged ions rather than singly charged ions. In addition, although the conclusions about the existence of different conformations were usually unambiguous, none of the methods were designed to give any detailed structural information on the various conformers observed. In this report, we describe the use of MALDI in conjunction with our recently developed ion chromatography (IC) technique (*11*). When combined with molecular mechanics-dynamics methods, these data provide unambiguous structural information on singly charged cationized macromolecules in the gas phase.

We investigated the gas-phase structure of various polyethylene glycol (PEG) polymers in the range PEG9 to PEG19 (that is, from 9 to 19 $-(CH_2CH_2O)-$ monomer units). These are ideal systems for an initial study because they give a range of molecules whose connectivities are known and that change in a known way. Hence, the effect of chain length on conformation can be studied. A known series also provides a stringent test of the IC method as it must be able to reproduce and account for these changes without changing the molecular parameters used in modeling the system. Moreover, because PEG is cationized by Na^+ in our experiments, we can investigate the metal ion binding site (or sites) in a series of macromolecules of significant size. Finally, the distribution of PEG neutral species results in a distribution of the cationized polymers formed in the MALDI process, reducing the intensity of any one system by about an order of magnitude and providing a real test of the sensitivity of the method. The success of these experiments prompted application to biopolymers, and our initial work on the polypeptide bradykinin yielded parent ion signals an order of magnitude greater than for individual PEG systems, which made data acquisition much easier. These results, which will be discussed briefly here, will be published elsewhere (*12*).

Ions were made in a MALDI source built at the University of California at Santa Barbara, which is described elsewhere (*13*).

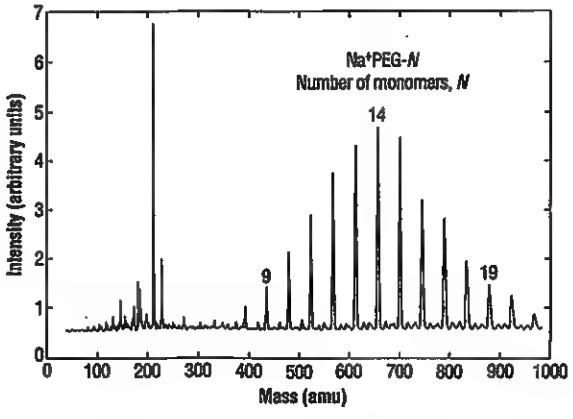

Fig. 1. A MALDI mass spectrum of a commercial PEG-600 sample present at 0.1% in a sinapinic acid matrix. All peaks below mass 300 (amu = atomic mass unit) are due to the matrix. A number of the Na^+-cationized PEG peaks are identified.

Department of Chemistry, University of California, Santa Barbara, CA 93106, USA.

*To whom correspondence should be addressed.

Briefly, the sample was deposited on a cylindrical drum that is attached to a screw thread. A synchronous motor slowly turned the screw such that a fresh area of sample on the drum was exposed for each laser shot. We used a Lambda Physik LPX-200 excimer laser running on N_2, yielding 10-ns pulses of ~1.5-mJ energy at 337 nm. For most studies, the sample was composed of a matrix of sinapinic acid and ~0.1% PEG-600. Ions emitted from the source were accelerated to 5 kV, mass-selected by a reverse–geometry sector mass spectrometer, decelerated to a few electron volts, and injected into the IC cell containing 5 torr of He at 300 K. The 10-ns laser pulse produced bursts of ions at the IC cell less than 10 μs in width, and no further gating was required. Arrival time distributions were obtained at the detector after passage through the quadrupole mass filter that follows the IC cell. Details of the instrument are given elsewhere (*14*).

A typical mass spectrum is shown in Fig. 1. A commercial sample of PEG-600 produced a series of peaks centered near a mass-to-charge ratio of 600 that corresponds to PEG species cationized by Na^+. Intensities were sufficient for IC studies of Na^+PEG9 to Na^+PEG19.

A typical arrival-time distribution (ion chromatagram) is given in Fig. 2 for Na^+PEG9. From distributions such as these, mobilities of the various Na^+-cationized PEG species can be obtained (*15*). The transport equations of an ion drifting through He gas under a uniform electric field can easily be solved (*16*), which yields the dashed line in Fig. 2 for an ion mobility of 4.2 $cm^2\ V^{-1}\ s^{-1}$; clearly, the agreement with experiment is excellent. The important point is that the IC peak can be fit essentially exactly with a single mobility. This fit excludes the existence of stable conformers that vary by more than 0.1 $cm^2\ V^{-1}\ s^{-1}$ from 4.2 $cm^2\ V^{-1}\ s^{-1}$ (that is, by more than 2.5%). These conformers would appear as obvious shoulders or as asymmetries in the experimental peak shape. Arrows in Fig. 2 are placed ±2.5% from the peak center, and no deviations from the expected peak shape were observed within these boundaries. However, the fit does not exclude rapidly interconverting isomers that yield an average mobility of 4.2 $cm^2\ V^{-1}\ s^{-1}$. Similar results were obtained for Na^+PEG10 to Na^+PEG19.

The question that now arises is: What is the structure of the conformer or set of conformers that gives rise to the IC spectra we obtain. We have discussed in detail the method we used to obtain such structures in our work on carbon clusters (*17*). In that work, we calculated a potential conformer structure by using either ab initio or semiempirical methods. The angle-averaged collision cross section of the conformer with He was then obtained with Monte Carlo methods. The mobility is simply inversely proportional to the cross section in the hard-sphere limit. If the mobility of the predicted structure was within 2% of the experimental value, then it became a candidate for the actual conformer structure. Usually, the agreement was within 1% for successful candidates.

The Na^+PEG systems considered here are too large for either ab initio or semiempirical methods, so instead we performed molecular mechanics calculations with the force field found in the Sybyl set of programs (*18*). We began with Na^+PEG9 and used the random selection aspect of the program to generate 400 stable conformers. Their relative energies varied over a range of ~60 kcal mol^{-1}, and the associated mobilities from ~4.3 to ~2.5 $cm^2\ V^{-1}\ s^{-1}$. Examination of the structures of the lowest energy conformers showed that all of them had multiple O atoms coordinated about the Na^+ center. A series of annealings and energy minimizations (*13*) generated the lowest energy structure. This structure is shown in Fig. 3 for Na^+PEG9. In order to best compare with experiment, we performed a 300 K molecular dynamics simulation on this 0 K structure for 200,000 fs. We calculated mobilities by sampling the instantaneous structure at 100-fs intervals (2000 mobility calculations in all), yielding a value of K_o = 4.20 ± 0.10 $cm^2\ V^{-1}\ s^{-1}$. The uncertainty given is the maximum spread obtained in the simulation. This value agrees very well with the experimental value of K_o = 4.18 ± 0.05 $cm^2\ V^{-1}\ s^{-1}$. No adjustable parameters were used to obtain a fit of the model to the experiment (*19–21*).

The structure shown in Fig. 3 is a stick-and-ball structure with artificial atom sizes selected to highlight the location of the Na^+ ion and the O atoms. The H atoms are excluded (for clarity). The PEG9 structure coils around the Na^+ ion such that five O atoms are nearest neighbors in a plane, and single additional O atoms both above and below the plane give a total of seven O nearest neighbors. Each O atom is ~2.2 Å from the Na^+ ion. A space-filling model in

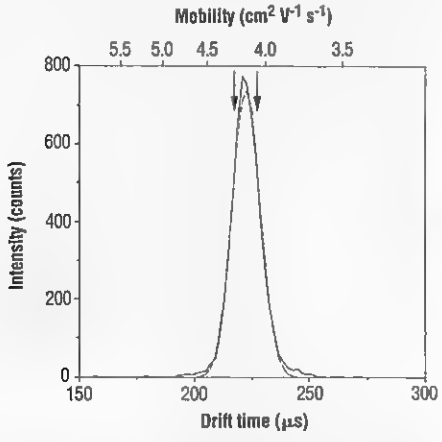

Fig. 2. An arrival time distribution (ion chromatagram) for Na^+PEG9. The solid line is the experimental result, and the dashed line is a fit obtained by solving the transport equations for a single species with a mobility of 4.2 $cm^2\ V^{-1}\ s^{-1}$. The two arrows indicate a shift in the peak center of ±2.5% (see text).

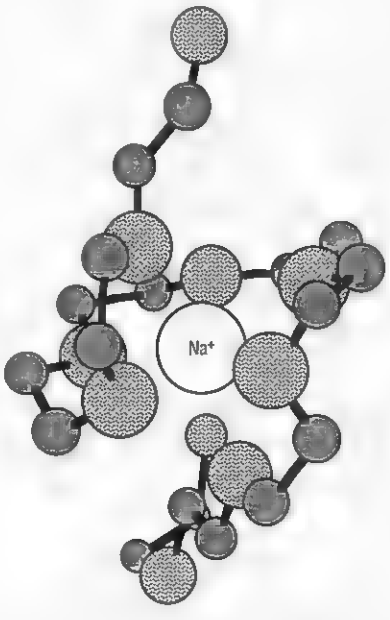

Fig. 3. A ball-and-stick structural representation of the lowest energy conformer of Na^+PEG9. The O atoms are shown as the larger speckled circles and the C atoms as the small, darker circles. The H atoms are not shown (for clarity). The sizes of the various atoms were chosen to highlight the interaction of Na^+ with the O atoms.

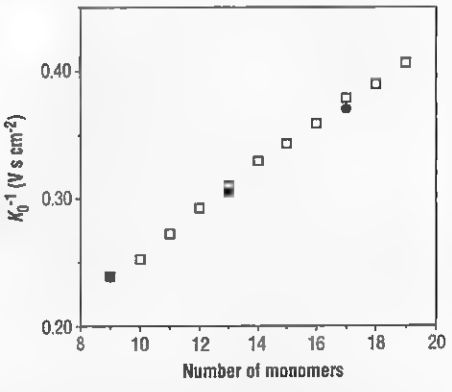

Fig. 4. A plot of K_o^{-1} versus number of monomers for the cationized PEG species Na^+PEG9 through Na^+PEG19. The open squares are the experimental data. The filled circles are the model-generated mobilities for Na^+PEG9, Na^+PEG13, and Na^+PEG17. The sizes of the points were chosen to include the uncertainties in the numbers.

which the van der Waals radii of the atoms are used indicates that the Na^+ ion is completely encased by the coiled PEG9.

The experimental data for other systems are given in Fig. 4 as a plot of K_o^{-1} versus the number of monomers. A regular, near-linear increase with monomer number is observed as expected for members of a single structural family (*17*). We have modeled Na^+PEG13 and Na^+PEG17 in addition to Na^+PEG9, and these three data points are shown in Fig. 4 for comparison. Excellent agreement was obtained between the model and experiment. Modeling of the complete series will be reported elsewhere (*13*).

The Sybyl molecular mechanics programs were also used to model the possible stable conformers of the neutral PEG9. A series of 400 stable conformers were randomly generated with resulting relative energies over a range of ~20 kcal mol^{-1}. Several of the more stable species were annealed and subjected to energy minimization. The most stable of these was then subjected to 200,000 fs of molecular dynamics at 300 K, and 2000 structures were extracted at 100-fs intervals. The mobilities these species would have generated if singly charged were in the range $K_o = 3.5 \pm 0.4$ cm^2 V^{-1} s^{-1}. This lower value of K_o indicates that a much more open structure is predicted for neutral PEG9 relative to Na^+PEG9, and the molecular dynamics simulation reveals that a much wider range of conformers is sampled at 300 K. Both results are consistent with rather weak intramolecular interactions in neutral PEG9 relative to Na^+PEG9.

A few words of comparison with our bradykinin results (*12*) are useful. Bradykinin is almost exclusively cationized with protons, rather than with Na^+ in our experiments, regardless of the matrix. Protons prefer to form localized bonds, and, if the charge is shared, they usually involve only two centers. Furthermore, bradykinin has two arginine units, one at the NH_2-terminus and one at the COOH-terminus, which are preferred sites of protonation (*22*). Hence, one might expect a more open structure for protonated bradykinin (a nine-residue peptide chain) than for Na^+-cationized PEG structures. Our modeling suggests that this is the case. The experimental mobility is 2.20 ± 0.05 cm^2 V^{-1} s^{-1}, and our preliminary modeling results, assuming protonation at arginine, yield a mobility of ~2.1 cm^2 V^{-1} s^{-1} for the lowest energy structure. The model result needs to be subjected to molecular dynamics averaging, and searches for other possible protonation sites need to be done. Nonetheless, the agreement is remarkably good and lends strong support both for the Sybyl molecular mechanics force field (*18*) and for our method for determining the van der Waals radii of the involved atoms (*19–21*).

REFERENCES AND NOTES

1. F. M. Richards, *Sci. Am.* **264**, 54 (January 1991).
2. M. Karas and F. Hillenkamp, *Anal. Chem.* **60**, 2299 (1988); R. C. Beavis and B. T. Chait, *Rapid Commun. Mass Spectrom.* **3**, 432 (1989); *ibid.*, p. 436.
3. C. M. Whitehouse, R. N. Dreyer, M. Yamashuta, J. B. Fenn, *Anal. Chem.* **57**, 675 (1985); J. B. Fenn, M. Mann, C. K. Meng, S. F. Wong, C. M. Whitehouse, *Science* **264**, 64 (1989).
4. See the special issue on mass spectrometry, *Acc. Chem. Res.* **27**, issue 11 (November 1994).
5. See, for example, B. T. Chait, R. Wang, R. C. Beavis, S. B. H. Kent, *Science* **262**, 89 (1993); K. Biemann, *Fresenius Z. Anal. Chem.* **343**, N1:25 (1992); *Annu. Rev. Biochem.* **61**, 977 (1992).
6. For leading references on alkali metals and peptides, see: R. B. Cody, J. I. Amster, F. W. McLafferty, *Proc. Natl. Acad. Sci. U.S.A.* **82**, 6367 (1985); L. M. Mallis and D. H. Russell, *Anal. Chem.* **58**, 1076 (1986); X. Tang, W. Eus, K. G. Standing, J. B. Westmore, *ibid.* **60**, 1791 (1988); R. P. Grese, R. L. Cerny, M. L. Gross, *J. Am. Chem. Soc.* **111**, 2835 (1989); J. A. Leary, T. D. Williams, G. Bott, *Rapid Commun. Mass Spectrom.* **3**, 192 (1989); L. M. Teesch and J. Adams, *J. Am. Chem. Soc.* **113**, 812 (1991).
7. For leading references on alkaline earth and transition metal ions, see: L. M. Teesch and J. Adams, *J. Am. Chem. Soc.* **112**, 4110 (1990); P. Hu and M. L. Gross, *ibid.* **114**, 9153 (1992); H. Zhoo, A. Reiter, L. M. Teesch, J. Adams, *ibid.* **115**, 2854 (1993); P. Hu and M. L. Gross, *ibid.*, p. 8821.
8. S. K. Chowdhung, V. Katta, B. T. Chalt, *ibid.* **112**, 9012 (1990); J. A. Loo, R. R. Ogorzalek-Loo, H. R. Udseth, C. G. Edmunds, R. D. Smith, *Rapid Commun. Mass Spectrom.* **5**, 101 (1991); R. Gueuremont, K. W. M. Sui, J. C. Y. LeBlanc, S. S. Berman, *J. Am. Soc. Mass Spectrom.* **3**, 216 (1992).
9. V. Katta and B. T. Chait, *Rapid Commun. Mass Spectrom.* **5**, 214 (1991); B. E. Winger, K. J. Light-Wahl, A. L. Rockwood, R. D. Smith, *J. Am. Chem. Soc.* **114**, 5897 (1992); D. Suekau *et al.*, *Proc. Natl. Acad. Sci. U.S.A.* **90**, 790 (1993).
10. T. Covey and D. J. Douglas, *J. Am. Soc. Mass Spectrom.* **4**, 616 (1993); K. A. Cox, R. K. Julian, R. G. Cooks, R. E. Kaiser, *ibid.* **5**, 127 (1994).
11. M. T. Bowers, P. R. Kemper, G. von Helden, P. A. M. van Koppen, *Science* **260**, 1446 (1993).
12. T. Wyttenbach, G. von Helden, M. T. Bowers, unpublished results.
13. G. von Helden, T. Wyttenbach, M. T. Bowers, *Int. J. Mass Spectrom. Ion Processes* (Al Nier special issue), in press.
14. P. R. Kemper and M. T. Bowers, *J. Am. Soc. Mass Spectrom.* **1**, 197 (1990).
15. ———, *J. Phys. Chem.* **95**, 5134 (1991).
16. E. A. Mason and E. W. McDaniel, *Transport Properties of Ions in Gases* (Wiley, New York, 1988).
17. G. von Helden, M.-T. Hsu, N. Gotts, M. T. Bowers, *J. Phys. Chem.* **97**, 8182 (1993).
18. M. Clark, R. D. Cramer III, N. van Opdenbosch, *J. Comput. Chem.* **10**, 982 (1989).
19. The van der Waals radii used were 1.09 Å for He, 1.51 Å for O, 1.10 Å for H, and 1.61 Å for C. The He and C van der Waals radii were the same as those used for very extensive C studies (*17*). The H and O radii were determined by He scattering calculations on CH_4 and $(C_2H_5)_2O$, respectively. More details are given in (*20*) and (*21*).
20. G. von Helden, E. Porter, N. G. Gotts, M. T. Bowers, *J. Phys. Chem.* (Mostafa El Sayed special issue), in press.
21. G. von Helden, thesis, University of California at Santa Barbara (1994).
22. G. S. Gorman, J. P. Speir, C. A. Turner, I. J. Amster, *J. Am. Chem. Soc.* **114**, 3986 (1992).

23. This work was supported under NSF grants CHE91-10752 and CHE94-21176 and by the Air Force Office of Scientific Research under grant FA 9620-93-1-0134.

13 October 1994; accepted 10 January 1995

Control of IκB-α Proteolysis by Site-Specific, Signal-Induced Phosphorylation

Keith Brown, Susan Gerstberger, Louise Carlson, Guido Franzoso, Ulrich Siebenlist*

IκB-α inhibits transcription factor NF-κB by retaining it in the cytoplasm. Various stimuli, typically those associated with stress or pathogens, rapidly inactivate IκB-α. This liberates NF-κB to translocate to the nucleus and initiate transcription of genes important for the defense of the organism. Activation of NF-κB correlates with phosphorylation of IκB-α and requires the proteolysis of this inhibitor. When either serine-32 or serine-36 of IκB-α was mutated, the protein did not undergo signal-induced phosphorylation or degradation, and NF-κB could not be activated. These results suggest that phosphorylation at one or both of these residues is critical for activation of NF-κB.

Proteolytic degradation of IκB-α is essential for activation of NF-κB (*1–4*). When degradation is blocked by certain protease inhibitors that target proteasomes, activation of NF-κB is prevented. Physiologic stimulation also induces phosphorylation of IκB-α (*1–7*), but the significance of this phosphorylation for activation of NF-κB in cells has remained unclear. Induced phosphorylation does not in itself dissociate complexes of IκB-α and NF-κB in vivo (*1, 2, 4, 7*). The question arises as to how proteolysis of IκB-α is triggered.

To identify regions in IκB-α essential for signaling and degradation, we systematically mutated the human IκB-α gene and stably transfected the altered genes into mouse EL-4 T lymphocytes (*8–10*). Human IκB-α was distinguished from endogenous murine IκB-α by its slower mobility on SDS gels. The exogenous human wild-type IκB-α and endogenous murine IκB-α were degraded with similar kinetics upon cellular stimula-

Laboratory of Immunoregulation, National Institute of Allergy and Infectious Diseases, National Institutes of Health, Building 10, Room 11B16, Bethesda, MD 20892–1876, USA.

*To whom correspondence should be addressed.

tion with tumor necrosis factor–α (TNF-α) (Fig. 1A) or phorbol 12-myristate 13-acetate (PMA) + ionomycin (Fig. 1B). Furthermore, the human IκB-α was phosphorylated in a signal-dependent manner, as indicated by the characteristic shift in electrophoretic mobility that accompanies signal-induced phosphorylation of endogenous IκB-α from human cells (*2*) (Fig. 2, A and D). To block proteolysis in the latter experiments, we added calpain inhibitor I to the cells (*11*). Although murine IκB-α was also phosphorylated upon stimulation (see below), only a small change in mobility was observed. The proteolysis and phosphorylation tests established that permanently transfected human wild-type IκB-α is fully signal-responsive in these cells.

We then tested various deletions and point mutants of human IκB-α in EL-4 cells (*10*). A deletion mutant missing the NH_2-terminal 54 amino acids (ΔN) was neither proteolyzed nor phosphorylated in response to signals (Figs. 1B and 2B), but still fully inhibited NF-κB (Fig. 3A). We therefore investigated potential phosphoacceptor sites within the deleted portion. IκB-α containing a Ser^{32}→Gly mutation (mt^{32}) was not degraded upon stimulation by TNF-α or PMA + ionomycin (Fig. 1D) (*12*) nor did it undergo the characteristic mobility shift upon cellular stimulation, suggesting a defect in signal-induced phosphorylation (Fig. 2D). IκB-α containing a Ser^{36}→Ala mutation (mt^{36}) behaved similarly (Figs. 1E and 2E). Both mutants still inhibited NF-κB, as determined by transient transfection of human NTera-2 embryonal carcinoma cells with a κB-dependent reporter plasmid (*9*) (Fig. 3A) and by in vitro DNA binding assays (Fig. 3B) (*12*). The mt^{32} IκB-α was also precipitated from EL-4 cell extracts with antibodies against the p65 subunit of NF-κB, regardless of whether cells were stimulated (Fig. 3C). We conclude that a mutation at either Ser^{32} or Ser^{36} (or deletion of the NH_2-terminus) has no effect on the inhibitory function of IκB-α but completely abolishes the signal-induced, phosphorylation-dependent shift in mobility and the degradation of IκB-α.

Mutations of all other potential phosphoacceptor Ser, Thr, and Tyr residues in the NH_2-terminal 89 residues of IκB-α (the region NH_2-terminal to the ankyrins and the beginning of the ankyrin domain) did not block signal-induced phosphorylation or degradation of the protein, nor did mutations of several other residues located elsewhere in the protein (*13*). These results support the hypothesis that Ser^{32} and Ser^{36} mutants directly blocked phosphorylation at one or both of these sites. (*14*). Proteolysis of the inhibitor also appears to require sequences at the COOH-terminus of IκB-α. A mutant missing the 41 COOH-terminal residues (ΔC) was not proteolyzed in response to signals but was phosphorylated (Figs. 1C and 2C), indicating that induced phosphorylation is necessary but not sufficient for proteolysis. The ΔC deletion eliminated sequences rich in Pro, Glu/Asp, Ser, and Thr residues (PEST sequences), which are often found in proteins that turn over rapidly (*15, 16*) and which may be necessary for induced proteolysis of IκB-α. The ΔC mutant still inhibited NF-κB activity in transfection experiments and retained its ability to bind p65, but it did not inhibit DNA binding of NF-κB in vitro (Fig. 3B) (*12, 17*). Thus, cytoplasmic retention of NF-κB and inhibition of DNA binding appear to be separable functions of IκB-α, with the latter requiring additional COOH-terminal sequences.

The mutations blocking signal-induced phosphorylation and proteolysis also prevented activation of NF-κB. We demonstrated this in NTera-2 cells, which do not express endogenous NF-κB or IκB-α (Fig. 3A) (*9*). Transactivation of a κB-driven reporter, which is dependent on cotransfection of the p65 subunit of NF-κB, was inhibited by cotransfection of wild-type IκB-α as well as by the mutants ΔN, mt^{32}, and mt^{36}. Upon stimulation with PMA + ionomycin, inhibition of NF-κB transactivation was relieved in the cells transfected with wild-type IκB-α, but not in those transfected with the signal-defective mutants.

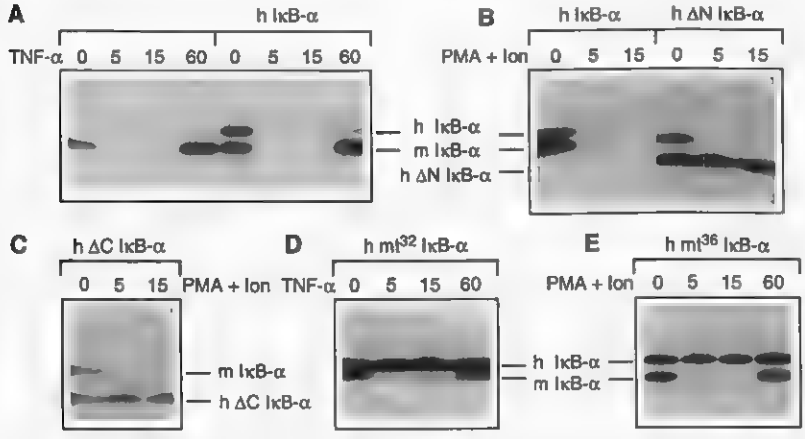

Fig. 1. (**A** to **E**) Signal-induced proteolysis of endogenous murine (m) and exogenous human (h) IκB-α in murine EL-4 T cells. Immunoblots had equal amounts of whole-cell extracts in each lane. Untransfected cells (A, left) or cells stably transfected (*8*) with the indicated IκB-α constructs (*10*) were stimulated with murine TNF-α (2000 U/ml; Genzyme, Cambridge, Massachusetts); or PMA (40 ng/ml; Sigma, St Louis, Missouri) and ionomycin (Ion, 2 μM, Calbiochem, San Diego, California). The numbers above the lanes indicate the period of time (in minutes) between cell stimulation and harvest. Blots A, B, D, and E were probed with rabbit polyclonal antibody directed against the COOH-terminus (amino acids 230 to 315) of h IκB-α. Blot C was probed with rabbit polyclonal antibody against full-length h IκB-α. The mobilities of h IκB-α, mt^{32}, and mt^{36} were similar. In (A), (D), and (E), the time course extends to 60 min after stimulation, at which time m IκB-α has already been resynthesized. This observation is explained by the rapid activation of endogenous m (but not exogenous h) IκB-α transcription by activated NF-κB released through degradation of IκB-α protein (*5*).

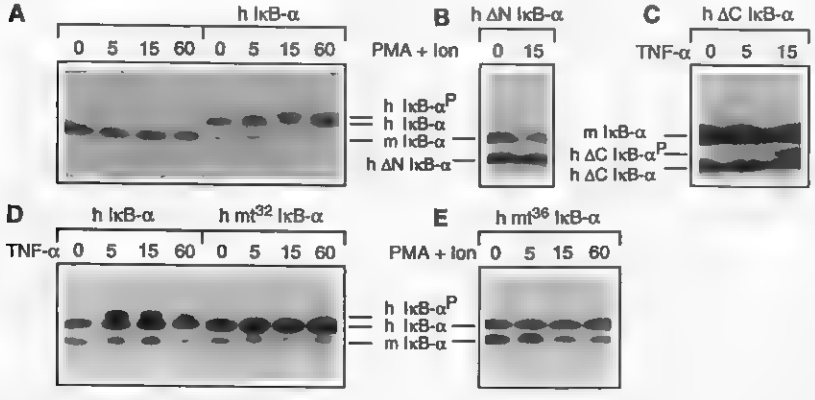

Fig. 2. (**A** to **E**) Signal-induced phosphorylation of h IκB-α in murine EL-4 T cells. Immunoblots were prepared as in Fig. 1. Cells were preincubated for 30 min with Calpain Inhibitor (100 μM, Boehringer, Indianapolis, Indiana) (*2*) prior to stimulation with mTNF-α or PMA + Ion, and later extracted in the presence of phosphatase inhibitors (*2, 5*). The signal-induced phosphorylated species of h IκB-α (h IκB-$α^P$) migrates slightly slower than h IκB-α.

Two-dimensional gel analyses were performed to separate phosphoisoforms of metabolically labeled human IκB-α (*18*). When immunoprecipitated from unstimulated EL-4 cells, ^{35}S-labeled wild-type human IκB-α resolved into several isoforms, revealed as a string of spots (Fig. 4A). Similar isoforms were also observed with murine IκB-α from unstimulated cells (*18*) and with mt^{32} (Fig. 4B). The spots represent distinct IκB-α phosphoisoforms that differ in the extent of phosphorylation. With prior phosphatase treatment, the spots collapsed into a single spot (*18*). Metabolic labeling with [^{32}P]orthophosphate confirmed that IκB-α was phosphorylated in unstimulated cells, with the more phosphorylated isoforms represented by the more intense spots (Fig. 4C). The significance of this constitutive phosphorylation is unknown.

Upon cellular stimulation, the constitutive phosphoisoforms of IκB-α were further phosphorylated, resulting in the appearance of additional spots with slower mobility in the second (size) dimension. The shift of these new spots toward a lower pH in the first dimension was consistent with a more negative charge (Fig. 4A). This was confirmed with ^{32}P-labeled IκB-α (Fig. 4C). The apparent magnitude of the shift in the first dimension suggests that more than one phosphate was added in response to signals (Fig. 4, A and C). In contrast to wild-type IκB-α, the mt^{32} (Fig. 4B) ΔN, and mt^{36} mutants (*18*) exhibited no apparent phosphorylation changes in response to cellular stimulation.

These data indicate that signal-induced phosphorylation of IκB-α is necessary for proteolysis of the inhibitor and for activation of NF-κB. Conservative mutations at either Ser^{32} or Ser^{36} blocked phosphorylation and degradation of IκB-α. These residues in IκB-α have been highly conserved through evolution (*19*). The most direct interpretation of our data is that NF-κB activating signals lead to phosphorylation, possibly at both Ser^{32} and Ser^{36} (*20*), which in turn represents a recognition signal that is necessary but not sufficient for proteolysis. Proteolysis of IκB-α requires additional sequences, including a COOH-terminal PEST region. Site-specific, signal-induced phosphorylation of proteins may be a general mechanism for rapidly altering protein stability in response to extracellular stimuli or during the cell cycle.

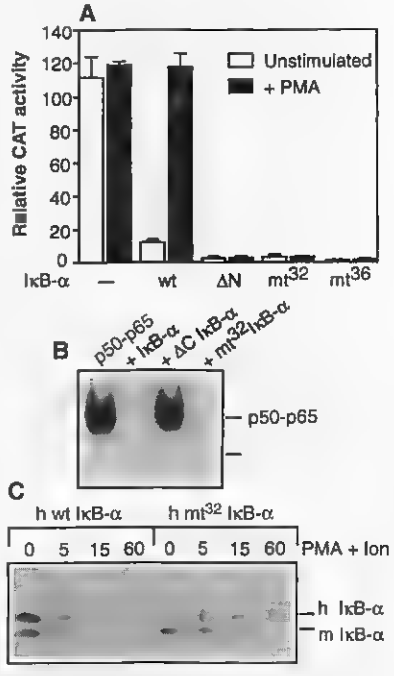

Fig. 3. Functional interaction of h IκB-α mutants with NF-κB. (**A**) Inhibition of NF-κB activation by h IκB-α Ser^{32} or Ser^{36} mutants. NTera-2 cells were transiently transfected with NF-κB p65 (0.2 μg, PMT2T-p65) and with a chloramphenicol acetyltransferase (CAT) reporter plasmid (5 μg) containing the κB site derived from human immunodeficiency virus (HIV) (*9*). Wild-type (wt) h IκB-α and h IκB-α mutants ΔN, mt^{32}, and mt^{36} (0.1 μg each on vector PMT2T) were cotransfected. Cells were stimulated for 6 hours with PMA (10 ng/ml) and 36 hours after transfection, they were harvested, extracted, and assayed for CAT activity (*9*). The values shown are the means of three independent experiments. Relative CAT activity refers to fold transactivation relative to cells transfected with reporter plasmid alone. (**B**) Inhibition of binding of NF-κB to κB-DNA by h IκB-α mutants. Extracts of NTera-2 cells cotransfected with NF-κB p50 and p65 (3 μg each vector) and with IκB-α constructs (4 μg each vector) were tested in electrophoretic mobility shift assays for binding to a ^{32}P-labeled palindromic κB DNA probe (*9*). The position of p50 homodimers (only faintly visible) is indicated by the mark below the p50-p65 band. (**C**) Physical association of h wt IκB-α and h mt^{32} IκB-α with endogenous murine NF-κB p65. Murine EL-4 T cells stably transfected with these IκB-α constructs were stimulated with PMA (40 ng/ml) + Ion (2 μM). After the indicated period of time (0 to 60 min), they were extracted and immunoprecipitated with protein A–Sepharose beads (Pharmacia, Piscataway, New Jersey) and rabbit polyclonal antibody directed against amino acids 103 to 194 of human p65. Washed precipitates were subjected to electrophoresis, immunoblotted, and probed with rabbit polyclonal antibodies directed against residues 230 to 315 of h IκB-α and ^{125}I-labeled protein A (Dupont, Boston, Massachusetts). The presence of cycloheximide (20 μg/ml) during stimulation blocked the resynthesis of m IκB-α that was usually observed within 60 min (see Fig. 1).

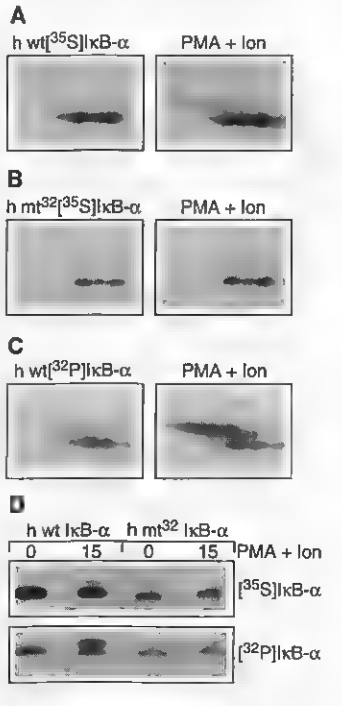

Fig. 4. (**A** to **C**) Two-dimensional gel electrophoresis of h wt IκB-α and h mt^{32} IκB-α. Murine EL-4 T cells stably transfected with these IκB-α constructs were labeled with [^{35}S]methionine plus [^{35}S]cysteine (1 mCi/ml each) or with [^{32}P]orthophosphate (2 mCi/ml) (Dupont, Boston, Massachusetts) for 60 min in the presence of Calpain Inhibitor I (200 μM). Half of each labeled cell suspension was then stimulated for 15 min with PMA (50 ng/ml) plus Ion (4 μM) and extracts were prepared in the presence of phosphatase inhibitors (*2, 5*). Extracts were then immunoprecipitated with a rabbit polyclonal antibody directed against amino acids 6 to 20 of h IκB-α (Santa Cruz Biotechnology, Inc., Santa Cruz, California). This antibody did not cross-react with endogenous m IκB-α (*12*). Immunoprecipitates were then subjected to two-dimensional gel electrophoresis (*18*). The horizontal axis represents the isoelectric focusing dimension. The more acidic species are on the left and the more basic species are on the right. The vertical axis represents the size-separation dimension. (**D**) One-dimensional gel electrophoresis of the ^{35}S- and ^{32}P-labeled h IκB-α immunoprecipitates shown in (A) to (C).

REFERENCES AND NOTES

1. U. Siebenlist, G. Franzoso, K. Brown, *Annu. Rev. Cell Biol.* **10**, 405 (1994).
2. Y.-C. Lin, K. Brown, U. Siebenlist, *Proc. Natl. Acad. Sci. U.S.A.* **92**, 552 (1995).
3. V. J. Palombella, O. J. Rando, A. L. Goldberg, T. Maniatis, *Cell* **78**, 773 (1994).
4. E. B.-M. Traenckner, S. Wilk, P. Baeuerle, *EMBO J.* **13**, 5433 (1994).
5. K. Brown, S. Park, T. Kanno, G. Franzoso, U. Siebenlist, *Proc. Natl. Acad. Sci. U.S.A.* **90**, 2532 (1993).
6. A. A. Beg, T. S. Finco, P. V. Nantermet, A. S. Baldwin, *Mol. Cell. Biol.* **13**, 3301 (1993); S.-C. Sun, P. A. Ganchi, C. Béraud, D. W. Ballard, W. C. Greene, *Proc. Natl. Acad. Sci. U.S.A.* **91**, 1346 (1994).
7. S.-C. Sun, J. Elwood, C. Béraud, W. C. Greene, *Mol. Cell. Biol.* **14**, 7377 (1994); T. S. Finco, A. A. Beg, A. S. Baldwin, *Proc. Natl. Acad. Sci. U.S.A.* **91**, 11884 (1994).
8. The IκB-α genes were transfected into EL-4 cells on vector PMT2T (*9*) by electroporation [20 μg DNA and 10^7 cells, Bio-Rad (Hercules, CA), 250 V, 960 μF], together with a plasmid conferring neomycin (neo) resistance (2 μg). Stable neo^r transfectants were selected by incubation of the electroporated cells for 3

to 4 weeks in medium supplemented with geneticin G418 [(Gibco-BRL, Gaithersburg, MD), at 400 μg/ml for 1 week; 200 μg/ml, 2 to 3 weeks] and then screened for human IκB-α by immunoblotting. The results with each transfected IκB-α species were confirmed with independently transfected cell clones.

9. V. Bours *et al.*, *Mol. Cell. Biol.* **12**, 685 (1992); G. Franzoso *et al.*, *Nature* **359**, 339 (1992); V. Bours *et al.*, *Cell* **72**, 729 (1993).
10. We constructed the ΔN and ΔC IκB-α mutants by cloning into PMT2T (*9*) the 1296–base pair (bp) Xho I–Eco RI fragment and the 921-bp Eco RI–Xmn I fragment, respectively, of the human gene (*15*). Point mutants of IκB-α were obtained in a Bluescript plasmid (Stratagene, La Jolla, CA) containing nucleotides 1 to 1550 of IκB-α complementary DNA (*15*) by site-directed mutagenesis [P. Bressler *et al.*, *J. Virol.* **67**, 288 (1993)]; the mutants were then cloned into PMT2T as 1550-bp Eco RI fragments encoding full-length IκB-α.
11. To permit detection of the newly phosphorylated IκB-α in this experiment, we included phosphatase inhibitors during cell extraction (*2*, *5*). To enhance detection, we trapped the phosphorylated intermediate by blocking proteolysis with calpain inhibitor I (*2*).
12. K. Brown, S. Gerstberger, L. Carlson, G. Franzoso, U. Siebenlist, unpublished data.
13. These include all four other potential phosphoacceptor sites within the NH_2-terminal 89 amino acids (residues Tyr^{42}, Ser^{63}, Thr^{71}, and Ser^{76}) and other sites throughout the ankyrin and COOH-terminal domain. Of note, mutation of the protein kinase C consensus site (residues Ser^{262} and Thr^{263}) (*15*) did not prevent activation of NF-κB (*12*).
14. Proteolytic mapping experiments confirmed that induced phosphorylation of IκB-α occurred at a site or sites that are NH_2-terminal to the ankyrin domain (*12*). Thus together with the observation that mutations of all other potential phosphorylation sites within the NH_2-terminal domain of IκB-α did not block signaling indicates that the possibility that the Ser^{32} and Ser^{36} mutations act directly at one or both of these sites to block phosphorylation.
15. S. Haskill *et al.*, *Cell* **65**, 1281 (1991).
16. S. Rogers, R. Wells, M. Rechsteiner, *Science* **234**, 364 (1986).
17. A similar ΔC mutant has previously been shown to inhibit DNA binding of NF-κB in vitro [E. N. Hatada, M. Naumann, C. Scheidereit, *EMBO J.* **12**, 2781 (1993)].
18. Two-dimensional gel electrophoresis was performed as described [P. H. O'Farrell, *J. Biol. Chem.* **250**, 4007 (1975)] by Kendrick Labs, Inc. (Madison, WI). The gels of ^{35}S-labeled murine IκB-α revealed constitutive phosphoisoforms analogous to those of human IκB-α. These experiments also showed that the murine IκB-α was phosphorylated in response to signals (shown by a shift in charge toward negative pH in the first dimension) and that the induced phosphorylation of this species resulted in only a minor shift in apparent size (*12*). Analyses of the ΔN and mt^{36} mutants yielded results similar to those obtained with mt^{32} (*12*). Phosphatase treatment resulted in a single spot (*12*). Endogenous IκB-α from human cells was indistinguishable from exogenously expressed human IκB-α on these gels.
19. R. de Martin *et al.*, *EMBO J.* **12**, 2773 (1994).
20. It remains to be determined if one or both serines are phosphorylated. Mutation of one of these closely spaced serines may block phosphorylation of the other; even if both serines are phosphorylated, their phosphorylation may be linked.
21. We thank K. Kelly and A. S. Fauci for review of the manuscript, A. S. Fauci for continued support, and Y. Ward for expert help and advice.

30 December 1994; accepted 9 February 1995

Requirement of RNA Polymerase III Transcription Factors for in Vitro Position-Specific Integration of a Retroviruslike Element

Jacqueline Kirchner, Charles M. Connolly, Suzanne B. Sandmeyer*

The yeast retroviruslike element Ty3 inserts at the transcription initiation sites of genes transcribed by RNA polymerase III (Pol III). An in vitro integration assay was developed with the use of Ty3 viruslike particles and a modified *SUP2* tyrosine transfer RNA ($tRNA^{Tyr}$) gene target. Integration was position-specific and required Ty3 integrase, Pol III transcription extract, and a transcriptionally competent tRNA gene. Use of individual transcription factor (TF) IIIB–, TFIIIC-, and Pol III–containing fractions showed that TFIIIB and TFIIIC, together, were sufficient for position-specific Ty3 integration, but not for transcription. This report demonstrates that in vitro integration of a retroelement can be targeted by cellular proteins.

Integration of replicated DNA into the host genome is essential for retroviruses and retrotransposons. Integration is nonrandom, but the mechanisms that determine the positions of integration remain poorly defined [reviewed in (*1*, *2*)]. DNA sequence, chromatin structure, and the presence of host cell proteins can influence target site selection. On the basis of some in vivo studies, retroviral integration appears to occur preferentially into regions that contain deoxyribonuclease I (DNAase I) hypersensitive sites and regions that are transcriptionally active. A study of avian leukosis virus integration in vivo suggested that most or all of the cellular genome was accessible to integration machinery, but that regional and site preferences existed (*3*). In a series of selected integrations, the yeast retroviruslike element Ty1 integrated with a preference for the 5′ portions of the three RNA Pol II–transcribed genes examined (*4*). In addition, unselected transposition of Ty1 into chromosome III revealed an insertion bias for regions near tRNA genes and outside of open reading frames; this pattern was not observed in vitro with a naked DNA substrate (*5*). These findings have implicated host DNA-associated proteins in integration site selection.

DNA structure influences retroviral integration site selection. This was suggested by a study that identified in vivo integration sites in DNA fragments containing bends (*6*). In addition, in vitro data indicate that integration occurs preferentially into particular DNA structures. Integration mediated by human immunodeficiency virus (HIV) pre-integration complexes or purified integrase (IN) occurred nonrandomly into unmodified, naked DNA and preferentially into runs of CpG modified by 5-methylation of cytosine (*7*). With nucleoprotein complexes of murine leukemia virus (MLV), integration into naked DNA also occurred nonrandomly and more frequently into the exposed major groove of DNA assembled into nucleosomes (*8*). Moreover, DNA positions predicted to be distorted within the nucleosome were used preferentially for integration mediated by HIV IN (*9*). Preferred integration into static or induced bends that were not associated with nucleosomes occurred with both MLV and HIV IN (*10*).

Ty3, a retroviruslike element in *Saccharomyces cerevisiae*, integrates solely upstream of genes transcribed by Pol III. The gene-proximal joint in the host DNA occurs within one to three nucleotides of the transcription initiation site (*11*, *12*). On the basis of in vivo experiments, it has been suggested that integration is mediated by a protein-protein interaction between the Ty3 integration complex and the Pol III transcription complex. To identify cellular factors required for Ty3 integration, we developed an in vitro assay. Ty3 viruslike particles (VLPs), analogous to retroviral core particles, were isolated as a complex fraction containing Ty3 RNA, replicated DNA, and the mature Ty3 proteins, including IN (*13*). The target plasmid, pDLC374 (Fig. 1A), was used previously as a target for Ty3 transposition in vivo monitored by genetic selection (*12*) or by a polymerase chain reaction (PCR) assay (*14*). This plasmid contained the yeast *HIS3* gene, a 2-μm plasmid origin of replication, and a modified version of the *SUP2* $tRNA^{Tyr}$ gene cloned into pIBI20. To reconstitute the natural genomic targets of Ty3, we prepared a Pol III transcription extract from yeast cells (*15*). The BioRex70 500 mM NaCl fraction (BR500) from this preparation was used together with Ty3 VLPs and the tRNA gene target plasmid for in vitro integration reactions (*16*). DNA was isolated from each reaction and amplified by PCR with primers

Department of Microbiology and Molecular Genetics, University of California, Irvine, CA 92717, USA.

*To whom correspondence should be addressed.

complementary to the *HIS3* gene (primer set 284-285) to quantitate the amount of pDLC374, or with primers complementary to Ty3 and the tDNA (primer set 278-279) to detect position-specific integration (Fig. 1A) (*17*). PCRs were performed previously with each primer set and either pDLC374 or pTM42, a pDLC374 derivative which has a Ty3 insertion in divergent orientation immediately upstream of the transcription initiation site of the tRNA gene (*14*). A 474–base pair (bp) product from the 278-279 PCR was detected for pTM42 but not for pDLC374. The 240-bp product from the *HIS3* primers (284-285 PCR) was detected for both plasmid templates.

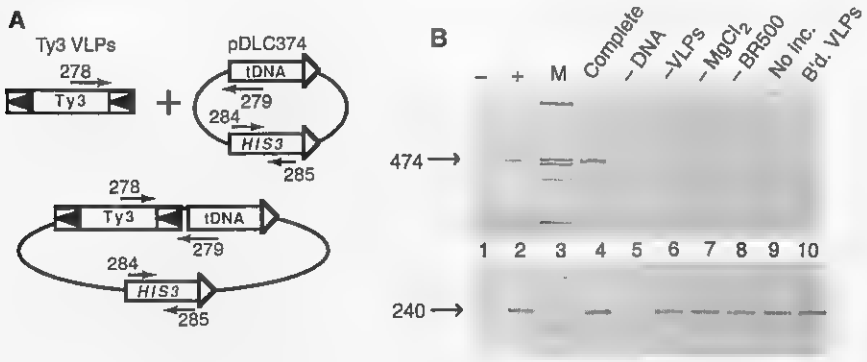

Fig. 1. Ty3 VLPs mediate integration in vitro. (**A**) Diagram for detection of in vitro integration of Ty3 by a PCR assay. PCR primers and their positions in the Ty3 and the modified *SUP2* $tRNA^{Tyr}$ sequences are shown. If Ty3 integration occurs into target plasmid pDLC374 upstream of the tRNA gene, in the divergent orientation, and at the insertion site used most frequently in vivo (*12*), primer 279 spans the Ty3-tDNA junction. PCR amplification of the resulting integration product with primer set 278-279 produces a 474-bp product. Primer set 284-285 amplifies a 240-bp fragment in the *HIS3* gene. (**B**) In vitro integration. Integration reactions were performed (*16*) and analyzed by PCR (*17*). The lane numbers refer to both upper and lower panels. Upper panel, products from 278-279 Ty3-specific PCR with 8 ng of template; lower panel, products from 284-285 *HIS3*-specific PCR with 0.1 ng of template (lanes 1 and 5, no DNA). Lane 4, standard integration reaction. Lane 7, $MgCl_2$ was omitted and 1 mM EDTA added. Other omissions from the integration reaction were as indicated above each lane. No inc. indicates that the 30°C incubation was omitted, and B'd. indicates that the VLPs were boiled for 10 min. In all figures of PCR products, M indicates size markers (λ DNA digested with Pst I), and the – and + signs refer to control reactions for the PCR assay (no template and 0.1 ng of pTM42, respectively). PCR product sizes are indicated to the left in base pairs.

Fig. 2. Integration requires VLPs with functional IN. VLPs were isolated from yeast cells expressing wild-type (WT) Ty3 or Ty3 with mutations in IN: D225E, E261D, or both. Mutant VLPs were used in standard integration reactions in parallel with WT VLPs as follows: WT, lanes 3 to 5; D225E, lanes 6 to 8; E261D, lanes 9 to 11; D225E + E261D, lanes 12 to 14. Integration reactions included 5 mM $MgCl_2$ (lanes 3, 6, 9, and 12), 10 mM $MgCl_2$ (lanes 4, 7, 10, and 13), or 10 mM $MgCl_2$ and boiled VLPs (lanes 5, 8, 11, and 14). The lane numbers refer to both upper and lower panels. Upper panel, 278-279 PCR with 6 ng of DNA; lower panel, 284-285 PCR with 0.1 ng of DNA. PCR product sizes are indicated to the right in base pairs.

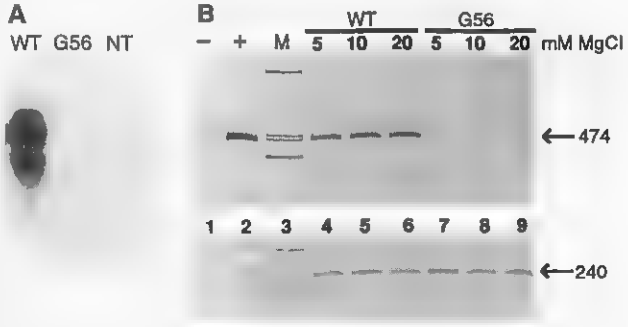

Fig. 3. In vitro integration depends on the presence of BR500 transcription extract. (**A**) Transcription assays. The templates for transcription were 400 ng of pDLC374 (WT) or the G56 mutant (G56). NT indicates no template. Assays were performed as in (*15*) except that the reactions had 250 μM adenosine triphosphate, uridine triphosphate, and cytidine triphosphate; 15 μM guanosine triphosphate (GTP); and 10 μCi [α-^{32}P]GTP (3000 cpm/mmol, Amersham) and were incubated at 30°C. There was 100 μg of BR500 protein in each reaction. (**B**) Integration reactions. Standard integration reactions (*16*) were performed with WT (lanes 4 to 6) and G56 (lanes 7 to 9) targets in the presence of 5, 10, or 20 mM $MgCl_2$. The lane numbers refer to both upper and lower panels. Upper panel, 278-279 PCR with 2 ng of DNA; lower panel, 284-285 PCR with 0.1 ng of DNA. PCR product sizes are indicated to the right in base pairs.

The dependence of the integration reaction on the presence of the BR500 extract suggested that integration in vitro depended on the ability of the tDNA to form a tran-

In vitro integration reactions were performed with the standard conditions as described (*16*) or with variations in order to identify essential reaction components (Fig. 1B). When the standard integration reaction conditions were used, the 474-bp 278-279 PCR product was observed, which indicated that integration occurred upstream of the tRNA gene. Integration required target DNA, VLPs, and a divalent cation. No integration occurred if the incubation time was 0 min or if the VLPs were boiled for 10 min before being added. There was no detectable integration in the absence of BR500 transcription extract, suggesting that a cellular protein or proteins were required for the position-specific integration. Differences in the amount of the 474-bp product were not the result of variation in the amount of DNA template for the PCR as demonstrated by equivalent amounts of the control 240-bp *HIS3* product. The 278-279 PCR products of several integration samples were compared with the 278-279 PCR products of a serial dilution of pTM42 DNA in pDLC374 DNA. On the basis of this comparison, integration was estimated to occur into less than 5% of the target DNA.

To verify that integration was the result of Ty3 IN activity, we isolated VLPs from cells expressing Ty3 with mutations in the IN protein. The conserved motif Asp-$X_{(39-58)}$-Asp-$X_{(35)}$-Glu occurs within the putative catalytic domain of IN in retroviruses and retroviruslike elements, and the invariant Asp and Glu residues are required for IN catalysis in vitro (*18*) and in vivo (*19*). Mutations engineered in Ty3 IN by site-directed mutagenesis changed the second Asp residue of this motif (amino acid position 225) (*20*) to Glu, and the Glu (amino acid position 261) to Asp. The mutations were introduced separately and in combination. The IN mutants produced wild-type amounts of mature Ty3 proteins and replicated DNA, but they did not transpose in vivo (*21*). When used in standard integration reactions in parallel with wild-type VLPs, the mutant VLPs were unable to catalyze integration (Fig. 2). Thus, in vitro, as in vivo, position-specific integration required Ty3 IN activity.

scription complex, as had been observed in vivo (*12*). To test this directly, we introduced a mutation into the tDNA promoter. Two internal promoter elements (box A and box B) in tRNA genes mediate the binding of the Pol III transcription factors TFIIIC and TFIIIB. TFIIIC binds first to the box A and box B sequences, then mediates the binding of initiation factor TFIIIB (*22*). We introduced a mutation by site-directed mutagenesis at the position in the modified *SUP2* $tRNA^{Tyr}$ gene corresponding to position 56 in the wild-type $tRNA^{Tyr}$ molecule. This mutation (G56) altered the first absolutely conserved cytosine in the box B promoter element, replacing it with guanine. The G56 mutation causes a decrease in the binding of TFIIIC to the *SUP4* $tRNA^{Tyr}$ gene in vitro to approximately 0.3% of wild-type amounts (*23*), which results in a decrease in transcription of *SUP4* $tRNA^{Tyr}$ in vivo to 5% of wild-type amounts (*24*). This mutation inactivates the *SUP2* $tRNA^{Tyr}$ gene as a target for Ty3 integration in vivo (*12*). In vitro, the modified *SUP2* $tRNA^{Tyr}$ gene with a wild-type box B was transcribed by the BR500 extract, but the G56 mutant was not (Fig. 3A). The G56 mutant was not used as a target for position-specific integration (Fig. 3B, lanes 7 to 9). These data showed that in vitro, as in vivo, integration required an intact box B. This result is consistent with the dependence of Ty3 integration on a Pol III transcription factor (or factors), Pol III, or both.

Integration into the modified *SUP2* $tRNA^{Tyr}$ gene with a wild-type or G56 mutant box B was also examined by performing the PCR with primers that did not anneal to the Ty3-target junction (*21*). With this integration position-independent primer set, a product of the predicted size for Ty3 integration immediately upstream of the tRNA gene was formed when the target was wild-type, but not when it was the G56 mutant. It is unlikely that our system can detect single insertions; thus, we cannot address the possibility that some insertions occur nonspecifically. However, the major site of in vitro integration detected with these primers was immediately upstream of the transcription initiation site.

To determine which Pol III transcription components were required for integration, we separated the BR500 extract on a DEAE Sephadex column into TFIIIB-, TFIIIC-, and Pol III–containing fractions (*15*). The fractions were tested in transcription reactions with pDLC374 (Fig. 4A). In vitro transcription activity was dependent on the presence of all three fractions. Transcription was not observed with the G56 mutant template or in the absence of template. The DEAE fractions were added to integration reactions in all combinations (Fig. 4B). No single fraction was sufficient for integration. Integration was observed when all three fractions were present, as expected, but also when only TFIIIC and TFIIIB were added. When Pol III was included, the amount of integration was lower. This result was obtained in duplicate experiments for three preparations of extract. Because TFIIIC is required to load TFIIIB onto the tDNA, these data do not address whether the role of TFIIIC in integration is direct or indirect, that is, as a loading factor.

The simplest model to explain the position-specific integration of Ty3 is that a protein-protein interaction occurs between some component of TFIIIB, either alone or together with TFIIIC, and the Ty3 integration complex. A tRNA gene that had reduced transcriptional activity as a result of mutations at the initiation site was competitive as a target for integration in vivo (*12*). That result suggested that transcription is not rate-limiting for transposition and is consistent with the in vitro result which showed that Pol III is not required for integration. The decrease in integration in the presence of Pol III may be the result of a competition between Pol III and the integration complex for contact with the TFIII(C+B)-tDNA complex.

In addition to a protein-protein interaction, there may be a DNA structural component to Ty3 integration. TFIIIC and TFIIIB bend the tDNA upon binding to the promoter elements and 5′ flanking region (*25*). The data are consistent with the center of the bend being positioned near the transcription start site. In addition, the initiation site is DNAase I–hypersensitive (*15*). DNA distortion in this region may facilitate access or activity of the Ty3 integration complex. Kinked and unwound regions of DNA appear to be used preferentially for retroviral integration, and distortion of DNA is an inherent feature in the activity of other endonucleases, for example Eco RI (*26*), and recombinases, for example FLP (*27*).

Ty3 is the most specific among well-studied retroelements in its pattern of integration, yet characterization of its mechanism of integration may elucidate the basis of more subtle integration patterns of retroviruses and other retroviruslike elements. The results presented here show the dependence of Ty3 position-specific integration on Pol III transcription factors. Retroviral and Ty1 integrations display some preference for transcribed regions and transcription initiation regions, respectively, and thus could be facilitated by interaction with transcription factors. HIV IN interacts with a human gene product (Inl1) which has a region similar to one in the yeast transcription factor Snf5p and stimulates the joining activity of IN in vitro (*28*). Targeting of Ty3 preintegration complexes by transcription factors is compatible with a retroviral mechanism of integration and suggests a basis for the observed insertion of retroviruses into preferred positions in host genomes.

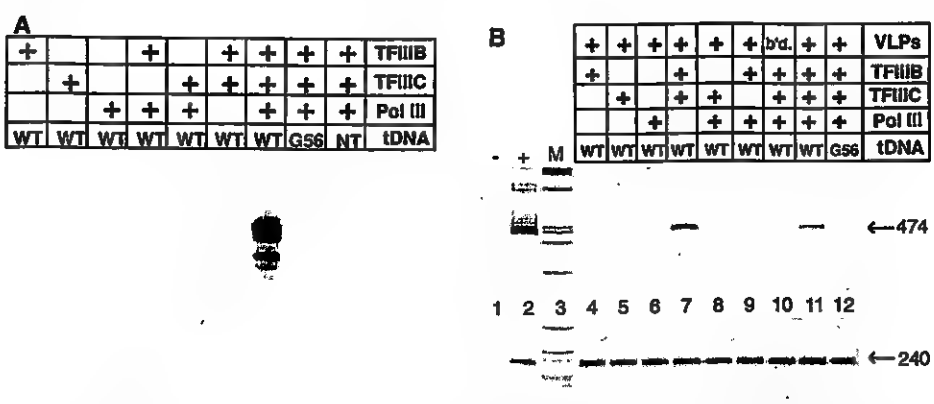

Fig. 4. In vitro integration depends on the presence of TFIIIC- and TFIIIB-containing fractions. **(A)** Transcription assays. Reactions were as described in the legend for Fig. 3A except 9 μl of each TFIIIC-, TFIIIB-, or Pol III–containing fraction (as indicted by the + sign) replaced the BR500 extract. **(B)** Integration reactions. Standard integration reaction conditions (*16*) were used except 9 μl of each TFIIIC-, TFIIIB-, or Pol III–containing fraction replaced the BR500 extract. B'd. indicates that VLPs were boiled for 10 min before being added. The lane numbers refer to both upper and lower panels. Upper panel, 278-279 PCR with 2 ng of DNA; lower panel, 284-285 PCR with 0.1 ng of DNA. PCR product sizes are indicated to the right in base pairs.

REFERENCES AND NOTES

1. S. B. Sandmeyer, L. J. Hansen, D. L. Chalker, *Annu. Rev. Genet.* **24**, 491 (1990).
2. R. Craigie, *Trends Genet.* **8**, 187 (1992).
3. E. S. Withers-Ward, Y. Kitamura, J. P. Barnes, J. M. Coffin, *Genes Dev.* **8**, 1473 (1994).
4. H. Eibel and P. Philippsen, *Nature* **307**, 386 (1984); G. Natsoulis, W. Thomas, M.-C. Roghmann, F. Winston, J. D. Boeke, *Genetics* **123**, 269 (1989); S. W. Liebman and G. Newnam, *ibid.* **133**, 499 (1993).
5. H. Ji *et al.*, *Cell* **73**, 1007 (1993).
6. E. Milot, A. Belmaaza, E. Rassart, P. Chartrand, *Virology* **201**, 408 (1994).
7. Y. Kitamura, Y. M. H. Lee, J. M. Coffin, *Proc. Natl. Acad. Sci. U.S.A.* **89**, 5532 (1992).
8. P. M. Pryciak and H. E. Varmus, *Cell* **69**, 769 (1992);

P. M. Pryciak, A. Sil, H. E. Varmus, *EMBO J.* **11**, 291 (1992).
9. D. Pruss, F. D. Bushman, A. P. Wolffe, *Proc. Natl. Acad. Sci. U.S.A.* **91**, 5913 (1994).
10. H.-P. Muller and H. E. Varmus, *EMBO J.* **13**, 4704 (1994).
11. D. L. Chalker and S. B. Sandmeyer, *Genetics* **126**, 837 (1990).
12. ———, *Genes Dev.* **6**, 117 (1992).
13. L. J. Hansen, D. L. Chalker, K. J. Orlinsky, S. B. Sandmeyer, *J. Virol.* **66**, 1414 (1992).
14. T. M. Menees and S. B. Sandmeyer, *Mol. Cell. Biol.* **14**, 8229 (1994).
15. G. A. Kassavetis, D. L. Riggs, R. Negri, L. H. Nguyen, E. P. Geiduschek, *ibid.* **9**, 2551 (1989).
16. The VLPs were isolated as described (*13*) with a sucrose step gradient. The VLP protein from 1 liter of cells (~330 μg) was resuspended in 40 μl of buffer [13.5 mM KCl, 9 mM Hepes (pH 7.8), 4.5 mM $MgCl_2$, and 10% glycerol] and kept on ice until used. A standard integration reaction consisted of 2 μl of resuspended VLP protein, 400 ng of pDLC374 (0.075 pmol), 20 mM Hepes (pH 7.8), 65 mM KCl, 1 mM dithiothreitol, 5 μl of BR500 transcription extract (at a final concentration of 1.8 to 2.0 mg/ml), and 10 mM $MgCl_2$ in a 50-μl reaction volume. If $MnCl_2$ replaced $MgCl_2$ in the reaction, integration was severely decreased (*21*). Per reaction, the VLPs provided 0.18 to 0.34 pmol of IN and 0.03 to 0.07 pmol of replicated Ty3 DNA (determined by comparison with standards). Reaction components were assembled on ice then incubated at 30°C for 30 min. Reactions were stopped by addition of proteinase K to a final concentration of 0.2 mg/ml, SDS to 0.2%, and EDTA (pH 8.0) to a concentration twice that of $MgCl_2$ in the integration reaction, then incubated at 37°C for 30 min. When necessary, $MgCl_2$ was added with the stop buffer to equalize the concentration of $MgCl_2$ in different samples.
17. The DNA from each integration reaction was isolated and quantitated by fluorometric analysis with a Mini TKO 100 DNA Fluorometer (Hoeffer Scientific). The PCR conditions for amplification of *HIS3* were similar to those described previously (*14*) except that the reactions with primer set 284-285 included 0.05 mM deoxynucleotide triphosphates (dNTPs) and 0.1 ng of template DNA and 18 cycles were run. The PCR conditions for detection of integration were similar to those described previously (*14*) except that the reactions with primer set 278-279 included 0.5 mM dNTPs, 3.5 mM $MgCl_2$, and 1 to 10 ng of template DNA (depending on the linear range, determined for each set of integration reactions). Primer 278 is complementary to nucleotides 444 to 418 of Ty3 on the transcribed strand. Primer 279 is complementary to the modified *SUP2* $tRNA^{Tyr}$ gene at nucleotides +25 to −5 on the transcribed strand (+1 corresponds to the transcription start site) and its 3′-most two nucleotides are complementary to Ty3 nucleotides 1 and 2 on the minus strand. The 278-279 PCR detected as little as 1×10^{-5} ng of pTM42 in the presence of 2 ng of pDLC374. The PCR products were analyzed by native polyacrylamide gel electrophoresis on 8% gels and visualized by transillumination with ultraviolet light after staining with ethidium bromide. Photographs were taken with Polaroid film (type 55), and the negatives were used for the figures presented here. For 284-285 PCRs, the negative was scanned with an LKB Ultroscan II Laser Densitometer (Pharmacia) to determine the band intensity for quantitation before the 278-279 PCR.
18. J. Kulkosky, K. S. Jones, R. A. Katz, J. P. G. Mack, A. M. Skalka, *Mol. Cell. Biol.* **12**, 2331 (1992); A. Engelman and R. Craigie, *J. Virol.* **66**, 6361 (1992); D. C. van Gent, A. A. M. Oude Groeneger, R. H. A. Plasterk, *Proc. Natl. Acad. Sci. U.S.A.* **89**, 9598 (1992); M. R. Drelich, R. Wilhelm, J. Mous, *Virology* **188**, 459 (1992); A. D. Leavitt, L. Shiue, H. E. Varmus, *J. Biol. Chem.* **268**, 2113 (1993)
19. C.-G. Shin, B. Taddeo, W. A. Haseltine, C. M. Farnet, *J. Virol.* **68**, 1633 (1994); P. M. Cannon, W. Wilson, E. Byles, S. M. Kingsman, A. J. Kingsman, *ibid.*, p. 4768; B. Taddeo, W. A. Haseltine, C. M. Farnet, *ibid.*, p. 8401; M. Wiskerchen and M. A. Muesing, *ibid.* **69**, 376 (1995)
20. J. Kirchner and S. B. Sandmeyer, *ibid.* **67**, 19 (1993).
21. ———, unpublished results.
22. E. P. Geiduschek and G. P. Tocchini-Valentini, *Annu. Rev. Biochem.* **57**, 873 (1988), and references therein; R. J. White, *RNA Polymerase III Transcription* (CRC Press, Boca Raton, FL, 1994), chap. 5, and references therein.
23. R. E. Baker, O. Gabriel sen, B. D. Hall, *J. Biol. Chem.* **261**, 5275 (1986)
24. D. S. Allison, S. H. Goh, B. D. Hall, *Cell* **34**, 655 (1983).
25. T. Leveillard, G. A. Kassavetis, E. P. Geiduschek, *J. Biol. Chem.* **266**, 5162 (1991).
26. J. A. McClarin *et al.*, *Science* **234**, 1526 (1986).
27. C. J. E. Schwartz and P. D. Sadowski, *J. Mol. Biol.* **205**, 647 (1989).
28. G. V. Kalpana, S. Marmon, W. Wang, G. R. Crabtree, S. P. Goff, *Science* **266**, 2002 (1994).
29. We thank T. M. Menees for communicating results before publication and for helpful discussions. We also thank H.-P. Muller, H. E. Varmus, G. V. Kalpana, and S. P. Goff for communicating results before publication. Supported by NIH grant 33281 to S.B.S.

17 October 1994; accepted 20 January 1995

Glutamate Receptor RNA Editing in Vitro by Enzymatic Conversion of Adenosine to Inosine

Susan M. Rueter,* Colleen M. Burns,* Sarah A. Coode, Paramita Mookherjee, Ronald B. Emeson†

RNA encoding the B subunit of the α-amino-3-hydroxy-5-methyl-4-isoxazolepropionic acid (AMPA) subtype of ionotropic glutamate receptor (GluR-B) undergoes a posttranscriptional modification in which a genomically encoded adenosine is represented as a guanosine in the GluR-B complementary DNA. In vitro editing of GluR-B RNA transcripts with HeLa cell nuclear extracts was found to result from an activity that converts adenosine to inosine in regions of double-stranded RNA by enzymatic base modification. This activity is consistent with that of a double-stranded RNA-specific adenosine deaminase previously described in *Xenopus* oocytes and widely distributed in mammalian tissues.

The editing of mRNA transcripts is an important mechanism for augmenting the flexibility of eukaryotic gene expression (*1*). The A→G conversion seen in mRNAs encoding glutamatergic ion channel subunits exemplifies the functional relevance of this posttranscriptional modification (*2*). Glutamate receptors of the AMPA subtype are generated by the assembly of GluR-A, -B, -C, and -D subunits into homo- and heteromeric channels (*3*). A single positively

Department of Pharmacology, Vanderbilt University School of Medicine, Nashville, TN 37232-6600, USA.

*These authors contributed equally to this work.
†To whom correspondence should be addressed.

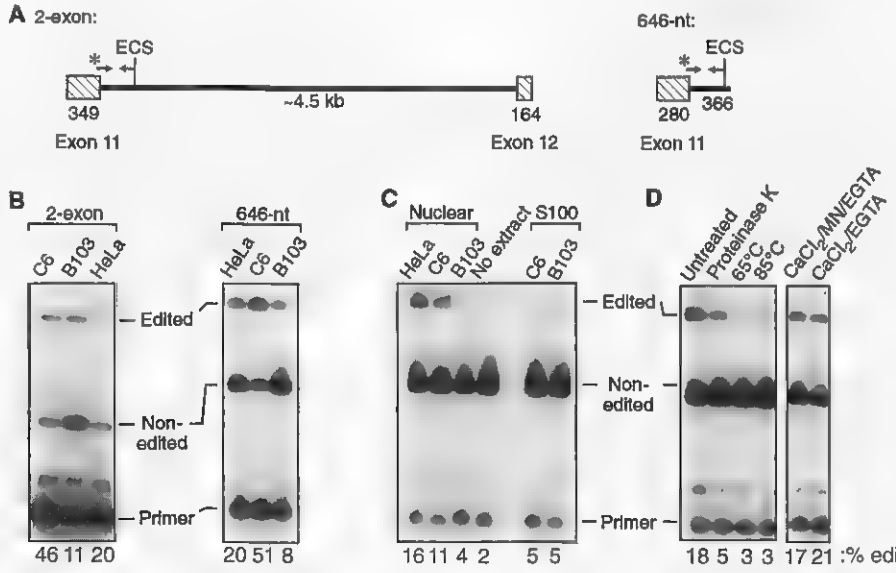

Fig. 1. In vivo and in vitro editing of GluR-B transcripts. (**A**) Schematic of GluR-B transcription units indicating the Q/R site (asterisk) and inverted repeat (arrows). (**B**) Primer-extension analyses of RNA from cells permanently transfected with GluR-B transcription units. (**C**) Primer-extension analyses of the 646-nt in vitro reaction products with nuclear and S100 extracts from the indicated cells. (**D**) Primer-extension analyses of in vitro reaction products generated in HeLa cell nuclear extracts pretreated as indicated. MN, micrococcal nuclease. The numbers at the base of each gel indicate the percent of A→G conversion (editing efficiency).

charged Arg residue within the second hydrophobic domain (TMII) of the GluR-B subunit is responsible for the linear current-voltage relation and low divalent cation permeability demonstrated by the AMPA receptor (*4*). This critical Arg is produced by a posttranscriptional modification that is represented by conversion of a genomically encoded Gln codon (CAG) to an Arg codon (CGG) in the GluR-B complementary DNA (cDNA) (*2*). Intron 11, immediately downstream of the edited position (Q/R site), is essential for accurate and efficient RNA editing (*5*). This intron contains 10 nucleotides (nt) that are complementary to the exonic sequence immediately surrounding the Q/R site. It has been proposed that this editing site complementary sequence (ECS), as well as an imperfect inverted repeat, contributes to the formation of an RNA duplex within the GluR-B primary RNA transcript (pre-mRNA) that is critical for editing (*5*).

To characterize the molecular events involved in GluR-B RNA editing, we developed a model system with transfected cell lines that exhibit RNA processing patterns analogous to those observed in vivo. Human epithelial (HeLa), rat glioma (C6), and rat neuronal (B103) cell lines were assessed for their ability to edit a permanently transfected GluR-B transcription unit extending from exon 11 through exon 12 (2-exon; Fig. 1A) (*6*, *7*). All three cell lines were capable of editing RNAs derived from this exogenous GluR-B minigene (Fig. 1B). Experiments with a 646-nt GluR-B transcription unit extending from –256 to +390 relative to the Q/R site demonstrated that this RNA substrate contains sufficient regulatory information for efficient editing (Fig. 1B) (*5*).

We developed an in vitro editing system with extracts from C6, HeLa, and B103 cells (*8*) and the 646-nt RNA substrate (*9*). The reaction products were amplified by the RNA template–specific polymerase chain reaction (RS-PCR) and analyzed by primer extension (*10*). The HeLa cell nuclear extracts showed 16 ± 3% A→G conversion (n = 4), whereas the C6 and B103 nuclear and cytoplasmic extracts exhibited lower editing efficiencies (Fig. 1C). Pretreatment of HeLa nuclear extracts with proteinase K or incubation at high temperatures abrogated editing, suggesting that a protein or proteins are required, whereas pretreatment with micrococcal nuclease had no effect (Fig. 1D) (*11*).

To assess the specificity of editing, we compared the editing patterns of various GluR-B RNA substrates in different editing systems (Table 1). Rat brain pre-mRNA transcripts showed extensive editing at the Q/R site (99%), and additional A→G replacements were identified at intronic "hot spots" (positions +60 and +262 through +264) which are predicted to reside in roughly equivalent positions on opposite sides of the RNA duplex (*5*). Editing within the exon at +4 was also seen in 38 of 100 cDNAs, altering the wobble position of a

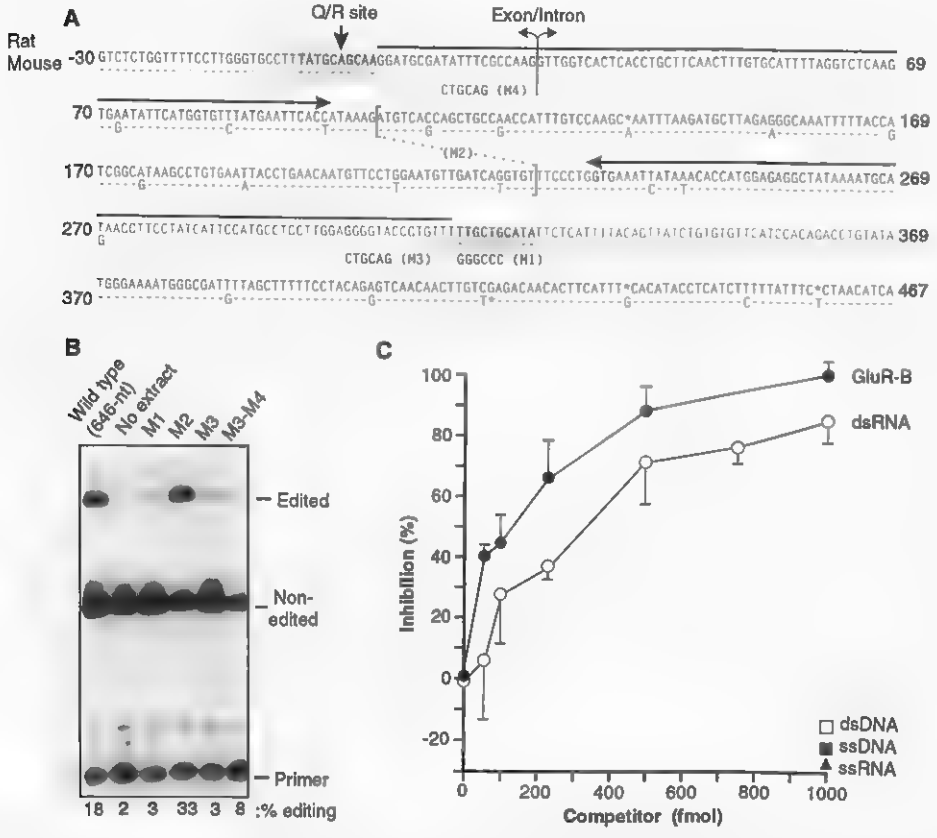

Fig. 2. Dependence of in vitro RNA editing activity on a double-stranded RNA (dsRNA) substrate. (**A**) Nucleotide sequence alignment of rat and mouse GluR-B genes in the proximal region of intron 11; gaps (asterisks) have been introduced for alignment purposes and dashes represent sequence identity. The imperfect inverted repeat is shown with overlying arrows. The complementary regions surrounding the Q/R site and the ECS are indicated with gray boxes. (**B**) Editing analyses of in vitro reaction products with mutant GluR-B RNA substrates. (**C**) Effect of single- and double-stranded nucleic acid competitors on the inhibition of in vitro GluR-B editing activity. The percentage of editing in the absence of competitor was 16.6 ± 4.4% (n = 7) (not shown); GluR-B RNA (●), dsRNA (○), dsDNA (□), ssDNA (■), and ssRNA (▲). Error bars represent the standard error from at least three independent experiments.

Table 1. Quantitation of GluR-B RNA editing patterns by direct nucleotide sequence analysis. RNAs were subjected to reverse transcription–PCR amplification, subcloned into pBKSII⁻, and sequenced. The nucleotide position (relative to the Q/R site), the percentage of cDNA isolates containing an A→G replacement, and the number of individually sequenced cDNA isolates are indicated. Intronic sites demonstrating <2% editing from all RNA sources have been omitted. The error rate for Taq polymerase misincorporation was estimated to be 0.06% (17 errors per 30,000 bases sequenced), on the basis of sequence discrepancies other than A→G conversions.

Editing system	GluR-B RNA substrate	No. of cDNAs sequenced	Editing (%) at nucleotide position													
			0	4	45	46	60	242	243	255	262	263	264	265	272	306
Rat brain	Endogenous	100	99	38	8	3	67	3	4	7	36	67	10	2	2	1
C6 cells	Endogenous	55	36	2	0	0	29	2	5	0	2	4	2	0	0	2
C6 cells	2-exon	50	46	2	0	0	2	0	0	2	8	6	2	2	0	0
HeLa cells	646-nt	100	24	3	0	0	7	0	0	0	2	0	1	0	0	0
HeLa extract	646-nt	100	26	0	0	0	13	0	0	0	1	0	1	0	0	0

Gln codon from CAA to CAG. Endogenous GluR-B transcripts in C6 cells, transfection-derived transcripts from C6 and HeLa cells, and in vitro reaction products exhibited the greatest amount of editing at the Q/R site; the extent of editing at other sites was markedly reduced in these systems (Table 1).

DNA sequence comparisons between the rat and mouse GluR-B genes have indicated extensive conservation of nucleotide sequence in the proximal region of intron 11 (Fig. 2A). To examine the cis-active elements required for in vitro editing, we introduced a series of mutations (M1 to M4) into highly conserved regions surrounding the Q/R site in the 646-nt GluR-B RNA substrate (Fig. 2, A and B) (*12*). Insertion of an Apa I restriction site into the ECS (M1) abolished editing at the Q/R site (Fig. 2B) as previously observed (*5*). Deletion of 120 nt between the inverted repeat sequences (M2; Fig. 2A, brackets) increased editing efficiency. Disruption of the RNA duplex by introduction of a Pst I restriction site within the second half of the inverted repeat (+301 to +306; M3) reduced editing to background levels (3 ± 1%), whereas introduction of a second Pst I site (+13 to +18; M3-M4) to restore the duplex slightly restored editing efficiency (8 ± 1%). These observations suggest that an RNA duplex structure is critical for editing activity.

We further characterized the sequence requirements for in vitro editing of GluR-B RNA by addition of single-stranded (ss) and double-stranded (ds) nucleic acid competitors. An RNA substrate containing 646 nt of the GluR-B sequence and a 3′ extension, derived from the pRC/CMV (cytomegalovirus) expression plasmid, was used to differentiate between the editing of the RNA substrate and the competitor GluR-B–derived sequences (*13*). Wild-type GluR-B RNA competitor (646 nt) inhibited editing in a concentration-dependent manner (Fig. 2C); a dsRNA of unrelated sequence also inhibited editing, although with decreased potency. In contrast, dsDNA, ssDNA, and ssRNA had no effect on editing.

The competition experiments suggested that the editing of GluR-B transcripts is dependent on a dsRNA substrate with little sequence specificity. This property is similar to the activity of a dsRNA-specific adenosine deaminase that acts on dsRNA but not ssRNA, ssDNA, or dsDNA (*14*). This enzyme (dsRAD or DRADA) converts adenosine to inosine (I) by hydrolytic deamination of adenosine in regions of dsRNA (*1*, *14*). This modified nucleotide could serve as a template for the incorporation of cytosine by reverse transcriptase and produce a codon that alters the coding potential of GluR-B mRNA from Gln to Arg (*1*, *5*). To investigate this possibility, we used thin-layer chromatography (TLC) to analyze the in vitro reaction products generated from an RNA substrate uniformly labeled with [α-^{32}P]adenosine 5′-triphosphate (ATP). The reaction products included a radiolabeled species that comigrated with inosine 5′-monophosphate (IMP) upon digestion with nuclease P1 (Fig. 3A) (*15*, *16*). RNA incubated in the absence of nuclear extract produced a markedly reduced IMP signal. These results suggest that the editing of GluR-B transcripts involves the production of inosine rather than guanosine during the course of the reaction, altering a genomically encoded Gln codon (CAG) to an Arg codon (CIG) in the GluR-B mRNA. Quantitative phosphorimager analysis of the radiolabeled species migrating at the positions of adenosine 5′-monophosphate (AMP) and IMP demonstrated an editing efficiency of 18%, in good agreement with the 14% editing determined by primer extension analyses. Nucleotide sequence analyses of the in vitro reaction product revealed editing solely at the Q/R site and position +60 (Table 1). Although a low level of IMP formation was observed in the absence of nuclear extract (Fig. 3A), sequence analyses of 50 cDNAs generated from this reaction did not reveal the presence of edited nucleotides. Because there are no known polymerases that incorporate nucleotides into a polynucleotide chain without a 5′-phosphate group, these results also suggest that the editing of GluR-B transcripts is not mediated by a mechanism of nucleoside excision and replacement in which the phosphodiester backbone of the RNA is cleaved and then esterified.

To exclude the possibility that IMP is produced by transglycosylation (base exchange) (*17*), we used an RNA uniformly labeled with [2,8-^{3}H]ATP as the substrate in the in vitro editing reaction (*15*, *16*). The radiolabeled reaction products from the nuclease P1 digest migrated with the internal standards for AMP and IMP (Fig. 3B). The generation of purine ring–labeled [2,8-^{3}H]IMP in this assay demonstrates that the processing of GluR-B transcripts does not involve base exchange, but rather an enzymatic base modification converting adenosine to inosine.

We have demonstrated that the editing of GluR-B RNA transcripts is dependent on a dsRNA-specific activity that converts adenosine to inosine by enzymatic base modification. The apparent nonselectivity of dsRAD compared with the efficiency of GluR-B editing at the Q/R site in rat brain (>99%) suggests that if a dsRAD-like activity is responsible for GluR-B editing, additional specificity factors may be involved (*5*). More recent studies of adenosine preference by dsRAD have indicated a high selectivity for specific adenosine residues within a short RNA duplex (*18*), alleviating the requirement for additional specificity factors. In addition to modifications of GluR-B at the Q/R site, RNA editing is responsible for A→G (I) conversions in RNAs encoding other AMPA and kainate receptor subunits (*2*), suggesting that a dsRAD-like activity may be responsible for the posttranscriptional modification of mRNAs encoding multiple glutamate receptor subunits.

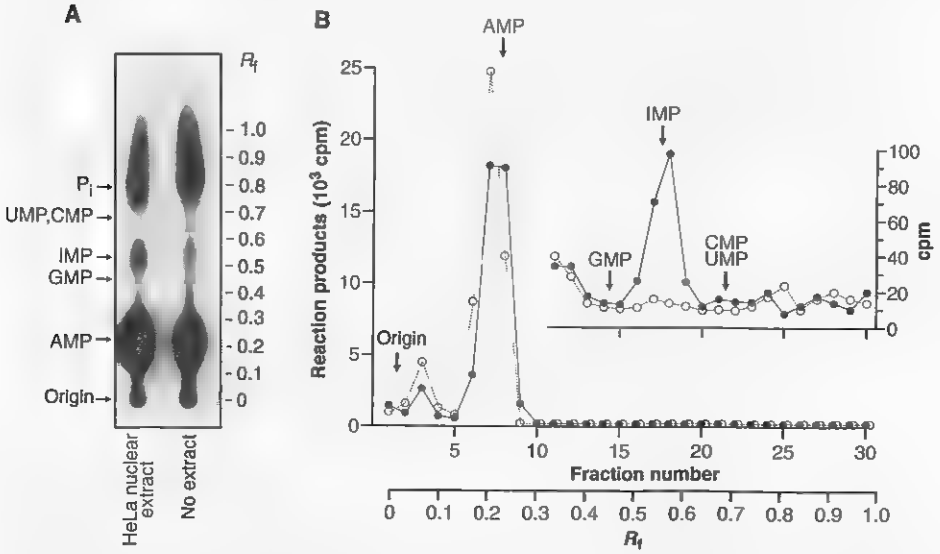

Fig. 3. Association of in vitro editing with an enzymatic adenosine-to-inosine conversion. (**A**) TLC analysis of an [α-^{32}P]ATP–labeled RNA substrate incubated in vitro. The migration positions of 5′-nucleoside monophosphate standards and their relative mobility (R_f) are indicated. P_i, inorganic phosphate. (**B**) TLC analysis of a [2,8-^{3}H]ATP–labeled RNA substrate incubated in vitro. Recovery of radioactivity for samples with (●) and without extract (○) was 94 and 98%, respectively. The inset contains an expanded *y* axis (counts per minute).

REFERENCES AND NOTES

1. B. Bass, in *The RNA World*, R. F. Gesteland and J. F. Atkins, Eds. (Cold Spring Harbor Laboratory Press, Cold Spring Harbor, NY, 1993), chap. 15.
2. B. Sommer, M. Kohler, R. Sprengel, P. H. Seeburg, *Cell* **67**, 11 (1991); H. Lomeli et al., *Science* **266**, 1709 (1994); M. Kohler, N. Burnashev, B. Sakmann, P. Seeburg, *Neuron* **10**, 491 (1993); J. Egebjerg and S. F. Heinemann, *Proc. Natl. Acad. Sci. U.S.A.* **90**, 755 (1993).
3. N. Nakanishi, N. A. Shneider, R. Axel, *Toxicon* **28**, 1333 (1990); K. Keinänen *et al.*, *Science* **249**, 556 (1990); J. Boulter *et al.*, *Neuron* **3**, 589 (1989); K. Sakimura *et al.*, *FEBS Lett.* **272**, 73 (1990).
4. R. I. Hume, R. Dingledine, S. F. Heinemann, *Science* **253**, 1028 (1991); R. Dingledine, R. Hume, S. Heinemann, *J. Neurosci.* **12**, 4080 (1992); T. Verdoorn, N. Burnashev, H. Monyer, P. Seeburg, B. Sakmann, *Science* **252**, 1715 (1991); M. Mishina *et al.*, *Biochem. Biophys. Res. Commun.* **180**, 813 (1991).
5. M. Higuchi *et al.*, *Cell* **75**, 1361 (1993); J. Egebjerg, V. Kukekov, S. F. Heinemann, *Proc. Natl. Acad. Sci. U.S.A.* **91**, 10270 (1994).
6. We established permanently transfected polyclonal cell lines by using calcium phosphate coprecipitation with a eukaryotic expression vector (pRC/CMV; Invitrogen) containing a 5-kb (2-exon) or 646–base pair (bp) GluR-B transcription unit. Total RNA was prepared by the guanidinium isothiocyanate method (*7*). Total RNA (2.5 μg) was reverse transcribed with an intronic antisense primer (+390 to +407 relative to the Q/R site); PCR amplification of cDNA was achieved with the initial cDNA synthesis primer and an expression vector–specific primer (5′-CTGGCTTATCGAAATTAATACGAC-3′). The product was purified on a 0.8 or 2% agarose gel and 2 pmol was annealed to a γ-^{32}P–labeled 17-nt oligomer antisense primer corresponding to positions +3 to +19. The primer was extended in the presence of 40 mM tris-HCl (pH 7.5), 50 mM NaCl, 20 mM $MgCl_2$, 3.6 mM $MnCl_2$, 200 μM each of deoxyadenosine 5′-triphosphate, deoxyguanosine 5′-triphosphate, and deoxycytidine 5′-triphosphate, and 1200 μM dideoxythymidine 5′-triphosphate by using 1.6 U of Sequenase (United States Biochemicals) for 10 min at 37°C. Primers annealed to nonedited and edited sequences were extended to the first or second upstream A, generating products of 20 and 24 nt, respectively; the resulting products were separated on a 20% acrylamide–7 M urea gel. Editing was quantified with a Molecular Dynamics phosphorimager.
7. F. Ausubel *et al.*, Eds., *Current Protocols in Molecular Biology* (Wiley, New York, 1989).
8. D. M. Driscoll, J. K. Wynne, S. C. Wallis, J. Scott, *Cell* **58**, 519 (1989); J. H. Wu, C. F. Semenkovich, S. H. Chen, W. H. Li, L. Chan, *J. Biol. Chem.* **265**, 12312 (1990). Nuclear and S100 extracts were prepared as in (*7*). The standard in vitro assay (20 μl) contained 50 fmol of RNA substrate, 50 μg of nuclear or S100 extract protein, 10 mM Hepes (pH 7.9), 10% glycerol, 50 mM KCl, 50 mM EDTA, and 0.25 mM dithiothreitol. The reactions were incubated at 30°C for 3 hours.
9. For synthesis of the in vitro RNA substrate, a 646-bp DNA fragment corresponding to positions −256 to +390 was cloned into the transcription vector pBK-SII⁻ (Stratagene) and linearized with Bam HI. RNA labeled with [α-^{32}P]uridine 5′-triphosphate (UTP) was transcribed (specific activity = 2.2 x 10^6 cpm/mmol) with T3 RNA polymerase. The reaction was treated with 10 U of ribonuclease-free deoxyribonuclease (Promega) at 37°C for 40 min, extracted with phenol-chloroform (1:1), and precipitated with ethanol.
10. In vitro products were amplified by RS-PCR [A. R. Shuldiner, R. Perfetti, J. Roth, in *PCR Protocols: Current Methods and Applications*, B. A. White, Ed. (Humana, Totowa, NJ, 1993), pp. 169–176]. The cDNA was synthesized with an antisense oligonucleotide containing a 5′-terminal extension (5′-AATCCGGATTGCCCGGAACGTCTTGGCGAAATATCGCATCCTTGC-3′). The cDNA products were selectively amplified with an antisense PCR primer unique to the RNA-derived cDNA extension sequence. Hybridization and extension of a [γ-^{32}P]-labeled 15-nt oligomer sense primer (−18 to −4) in the presence of dideoxy-ATP generated products of 19 and 22 nt for nonedited and edited transcripts, respectively.
11. Protease sensitivity and thermolability studies were performed by preincubation of HeLa cell nuclear extracts (50 μg) with 1 μg of proteinase K for 20 min at 37°C or by preincubation at elevated temperature (65°C and 85°C) for 10 min, respectively. Micrococcal nuclease sensitivity was determined by pretreatment of extracts with $CaCl_2$ (0.75 mM final concentration) and 13.5 U of micrococcal nuclease (Pharmacia) for 10 min at room temperature. Micrococcal nuclease was inactivated by the addition of EGTA (2.5 mM final concentration).
12. Construction of mutant GluR-B RNA substrates was performed by oligonucleotide-directed mutagenesis in pBKSII⁻ (Stratagene) as previously described (*7*).
13. In competition studies, cDNA was synthesized with an oligonucleotide complementary to the pRC/CMV-derived 3′ extension of the GluR-B RNA substrate. The ssDNA competitor (81 nt) was an oligonucleotide derived from the neomycin resistance gene (pRC/CMV); the dsDNA competitor (178 bp) was obtained by PCR amplification of pBKSII⁻ polylinker. The ssRNA competitors were transcribed in the presence of [α-^{32}P]UTP (specific activity = 2.2 x 10^6 cpm/mmol) from pBKSII⁻ linearized with Xba I (93 nt) or Xho I (97 nt). The dsRNA competitor was produced by annealing the ssRNAs in 80% formamide, 40 mM Pipes (pH 6.4), 400 mM NaCl, and 1.25 mM EDTA for 14 to 16 hours at 25°C. Residual ssRNA was removed by ribonuclease A digestion (25 μg/ml) (*7*). The dsRNA was purified on an 8% nondenaturing acrylamide gel and eluted by incubation in 1 M ammonium acetate, 10 mM tris-HCl (pH 7.6), and 1 mM EDTA for 2 hours at 4°C.
14. B. L. Bass and H. Weintraub, *Cell* **48**, 607 (1987); R. W. Wagner and K. Nishikura, *Mol. Cell. Biol.* **8**, 770 (1988); U. Kim and K. Nishikura, *Semin. Cell. Biol.* **4**, 285 (1993).
15. The 646-nt RNA substrate was transcribed in the presence of [α-^{32}P]ATP (800 Ci/mmol) or [2,8-^{3}H]ATP (30 Ci/mmol) (RNA specific activity, 4.9 x 10^{10} and 9.6 x 10^9 cpm/mmol, respectively). After the standard in vitro reaction, one-half of the product was used to quantitate GluR-B RNA editing by the RS-PCR primer extension assay, and the remainder of the reaction was resuspended in 50 mM sodium acetate (pH 5.3), digested with nuclease P1 at 37°C for 2 hours, and spotted onto a cellulose TLC plate (Sigmacell Type 100). Chromatography proceeded for ~6 hours in 0.1 M NaH_2PO_4 (pH 6.8), ammonium sulfate, and *n*-propanol (100:60:2, v/w/v) as described (*16*). The migration positions of nucleoside monophosphate standards were determined by ultraviolet light absorption, and the migration positions of the [^{32}P]-labeled products were detected by autoradiography and quantitated with a Molecular Dynamics phosphorimager. For detection of [^{3}H]-labeled reaction products, 0.5-cm cellulose fractions from the TLC plate were counted by liquid scintillation spectrometry.
16. M. Silberklang, A. M. Gillum, U. L. RajBhandary, *Methods Enzymol.* **59**, 58 (1979).
17. G. A. Garcia, K. A. Koch, S. Chong, *J. Mol. Biol.* **231**, 489 (1993); M. S. Elliott and R. W. Trewyn, *J. Biol. Chem.* **259**, 2407 (1984).
18. A. G. Polson and B. L. Bass, *EMBO J.* **13**, 5701 (1994).

19. We thank J. Lu, J. Patton, R. Breyer, and B. Wadzinski for critical reading of the manuscript and J. Patton for providing HeLa cell extracts. Supported by grants from the National Parkinson Foundation and NIH (ES00267).

30 December 1994; accepted 9 February 1995

Involvement of CRAF1, a Relative of TRAF, in CD40 Signaling

Genhong Cheng,* Aileen M. Cleary,* Zheng-sheng Ye,* David I. Hong, Seth Lederman, David Baltimore†

CD40 is a receptor on the surface of B lymphocytes, the activation of which leads to B cell survival, growth, and differentiation. A yeast two-hybrid screen identified a gene, *CRAF1*, encoding a protein that interacts directly with the CD40 cytoplasmic tail through a region of similarity to the tumor necrosis factor–α (TNF-α) receptor–associated factors. Overexpression of a truncated *CRAF1* gene inhibited CD40-mediated up-regulation of CD23. A region of *CRAF1* was similar to the TNF-α receptor–associated factors TRAF1 and TRAF2 and so defined a shared TRAF-C domain that was necessary and sufficient for CD40 binding and homodimerization. The CRAF1 sequence also predicted a long amphipathic helix, a pattern of five zinc fingers, and a zinc ring finger. It is likely that other members of the TNF receptor superfamily use *CRAF*-related proteins in their signal transduction processes.

CD40 (*1*) is a receptor on B cells that interacts with the helper T cell surface protein CD40L (CD40 ligand, also known as T-BAM, gp39, or TRAP) (*2–4*). CD40L is found particularly on lymphoid follicle CD4⁺ T lymphocytes, where it delivers a contact-dependent signal that stimulates B cell survival, growth, and differentiation (*2–4*). Signaling through CD40 rescues B cells from apoptosis induced by Fas (CD95) or by cross-linking of the immunoglobulin M (IgM) complex (*5*); it also induces B cells to differentiate and to undergo Ig isotype switching (*3*) and to express CD80 (B7 or BB-1) (*6*). The crucial role of CD40L-CD40 interaction is illustrated by humans with defects in CD40L, who manifest a serious immune deficiency syndrome, the X-linked hyper-IgM syndrome (HIGMX-1), characterized by an absence of IgG, IgA, and IgE, elevated IgM, and no lymphoid

G. Cheng and D. Baltimore, Department of Biology, Massachusetts Institute of Technology, 77 Massachusetts Avenue, Cambridge, MA 02139, USA.
A. M. Cleary, D. I. Hong, S. Lederman, Department of Medicine, Columbia University, New York, NY 10032, USA.
Z.-s. Ye, Rockefeller University, 1230 York Avenue, New York, NY 10021, USA.

*These authors contributed equally to this work.
†To whom correspondence should be addressed.

follicles (*7*). The essential roles of CD40L and CD40 in the phenotype of HIGMX-1 syndrome has been confirmed by targeted disruption of either CD40L (*8*) or CD40 (*9*) in mice. In addition to B cells, CD40 is also expressed by follicular dendritic cells (*10*), dendritic cells (*11*), activated macrophages (*12*), epithelial cells (including thymic epithelium) (*13*), and a variety of tumor cells.

Stimulation of CD40 causes the tyrosine phosphorylation of multiple substrates including Src family kinases such as p53-p56^{lyn}, activates multiple serine-threonine–specific protein kinases, and induces the phosphorylation of phospholipase C-γ2 and of phosphoinositide-3′ kinase (*14*). The initial stage of signaling by CD40, however, is not yet characterized. Because the murine CD40 cytoplasmic tail is necessary for signaling (*15*), we have used the yeast two-hybrid system in an effort to identify complementary DNAs (cDNAs) encoding protein domains that can bind to the tail (*16*). From 2 × 10^6 clones of a murine 70Z pre-B cell cDNA library (*17*), one (C26) was isolated that met all specificity criteria for binding to the cytoplasmic tail of CD40 in yeast. The C26 cDNA fragment was sequenced and no identical gene was evident in the databases. We call this gene *CRAF1* for CD40 receptor–associated factor 1. By Northern (RNA) blot analysis, *CRAF1* was expressed in B cell lines representing different stages of B cell differentiation; in addition, it was expressed in all murine tissues examined, including brain, heart, lung, liver, kidney, muscle, small intestine, spleen, and thymus (*18*). Thus, it may well serve functions in other pathways.

Mouse and human cDNA libraries were screened to isolate cDNA clones encoding the entire open reading frame of a murine 567–amino acid and a human 568–amino acid protein. The two sequences share 96% identity, with the differences concentrated near the NH_2-terminus, indicating that *CRAF1* is evolutionarily conserved, particularly in its COOH-terminal 400 amino acids (Fig. 1). The CRAF1 sequence is similar to that of TNF-α receptor–associated factors 1 and 2 (TRAF1 and TRAF2), which can complex with the cytoplasmic tail of TNF-α receptor II (TNFαRII) (*19*). The COOH-terminus of CRAF1 is related by sequence to each of these TRAF proteins for 150 amino acids, wherein CRAF1 is 59 and 62% identical to TRAF1 or TRAF2, respectively (Fig. 2) (*19*). This homology subdivides what was termed the "TRAF domain," excluding a more NH_2-terminal putative coiled-coiled subdomain (TRAF-N) with which CRAF1 shares only 16 or 12% homology and defines a "TRAF-C" (for COOH-terminal) domain. Because the extracellular domains of CD40 and TNFαRII are homologous, as are their ligands, these data suggest that they may make use of related but distinct signaling molecules. However, the cytoplasmic domains of CD40 and TNFαRII contain no apparent sequence homology, which suggests that the particular contacts involved in binding the signaling molecules to the receptors have diverged.

In addition to the TRAF-C domain, sequence analysis of the CRAF1 protein revealed three potential domains: an amphipathic helix, a string of Zn fingers, and a Zn ring finger domain (Fig. 2A). A helical wheel representation of the putative helix (Fig. 2B) shows that isoleucine (or occasionally leucine) repeats every seven residues through eight consecutive repeats, which implies the presence of a isoleucine zipper in analogy to the leucine zipper seen in other

Fig. 1. Predicted amino acid sequences of mouse (M) and human (H) CRAF1 (22). The full-length mouse sequence is shown and numbered. The human sequence has one more amino acid than that of the mouse (indicated with a dot), but all numbers here refer to the mouse sequence. Dashes indicate positions in the human sequence that are identical to those in the mouse. The C26 clone obtained from the yeast two-hybrid screen contained the COOH-terminal region of CRAF1 starting from the position marked with an arrow. The cDNA nucleotide sequences are deposited in GenBank with accession numbers U21050 and U21092.

```
M  MESSKKMDAAGTLQPNPPLKLQPDRGAG.SVLVPEQGGYKEKFVKTVEDK   49
H  --------SP-A--T------HT--S--TP-F------------------

M  YKCEKCRLVLCNPKQTECGHRFCESCMAALLSSSSPKCTACQESIIKDKV   99
H  ------H----S-------------------------------V----

M  FKDNCCKREILALQVYCRNEGRGCAEQLTLGHLLVHLKNECQFEELPCLR  149
H  --------------I-----S-----------------D-H------V-

M  ADCKEKVLRKDLRDHVEKACKYREATCSHCKSQVPMIKLQKHEDTDCPCV  199
H  P-----------------------------------A-----------

M  VVSCPHKCSVQTLLRSELSAHLSECVNAPSTCSFKRYGCVFQGTNQQIKA  249
H  ------------------------------------------------

M  HEASSAVQHVNLLKEWSNSLEKKVSLLQNESVEKNKSIQSLHNQICSFEI  299
H  ------------------------------------------------

M  EIERQKEMLRNNESKILHLQRVIDSQAEKLKELDKEIRPFRQNWEEADSM  349
H  ------------------------------------------------

M  KSSVESLQNRVTELESVDKSAGQAARNTGLLESQLSRHDQTLSVHDIRLA  399
H  ----------------------V---------------M---------

M  DMDLRFQVLETASYNGVLIWKIRDYKRRKQEAVMGKTLSLYSQPFYTGYF  449
H  ------------------------------------------------

M  GYKMCARVYLNGDGMGKGTHLSLFFVIMRGEYDALLPWPFKQKVTLMLMD  499
H  ------------------------------------------------

M  QGSSRRHLGDAFKPDPNSSSFKKPTGEMNIASGCPVFVAQTVLENGTYIK  549
H  ------------------------------------------------

M  DDTIFIKVIVDTSDLPDP                                  567
H  ------------------
```

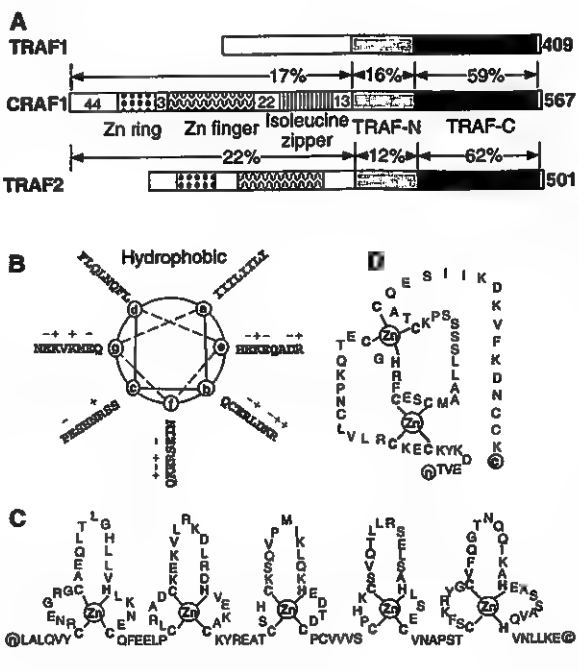

Fig. 2. Potential structural domains of CRAF1 (22). (**A**) Diagrams of three TRAF family members. Percentages of amino acid identity between CRAF1 and either TRAF1 or TRAF2 are shown. The TRAF domain was defined in the COOH-terminal region of TRAF1 and TRAF2 (*19*) (residues 356 to 562 for CRAF1) but can be subdivided into TRAF-N and TRAF-C subregions according to sequence homology with CRAF1 as well as by the mapping assays shown in Fig. 3. For CRAF1, the number of amino acids between homologous regions is indicated. (**B**) Helical wheel representation of residues 287 to 342 of CRAF1. The wheel starts with the inner residue Ile^{287} at position a and finishes with the outer residue Asn^{342} at position g; "+" and "−" denote change of amino acid residues. (**C**) Predicted Zn fingers corresponding to residues 110 to 264 of CRAF1. (**D**) Zn finger from residues 45 to 106 of CRAF1. n, NH_2-terminus; c, COOH-terminus.

proteins (*20*). The wheel also indicates that the position next to the zipper is always hydrophobic or uncharged, whereas the other positions around the wheel include multiple charged residues and few hydrophobic ones. This strongly suggests an amphipathic structure that could be an interaction site for another such helix.

There are five repeats of potential Zn fingers just NH_2-terminal to the isoleucine repeats (Fig. 2C). However, the four amino acids that would contact the metal are arranged in the unique pattern Cys-X_{2-6}-Cys-$X_{11,12}$-His-X_{3-7}-Cys(His), instead of Cys-X_{2-4}-Cys-$X_{12,13}$-His-X_{2-4}-His, which is seen in classic Zn fingers (*21*). At the COOH-terminal edge of finger 2 is a sequence (KACKYR) (*22*) that could bind to DNA, which suggests that CRAF1 might be a DNA binding protein. In the TRAF2 protein, we found five fingers with the same pattern of repeats seen in the CRAF1 protein but with weak overall similarity (Fig. 2A), suggesting that these structural units may represent a subclass of Zn finger motifs in this type of signaling molecule. In addition, a Zn ring structure was also evident in the NH_2-terminus of CRAF1 (Fig. 2D) (*23*). This ring motif has been recognized in over 40 proteins that have diverse functions related to DNA mechanics, including recombination, repair, and transcription regulation (*24*). These structural data suggest that CRAF1 could directly transmit CD40 signals to the nucleus.

To further map the region of CRAF1 that interacts with the CD40 cytoplasmic tail, we generated four deletion mutants of the C26 cDNA and studied them in the yeast system for their ability to bind to the CD40 cytoplasmic tail. The TRAF-C subdomain of CRAF1 was necessary and sufficient for CRAF1 to interact with CD40 (Fig. 3). Moreover, the CRAF1 protein in yeast could interact with itself, forming homodimers or oligomers, also mediated by the TRAF-C domain (Fig. 3). Quantitative analysis of β-galactosidase expression indicated that the affinity of the TRAF-C domain of CRAF1 to bind to CD40 and to dimerize with itself was not increased by addition of the rest of the TRAF domain. We therefore suggest that the COOH-terminal portion of the TRAF domain may function as an individual unit (the TRAF-C domain) that is involved in both binding to the receptor tail and mediating dimerization.

To determine if the CD40-binding domain of CRAF1 can play a functional role in mammalian cells, we examined whether overexpression of the C26 partial cDNA fragment would act as a dominant negative protein, inhibiting CD40 signaling presumably by prevention of the binding of the endogenous protein to the CD40 tail. Ramos 2G6 cells (*25*) can be induced to up-regulate

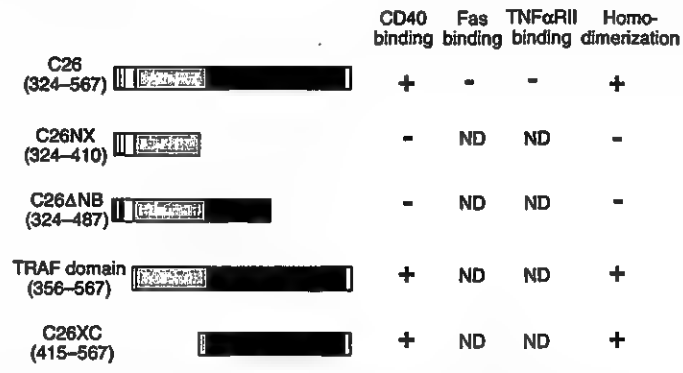

Fig. 3. Mapping the CD40 binding and homodimerization domain of CRAF1. C26NX and C26XC represents fragments from the NH_2-terminus of C26 to the internal Xho I site and from the Xho I site to the COOH-terminus of CRAF1, respectively. C26ΔNB was made by deletion of the Nco I–Bgl II fragment in the 3′ untranslated region of the C26 cDNA clone. The full TRAF domain of CRAF1 was synthesized by the polymerase chain reaction with the use of plaque-forming units of DNA polymerase. Various DNA fragments were ligated in-frame into yeast expression vectors encoding either the LexA DNA-binding domain (LexA) or the transcriptional activation domain (TAD). For CD40 binding assays, the LexA construct containing the CD40 cytoplasmic tail and various TAD fusion constructs were cotransfected into yeast strain EGY48 along with the lacZ-containing reporter vector (pSH18-34). Colonies that grew up on synthetic dextrose plates without tryptophan, uracil, and histidine were replica-plated to plates with or without leucine and tested for galactose-inducible blue color in the presence of x-gal. LexA constructs containing the cytoplasmic tails of Fas and TNFαRII were also included in the same experiments to test their interaction with the C26 clone. For dimerization assays, various LexA fusion constructs containing different fragments of C26 were used in every combination with various TAD fusion constructs. Transformants that grew on plates lacking leucine and that showed galactose-inducible blue are marked "+"; this was further confirmed by β-galactosidase assays with the use of yeast grown in liquid cultures (*34*). Transformants that grew only on plates containing leucine but that did not show blue on x-gal plates are marked "−"; ND, experiments not done.

surface CD23 molecules in a contact-dependent fashion that depends on CD40L interaction with CD40 (*3*). Therefore, a cDNA construct was generated that drives the expression of a polyhistidine/C26 fusion protein (pEBVHis/C26) in mammalian cells (*26*). As a negative control for the effects of C26, the β-galactosidase gene was expressed as a fusion protein in the same vector (pEBVHis/lacZ) (Invitrogen). These constructs were electroporated into Ramos 2G6 cells, and clones expressing a large amount of pEBVHis/C26 mRNA were prepared (Fig. 4A). CD40L-expressing cells (293.CD40L) were then cultured with Ramos 2G6 cells that either were not transfected or were stably expressing pEBVHis/lacZ or pEBVHis/C26 (*27*). The control and pEBVHis/lacZ-transfected Ramos lines up-regulated CD23; this effect was inhibited by a monoclonal antibody (mAb) to CD40L (mAb 5C8). In contrast, the ability of the pEBVHis/C26 transfectants to up-regulate CD23 in response to CD40L-CD40 signals was diminished. The inhibition of CD23 up-regulation by pEBVHis/C26 was relatively specific because recombinant interleukin-4 (rIL-4)–induced up-regulation of CD23 was not affected (Fig. 4B). Similar effects were seen in all three subclones of pEBVHis/C26 transfectants. Thus, the COOH-terminal region of CRAF1 represented in the C26 cDNA could block the CD40 triggering of Ramos cells, suggesting that CRAF1 participates in CD40 signaling.

CD40 is a type I transmembrane glycoprotein belonging to the TNF receptor superfamily. Besides CD40, 11 other proteins have been identified in this superfamily, which includes TNF receptors I and II, the nerve growth factor (NGF) receptor, and Fas (*28*). Members within this family share sequence similarity through their extracellular regions that contain multiple cysteine-rich pseudorepeats. The common structural framework of the extracellular domain is reflected in the ability of the TNF receptor superfamily members to interact with a parallel family of TNF-related cytokine ligands. To date, eight such ligands (including TNF-α, CD40L, and FasL) have been cloned that share extensive sequence identity and exist as secreted cytokines or type II transmembrane ligands (*28*).

The functions of TNF receptor superfamily members are very divergent. They range from general acute phase responses and lymphocyte activation to nerve cell growth. In some circumstances, they have opposite roles. For instance, Fas and TNFαRI can cause apoptosis upon ligand stimulation, whereas CD40 and NGF receptors can rescue cells from apoptosis (*29*). In addition, stimulation of either TNFαRI, TNFαRII, or CD40 receptor activates nuclear factor kappa B (*30*). Because CRAF1 is very similar to TRAF1 and TRAF2, a family of signal transduction proteins (the TRAF family) probably exists as downstream signal transducers of the TNF receptor superfamily. It is likely that direct binding between members of the TNF receptor family and the TRAF family will be specific because the cytoplasmic tails of these TNF receptor superfamily members are relatively short and show little or no sequence homology. Consistent with this

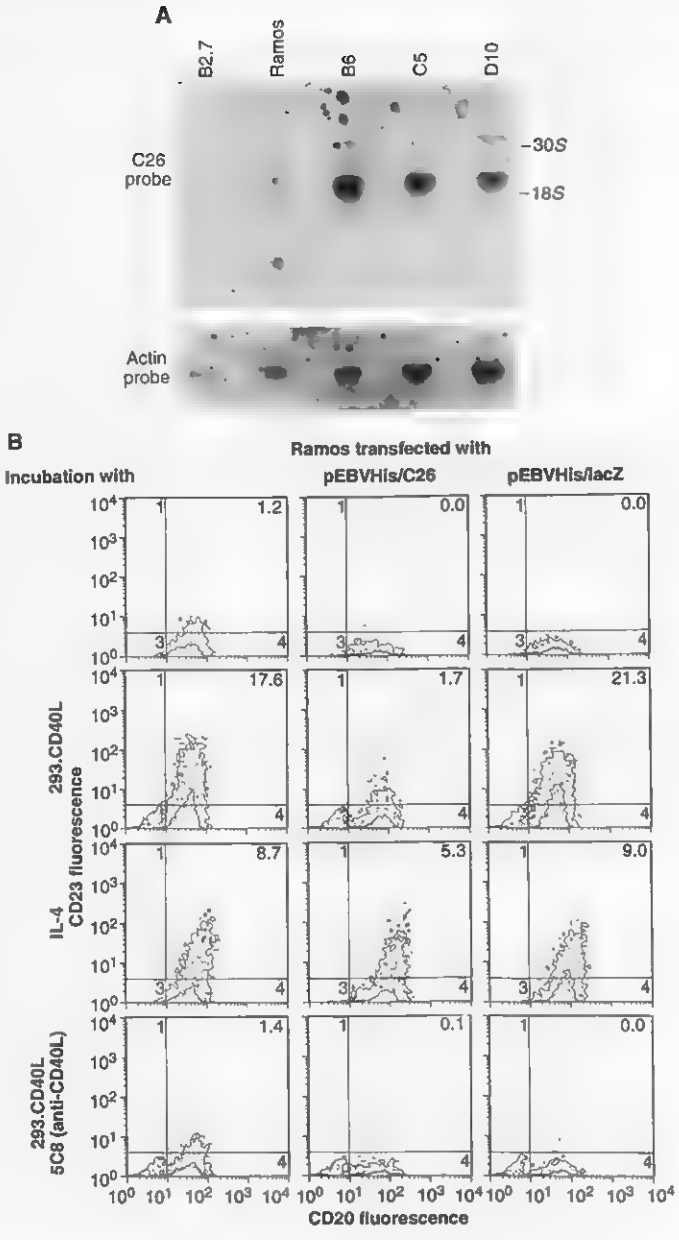

Fig. 4. Effect of C26 fusion proteins on CD40L: CD40-induced CD23 up-regulation. (**A**) Northern blot analysis of Ramos 2G6 transfectants. Total RNA (2 μg) from the Jurkat T cell line (B2.7) was used for markers. In other lanes, polyadenylate-containing RNA (0.75 μg per lane) was obtained from the untransfected Ramos 2G6 clone (Ramos) or pEBVHis/C26 Ramos transfectants (B6, C5, or D10). RNA blots of control and transfected cell lines were probed with C26 cDNA or an actin probe. (**B**) Two-color fluorescence-activated cell sorting analysis of Ramos 2G6 and Ramos 2G6 transfectants (pEBVHis/C26 or pEBVHis/lacZ) after 18 to 24 hours of culture with medium (−), 293.CD40L cells, rIL-4, or 293.CD40 cells plus anti-CD40L mAb 5C8 (as indicated). The *x* and *y* axes represent CD20 and CD23 fluorescence, respectively. The percentage of $CD20^+$ cells that express CD23 is indicated in the upper right-hand corner of each contour map. The D10 clone of pEBVHis/C26 is shown.

notion, we found that the COOH-terminal segment of CRAF1 does not interact with the tail of Fas or with TNFαRII (Fig. 3). However, the fact that the members of the TRAF family can form either homodimers or heterodimers could result in extensive diversity and specificity in their signal transduction pathways. It is even possible that apoptosis and cell survival may be determined by an equilibrium of dimerization between TRAF family members.

The functional consequences of CD40 signaling are different for B cells at different stages of differentiation (*31*). CD40 crosslinking causes resting B cells to enter into the cell cycle, enhances the proliferative rate of some chronic lymphocytic leukemia B cells, induces some B lymphoma cells to apoptose, and prevents germinal center B cells from apoptosis (*14*). However, CRAF1 is expressed at all stages of B cell differentiation and may be ubiquitous. It could have more specific partners or specifity may be a result of how a common signal is interpreted in a given cell.

Note added in proof: After submission of our paper, Hu *et al.* (*32*) and Mosialos *et al.* (*33*) described proteins that interact with the cytoplasmic tail of CD40. Their proteins are identical to CRAF1.

REFERENCES AND NOTES

1. S. Paulie *et al.*, *Cancer Immunol. Immunother.* **20**, 23 (1985); E. A. Clark and J. A. Ledbetter, *Proc. Natl. Acad. Sci. U.S.A.* **83**, 4494 (1986); I. Stamenkovic, E. A. Clark, B. Seed, *EMBO J.* **8**, 1403 (1989).
2. S. Lederman *et al.*, *J. Exp. Med.* **175**, 1091 (1992); R. J. Armitage *et al.*, *Nature* **357**, 80 (1992); D. Graf, U. Korthauer, H. W. Mages, G. Senger, R. A. Kroczek, *Eur. J. Immunol.* **22**, 3191 (1992), J. F. Gauchat *et al.*, *FEBS Lett.* **315**, 259 (1993).
3. S. Lederman *et al.*, *J. Immunol.* **149**, 3817 (1992).
4. D. Hollenbaugh *et al.*, *EMBO J.* **11**, 4313 (1992).
5. T. Tsubata, J. Wu, T. Honjo, *Nature* **364**, 645 (1993); N. J. Holder *et al.*, *Eur. J. Immunol.* **23**, 2368 (1993); S. L. Parry, J. Hasbold, M. Holman, G. G. B. Klaus *J. Immunol.* **152**, 2821 (1994); A. M. Cleary, S. M. Fortune, L. Chess, S. Lederman, unpublished results
6. M. J. Yellin *et al.*, *J. Immunol.* **153**, 666 (1994).
7. R. C. Allen *et al.*, *Science* **259**, 990 (1993); U. Korthäuer *et al.*, *Nature* **361**, 539 (1993); J. P. DiSanto *et al.*, *ibid.*, p. 541; A. Aruffo *et al.*, *Cell* **72**, 291 (1993); R. E. Callard *et al.*, *J. Immunol.* **153**, 3295 (1994); N. Ramesh *et al.*, *Int. Immunol.* **5**, 769 (1993).
8. J. Xu *et al.*, *Immunity* **1**, 423 (1994).
9. T. Kawabe *et al.*, *ibid.*, p. 167.
10. F. Schrieve *et al.*, *J. Exp. Med.* **169**, 2043 (1989); E. A. Clark, K. H. Grabstein, G. L. Shu, *J. Immunol.* **148**, 3327 (1992).
11. D. N. Hart and J. L. McKenzie, *J. Exp. Med.* **168**, 157 (1988).
12. M. R. Alderson *et al.*, *ibid.* **178**, 669 (1993).
13. A. H. Galy and H. Spits, *J. Immunol.* **149**, 775 (1992).
14. F. H. Durie, T. M. Foy, S. R. Masters, J. D. Laman, R. J. Noelle, *Immunol. Today* **15**, 406 (1994).
15. S. Inui *et al.*, *Eur. J. Immunol.* **20**, 1747 (1990).
16. The bait for the yeast two-hybrid screen was a LexA fusion protein containing the cytoplasmic tail of the mouse CD40 receptor (from residue 219 to the COOH-terminus).
17. The cDNA library for the yeast two-hybrid screen was a mixture of oligo(dT) and random primed cDNAs constructed into the yeast expression vector YSD, which is a centromere-based, galactose-induced yeast expression vector containing the VP16 transcription activation domain. Half of the mRNA used for cDNA synthesis was isolated from uninduced 70Z cells, and the other half was from 70Z cells that were induced with lipopolysaccharide for 12 hours. The primary library contained about 8×10^5 individual clones, with an average insert size of 0.9 kb.
18. G. Cheng, Z. S. Ye, D. Baltimore, unpublished results.
19. M. Rothe, S. C. Wong, W. J. Henzel, D. V. Goeddel, *Cell* **78**, 681 (1994).
20. W. H. Landschulz, P. F. Johnson, S. L. McKnight, *Science* **240**, 1759 (1988).
21. R. M. Evans and S. M. Hollenberg, *Cell* **52**, 1 (1988).
22. Abbreviations for the amino acid residues are A, Ala; C, Cys; D, Asp; E, Glu; F, Phe; G, Gly; H, His; I, Ile; K, Lys; L, Leu; M, Met; N, Asn; P, Pro; Q, Gln; R, Arg; S, Ser; T, Thr; V, Val; W, Trp; and Y, Tyr.
23. P. S. Fremont, I. M. Hanson, J. Trowsdale, *ibid.* **64**, 483 (1991).
24. P. N. Barlow, B. Luisi, A. Milner, M. Elliott, R. Everett, *J. Mol. Biol.* **237**, 201 (1994).
25. J. P. Siegel and H. S. Mostowski, *J. Immunol. Methods* **132**, 287 (1990).
26. The C26 cDNA fragment was cut with Eco RI–Hinc III from yeast vector YSD, ligated into Bluescript IISK+ (Stratagene), and then recloned in-frame into the pEBVHisA vector (Invitrogen), with the use of Bam HI and Kpn I cuts, to create pEBVHis/C26. Stable Ramos cell lines containing either this construct or the control construct (pEBVHis/lacZ) were isolated by electroporation and hygromycin selection.
27. Either 2×10^5 Ramos B cells or Ramos B cells transfected with pEBVHis/C26 or pEBVHis/lacZ were incubated for 18 to 24 hours in 0.2 ml of medium alone, in rIL-4 at a concentration of 25 ng/ml, or in the presence of 5×10^4 293.CD40L cells. In some cases, mAb 5C8 (anti-CD40L) was added. Cells were then washed and incubated with saturating concentrations of mAb Leu-16 (anti-CD20) conjugated to fluorescein isothiocyanate (Becton Dickinson) and mAb to CD23 conjugated to phycoerythrin (Biosource International) for 45 min at 4°C in the presence of heat-aggregated IgG (80 μg/ml) (International Enzyme). Cells were washed to remove unbound antibody before fluorescence intensity was measured on a FACSCAN cytofluorograph (Becton Dickinson) with Consort 30 software
28. C. A. Smith, T. Farrah, R. G. Goodwin, *Cell* **76**, 959 (1994).
29. N. Itoh *et al.*, *ibid* **66**, 233 (1991); L. A. Taraglis, T. M.

Ayres, G. H. W. Wong, D. V. Goeddel, *ibid.* **74**, 845 (1993).
30. M. Grilli, J. J.-S. Chiu, M. J. Lenardo, *Int. Rev. Cytol.* **143**, 1 (1991); I. Berberich, G. L. Shu, E. A. Clark, *J. Immunol.* **153**, 4357 (1994).
31. J. Gordon, M. J. Millsum, G. R. Guy, J. A. Ledbetter, *J. Immunol.* **140**, 1425 (1988); M. F. Gruber, J. M. Bjorndahl, S. Nakamuar, S. M. Fu, *ibid.* **142**, 4144 (1989); M. K. Spriggs *et al.*, *J. Exp. Med.* **176**, 1543 (1992); P. Lane *et al.*, *ibid.* **177**, 1209 (1993); D. H. Crawford and D. Catovsky, *Immunology* **80**, 40 (1993); A. W. Heath *et al.*, *Cell Immunol.* **152**, 468 (1993); Y.-J. Liu *et al.*, *Nature* **342**, 929 (1989).
32. H. M. Hu, K. O'Rourke, M. S. Boguski, V. M. Dixit, *J. Biol. Chem.* **269**, 30069 (1994).
33. G. Mosialos *et al.*, *Cell* **80**, 389 (1995).
34. J. H. Miller, in *Experiments in Molecular Genetics*, C. S. H. L. Press, Ed. (Cold Spring Harbor Laboratory, Cold Spring Harbor, NY, 1972).
35. We thank P. Svec and T. Hawkins for their help in sequencing and J. Jacob for critical reading of the manuscript. G.C. and Z.-Y. are recipients of an Irvington House Institute fellowship and a Leukemia Society special fellowship, respectively. S.L. is an Arthritis Investigator of the Arthritis Foundation. D.B. is an American Cancer Society Research Professor. A.M.C. is supported by the Medical Scientist Training Program grant 5-T32-GM07367. S.L., A.M.C., and D.I.H. are also supported in part by Biogen, Cambridge, MA. This work was supported by National Institute of Allergy and Infectious Diseases grant A122346 (D.B.) and by National Cancer Institute (NCI) grant R01-CA55713 to S.L.

22 November 1994; accepted 2 February 1995

Crystal Structure of the Tetramerization Domain of the p53 Tumor Suppressor at 1.7 Angstroms

Philip D. Jeffrey, Svetlana Gorina, Nikola P. Pavletich

The p53 protein is a tetrameric transcription factor that plays a central role in the prevention of neoplastic transformation. Oligomerization appears to be essential for the tumor suppressing activity of p53 because oligomerization-deficient p53 mutants cannot suppress the growth of carcinoma cell lines. The crystal structure of the tetramerization domain of p53 (residues 325 to 356) was determined at 1.7 angstrom resolution and refined to a crystallographic *R* factor of 19.2 percent. The monomer, which consists of a β strand and an α helix, associates with a second monomer across an antiparallel β sheet and an antiparallel helix-helix interface to form a dimer. Two of these dimers associate across a second and distinct parallel helix-helix interface to form the tetramer.

The p53 tumor suppressor (*1*), a tetrameric protein that can bind to specific DNA sequences (*2*) and activate gene expression (*3*, *4*), plays a central role in a cell's response to tumorigenic events. p53 can induce cell cycle arrest in response to DNA damage and thus can prevent genetic alterations such as chromosomal rearrangements and gene amplifications (*5*). In addition to coordinating the DNA damage response, p53 can also induce apoptosis in response to the activation of oncogenes such as c-Myc and E1A (*6*). These findings suggest that p53 exerts its tumor suppressing effects by responding to events that may lead to the abnormal proliferation of cells.

The p53 protein has multiple domains with the DNA binding, transactivation, and tetramerization functions residing in separate domains. The sequence-specific DNA binding activity resides in the central portion which folds into a compact structural domain [core domain, residues 102 to 292 (*7*–*9*)]; the transactivation function resides in the loosely folded NH_2-terminal portion [residues 1 to 44 (*3*, *7*)]; and the tetramerization function resides in a structural domain in the COOH-terminal portion of the protein [residues 320 to 356 (*7*, *9*–*11*)]. Consistent with its tetrameric oligomerization state, the p53 protein binds DNA sites that contain four repeats of the pentamer sequence motif Pu-Pu-Pu-C-(A/T) (*2*).

DNA binding and transactivation are the critical mediators of p53's biological effects because tumor-derived p53 mutants defective in suppressing growth are also defective in DNA binding and transactivation (*3*). In vitro, tetramerization is not essential for DNA binding, and the isolated core domain can bind DNA with approximately one-fifth the affinity of intact p53 (*7*). In vivo, however, oligomerization-deficient p53 cannot efficiently transactivate from genomic p53 binding sites in transient transfection assays (*12*), and it cannot suppress the growth of carcinoma cell lines (*12*, *13*). This suggests that there is a tight threshold for in vivo p53 activity and that oligomerization is required to maintain this activity above threshold (*12*). These findings are analogous to those obtained with several tumorigenic mutants of p53 which bind to DNA with reduced affinity but fail to suppress growth in vivo (*14*).

Using a peptide that corresponds to residues 320 to 356 of p53 (*15*), we have obtained three crystal forms of the tetramer and have determined the structure by the multiple isomorphous replacement method (MIR) (*15*). The quaternary structures in the three crystal forms are essentially identical; therefore, our discussion of the tetramer structure will focus on the tetragonal crystal form that diffracts to beyond 1.7 Å resolution and has been refined to a crystallographic *R* factor of 19.2% (Table 1 and Fig. 1).

The crystal structure of the tetramer reveals that the oligomerization domain contains a β strand from residue 326 to 333 and an α helix from residue 335 to 354. The β strand and the α helix form a V-shaped structure with the helix axis being roughly antiparallel to the direction of the β strand. The transition from the β strand to the α helix occurs over a single residue, Gly^{334}, with the backbone amide nitrogen of the glycine making the last β sheet hydrogen bond and the backbone carbonyl making the first α helical hydrogen bond. The backbone conformation ($\phi = 98°$, $\psi = 130°$) in this hinge region is unique to the glycine amino acid, and it is energetically unfavorable for other amino acids. Consistent with its role as a critical hinge residue between the β strand and the α helix, Gly^{334} is conserved across species (*16*) and is one of the few oligomerization domain residues that has been found to be mutated in tumors (*17*). Flanking the Gly^{334} hinge region, there are hydrophobic interactions between the α helix and the β strand involving the side chains of Ile^{332}, Phe^{338}, and Phe^{341}.

The tetramer has 222-point symmetry (three mutually perpendicular twofold rotation axes), with each of the four monomers being in an identical environment (Fig. 2). The tetragonal crystal form has one monomer in the asymmetric unit, and the three twofold symmetry axes of the tetramer coincide with crystallographic symmetry. The twofold axes intersect at the center of the tetramer near the side chain of Leu^{344}. In the

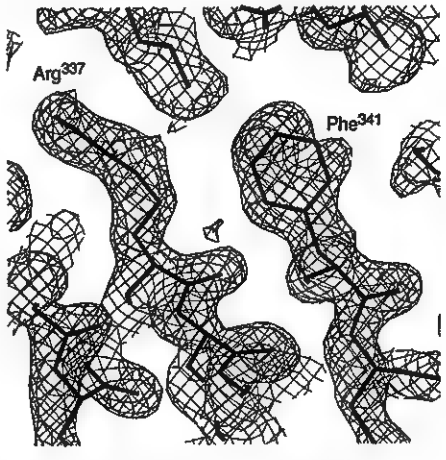

Fig. 1. Multiple isomorphous replacement (MIR) electron density map calculated with phases from the program SQUASH (*34*) at 2.0 Å and contoured at 1.0σ. The Arg^{337} and Phe^{341} residues are labeled. The helix axis is approximately horizontal in the figure.

Cellular Biochemistry and Biophysics Program, Memorial Sloan-Kettering Cancer Center, New York, NY 10021, USA.

Table 1. Data collection and analysis. The peptide of the p53 tetramerization domain crystallizes in space group *P*422 with cell dimensions of $a = b = 45.45$ Å and $c = 33.03$ Å (*15*) and has one monomer in the asymmetric unit. All native and derivative data were collected from the same crystal at room temperature on an RAXIS IIc area detector. Heavy atom derivatives were prepared by successive soaking of the crystal in heavy atom solutions containing 3 M sodium formate, 0.5 M ammonium sulfate, and 100 mM Hepes-Na^+ (pH 7.5) and the following heavy atom compounds: 3 mM silver nitrate for 3 hours (silver-1 derivative); 6 mM silver nitrate for 3 hours (silver-2 derivative); and 5 mM lead chloride for 4 hours (silver + lead derivative). Initial multiple isomorphous replacement (MIR) phases calculated with the PHASES program package (*33*) had a mean figure of merit of 0.48 to 2.0 Å, and they were improved by using Sayre's equation, density modification by histogram matching, and solvent flattening with the program SQUASH (*34*). The model was built into MIR electron density maps with the program CHAIN (*35*) and was refined with the program X-PLOR (*31*). An overall anisotropic temperature factor correction was applied to the native data set in the final stages of the refinement.

Item	Native	Silver-1	Silver-2	Silver + lead
Resolution (Å)	1.7	2.0	2.0	2.2
Observed reflections	20115	11320	11284	10201
Unique reflections	3950	2274	2547	1948
Data coverage (%)	98.9	87.4	98.3	99.1
R_{sym} (%)*	3.7	4.4	6.5	6.2
MIR analysis				
Resolution (Å)		2.0	2.0	2.2
Isomorphous difference†		0.069	0.102	0.128
Phasing power‡		1.73	1.64	0.73
Cullis *R* factor§		0.493	0.488	0.656
Refinement				
Resolution (Å)	6.0–1.7			
R factor‖	0.192			
Reflections with $\|F\| > 1\sigma$	3815			
Total number of atoms	306			
Water molecules	48			
rms on bond lengths (Å)¶	0.013			
rms on bond angles (°)¶	1.27			
rms on *B* values (Å²)¶	5.4			

*$R_{sym} = \Sigma_h\Sigma_i|I_{h,i} - I_h|/\Sigma_h\Sigma_i I_{h,i}$, where I_h is the mean intensity of the i observations of the unique reflection h. †Isomorphous difference $= \Sigma|F_{PH} - F_P|/\Sigma F_{PH}$, where F_{PH} and F_P are the derivative and native structure factor amplitudes, respectively. ‡Phasing power $= \{\Sigma F_{H(calc)}^2/\Sigma|F_{PH(obs)} - F_{PH(calc)}|^2\}^{1/2}$. §Cullis *R* factor $= \Sigma||F_{PH} \pm F_P| - F_{H(calc)}|/\Sigma|F_{PH} - F_P|$ for centric reflections, where $F_{H(calc)}$ is the calculated heavy atom structure factor. ‖*R* factor $= \Sigma|F_{obs} - F_{calc}|/\Sigma F_{obs}$. ¶The rms deviation in *B* values is the rms deviation in the temperature factors between bonded atoms. The rms deviations for bond lengths and bond angles is the rms deviation from ideal stereochemical values.

Table 2. Summary of interactions between monomer A and monomers B, C, and D. Hydrogen bonds and salt links were assigned between polar or charged groups separated by less than 3.0 Å. Buried surface areas are those buried on monomer A by the other monomers, calculated with a spherical probe with a 1.7 Å radius (*36*). Interhelical angles were calculated from helix axes determined with the Cα atoms of residues 336 to 354. Interhelical distances represent the closest approach of the helical axes.

Item	Interactions with monomer		
	B	C	D
Van der Waals contacts	164	35	8
Hydrogen bonds	8	0	0
Salt links	2	2	0
Buried surface area (Å²)	1138	360	108
Interhelical angles (°)	162	80	103
Interhelical distances (Å)	12.0	8.4	12.7

tetramer, each of the four monomers (A, B, C, and D) has three distinct interfaces with the other monomers. The A-B interface is more extensive than the A-C or A-D interfaces (Table 2), and the tetramer can therefore be regarded as a dimer formed through the association of the AB and CD dimers.

The monomers within the AB (or CD) dimer associate in a nearly antiparallel manner by means of their β strands and their α helices (Fig. 2). The strands form a highly twisted, two-stranded antiparallel β sheet, and the helices associate with a 161° angle, which is characteristic of other helix bundle proteins (*18*). In the dimer, the polypeptide chains are intertwined, with the β strand of A packing against the α helix of B. The association of the A and B monomers relies heavily on the eight backbone hydrogen bonds of the β sheet (Table 2). In addition, there is a small hydrophobic core consisting of the buried side chains of Ile^{332} and Phe^{341} and the partially buried side chains of Phe^{338} and Leu^{330} from each monomer (Fig. 3). We also observed an intermonomer salt link between Arg^{337} and Asp^{352} and an intermonomer hydrogen bond between Tyr^{327} and Arg^{333}.

The AB and CD dimers associate through their α helices to form the AB-CD tetramer (Fig. 2). The β strands are on the outside of the tetramer and are not involved in dimer-dimer interactions. The interactions between the two dimers are primarily hydrophobic in nature and involve the buried side chains of Ala^{347}, Phe^{341}, and Leu^{344} (Phe^{341} is also involved in the AB dimer hydrophobic core) and the partially buried side chains of Met^{340}, Leu^{348}, and Leu^{350} (Table 2 and Fig. 3). The helices from monomers A and C (or B and D) approach closely at Ala^{347} (Cα–Cα distance of 5.1 Å) across one of the symmetry axes. The short side chain of the alanine residue appears to be important for this interface because it allows for the close approach of the α helices. The A and C helices are "parallel" to each other but have a large interhelical angle of 81°. This arrangement of the helices is atypical of helix bundle or leucine zipper motifs where the helices have smaller interhelical angles.

The quaternary structure of the tetramer is very similar in all three crystal forms. The Cα atoms of the four helices in the tetragonal crystal form can be superimposed on those of the two hexagonal crystal forms with typical root-mean-square (rms) deviations of 0.9 Å for the helical regions (*19*). There is thus no indication that either crystallization conditions or crystal packing forces have perturbed the quaternary structure of the tetramer to any significant extent. However, we observed significant differences when we compared the crystal structure to a structure determined by nuclear magnetic resonance (NMR) spectroscopy (*20*) [see the technical comment in this issue for a discussion of the differences (*21*)]. A second NMR structure published recently (*22*) is more similar to our crystal structure (*23*).

The crystal structure presented in this report has implications for understanding why the oligomerization domain is rarely mutated in tumors, even though it appears to be necessary for p53's growth suppression activity. Less than 1% of the tumor-derived mutations are found in the tetramerization domain (*17*), and this has been interpreted to reflect selection for mutations which, while disrupting DNA binding, allow the mutant p53 to form inactive hetero-oligomers with the product of the remaining wild-type allele and to abrogate its function in a dominant negative fashion (*10*, *24*). This gain of function has been demonstrated in cell culture by overexpressing the mutant proteins (*10*, *25*), but it is not clear whether this effect contributes to neoplastic transformation and to the low frequency of tumor-derived mutations in this region.

An alternative hypothesis that is supported by the crystal structure is that few single amino acid mutations can adequately interfere with oligomerization to bring the DNA binding and transactivation activity of p53 below the threshold required for in vivo effects. Several observations support this hy-

pothesis. First, tetramerization of p53 may be redundant because dimerization appears to be sufficient for in vivo p53 activity. A dimeric p53 constructed by replacing the tetramerization domain with the coiled-coil dimerization domain of GCN4 has growth suppression activity like that of wild type (*12*). Second, the crystal structure of the tetramerization domain reveals that tetramerization involves two distinct dimerization interfaces, with one of the interfaces having extensive main chain hydrogen bonds (Fig. 3). It is conceivable, then, that most single amino acid changes cannot adequately destabilize both dimer interfaces to result in the complete dissociation to monomers. Third, whereas the majority of the mutations in the core DNA binding domain are missense mutations, those in the tetramerization domain are predominantly chain termination mutations [18 out of 22 mutations found in this region are either frameshift or chain termination mutations (*17*)]. Fourth, the NH_2-terminal transactivation domain of p53, which is essential for p53's growth suppression activity, is also rarely mutated in tumors. Systematic site-directed mutagenesis studies of this region have shown that two independent mutations are required to produce the same phenotype as a single tumor-derived mutation in the core DNA binding domain (*26*), making the inactivation of the transactivation domain a rare mutagenic event.

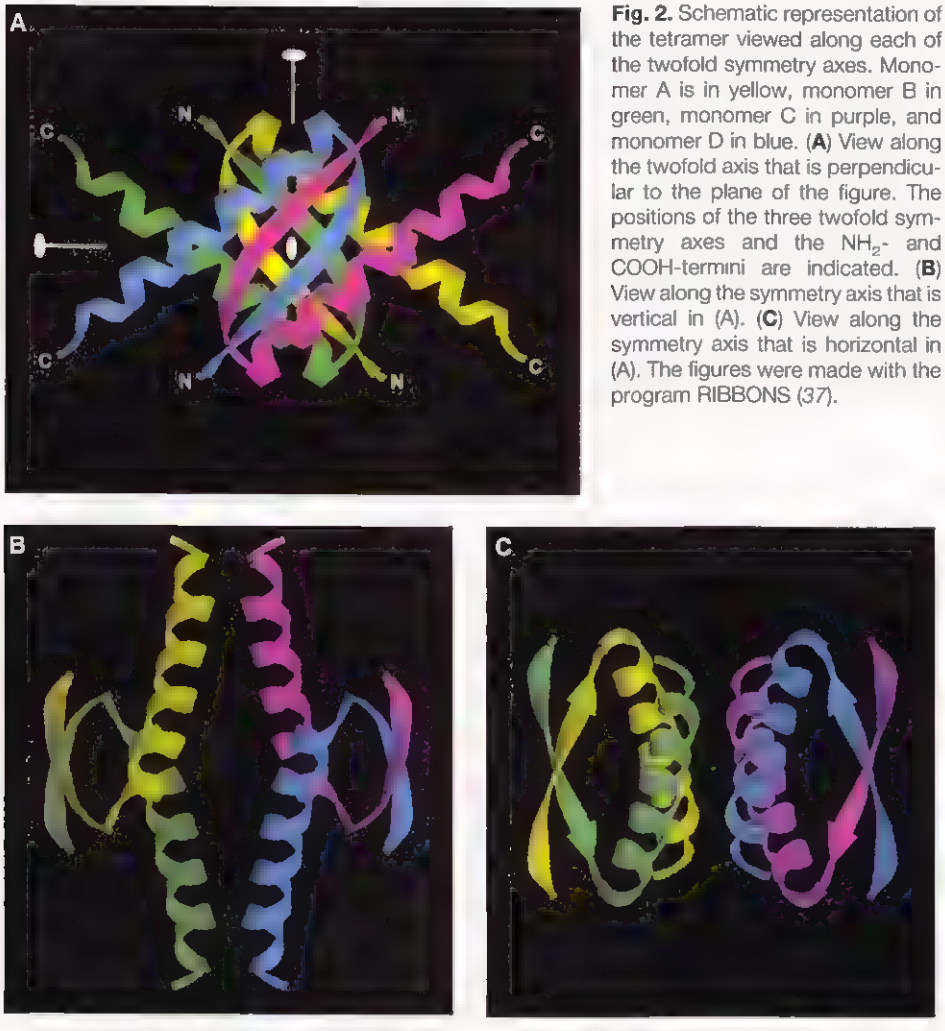

Fig. 2. Schematic representation of the tetramer viewed along each of the twofold symmetry axes. Monomer A is in yellow, monomer B in green, monomer C in purple, and monomer D in blue. (**A**) View along the twofold axis that is perpendicular to the plane of the figure. The positions of the three twofold symmetry axes and the NH_2- and COOH-termini are indicated. (**B**) View along the symmetry axis that is vertical in (A). (**C**) View along the symmetry axis that is horizontal in (A). The figures were made with the program RIBBONS (*37*).

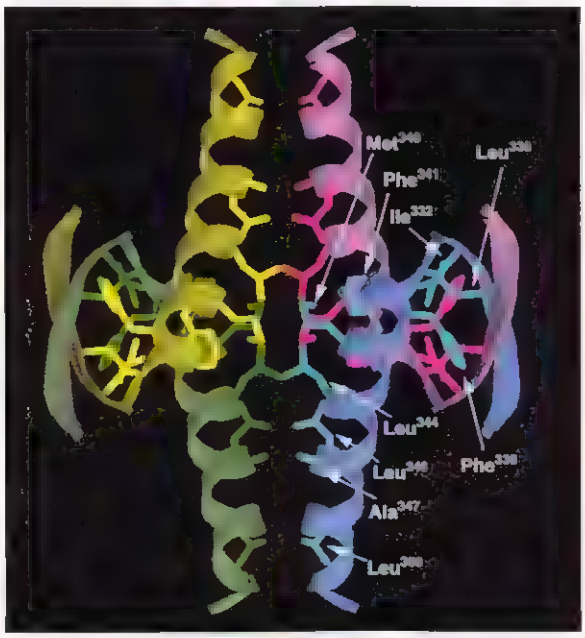

Fig. 3. Schematic representation of the tetramer showing the residues that make up the hydrophobic cores of the AB dimer and the AB-CD tetramer in the coloring scheme of Fig. 2. Eight side chains (four from each monomer) form the hydrophobic core at the AB dimer interface. Twenty side chains (five from each monomer) form the hydrophobic core at the AB-CD tetramer interface.

To obtain insights into the structure of the intact p53-DNA complex, we have constructed a model using the crystal structure of a dimeric p53 core domain–DNA complex published recently [residues 94 to 312 (*27*)], and the crystal structure of the tetramerization domain reported in this study (Fig. 4). In this model, four core domain molecules bind on the same face of the DNA, with their COOH-termini extending through the major groove and ending at the opposite face of the DNA. The tetramerization domains occur near the face of the DNA that is opposite to where the core domains bind. The arrangement of the four core domains is of lower symmetry than the arrangement of the four tetramerization domains, having only one twofold symmetry axis compared with the three mutually perpendicular twofold axes of the tetramerization domains. The core and oligomerization domains are connected through a 30-residue linker that is highly sensitive to proteolytic digestion and thus appears to be flexible or loosely folded (*7*). This linker can adequately span the distance between the core and oligomerization domains which, depending on the precise position and orientation of the oligomerization domain, could be 10 to 40 Å (a 30–amino acid peptide could be up to 100 Å long in a fully extended conformation). The length and apparent flexibility of the linker suggests that the oligomerization domains may not have a well-defined position and orientation with respect to the core domain–DNA complex.

The COOH-terminal portion of p53 has been shown to have an affinity for nucleic

Fig. 4. Model of the core domain–DNA–tetramerization domain complex with the DNA axis perpendicular to the plane of the figure. The four core domains and the four tetramerization domains are colored separately and the DNA is colored gray. The model was constructed by using the crystal structure of the dimeric core domain–DNA complex (*27*), aligned on a B-form DNA model having a consensus tetrameric binding site (*2*), and the crystal structure of the oligomerization domain. The COOH-termini of the four core domains and the NH_2-termini of the tetramerization domains are indicated. The two domains are connected by means of a 30–amino acid long flexible linker, and it is likely that the oligomerization domain does not have a well-defined position with respect to the core domain–DNA complex.

acids. In particular, a 25–amino acid basic region immediately after the oligomerization domain has been proposed to interact nonspecifically with double- and single-stranded nucleic acids (*7*, *9*, *28*, *29*). In our model of the core domain–tetramerization domain–DNA complex (Fig. 4), the oligomerization domain is in close proximity to the DNA. This raises the possibility that the COOH-terminal portion of p53 may interact with DNA and may modulate the sequence-specific DNA binding activity. It has been proposed that the basic region may inhibit p53's sequence-specific DNA binding activity because deletion of the basic region or the binding of an antibody to this region appears to enhance DNA binding activity in vitro (*30*). Our model suggests that this inhibition may occur through the nonspecific interaction of the COOH-terminal region with the DNA. The basic regions could either mask the specific binding sites of the core domains, or they could interfere with the correct relative alignment of the two domains, for example, by intertwining the linker. In this respect, productive DNA binding by p53 may involve a competition between the sequence-specific DNA binding activity of the core domain and the nonspecific DNA binding activity of the COOH-terminal domain.

REFERENCES AND NOTES

1. A. J. Levine, J. Momand, C. A. Finlay, *Nature* **351**, 453 (1991); B. Vogelstein and K. W. Kinzer, *Cell* **70**, 523 (1992).
2. J. P. Bargonetti, N. Friedman, S. E. Kern, B. Vogelstein, C. Prives, *Cell* **65**, 1083 (1991); S. E. Kern *et al.*, *Science* **252**, 1708 (1991); W. D. Funk, D. T. Pak, R. H. Karas, W. E. Wright, J. W. Shay, *Mol. Cell. Biol.* **12**, 2866 (1992); W. S. El-Deiry, S. E. Kinzler, J. A. Pietenpol, K. W. Kinzler, B. Vogelstein, *Nature Genet.* **1**, 45 (1992).
3. S. Fields and S. K. Jang, *Science* **249**, 1046 (1990); L. Raycroft, H. Wu, G. Lozano, *ibid.*, p. 1049; G. Farmer *et al.*, *Nature* **358**, 83 (1992); T. Unger, M. M. Nau, S. Segal, J. D. Minna, *EMBO J.* **11**, 1383 (1992).
4. S. E. Kern *et al.*, *Science* **256**, 827 (1992).
5. M. B. Kastan *et al.*, *Cell* **71**, 587 (1992); Y. Yin, M. A. Tainsky, F. Z. Bischoff, L. C. Strong, G. M. Wahl, *ibid.* **70**, 937 (1992); L. R. Livingstone *et al.*, *ibid.*, p. 923; L. Hartwell, *ibid.* **71**, 543 (1992).
6. H. Hermeking and D. Eick, *Science* **265**, 2091 (1994); S. W. Lowe and H. E. Ruley, *Genes Dev.* **7**, 535 (1993); X. Wu and A. J. Levine, *Proc. Natl. Acad. Sci. U.S.A.* **91**, 3602 (1994); H. Symonds *et al.*, *Cell* **78**, 703 (1994).
7. N. P. Pavletich, K. A. Chambers, C. O. Pabo, *Genes Dev.* **7**, 2556 (1993).
8. J. Bargonetti, J. J. Manfredi, X. Chen, D. R. Marshak, C. Prives, *ibid.*, p. 2565.
9. Y. Wang *et al.*, *ibid.*, p. 2575.
10. E. Shaulian, A. Zauberman, D. Ginsberg, M. Oren, *Mol. Cell. Biol.* **12**, 5581 (1992).
11. H. W. Sturzbecher *et al.*, *Oncogene* **7**, 1513 (1992).
12. J. A. Pietenpol *et al.*, *Proc. Natl. Acad. Sci. U.S.A.* **91**, 1998 (1994).
13. When overexpressed, oligomerization-deficient p53 is capable of low levels of transactivation in transient transfection assays (*9*).
14. D. J. Park *et al.*, *Oncogene* **9**, 1899 (1994).
15. The initial identification of the tetramerization domain of p53 by proteolytic digestion has been described (*7*). A peptide corresponding to residues 311 to 367 of p53 was used in initial crystallization trials but failed to yield diffraction-quality crystals. Further digestion of the 311–367 peptide by subtilisin yielded a major fragment which was identified by NH_2-terminal sequencing and mass spectrometry to correspond to residues 320 to 356. This region of p53 is conserved across species (7 of the 32 residues are invariant, and many of the remaining ones involve conservative substitutions) and is delimited by sequences that are variable and contain deletions and insertions in other species (*16*). The proteolytic fragment was purified to near homogeneity according to procedures reported for the 311–367 peptide (*7*), and it yielded three crystal forms in hanging drop vapor diffusion crystallization experiments. A tetragonal form in space group $P422$ ($a = b = 45.45$ Å, and $c = 33.03$ Å) was grown from 3 M sodium formate, 0.5 M ammonium sulfate, and 50 mM tris-HCl (pH 8.8); a hexagonal form (form I) in space group $P6_122$ ($a = b = 79.8$ Å, and $c = 49.9$ Å) was grown from 6 M sodium formate, and 100 mM Hepes-Na^+ (pH 7.5); and a second hexagonal form (form II) in space group $P6_122$ ($a = b = 138.6$ Å, and $c = 49.9$ Å) was grown from 28% polyethylene glycol (PEG) 400 and 100 mM Hepes-Na^+ (pH 7.5). The tetragonal crystal form contained one monomer per asymmetric unit and diffracted to beyond 1.7 Å resolution. Hexagonal form I contained one dimer (AB dimer) per asymmetric unit and diffracted to 2.8 Å. Hexagonal form II contained three dimers (AB dimers) per asymmetric unit and diffracted to 3.0 Å. The structure of the tetragonal form was determined by the MIR method, and the statistics from the crystallographic analysis are presented in the text. The structure of the hexagonal form I was also determined by the MIR method. Briefly, we calculated MIR phases for the hexagonal form I by using four heavy atom derivatives (lead chloride, samarium acetate, silver nitrate, and dipotassiumhexabromoplatinate), and the phases had a mean figure of merit of 0.49 at 3.0 Å resolution. Solvent-flattened MIR maps had clear electron density for the helical residues 336 to 352 but had poor electron density for the β sheet region. The structure has been partially refined with X-PLOR (*31*) and has a crystallographic R factor of 29.9% for 6.0 to 2.9 Å data (1845 reflections with $|F| > 2\sigma$; rms deviation in bond lengths = 0.020 Å, and in bond angles = 2.2°). The β sheet region, which had poor electron density in the MIR map, has high temperature factors in the partially refined model, and it appears to be disordered in the hexagonal crystal form I (we presume that this is due to the lack of crystal-packing contacts in this region). The structure of the hexagonal form II was determined by molecular replacement with the programs MERLOT and BRUTE (*32*), with the dimer model from the hexagonal form I crystal structure. In the hexagonal form II structure the α helices are well defined, but the β sheet regions exhibit the same disorder apparent in the hexagonal form I structure.
16. T. Soussi, C. C. Fromentel, P. May, *Oncogene* **5**, 945 (1990).
17. M. S. Greenblatt, W. P. Bennett, M. Hollstein, C. C. Harris, *Cancer Res.* **54**, 4855 (1994); Database of p53 mutations, European Molecular Biology Laboratory Data Library (1994).
18. D. W. Banner, M. Kokkinidis, D. Tsernoglou, *J. Mol. Biol.* **196**, 657 (1987).
19. Only the Cα atoms of the helices (residues 338 to 350) were used in the superposition because the β sheet regions appear to be partially disordered in the hexagonal crystal forms.
20. G. M. Clore *et al.*, *Science* **265**, 386 (1994).
21. G. M. Clore *et al.*, *ibid.* **267**, 1515 (1995).
22. W. Lee *et al.*, *Nature Struct. Biol.* **1**, 877 (1994).
23. The initial NMR structure (*20*) has a rms deviation of Cα atoms of 3.1 Å when superimposed on the crystal structure (residues 325 to 350). This deviation is primarily due to a 36° difference in the orientation of the AB dimer relative to the CD dimer. A revision of that structure (*21*) has a rms deviation of only 1.2 Å. The second NMR structure published recently (*22*) has a rms deviation of 1.5 Å.
24. J. Milner and E. A. Medcalf, *Cell* **65**, 765 (1991).
25. P. Hinds, C. Finlay, A. J. Levine, *J. Virol.* **63**, 739 (1989); P. W. Hinds *et al.*, *Cell Growth Differ.* **1**, 571 (1990); O. Halvey, D. Michalovitz, M. Oren, *Science* **250**, 113 (1990); D. Dittmer *et al.*, *Nature Genet.* **4**, 42 (1993).
26. J. Lin, J. Chen, B. Elenbaas, A. J. Levine, *Genes Dev.* **8**, 1235 (1994).
27. Y. Cho, S. Gorina, P. D. Jeffrey, N. P. Pavletich, *Science* **265**, 346 (1994).
28. P. Oberosler, P. Hloch, U. Ramsperger, H. Stahl, *EMBO J.* **12**, 2389 (1993).
29. L. Wu, H. J. Bayle, B. Elenbaas, N. P. Pavletich, A. J. Levine, *Mol. Cell. Biol.*, **15**, 497 (1995).
30. T. R. Hupp, D. W. Meek, C. A. Midgley, D. P. Lane,

Cell **71**, 875 (1992).
31. A. T. Brünger, J. Kuriyan, M. Karplus, *Science* **235**, 458 (1987); A. T. Brünger, *X-PLOR v3.1 Manual* (Yale Univ. Press, New Haven, CT, 1990).
32. P. M. D. Fitzgerald, *J. Appl. Crystallogr.* **21**, 273 (1988); M. Fujinaga and R. J. Read, *ibid.* **20**, 273 (1987).
33. W. Furey and S. Swaminathan, *Am. Crystallogr. Assoc. Meet. Abstr. Ser. 2* **18**, 73 (1990).
34. K. Y. J. Zhang, *Acta Crystallogr.* **D49**, 213 (1993).
35. J. S. Sack, *J. Mol. Graph.* **6**, 224 (1988).
36. M. L. Connolly, *J. Appl. Crystallogr.* **16**, 548 (1983).
37. M. Carson, *ibid.* **24**, 958 (1991).
38. Supported by National Cancer Institute grant CA08748-29, the Dewitt Wallace Foundation, and the Pew Charitable Trusts (N.P.P.). Coordinates have been deposited with the Brookhaven Protein Data Bank.

4 November 1994; accepted 12 January 1995

Pineal Opsin: A Nonvisual Opsin Expressed in Chick Pineal

Marianna Max,* Peter J. McKinnon, Kenneth J. Seidenman, R. Keith Barrett, Meredithe L. Applebury, Joseph S. Takahashi, Robert F. Margolskee

Pineal opsin (P-opsin), an opsin from chick that is highly expressed in pineal but is not detectable in retina, was cloned by the polymerase chain reaction. It is likely that the P-opsin lineage diverged from the retinal opsins early in opsin evolution. The amino acid sequence of P-opsin is 42 to 46 percent identical to that of the retinal opsins. P-opsin is a seven-membrane spanning, G protein–linked receptor with a Schiff-base lysine in the seventh membrane span and a Schiff-base counterion in the third membrane span. The primary sequence of P-opsin suggests that it will be maximally sensitive to ~500-nanometer light and produce a slow and prolonged phototransduction response consistent with the nonvisual function of pineal photoreception.

All identified vertebrate opsins fit into four major groups based on conservation at the protein level, epitomized by chick green, blue, violet, and red opsins (*1*, *2*). The order of divergence of these groups is not well resolved. The green opsin cluster contains as a subgroup the rod opsins (rhodopsin) used for scotopic vision (*2*). Within the red cluster multiple duplication events gave rise to closely related "green" opsins in Old World primates and some fish (*3*). Opsins within a given class share ~65 to 95% amino acid identity, whereas identity among classes is only ~40 to 50%.

The chick pineal is thought to contain a rhodopsin-like photoreceptor with a maximal sensitivity at 500 nm (*4*), based on the action spectrum for light-induced suppression of *N*-acetyltransferase activity, which reduces melatonin synthesis. Two other pieces of evidence also suggest that the pineal gland contains an opsin-like protein: (i) Vitamin A depletion from cultured pineal cells reduces light-mediated suppression of melatonin synthesis, suggesting the action of a vitamin A–based pigment (*5*) (presumably an opsin-bound chromophore) and (ii) immunocytochemistry indicates the presence of one or more opsin-like proteins in avian pinealocytes (*6*).

To identify the opsin or opsins expressed in pineal, we used degenerate oligonucleotide primers and reverse transcriptase–polymerase chain reaction (RT-PCR) (*7*) to amplify and clone opsin-like complementary DNAs (cDNAs) from chick pineal. Using primers to conserved regions flanking the Schiff-base lysine in the seventh transmembrane domain, we recovered three distinct opsin-like cDNAs: chick red opsin, chick green opsin, and a previously unidentified opsin [pineal opsin (P-opsin)]. Ribonuclease (RNase) protection (*8*) detected abundant P-opsin RNA but no retinal opsin RNAs in pineal (Fig. 1A) (*9*). RNase protection detected no expression of P-opsin transcript in chick retinal RNA although, as expected, red, green, blue, violet, and rhodopsin transcripts were detected. Neither P-opsin nor retinal opsin RNAs were detected in chick brain by RNase protection. In situ hybridization (*10*) demonstrated expression of P-opsin in most pinealocytes (Fig. 1, B and C), but not in chick retina. Thus, P-opsin is an abundant pineal transcript absent from retina.

A pineal-specific cDNA library was

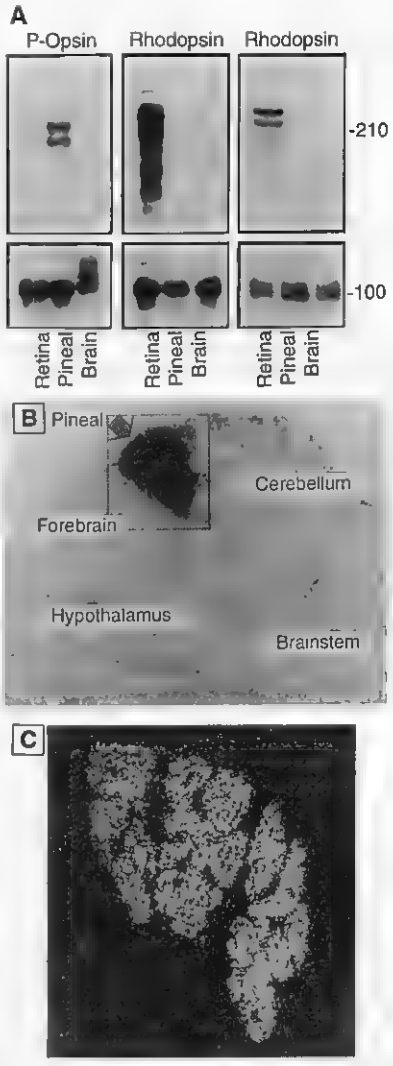

Fig. 1. Expression of P-opsin mRNA. (**A**) RNase protection assay (*8*) with RNA (~30 μg) from chick pineal, retina, or brain. (Left) Exposure for 8 hours shows abundant P-opsin expression in pineal but no expression elsewhere. (Middle) Eight-hour exposure shows that rhodopsin is not expressed in pineal; however, its protected product in retina appears to smear due to overexposure. (Right) Four-hour exposure of the rhodopsin protection shows the appropriate P-opsin bands in retina at ~210 bp. In other RNase protection assays, protected products were detected with probes made from chick green, red, blue, and violet opsins in retinal RNA but not in pineal RNA. All probes include 70 bp of vector sequence: No full-length probe could be detected after RNase digestion, indicating that only sequence-specific probe fragments of the correct size were protected. All protections included an actin standard (100-bp product) to control the amount of target RNA in each assay. (**B**) Autoradiograph of in situ hybridization (*10*) of ^{33}P-labeled P-opsin probe to a sagittal section of chick brain including attached pineal. The dotted square around the pineal gland corresponds to the view in (C). (**C**) Dark field view (40× magnification) of the boxed area of the section in (B) after the slide was dipped in emulsion (NTB 2 from Kodak), exposed for 2 weeks, and developed. The label is restricted to the pineal. Retina is not labeled by this probe and the sense probe control does not label the brain, pineal, or retina.

M. Max, Roche Institute of Molecular Biology, Roche Research Center, Hoffmann-LaRoche, Nutley, NJ 07110, USA, and National Science Foundation Center for Biological Timing, Department of Neurobiology and Physiology, Northwestern University, 2153 North Campus Drive, Evanston, IL 60208, USA.
P. J. McKinnon and R. F. Margolskee, Roche Institute of Molecular Biology, Roche Research Center, Hoffmann-LaRoche, Nutley, NJ 07110, USA.
K. J. Seidenman, R. K. Barrett, J. S. Takahashi, National Science Foundation Center for Biological Timing, Department of Neurobiology and Physiology, Northwestern University, 2153 North Campus Drive, Evanston, IL 60208, USA.
M. L. Applebury, Harvard Medical School, Howe Laboratories, 243 Charles Street, Boston, MA 02114, USA.
*To whom correspondence should be addressed.

screened with the cloned P-opsin PCR product (*11–13*) to obtain a full length P-opsin clone. The longest clone [1696 base pairs (bp)] with a plausible transcription start site and ATG sequence contained two stretches of open reading frame that together encode an opsin-like protein of 351 amino acid residues (Fig. 2A). We confirmed that this clone is full length by primer extension (*11*). This clone contains a 181-bp unprocessed intron (based on alignment with retinal opsin cDNAs) that was not present in the

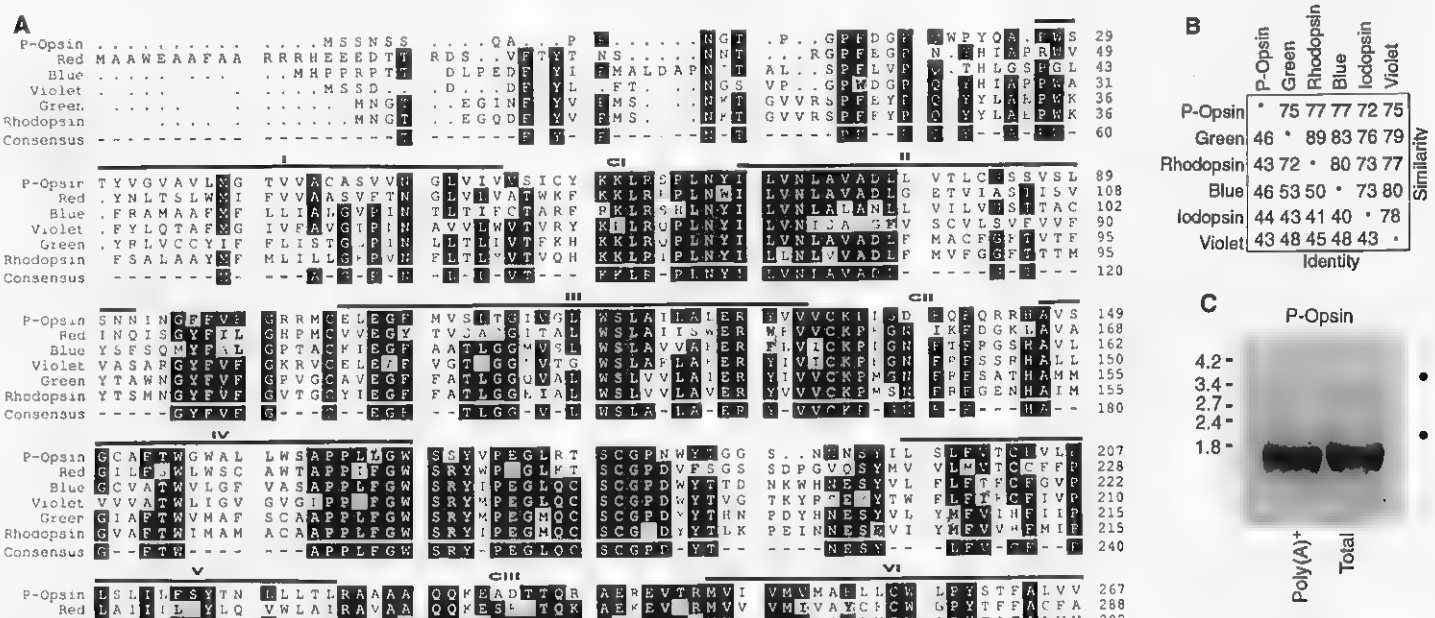

Fig. 2. Comparison of the P-opsin amino acid sequence (*12*) to that of the chick retinal opsins (*2*). (**A**) An optimized alignment of the P-opsin amino acid sequence to that of the chicken retinal opsins [single-letter code (*30*)]. Regions of amino acid identity are represented by white letters boxed in black. Conservative substitutions are shown by black letters boxed in gray. Unboxed black letters correspond to nonconsensus regions. Dots correspond to gaps introduced in the sequence to optimize alignment. A line showing consensus of four or more amino acid residues appears along the bottom (white letters boxed in black). Bars along the top of the alignment indicate transmembrane regions (I to VII) and cytoplasmic loops (CI to CIV). The alignment was determined iteratively by the Bestfit routine of the Wisconsin GCG software package (*15*) with modifications by eye for best fit of the divergent NH_2- and COOH-terminal regions. (**B**) Amino acid relatedness of chick opsins. The percent of identity between any two opsins is shown below the diagonal and the percent of similarity (identities and conservative changes) between any two opsins is shown above the diagonal. (**C**) Northern blot (*11*, *14*) of pineal polyadenylated (3 μg) and total (30 μg) RNA labeled with P-opsin cDNA probe. Numbers on the left of the blot show the size of DNA markers (in kilobases) and the dots to the right of the blot show the positions of chick ribosomal RNA bands.

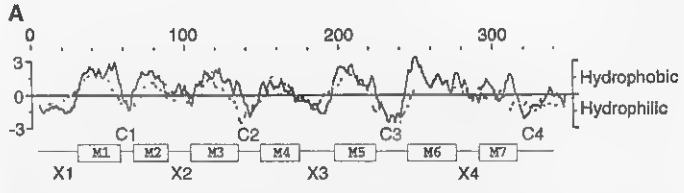

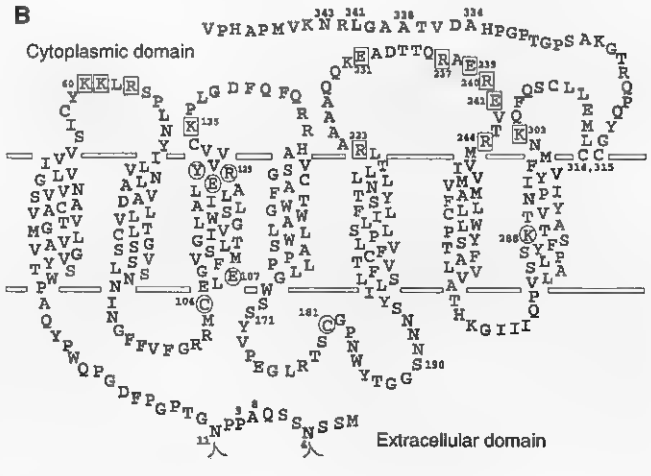

Fig. 3. Predicted secondary structure of P-opsin (**A**) The Kyte-Doolittle (*15*) hydrophobicity profile of P-opsin with the putative transmembrane regions (M1 to M7), cytoplasmic loops (C1 to C4), and extracellular regions (X1 to X4) indicated (**B**) The proposed secondary structure of P-opsin embedded within the membrane (represented by the two double lines). The cytoplasmic domain is shown to have four loops homologous to those of the other opsins; this face of the molecule is expected to interact with one or more G proteins (*16*). The regions below the bottom double line are presumed to be extracellular (rather than intradiscal) because pinealocytes have modified cone-like disk membranes rather than rod-like disks (*6*). Numbered amino acids are discussed in the text.

shorter clones. The predicted size of the fully processed transcript is 1515 bp, which corresponds to the size of the band detected by northern (RNA) blot (*11*, *14*) of pineal RNA (Fig. 2C). The predicted amino acid sequence is 42 to 46% identical with that of retinal opsins (Fig. 2B), suggesting that P-opsin does not fit into any of the previously identified classes of opsin genes.

P-opsin is a typical seven-membrane spanning protein like the retinal opsins and other GTP-binding protein (G protein)–linked receptors (Fig. 3A) (*15*). Regions of conservation in the retinal opsins are largely conserved in P-opsin (Fig. 2A). The following observations suggest a functional similarity between P-opsin and the retinal opsins (Fig. 3B): (i) a lysine (K288) in the appropriate position within the seventh membrane spanning region to act as the Schiff-base linkage with 11-*cis* retinal (*16*); (ii) a glutamic acid (E107) within the third membrane span to serve as the Schiff-base counterion (*16*); (iii) a pair of cysteines (C104 in the third membrane span and C181 in the third extracellular loop) which are thought to promote folding and in rhodopsin to stabilize the meta II form (*16*, *17*); (iv) predicted N-linked glycosylation sites (N4, N11) (*16*); (v) a pair of cysteines (C314,315) in the carboxyl tail that are palmitoylated in rhodopsin and anchor the tail to the membrane and thus form a fourth cytoplasmic

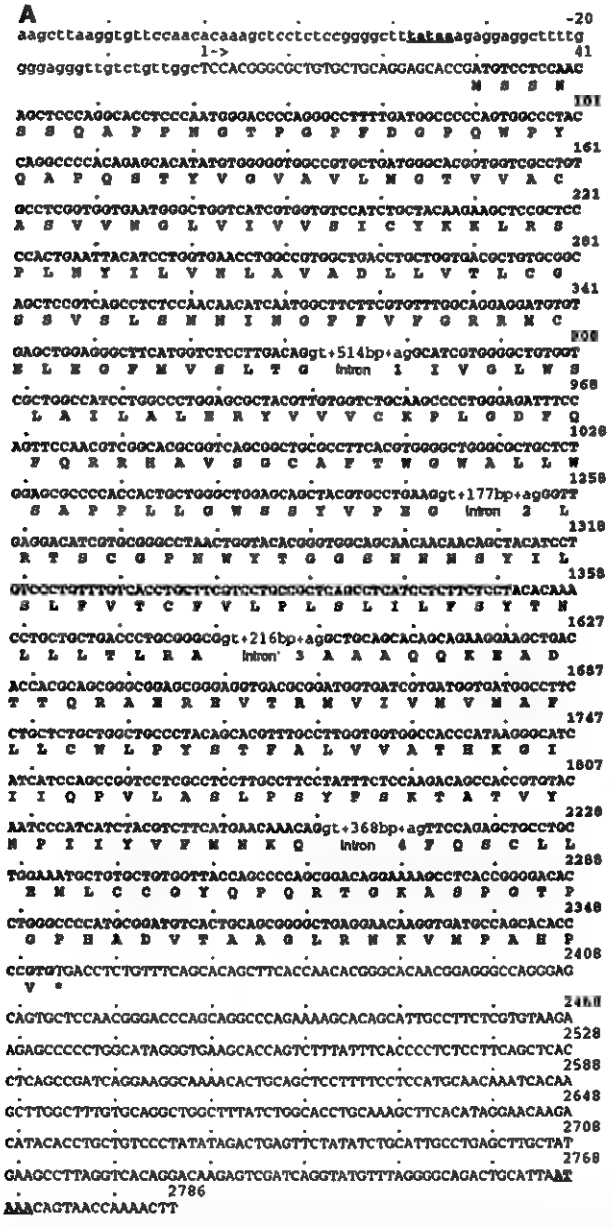

Fig. 4. The genomic structure of P-opsin and the evolutionary relationship of P-opsin to the retinal opsins. (**A**) Coding sequence from P-opsin genomic clone GP3 (*22*) as well as some 5′ flanking DNA −79 bp 5′ of the transcription start site and extending to the end of the coding sequence. DNA encoding protein is shown in uppercase bold typeface and the amino acid translation appears below. The positions of the introns are shown in lowercase nonbold typeface. Included are the intron-exon splice donor sites and the number of bases in between. The 5′ and 3′ untranslated regions are shown in uppercase nonbold typeface. The putative TATAA box is shown in bold and underlined in the 5′ flanking region as is the polyadenylation signal sequence in the 3′ untranslated region. (**B**) The reconstructed phylogenetic tree of vertebrate opsins including P-opsin. The tree was reconstructed with the PHYLIP package of programs (*1*, *23*). The tree is unrooted. Initial trees constructed with a selection of invertebrate opsins indicated that invertebrate opsins are strongly resolved from vertebrate opsins; thus, *Drosophila* opsin was chosen as the outgroup to draw the tree. Numbers in parentheses at each node show the number of trees with this pairing (n = 100 sample sets). Values of <60% pairing indicate that the appropriate pairing is unresolved and pairing of <70% is weak. All sequences are available through GenBank. Species designations are as follows: CAV, cavefish (*Astyanax fasciatus*); ZEF, zebrafish (*Brachydanio rerio*); GOF, goldfish (*Carassius auratus*); SGB, sandgoby (*Pomatoschistus mintus*); FRG, frog (*Rana pipiens*); XEN, (*Xenopus laevis*); XLTAD, tadpole (*X. laevis*); CHK, chick (*Gallus gallus*); BOV, cow (*Bos taurus*); OVI, sheep (*Ovis aries*); MUR, mouse (*Mus musculus*); CG, hamster (*Cricetulus griseus*); HUM, human (*Homo sapiens*); Can, dog (*Canis familieris*); LNP, lamprey (*Lampetra japonica*); GEC, lizard (*Gekko gekko*); ANC, lizard (*Anolis carolinensis*); CJAC, marmoset (*Calithrix jaccus*); and DRMGH1, fruit fly Rh1-6 (*Drosophila melanogaster*). The number after the P in the gene designation indicates absorption maxima. Other abbreviations are as follows: RHO, rhodopsin; GR, green. Major groupings agree with previous opsin phylogenetic trees (*1*, *2*), consistent with the suggestion that P-opsin is a separate lineage (that is, a fifth major group) within the vertebrate opsin family.

loop (*16*); (vi) a ERY or DRY (E128-Y130) motif in the third membrane span that is thought to participate in receptor–G-protein interactions (*16*); and (vii) several charged amino acids in the cytoplasmic loops (K60, K61, R63, K135, R223, E231, K237, E239, R240, E241, R244, K303) conserved in the chick retinal opsins and thought to be important for G-protein activation (*18*).

P-opsin also has several unique features when compared to the retinal opsins. The multiple serines and threonines in the carboxyl tail of the retinal opsins are not present in P-opsin (amino acids 334, 338, 341, and 343). These residues are phosphorylated in metarhodopsin by rhodopsin kinase, which increases the affinity of rhodopsin for S-antigen (arrestin) and decreases its affinity for transducin (thereby shutting off the transduction cascade) (*19*). P-opsin may be inactivated by a different mechanism or it may produce a prolonged light response as observed in arrestin mutants of *Drosophila* (*20*). In addition, P-opsin has an alanine at amino acid 232 rather than the conserved serine present in the retinal opsins. In rhodopsin this mutation reduces its ability to activate rod transducin by half (*21*), suggesting that the interaction of P-opsin with its G-protein partner may be similarly altered.

A chicken genomic library was screened with the P-opsin cDNA as a probe (*11*, *13*, *22*). We obtained 12 positive clones, one of which (GP3) contained the entire protein-coding region (Fig. 4A). The genomic organization of the P-opsin gene is similar to that of the short-wavelength opsin genes (it has five exons rather than the six exons of the red and red-like green opsins) except that the position of the second intron is displaced 15 nucleotides in the 3′ direction.

A preliminary evaluation of the evolutionary relationship of P-opsin to the retinal opsins was assessed by the neighbor-joining method with the PHYLIP package of programs (*1*, *23*). Individual runs with the full fixed alignment of sequences often pair P-opsin with the red and red-like green branch of the opsin phylogenic tree (putative node A′, Fig. 4B), but when bootstrap resampling is applied, P-opsin pairs more often with the blue, violet, green, and rhodopsin branch of the tree (node A), consistent with its genomic organization (Fig. 4A). However, this pairing occurs only 56 out of 100 times, which is inadequate to resolve the node. The phylogenic tree analysis suggests that P-opsin branches early from the other opsin groups but does not resolve its pairing. Several other pairings in this tree are also not adequately resolved, particularly the blue and violet clusters and the nodes marked B to F. Some of these nodes (including the node giving rise to P-opsin) may be better resolved as more opsin sequences become available.

Although no attempt was made in this tree to equate node position with evolutionary time, several lines of evidence suggest that the divergence of each of the major opsin groups occurred before the vertebrate radiation. (i) Homologous genes for each group are found across multiple vertebrate classes. (ii) Identity between groups is greater at the nucleotide level than at the amino acid level, suggesting selection for functional divergence by amino acid substitution in critical regions. (iii) The genomic structure is highly conserved between groups. Based on the homology of P-opsin with the retinal opsins (and assuming that evolutionary rates are equivalent among vertebrate opsin genes), it appears that the P-opsin gene is at least as old as the vertebrate lineage.

The function of P-opsin may differ significantly from that of the retinal opsins because photoreception in pineal cells seems to differ in important ways from that of retinal photoreceptors. Pineal cells retain the ability to respond to light after many days in dispersed cell culture and with repeated exposure to bright light (*24*), despite the apparent absence of any retinal isomerase or retinal pigment epithelium (RPE) equivalent cell type [RPE cells appear to be the sole site of re-isomerization of all-*trans* retinal to 11-*cis* in vertebrate retina and thus are required for regeneration of active retinal chromophore after photobleaching (*25*)]. Perhaps pineal opsin or opsins can bind all-*trans* retinal and photoconvert it to 11-*cis* as do the invertebrate pigments (*26*).

The pineal shows two responses to light (both of which are maximally sensitive near 500 nm) (*4*, *27*): (i) Melatonin synthesis is acutely suppressed and (ii) the phase of the circadian rhythm of melatonin production is shifted (entrainment). Several lines of evidence suggest that two separate transduction pathways mediate these responses. The acute transduction pathway is sensitive to pertussis toxin and to vitamin A depletion, whereas the entrainment pathway is not (*5*, *24*, *28*). One would expect that P-opsin could mediate one or both of these transduction pathways. The identification and cloning of P-opsin should provide the means to study the molecular mechanisms underlying nonvisual phototransduction.

Note added in proof: Subsequent to submission of our manuscript, Okano *et al.* (*29*) reported the cloning of an opsin cDNA (named pinopsin) that is expressed in chick pineal. The inferred amino acid sequences of P-opsin and pinopsin differ at only 2 positions out of 351, suggesting that they are the same gene products.

REFERENCES AND NOTES

1. M. L. Applebury, in *Molecular Evolution of Physiological Processes*, D. M. Fambough, Ed. (Rockefeller Press, New York, 1994), pp. 235–248.
2. T. Okano, D. Kojima, Y. Fukada, Y. Shichida, T. Yoshizawa, *Proc. Natl. Acad. Sci. U.S.A.* **89**, 5932 (1992); S.-Z. Wang, R. Adler, J. Nathans, *Biochemistry* **31**, 3309 (1992).
3. J. Nathans, D. Thomas, D. S. Hogness, *Science* **232**, 193 (1986); R. E. Ibbotson, D. M. Hunt, J. K. Bowmaker, J. D. Mollon, *Proc. R. Soc. London Ser. B.* **247**, 145 (1992); R. Yokoyama and S. Yokoyama, *Proc. Natl. Acad. Sci. U.S.A.* **87**, 9315 (1990).
4. T. Deguchi, *Nature* **290**, 706 (1981).
5. M. Zatz, *J. Neurochem.* **62**, 2001 (1994).
6. M. Araki, Y. Fukada, Y. Shichida, T. Yoshizawa, F. Tokunaga, *Dev. Brain Res.* **65**, 85 (1992); B. Vigh, I. Vigh-Teichman, P. Rohlich, B. Aros, *Z. Mikrosk-Anat. Forsch.* **96**, 113 (1982).
7. S. K. McLaughlin, P. J. McKinnon, R. F. Margolskee, *Nature* **357**, 563 (1992); P. Chomczynski and N. Sacchi, *Anal. Biochem.* **162**, 156 (1987). First-strand cDNAs were made from pineal and retinal total RNA from chickens (on a 12-hour light:12-hour dark cycle). RNA was harvested at 3-hour intervals and pooled. PCR products were amplified (Taq polymerase; Perkin-Elmer, Branchburg, NJ) from pineal and retinal cDNAs with the following degenerate primers: CCGGATCCACICA(A/G)AA(A/G)GCIGA and CCGAATTCAA(T/G)TG(T/G)(T/G)(T/C)T(A/G)TTCAT (restriction sites used to facilitate cloning are underlined). PCR products were cloned into Eco RI and Bam HI sites of pBluescript II KS+ (Stratagene, La Jolla, CA) and then sequenced on an Applied Biosystems 373A automated DNA sequencer. Primers for PCR and sequencing were made with a 380B Applied Biosystems oligonucleotide synthesizer.
8. P. A. Kreig and D. A. Melton, *Methods Enzymol.* **155**, 397 (1987). The following regions of P-opsin and the chick retinal opsins were amplified by PCR from either pineal or retinal cDNA: P-opsin (amino acids 235 to 305), rhodopsin (amino acids 243 to 313), green (amino acids 243 to 313), red (amino acids 256 to 326), blue (amino acids 54 to 108), and violet (amino acids 189 to 282). A chick β-actin PCR product was also amplified (amino acids 220 to 253). The PCR products were digested with restriction endonucleases and cloned into pBluescript II KS+ or SK−. The identity of all clones was confirmed by sequencing. P-opsin, red, and green were amplified from pineal cDNA; blue, violet, and β-actin were amplified from retinal cDNA; and rhodopsin was amplified from a full-length retinal rhodopsin clone. The following primers were used to generate the opsin and actin probes. P-opsin, green, red, and rhodopsin: CCGGATCCACICA(A/G)AA(A/G)GCIGA and CCGAATTCAA(T/G)TG(T/G)(T/G)(T/C)T(A/G)TTCAT; blue opsin, CACGAATTCCTCCTCATCGCTTTGGGG and CACCTCGAGCATCTGCGAGAAGCTGTA; violet opsin, CACGAATTCGTGGGCACGAAATACCGC and CACCTC GAGGCGGAGGTCCAAGCCGTG; and β-actin, CCGGATCCGAGTCCTGTGGTAT and CCGAATTCGTACCACGAGACAG. Antisense RNA probes for RNase protection assays were generated as follows. Red, green, P-opsin, and β-actin cDNA clones were linearized with Bam HI, then [^{32}P]UTP (uridine triphosphate)–containing transcripts were generated by T3 RNA polymerase. Blue and violet cDNA clones were linearized with Eco RI, then [^{32}P]UTP transcripts were generated by T7 RNA polymerase.
9. Although RNase protection assays failed to detect the retinal pigments in pineal that were amplified by PCR (red and green), there appear to be a small number of rhodopsin and iodopsin immunoreactive cells in the pineal (*6*). This suggests that the pineal may express some retinal opsins in a small subset of cells detectable by PCR but not by RNase protection assay.
10. S. K. McLaughlin and R. F. Margolskee, *Biotechniques* **15**, 506 (1993). For in situ hybridization ^{33}P-labeled RNA probes were transcribed from a linearized full-length P-opsin cDNA clone by T7 RNA polymerase (antisense) or T3 RNA polymerase (sense).
11. T. Maniatis, E. F. Fritsch, J. Sambrook, *Molecular Cloning: A Laboratory Manual* (Cold Spring Harbor Laboratory, Cold Spring Harbor, New York, ed. 2, 1989).
12. An oligo(dT)-primed pineal cDNA library was constructed in the Lambda Zap II vector (Stratagene) from polyadenylated [poly(A)$^+$]RNA obtained from pineal cells in culture (12-hour light:12-hour dark) harvested just before lights off on the third day. The library was

screened with a ^{32}P-labeled probe generated by PCR, with the 210-bp P-opsin cDNA obtained by RT-PCR as template. Filters were hybridized with the probe overnight at 65°C in Church buffer (*13*) and washed at high stringency in 0.2× saline sodium citrate (SSC), 0.5% SDS at 65°C. More than 30 individual partial P-opsin cDNA clones and one full-length clone were obtained (ranging in size from 800 to 1696 bp). Some of the partial clones (~1/3) had the sequence CAG (glutamine) for amino acid 28 rather than TGG (tryptophan). This may be due to a polymorphism in the population or to RNA editing.

13. G. M. Church and W. Gilbert, *Proc. Natl. Acad. Sci. U.S.A.* **81**, 1991 (1984).
14. The probe for Northern blot analysis was made by incorporating [^{32}P]dCTP (deoxycytidine triphosphate) into a 210-bp PCR product by amplifying P-opsin cDNA (amino acids 235 to 305).
15. I. Kyte and R. F. Doolittle, *Biology* **157**, 105 (1982); J. Devereaux, P. Haeberli, O. Smithies, *Nucleic Acids Res.* **12**, 387 (1984). The secondary structure of P-opsin was extrapolated from its hydrophobicity on the basis of a similar plot of bovine rhodopsin (*16*).
16. H. G. Khorana, *J. Biol. Chem.* **267**, 1 (1992).
17. F. F. Davidson, P. C. Loewen, H. G. Khorana, *Proc. Natl. Acad. Sci. U.S.A.* **91**, 4029 (1994).
18. E. M. Ross, *Neuron* **3**, 141 (1989).
19. H. Kühn, *Prog. Retinal Res.* **3**, 123 (1984); U. Wilden, S. W. Hall, H. Kühn, *Proc. Natl. Acad. Sci. U.S.A.* **83**, 1174 (1986).
20. P. J. Dolph *et al.*, *Science* **260**, 1910 (1993).
21. R. R. Franke, T. P. Sakmar, M. Graham, H. G. Khorana, *J. Biol. Chem.* **267**, 14767 (1993).
22. Genomic clone GP3 and others were obtained by screening of a chicken genomic library contained in Lambda Fix II (Stratagene) with a random-primed probe made from the full-length P-opsin cDNA clone. After overnight hybridization at 65°C in Church buffer, filters were washed at high stringency (0.2× SSC, 0.5% SDS, 65°C). Lambda DNA from purified positive plaques was subcloned into pBluescript II KS+, mapped by restriction endonuclease digestion, and sequenced. Both of the genomic clones that were sequenced through this region contain the sequence CAG (glutamine) at amino acid 28 rather than TGG (tryptophan) as found in the majority of cDNAs (*12*).
23. Tree reconstruction was performed as described in figure 3 of (*1*) with PHYLIP version 3.5c, assembled by J. Felsenstein [*Cladistics* **5**, 164 (1989)]. An alignment of sequences was generated by McCAW [M. O. Dayhoff, R. M. Schwartz, B. C. Orcutt, *Atlas of Protein Sequencing and Structure*, M. O. Dayhoff, Ed. (National Bioscience Research Foundation, Washington, DC, 1978), vol. 5, p. 345; G. D. Schuler, S. F. Altschul, D. J. Lipman, *Protein Struct. Funct. Genet.* **9**, 180 (1991)], with minor adjustments made by hand. Distance matrices were calculated with PRODIST, which uses the Dayhoff PAM 001 matrix. NEIGHBOR was used to generate pairwise groupings with the neighbor-joining method described by N. Saitou and M. Nei [*Mol. Biol. Evol.* **4**, 406 (1987)]. Randomization of sequence entry order had no effect on tree reconstruction. Bootstrapping (SEQBOOT) generated multiple (n = 100) randomly resampled data sets from the alignment [J. Felsenstein, *Evolution* **39**, 783 (1985); *Annu. Rev. Genet.* **22**, 521 (1988)]. CONSENSE produced a consensus tree from the data set. No attempt was made to associate branch length with amino acid substitution rate. Similar results were obtained using the accepted-mutation parsimony (AMP) method of Kolakowski and Rice, available by e-mail at lfk@receptor.MGH.Harvard.Edu.
24. J. S. Takahashi, N. Murakami, S. S. Nikaido, B. L. Pratt, L. M. Robertson, *Recent Prog. Horm. Res.* **45**, 279 (1989).
25. J. G. Flannery, W. O'Day, B. A. Pfeffer, J. Horwitz, D. Bok, *Exp. Eye Res.* **51**, 717 (1990).
26. S. Yarfitz and J. B. Hurley, *J. Biol. Chem.* **269**, 14329 (1994).
27. T. Deguchi, *Science* **203**, 1245 (1979); L. M. Robertson and J. S. Takahashi, *J. Neurosci.* **8**, 12 (1988); *ibid.*, p. 22.
28. M. Zatz and D. A. Mullen, *Brain Res.* **453**, 63 (1988).
29. T. Okano, T. Yoshizawa, Y. Fukada, *Nature* **372**, 94 (1994).
30. Abbreviations for the amino acid residues are as follows: A, Ala; C, Cys; D, Asp; E, Glu; F, Phe; G, Gly; H, His; I, Ile; K, Lys; L, Leu; M, Met; N, Asn; P, Pro; Q, Gln; R, Arg; S, Ser; T, Thr; V, Val; W, Trp; and Y, Tyr.
31. We thank L. F. Kolakowski for constructing evolutionary trees by the AMP method, J. Kornhauser and A. Opper for performing in situ hybridization, J. Florez for pineal cell cultures to make ZT 12 cDNA library, and R. Wurzberger for sequencing and oligonucleotide synthesis. Supported by NIH grants MH39592 and EY08467 to J.S.T., MH10287 to K.J.S., MH10225 to M.M., MH10369 to R.K.B., and EY04801 to M.L.A.

13 September 1994; accepted 21 December 1994

Massive Cell Death of Immature Hematopoietic Cells and Neurons in Bcl-x–Deficient Mice

Noboru Motoyama,* Fanping Wang,* Kevin A. Roth,* Hirofumi Sawa, Kei-ichi Nakayama, Keiko Nakayama, Izumi Negishi, Satoru Senju, Qing Zhang, Satoshi Fujii, Dennis Y. Loh†

bcl-x is a member of the *bcl-2* gene family, which may regulate programmed cell death. Mice were generated that lacked Bcl-x. The Bcl-x–deficient mice died around embryonic day 13. Extensive apoptotic cell death was evident in postmitotic immature neurons of the developing brain, spinal cord, and dorsal root ganglia. Hematopoietic cells in the liver were also apoptotic. Analyses of *bcl-x* double-knockout chimeric mice showed that the maturation of Bcl-x–deficient lymphocytes was diminished. The life-span of immature lymphocytes, but not mature lymphocytes, was shortened. Thus, Bcl-x functions to support the viability of immature cells during the development of the nervous and hematopoietic systems.

Apoptosis (programmed cell death) is a poorly understood process that occurs in many tissues during early development and throughout adult life in many organisms. The protooncogene *bcl-2*, whose gene product inhibits certain forms of apoptosis (*1*), is widely expressed during mouse development and in long-lived cells such as neurons and stem cells of many tissues in an adult mouse (*2*). Although early embryonic lethality was expected on the basis of its expression pattern, *bcl-2*–ablated mice were shown to remain viable, and major abnormalities were limited to the hair color, polycystic kidney development, and decreased lymphoid cell life-span (*3*, *4*). In particular, the nervous system developed normally. These findings may be attributed to redundancy, because *bcl-2* is only one of a larger family of related genes (*5*, *6*). As expected, other members of the *bcl-2* family can inhibit apoptosis in in vitro assays (*5*, *6*).

bcl-x, a member of the *bcl-2* gene family, can be alternatively spliced to produce two protein isoforms (Bcl-x_L and Bcl-x_S), one of which (Bcl-x_L) inhibits apoptosis (*6*). Bcl-x in mice is expressed highly during development and in the brain, thymus, and kidney in adult, predominantly in the Bcl-x_L form (*7*, *8*). To elucidate the functional and developmental role of Bcl-x, we used homologous recombination in embryonic stem (ES) cells to generate mice lacking both Bcl-x_L and Bcl-x_S (*9*) (Fig. 1). Heterozygous

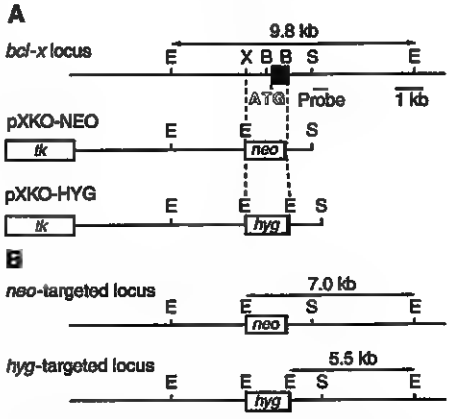

Fig. 1. Target disruption of the *bcl-x* gene (*9*). **(A)** Genomic structure surrounding coding exon of mouse *bcl-x*, and structure of the pXKO-NEO and pXKO-HYG targeting vectors. The position of translation initiation site is shown (ATG). **(B)** Predicted structure of the targeted *bcl-x* locus. The location of the hybridization probe, a 0.4-kb Kpn I–Pst I fragment, and expected sizes of the Eco RV fragments that hybridize with the probe are indicated. B, Bam HI; E, Eco RV; S, Spe I; X, Xho I. The restriction map of Bam HI is not complete.

N. Motoyama, F. Wang, K.-i. Nakayama, K. Nakayama, I. Negishi, S. Senju, Q. Zhang, D. Y. Loh, Howard Hughes Medical Institute and Departments of Medicine, Genetics, and Molecular Microbiology, Washington University School of Medicine, St. Louis, MO 63110, USA.
K. A. Roth, Departments of Pathology, Molecular Biology, and Pharmacology, Washington University School of Medicine, St. Louis, MO 63110, USA.
H. Sawa and S. Fujii, Division of Cardiovascular Medicine, Washington University School of Medicine, St. Louis, MO 63110, USA.

*These authors contributed equally to this report.
†To whom correspondence should be addressed.

mutant mice (*bcl-x*$^{+/-}$) were healthy and normal in size. Homozygous mutant mice (*bcl-x*$^{-/-}$) died around 13 days of gestation (E13) (Table 1).

Embryos from E11.5, 12.5, and 13.5 *bcl-x*$^{-/-}$, *bcl-x*$^{+/-}$, and wild-type mice were histologically examined. E11.5 *bcl-x*$^{-/-}$ mice were histologically similar to heterozygotes and wild-type mice with one major exception. Throughout the brain and spinal cord in the regions containing postmitotic, differentiating neurons, there was extensive cell death. In the most mature regions of the E11.5 nervous system, the rostral spinal cord and brain stem, there were large areas containing pyknotic nuclei, karyorrhectic debris, and frequent phagocytic cells with engulfed debris (Fig. 2). The histologic appearance of the degenerative zones in the *bcl-x*$^{-/-}$ mice resembles that seen in regions of naturally occurring neuronal cell death (*10*); however, the magnitude of cell death and its neuroanatomic distribution exceeds that seen in wild-type and heterozygote littermates.

By E12.5, extensive areas of neuronal degeneration were seen throughout the maturing *bcl-x*$^{-/-}$ brain, including the diencephalon, midbrain, and caudal spinal cord. Although naturally occurring neuronal cell death was seen in E12.5 wild-type and heterozygote mice in regions such as the rostral spinal cord and dorsal root ganglia, there was no evidence of massive, diffuse cell death as seen in the *bcl-x*$^{-/-}$ mice.

The degenerative changes in the *bcl-x*$^{-/-}$ nervous system appeared to be localized to regions of differentiating neurons. Because these mice had already died before mature neuronal phenotypes could be identified by histologic stains, we further characterized the zones of death by microtubule-associated protein 2 (MAP2) immunoreactivity (Fig. 2, F to H). The MAP2 protein is neuron-specific and is expressed during embryonic brain development (*11*). Immunohistochemical staining of E11.5 and 12.5 wild-type and *bcl-x*$^{-/-}$ brain and spinal cord showed that cells in the mitotically active ventricular zone lacked MAP2 immunoreactivity, but that more peripherally located differentiating cells possessed strong MAP2 staining. The vast majority of degenerating cells, identified by bisbenzamide staining, were located in MAP2-positive regions. The identification of the bisbenzamide-positive apoptotic cells in the *bcl-x*$^{-/-}$ nervous system as neurons is further supported by recent in vitro experiments. After 2 days in 2% fetal calf serum containing medium, primary dissociated E12.5 *bcl-x*$^{-/-}$ telencephalic cell cultures contained three times as many condensed or clumped bisbenzamide-labeled nuclei and only 30% of the number of neurofilament heavy chain immunoreactive neurons as heterozygote and wild-type cultures (*8*). These results also suggest that

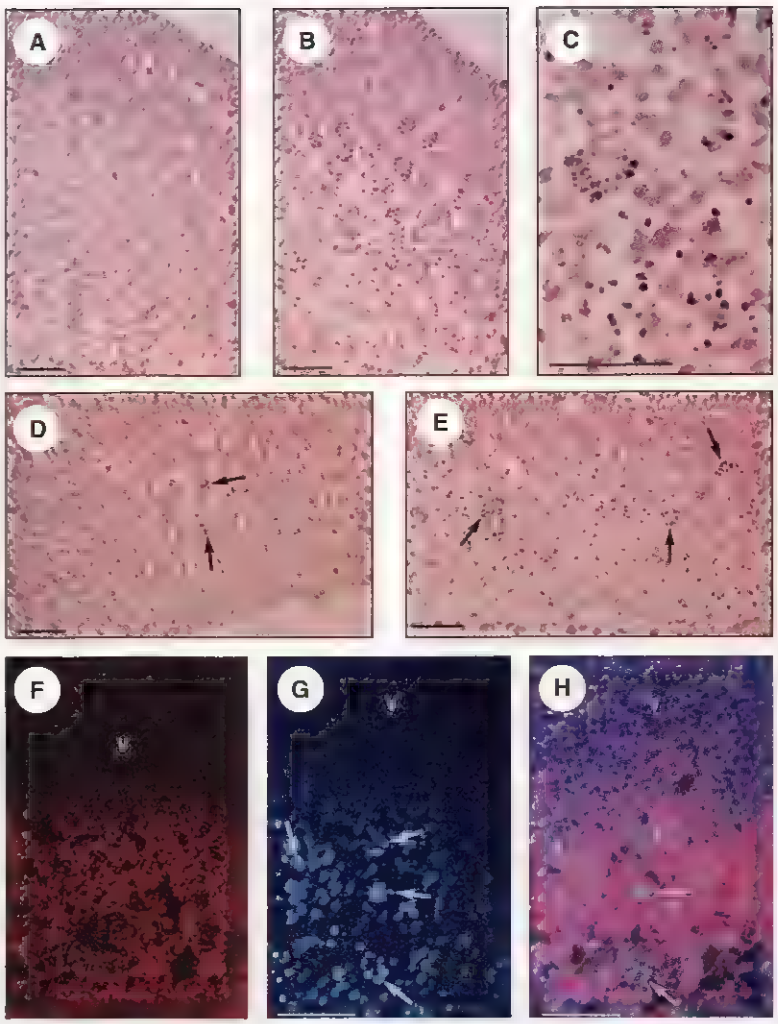

Fig. 2. Histologic appearance of E11.5 wild-type (A and D) and *bcl-x*$^{-/-}$ (B, C, and E) brainstem (A to C) and spinal cord (D and E) (*25*). A hematoxylin-eosin–stained section of the rostral pons from a wild-type mouse (**A**) shows immature neuroepithelial cells adjacent to the fourth ventricle (upper right corner) and ventrally located differentiating cells. A similarly located section from a *bcl-x*$^{-/-}$ animal (**B**) reveals extensive cell death of the differentiating neuroepithelial cells. High magnification (**C**) shows pyknotic nuclei, karyorrhectic debris, and distended phagocytic cells. A sagittal section of the rostral spinal cord from a wild-type mouse (**D**) shows occasional pyknotic nuclei and phagocytic cells in the ventral spinal cord (indicated by arrows). In comparison, the spinal cord of a *bcl-x*$^{-/-}$ mouse (**E**) contains enormous numbers of dead cells and phagocytes. MAP2 immunolabeling (F and H) and bisbenzamide staining (G and H) of E12.5 *bcl-x*$^{-/-}$ brainstem (F to H). The ventricular zone (labeled V) shows little MAP2 immunoreactivity, whereas cells located in the ventral medulla possess strong, bright red–fluorescent MAP2 immunoreactivity (**F**). Bisbenzamide staining (**G**) shows normal diffuse blue fluorescent nuclear staining of the ventricular zone cells (labeled V) and numerous clumped, fragmented, bright blue–white fluorescent nuclei (indicated by arrows) in the ventral medulla. Double exposure of MAP2 immunofluorescence and bisbenzamide labeling (**H**) shows weak MAP2 staining of the densely packed, immature cells of the ventricular zone (labeled V) and strong MAP2 labeling of cells in the differentiated zone, including some cells with abnormal bisbenzamide-stained nuclei (indicated by short arrows). Clusters of abnormal bisbenzamide-stained nuclei can be seen within phagocytes (indicated by arrows). Scale bars, 50 μm.

Table 1. Embryonic lethality of Bcl-x null mutation (*23*).

Age (days)	Number in litter	Total conceptuses	Number of normal-looking embryos	Genotype of normal embryos			Number of abnormal embryos*
				+/+	+/−	−/−	
E11.5-12.0	3	27	27	10	10	7	0
E12.5-13.0	4	37	36	13	16	7	1
E13.5-14.0	4	35	23	9	14	0	12
E14.5-15.0	1	10	9	3	6	0	1
E15.5-16.0	2	15	12	3	9	0	3

*All abnormal embryos were homozygous mutant (*bcl-x*$^{-/-}$) mice and had already died.

the increased neuronal death observed in the *bcl-x*$^{-/-}$ nervous system in vivo represents a primary event and is not simply secondary to the hematopoietic dysfunction described below.

To further define the degenerative changes observed in *bcl-x*$^{-/-}$ embryos, we stained sections of E12.5 mutant and wild-type mice by the terminal-deoxytransferase (TdT)–mediated deoxyuridine triphosphate (dUTP)–biotin nick end-labeling (TUNEL) method to identify apoptotic cells (*12*) (Fig. 3). In wild-type mice, occasional TUNEL-labeled nuclei were observed in the spinal cord and dorsal root ganglia. In comparison, mutant mice had an increase in the number of TUNEL-labeled nuclei in these sites, as well as in nonproliferative zones throughout the central nervous system (*8*). We also found a threefold increase in TUNEL-labeled nuclei in histologically identifiable hematopoietic cells in E12.5 *bcl-x*$^{-/-}$ liver compared to heterozygote and wild-type tissue (Fig. 3, C and D). To address the localization of *bcl-x* transcripts, we detected mRNA in E12.5 wild-type tissue sections by in situ hybridization (Fig. 4). Consistent with our findings that differentiating neurons in the intermediate zone and hematopoietic cells in the liver showed extensive apoptosis in *bcl-x*$^{-/-}$ mice, the *bcl-x* mRNA was expressed in those regions in wild-type mice. Because much of the observed cell death in the *bcl-x*$^{-/-}$ nervous system occurred prior to, or coincident with, terminal differentiation, it is unlikely that lack of target-derived neurotrophic factors or synaptic activity could account for the neuronal destruction. These findings suggest that programmed cell death in the developing brain and hematopoietic system is critically dependent on Bcl-x expression.

The lymphoid system is the second tissue where extensive apoptosis occurs and was found to be severely affected in the Bcl-2–deficient mice (*3*, *4*). Because of early embryonic lethality, we could not study the effect of Bcl-x absence on lymphocytes in the germline mutant mice. To study the function of Bcl-x in lymphocytes, we used the double-knockout method (*9*, *13*, *14*). We injected the *bcl-x*$^{-/-}$ ES or parental wild-type ES cells into the blastocysts from C57BL/6 (B6) and recombination activating gene–2 (RAG-2)–deficient mice to generate chimeric mice (B6 and RAG-2 chimeric mice, respectively).

In the chimeric mice, the maturation of *bcl-x*$^{-/-}$ T and B cells was reduced. In the thymus, there was a reduction in the proportion of mature CD4$^+$ or CD8$^+$ single positive (SP) thymocytes (Fig. 5A and Table 2). The thymocytes that did differentiate were derived from injected *bcl-x*$^{-/-}$ ES cells, as determined by Southern (DNA) blot analy-

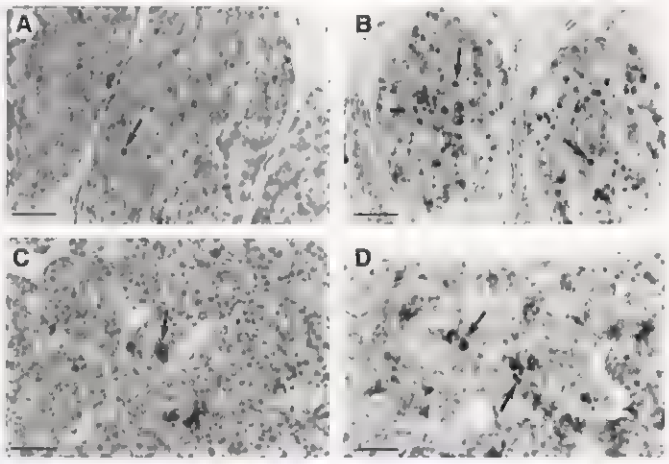

Fig. 3. TUNEL staining of E12.5 wild-type (A and C) and *bcl-x*$^{-/-}$ (B and D) dorsal root ganglia (A and B) and liver (C and D) (*26*). Scattered TUNEL-positive nuclei are seen in the wild-type dorsal root ganglia (**A**) and are greatly increased in the *bcl-x*$^{-/-}$ ganglia (**B**), which also appear shrunken. The frequency of TUNEL-positive nuclei in liver hematopoietic elements is low in wild-type mice (**C**) compared to *bcl-x*$^{-/-}$ mice (**D**). Scale bars, 50 μm.

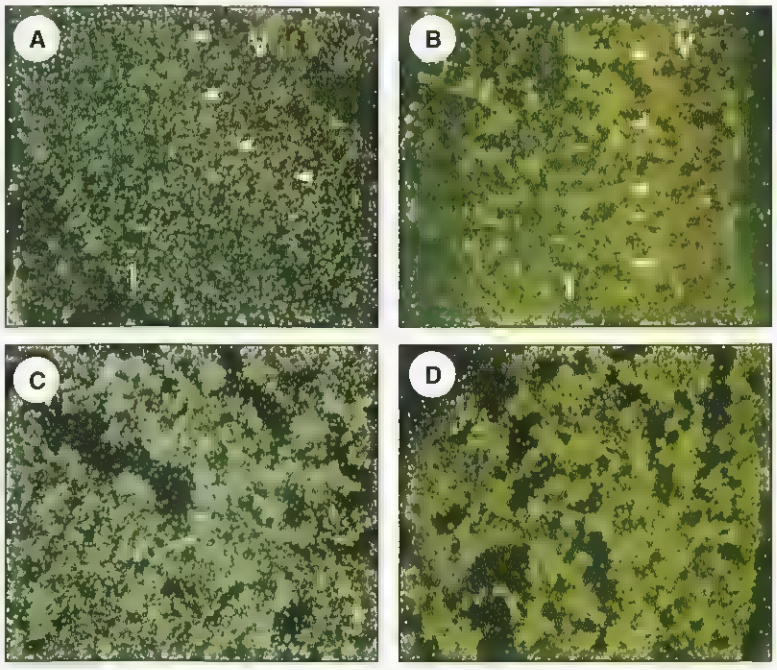

Fig. 4. In situ hybridizations of E12.5 wild-type (A and C) and *bcl-x*$^{-/-}$ (B and D) brain (A and B) and liver (C and D) (*27*). *bcl-x* mRNA was highly localized in the intermediate zone (labeled I) of the developing brain (**A**) and in the liver (**C**) of the wild-type mice. In comparison, *bcl-x*$^{-/-}$ mice had few grains similar to background level (**B** and **D**). Arrowheads indicate the border between ventricular (labeled V) and intermediate zones. Left side, intermediate zone; right side, ventricular zone.

Table 2. Proportion of lymphocyte populations in chimeric mice (*24*). Data show the proportion among Ly9.1$^+$ lymphocytes in B6 chimeric mice. SP, single positive; DP, double positive; BM, bone marrow; and LN, lymph node.

Genotype	Thymocytes		BM cells		LN cells		Splenocytes	
	SP	DP	B220$^+$IgM$^-$	B220$^+$IgM$^+$	T	B	T	B
Wild-type	21.8 ± 4.2 (n = 8)	73.3 ± 3.8 (n = 8)	50.8 ± 3.1 (n = 4)	26.2 ± 1.9 (n = 4)	63.0 ± 7.0 (n = 8)	33.3 ± 5.5 (n = 8)	64.4 ± 7.0 (n = 6)	21.0 ± 4.1 (n = 8)
bcl-x $^{-/-}$	14.3 ± 2.4 (n = 10)	78.4 ± 4.9 (n = 10)	27.8 ± 4.2 (n = 4)	10.0 ± 3.7 (n = 4)	58.2 ± 9.5 (n = 10)	30.4 ± 5.1 (n = 8)	39.4 ± 7.3 (n = 6)	14.1 ± 4.1 (n = 8)

sis (*8*, *15*). In the bone marrow (BM), the proportion of mature B cells was reduced (Fig. 5B and Table 2). In the B6 chimeric mice, the proportion of $B220^{dull}IgM^-$ cells was decreased (Table 2). This decrease was not evident in the RAG-2 chimeric mice because $B220^{dull}IgM^-$ cells were also derived from RAG-2 blastocysts (*14*). Forward scatter parameter analysis (*16*) showed that small pre-B cells rather than the large pro-B cells in the $B220^{dull}IgM^-$ population were preferentially decreased in both the B6 and RAG-2 chimeric mice (Fig. 5C) (*8*). In contrast, lymph node (LN) and spleen cells of *bcl-x*$^{-/-}$ chimeric mice showed normal population distribution, although the ratios of mature T and B cells were decreased (Table 2). Thus, *bcl-x*$^{-/-}$ lymphocytes can differentiate into mature cells, although the total number of mature lymphocytes generated is decreased.

Thymocytes, BM, and LN cells were cultured for examination of in vitro life-span. Among thymocytes, *bcl-x*$^{-/-}$ TCR^{med} cells, but not TCR^{hi} cells, died more quickly than controls (Fig. 6, A and B). Most *bcl-x*$^{-/-}$ double-positive (DP) thymocytes disappeared during a 48-hour culture (Fig. 5A). The *bcl-x*$^{-/-}$ $B220^+$ BM cells behaved similarly (Fig. 6D). On the basis of staining patterns of B220 versus IgM or of B220 versus IgD (*8*), $B220^{dull}IgM^-$ and immature B cells ($B220^{dull}IgM^+IgD^-$ cells) were involved (Fig. 5B). However, life-spans of mutant LN T and B cells were comparable to those of controls (Fig. 6, C and E), whereas mature T and B cells in *bcl-2*$^{-/-}$ LN cells are mostly apoptotic (*3*, *4*, *17*). Thus, the absence of Bcl-x affects the life-span and apoptosis of developing immature lymphoid cells rather than of their mature counterparts, whereas in the *bcl-2*$^{-/-}$ mice this pattern is reversed (*3*, *4*, *17*).

The abnormality we observed in the lymphoid system is similar to that which occurs in c-*abl*–deficient mice (*18*). Similarly, the abnormalities found in the nervous and hematopoietic systems are similar to those observed in *rb*-deficient mice (*19*). In the *rb*-deficient mice, differentiating neurons die in the brain and spinal cord, and hematopoiesis in the liver is abnormal. However, unlike in *rb*$^{-/-}$ brain, increased mitosis was not observed in *bcl-x*$^{-/-}$ brain. The c-Abl protein interacts physiologically with Rb protein (*20*), and both may be involved in cell cycle controls (*21*, *22*). These similarities and observations suggest the possibility of a functional connection between Bcl-x, c-Abl, and Rb.

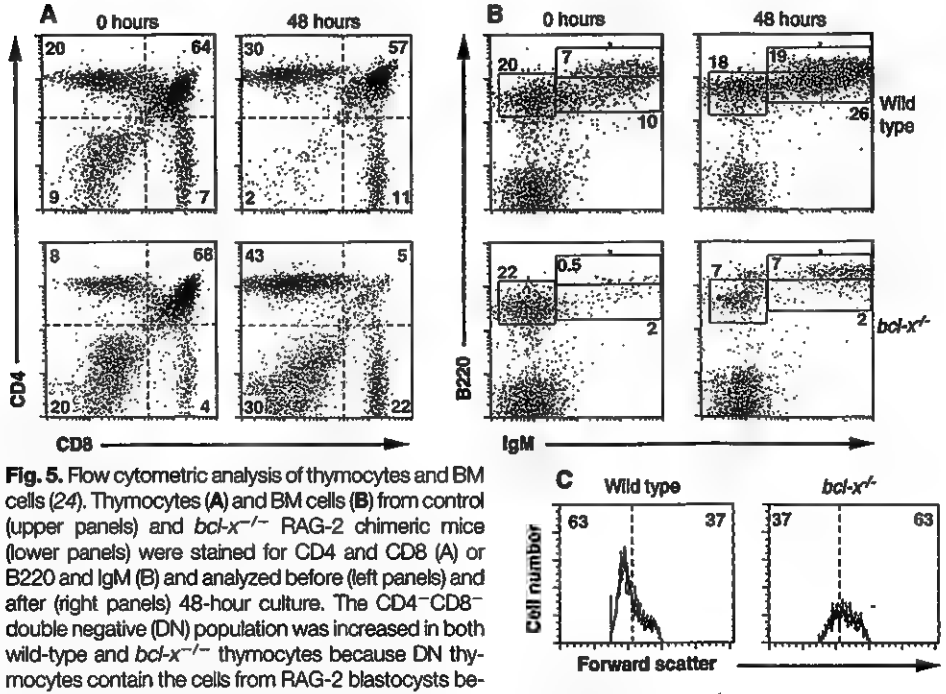

Fig. 5. Flow cytometric analysis of thymocytes and BM cells (*24*). Thymocytes (**A**) and BM cells (**B**) from control (upper panels) and *bcl-x*$^{-/-}$ RAG-2 chimeric mice (lower panels) were stained for CD4 and CD8 (A) or B220 and IgM (B) and analyzed before (left panels) and after (right panels) 48-hour culture. The $CD4^-CD8^-$ double negative (DN) population was increased in both wild-type and *bcl-x*$^{-/-}$ thymocytes because DN thymocytes contain the cells from RAG-2 blastocysts besides those from ES clones (*14*). BM cells (**C**) from control (left panel) and *bcl-x*$^{-/-}$ B6 chimeric mice (right panel) were gated on $Ly9.1^+B220^{dull}$,IgM^- population and cell size by forward scatter analysis.

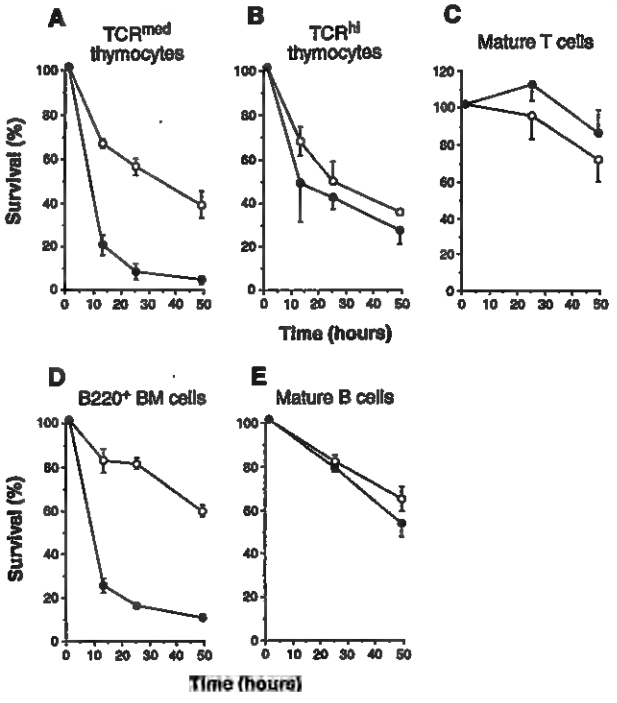

Fig. 6. In vitro cell survival of thymocytes and BM and LN cells. Assays were performed as described (*3*). TCR^{med} (**A**), TCR^{hi} thymocytes (**B**), LN T cells (**C**), $B220^+$ BM cells (**D**), and LN B cells (**E**) from *bcl-x*$^{-/-}$ (closed circles) and control (open circles) B6 chimeric mice were cultured for the indicated times. Experiments shown were done with three knockout and three control chimeras. Experiments were also performed with chimeras derived from different independent ES cell lines with similar results.

REFERENCES AND NOTES

1. D. L. Vaux, *Proc. Natl. Acad. Sci. U.S.A.* **90**, 786 (1993); E. Cuende *et al.*, *EMBO J.* **12**, 1555 (1993); T. E. Allsopp, S. Wyatt, H. F. Paterson, A. M. Davies, *Cell* **73**, 295 (1993); A. Batistatou, D. E. Merry, S. J. Korsmeyer, L. A. Greene, *J. Neurosci.* **13**, 4422 (1993); L.-T. Zhong *et al.*, *Proc. Natl. Acad. Sci. U.S.A.* **90**, 4533 (1993); M. Dubois-Dauphin, H. Frankowski, Y. Tsujimoto, J. Huarte, J.-C. Martinou, *ibid.* **91**, 3309 (1994).
2. D. M. Hockenbery, M. Zutter, W. Hickey, M. Nahm, S. J. Korsmeyer, *Proc. Natl. Acad. Sci. U.S.A.* **88**, 6961 (1991); D. P. LeBrun, R. A. Warnke, M. L. Cleary, *Am. J. Pathol.* **142**, 743 (1993); D. Veis-Novack and S. J. Korsmeyer, *ibid.* **145**, 61 (1994); D. E. Merry, D. J. Veis, W. F. Hickey, S. J. Korsmeyer, *Development* **120**, 301 (1994).
3. K.-i. Nakayama *et al.*, *Science* **261**, 1584 (1993).
4. K. Nakayama *et al.*, *Proc. Natl. Acad. Sci. U.S.A.* **91**, 3700 (1994); D. J. Veis, C. M. Sorenson, J. R. Shutter, S. J. Korsmeyer, *Cell* **75**, 229 (1993).
5. G. T. Williams and C. A. Smith, *Cell* **74**, 777 (1993); E. Y. Lin, A. Orlofsky, M. S. Berger, M. B. Prystowsky, *J. Immunol.* **151**, 1979 (1993).
6. L. H. Boise *et al.*, *Cell* **74**, 597 (1993).
7. M. Gonzalez-Garcia *et al.*, *Development* **120**, 3033 (1994); W. Fang, J. J. Rivard, D. L. Mueller, T. W. Behrens, *J. Immunol.* **153**, 4388 (1994); S. Krajewski *et al.*, *Cancer Res.* **54**, 5501 (1994).
8. N. Motoyama, K. A. Roth, D. Y. Loh, unpublished observations.
9. Genomic DNA containing the *bcl-x* locus was isolated from a library of mouse strain 129 DNA (Strat-

agene). A 1.8-kb Xho I–Bam HI fragment containing most of the Bcl-x coding region was replaced with either a PGK-*neo* polyadenylate [poly(A)] cassette or a PGK-*hyg* poly(A) cassette. The targeting vectors, pXKO-NEO and pXKO-HYG, contain a 6.0-kb region of homology 5′ and 1.0 kb 3′ of the drug-resistance markers and a PGK-*tk* poly(A) cassette. Transfections and selections were performed as described (*3*). DNAs prepared from ES cells were digested with Eco RV, transferred to a nylon membrane, and then hybridized with the 0.4-kb Kpn I–Pst I probe that flanked the 3′ homology region. Expected sizes for wild-type *bcl-x*, mutant *bcl-x* by pXKO-NEO, and mutant *bcl-x* by pXKO-HYG are 9.8, 7.0, and 5.5 kb and were detected in wild-type, *bcl-x*$^{+/-}$, and *bcl-x*$^{-/-}$ ES clones, respectively.

10. R. W. Oppenheim, *Annu. Rev. Neurosci.* **14**, 453 (1991).
11. B. Riederer and A. Matus, *Proc. Natl. Acad. Sci. U.S.A.* **82**, 6006 (1985); R. P. Tucker, L. I. Binder, A. I. Matus, *J. Comp. Neurol.* **271**, 44 (1988).
12. Y. Gavrieli, Y. Sherman, S. A. Ben-Sasson, *J. Cell Biol.* **119**, 493 (1992).
13. A. Jakobovits *et al.*, *Proc. Natl. Acad. Sci. U.S.A.* **90**, 2551 (1993).
14. J. Chen, R. Lansford, V. Stewart, F. Young, F. W. Alt, *ibid.*, p. 4528; J. Chen *et al.*, *Immunity* **1**, 65 (1994).
15. ES-derived thymocytes were purified with an antibody to CD8 (anti-CD8) and magnetic beads from *bcl-x*$^{-/-}$ or wild-type RAG-2 chimeric mice as described (*3*). DNAs prepared from the purified CD8-positive thymocytes were subjected to Southern blot analysis as described above.
16. D. Kitamura *et al.*, *Cell* **69**, 823 (1992).
17. K.-i. Nakayama, K. Nakayama, L. B. Dustin, D. Y. Loh, in preparation.
18. V. L. J. Tybulewicz, C. E. Crawford, P. K. Jackson, R. T. Bronson, R. C. Mulligan, *Cell* **65**, 1153 (1991); P. L. Schwartzberg *et al.*, *ibid.*, p. 1165.
19. E. Y.-H. P. Lee *et al.*, *Nature* **359**, 288 (1992); T. Jacks *et al.*, *ibid.*, p. 295; A. R. Clarke *et al.*, *ibid.*, p. 328.
20. P. J. Welch and J. Y. J. Wang, *Cell* **75**, 779 (1993).
21. D. W. Goodrich, N. P. Wang, Y.-W. Qian, E. Y.-H. P. Lee, W.-H. Lee, *ibid.* **67**, 293 (1991).
22. C. L. Sawyers, J. McLaughlin, A. Goga, M. Havlik, O. Witte, *ibid.* **77**, 121 (1994).
23. One of four *bcl-x*$^{-/-}$ mice at E12.5 and two E13.5 *bcl-x*$^{-/-}$ mice were examined histologically and showed autolytic changes throughout the embryonic tissues indicative of intrauterine death. Careful examination of the three viable E12.5 *bcl-x*$^{-/-}$ embryos showed no obvious gross fetal abnormality, and histologic examination of two E12.5 *bcl-x*$^{-/-}$ placentas showed normal maternal and fetal components. In the embryonic mouse, yolk-sac–derived nucleated red blood cells begin to disappear from the circulation around E12, when the liver becomes the principal source of hematopoietic activity [M. H. Kaufmann, *The Atlas of Mouse Development* (Academic Press, San Diego, CA, 1992), p. 128]. Because the *bcl-x*$^{-/-}$ mice were paler, died at approximately E13, and showed a marked increase in TUNEL-labeled nuclei in the hematopoietic elements of the liver, it is possible that a defect in hepatic hematopoiesis, coupled with declining numbers of yolk sac–derived red cells, produces hypoxic damage to the embryo, resulting in death.
24. Thymocytes and BM and LN cells (1 × 10^6 cells each) were prepared from wild-type and *bcl-x*$^{-/-}$ B6 chimeric mice and were stained with anti-Ly9.1–fluorescein isothiocyanate (FITC), and anti-CD4–phycoerythrin (PE) and anti-CD8–biotin, or anti-B220–PE and anti-immunoglobulin M (IgM)–biotin (PharMingen). For RAG-2 chimeric mice, cells were stained with anti-CD8–FITC and anti-CD4–PE, or anti-IgM–FITC or anti-IgD–FITC (Southern Biotechnology) and anti-B220–PE. Biotin conjugate was revealed by RED 613-streptavidin (Gibco BRL). Dead cells were excluded by staining with propidium iodide (Boehringer Mannheim). Flow cytometric analysis was done on FACScan computer and software (Becton Dickinson).
25. Whole embryos were fixed in 4% paraformaldehyde and embedded in paraffin, and 5-μm-thick sagittal sections were cut at multiple levels. Sections were alternatively stained with hematoxylin-eosin and with cresyl violet. Unstained sections were processed for immunostaining as described [M. L. Hermiston, C. B. Latham, J. I. Gordon, K. A. Roth, *J. Histochem. Cytochem.* **40**, 1283 (1992)]. A mouse monoclonal antibody to MAP2 (Sigma) was used at a dilution of 1:1000 to detect differentiating neurons. Primary antibodies were detected with a CY-3-conjugated donkey antiserum to mouse IgG (Jackson Immunoresearch Laboratories). Omission of the primary antibody resulted in only weak, nonspecific labeling of the blood vessels. After immunolabeling, sections were incubated for 10 min at room temperature in bisbenzamide (0.04 μg/ml) (Hoechst 33258, Sigma) to label cell nuclei. Slides were viewed and photographed with a Zeiss Axioskop fluorescence microscope.
26. Apoptotic cells were identified by the TUNEL method (*12*) modified to detect incorporated digoxygenin-dUTP with either alkaline phosphatase or gold-conjugated sheep antibody to digoxygenin.
27. In situ hybridizations were performed as described [H. Sawa, B. E. Sobel, S. Fujii, *Circ. Res.* **73**, 671 (1993)]. For construction of RNA probes, pBluescript SKII+ plasmid containing a 0.8-kb mouse *bcl-x* complementary DNA insert was linearized by restriction digestion with Xho I or Not I (for antisense and sense, respectively) and transcribed with T7 or T3 RNA polymerase in the presence of ^{35}S-labeled uridine triphosphate (UTP).
28. We thank F. W. Alt for RAG-2–deficient mice, P. Mombaerts for E14 ES cell line, J. Y. J. Wang for helpful suggestions, and L. B. Dustin and I. T. Chan for critical reading of the manuscript. Supported by the Howard Hughes Medical Institute (D.Y.L.) and the Japan Society for the Promotion of Science (N.M.).

2 November 1994; accepted 9 February 1995

Synaptic Desensitization of NMDA Receptors by Calcineurin

Gang Tong,* Dawn Shepherd, Craig E. Jahr†

Desensitization is a phenomenon that is common to many ligand-gated ion channels but has been demonstrated only rarely with physiological stimulation. Numerous studies describe desensitization of the *N*-methyl-D-aspartate (NMDA) subtype of glutamate receptor by exogenous agonists, but whether synaptic stimulation causes desensitization has been unknown. Synaptic stimulation of NMDA receptors on rat hippocampal neurons resulted in desensitization that was prevented by intracellular 1,2-bis(*o*-aminophenoxy)ethane-*N*,*N*,*N*′,*N*′-tetraacetic acid (BAPTA), adenosine-5′-*O*-(3-thiotriphosphate) (ATP-γ-S), or inhibitors of phosphatase 2B (calcineurin), but not by inhibitors of phosphatases 1 and 2A or of tyrosine phosphatases. Synaptic NMDA receptors may fluctuate between phosphorylated and dephosphorylated forms, depending on the rate of synaptic stimulation and the magnitude of the associated influx of calcium through NMDA receptors.

The magnitude of Ca^{2+} influx through synaptically activated NMDA receptor channels not only affects the amplitude and lifetime of long-term synaptic plasticity at certain central synapses, but also is a factor in whether subsequent synaptic strength is increased or decreased (*1*–*3*). Several species of protein phosphatases cause diminished NMDA channel activity (*4*–*6*), which may result in decreased Ca^{2+} influx during synaptic stimulation. In addition, calcineurin activity stimulated by brief elevations of intracellular Ca^{2+} concentration (*7*) causes the development of a glycine-insensitive form (*8*, *9*) of NMDA receptor desensitization. Because NMDA receptor channels are very permeable to Ca^{2+} (*10*), synaptic activation may enable this form of desensitization and may result in a negative feedback of NMDA receptor synaptic activation. If desensitization is enhanced by synaptic stimulation, the decrease in ion flux will result in smaller intracellular Ca^{2+} transients that could shift the balance between long-term potentiation (LTP) and long-term depression (LTD) of synaptic strength (*1*–*3*).

Isolated cultured rat hippocampal neurons make synapses onto themselves (*11*) and were used to measure NMDA receptor desensitization induced by synaptic stimulation. The synapses were conditioned by stimulating them four times within 75 ms (*12*) and were tested with a single stimulus after a variable interval (0.8 to 7.5 s). The depression of the test excitatory postsynaptic current (EPSC) relative to the first conditioning EPSC could result from a combination of a lower presynaptic release probability (synaptic depression or presynaptic inhibition) and a decreased sensitivity of postsynaptic receptors (desensitization). The amount of depression resulting from NMDA receptor desensitization was estimated by comparing the amplitudes of test EPSCs conditioned by the four-pulse conditioning stimulus delivered in the presence or absence of the competitive antagonist of the NMDA receptor, D-2-amino-5-phosphonopentanoic acid (D-AP5, 100 μM) (Fig. 1A). In the presence of D-AP5, glutamate released by

G. Tong and C. E. Jahr, Vollum Institute and Department of Cell Biology and Anatomy, Oregon Health Sciences University, Portland, OR 97201–3098, USA.
D. Shepherd, Vollum Institute, Oregon Health Sciences University, Portland, OR 97201–3098, USA.

*Present address: Department of Pharmacology, University of California, San Francisco, CA 94143, USA.
†To whom correspondence should be addressed.

conditioning stimuli will not bind to NMDA receptors, and thus agonist-induced desensitization will not occur. We rapidly removed D-AP5 from the synapse by switching to a solution without D-AP5 after the last conditioning stimulus (*13*). Because the probability of release from individual release sites is about 0.5 or lower (*14*), four conditioning stimuli were used to maximize the percentage of release sites (and thus NMDA receptors) that were activated. In saturating concentrations of glycine (20 μM), the test EPSC evoked 1.5 s after delivery of the conditioning stimuli was 78.7 ± 2.0% of the test EPSC evoked after the conditioning stimuli that were applied while D-AP5 was present. This observation indicates that synaptic activation of NMDA receptors results in receptor desensitization that is glycine-insensitive.

These experiments were repeated in an extracellular solution containing 1 mM Mg^{2+} because, at this physiological concentration, Mg^{2+} blocks more than 95% of the NMDA receptor current (and thus Ca^{2+} influx) at a holding potential of −70 mV and about 80% of the current at −40 mV (*15*). When the membrane potential was held at −40 mV for 100 ms after delivery of the conditioning stimuli to approximate normal synaptic transmission, the test EPSC evoked 1.5 s after delivery of the conditioning stimuli was 84.4 ± 3.2% of the test EPSC evoked after the conditioning stimuli that were applied while D-AP5 was present (paired *t* test, $P < 0.005$, $n = 5$) (Fig. 1B). Therefore, the amount of calcium influx in physiological conditions is sufficient to densensitize NMDA receptors. However, when the membrane potential was held at −70 mV continuously, the test EPSCs in the presence and absence of D-AP5 were indistinguishable (100.8 ± 3.0%, $n = 8$). Therefore, partial relief of Mg^{2+} inhibition of NMDA channels is necessary for synaptic activation of NMDA receptor desensitization.

The time course of recovery from desensitization (Fig. 1C) was very similar to that in outside-out patches (*8*, *9*); complete recovery required more than 7.5 s. Periods between conditioning and test EPSCs shorter than 0.8 s were not tested because of the slow decay of synaptic current evoked by the conditioning stimuli, which interfered with the measurement of desensitization, and because of the finite time required to completely wash away D-AP5. Because desensitization in outside-out patches is greatest at much shorter intervals (*8*, *9*), it is likely that shortly after the conditioning stimuli were applied, desensitization was more profound than it was 0.8 s later.

We also monitored (*S*)-α-amino-3-hydroxy-5-methyl-4-isoxazolepropionic acid (AMPA) receptor EPSCs to control for possible effects of NMDA receptor stimulation on presynaptic release probability—for example, through the action of retrograde transmitters (*3*). Conditioning stimuli were applied in the presence and absence of D-AP5, as described above, but in the absence of AMPA receptor blockers. The test stimulus was given in the presence of D-AP5 so

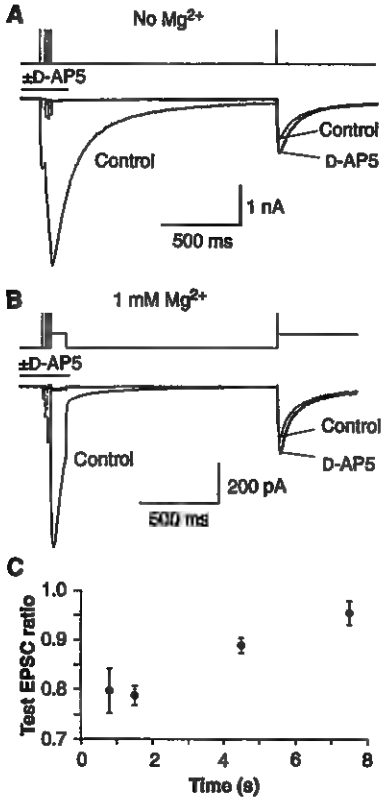

Fig. 1. Glycine-insensitive synaptic desensitization of NMDA receptors. (**A**) In the absence of extracellular Mg^{2+}, four conditioning NMDA receptor EPSCs were evoked in rapid succession (*12*) in the presence (thick line) or absence (control; thin line) of 100 μM D-AP5; a test EPSC was evoked 1.5 s later (more than 1 s after switching to a solution without D-AP5). The top trace indicates the voltage command protocol used to stimulate the synapse. The holding potential was −70 mV. (**B**) Similar protocol to that used in (A), but in the continuous presence of 1 mM extracellular Mg^{2+} and with voltage jumps to −40 mV (as shown in the upper trace) to allow partial relief of inhibition of NMDA channels during conditioning and test EPSCs. Responses recorded in the continuous presence of D-AP5 were subtracted to remove voltage jump leak currents. (**C**) The time course of recovery from desensitization is plotted as the ratio of the test EPSCs evoked following conditioning stimuli that were delivered in the absence and presence of D-AP5, respectively. EPSC amplitudes were measured from the base line value before delivery of the conditioning stimuli and thus underestimate the degree of desensitization. The two sets of responses were interleaved in time to control for time-dependent changes in synaptic strength.

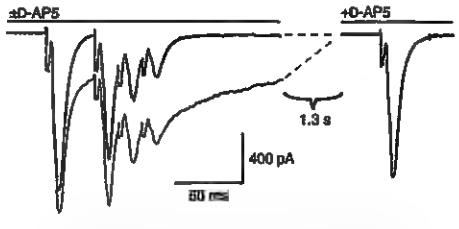

Fig. 2. Activation of NMDA receptors does not alter presynaptic release. The same stimulation protocol as in Fig. 1A was used in the absence of AMPA receptor blockers. Test EPSCs are superimposed. The interval between the first conditioning stimulus and the test stimulus was 1.5 s; the gap in records is 1.3 s.

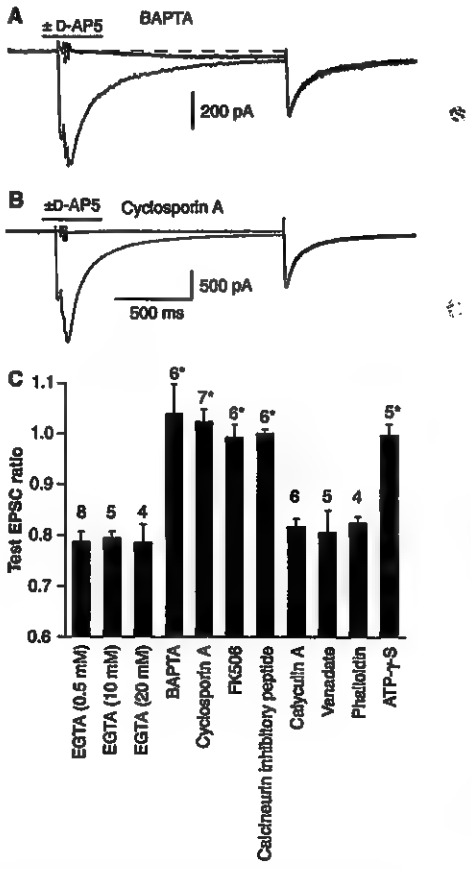

Fig. 3. Synaptic desensitization is prevented by internal BAPTA and calcineurin inhibitors. (**A**) The same protocol as that used in Fig. 1A, with an intracellular solution containing 20 mM BAPTA instead of EGTA. The small current that developed after washout of D-AP5 (dotted line is base line) was seen in 37 of 85 recordings and was caused, at least in part, by an increased frequency of spontaneous EPSCs (*23*). (**B**) EPSCs recorded with 200 nM cyclosporin A in external and internal solutions. (**C**) Graph of the ratio of the amplitudes of test EPSCs recorded after conditioning stimuli were applied in the absence or presence of D-AP5. The interval between the first conditioning stimulus and the test stimulus was 1.5 s. The number of cells in each category is printed above the bars. Asterisks indicate significant differences ($P < 0.01$) from the 0.5 mM EGTA condition (analysis of variance). Error bars represent SEM.

that the AMPA receptor EPSC could be recorded in isolation (Fig. 2). Activation of NMDA receptors by the conditioning stimuli had no effect on the amplitude of the AMPA receptor test EPSC (100.1 ± 1.6%, n = 6). AMPA receptor EPSCs recorded in the presence of 2 mM extracellular Mg^{2+} to block NMDA receptor currents were not affected by 100 μM D-AP5 (n = 4).

In outside-out patches, the fast phase of development of glycine-insensitive desensitization is blocked by internal BAPTA, by ATP-γ-S, and by inhibitors of calcineurin (*7*). We used the same manipulations to block the synaptic form of desensitization. Although there was no difference in the amount of desensitization in recordings with 0.5 to 20 mM internal EGTA, 20 mM internal BAPTA blocked desensitization (Fig. 3, A and C). Addition of the specific inhibitors of calcineurin, cyclosporin A (200 to 500 nM), FK506 (200 to 500 nM), or calcineurin inhibitory peptide (270 μM) (*16*), blocked synaptic desensitization after 4 to 7 min of recording (Fig. 3, B and C). Synaptic desensitization was not prevented by calyculin A (200 nM), a phosphatase 1 and 2A inhibitor (*17*); by intracellular vanadate (1 mM), a tyrosine phosphatase inhibitor (*18*); or by phalloidin (1 μM), which stabilizes filamentous actin (*19*) and has been shown to prevent Ca^{2+}-dependent rundown of the NMDA receptor (*20*) (Fig. 3C). However, inclusion of 1 mM ATP-γ-S in the internal solution blocked desensitization within 4 to 6 min of the start of recordings (Fig. 3C).

These results indicate that the phosphorylation state of the NMDA receptor, or of an associated protein, alters NMDA receptor desensitization. Because synaptic desensitization is dependent on Ca^{2+} influx through NMDA receptor channels and subsequent activation of calcineurin, synaptic NMDA receptor complex may be dephosphorylated with each quantum of released transmitter. Inhibition of the effect of Ca^{2+} influx by chelation required the extremely fast binding properties of BAPTA (*21*); EGTA at concentrations that result in smaller amounts of free Ca^{2+} at equilibrium did not block synaptic desensitization. This observation suggests that the site of action of Ca^{2+} is very close to the cytoplasmic face of synaptic NMDA receptor channels. Calcineurin is reported to be associated with postsynaptic densities (*22*); this provides the spatial specificity for this mechanism.

Because recovery from desensitization requires several seconds, regulation of NMDA receptor function by this mechanism may be strong enough to significantly alter Ca^{2+}-dependent processes invoked by repetitive synaptic activity. The balance between homosynaptic LTD and LTP in the hippocampus depends in part on the magnitude of the increase of intracellular Ca^{2+} concentration as a result of influx through NMDA channels (*1–3*). Low-frequency stimulation (1 Hz) increases the intracellular Ca^{2+} concentration sufficiently to induce a calcineurin-dependent homosynaptic LTD (*2*), whereas high-frequency stimulation (100 Hz) raises Ca^{2+} to concentrations at which other Ca^{2+}-dependent reactions predominate and produce LTP (*3*). Thus, inhibition of induction of LTD by calcineurin blockers (*2*) may in part be a result of decreased NMDA receptor desensitization leading to greater intracellular Ca^{2+} concentrations during low-frequency stimulation.

REFERENCES AND NOTES

1. S. M. Dudek and M. F. Bear, *Proc. Natl. Acad. Sci. U.S.A.* **89**, 4363 (1992).
2. R. M. Mulkey *et al.*, *Nature* **369**, 486 (1994).
3. M. F. Bear and R. C. Malenka, *Curr. Opin. Neurobiol.* **4**, 389 (1994).
4. L.-Y. Wang *et al.*, *Nature* **369**, 230 (1994).
5. D. N. Lieberman and I. Mody, *ibid.*, p. 235.
6. Y. T. Wang and M. W. Salter, *ibid.*, p. 233.
7. G. Tong and C. E. Jahr, *J. Neurophysiol.* **72**, 754 (1994).
8. W. Salther *et al.*, *Neuron* **4**, 725 (1990); I. V. Chizhmakov *et al.*, *J. Physiol. (London)* **448**, 453 (1992).
9. R. A. J. Lester and C. E. Jahr, *J. Neurosci.* **12**, 635 (1992).
10. M. L. Mayer *et al.*, *ibid.* **7**, 3230 (1987); P. Ascher and L. Nowak, *J. Physiol. (London)* **399**, 247 (1988); C. E. Jahr and C. F. Stevens, *Nature* **325**, 522 (1987); C. Rosenmund *et al.*, *J. Neurophysiol.* **73**, 427 (1995).
11. J. M. Bekkers and C. F. Stevens, *Proc. Natl. Acad. Sci. U.S.A.* **88**, 7834 (1991). Whole-cell recordings of autaptic currents and miniature EPSCs were made (Axopatch-1D) with low-resistance patch pipettes (0.5 to 2.5 megohms) containing 150 mM potassium gluconate, 10 mM NaCl, 10 mM Hepes, 0.5 mM EGTA (except where noted), 4 mM magnesium adenosine triphosphate, and 0.2 mM guanosine triphosphate, adjusted to pH 7.3 with KOH. Control extracellular solution contained 160 mM NaCl, 3 mM KCl, 5 mM Hepes, 2 mM $CaCl_2$, 20 μM glycine, 5 μM 2,3-dihydroxy-6-nitro-7-sulfamoyl-benzo(F)quinoxaline (NBQX), and 50 to 100 μM picrotoxin, adjusted to pH 7.4 with NaOH. Autaptic EPSCs were evoked with voltage jumps to −20 or 0 mV from a holding potential of −60 to −90 mV (durations of 0.3 to 2 ms). Currents were sent through a low-pass filter at 0.5 to 10 kHz and were digitally sampled at 1 to 50 kHz. Series resistance compensation (80 to 100%) was used in all experiments. All experiments were performed at 22° to 24°C. Data are expressed as mean ± SEM.
12. The first two stimuli of the conditioning train were delivered 35 ms apart to allow for accurate measurement of the amplitude of the first EPSC. The second to fourth stimuli were delivered 20 ms apart.
13. Solution changes were made with gravity-fed flow tubes (*7*, *9*).
14. N. A. Hessler *et al.*, *Nature* **366**, 569 (1993); C. Rosenmund *et al.*, *Science* **262**, 754 (1993).
15. C. E. Jahr and C. F. Stevens, *J. Neurosci.* **10**, 3178 (1990).
16. J. Kunz and N. N. Hall, *Trends Biochem. Sci.* **18**, 334 (1993); Y. Hashimoto, B. A. Perrino, T. R. Soderling, *J. Biol. Chem.* **265**, 1924 (1990). FK506 was added to the external solution, calcineurin inhibitory peptide was added to the internal solution, and cyclosporin A was added to both solutions.
17. H. Ishihara *et al.*, *Biochem. Biophys. Res. Commun.* **159**, 871 (1989). Calyculin A was added to the external solution.
18. G. Swarup *et al.*, *ibid.* **107**, 1104 (1982).
19. J. A. Cooper, *J. Cell Biol.* **105**, 1473 (1987).
20. C. Rosenmund and G. L. Westbrook, *Neuron* **10**, 805 (1993).
21. R. Pethig *et al.*, *Cell Calcium* **10**, 491 (1989).
22. S. Goto *et al.*, *Brain Res.* **397**, 161 (1986).
23. In two cells that exhibited the development of this current after washout of D-AP5, the frequencies of AMPA receptor spontaneous EPSCs (in the presence of D-AP5 and 2 mM Mg^{2+}) recorded after the four-pulse conditioning stimulus was delivered were two and four times, respectively, the unstimulated frequency. In an additional cell, the frequency increased to a point where spontaneous events summated and could not be counted. It is unlikely that free glutamate remained in the cleft after delivery of the conditioning stimulus because the D-AP5 was washed out in this interval; this result suggests that the synaptic clefts were well perfused.

24. Supported by NIH grant NS21419.

29 August 1994; accepted 21 December 1994

Storage of 7 ± 2 Short-Term Memories in Oscillatory Subcycles

John E. Lisman* and Marco A. P. Idiart

Psychophysical measurements indicate that human subjects can store approximately seven short-term memories. Physiological studies suggest that short-term memories are stored by patterns of neuronal activity. Here it is shown that activity patterns associated with multiple memories can be stored in a single neural network that exhibits nested oscillations similar to those recorded from the brain. Each memory is stored in a different high-frequency ("40 hertz") subcycle of a low-frequency oscillation. Memory patterns repeat on each low-frequency (5 to 12 hertz) oscillation, a repetition that relies on activity-dependent changes in membrane excitability rather than reverberatory circuits. This work suggests that brain oscillations are a timing mechanism for controlling the serial processing of short-term memories.

Some forms of short-term memory appear to be stored by neurons that continue to fire after they are excited by a brief input (*1*). Hebb and others (*2*) proposed that such firing is sustained by reverberation of electrical activity in neuronal loops. We now demonstrate the feasibility of an alternative mechanism that is based on known properties of hippocampal and cortical neurons: Firing is sustained by an increase in mem-

brane excitability (3, 4) that is refreshed on each cycle of a network oscillation. We also show that a simple oscillatory neuronal network that incorporates this mechanism can store multiple short-term memories, in accordance with psychophysical experiments showing that humans can store 7 ± 2 short-term memories (5). The model is based on the properties of known brain oscillations and suggests a specific role for these oscillations in memory function.

A mechanism by which firing can be maintained during short-term memory is suggested by recent biophysical measurements of the effects of acetylcholine and serotonin, neuromodulators that are released during periods of brain oscillation (6). In the absence of these neuromodulators, firing induces an afterhyperpolarization, which results in a transient decrease in excitability. However, in their presence, firing induces an afterdepolarization (ADP), which results in a transient increase in excitability (3). This ADP is too brief to account for the duration of short-term memory, but it is long enough to store information between cycles of oscillations in the theta-alpha range (5 to 12 Hz). Thus, if the ADP triggered in one cycle promoted firing in the next, the ADP would be refreshed during each cycle and firing could be maintained for many cycles. To examine this putative storage role of the ADP, we performed computer simulations. Each neuron (Fig. 1A) was assumed to receive a suprathreshold excitatory input that carries the information to be stored and an input that generates a subthreshold low-frequency oscillation. The simulations show (Fig. 1A) that after a neuron is excited by a single brief input, it fires on subsequent oscillatory cycles, thereby performing a storage function. A single memory could be stored by the spatial pattern of firing in a group of such neurons.

We next elaborated on this model to account for the ability of the brain to store approximately seven short-term memories (5) (Fig. 2A). An important clue regarding the underlying mechanisms is provided by experiments performed by Sternberg (7): A subject was exposed to a list of items and then to a test item. The subject pressed a button to indicate whether the test item was on the list and the reaction time was measured. For each additional item on the list, the reaction time increased by ~38 ms (Fig. 2B), an observation that is consistent with a serial scan process. This time increment corresponds to a cycle of a high-frequency brain oscillation in the beta-gamma range (8). If seven cycles of high-frequency oscillation were nested together by a low-frequency oscillation, the nesting oscillation would be in the range of alpha-theta oscillations (5 to 12 Hz). Thus, different memories may be stored in different high-frequency ("40 Hz") subcycles of a low-frequency oscillation. This possibility is strengthened by recent observations in cor-

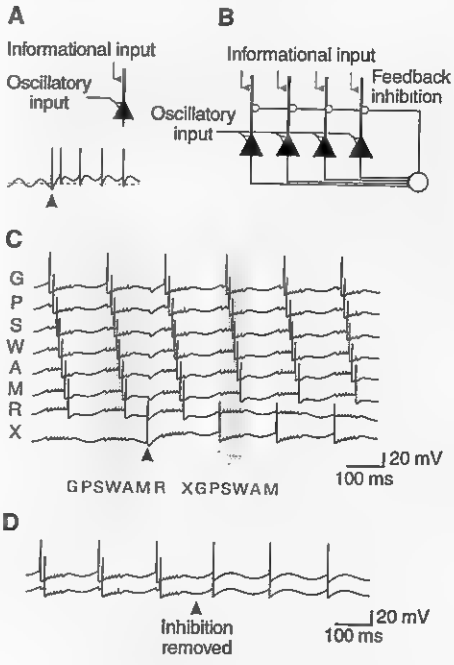

Fig. 1. (**A**) The ADP allows information storage in a single cell. The neuron receives a suprathreshold informational input and a second, subthreshold input that induces the membrane potential to oscillate at theta frequency (negative phase due to inhibition). Simulations (23) show membrane potential before and after informational input (arrowhead). (**B**) Network in which pyramidal cells make converging excitatory synapses onto an inhibitory interneuron that produces feedback inhibition of pyramidal cells. (**C**) The network can maintain the firing and correct phase of seven groups of cells that are active during different subcycles of the low-frequency oscillation. Each trace illustrates the synchronous firing of a group of cells whose spatial pattern encodes the memory of a letter. The dashed lines during the second and fourth theta cycles show the different subcycles. The limited memory capacity of the network is demonstrated by its failure to store eight memories. Input of the memory X is successful (arrowhead), but R is lost. (**D**) If feedback inhibition is removed (arrowhead), the "40-Hz" oscillation and phase information is rapidly lost. The two traces represent two of the seven memories stored in the network. A small phase difference (too small to be shown) persists for one cycle after removal of inhibition.

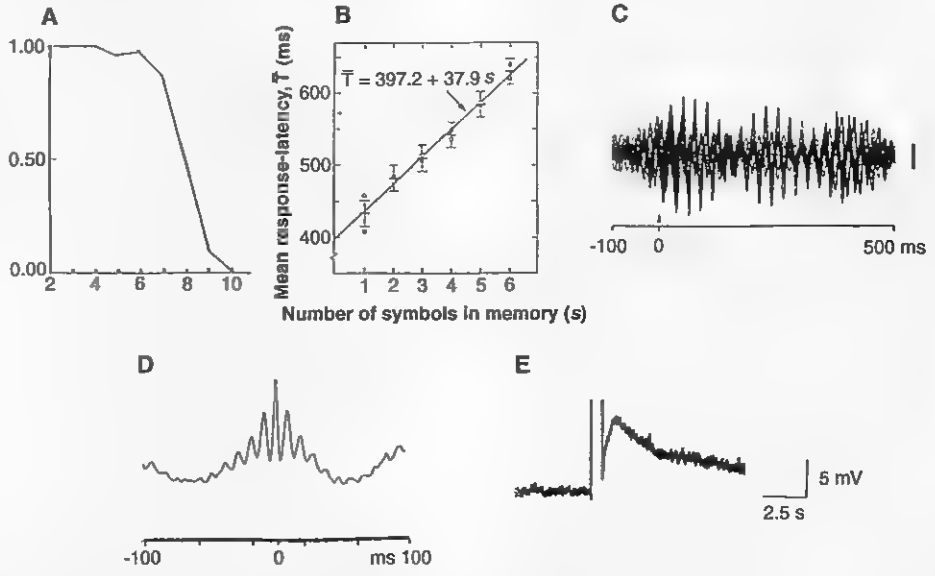

Fig. 2. Psychophysical and physiological data relevant to the model of short-term memory (**A**) Human short-term memory capacity for list items. Probability of correct recall of entire list (*y* axis) as a function of list size (*x* axis). [Reproduced with permission from (24)] (**B**) Evidence for exhaustive serial scanning of the memory list. The subject responds if the test item is on the stored list. Response time is plotted as a function of the number of symbols in memory. [Reproduced with permission from (7)] (**C**) Nested oscillations demonstrated in a magnetoencephalographic recording of human cortical responses evoked by an acoustic stimulus. [Reproduced with permission from (9)] (**D**) Nested oscillations recorded from the hilar region of the rat hippocampus. The record is an average, triggered on high-frequency peaks of the waveform. [Reproduced with permission from Bragin *et al.* (10)] (**E**) ADP recorded with an intracellular microelectrode from a cortical pyramidal cell. The large initial deflection is due to a current pulse that evokes action potentials. After the end of current injection, the ADP rises slowly and then falls (previously unpublished record provided by R. Andrade).

J. E. Lisman, Department of Biology and Center for Complex Systems, Brandeis University, Waltham, MA 02254, USA.
M. A. P. Idiart, Department of Physics and Center for Complex Systems, Brandeis University, Waltham, MA 02254, USA.

*To whom correspondence should be addressed at: Center for Complex Systems, Brandeis University, Waltham, MA 02254, USA.

tex (Fig. 2C) and hippocampus (Fig. 2D) showing that approximately seven high-frequency subcycles are nested in a low-frequency oscillation (*9*, *10*).

Could the ADP provide a mechanism for storing different memories in different subcycles? An important feature of the ADP is its slow rise (Fig. 2E). The most excitable cells are therefore not those that just fired, but those that fired earliest. More specifically, the most excitable cells in the first subcycle of a low-frequency oscillation would be those that fired on the first subcycle of the previous low-frequency cycle. Similarly, the most excitable cells in the second subcycle would be those that fired on the second subcycle of the previous cycle. The slow increase in the ADP thus provides ramps of excitation that could serve as a basis for ordering multiple memories (*11*). Figure 1B shows a network of cells, each of which can generate an ADP. The neurons receive continuous oscillatory input and pooled feedback inhibition (*10*), the function of which is to partition a cycle into subcycles. The first part of the simulation (Fig. 1C, left of arrowhead) shows that a network with these properties can faithfully store seven nonoverlapping (*12*) memories. The memories were previously loaded into the network by brief activation of informational inputs. Each memory is represented by a group of cells that fire simultaneously during a particular subcycle. When a different group of cells is briefly presented with the eighth pattern, X, at its informational inputs (Fig. 1C, arrowhead), this group then fires on the first subcycle of each subsequent cycle. Previous memories are shifted back one subcycle, and the memory pattern stored in the last subcycle, R, is lost [for alternative assumptions and ideas concerning readout, see (*13*, *14*)]. The number of memories that can be stored without loss depends on variables that we have adjusted in order to limit the number to seven, in accord with average human performance (*5*). This simulation demonstrates that the network shown in Fig. 1B can store multiple memories and keep them separate by phase (oscillatory subcycles). The number of short-term memories that can be stored is limited by the number of subcycles that fit within a low-frequency cycle. In the model, the presence of subcycles is dependent on the feedback inhibition (Fig. 1D).

Systematic changes in the phase of cell firing occur as new information is introduced into the network (Fig. 1C). The observation of systematic phase changes in hippocampal place cells (*15*) thus suggests that the storage mechanism we have modeled may be applicable to the hippocampus. A second important feature of the model is the property of time compression: Sequential memories inserted over many seconds are recreated in the network at intervals of ~25 ms (Fig. 1C). Such compression might enable the *N*-methyl-D-aspartate subtype of glutamate receptor channel, which exhibits an associational mechanism with a 100-ms time scale, to form associations between events that occurred at much greater intervals.

Our model is consistent with the previous proposal (*16*, *17*) that the phase of cell firing in oscillatory networks can be used to distinguish different activity patterns. However, our model predicts that cells are not likely to fire on sequential 40-Hz subcycles because different subcycles represent different information. The available data appear consistent with this view (*18*) and recent experiments show directly that sequential 40-Hz waves relate to different rather than identical perceptual information (*19*). Another prediction is that memory patterns repeat on each low-frequency brain oscillation. Consistent with this view is the observation that brief sensory stimulation or cortical electrical stimulation produces electroencephalogram afterdischarges that repeat at the low-frequency, alpha rhythm (*20*). The model could be further tested by artificially exciting single cells. Because the proposed memory mechanism is based on an intrinsic neuronal property, the ADP, the model predicts that a cell should continue to fire on subsequent oscillatory cycles. The analysis of electrical events during short-term memory tasks (*21*) should provide a further basis for testing the ideas proposed here.

Note added in proof: We have recently become aware of a report (*22*) showing oscillatory activity ~4 Hz during a short-term memory task.

REFERENCES AND NOTES

1. J. M. Fuster and J. P. Jervey, *J. Neurosci.* **2**, 361 (1982); S. Funahashi, C. J. Bruce, P. S. Goldman-Rakic, *J. Neurophysiol.* **61**, 331 (1989).
2. D. O. Hebb, *The Organization of Behavior* (Wiley, New York, 1949); D. J. Amit, *Modeling Brain Function* (Cambridge Univ. Press, Cambridge, 1989); D. J. Amit, N. Brunel, M. V. Tsodyks, *J. Neurosci.* **14**, 6435 (1994); D. Zipser, B. Kehoe, G. Littlewort, J. Fuster, *ibid.* **13**, 3406 (1993).
3. Cholinergic induction of an ADP is described by R. Andrade [*Brain Res.* **548**, 81 (1991)], M. Caeser, D. A. Brown, B. H. Gahwiler, and T. Knopfel [*Eur. J. Neurosci.* **5**, 560 (1993)], and J. F. Storm [*J. Physiol. (London)* **409**, 171 (1989)]. The similar effects of serotonin are described by R. Araneda [*Neuroscience* **40**, 399 (1991)].
4. D. Horn and M. Usher [*Neural Comput.* **3**, 31 (1991); in *Advances in Neural Information Processing Systems*, J. E. Moody, S. J. Hanson, P. Lippmann, Eds. (Morgan & Kaufmann, San Mateo, CA, 1994), vol. 4, pp. 125–132] explore related ideas concerning the retrieval of multiple memories by oscillatory networks.
5. G. A. Miller, *Psychol. Rev.* **63**, 81 (1956).
6. Interaction of the ADP with brain oscillations is likely, given (*3*) and the evidence for the participation of acetylcholine and serotonin in brain oscillations [M Stenade, R. Curro Dossi, D. Pare, G. Oakson, *Proc. Natl. Acad. Sci. U.S.A.* **88**, 4396 (1991); B. Bland, *Prog. Neurobiol.* **26**, 1 (1986)].
7. S. Sternberg, *Science* **153**, 652 (1966)
8. Scan time/memory (s = 38 ms/memory) (*6*) may be the sum of true scan time/memory and a time, T/memory, imposed by other costs of increasing complexity. T = 13 ms/memory can be estimated when the number of memories exceeds capacity from the data of D. Burrows and R. Okada [*Science* **188**, 1031 (1975)]. In this instance, true retrieval time/memory would equal 25 ms (38 ms − 13 ms) and implicate a 40-Hz oscillation.
9. R. Llinas and U. Ribary, *Proc. Natl. Acad. Sci. U.S.A.* **90**, 2078 (1993).
10. A. Bragin *et al.*, *J. Neurosci.* **15**, 47 (1995). A related study showing both theta and 40-Hz oscillations was performed by I. Soltesz and M. Deschenes [*J. Neurophysiol.* **70**, 97 (1993)].
11. If additional spikes are superposed on an existing ADP, a hyperpolarizing event is evoked. This afterhyperpolarization decays within 500 ms, thereby generating a positive ramp to a final depolarized level (R. Andrade, personal communication). It is therefore reasonable to model the upward ramp of the ADP as being reinitiated with each spike.
12. With nonoverlapping memories, a given cell only participates in a single pattern. If memories overlap, cells should fire on multiple subcycles. However, the ADP could only cause firing on one subcycle. The "missing" signal could conceivably be filled in if recurrent modifiable excitatory collaterals are present (*17*). Understanding such collaterals is also of importance to the transition to long-term memory and to the formation of associations between different memory patterns. The ADP and rapidly modifiable synapse may both be involved in short-term memory.
13. As modeled, loss of previous memories occurs as a direct result of entry of new information. There is some support for such an effect in human memory [R. C. Atkinson and R. M. Shiffrin, in *The Psychology of Learning and Motivation: Advances in Research and Theory*, K. W. Spence, and J. T. Spence, Eds. (Academic Press, San Diego, CA, 1968), vol. 2, pp. 89–105]. Alternatively, some psychological measurements are more consistent with a passive decay process [A. Wingfield and D. L. Byrnes, *Science* **176**, 690 (1972)]. If one assumes a sharp decay process after ~1.5 s and the loading of new memories at the end of the memory stack, the phase of memory becomes earlier as new memories are entered, rather than later as in Fig. 1C.
14. Further assumptions are required to predict reaction time during memory readout in the Sternberg task. One model is that presentation of the test item resets the low-frequency oscillation and initiates the sequential readout of memory-containing subcycles; the greater the number of subcycles that contain memories, the longer the reaction time.
15. J. O'Keefe and M. L. Recce, *Hippocampus* **3**, 317 (1993); W. E. Skaggs, M. A. Wilson, B. L. McNaughton, *Soc. Neurosci. Abstr.* **19**, 795 (1993). Phase of firing advances with time [for comparison see (*13*)].
16. W. Singer, *Annu. Rev. Physiol.* **55**, 349 (1993).
17. C. von der Malsburg, *Biol. Cybernet.* **54**, 29 (1986).
18. There is some indication that cells can fire on multiple sequential cycles of 40-Hz oscillations [A. K. Kreiter and W. Singer, *Eur. J. Neurosci.* **4**, 369 (1992)], but generally this has not been observed [C. Koch and F. Crick, in *Some Further Ideas Regarding the Neuronal Basis of Awareness in Large Scale Neuronal Theories of the Brain*, C. Koch and J. L. Davis, Eds. (MIT Press, Cambridge, MA, 1994), pp. 93–109.
19. M. Joliot, U. Ribary, R. Llinas, *Proc. Natl. Acad. Sci. U.S.A.* **91**, 11748 (1994)
20. H.-T. Chang, *J. Neurophysiol.* **13**, 235 (1950).
21. A crucial question that remains unclear is whether spike trains recorded during memory tasks (*1*) are dependent on an oscillatory storage process. Simultaneous recordings of spike trains and field potentials, as in (*15*), may be required to settle this issue. Magnetoencephalographic and electroencephalo-

gram measurements during short-term memory tasks are described by L. Kaufman, S. Curtis, J. Z. Wang, and S. J. Williamson [*Electroencephalogr. Clin. Neurophysiol.* **82**, 266 (1992)] and M. Fahle, J. Albrecht, H. Buelthoff, and D. Braun [*Soc. Neurosci. Abstr.* **20**, 319 (1994)].

22. K. Nakamura, A. Mikami, K. Kubota, *Neuroreports* **3**, 117 (1992).
23. Pyramidal cells are modeled as identical integrate-and-fire neurons. The membrane potential for each pyramidal cell is given by

$$\tau_v dV_i(t)/dt = -V_i(t) + V^{rest} + V^{osc}(t) + V_i^{ADP}(t) + V^{inh}(t)$$

and it is reset to $V^{rest} = -60$ mV when it exceeds $V^{thresh} = -50$ mV, the threshold for spike generation. Because it does not change the qualitative features of the model, we assume that τ_v is small compared to any other time constant, so that

$$V_i(t) \approx V_{rest} + V^{osc}(t) + V_i^{ADP}(t) + V^{inh}(t)$$

The inhibitory interneuron is not explicitly modeled; it is activated by each spike in a pyramidal cell and it inhibits all pyramidal cells. This inhibition is assumed to be a linear superposition of inhibitory postsynaptic potentials, such that $V^{inh}(t) = \Sigma\, \alpha(t - t_n)$, where t_n is the time of the nth spike in the network and α is the alpha function, $\alpha(t) = A^*(t/\tau)^*\exp(1 - t/\tau)$, with $A^{inh} = -4$ mV and $\tau^{inh} = 5$ ms. V_i^{ADP} increases from zero after each action potential in cell i (*11*) with an alpha function of amplitude $A^{ADP} = 10$ mV and a time constant of $\tau^{ADP} = 200$ ms. The oscillatory input is $V^{osc}(t) = B^*\sin(2\pi ft)$, with $f = 6$ Hz and $B = 5$ mV. A memory is inserted through informational inputs at a single negative peak of the cycle. The brief input is sufficient to activate the cells and evoke an ADP.

24. H. S. Oberly, *Am. J. Psychol.* **40**, 295 (1928).
25. Supported by the W. M. Keck Foundation and NIH grant NS27337. We thank L. Abbott, S. Sternberg, G. Buzsaki, and M. Kahana for extensive discussions. We extend special thanks to R. Llinas for pointing out Miller's work on memory limits.

13 September 1994; accepted 5 January 1995

TECHNICAL COMMENTS

Interhelical Angles in the Solution Structure of the Oligomerization Domain of p53: Correction

We recently presented the solution structure of the oligomerization domain (residues 319–360) of the tumor suppressor p53 using an multidimensional heteronuclear-edited and -filtered nuclear magnetic resonance (NMR) spectroscopy (*1*). The structure comprised a dimer of dimers, each dimer being formed by two antiparallel helices and an antiparallel β sheet. The two dimers were arranged approximately orthogonal to each other such that the tetramer formed a four-helical bundle with the antiparallel β sheets lying on opposing faces of the molecule. After the determination of the NMR structure, the crystal structure of the oligomerization domain was solved by Nikola Pavletich and his colleagues and kindly provided to us for comparison (*2*). While the overall topology of the tetramer was the same in the NMR and x-ray structures, a difference in the orientation of the two dimers (that is between the AC dimer and the BD dimer) was observed. Specifically, the angle between the long axes of helices A and B was 114° in the solution structure versus 80° in the crystal structure. Thus, while the structure of the dimer was similar, the root-mean-square (rms) difference between our proposed NMR structure and the x-ray structure for the complete tetramer was large (3 Å). This difference involves a rigid body rotation of one dimer relative to the other about the symmetry axis of the tetramer and is readily appreciated from the ribbon diagrams of the original NMR structure and the x-ray structure (Fig. 1, A and B, respectively). It is important to determine whether a genuine difference between solution and crystal structures exists, or whether a misinterpretation of the NMR data could be the cause of this discrepancy.

To this end, we reexamined our nuclear Overhauser enhancement (NOE) data obtained from both the four-dimensional (4D) $^{13}C/^{13}C$-separated and three-dimensional (3D) ^{13}C-separated/^{12}C-filtered NOE spectra. We found that, although the partitioning of the intersubunit NOEs was correct, there were three errors in NOE assignments involving contacts between the A and B subunits (and by symmetry between the C and D subunits). Specifically, the weak NOEs between Lys^{351} CεH(A) and Met^{340}-CγH(B), Lys^{351}CδH(A) and Met^{340}-CαH(B), and Lys^{351}CγH(A) and Met^{340}-CαH(B), which were only identified in the 4D $^{13}C/^{13}C$-separated NOE spectrum, were a

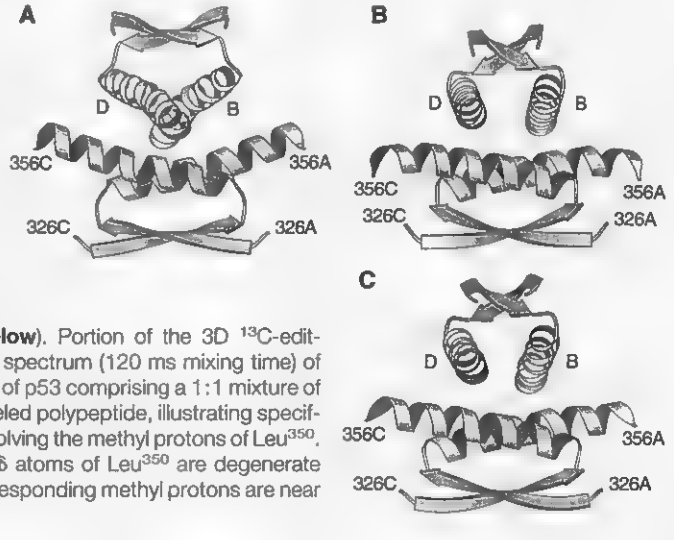

Fig. 1 (right). Ribbon diagrams of **(A)** the original average NMR structure, **(B)** the x-ray structure, and **(C)** the new average NMR structure (*3*). The angle between helices A and B, which describes the orientation of the two dimers, is 114° in (A), 80° in (B), and 78° in (C). The figure was generated with the program MOLSCRIPT (*7*).

Fig. 2 (below). Portion of the 3D ^{13}C-edited(F_2)/^{12}C-filtered(F_3) NOE spectrum (120 ms mixing time) of the oligomerization domain of p53 comprising a 1:1 mixture of unlabeled and $^{13}C/^{15}N$-labeled polypeptide, illustrating specifically intersubunit NOEs involving the methyl protons of Leu^{350}. The ^{13}C shift of the two Cδ atoms of Leu^{350} are degenerate and the ^1H shifts of the corresponding methyl protons are near degenerate.

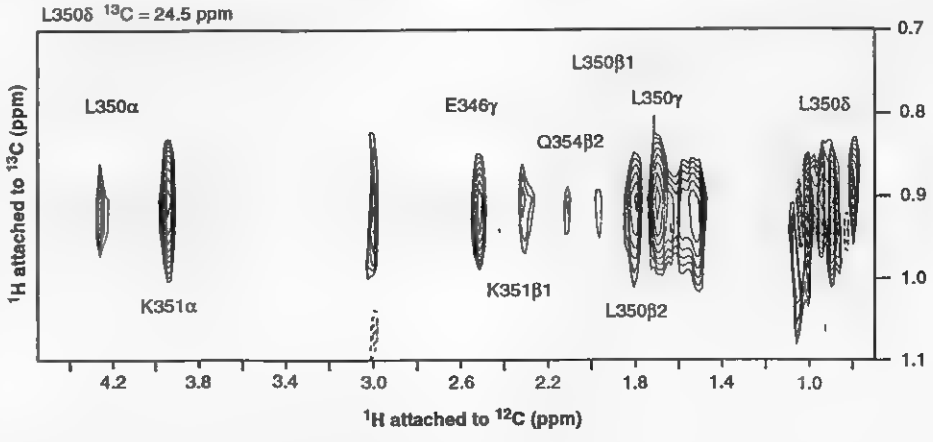

result of spectral artifacts. Also, key intersubunit NOEs between helices A and B involving the methyl groups of Leu^{350}CδH had been omitted from the NOE restraints list. These included a strong NOE from Leu^{350}-CδH(A) to Lys^{351}CαH(B), as well as weak NOEs to Lys^{351}Cβ1H(B) and Gln^{354}-Cβ2H(B) (Fig. 2). Even when the three incorrect NOEs were omitted and the structures recalculated, the orientation of the two dimers differed by 25° from that in the crystal structure. Introduction of the new NOEs, however, fully corrected this situation, as can be seen from the ribbon diagram of the new average NMR structure (Fig. 1C) (3).

As a result of these corrections, the difference between the average backbone coordinates of the new ensemble of NMR structures and the crystal structure for the residues visible in the electron density map is 1.2 Å for the whole tetramer. The precision of the NMR backbone coordinates is 0.45 Å which, assuming no errors in the experimental restraints, translates into a mean coordinate accuracy of 0.9 to 1.1 Å (4). Hence, the two structures are essentially identical within the errors of the present NMR coordinates.

It is instructive to examine the source of the errors in our earlier study (1). Conventionally, in a single chain protein, errors in NOE assignments manifest themselves by inconsistencies. In this particular case, this was not evident, as excellent agreement between the calculated and input values of the NOE, torsion and coupling constant restraints, good nonbonded contacts, and small deviations from idealized covalent geometry, were obtained. Complete cross-validation (5) was of little help, as it did not result in a significant change in the structure because the target function also incorporated symmetry restraints. Finally, the fourfold degeneracy reduced the number of unique NOEs by a factor of 4, thereby increasing the difficulty in ascertaining errors.

Why were three key intersubunit NOEs, Leu^{350}CδH(A) to Lys^{351}CαH(B), Lys^{351}-Cβ1H(B) and Gln^{354}Cβ2H(B), omitted from the restraint list, and why did their omission result in a large reorientation of the two dimers? First, the problem with our proposed structure reflected to some extent the limitation of the NMR technique itself, as the main structural parameter, and the only one involved in determining long-range order, involves short (<5 Å) interproton distances derived from the NOEs. As the number of observed NOEs between the A and B dimers is limited to 24, propagation of errors can easily occur. This may have been further compounded by our representing the nonbonded contacts by only a repulsive term, which worked to reduce the contact area between the two dimers. Second, two of the crucial NOEs involve two neighboring residues for which intrasubunit NOEs would occur, although in the 3D ^{13}C-edited/^{12}C-filtered NOE spectrum carried out on the unlabeled-labeled heterotetramer, these should not be observable. We noticed, however, experimental problems with this spectrum. For example, strong cross peaks were observed from the methyl protons of Ala^{353} and Ala^{355} to their respective CαH protons despite the fact that the intersubunit separation between these two proton pairs was more than 14 Å. Consequently, we attributed these peaks to artifacts arising from intrasubunit NOEs, possibly as a result of incomplete ^{13}C labeling. The Leu^{350}CδH to Lys^{351}CαH and Lys^{351}Cβ1H peaks were thought to reflect a similar situation. Third, in a single-chain protein, the angle between structural elements corresponding to the two dimers would also be restricted by the limitations imposed by covalent geometry. Last, in a contiguous single polypeptide chain, the three crucial NOEs would correspond to 12 unique NOEs.

The reason for the profound effect of these additional restraints lies to some degree in the orthogonal packing of the two dimers. The large majority of NOE restraints are at the center of the helices, whereas many of those involving Leu^{350}-CδH lie at the end of the helices, thereby exerting more leverage on the overall interhelix orientation.

What are the consequences of the correction in angle between the two dimers? First, the overall topology of the tetramer remains the same, and the main thrust and conclusions of our article (1) are unaffected. From a structural viewpoint, however, the packing of the two dimers is slightly better in the new NMR structure and in the crystal structure than in the one we proposed originally (1).

After the submission of this comment, Lee *et al.* (6) also published an NMR structure of the oligomerization domain. The angle between helices A and B in this structure was 55° to 60° [figure 8D in (6)] compared with 80° and 78° in the x-ray and new NMR structures, respectively, and 114° in the original NMR structure. This illustrates the high degree of technical difficulty in solving the structure of this symmetrical homotetramer by NMR.

G. Marius Clore
James G. Omichinski
Laboratory of Chemical Physics, National Institute of Diabetes and Digestive and Kidney Diseases, National Institutes of Health, Bethesda, MD 20892, USA
Kazuyasu Sakaguchi
Nicola Zambrano
Hiroshi Sakamoto
Ettore Appella
Laboratory of Cell Biology, National Cancer Institute, National Institutes of Health, Bethesda, MD 20892, USA
Angela M. Gronenborn
Laboratory of Chemical Physics, National Institute of Diabetes and Digestive and Kidney Diseases

REFERENCES AND NOTES

1. G. M. Clore *et al.*, *Science* **265**, 386 (1994).
2. P. D. Jeffrey, S. Gorina, N. P. Pavletich, *ibid.* **267**, 1498 (1995). N. P. Pavletich, personal communication.
3. The structural statistics are as follows: A total of 35 simulated annealing structures were calculated as described in (1) on the basis of a total of 3268 approximate interproton distance restra nts comprising 2404 intrasubunit restraints (744 intraresidue, 844 sequential $|i-j| = 1$, 744 medium range $1 < |i-j| \leq 5$, and 72 long range $|i-j| > 5$ restraints) and 864 intersubunit restraints (758 for the AC and BD dimers, 96 for the AB and CD dimers, and 10 for the AD and BC dimers), supplemented by 128 distance restraints for 64 intrasubunit hydrogen bonds, 24 distance restraints for 12 intersubunit hydrogen bonds, 144 ^{3}JHNα coupling constant restra nts, and 268 torsion angle restraints (144 φ, 104 χ_1, and 20 χ_2). The precision of the structures (defined as the average atomic rms difference between the individual simulated annealing structures and the mean coordinates) is 0.45 Å for the backbone atoms and 0.84 Å for all atoms for residues 326 to 356. (Residues 319–325 at the NH_2-terminus and 357–360 at the COOH-terminus are disordered in solution.) The rms deviations from the experimental restraints are as follows: 0.053 ± 0.003 Å, 0.27 ± 0.02 Hz, and 0.23 ± 0.15°, for the distance, coupling constant, torsion angle, Cα shift, and Cβ shift restraints, respectively. The deviations for idealized covalent geometry are 0.002 ± 0.0001 Å, 0.446 ± 0.010°, and 0.335 ± 0.069° for bond, angle, and improper torsion terms. The coordinates of the 35 simulated annealing structures, and those of the restrained regularized mean structure, together with the experimental NMR restraints and the ^{1}H, ^{13}C, and ^{15}N chemical shift assignments have been deposited in the Brookhaven Protein Data Bank (accession code numbers 1OLH, 1OLG, and 1OLH_MR, respectively).
4. G. M. Clore, M. A. Robien, A. M. Gronenborn, *J. Mol. Biol.* **231**, 82 (1993).
5. A. T. Brünger *et al.*, *Science* **261**, 328 (1993).
6. W. Lee *et al.*, *Nature Struct. Biol.* **1**, 877 (1994).
7. P. J. Kraulis, *J. Appl. Crystallogr.* **24**, 946 (1991).

16 November 1994; accepted 9 January 1995

A New Breed of
Molecular Biology Products

Get this catalogue and increase your molecular biology *savoir-faire.*

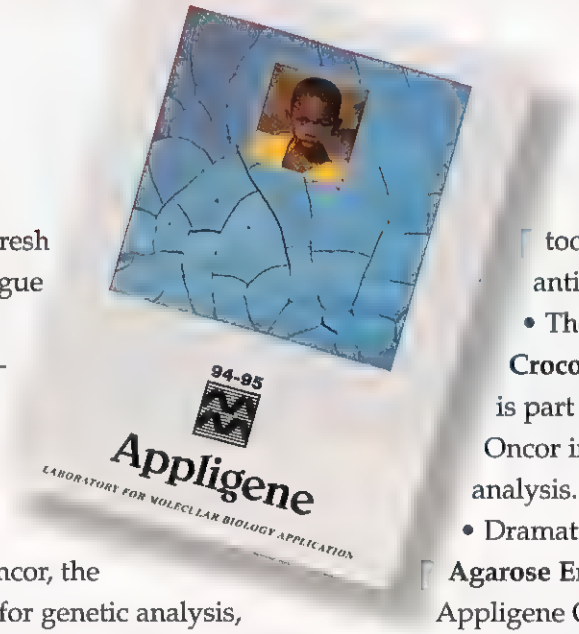

Here's informative reading fresh from France: an exciting catalogue of innovative instruments, systems and reagents manufactured by Appligene, one of Europe's leading molecular biology companies.

These products are now marketed and supported by Oncor, the leading developer of products for genetic analysis, among them the breakthrough **ApopTag**™ *In Situ* Apoptosis Detection Kit.

• **Penetratin**™ **1**, a patented 16 amino acid peptide, delivers DNA and peptides directly to the cell nucleus and is the newest Appligene Oncor tool for gene targeting and antisense research.

• The versatile, oil-free **Crocodile III** temperature cycler is part of a full line of Appligene Oncor instrumentation for DNA analysis.

• Dramatically clear **Infinity**™ **Agarose Enhancer** is among many Appligene Oncor products for DNA isolation, electrophoresis and blotting.

Be savvy. Call us for a catalogue now. We'll get it to you *tout de suite.*

oncor®

For Research Use Only Not for use in diagnostic procedures.
Penetratin™ is a trademark of Appligene. Infinity™ and ApopTag™ are trademarks of Oncor, Inc.

209 Perry Parkway
Gaithersburg,
MD 20877

1-800-77-ONCOR
301-963-3500
Fax: 301-926-6129

Circle No. 23 on Readers' Service Card

THE ICE AGE IS OVER.

New EasyTides™ ambient shipped radiolabeled nucleotides from DuPont NEN.

- Easy to use. Shipped in NENSURE™ vials without dry ice. No need to thaw, just store in the refrigerator at 4°C.
- Easy to see. Colored with an inert dye for easier pipetting.
- Easy on the environment. Less bulky packaging, and no Styrofoam® to recycle.

EasyTides perform like the products you use now. Available in ^{32}P, ^{33}P, and ^{35}S-nucleotides. Try EasyTides the next time you order. For information or to order, call 1-800-551-2121. Or call FaxBack at 1-800-666-6527 and request document 9001.

United States 1-800-551-2121 • Canada 1-800-387-8391 • Australia +61 (008) 257149 • Belgium +32 (02) 7242717
Denmark +45 31506610 • France (01) 6982 5450 • Germany +49-6172-872600 • Italy (02) 25302 481/483
Japan +81 (03) 3224-8763 • Latin America/Asia Pacific Fax +1 (617) 426-2464 • Netherlands +31 (073) 206550
Sweden +46 (08) 7503700 • Switzerland +41 (01) 8410330 • United Kingdom +44 (0438) 734865

DUPONT

DuPont NEN®

Manufactured under an ISO 9001 quality system registered by UL® and approved by BSI.
Styrofoam® is a registered trademark of the Dow Chemical Company.

When synthesizing quality custom primers, we extract something extra from every base.

Save a dollar a base or more with new GIBCO BRL Custom Primers.

GIBCO BRL CUSTOM PRIMERS™ $1.19 PER BASE PLUS SETUP*

At just $1.19 a base plus setup, new GIBCO BRL Custom Primers offer substantial savings – $20 or more on an average 20-mer – with all the quality you need for confident use.

New Parallel Array Synthesis™ Technology – greater efficiency, lower cost.

Using new Parallel Array Synthesis™ technology, we produce and purify hundreds of custom primers simultaneously. The result is production capacity unmatched by any supplier to deliver the lowest possible price. And, whether your order is for two primers or two hundred, we'll ship within 48 hours of order – in formats that fit your research needs, from single vials to 96-tube arrays.

The quality you have to have, at about half the price.

Highly automated computer-controlled production and continuous monitoring of coupling efficiencies throughout synthesis ensure you of the highest quality primers. And, like all GIBCO BRL products, new Custom Primers come backed by the commitment to technical excellence that's made our name synonymous with scientific achievement.

But even more, they come with a new level of savings that's breaking ground all its own.

Start saving today. Call for ordering information and our easy fax order form at **800-828-6686**.

*Setup Charge $5.00 for Deprotected or $10.00 for Deprotected/Desalted primers.

LIFE TECHNOLOGIES™

Producer of GIBCO BRL Products

To Order/TECH-LINE℠: (800) 828-6686 Facsimile: (800) 331-2286

Corporate Headquarters
8717 Grovemont Circle
P.O. Box 6009
Gaithersburg, MD 20884-9980 U.S.A.
(301) 840-8000

U.S.A. Orders
P.O. Box 68
Grand Island, NY 14072-0068 U.S.A.
Facsimile: (800) 331-2286
To Order/TECH-LINE: (800) 828-6686

U.S.A. Office for Latin America
To Order/TECH-LINE: (301) 840-4027
Facsimile: (301) 258-8238

Canada Orders
Burlington, Ontario L7P 1A1 Canada
To Order: (800) 263-6236
Facsimile: (800) 387-1007

TECH-LINE℠ and the Life Technologies logo are marks of Life Technologies, Inc. For research use only. Not intended for human or animal diagnostic or therapeutic use. © 1994 Life Technologies, Inc.

Why do an assay in several places when you can do it all right here.

Incubate, filter, precipitate, immobilize, harvest and detect directly in the MultiScreen assay plate. Compared to conventional methods, its 96 discrete filter tubes reduce reagent usage by 50–90%, and radioactive waste by >95%. Compatibility with direct microplate scintillation counters dramatically improves throughput.

MultiScreen handles every assay step. Its patented underdrain assures reliable, multiple incubations. To remove supernatant, just apply vacuum to wash or quantitatively collect filtrate. Easily transfer filters directly into vials for radiodetection.

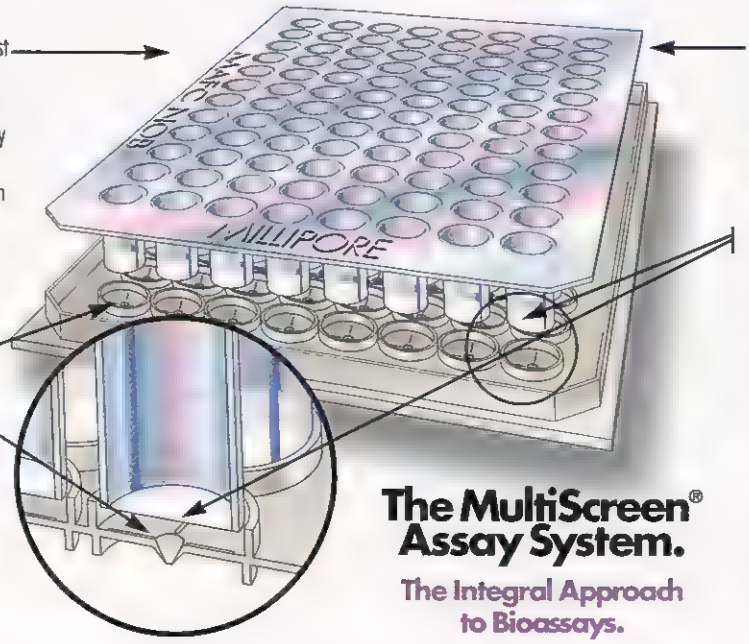

Whether you're doing receptor binding, second messenger studies, cell culture and proliferation or immunoassays, MultiScreen has been proven faster, simpler, and more efficient.

Let Millipore's Technical Service help you choose the optimum membrane or filter for your assay—glass fiber, cellulosic or charged membranes, Immobilon™ series, low-binding Durapore® and more.

The MultiScreen® Assay System.

The Integral Approach to Bioassays.

MILLIPORE

Call or fax for a complete technical package or to arrange a demo. •U.S. and Canada: 1-800-645-5476 •Japan: (03) 3474-9111 •European headquarters in Paris, fax: 33.1.30.12.71.83
Internet Lab Catalogue: access URL menu, type: http://www.millipore.com

Circle No. 21 on Readers' Service Card

Don't let small sample dialysis get out of hand.

Take control with the new Pierce Slide-A-Lyzer™ Dialysis Cassettes!

Load a sample for dialysis easier and faster than ever with this revolutionary new system. The new Pierce Slide-A-Lyzer™ Dialysis Cassette replaces the mess and hassles of conventional tubing with a more convenient, more effective approach.

1.

No more boiling, soaking, tying, or clamping - all you need is a syringe to load and remove your sample from these ready-to-use, disposable cassettes. The exclusive cassette design gives you total sample control, good surface-to-volume ratio and consistently reliable sample recovery. For even greater convenience, use the accessory Buoys to float your sample during dialysis, and as a bench-top cassette stand during loading and recovery.

2.

3.

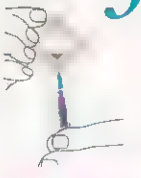

Pierce Slide-A-Lyzer™ Cassettes have a 0.5 - 3.0 ml sample capacity, 10,000 molecular weight cut-off, and are ideal for routine dialysis of protein, nucleic acid and carbohydrate samples.

Product #	Description	U.S. Price
66425	**Slide-A-Lyzer™ 10K Dialysis Cassettes*, 10 pack** Contains: 10 cassettes (10,000 Molecular Weight Cut-off, 0.5 - 3.0 ml sample capacity)	$49
66430	**Slide-A-Lyzer™ Buoys, 10 pack**	$12
66490	**Slide-A-Lyzer™ Syringe and 18G Needle Accessories, 10 pack** Contains: 10 each of 5 cc single-use, sterile, polypropylene syringes with Luer-Lok® tips and single-use, sterile, 18-gauge, 1" needles compatible for use with the Slide-A-Lyzer™ Dialysis Cassette. Ideal for nucleic acid applications.	$9

Call for your FREE copy of Pierce's Life Science & Analytical Research Products or Molecular Biology Catalog!

To order in the U.S.A.: Pierce • 3747 N. Meridian Rd. • P.O.Box 117 • Rockford, IL 61105 • **Telephone: 800.874.3723 FAX: 800.842.5007**
European Office: Pierce Europe B.V. • P.O. Box 1512 • 3260 BA Oud Beijerland • The Netherlands • Telephone: 31.1860.19277 FAX: 31.1860.19279

European Distributors:
Austria 018891819 · Belgium 03646553 · Denmark 44948822 · France 070038855 · Germany 0224196850 · Italy 025097220 · Holland 0206113133 or 076795795 · Norway 2272200 · Spain 07290333 · Switzerland 0217287772 · United Kingdom 0244382525 · Sweden 087460035

Outside Europe and the U.S., contact Pierce U.S. for your local Pierce distributor. Telephone: 815.968.0747 FAX: 815.968.0448

PIERCE
a Perstorp Biotec Company

© Pierce Chemical Company, 1994. * Patent Pending

Circle No. 6 on Readers' Service Card

No Compromises!

Dynabeads® solid-phase DNA sequencing

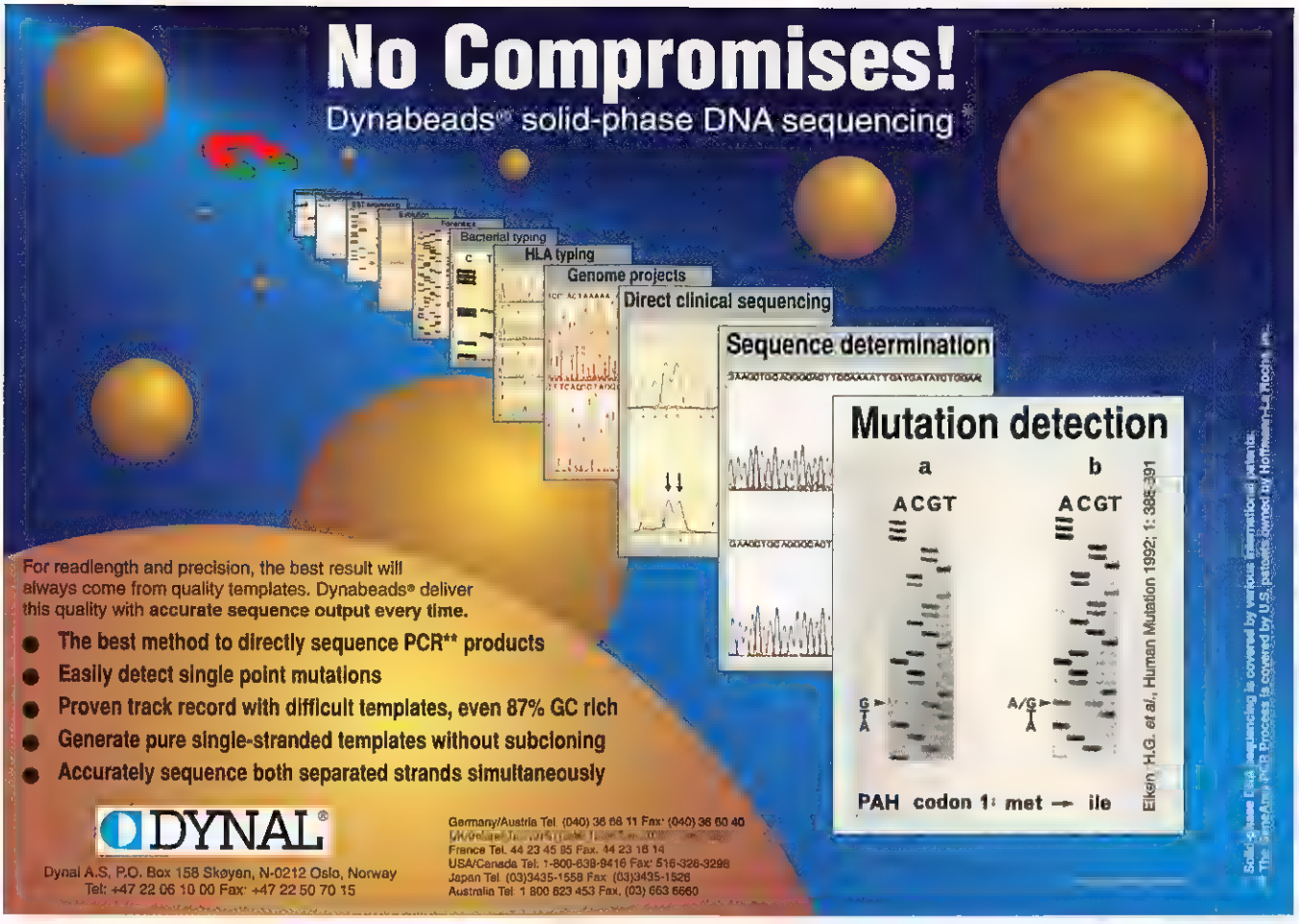

For readlength and precision, the best result will always come from quality templates. Dynabeads® deliver this quality with accurate sequence output every time.

- The best method to directly sequence PCR** products
- Easily detect single point mutations
- Proven track record with difficult templates, even 87% GC rich
- Generate pure single-stranded templates without subcloning
- Accurately sequence both separated strands simultaneously

DYNAL®

Dynal A.S, P.O. Box 158 Skøyen, N-0212 Oslo, Norway
Tel: +47 22 06 10 00 Fax: +47 22 50 70 15

Germany/Austria Tel. (040) 36 68 11 Fax: (040) 36 60 40
France Tel. 44 23 45 85 Fax. 44 23 18 14
USA/Canada Tel: 1-800-638-9416 Fax: 516-326-3298
Japan Tel. (03)3435-1558 Fax (03)3435-1526
Australia Tel. 1 800 623 453 Fax. (03) 663 6660

Solid-phase DNA sequencing is covered by various international patents.
The SureAmp PCR Process is covered by U.S. patents owned by Hoffmann-La Roche Inc.

Circle No. 17 on Readers' Service Card

MOLECULAR RESEARCH CENTER, INC. *presents*

SMART SOLUTIONS

The most reliable and cost-effective reagents for DNA and RNA isolations. Using separation technology based on the recognition of target molecules by a liquid phase, these innovative reagents outperform traditional DNA and RNA isolation methods. No enzymatic treatments! No columns! No prolonged protocols!

DNAzol™, a new standard of simplicity and effectiveness in the isolation of high quality genomic DNA developed by P. Chomczynski.

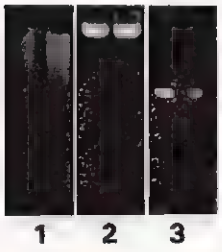

- Requires only 10 - 30 minutes
- Effective with cells, tissue and liquid samples, including blood.
- No phenol or other toxic agents
- Isolated DNA ② is ready for Southern blotting, restriction analysis ①, PCR ③, molecular cloning and other applications.

TRI REAGENT®, the most advanced version of the single-step method of RNA isolation.

- Isolates high quality total RNA in less than one hour
- Can be used to simultaneously isolate RNA, DNA and proteins
- Effective with cells, tissue and liquid samples, including blood.
- Isolated RNA ⑤ is ready for Northern blotting ④, RT-PCR ⑥, and other applications

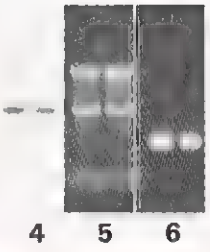

For information or to place an order from USA, Canada and countries not listed below call 1-800 452-9868, 513-841-0900 or Fax 513-841-0080.

MRC
MOLECULAR RESEARCH CENTER, INC
5645 Montgomery Rd. Cincinnati, OH 45212

AUSTRALIA: A.G.P. Technologies Pty Ltd 61-7-3419702 Fax 61-7-841-3422; **FRANCE:** Euromedex 33-88-180722 Fax 33-88-180725; **GERMANY:** BioTech Trade & Service GmbH 49-6227-51308 Fax 49-6227-53694, **INDIA:** Lab Care Products 91-11-6425156 Fax 91-11-6425156, **ISRAEL:** Tal Ron 972-8-472563 Fax 972-8-471156; **ITALY:** B o-Optica Milano SpA 39-2-2640274 Fax 39-2-2153000; **KOREA:** Choong Il Chemical, Inc 822-2946411 Fax 822-2936556; **MALAYSIA:** Technicvest Sdn. Bhd 603-6320998 Fax 603-632-0994; **SWITZERLAND:** Lucerna Chem Ag 41-41-369636 Fax 41-41-369656; **TAIWAN:** Pan Asia Biomedical Technology, Inc. 886-2-7418169 Fax 886-2-7764372; **UNITED KINGDOM:** Molecular Research Centre Oxford 44-993-706736 Fax 44-865-351511.

Circle No. 3 on Readers' Service Card

The latest edition of the New England Biolabs catalog provides a host of new features and is an easy-to-use reference guide. Pick up your copy and catch the wave of new products on the rise:

- **171 Restriction Endonucleases** including 12 new and over 80 recombinant enzymes
- **Recombinant Fse I:** an 8-base cutter, GGCCGG/CC
- **9°N$_m$ DNA Polymerase:** A recombinant thermostable DNA Polymerase with a reduced level of 3'→ 5' exonuclease activity
- **Klenow Fragment (3 → 5 exo$^-$):** for dideoxy sequencing and random primer labeling
- **LITMUS™ multipurpose cloning vectors**
- **An expanded line of Protein Modification Products** including endo- and exoglycosidases, protein kinases, protein phosphatases, inhibitors and substrates, and protein molecular weight markers
- **Code20™ Cassette Mutagenesis Kit** for inserting or substituting all single 20 amino acid codons at specific sites in DNA
- **polyA Spin™ mRNA Isolation Kit** for the isolation of full-length poly(A)$^+$ eukaryotic mRNA using spin columns pre-packed with microcrystalline oligo(dT) cellulose

Call New England Biolabs to be sure you have your very own copy.

New Products on the Rise

New England Biolabs 1995 Catalog

- **New England Biolabs Inc.** 32 Tozer Road, Beverly, MA 01915 USA 1-800-NEB-LABS Tel. (508) 927-5054 Fax (508) 921-1350 email: info@neb.com
- **New England Biolabs Ltd., Canada** Tel. (800) 387-1095 (905) 672-3370 Fax (905) 672-3414 email: info@ca.neb.com
- **New England Biolabs GmbH, Federal Republic of Germany** Tel. (0130) 83 30 31 (06196) 3031 Fax (06196) 83639 email: info@de.neb.com
- **New England Biolabs (UK) Ltd.** Tel. (0800) 31 84 86 (01462) 420616 Fax (01462) 421057 email: info@uk.neb.com

DISTRIBUTORS: Australia (075) 94-0299; Belgium (0800)1 9815; Brazil (011) 66-3585; Denmark (31) 56 20 00; Finland (90) 420-8877; France (1) 34 60 24 24; Greece (01) 5226547; Hong Kong 649-9988; India (542) 311473; Israel (03) 5351205; Italy (02) 38103171; Japan (03) 3272-0671; Korea (02) 556-0311; Mexico (5) 519-3463; Netherlands (033) 95 00 94; New Zealand (09) 418-3839; Norway 22 22 84 1; Singapore 4457927; Sweden (08) 7348300; Switzerland (061) 481 47 13; Taiwan (02) 8802913

NEW ENGLAND BioLabs®

20 years and beyond.

Circle No. 71 on Readers' Service Card

A New Spin On PCR Cleanup.

Spin. Spin. Done.

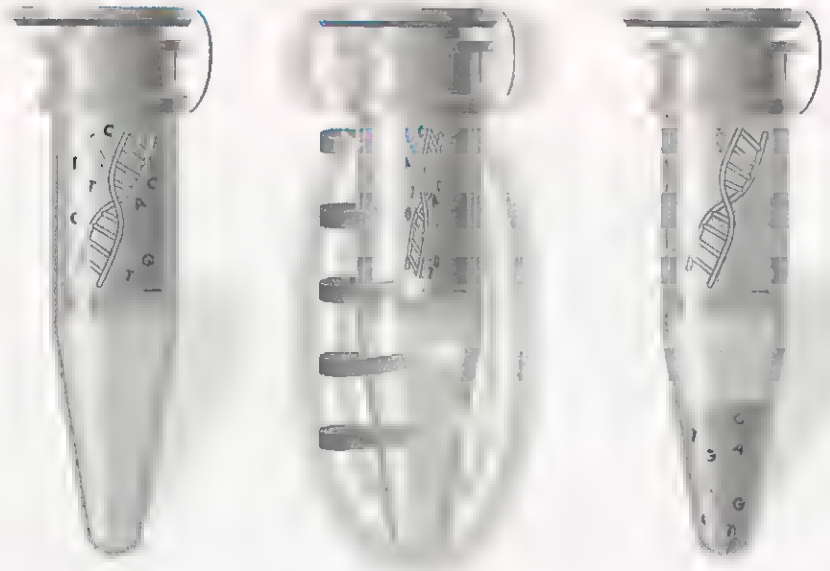

Now you can separate primers and dNTPs from PCR-amplified fragments in just two, five-minute spins in your centrifuge. Simply use Millipore's Ultrafree®-MC (30K Nominal Molecular Weight Limit) centrifugal filters—and your sample is ready. There's no need to run additional purification procedures. No separation method is faster or easier—or gives you higher recovery of amplified product.

Want to give it a whirl? Give us a call and we'll send you a free Ultrafree-MC sample. US and Canada, 1-800-MILLIPORE ext. 8017. Japan, fax to (03) 3474-9141. Europe (fax to our Paris headquarters), +33.1.30.12.71.83.

MILLIPORE

Internet Lab Catalogue: access URL menu, type: http://www.millipore.com

© 1994 Millipore Corporation

Circle No. 37 on Readers' Service Card

HEAT SHOCK / STRESS RESPONSE

THE LARGEST SELECTION OF STRESS RESPONSE BIOCHEMICALS

Antibodies Proteins Probes Vectors

Does your area of study involve stress proteins?

Many Do!

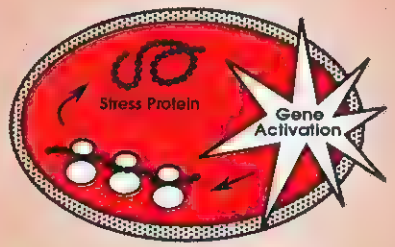

Disease States
Fever
Hypertrophy
Inflammation
Oxidant Injury
Ischemia
Viral Infection
Malignancy

Normal Cellular Influences
Cell Cycle
Development & Differentiation
Growth Factors
Molecular Chaperones

Environmental Stressors
Amino Acid Analogues
Chemotherapeutic Agents
Heat Shock
Inhibition of Energy Metabolism
Transition Heavy Metals

StressGen BIOTECHNOLOGIES CORP.

120-4243 Glanford Avenue, Victoria, B.C., CANADA V8Z 4B9

For a Free Catalog or Information Call
Toll Free (US): (800) 661-4978
Tel: (604) 744-2811 Fax: (604) 744-2877

AMS BIOTECH. LTD., **DENMARK, NORWAY, SWEDEN** - Tel: 46-8-630-0232. **SPAIN** - Tel: 34-1-433-6643. **SWITZERLAND** - Tel: 41-91-50-55-22 • BIOCLONE PTY. LTD., **AUSTRALIA, NEW ZEALAND** - Tel: 61-2-517-1966 • BIOMOL GmbH, **GERMANY** - Tel: 49-40-85-32-800 • BIOQUOTE LTD., **UNITED KINGDOM** - Tel: 44-904-431-402 • CASHMERE SCI. CO., **TAIWAN** - Tel: 886-2-821-3004 • CAIRO CHEM CO., **EGYPT** - Tel: 02-3615525 • DIAGNOSTIC BROKERS ASSOC., **ITALY** - Tel: 39-2-264-145-76 • ENCO SCI. SVC., **ISRAEL** - Tel: 972-3-934-9922 • ESSENCE INTL. CORP., **KOREA** - Tel: 82-2-577-5383 • FARMALEX S.A., **GREECE** - Tel: 30-1-64-45-612 • FENG JIH CO. LTD., **TAIWAN** - Tel: 886-2-647-8855 • FUNAKOSHI CO. LTD., **JAPAN** - Tel: 81-3-5684-1622 • KUBERAN ENT., **MALAYSIA** - Tel: 3-7573785 • KORAM BIOTECH. CORP., **KOREA** - Tel: 82-2-556-0311 • PROTECH CO. LTD., **TAIWAN** - Tel: 886-2-3810844 • SANBIO BV., **BELGIUM, THE NETHERLANDS, AND LUXEMBOURG** - Tel: 31-4182-51115 • SPACE, **ITALY** - Tel: 39-2-25-75-377 • SZABO, **AUSTRIA** - Tel: 43-1-409-39-610 • TEBU, **FRANCE** - Tel: 33-1-34-84-62-52

Circle No. 74 on Readers' Service Card

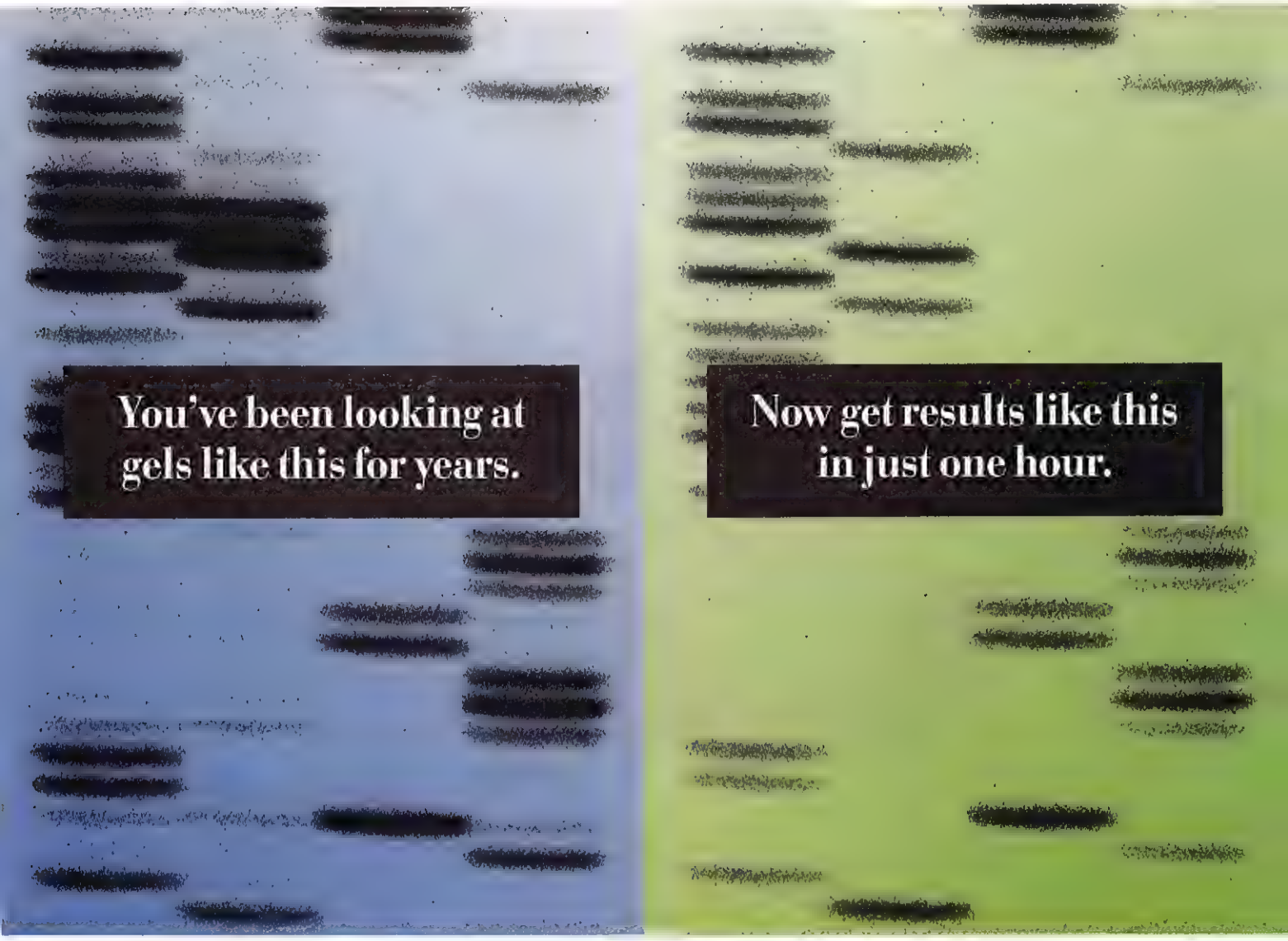

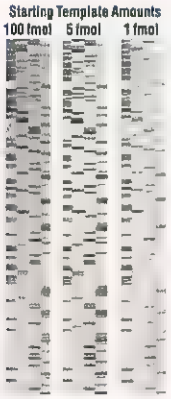

DNA sequence obtained with the AmpliCycle Sequencing Kit and the GC-rich control template, pBSMB. ^{33}P end-labeled primer.

For superior sequencing results directly from any template source—PCR products, plaques, colonies, ss or dsDNA—use the AmpliCycle™ Sequencing Kit from Perkin-Elmer.

This kit features AmpliTaq® DNA Polymerase, CS, a novel enzyme specifically developed for cycle sequencing. It provides ladders with even band intensities, low background, and fewer false terminations using ^{32}P, ^{33}P, or ^{35}S.

Accurate DNA sequences can be determined with as little as one hour exposure or from as little as 1 fmol of template. By adjusting the amount of template and label, protocols can be optimized for sensitivity or isotope conservation, with end-labeling or direct incorporation.

Perkin-Elmer's performance guarantee backs every AmpliCycle Sequencing Kit. The integrated resources of our Applied Biosystems Division offer the most comprehensive range of systems, technologies, and support in PCR, genetic analysis, nucleic acid synthesis, and protein research.

Now get sequencing results in just one hour by calling 1-800-327-3002 in the U.S. For PCR technical support, call 1-800-762-4001. For more information, call 1-800-345-5224. Outside the U.S., call or fax your local Perkin-Elmer representative.

PERKIN ELMER

Europe Langen Germany Tel: (0) 6103-708-0 Fax: (0) 6103-708-210
Canada Mississauga, Canada Tel: 905-821-8183 Fax: 905-821-8246
Japan Tokyo, Japan Tel: (0473) 80-8500 Fax: (0473) 80-8505
Latin America Mexico City, Mexico Tel: 52-5-651-7077 Fax: 52-5-593-6223
Australia Melbourne, Australia Tel: (03) 212-8585 Fax: (03) 212-8502

Perkin-Elmer PCR reagents are developed and manufactured by Roche Molecular Systems, Inc., Branchburg, New Jersey, U.S.A.

Roche

Perkin-Elmer is a registered trademark of The Perkin-Elmer Corporation. AmpliCycle is a trademark and AmpliTaq is a registered trademark of Roche Molecular Systems, Inc. The GeneAmp PCR process is covered by U.S. patents owned by Hoffmann-La Roche, Inc. and F. Hoffmann-La Roche Ltd.

ACGT!

That's worthy of a prize.

Pharmacia Biotech & SCIENCE Prize for Young Scientists
IN MOLECULAR BIOLOGY 1995

Perhaps you don't have to be quite this young, but in recognition of the work which is done during preparation for a doctorate, Pharmacia Biotech and SCIENCE are joining forces to encourage scientists at the start of their careers. This major new world-wide prize will include $20,000 awarded to the best young scientist of the year, with up to 7 further prizes of $5,000 each.

For 115 years SCIENCE has been one of the world's leading scientific journals, promoting science, through print, exhibitions and conferences.

Pharmacia Biotech, as one of the pioneers of biotechnology, is committed to serving the changing needs of the international scientific community.

Call for entries

You must be a recent Ph.D. graduate (awarded between January 1st and December 31st 1994) working in molecular biology. Submissions must be in the form of a 1000 word essay, in English, on your thesis, high-lighting the significance of its contribution and overall implications in the field. The winning essay will be published in SCIENCE.
Closing date for entries is July 5th 1995.
The prizes will be presented in Stockholm, Sweden, during December 1995.

Full details can be requested from the administrator, at the address below, or via
Internet on: science_editors@aaas.org (US/ROW enquiries)
science@science-int.co.uk (European enquiries)

SCIENCE

The Award Committee:
Pharmacia Biotech & SCIENCE Prize for Young Scientists

US/ROW enquiries - 1333 H Street NW, Washington, DC 20005, USA
Fax 202 408 8015

Pharmacia Biotech

European enquiries - Science International, 14 George IV Street, CAMBRIDGE, CB2 1HH, UK Fax +44 1223 302068

Circle No. 60 on Readers' Service Card

Porsche Power on Your PC, or Mac, or Sun Workstation.

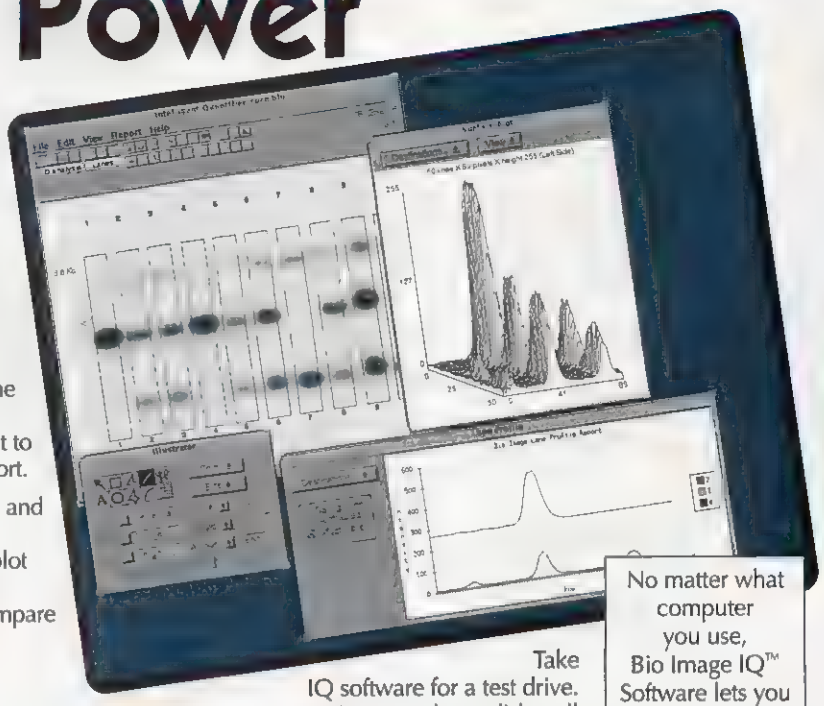

If you use electrophoresis in your research, chances are you're not taking full advantage of the technique by using image analysis – probably because the software you tried was either difficult to use or limited in what applications it could support.

Perform a wide variety of analytical tasks quickly and easily with Bio Image IQ™ Software. This menu-driven package supports whole band 1-D, 2-D, blot analysis, and colony / plaque counting. Prepare reports, annotate images for publication, and compare data in your favorite spreadsheet and database programs – all without leaving your keyboard.

IQ Software offers these key advantages:

- ***Self-installing and self-tutoring – No training required***
- ***Available for Windows 3.1, Macintosh and Sun***
- ***Network ready – Import images from multiple sources; export data to multiple destinations.***

Take IQ software for a test drive. To receive your demo disk, call **1-800-BIO-IMAGE** or fax (313) 930-0990 or E mail sales@bioimage.com.

Bio Image

No matter what computer you use, Bio Image IQ™ Software lets you take full advantage of electrophoresis by making image analysis powerful yet easy-to-use.

Circle No. 64 on Readers' Service Card

Creative Solution #3

Quick Sample Recovery from Agarose

Extract DNA or RNA from agarose gel slices fast, with convenient Micropure™ separators. To concentrate as well, combine with Microcon® microconcentrators and process your gel slices in under 10 minutes. Get high recovery in a single centrifuge spin at up to 14,000 × g.

Discover Amicon's creative solutions in membrane separation, based on our unique experience.

We'd like to send you 19 of them now!

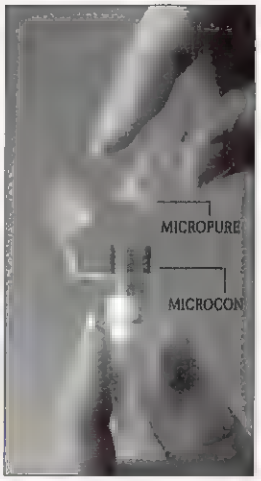

For more information and protocols, please call 1-800-343-1397

amicon®
a GRACE company

Amicon, Inc., 72 Cherry Hill Drive, Beverly, MA 01915

Circle No. 42 on Readers' Service Card

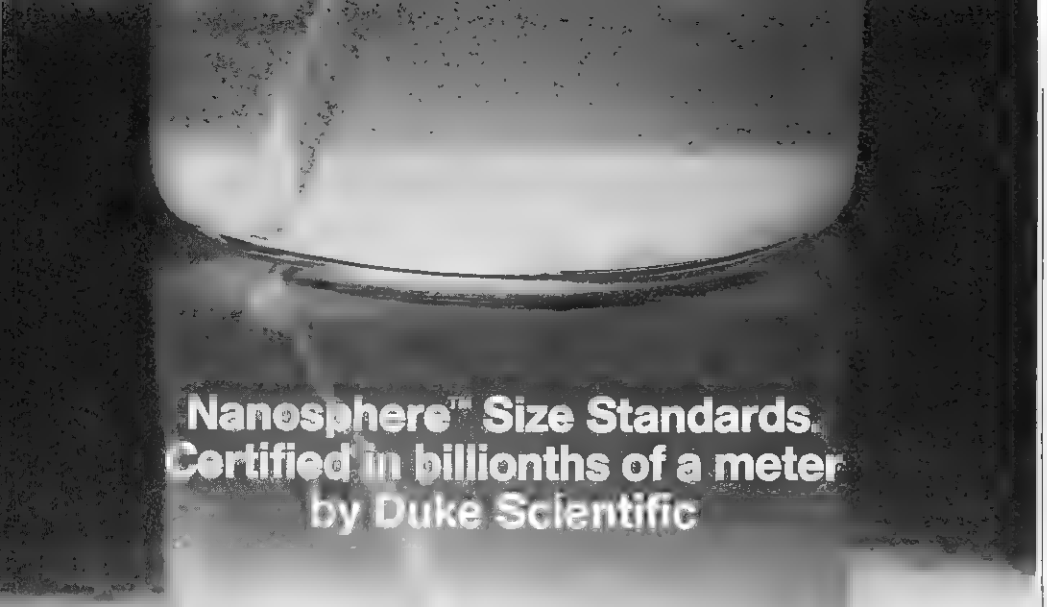

Nanosphere™ Size Standards. Certified in billionths of a meter by Duke Scientific

Nanosphere Size Standards are calibrated in billionths of a meter (nanometers) and are available in 22 sizes from 21 to 900nm—all traceable to the National Bureau of Standards. Nanospheres are part of our complete line of spherical particles from 0.02 to 2000 micrometers in diameter. They are used as standards for instrument calibration, quality control, filter checking, and in numerous biotechnology applications. At Duke Scientific—established in 1971—we have the expertise and resources to meet any of your requirements for microspheres and particles. Call us today for information.

Duke Scientific Corporation

2463 Faber Place, P.O. Box 50005, Palo Alto, CA 94303, Toll Free (800) 334-3883, in CA (415) 424-1177, Fax (415) 424-1158

Circle No. 46 on Readers' Service Card

Resource Directory of Scientists and Engineers with Disabilities

The American Association for the Advancement of Science Project on Science, Technology, and Disability invites scientists and engineers with disabilities to be included in the third edition of the *Resource Directory of Scientists and Engineers with Disabilities*. Potential candidates for the directory must hold, or be working toward, a degree in a scientific, engineering, or medical discipline, or currently be employed in a scientific field.

Funded by the National Science Foundation, the project's *Resource Directory of Scientists and Engineers with Disabilities* has assisted hundreds of individuals enter and advance in scientific disciplines. The directory helps to connect persons with disabilities and their families with professors, teachers, and counselors who can serve as role models and mentors.

The *Resource Directory* lists scientists, mathematicians, and engineers from all parts of the country with their disciplines, degrees, and disabilities. Individuals include professionals who were born with a disability, and those who acquired their disability mid-career. Persons listed in the directory are also asked to consult for academia, government agencies, and industry as well as serve on peer review panels and symposia.

Established in 1975, the AAAS Project on Science, Technology, and Disability has sought and shared expert advice from scientists and engineers with disabilities. Since the passage of the Americans with Disabilities Act (ADA), the AAAS *Resource Directory* has become a valuable source of expertise.

To be included in the *Directory* we are asking candidates to forward the following information: ***Name, Address, Phone number, Disciplines, Degrees, and brief description of their current work*** to the attention of Laureen Summers, Program Associate; or Patricia Thompson, Editorial Assistant, AAAS, 1333 H Street, N.W., Washington, DC 20005 or information can also be sent via fax to 202-371-9849. For additional information please call (202) 326-6645 (v/tdd).

WE NEED YOUR HELP!

EXPLORE WITH AAAS in 1995

- **Mexico's Copper Canyon**, April 22–29. Led by Mexican historian Pedro Palma. *$1,890 plus air*
- **Backroads China**, May 26–June 9. Discover a China that is hinted about, and almost never seen. Led by Dr. Chris Carpenter and Prof. Wang Zhijun of the Chinese Academy of Sciences. *$2,295 plus air*
- **Lake Baikal & the Great Siberian Tiaga**, July 9–23 & Sept. 3–17. Led by Dr. Vladimir Fialkov, Baikal Museum Director, and Dr. Victor Kuzenavov, Irkutsk Botanic Garden Director. A superb exploration of Lake Baikal and more. *$2,495 plus air*
- **Impressions of a Swedish Summer**, August 17–27. *$2,295 plus air*
- **Columbia River Cruise**, Oct. 27–Nov. 2. With lectures by AAAS scientist Dr. Marvin Beeson, explore the land of Lewis & Clark, the Columbia and Snake Rivers. *from $1,990 plus air*
- **South Georgia Islands & Antarctica**, Nov. 29–Dec. 20. Led by wildlife biologist Narca Moore-Craig, explore South Georgia, the Falklands, Antarctic Peninsula, and more. *from $5,995 plus air*
- **Sea of Cortez**, December 27–January 3, 1996. A fifth repeat of this popular holiday adventure, led by Dr. Roger Luckenbach. *from $2,370 plus air*
- **Antarctica & the Falkland Islands**, Jan. 25–Feb. 8, 1996. With lectures by Dr. Gunter Weller. A repeat of our popular expedition on board *M/V Alla Tarasova*. *from $5,395 from Miami*

Call Today for Trip Brochures!

(800) 252-4910

AAAS *Travels*

Exclusively for AAAS by BETCHART

A leading operator of travel for non-profits since 1981

17050 Montebello Road
Cupertino, CA 95014-5435

BOOK REVIEWS

Hydraulics Under Fire

Structures in the Stream. Water, Science, and the Rise of the U.S. Army Corps of Engineers. TODD SHALLAT. University of Texas Press, Austin, 1994. xii, 276 pp., illus. $34.95.

Not long ago, while explaining to a relative some contract work I was performing for the Office of History of the Army Corps of Engineers, I was surprised at the cool, almost hostile reaction that my mention of the Corps evoked. Apparently the Corps is not too popular in some parts of New Jersey. It is a reaction with which Todd Shallat is familiar. "I live in Idaho on a tributary of the Snake," he begins his preface, "where the U.S. Army Corps of Engineers is widely misunderstood and despised."

It is in large part to explain this hostility that Shallat, director of the public history program at Boise State University, has written his impressive, groundbreaking *Structures in the Stream*. Shallat uses federal water policy as the thread by which he examines the early history of the Army Corps of Engineers from its origins in the 18th century through the Mississippi Delta dispute of the late 19th century. The result is a succinct, analytical, and well-documented study that is, Shallat writes, "my way of thinking through the connection between science, technology, and political power."

Intriguingly, Shallat traces the origins of the controversy to a sharp cultural and technological division within the American engineering community. Heavily influenced from the start by the French tradition of engineering, American military engineers adhered to the French emphasis on centralized national planning, government financing, and military justification for internal improvement projects. They also adopted French engineering practices and technology, which emphasized the use of scientific methods and theory as the basis for application. American cadets studied French science and read French texts at West Point, and as commissioned officers they often traveled to France for additional study; so it is hardly surprising that they favored French ideas and methods in hydraulic engineering.

This Continental orientation put the Corps at odds with the mainstream of early American building culture, which, true to the British tradition of engineering, favored locally and privately financed projects that were justified on commercial grounds and carried out by self-taught gentleman-mechanics. Civilian American engineering practice, like that of the British, was based largely on empirical knowledge and rules of thumb and tended to follow British ideas and techniques. To civilian builders, and to much of the rest of American society, the Corps of Engineers seemed elitist, bureaucratic, and even threatening to American democratic institutions; while the Corps's technology seemed too theoretical, impractical, and unnecessarily expensive.

These cultural and technological conflicts played themselves out in political battles between the proponents and opponents of federal sponsorship of internal improvements throughout the 19th century. The Corps of Engineers was—and remains—far more involved in these early contests than has usually been recognized. One of Shallat's most cogent points is that however apolitical and neutral technicians may profess to be, they hold power by virtue of their expert knowledge, their control of information, and their role as implementers of government programs.

"Critics have long denounced the 'pork-barrel' ties that bind the Corps to the Senate and House." [From *Structures in the Stream*; courtesy of the *Arkansas Democratic Gazette* and George Fisher]

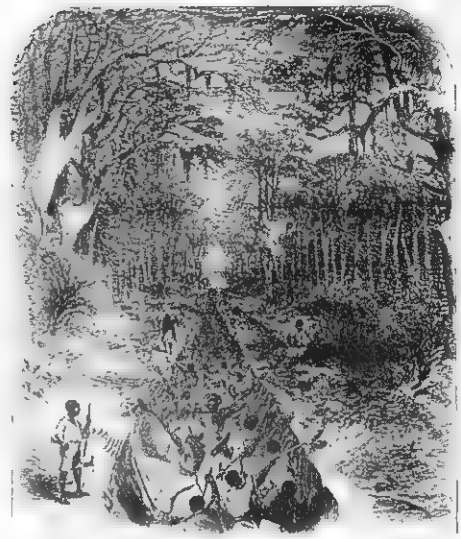

"Canal at Delta Point, 1862. Laboring in blistering heat, 1,200 slaves toiled alongside Union soldiers in an aborted attempt to bypass Confederate guns by cutting through a bend in the Mississippi River near Vicksburgh." [From *Structures in the Stream*; courtesy of the Boise Public Library]

"Ultimately, the power to quote statistics and package information shaped government as much as the shifting mandates of Congress and the ambiguous directives of law" (p. 156). The Corps promoted a grand vision of centralized planning and military-sponsored public works via the recommendations of individual officers and boards, such as the Board of Engineers for Internal Improvements in the 1820s. Disputes such as those over the Chesapeake & Ohio Canal and later the Mississippi River projects were as much about the Corps's philosophy and outlook as about its technology. The Army did succeed in establishing early its claim to jurisdiction over federal waterways projects, but the French tradition did not entirely prevail; public hostility to that tradition "helps explain why the United States remains one of the very few industrialized countries without a central planning authority or an intelligible national plan" (p. 6).

Given the partisan or polemical nature of much of the literature on the Corps of Engineers, *Structures in the Stream* is refreshingly balanced and objective. Shallat equivocates on the Corps's ultimate legacy. The Corps, he notes, is indeed authoritarian, hidebound, and often resistant to innovation, as its critics maintain; but it has also embraced innovation at other times, promoted the nation's commerce and safety, and advanced the concept of rational planning (for better or worse). "In the end," Shallat concludes, "there is no simple way to characterize Corps engineering. Cautious, responsive, despotic, opportunistic—

the engineers, after two hundred years, have learned to straddle the contradictions built into our nation state" (p. 207).

Philip L. Shiman
History Department,
Duke University,
Durham, NC 27706, USA

■

Workings of HIV

HIV and the Pathogenesis of AIDS. JAY A. LEVY. ASM Press, Washington, DC, 1994. xiv, 359 pp., illus., + plates. Paper, $49; to American Society for Microbiology members, $39.

That human immunodeficiency virus causes AIDS has long been evident from its global and detailed epidemiology; for example, about 50 percent of HIV-infected hemophiliacs have developed AIDS thus far, whereas no HIV-negative hemophiliac has done so. Just how HIV causes AIDS has seemed more mystifying, although the salient clues have been there from the beginning. In 1981 Michael Gottlieb reported that AIDS patients exhibited a severe depletion of CD4-positive T-helper lymphocytes, and in 1984 David Klatzmann showed that these very cells are selectively sensitive to infection by HIV. Thus their depletion is explained by HIV infection, due either to the cytopathic effects of the virus itself or, more likely, to destruction by HIV-specific CD8-positive cytotoxic T lymphocytes. At first it seemed puzzling how few HIV-infected cells were detectable in peripheral blood at any one time. But by 1986 Klara Tenner-Racz had shown that the lymph nodes of asymptomatic HIV-positive people are actually chockablock with HIV, which is not a latent infection at all. In fact, the viral burden is high in many individuals. As George Shaw's and David Ho's groups recently reported, the turnover of HIV and HIV-infected cells is so rapid that it is a wonder how the immune system maintains its integrity for many years in the face of this viral onslaught. We may ask, therefore, why such an effective immune response is not successful in clearing the virus altogether? Yet if it cannot, why does it keep the more severe effects of HIV at bay so long, and what co-factors herald progression to AIDS? These questions about HIV pathogenesis are germane both to vaccine development and to therapeutic strategies to prevent or delay AIDS.

Jay Levy's monograph on HIV and the pathogenesis of AIDS tells you everything about HIV infection you might wish to find out without tackling the daunting literature on AIDS, which generates thousands of new research reports each year. It is a considerable achievement that one scholar could grasp the entire subject and distill our knowledge of it in 12 concise chapters and some 2000 references. Levy was a pioneer of HIV isolation and characterization, and he and his colleagues at the University of California at San Francisco have made signal contributions to the understanding of HIV in the brain, of HIV tropism, and of the role of CD8 cells in controlling infection. In this volume he has kept abreast of the ever-burgeoning field in a remarkably informed and balanced way. Indeed, I would have preferred him to be more opinionated about controversial aspects of HIV infection, as he can be in informal discussions, for that is a privilege of the single-author book amid so many multi-author volumes.

Levy moves from a description of HIV to features of transmission, the cell and molecular biology of infection, the enormous genetic and phenotype heterogeneity of HIV and its variable tropism for lymphocytes, macrophages, and dendritic cells, to the host's immune responses. He describes the pathogenesis of HIV not only in the immune system itself but also in the central nervous system, gastrointestinal tissue, and other organs. He does not dwell in detail on the various opportunistic infections that result from AIDS but includes a useful chapter on AIDS-related cancers. The final chapters deal with the prognosis for long-term survival featuring non-progressors and how antiviral approaches linked with immune modulation might form the pattern of future treatment.

The text is clearly illustrated with mainly black-and-white diagrams (and some colorful histopathology), useful boxed tables and lists, and appendixes on the clinical categories and classifications of AIDS. This volume will be valuable to the seasoned virologist, immunologist, or physician and to the newcomer to AIDS research alike.

Robin A. Weiss
Chester Beatty Laboratories,
Institute of Cancer Research,
London SW3 6JB, UK

■

Patterns of Peopling

The History and Geography of Human Genes. L. LUCA CAVALLI-SFORZA, PAOLO MENOZZI, and ALBERTO PIAZZA. Princeton University Press, Princeton, NJ, 1994. xiv, 1032 pp., illus. $150 or £150.

In 1978 the authors of this volume, in a paper in this journal, helped reinvigorate interest in the analysis of geographic patterns of genetic variation as a method for inferring pattern and process in the evolution and history of human populations. The paper, and the cover of the issue of *Science* that contained it, became well known as having introduced the method of synthetic gene-frequency maps. The present volume is the culmination of a 20-year collaboration to document the extent and patterning of human genetic variation using classical markers. According to the authors, the "book was started with the desire to analyze the geography of human genes, using new techniques we have developed for the purpose of studying ancient human migrations."

Cavalli-Sforza and colleagues have compiled an unprecedented array of genetic data on the world's populations. The original database consisted of over 76,000 allele frequencies from 6633 separate samples. The authors exercised a mixture of culling and pooling strategies to reduce the database to a more analytically manageable 491 populations with observations on over 120 alleles. Although the criteria applied in this culling and pooling of samples are left frustratingly vague, the appendixes make clear which populations are used in the basic analyses presented throughout the book.

The largest section—the second half—of this compendium consists of more than 500 gene-frequency maps. For each allele for which sufficient observations are available there is a map reflecting the world distribution of its frequency, as well as separate maps displaying the allele frequency diversity on separate continents: Africa, Asia, Europe, America, and the Pacific Islands, including Australia and New Guinea. The maps include the geographic location of each population from which data are used, symbols intended to help the reader judge the fit between the original data and the map, and three small graphs, one summarizing the descriptive statistics of the distribution of the allele frequencies, one showing the sample sizes, and a variogram, a standardized method of indicating the relationship between geography and genetic variation. In addition to these single-gene maps, color maps reflecting the conjoint distribution of the first three principal-component scores of allele frequencies are also given for the world and the five continental areas.

The single-gene maps are an impressive summation of genetic data. Valuable as I believe they are, however, they should be viewed with considerable caution. The map of *HLAA*2* for the Americas is illustrative. The portion of the map of North America north of Mexico is based on only 10 data points: two in western Alaska, two on the Arctic coast of Canada, one in the U.S. southeast, and five clustered closely in the U.S. southwest. Additionally, Greenland is represented by a single observation on the

east coast. The map of this gene indicates a regular clinal pattern emanating from the core of high frequencies in the U.S. southwest to lower frequencies in the Arctic and eastern Greenland, yet for most of this vast geographic expanse no data are actually available. All six of the displayed levels of variation in this map are represented in this geographic space, including three separate levels in Greenland, where only a single population is represented for this allele. In some of their other maps, admittedly with a more uniform distribution of data points, such clinial distributions are used as a basis for inferences regarding ancient migrations and settlements. Though in general such inferences are reserved for the interpretation of synthetic maps of principal components, they amplify the problem of visual geographic display from sparse data.

The authors are most familiar with this problem, which invariably arises in analyzing geographic variation in gene frequencies. Should one opt for maximizing number of genetic systems (alleles) or number of populations sampled? It is not possible to do both; maximizing one inevitably reduces, usually dramatically, the other. This asymmetry stems from the fact that there has never been a standard set of markers to be typed in all groups studied. Haphazard data collection has made it impossible to directly compare large numbers of populations for the same (large) set of genetic polymorphisms. The authors recognize and lament this fact and use the opportunity to lobby for greater coordination, and standardization, in the collection of population data on the DNA polymorphisms now being carried on worldwide. They have attempted a compromise in this book by initially maximizing the number of genes available for analysis, critical for many types of genetic (for example, phylogenetic) analysis, and then not eliminating populations just because they lack data on one or more systems. The authors argue that comparing populations differing in the systems available should not introduce substantive bias so long as the number of genes is large, the overlap of systems between populations compared is substantial, and the lack of observations on any particular system is essentially random. This is a cogent and practical argument, I believe, but the 24% missing data in the full data array should give pause.

Whatever deficiencies may obtain in the individual gene maps, they are usually clearly acknowledged. Questions raised by the peculiarities of the geographic distribution of alleles are frequently the subject of more detailed analyses and hypothesis tests in the other major portion of the volume, eight chapters of description and analysis of the data upon which the maps are based. The first of these chapters is essential reading, since it delineates the nature of the data employed and analytical methods used. The last, an epilogue, provides less a summary of what has gone before or an introduction to the maps to follow than a position statement on the nature of multidisciplinary genetic research and where it may, and should, go, including a reiteration of the authors' support for the Human Genome Diversity Project.

Between these chapters are summaries of the analysis of the pattern of diversity of allele frequencies on a global scale and treatments of each of the continental areas. The format of these chapters is uniform: an archeological and linguistic introduction is followed by a genetic distance analysis (F_{ST} is used as the distance statistic throughout). The genetic distances are used as the basis of a phylogenetic analysis with an average linkage tree as the core. Finally, a series of principal-component and synthetic gene-frequency maps are displayed and discussed with respect to the previous analyses and observed gene frequency patterns.

The treatment of world genetic diversity in chapter 2 is based on a subsample of only 42 populations, albeit with a large number of alleles analyzed. Fourteen of the samples are from Asia, but no other continent is characterized by more than seven. Nevertheless, "the most important conclusion in this section is that the greatest difference in the human species is between Africans and non-Africans . . ." (p. 83). This conclusion is at variance with some earlier analyses from these authors but concordant with a growing number of studies based on DNA markers and sequences, briefly reviewed here. The reasons for the discrepancy with earlier studies are examined and the discrepancy is attributed to the inclusion of too few genes in prior analyses.

The authors are at pains here and in the chapters on individual continents to document the correlation between patterns of genetic and linguistic variation. It is unquestionably true that language may both facilitate and impede genetic exchange, thus imposing a similarity on genetic and linguistic distributions. However, the use of linguistic affinity as one of the criteria for pooling separate samples from local geographic areas would seem to weaken the analyses demonstrating close association of genetic and linguistic variation.

Space precludes accounts of the analyses and conclusions for all continental areas, but the chapter on the Americas may serve as example. In general, analytical results illustrate a reasonably clear relationship of gene frequency variation to geography for North American groups, whereas South America is characterized by extreme genetic diversity, with little correlation with geography or linguistics. This pattern is interpreted as reflecting extreme drift among populations of this continent, in accordance with results by earlier workers. In North America, Athapaskan groups are shown to be more similar to Eskimos than to other Amerinds, a confirmation of earlier work of these authors and others. The greater correspondence among genes, geography, and language in North Amerinds is taken to reflect the discrete nature of early migrations. The authors clearly adopt and support the three-migration theory of Amerindian origins, based in part on the tripartite linguistic classification of Amerinds by Greenberg: Amerind, Na-Dene, and Eskimo-Aleut. Moreover, the au-

Vignettes: Comestibles

My meal . . . was very agreeable, surpassing anything found at the table of the wealthy. Good, fat, well-boiled venison, taken with pure honey, is as great an excitant of the power of the *sensorium commune* in the human species as a pure solution of sulph[uric] copper is to excite the power of a clean galvanic battery.

—*Gideon Lincecum*, in *Adventures of a Frontier Naturalist: The Life and Times of Dr. Gideon Lincecum* (Jerry Bryan Lincecum and Edward Hake Phillips, Eds.; Texas A&M University Press)

I would ask anybody to name some attribute of milk besides purity. Yes, whiteness is bound to be one. "Whiteness" and "purity." Atoms would be way up at the top, but an atomic description of milk is still a long way beyond us. . . . As to the scientific account of cheese-making, until recently the way you learned to make cheddar or brie was to go and apprentice yourself to the best brie-making farmer in Brie. There wasn't any way to go to Cornell and find out. You could go there and make cheese all right, but by God it was sure not brie.

—*Philip Morrison*, in *Nothing Is Too Wonderful to Be True* (AIP Press)

thors argue that the analysis of gene-frequency diversity in America is rather more consistent with an earlier Amerind entry (15,000 to 30,000 years ago) than many American archeologists are ready to acknowledge.

The book contains three appendixes. The first two provide allele frequencies for the 42 populations used in the global analysis, and for the 491 populations in the full database. Appendix 3 lists the primary sources from which the gene frequency data were obtained.

There is much to relish and much to challenge in this volume. Many will question the use of specific analytical methods (choice of distance statistic, tree-construction method, and synthetic map surface construction methods) or be frustrated at the ambiguities of sample pooling or the limitations of the analyses presented. For many, the lack of clear-cut criteria upon which a number of analytical decisions, such as the deletion of samples due to admixture, were made will be troubling. Similarly, "when points for calculating variogram curves were too few, the variogram was omitted from the gene maps" (p. 124). The criteria employed to make this judgment are not obvious, nor is the rationale for producing a map from what may be presumed to be very sparse and irregularly distributed observations.

These reservations, however, are modest. This is an impressive display of synthesis and analysis. Arguments regarding methods and approaches will be trivial if the original data are made available to other researchers as is implied in chapter 1. This is the most comprehensive treatment of human genetic variation available. If it provokes many to challenge its conclusions and hypotheses with increasingly sophisticated analyses, and I believe it will, it will likely play an important role in future research in anthropological genetics. It is especially appropriate that such a complete summary of the classical blood-group, serum-protein, and enzyme markers appears now, as we are rapidly generating the next generation of human genetic diversity data at the nucleotide level. Many of the deficiencies to be found in this volume are the deficiencies of data collection, of standardization, and ultimately of comparability. As the authors clearly note, we should learn from these deficiencies and coordinate, to a much greater degree than in the past, the nature of the genetic data now being accumulated on DNA markers. This is a lesson worth learning, and one that is clearly presented here.

Dennis H. O'Rourke
Department of Anthropology,
University of Utah,
Salt Lake City, UT 84112, USA

Books Received

The Asian City. Processes of Development, Characteristics and Planning. Ashok K. Dutt *et al.*, Eds. Kluwer, Norwell, MA, 1994. xvi, 392 pp., illus. $176 or £116 or Dfl. 275. GeoJournal Library, vol. 30.

Atlas of Compact Groups of Galaxies. Paul Hickson. Gordon and Breach, Langhorne, PA, 1994 (distributor, International Publishers Distributor, Brooklyn, NY). viii, 221 pp., illus. $68 or £44 or ECU 57; paper, $32 or £21 or ECU 27.

Automotive Sensors. M. H. Westbrook and J. D. Turner. Institute of Physics, Philadelphia, 1994. xviii, 253 pp., illus. $149 or £75. Sensors Series.

Basic Mechanisms of Physiologic and Aberrant Lymphoproliferation in the Skin. W. Clark Lambert, Benvenuto Giannotti, and Willem A. van Vloten, Eds. Plenum, New York, 1994. xii, 651 pp., illus. $135. NATO ASI Series A, vol. 265. Based on a workshop, San Miniato, Pisa, Italy, Oct. 1991.

The Bell Curve. Intelligence and Class Structure in American Life. Richard J. Herrnstein and Charles Murray. Free Press (Macmillan), New York, 1994. xxvi, 845 pp., illus. $30.

Beta$_3$-Adrenergic Agonism. A New Concept in Human Pharmacotherapy. Daniel E. Goldberg and William H. Frishman. Futura, Armonk, NY, 1994. x, 198 pp., illus. $35.

Blondes in Venetian Paintings, the Nine-Banded Armadillo, and Other Essays in Biochemistry. Konrad Bloch. Yale University Press, New Haven, CT, 1995. xiv, 261 pp., illus. $30.

The Book of Genesis. Exploring Realistic Neural Models with the GEneral NEural Simulation System. James M. Bower and David Beeman. Springer-Verlag, New York, 1994. xx, 409 pp., illus. $49.95.

The Book of Ingenious and Diabolical Puzzles. Jerry Slocum and Jack Botermans. Times, New York, 1995. viii, 152 pp., illus. $19.50.

The Brackish-Water Fauna of Northwestern Europe. An Identification Guide to Brackish-Water Habitats, Ecology and Macrofauna for Field Workers, Naturalists and Students. R. S. K. Barnes. Cambridge University Press, New York, 1994. xvi, 287 pp., illus. $64.95; paper, $24.95.

Circuits of the Mind. Leslie G. Valiant. Oxford University Press, New York, 1994. xvi, 237 pp., illus. $49.95.

Complex Dynamics. R. Livi, J.-P. Nadal, and N. Packard, Eds. Nova, Commack, NY, 1994. viii, 310 pp., illus. $97. Les Houches Series. From a workshop, Les Houches, France, Mar. 1990.

Computational Analysis of Visual Motion. Amar Mitiche. Plenum, New York, 1994. xvi, 235 pp., illus. $65. Advances in Computer Vision and Machine Intelligence.

Condensed Matter Theories. Vol. 9. John W. Clark, Khan A. Shoaib, and Abdullah Sadiq, Eds. Nova, Commack, NY, 1994. xvi, 543 pp., illus. $98.

Coping with War-Induced Stress. The Gulf War and the Israeli Response. Zahava Solomon. Plenum, New York, 1994. xxvi, 254 pp., illus. $39.50. Plenum Series on Stress and Coping.

Cultivating Crisis. The Human Cost of Pesticides in Latin America. Douglas L. Murray. University of Texas Press, Austin, 1995. xiv, 177 pp., illus. $35; paper, $17.95.

The Cultures of Science. Marjorie Senechal, Ed. Nova, Commack, NY, 1994. viii, 93 pp., illus. $49. From a symposium series, Oct. 1992.

Cytokines in Human Multiple Myeloma. Bernard Klein, Régis Bataille, and Jean Luc Harousseau. Landes, Georgetown, TX, 1994 (distributor, CRC Press, Boca Raton, FL). viii, 116 pp., illus. $89.95. Medical Intelligence Unit.

Dioxins and Health. Arnold Schecter. Plenum, New York, 1994. xxii, 710 pp., illus. $125.

DNA Structure and Function. Richard R. Sinden. Academic Press, San Diego, CA, 1994. xxiv, 398 pp., illus. $49.95.

Drug Use and Abuse. Stephen A. Maisto, Mark Galizio, and Gerard J.Conners. 2nd ed. Harcourt Press (Harcourt Brace), Fort Worth, TX., 1994. xx, 500 pp., illus. Paper, $15.95.

Environmental Deceptions. The Tensions Between Liberalism and Environmental Policymaking in the United States. Matthew Alan Cahn. State University of New York Press, Albany, 1995. xii, 179 pp. $19.95. SUNY Series in International Environmental Policy and Theory.

Environmental Health Risks and Public Policy. Decision Making in Free Societies. David V. Bates. University of Washington Press, Seattle, 1995. xii, 117 pp., illus. $30; paper, $12.95. Jessie and John Danz Lecture Series.

The Environmental Imagination. Thoreau, Nature Writing, and the Formation of American Culture. Lawrence Buell. Harvard University Press, Cambridge, MA, 1995. xii, 587 pp., illus. $35.

Environmental Inequalities. Class, Race, and Industrial Pollution in Gary, Indiana, 1945-1980. Andrew Hurley. University of North Carolina Press, Chapel Hill, 1995. xx, 246 pp., illus. $39.95; paper, $16.95.

Equity Issues for Women in Archeology. Margaret C. Nelson, Sarah M. Nelson, and Alison Wylie, Eds. American Anthropological Association, Washington, DC, 1994. xii, 236 pp., illus. Paper, $25. Archeological Papers of the American Anthropological Association, no. 5.

Explorations Beyond the Machine. A Philosophy of Social Science for the Post-Newtonian Age. Ian T. King. Nova, Commack, NY, 1994. x, 277 pp. $69. Mamardashvili Series on Philosophy, Psychology and Sociology.

Exploring Social, Political and Economic Organization in the Zuni Region. Todd L. Howell and Tammy Stone, Eds. Arizona State University, Tempe, 1994. x, 130 pp., illus. Paper, $17.50. Anthropological Research Papers, no. 46.

The Human Endometrium. Carlo Bulletti, Erilo Gurpide, and Carlo Flamigni, Eds. New York Academy of Sciences, New York, 1994. xii, 500 pp., illus. $155. Annals of the New York Academy of Sciences, vol. 734. From a conference, Bologna, Italy, Sept. 1993.

The Human Volcano. Population Growth as Geologic Force. Jon Erickson. Facts on File, New York, 1995. x, 210 pp., illus. $24.95 or $C31.95. The Changing Earth Series.

Minding the Helm. Marine Navigation and Piloting. National Research Council Committee on Advances in Navigation and Piloting. National Academy Press, Washington, DC, 1994. xxii, 500 pp., illus. $54.95.

Modern Methods in Analytical Morphology. Jiang Gu and Gerhard W. Hacker, Eds. Plenum, New York, 1994. xii, 445 pp., illus. $125. From a workshop, Salzburg, Austria, Sept. 1992.

Molecular Genetics in Surgical Oncology. Jeffrey F. Moley and Steve H. Kim. Landes, Georgetown, TX, 1994 (distributor, CRC Press, Boca Raton, FL). vi, 112 pp., illus. $89.95. Medical Intelligence Unit.

More Than One Mystery. Explorations in Quantum Interference. Mark P. Silverman. Springer-Verlag, New York, 1994. xiv, 212 pp., illus.

Multisensor Integration and Fusion for Intelligent Machines and Systems. Ren C. Luo and Michael G. Kay, Eds. Ablex, Norwood, NJ, 1995. xvi, 688 pp., illus. $85.

The Muon Method in Science. V. P. Smilga and Yu. M. Belousov. Nova, Commack, NY, 1994. xii, 420 pp., illus. Proceedings of the Lebedev Physics Institute, vol. 219.

Patrick Suppes, Scientific Philosopher. Vol. 3, Language, Logic, and Psychology. Paul Humphreys, Ed. Kluwer, Norwell, MA, 1994. vii, 344 pp., illus. $146 or £116 or Dfl. 290. Synthese Library, vol. 235.

Peptidases and Neuropeptide Processing. A. Ian Smith, Ed. Academic Press, San Diego, CA, 1994. xvi, 407 pp., illus. $95. Methods in Neurosciences, vol. 23.

Photobiology in Medicine. Giulio Jori *et al.* Plenum, New York, 1994. x, 190 pp., illus. $75. NATO ASI Series A, vol. 272. From an institute, Alghers, Italy, Sept.-Oct. 1993.

Physical and Related Properties of 145 Timbers. Information for Practice. Jan F. Rujskijk and Peter B. Laming. Kluwer, Norwell, MA, 1994. viii, 380 pp., illus. $105 or £70 or Dfl. 170. TNO Building and Construction Research, Centre for Timber Research.

Physiology and Determination of Crop Yield. K. J. Boote *et al.*, Eds. American Society of Agronomy, Crop Science Society of America, and Soil Science Society of American, Madison, WI, 1994. xxii, 601 pp., illus. $66. Based on a symposium, Gainesville, FL, June 1991.

Simplified Building Design for Wind and Earthquake Forces. James Ambrose and Dimitry Vergun. 3rd ed. Wiley, New York, 1995. x, 355 pp., illus. $49.95. Parker/Ambrose Series of Simplified Design Guides.

DO YOU REALLY, REALLY, REALLY WANT TO MAKE A DINOSAUR?

DNA STAT-120

High Molecular > 150 Kb

- Less than a 2 hour procedure from start to finish
- Very high yield of pure high MW Genomic DNA
- Adapts easily to very small or large specimens
- No organic solvents, no centrifugation
- DNA good for southern blotting and cDNA libraries
- Gold-pak for PCR applications (cat. no. 4530)

50 ml - TL-4500 • 100 ml - TL-4510
200 ml - TL-4520

RNAzol™ B - Total RNA in 90 minutes

RNA STAT-60™ - Total RNA in less than 1 hour

RNA STAT-50™ LS - Single extraction reagent for total RNA from liquid samples

RNA STAT-30™ KIT - Total RNA/mRNA isolation kit

mRNA STAT-30™ KIT - poly a+mRNA isolation kit - oligo d T columns

Aquanase-Free™ Water - RNase, DNase, pyrogen free water for all molecular biology needs

DNA STAT-60

Low Molecular < 20 Kb

- Monophasic
- Non-poisonous, non-irritant, organic solvent
- Does not require ultracentrifugation
- No organic solvents, no centrifugation
- DNA good for PCR, southern blotting, and cDNA libraries

50 ml - TL-4200 • 100 ml - TL-4210
200 ml - TL-4220

TEL-TEST "B," INC.

P.O. Box 1421 • 1511 County Road 129 • Friendswood, Texas 77546
(713) 482-2672 • Customer Service: (800) 631-0600 / Outside Texas • FAX: (713) 482-1070

Circle No. 57 on Readers' Service Card

Stanford Graphics 3.0

The Ultimate Technical Graphics and Analysis Software

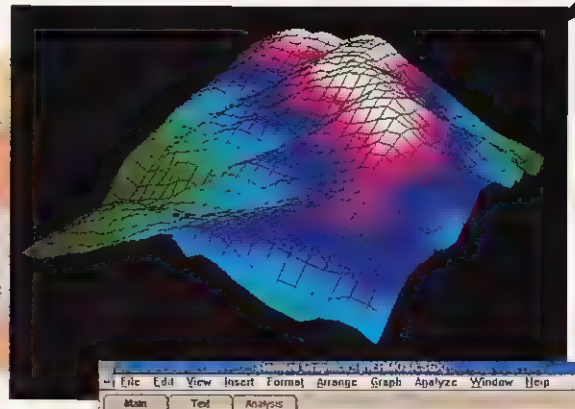

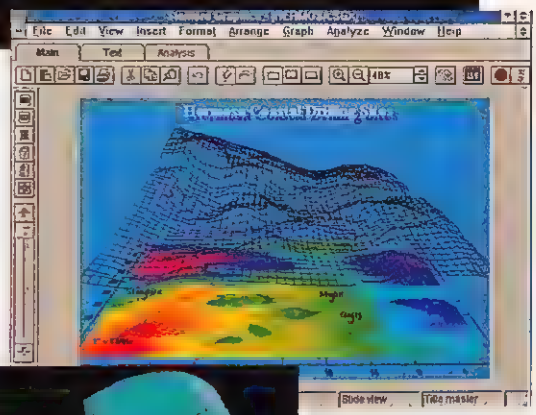

- Comprehensive statistical library of functions ever offered in a presentation package.
- Graph Gallery of 171 chart types for business, statistical and technical users.
- Interactive presentation-quality 2D and 3D graphics.
- Links large external data files to a 4-dimensional spreadsheet.
- Formula Visualizer graphically displays user-defined equations.
- Curve fitting, contouring, FFT's and data smoothing.
- Complete Windows compatibility, including DDE, OLE and True Type font support.

Rated #1 by PC Windows Magazine

Windows 3.1, & Windows NT Versions Available

Call for a FREE InfoPak today!

1-800-729-4723

Visual Numerics

phone (713) 954-6424 fax (713) 781-9260
e-mail: marketing@houston.vni.com
Mosaic URL: http://www.vni.com

STANFORD GRAPHICS Presentation & Data Analysis Software

Visual Numerics and Stanford Graphics are trademarks of Visual Numerics, Inc.
All other brand or product names are trademarks of their respective owners.

Circle No. 51 on Readers' Service Card

AD9582

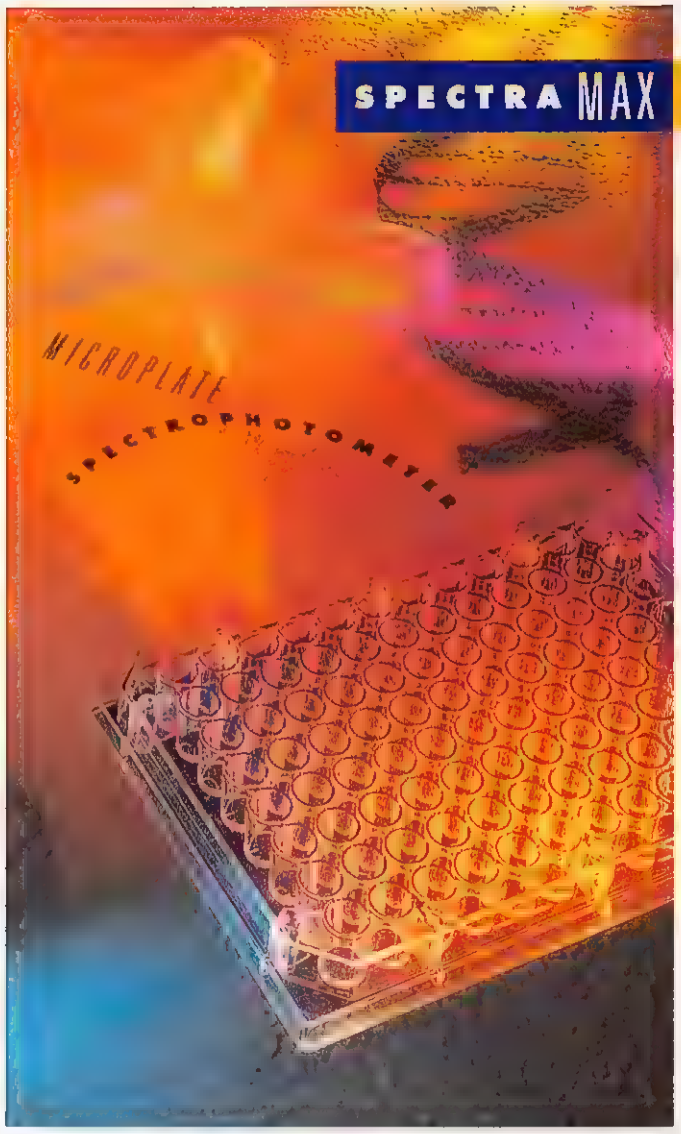

Now... Read DNA, RNA, and Proteins Directly

SPECTRAmax 250:
It's more than a Microplate Reader

SPECTRAmax™ 250 combines the tunability of a spectrophotometer with the efficiency of a microplate reader. Simplify your analysis using the speed and convenience of a microplate format.

Direct UV measurements in a microplate
Directly determine the concentration of up to 96 different DNA, RNA, or protein samples in a few seconds using a SPECTRAplate UV transparent disposable or quartz microplate. Protocols are included to measure the purity of DNA samples by calculating A 260/A 280 ratios. Use up to six different wavelengths to quantitate your samples.

UV/VIS Spectra Scans
Perform a spectral scan from 250-750 nm, in 1 nm increments, on all 96 wells of your microplate to determine the absorption maxima of your sample. Analyze column fractions or characterize the composition of inorganic samples.

New SOFTmax® PRO
The built-in spreadsheet capabilities of SOFTmax® PRO give you complete control of calculations and data presentation.

Discover the advantages of SPECTRAmax 250 – contact your local representative today at 1-800-400-9060

Tunable Wavelength

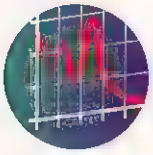
Spectra Analysis

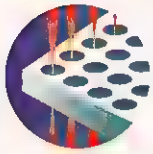
UV Transparent Microplate

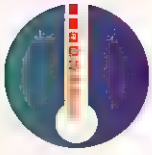
Precise Temp. Control

Molecular Devices
1311 Orleans Dr., Sunnyvale, CA 94089
(800) 400-9060

Circle No. 41 on Readers' Service Card

Call for a free sample

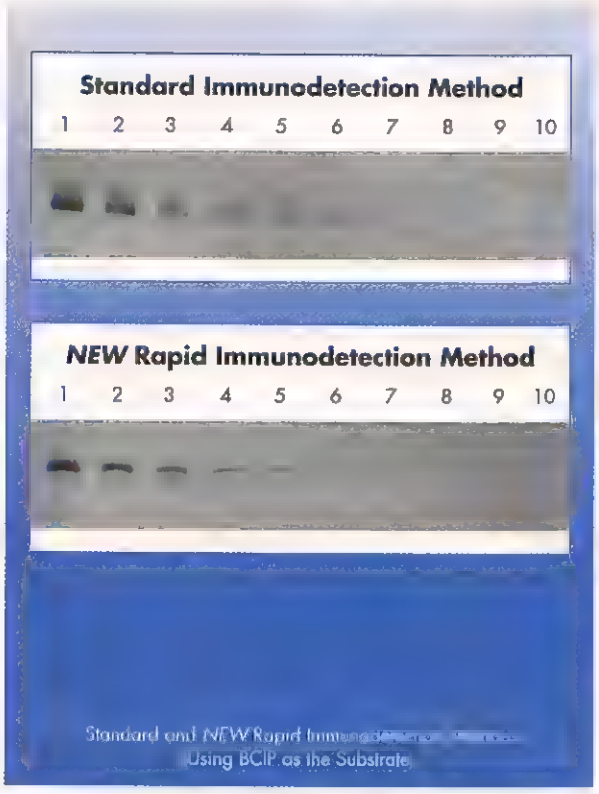
Standard Immunodetection Method
1 2 3 4 5 6 7 8 9 10
NEW Rapid Immunodetection Method
1 2 3 4 5 6 7 8 9 10
Using BCIP as the Substrate

Eliminate the blocking step in Western blots.

The standard immunodetection method for blotted proteins can be very time-consuming. That's because conventional membranes must be blocked to prevent non-specific antibody binding. Extensive washes are also required to reduce the background for a better signal-to-noise ratio.

Cut your detection time up to 2 hours with Immobilon-P™ Transfer Membranes from Millipore. Unique membrane properties eliminate the blocking step and dramatically reduce the number and length of washes required – without compromising specificity or sensitivity.

Call or fax to request a free sample of Immobilon-P Transfer Membranes and a copy of the new rapid protocol. U.S. and Canada call Technical Services: 1-800-MILLIPORE; Japan: (03) 3474-9111; European Headquarters in Paris, fax: 33.1.30.12.71.83.

MILLIPORE

Millipore Lab Catalogue on **Internet:** access **URL** menu and type: **http://www.millipore.com**

Circle No. 66 on Readers' Service Card

Introducing StatView 4.1 for your Power Macintosh

Analyzing data the StatView way is faster than ever!

StatView — now 4 to 10 times faster on your Power Macintosh!

Are you still trying to wring statistics from a spreadsheet? Or shuttling data back and forth among statistics, graphing, and presentation programs? We have a better way.

The StatView way

StatView is the best-selling, most award-winning data analysis package for the Macintosh. No other program combines data management, data analysis, graphing, drawing, and color presentation into a single easy-to-use package. If you need to go from raw data to a finished presentation, the easiest way is the StatView way.

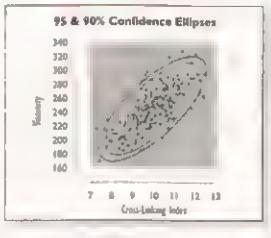

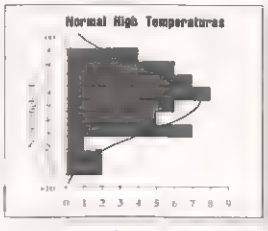

Now 4 to 10 times faster!

StatView is now accelerated for your Power Macintosh. (Of course it runs great on regular Macs, too.) Take advantage of this stellar performance increase — try StatView "native" on your Power Macintosh today. For more information on StatView 4.1, call us at **1-800-666-STAT**

ABACUS CONCEPTS
THE SIGNIFICANT DIFFERENCE™

© 1994 Abacus Concepts, Inc., 1918 Bonita Avenue, Berkeley, CA 94704-1014, tel: 510-540-1949, fax: 510-540-0260. StatView is a registered trademark and SuperANOVA is a trademark of Abacus Concepts, Inc. All other brands are property of their respective holders

Circle No. 61 on Readers' Service Card

The Gerontological Society of America and The Glenn Foundation for Medical Research Announce the Winners of the 1994 Glenn Foundation Award

James R. Smith, PhD and Olivia Pereira-Smith, PhD Huffington Center on Aging at Baylor College of Medicine

Drs. James R. Smith and Olivia Pereira-Smith were the recipients of the 1994 Glenn Foundation Award for a Significant Research contribution in the Biology of Aging. Drs. James R. Smith and Olivia Pereira-Smith were honored for their research into the molecular mechanisms of cell cycle control.

The $20,000 award was presented to Drs. Olivia Pereira-Smith and James R. Smith at The Gerontological Society of America's 47th Annual Scientific Meeting in November of 1994.

The Award is funded by the Glenn Foundation for Medical Research in Santa Barbara, California and administered by The Gerontological Society of America. The Society is the national multidisciplinary organization for researchers, educators and practitioners in aging.

The deadline for the 1995 Glenn Award selection process is May 8. For further information, contact:

Awards Coordinator
The Gerontological Society of America
1275 K Street, NW, Suite 350
Washington, DC 20005-4006
Tel: (202) 842-1275

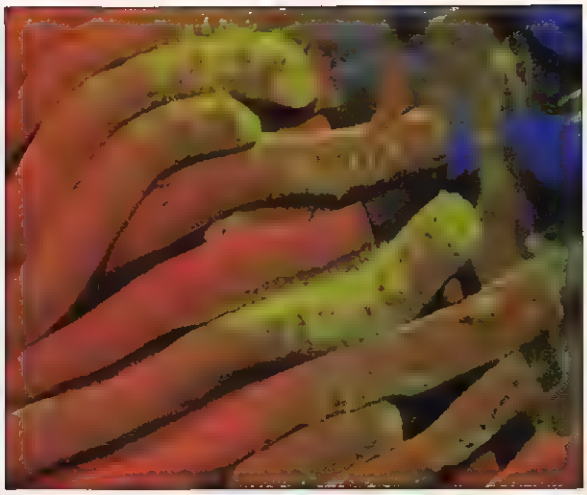

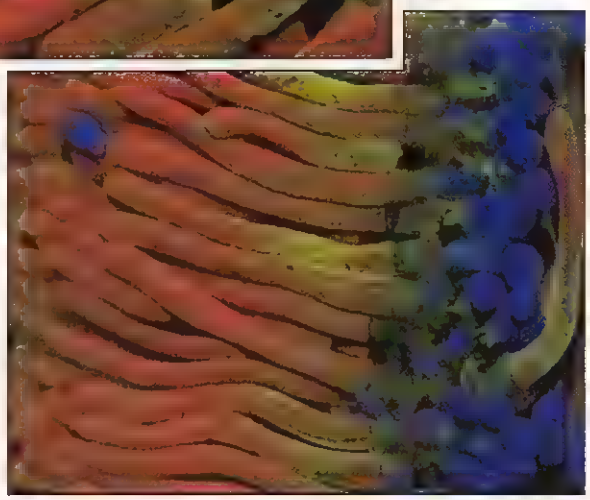

The Ultima 312™...

The Ultimate in Confocal Imaging

Introducing the Ultima 312™ Premium Laser Confocal Microscope System from Meridian Instruments, an instrument that treats your confocal data as it should be treated.

A high-performance point scanner, the Ultima 312 offers a **dynamic range of 12 bits per channel**. That means that even with particularly dim signals, the Ultima 312 provides 16 times the dynamic range of the best 8-bit systems, giving you images with more distinct contrasts. The result? More data content per image.

The Ultima 312 dramatically increases both the quality and the quantity of your data, as well as your confocal imaging options. It is well-suited for studies requiring **simultaneous detection of up to 3 channels**, as well as studies involving simultaneous (or sequential) **UV and visible laser excitation**.

Specimens ranging in size from bacteria to mice can be scanned using the instrument's **two scanning modes** — the aberration-free, on-axis StageScan™ mode (for scans of areas as large as 5.3 cm x 8.8 cm), or the high-speed DualScan™ combination galvanometric mirror and stage scanning mode (for faster scans of smaller areas). **Images can be as large as 1,536 x 1,536 pixels**, the largest available from any confocal intrument.

The Ultima 312 is controlled by a powerful Pentium microprocessor which automates such vital functions as pinhole alignment and calibration, an important benefit for researchers working in multi-user facilities.

The Ultima 312 Premium Laser Confocal Microscope System. 3 PMTs. 12-bit analog to digital conversion. Unlimited possibilities.

Contact the Meridian Instruments office nearest you for more information, or to schedule your personal demonstration of the Ultima 312, the ultimate laser confocal system.

3-D rendering of rod photoreceptors from the frog Xenopus laevis, showing the distribution of nuclei (blue), the visual pigment opsin (green), and glyco-conjugates containing N-acetyl glucosamine (red). Nuclei were stained with Hoechst; visual pigment was labeled with a monoclonal antibody to opsin, followed by a FITC-conjugated secondary antibody; and N-acetyl glucosamine was defined by lectin wheat germ agglutinin, conjugated to the fluorochrome Cy3. Top image reconstructed from 29 optical slices (51 x 48 μm), scanned at 0.5 μm Z-steps, bottom image reconstructed from 27 optical slices (102 x 96 μm), scanned at 1.0 μm Z-steps. (Sample courtesy of Dr. Brian Matsumoto, University of California at Santa Barbara.)

MERIDIAN
Instruments, Inc.

Meridian Instruments, Inc.
2310 Science Parkway
Okemos, Michigan 48864 USA
Phone: 800-247-8084
FAX: 517-349-5967

Meridian Instruments Europe
Industriepark—West 75
B-9100 St. Niklaas BELGIUM
Phone: 32-3-7801760
FAX 32-3-7781727

Meridian Instruments Far East K.K.
The Sonehara Building (2nd Floor)
2-23-3 Higashi Nihonbashi
Chuo-ku, Tokyo 103 JAPAN
Phone: 81-3-5820-3315
FAX: 81-3-5820-3316

Meridian Instruments Hong Kong, Ltd.
19th Floor, Room B
Sai Wan Ho Plaza
66-68 Shau Kei Wan Road
HONG KONG
Phone: 852-513-7333
FAX: 852-513-1299

Meridian Instruments Italia
Via Fabio Filzi, 12
20026 Novate Milanese ITALY
Phone: 39-2-3541444
FAX: 39-2-3541572

Distributors located in: Australia, Austria, Benelux, Finland, France, Israel, Korea, New Zealand, the People's Republic of China, Portugal, Spain, Sweden, Switzerland, Taiwan, and the United Kingdom.

©1994 Meridian Instruments Inc.

Circle No. 55 on Readers' Service Card

IMMUNODEFICIENT MICE

NU/NU CD-1® • NU/NU • BALB/c Nude
• NIH-III • Fox Chase SCID™ • SCID Beige

ISO 9002 SCSR INC. SEAL OF QUALITY CERTIFIED FIRM

Charles River
LABORATORIES

Contributing to the Search for Healthier Lives™

251 Ballardvale Street, Wilmington, MA 01887 **1-800-LAB-RATS**

© Charles River Laboratories, 1995 Fox Chase SCID is a trademark of the Fox Chase Cancer Center

Circle No. 26 on Readers' Service Card

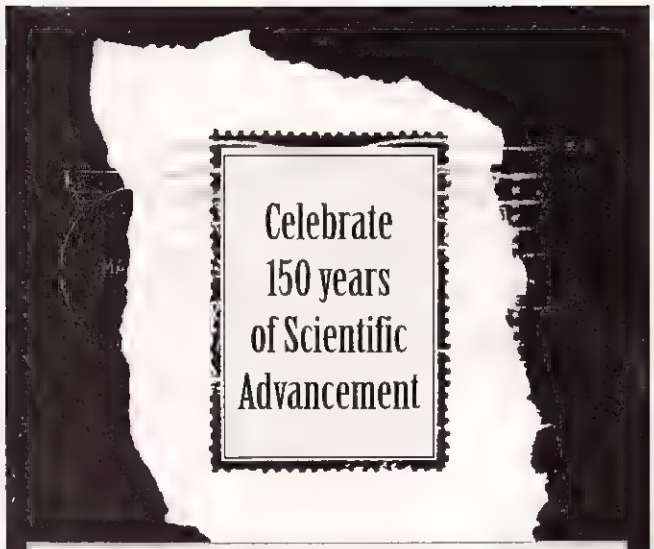

Celebrate 150 years of Scientific Advancement

In 1998, the American Association for the Advancement of Science (AAAS) will celebrate the 150th anniversary of its founding. A commemorative postage stamp would be a fitting tribute to the Association's historic efforts to promote the progress of science and engineering in the service of humankind.

BUT YOUR HELP IS ESSENTIAL.

We need letters expressing support for a AAAS commemorative stamp as well as ideas for the stamp's theme and design.

Please write promptly to:

The AAAS Commemorative Postage Stamp Committee
Office of Communications, Room 801
1333 H Street, NW, Washington, DC 20005

or call: 202-326-6440

Affordable Scientific Imaging Systems From UVP

GDS 7500 Shown

UVP, a world leader in ultraviolet and white light CCD scientific imaging technology, offers the scientific community an extensive range of PC and MAC based imaging systems to visualize, document and analyze gels, films or membranes.

Doc-It™ entry-level gel documentation system.

Grab-It™ image acquisition system utilizes your MAC or PC computer to create a dedicated gel documentation and densitometry system.

GDS5000 and GDS7500 complete gel documentation, image archiving, densitometry system ideal as a core location system with security log-on features, color applications, MAC and PC diskette image storage, ethernet network options, and image enhancements.

GelBase™/GelBlot™ Pro, GelSeq™, GelMatch™ analysis software for both Windows and MAC applications to perform molecular weight sizing, quantitation, 2D, 3D imaging, sequencing, analysis and RFLP analysis.

At UVP, we have over 62 years of experience serving the scientific community. With thousands of placements world wide, we offer the technical, sales and product support you deserve.

Call Today for A Demonstration Tomorrow.

UVP

UVP, Inc. Upland, CA
800-452-6788 (909)946-3197
Ultra Violet Products Limited
Cambridge, England *44 (0) 1223 420022

Visit UVP at AACR, booth 421
Circle No. 62 on Readers' Service Card

REPEL ALIEN INVADERS

Revco's Unique Deep Drawn CO_2 Incubators Fight Contamination

Deep in the dark recesses of most incubators, in crevassed corners and along welded seams, viruses, bacteria, molds and fungi are fighting for a foothold. If they are successful, it could mean shut-down for cleaning and decontamination. At best.

Worse, they might contaminate costly cultures. Worse still, they can cause irreparable damage and render the incubator useless.

But not in the seamless, deep-drawn interiors of Revco Ultima incubators. Manufactured without welds or sharp corners, these chambers offer no place to hide. A simple wipe of a cloth with cleaning agent eliminates the most tenacious invader.

Choose from stainless steel and copper seamless.

In Europe, the copper interiors are particularly popular because of their microbe-inhibiting effects. Beyond the corrosion-resistant barrier of stainless, copper provides an active shield to growth. With Revco, you have two tough choices.

Tough contamination-resistance is another sound reason laboratory cultures are safe in Revco incubators. For more information on the deep drawn tanks, sophisticated microprocessor controls, and other clear Revco advantages, call, write or circle the number below:

Revco Incubators. Safe and Sound.

REVCO

Revco Scientific • 1 Revco Drive Asheville, NC 28804
Phone: 800-252-7100 Fax: 704-645-3368

Circle No. 52 on Readers' Service Card

CYTOKINES ▪ ADHESION MARKERS ▪ T CELL RECEPTORS ▪ SOLUBLE RECEPTORS

T Cell Diagnostics Puts a Decade of Immunology Research in Your Hands.

The path your research takes is often dictated by the resources at hand. For 10 years, T Cell Diagnostics and our parent company, T Cell Sciences, have developed tools for novel explorations into human immunology.

High-Performance EIA Kits Lead the Way

Accurately quantitate cytokines and soluble receptors with our complete line of high-sensitivity, high-specificity immunoassay kits. Calibrated standards and easy-to-follow protocols ensure reproducible results in a few quick steps.

Obtain absolute CD4 and CD8 lymphocyte counts in your lab without flow cytometry by using the familiar TRAx® ELISA format.

High-Quality Mabs for High Specificity

Precisely identify T cell antigen receptors and adhesion markers by using our broad range of monoclonal antibodies and extensive applications expertise.

Measure Immune Profiles for Clinical Research

With our unique combination of products, you have the capability to study immune status in HIV, infectious disease, and organ transplantation.

Complete Support at Your Fingertips

Our experienced Technical Support Staff and Researchers will work closely with you to realize every advantage that our products bring to your lab.

Let us put a decade of immunology research in your hands. Call 1-800-624-4021 for our catalog.

T CELL DIAGNOSTICS

HELPING YOU EXPLORE THE IMMUNE RESPONSE

T Cell Diagnostics, Inc., 6 Gill Street Woburn, MA 01801 Tel 617-937-0890, 1-800-624-4021 *For Investigational Use Only Pending FDA clearance †Patents Pending, T Cell Diagnostics Inc ‡For Research Use Only

Circle No. 36 on Readers' Service Card

D C #564

Solvents Database

The Solvents Database (SOLV-DB) contains data on the physical and chemical properties, environmental fate, health and safety effects, and regulations concerning chemicals. Solvents can be selected by common name, synonym, CAS number, molecular formula, or SAX number. The database also includes information on chemical identity and vendors of solvents. Users can select criteria such as boiling point range and flammability to identify new alternative solvents and compare properties with the solvent being used. SOLV-DB runs on IBM-compatible computers with DOS 3.0 or higher; 2 megabytes of random access memory; 5.6 megabytes of hard disk space; and CGA, EGA, VGA, or compatible monitors. **Syracuse Research. Circle 138.**

Anti-Fouling Filtration

The centrifugal Centriprep Particle Separator is designed for removing debris such as cells, beads, and other particles from

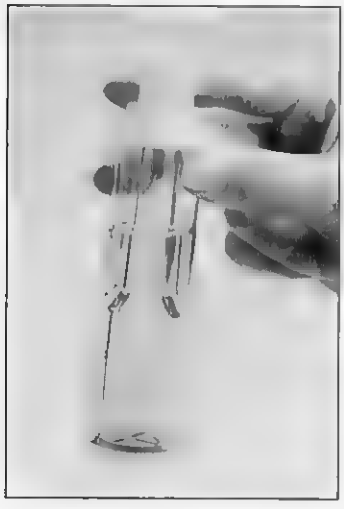

biological samples. During centrifugation, the device minimizes accumulation of particles on the membrane surface that would block the filter and diminish its effectiveness. Centrifugal force drives the suspended particles away from the filter surface while the pressure resulting from the centrifugation forces membrane-permeable material through the membrane. The device is capable of purifying up to 15 ml. Membrane porosity is 0.2 μm. **Amicon. Circle 139.**

Separation Media

Three new separation media for high-performance hydrophobic interaction chromatography are designed for fast, high resolution purification of proteins and peptides. Source 15ETH (ether), Source 15ISO (isopropyl), and Source 15PHE (phenyl) cover a wide range of selectivities. They maintain performance at large scale and thus can be used for the final stages of an industrial purification process in which trace contaminants and close variants need to be removed. The media can be packed in standard and high-performance laboratory scale columns. **Pharmacia Biotech. Circle 140.**

Monoclonal Antibodies

Six new monoclonal antibodies (mAbs) to matrix metalloproteinases (MMP) and two to tissue inhibitors of metalloproteinases (TIMP) are available. Members of the MMP family of enzymes are expressed at elevated levels in aggressive human tumor cells and have been implicated in the catalytic functions of extracellular proteolyses. The mouse mAbs are for MMP-1, MMP-2, MMP-3, MMP-9, TIMP-1, and TIMP-2. **Oncogene Science. Circle 141.**

A group of antibodies to chemokines includes human mAbs to interleukin-8 (IL-8), macrophage inflammatory protein (MIP)–1α, MIP-1β, and RANTES, and mouse mAbs to MIP-1α and MIP-1β. The line also includes recombinant human chemokines including IL-8, GROα, MIP-1α, MIP-1β, monocyte chemotactic protein–1 and RANTES. Recombinant mouse chemokines include MIP-1α and MIP-1β. **Sigma ImmunoChemicals. Circle 142.**

For studies of the immune system's regulatory control pathways, a mAb against the 55-kD Tac subunit of the human IL-2 receptor is suitable for various immunodection assays, including immunoprecipitation and immunohistochemistry. **Berkeley Antibody. Circle 143.**

Agarose Additive

Gels made with GelTwin Agarose Additive and agarose feature improved resolution in the 50- to 2000-bp range, increased loading capacity, and improved gel clarity. A gel containing 1% GelTwin and 0.5% agarose performs comparably to a 2% agarose gel, which results in significant cost savings and improved resolution. GelTwin outperforms expensive specialty agaroses for polymerase chain reaction analysis, according to the manufacturer. **J.T. Baker. Circle 144.**

Device Caps and Uncaps Vials

The Capitator, a device designed to take caps on and off threaded neck vials, bottles, test tubes, and T flasks, now accommodates two different ranges of cap sizes. In addition to the original range of caps from 0.5 to 1.5 inches in diameter, it can now be used for caps ranging in size from 1 to 2 inches. The device allows vials to be uncapped using one hand and can be used in a hood. It can be

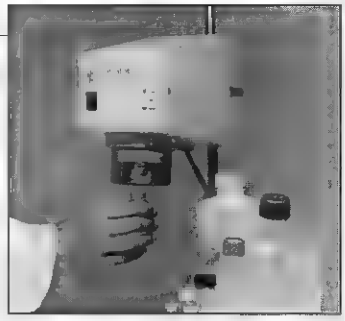

used for short-run production, multiple sample handling, working with robots, quality control applications, and in cell culture and microbiology labs. **Manostat. Circle 145.**

Literature

General Utility of the Mass Spectrometric Detector for the Analysis of Materials by Gas Chromatography is an application note that focuses on the advantages of this technology for analysis of complex molecular mixtures. It includes descriptions of 10 varied applications, ranging from analysis of perfume to testing of drugs of abuse. **Perkin-Elmer. Circle 146.**

SynChropak Bibliography contains more than 450 references on high-performance liquid chromatography applications involving biomolecules. Compounds are indexed alphabetically to facilitate methods development. **SynChrom. Circle 147.**

Culture with Confidence describes a line of water-jacketed CO_2 incubators designed to main ideal growth conditions for cell and tissue culturing applications. **Precision Scientific. Circle 148.**

GC Cryo-Trap Adds Cryo-Cooling Capabilities to your GC describes two programmable traps that can be interfaced to thermal desorption and head space gas chromatography systems. **Scientific Instrument Services. Circle 149.**

Higher Productivity, Better Results, and Lower Cost with Fully Compatible Automation describes a line of sample preparation and sample introduction products for chromatography. **Hewlett-Packard. Circle 150.**

Newly offered instrumentation, apparatus, and laboratory materials of interest to researchers in all disciplines in academic, industrial, and government organizations are featured in this space. Emphasis is given to purpose, chief characteristics, and availability of products and materials. Endorsement by *Science* or AAAS is not implied. Additional information may be obtained from the manufacturers or suppliers named by circling the appropriate number on the Readers' Service Card and placing it in a mailbox. Postage is free.

SCIENCE

PERSONNEL PLACEMENT

LINE CLASSIFIED ADVERTISEMENTS

Deadlines: Ads are due by Thursday, 10 a.m., 2 weeks prior to the issue date. *Science* is published each Friday, except the last Friday of the year. Call for holiday deadlines. Ads must be submitted in writing.

How to Submit a Classified Ad: Prepare double-spaced typewritten copy. Do not include any abbreviations. *Science* will edit and typeset ads according to *Science* guidelines. Include billing information, and desired publication date. Available categories: Positions Open, Meetings, Announcements, Courses and Training, Search Firms. *Science* cannot provide proofs of typeset line ads.

Mail, FAX or Email materials to:
Science Classified Advertising
1333 H Street, N.W., Room 814
Washington, DC 20005
Telephone: 202-326-6555
FAX: 202-682-0816
Internet Email: science_classifieds@aaas.org

Rates: Ads are $43 per line; $430 minimum. One line equals 52 characters and spaces; centered headings equal 32 characters and spaces. A 3% cash discount is granted to all prepaid ads.

Estimates: *Science* will provide a cost estimate for line ads. This is an approximate cost only. Allow for variation between estimated lines and actual typeset lines and resulting final cost. Purchase orders must allow for some degree of flexibility and/or adjustment.

Ads from Outside the U.S.: A discount of $30 will be offered to advertisers making payment in U.S. dollars by checks drawn on U.S. banks. Contact Gordon Clark at +44 223 302 067 (telephone) or +44 223 302 068 (FAX).

Credit Cards: *Science* accepts American Express, MasterCard and VISA. Discount does not apply to credit cards.

Cancellations: Deadline for cancellation is 10 a.m., Tuesday, 10 days prior to issue date.

DISPLAY PERSONNEL ADVERTISEMENTS

For rates and info. for fractional display ads call:

Deborah Cummings
Recruitment Advertising
Telephone: 202-326-6541
FAX: 202-682-0816

Janis Crowley
Recruitment Advertising Manager
Telephone: 212-496-7704
FAX: 202-682-0816

Gordon Clark
European Recruitment Advertising
Telephone: +44 223 302 067
FAX: +44 223 302 068

CONDITIONS: The AAAS encourages employers to actively recruit and employ underrepresented minority groups. *Science* reserves the right, at its discretion, to edit or decline to publish advertisements submitted to it.

POSITIONS OPEN

SENIOR FACULTY POSITIONS
Structure and Function of Macromolecules
University of Oklahoma Health Sciences Center
Department of Biochemistry and Molecular Biology

Under the leadership of the new Chairman, **Dr. Paul H. Weigel**, the Department of Biochemistry and Molecular Biology at the University of Oklahoma Health Sciences Center plans a significant expansion in the size and research activities of the Department. The search committee invites applications from established investigators with expertise in structure and function of macromolecules for several positions at the **ASSOCIATE** or **FULL PROFESSOR** level. Interested candidates must have a Ph.D. or equivalent degree and a strong publication record in physical biochemistry with sustained extramural support. Examples of appropriate areas of research are protein folding, assembly, protein-protein, protein-nucleic acid, protein carbohydrate and protein-membrane interactions. Knowledge of physical biochemical techniques, such as fluorescence spectroscopy, microcalorimetry, circular dichroism and NMR spectroscopy would be an asset. Successful candidates are expected to lead independent research programs, to participate in graduate and professional teaching programs and to serve as a resource for other faculty and students. There are six colleges in the University of Oklahoma Health Sciences Center, located on a 200 acre modern campus in Oklahoma City, with over 3,300 students and 2,200 faculty. A Biotechnology Park is under construction and work will begin shortly on a $45 million Biomedical Research Center. A letter of application, curriculum vitae, outline of current and future research activities, selected reprints and names of three references should be received by May 1, 1995, after which screening will begin with a possible starting date of September 1, 1995. Applications should be sent to: **John R. Sokatch, Chair, Search Committee, Department of Biochemistry and Molecular Biology, University of Oklahoma Health Sciences Center, P.O. Box 26901, Oklahoma City, OK 73190.** *The University of Oklahoma is an Equal Opportunity/Affirmative Action Employer.*

HIGHER PLANT ECOLOGIST
Memorial University of Newfoundland
Department of Biology

Applications are invited for a tenure-track position at the **ASSISTANT PROFESSOR** level in the Department of Biology commencing in September 1995. We are seeking a higher plant ecologist. The successful candidate will be expected to develop a strong research program, seek and secure external funding, supervise graduate students and teach courses at the undergraduate and graduate levels. Candidates must have a Ph.D. and preferably postdoctoral experience. Application, including curriculum vitae, statement of research directions, the names and addresses of three references, and copies of representative publications should be sent to: **Dr. T. R. Patel, Chair, Search Committee, Biology Department, Memorial University of Newfoundland, St. John's NF, A1B 3X9 Canada.** Screening of applications will begin on April 15, 1995. *In accordance with Canadian immigration requirements, this advertisement is directed towards Canadian citizens and permanent residents of Canada. Memorial University is committed to Employment Equity.*

ASSISTANT/ASSOCIATE PROFESSOR
TENURE-TRACK—MOLECULAR BIOLOGY

The Faculty of Dentistry, University of Western Ontario, is seeking an outstanding candidate with a strong background in molecular biology to join an interdisciplinary group in mineralized tissue research. The appointee is expected to develop or have already established a vigorous, externally funded research program complementing existing strengths in the biochemistry and physiology of mineralized tissues. Candidates should have a Ph.D. (or equivalent) and at least two years of postdoctoral experience. A commitment to teaching and contributions to administration are expected. Send curriculum vitae, selected reprints, outline of research plans and list of three referees to: **Dr. R. I. Brooke, Dean, Faculty of Dentistry, The University of Western Ontario, London, Ontario, N6A 5C1 Canada. FAX: 519-661-3875.** Position is subject to budget approval. *In accordance with Canadian immigration requirements, this advertisement is directed to Canadian citizens and permanent residents of Canada. The University of Western Ontario is committed to employment equity, welcomes diversity in the workplace, and encourages applications from all qualified individuals including women, members of visible minorities, aboriginal persons and persons with disabilities.*

POSITIONS OPEN

VETERINARY PHYSIOLOGIST

The Department of Veterinary Physiology and Pharmacology, College of Veterinary Medicine, Texas A&M University, invites applications for a tenure-track teaching position as an **ASSISTANT** or **ASSOCIATE PROFESSOR** of veterinary physiology and pharmacology. The requirements for this position are the D.V.M. and Ph.D. or equivalent degrees. Clinical experience is desirable. Preference will be given to candidates with exceptional teaching skills and expertise relating to the physiology of animals.

The successful candidate will devote the majority of his/her time to instruction of veterinary and undergraduate students and will be expected to teach in a variety of settings including large classroom lectures, small group discussions and teaching laboratory sessions. The opportunity to teach graduate students is also available. Expectations for the person filling this position include: effective interpersonal skills, a demonstrated and/or excellent potential for performance of scholarly activity (research and publications) relating to teaching and the ability to provide departmental leadership in the area of physiology education.

Interested candidates should submit a letter of intent outlining their academic interests and goals, a curriculum vitae, pertinent publications and a list of references to: **Dr. Jon F. Hunter, Department of Veterinary Physiology and Pharmacology, Texas A&M University, College Station, TX 77843-4466.** Inquiries may be directed to **Dr. Hunter** at: **409-845-7261** (telephone) or **409-845-6544** (FAX).

Review of applications will begin immediately and continue until the position is filled. *Texas A&M University is an Affirmative Action/Equal Opportunity Employer committed to excellence through diversity and encourages applications from minorities, women, veterans and persons with disabilities.*

FACULTY POSITION
Department of Biochemistry and Molecular Biology
Saint Louis University School of Medicine
Molecular Genetics/Human Genomics/
Gene Therapy/Transgenic Research

Applications are invited for a tenure-track position involving research and teaching at the **ASSISTANT** or **ASSOCIATE PROFESSOR** level. Applicants whose research might complement interdepartmental efforts bridging the areas of human genomic analysis, experimental aspects of gene therapy, and transgenic approaches to genetic analysis are encouraged to apply. We seek applicants who will complement ongoing research in molecular genetic, metabolic regulation, cellular biology, and/or physical biochemistry and can participate in the multidepartmental Cell and Molecular Biology Program at Saint Louis University School of Medicine. Excellent start-up funds and salary are available. Curriculum vitae, description of research plans, and at least three letters of recommendation should be sent to: **Search Committee, c/o Dr. William S. Sly, Chairman, Edward A. Doisy Department of Biochemistry and Molecular Biology, Saint Louis University School of Medicine, 1402 South Grand Boulevard, St. Louis, MO 63104.** *Saint Louis University is an Equal Opportunity/Affirmative Action Employer/Minority/Female/Veterans/Disabled.*

VIROLOGIST
ASSISTANT PROFESSOR
University of California, San Francisco

The F.I. Proctor Foundation in collaboration with the University of California, San Francisco (UCSF) Program in Biological Sciences is seeking exceptional candidates for a position of **ASSISTANT PROFESSOR.** Candidates should have a Ph.D. or M.D. degree and postdoctoral research experience in viral pathogenesis. Applicants should have outstanding potential for research and teaching, and will be expected to develop an independent research program. We are particularly interested in candidates with research programs related to mechanisms of herpesvirus pathogenesis.

Interested applicants should submit a curriculum vitae, summary of research interests, copies of major publications and three letters of recommendation by May 15, 1995, to:

Chair of Search Committee
F.I. Proctor Foundation, S-315
UCSF Medical Center
San Francisco, CA 94143-0412

UCSF is an Equal Opportunity and Affirmative Action Employer.

Tenure-Track And Postdoctoral Opportunities.

Listed below are some of the outstanding research training opportunities that are currently available at the National Institutes of Health.

Tenure-Track Position
Assistant Professor Equivalent

Developmental Neurobiology
Phillip G. Nelson, MD, PhD

Position is available to develop an independent program on the developmental regulation of neurotransmitter phenotypes at the molecular level. The program complements studies on neuronal differentiation. The candidate should have broad experience in neurosciences including neuroanatomy, molecular and cell biology, and protein-DNA interactions. Please submit a *curriculum vitae*, statement of research interests, and three letters of recommendation by April 15, 1995. Laboratory of Developmental Neurobiology (OE-72), NICHD, Building 49, Room 5A38, 49 CONVENT DR MSC 4480, BETHESDA MD 20892-4480.

Postdoctoral Positions

Functional Neuroanatomy
Miles Herkenham, PhD

Positions are available to apply molecular and histochemical techniques to study the neuroanatomical bases for the brain's response to peripheral cytokines, drugs of abuse (cannabinoids), or psychotherapeutic drugs. A strong background in neurobiology, molecular biology, immunology, or pharmacology is desired. Applicants must have less than five years of postdoctoral experience. Section on Functional Neuroanatomy (OE-72), NIMH, Building 36, Room 2D15, 36 CONVENT DR MSC 4070, BETHESDA MD 20892-4070.

Insulin Signal Transduction and Hypertension
Michael J. Quon, MD, PhD

Molecular mechanisms of insulin-stimulated glucose transport are being studied using a novel transfection system for adipose cells in primary culture*. Insights from these studies are being used to investigate the relationship between insulin resistance and hypertension at a molecular level. In particular, the role of insulin signaling in nitric oxide production by vascular endothelium is being studied. A strong background in molecular biology and/or cell biology is preferred. Applicants must have less than five years of postdoctoral experience. Hypertension Endocrine Branch (OE-72), NHLBI, Building 10, Room 8C-103, 10 CENTER DR MSC 1754, BETHESDA MD 20892-1754.

*(*PNAS* 91:5587-5591, 1994, *JBC* 269:27920-27924, 1994)*

Molecular Biology of Herpesviruses
Jeffrey I. Cohen, MD

The functions of herpesvirus genes are being studied and mutated viruses are being constructed and characterized *in vitro* and in animal models. These studies include viral genes that may interact with the immune system. Applicants should have experience in virology and molecular biology, and less than four years of postdoctoral experience. Laboratory of Clinical Investigation (OE-72), NIAID, Building 10, Room 11N228, 10 CENTER DR MSC 1888, BETHESDA MD 20892-1888.

Selective Transposon Insertion
Judith A. Kassis, PhD

Position available to study the selective insertion of transposable elements in *Drosophila*. The mechanism of selective insertion will be studied using genetic, molecular and biochemical techniques. Applicants must have experience in molecular biology, genetics or biochemistry, and have less than five years of postdoctoral experience. Laboratory of Developmental Biology (OE-72), FDA/CBER, Division of Cellular and Gene Therapies, (HFM-527), 1401 Rockville Pike, Rockville, MD 20852-1448.

Toxin and Ribonuclease Biology
Richard J. Youle, PhD

Ongoing research projects include engineering of toxic proteins into therapeutics for cancer and HIV; understanding the cell biology of ribonuclease cytotoxicity; study of the mechanisms of neuronal cell loss during development and disease; and exploring the biochemistry of apoptosis. Applicants should have a strong background in molecular or cell biology, and have less than five years of postdoctoral experience. Surgical Neurology Branch (OE-72), NINDS, Building 10, Room 5D37, 10 CENTER DR MSC 1414, BETHESDA MD 20892-1414.

Additional Postdoctoral Fellowship Opportunities

For an on-line listing of additional postdoctoral openings, you may access the NIH EDNET Bulletin Board POSTDOC conference via Internet **(wylbur.cu.nih.gov)** or modem (1,301-402-2221 or 1,800-358-2221) with parameters set at "7,Even,1". When connected to NIH, type in ",vt100" for terminal emulation, "F5E" for initials, and "AJL1" for account number.

The Postdoctoral Research Fellowship Opportunities catalog, which describes intramural laboratories at the NIH, is also available by request. An electronic version of the catalog may be accessed via the Internet using either the Gopher Information System **(gopher.nih.gov)** or the World Wide Web **(http://www.nih.gov/)**. When connected, select *Research Opportunities at the NIH Office of Education*. If you would like to request a catalog or have further questions, please contact the NIH Office of Education, Building 10, Room 1C129, 10 CENTER DR MSC 1158, BETHESDA MD 20892-1158, 301-402-1603, Fax 301-402-0483.

To Apply

If you hold a doctoral degree (e.g., PhD, MD/PhD, MD, DO, DDS, DMD or DVM) accompanied by previous laboratory research experience, and would like to be considered for one of these positions, please send a cover letter, *curriculum vitae*, bibliography, and statement of research interests to the address listed with each position. In addition, please arrange to have letters of recommendation sent from three scientists who can provide an evaluation of your qualifications.

NATIONAL INSTITUTES OF HEALTH

National Institutes Of Health

Office Of Education

The NIH is an Equal Opportunity Employer

POSITIONS OPEN

ASSISTANT/ASSOCIATE/FULL PROFESSOR
Agricultural Science and Technology Education

The Department of Education at Cornell University invites applications for two **TENURE-TRACK POSITIONS** to provide leadership for a teacher education program in agricultural science and technology. Successful applicants will cooperate with an existing program in science and mathematics teacher education, extend the mission of agricultural science and technology education beyond preservice teacher education to include public literacy about agriculture and food systems, and conduct high quality programs of research.

Qualifications include a Ph.D. in an appropriate field, teacher education experience, a demonstrated capacity for quality research, and a commitment to quality and leadership in the development of agricultural science and technology education. In addition, the successful candidates will possess a suitable mix of the following qualifications: knowledge of a relevant technical field such as plant science, environmental science, or agricultural engineering; competence in a relevant social or behavior science; knowledge of adult or extension education; or an interest in international applications. Cornell wishes to hire individuals who can bring innovative approaches to this field, and will consider applicants with a variety of backgrounds and training.

Applicants should submit a letter of application, curriculum vitae, a writing sample, and names and addresses of four references by April 1, 1995, to: **Dr. Kenneth Strike, Search Committee Chair, Department of Education, NYS College of Agriculture and Life Sciences, Kennedy Hall, Ithaca, NY 14853.**

CANCER MOLECULAR BIOLOGIST
The USC/Norris Comprehensive Cancer Center

The University of Southern California/Norris Comprehensive Cancer Center is recruiting a tenure-track faculty member for a joint appointment in the Departments of Surgery and Molecular Microbiology and Immunology or Biochemistry and Molecular Biology. We are looking for individuals at the **ASSISTANT PROFESSOR** or higher level with an interest in molecular biology and genetics of cancer. It is expected that in this position the recruit will develop an independent research program. The Cancer Center will provide the individual with a highly interactive environment and ample opportunities to collaborate with strong research groups interested in gene therapy, molecular epidemiology, gene regulation and tumor invasion and metastases. Salaries and start-up funds are highly competitive.

Send curriculum vitae, names of three references and summary of research interests to: **Dr. Peter A. Jones, Director, USC/Norris Comprehensive Cancer Center, 1441 Eastlake Avenue, NOR 815, Los Angeles, CA 90033.** *USC is an Affirmative Action/Equal Opportunity Employer.*

Biology. The Department of Biology at Merrimack College invites applications for two or three tenure-track positions at **ASSISTANT** or **ASSOCIATE PROFESSOR** level beginning September 1995. Candidates must possess a Ph.D. and undergraduate teaching experience in biochemistry, cell and molecular biology, developmental biology, genetics, immunology, environmental biology, or plant science. Expertise in more than one area is preferred. Demonstrated excellence in teaching and continued involvement in research, particularly that which could involve undergraduates, are expected. Teaching load is 12 contact hours per semester. The college is particularly interested in candidates who desire to teach in a small, interactive classroom environment emphasizing dialogue and inquiry on civilizational issues. Send curriculum vitae and three letters of reference by March 27, 1995, to: **Dr. Kathleen A. FitzPatrick, Chair, Department of Biology, Merrimack College, 315 Turnpike Street, North Andover, MA 01845. Email: Kfitzpatrick@merrimack.edu.** *Merrimack College is an Equal Opportunity Employer. Women and minorities are encouraged to apply.*

Histologist. Full-time **ASSISTANT** or **ASSOCIATE PROFESSOR** position available starting July 1, 1995, to teach Histology. Research and service are expected. Send curriculum vitae, research interests, and three letters of reference by April 1, 1995, to: **Dr. J. Alcala, Chairperson, Department of Anatomy, Ponce School of Medicine, P.O. Box 7004, Ponce, PR 00732. Telephone: 809-840-2575.** *The Ponce School of Medicine is an Affirmative Action/Equal Opportunity Employer.*

PARASITOLOGIST

The University of Illinois at Urbana-Champaign (UIUC) announces a full-time, tenure-track **ASSISTANT PROFESSOR** position in Parasitology within the Department of Veterinary Pathobiology in the College of Veterinary Medicine with a starting date of August 21, 1995. The successful applicant will have a Ph.D. and/or a D.V.M. with advanced academic training in parasitology. Duties will include teaching parasitology to veterinary and graduate students and the development of a strong research program. Appointments in the University of Illinois Laboratories for Veterinary Diagnostic Medicine and the Agricultural Experiment Station are available for an appointee who qualifies. Salary is negotiable and commensurate with qualifications.

Special consideration may be given to applicants with postdoctoral experience, demonstrable interest in veterinary parasitology or whose research interests will complement existing programs. Research strengths in the Department include studies on infectious diseases, molecular hemotropic disease, epidemiology, and pathology. There are opportunities for collaboration with other departments within the College, as well as departments in other colleges at UIUC.

Letters of application, curriculum vitae, and three letters of recommendation should be sent to: **Dr. C. J. Jones, Search Committee Chair, Department of Veterinary Pathobiology, College of Veterinary Medicine, 2001 South Lincoln Avenue, Urbana, IL 61801. Telephone: 217-333-0330.** To ensure full consideration, all materials should be received by May 1, 1995.

The University of Illinois is an Affirmative Action/Equal Opportunity Employer.

Environmental Virologist. The Department of Biology at New Mexico State University is seeking applicants for a tenure-track **ASSISTANT PROFESSOR** for as early as January 1996. Applicants must have a Ph.D. and postdoctoral research experience in virology or related field, such as microbiology or molecular biology. The successful candidate will be expected to develop a vigorous research program in the area of environmental virology. Teaching responsibilities will include courses in immunology and virology at the senior/graduate level and participation in an introductory biology or microbiology course. The department offers Bachelor's degrees in biology and microbiology and the M.S. and Ph.D. in biology. The individual selected may participate in the M.S./Ph.D. Graduate Program in Molecular Biology and the NIH-sponsored Minority Access to Research Careers and Minority Biomedical Research Support programs. Applicants should submit a curriculum vitae, statements of research and teaching interests, and the names, addresses, and telephone numbers of at least three references to: **Dr. Charlotte McCarthy, Search Committee, Department of Biology, Box 30001, Department 3AF, New Mexico State University, Las Cruces, NM 88003-8001.** Review of applications will begin April 21, 1995. *New Mexico State University is an Equal Employment Opportunity/Affirmative Action Employer. Offer of employment contingent upon verification of individual's eligibility for employment in the United States.*

SEARCH REOPENED
PLANT ECOLOGIST

The faculty of the University of Mississippi Department of Biology invites applications for a tenure-track, nine-month appointment as **ASSISTANT PROFESSOR.** Duties: Conduct research in specialty area; develop an extramurally funded research program; excel in undergraduate and graduate teaching, including introductory and specialty courses; direct graduate students; professional service; advise undergraduates. Research and teaching opportunities exist at the University of Mississippi Biological Field Station. Qualifications: Doctoral degree; research experience and publications in plant ecology; evidence of ability to obtain extramural funding. Applications reviewed immediately until position is filled. Position available: August 1995. Send a letter of application including a description of current research and future plans, teaching experience and interests, and a description of how your teaching and research might take advantage of opportunities at the Biological Field Station; a curriculum vitae; and three letters of reference to: **Dr. James Kushlan, Chair, Department of Biology, University of Mississippi, University, MS 38677. Telephone: 601-232-7204.**

The University of Mississippi is an Affirmative Action/Americans with Disabilities Act/Equal Opportunity Employer. Women and minorities are particularly encouraged to apply.

ASSISTANT PROFESSOR, Food Safety Microbiology. Tenure-track, academic year faculty position (60% research/40% teaching) available in the Department of Food Science and Technology, University of Nebraska. Candidate will conduct research on food safety microbiology, emphasizing molecular approaches to detection, pathogenesis, or control of pathogenic microorganisms in foods. Will be expected to seek external funding, advise graduate students, and participate in teaching food microbiology and related courses. Requires Ph.D. in Food Science, Microbiology, or related discipline. Postdoctoral or industry experience is highly desirable. Candidate will join a Department of 13 faculty, including three food microbiologists. Department is located in the new Food Industry Complex containing molecular biology, fermentation and bioprocessing, and tissue culture laboratories. The Food Industry Complex is among the best in the United States for food science research. Applicants should submit a letter of application, a statement of research interests, a curriculum vitae, transcripts, and have three letters of reference sent postmarked by June 1, 1995 (or until suitable candidate is identified), to: **Dr. Robert Hutkins, Chair, Search Committee, Department of Food Science and Technology, University of Nebraska, Lincoln, NE 68583-0919.** *University of Nebraska–Lincoln is committed to a pluralistic campus community through Affirmative Action and Equal Opportunity and is responsive to the needs of dual career couples. We assure reasonable accommodation under the Americans With Disabilities Act; contact Dr. Hutkins for more information.*

FACULTY POSITION IN CELL BIOLOGY

The Department of Cell Biology and Neuroscience of The University of Texas Southwestern Medical Center at Dallas seeks applications for a tenure-track position at the level of **ASSISTANT PROFESSOR.** Applicants must have a relevant Ph.D. or M.D. degree, appropriate postdoctoral training, and show evidence of firm commitment to a career in independent research. We are particularly interested in considering creative and highly motivated individuals who wish to apply contemporary cell and molecular techniques to elucidate at the cellular level the fundamental mechanisms of human disease. Responsibilities will also include teaching of medical and graduate students after the first year of employment.

Send curriculum vitae, a brief description of proposed research, and three letters of reference to: **Richard G. W. Anderson, Ph.D., Department of Cell Biology and Neuroscience, UT Southwestern, 5323 Harry Hines Boulevard, Dallas, TX 75235-9039.** *An Equal Opportunity/Affirmative Action Employer.*

PHYSICIAN/SCIENTIST
ASSISTANT PROFESSOR (TENURE-TRACK)

The Geographic Medicine Division and the Vaccine Development Center at the University of Maryland School of Medicine seek a physician scientist with molecular biology skills and experience as **ASSISTANT PROFESSOR** (tenure-track) of Medicine. The position requires that approximately one month each year be spent in clinical research (testing of vaccines) with the remainder of time devoted to basic laboratory research on the development of methods to study the molecular epidemiology of human malaria (major research thrusts within the Center). Prerequisites include M.D. with Board-certification in internal medicine and certification or eligibility in infectious diseases and demonstrable laboratory expertise in molecular biology of *Plasmodium falciparum.* An individual with malaria field experience is strongly preferred. Starting date circa August 1, 1995. Please send curriculum vitae to: **Dr. Robert Edelman, Associate Director, Clinical Studies, Center for Vaccine Development, University of Maryland School of Medicine, 10 South Pine Street, Baltimore, MD 21201.** *The University of Maryland at Baltimore encourages women and minorities to apply and is an Affirmative Action/Equal Employment Opportunity/ADA Employer.*

Pharmacology/Toxicology: **ASSISTANT PROFESSOR,** tenure-track position beginning July 1, 1995. Ph.D. in Pharmacology/Toxicology required. A degree in pharmacy is desirable. Team teaching of biomedical science and graduate courses, student advising, and extramural-supported scholarly research is expected. Submit letter of intent, curriculum vitae, statement of research interests, names, addresses and telephone numbers of three references to: **F. W. Fochtman, Ph.D., Chair, Search Committee, Department of Pharmacology/Toxicology, School of Pharmacy, Duquesne University, Pittsburgh, PA 15282.**

AMERICAN ASSOCIATION FOR CANCER RESEARCH SCIENTIFIC CONFERENCES

APRIL 1-6, 1995
Signal Transduction of Normal and Tumor Cells
Co-sponsored by the National Cancer Institute of Canada
Chairpersons: Anthony J. Pawson, Toronto, Ontario, Canada; André Veillette, Montreal, Quebec, Canada; Grant McFadden, Edmonton, Alberta, Canada
Banff Centre, Banff, Alberta, Canada

OCTOBER 14-18, 1995
Cytokines and Cytokine Receptors
Chairperson: Steven Gillis, Seattle, WA
The Sagamore, Bolton Landing (Lake George), NY

NOVEMBER 5-9, 1995
Cancer: The Interface Between Basic and Applied Research
Chairpersons: Bert Vogelstein, Baltimore, MD; Stephen H. Friend, Seattle, WA; John D. Minna, Dallas, TX
Stouffer Harborplace Hotel, Baltimore, MD

NOVEMBER 17-21, 1995
Novel Strategies Against Resistant Cancers
Chairpersons: Victor Ling, Toronto, Ontario, Canada; Daniel D. Von Hoff, San Antonio, TX
Sanibel Harbour Resort & Spa, Ft. Myers, FL

DECEMBER 2-6, 1995
The Molecular Basis of Gene Transcription
Chairperson: Tom Curran, Nutley, NJ
Hotel Del Coronado, Coronado (San Diego), CA

JANUARY 17-20, 1996
Cancer and the Cell Cycle
Joint Meeting with the Swiss Institute for Experimental Cancer Research
Chairpersons: Edward E. Harlow, Charlestown, MA; Viesturs Simanis, Lausanne, Switzerland
Location to be Announced in Lausanne, Switzerland

FEBRUARY 19-25, 1996
Cancer Susceptibility Genes and Molecular Carcinogenesis
Chairpersons: Curtis C. Harris, Bethesda, MD; Allan Balmain, Glasgow, Scotland; Kenneth Olden, Research Triangle Park, NC
Keystone Resort, Keystone, CO

MARCH 1-5, 1996
Proteases and Their Inhibitors in Cancer
Chairpersons: Lynn M. Matrisian, Nashville, TN; Bonnie F. Sloane, Detroit, MI
Marriott's Bay Point Resort, Panama City Beach, FL

APRIL 20-24, 1996
87th Annual Meeting
Chairperson: Lorraine J. Gudas, New York, NY
Washington D.C. Convention Center, Washington, D.C.
Abstract Deadline: December 1, 1995

JUNE 1996
Inducible Genomic Responses
Chairpersons: William T. Beck, Memphis, TN; John A. Hickman, Birmingham, England; Richard I. Morimoto, Evanston, IL
Location to be Announced

OCTOBER 1996
Novel Approaches in Blood and Marrow Transplantation
Second Annual Meeting of the American Society for Blood and Marrow Transplantation
Chairpersons: Joseph R. Bertino, New York, NY; Bruce R. Blazar, Minneapolis, MN
Location to be Announced

OCTOBER 1996
Carcinogenesis from Environmental Pollution: Assessment of Human Risks and Strategies for Prevention
Joint Meeting with International Agency for Research on Cancer
Chairpersons: Frederica Perera, New York, NY; Paul Kleihues, Lyon, France
Location to be Announced in Budapest, Hungary

OCTOBER 19-23, 1996
Programmed Cell Death
Chairperson: Stanley J. Korsmeyer, St. Louis, MO
The Sagamore, Bolton Landing (Lake George), NY

AACR members will receive brochures on the above special conferences as soon as they are available. Nonmembers should call or write:

American Association for Cancer Research
Public Ledger Building, Suite 816
150 South Independence Mall West
Philadelphia, PA 19106-3483
215-440-9300 • 215-440-9313 (FAX)

POSITIONS OPEN

ANATOMY AND PHYSIOLOGY POSITIONS
OHIO UNIVERSITY

The Department of Biological Sciences announces the availability of two non-tenure-track teaching positions at the **ASSISTANT PROFESSOR** level beginning September 1995; maximum employment is three years. Position No. 1 is for Human Physiology and Physiology of Exercise, and Position No. 2 is for Human Anatomy. Successful completion of the Ph.D. degree is required for both positions. These positions represent a significant teaching commitment in our large undergraduate curriculum. Responsibilities will include participation in lectures and laboratories. Collaborative research efforts with faculty are possible. Minimum salary for these positions is $30,000 for nine months plus a comprehensive benefits package. Applicants should send a curriculum vitae, transcripts, statement of teaching and research interests, the position(s) applied for, and three letters of recommendation by April 1, 1995, to: **Physiology/Anatomy Search, Jean Witkowski, Biological Sciences, 107A Irvine Hall, Ohio University, Athens, OH 45701.**

Ohio University is an Equal Opportunity/Affirmative Action Employer and women and minorities are encouraged to apply.

The Center for Neuroscience and the Department of Psychology at the University of California, Davis, invite applications for a tenure-track position at the **ASSISTANT PROFESSOR** level in the area of computational neuroscience. Candidates specializing in analytical approaches and predictive modeling of perceptual and/or motor circuitry in vertebrates are encouraged to apply. Postdoctoral experience is desirable. Ideal candidates would also incorporate neurophysiological, neuroanatomical, psychophysical, and/or cognitive-experimental techniques to test models. The appointee will be expected to teach undergraduate and graduate level courses in his/her areas of expertise. The University of California is interested in candidates who are committed to the highest standards of scholarship and professional activities. This position is open until filled, but applications must be received by May 1, 1995, to be assured full consideration.

Applicants should submit curriculum vitae, bibliography, a brief description of research interests and the names of at least three references to: **Michael S. Gazzaniga, Ph.D., Director, Center for Neuroscience, University of California, Davis, CA 95616.**

The University of California is an Equal Opportunity/Affirmative Action Employer with a strong institutional commitment to the achievement of diversity among its faculty and staff.

ENVIRONMENTAL SCIENTIST—DIRECTOR

Claremont McKenna College, a member of The Claremont Colleges, seeks to hire at the advanced level a **DIRECTOR** of the Roberts Environmental Center, an institute for research and undergraduate education in environmental problems. Responsibilities will include research (preferably applied biological research pertinent to Southern California), administration, and undergraduate teaching in environmental science. Prior experience in each of these areas is essential. Salary commensurate with experience. Claremont McKenna College is a small, selective liberal arts college that emphasizes economics and policy studies. Send a résumé and arrange to have three to five letters of recommendation forwarded to: **Anthony Fucaloro, Dean of the Faculty, Claremont McKenna College, 500 East 9th Street, Claremont, CA 91711-6400** by March 31, 1995. Review of applications will begin immediately and continue until the position is filled.

Claremont McKenna College is an Affirmative Action/Equal Opportunity Employer. Women and minority candidates are encouraged to apply.

CHAIR IN ORGANIC CHEMISTRY

The Swiss Federal Institute of Technology in Zurich (ETHZ) invites applications for a **CHAIR** in organic chemistry. Candidates should have an outstanding record in organic synthesis, preferably related to bio-organic problems. The candidate is expected to teach at all levels of organic chemistry.

Vigorous research, facility with teaching, and the willingness to collaborate with colleagues both within and outside ETHZ are prerequisites.

Please submit your application together with a curriculum vitae and a list of publications to: **President of ETH Zurich, Professor J. Nüesch, ETH Zentrum, CH-8092 Zurich,** no later than April 15, 1995. *Applications from young and women scientists are especially invited.*

PLANT MOLECULAR BIOLOGIST
BOYCE THOMPSON INSTITUTE

The Boyce Thompson Institute (BTI) at Cornell University invites applications for a **TENURE-TRACK ASSISTANT SCIENTIST** position in the Plant Molecular Biology Program. Candidates using molecular or genetic approaches to solve fundamental problems in plant biology are encouraged to apply. The successful candidate will be expected to establish a vigorous, independent research program which complements the activities of the Plant Molecular Biology Program, and to collaborate with other BTI and/or Cornell faculty. Submit curriculum vitae, statement of research goals, and three letters of reference by April 14, 1995, to: **Dr. H. Alan Wood, Chair, Search Committee, Boyce Thompson Institute, Tower Road, Ithaca, NY 14853 USA. Email: haw5@cornell.edu.**

BTI is an Affirmative Action/Equal Opportunity Employer. Women and minorities are encouraged to apply.

DEPARTMENT OF ANATOMY
Medical Sciences Campus
University of Puerto Rico

Applications are invited for a tenure-track faculty position, rank according to experience up to **ASSOCIATE PROFESSOR.** We seek an individual with teaching experience in gross anatomy, engaged in research in one or more of the following fields: functional morphology, developmental biology, ultrastructure, and cell biology. Teaching responsibilities include gross anatomy and graduate courses in the individual's specialty. The successful candidate will have an ongoing research program and willingness to seek external funding. Applicants should send curriculum vitae and summary of current research to: **John G. H. Cant, Director, Department of Anatomy, Medical Sciences Campus, University of Puerto Rico, G.P.O. Box 365067, San Juan, PR 00936-5067. Telephone: 809-758-2525, ext. 1501; FAX: 809-767-0788.** Review of applications will begin immediately and continue until the position is filled. *The University of Puerto Rico is an Equal Opportunity/Affirmative Action Employer.*

CHAIR of Biology: Search extended. Alfred University seeks a division chair in either molecular biology or "whole organism" plant science. Requires strong commitment to undergraduate teaching and advising. Research expectations consonant with active undergraduate research program in small liberal arts environment. Successful candidate will have teaching and scholarly record compatible with appointment as full professor and a desire to provide leadership for curricular change. Knowledge of pre-medical programming and success in obtaining extramural funding are desirable. Ph.D. required. Salary and benefits competitive. Women and minorities encouraged to apply. Review of applications will begin March 25, 1995, and continue until position is filled. Send curriculum vitae and three letters of recommendation to: **Dr. C. R. Grontkowski, Acting Chair of Biology, Alfred University, Alfred, NY 14802.** *An Equal Opportunity/Affirmative Action Employer.*

FACULTY POSITION
ISCHEMIA-REPERFUSION RESEARCH

The Department of Anesthesia at Brigham and Women's Hospital, Harvard Medical School has one position for a **FULL-TIME RESEARCHER** to study mechanisms of ischemia-reperfusion injury, preferably with a focus on the role of neutrophils. The position is within a newly established Ischemia-Reperfusion Center, to join two other investigators in established research space. The Anesthesia Research Laboratories are comprised of 15 independent investigators working in molecular neuropharmacology, pain research, muscle mechanics and cardiac electrophysiology. Academic rank will be commensurate with experience and status. Applicants should send a letter describing their interests, a curriculum vitae and have three letters of recommendation forwarded to:

Professor Gary R. Strichartz
Vice Chairman for Research
Department of Anesthesia Research Laboratories
Brigham and Women's Hospital
Harvard Medical School
75 Francis Street
Boston, MA 02115

Harvard Medical School/Brigham and Women's Hospital are Equal Opportunity/Affirmative Action Employers. Women and minority candidates are especially encouraged to apply.

TEXAS A&M UNIVERSITY
SEA GRANT COLLEGE PROGRAM
College of Geosciences and Maritime Studies

Applications are invited for the position of **DIRECTOR** of the Texas A&M University (TAMU) Sea Grant College Program to begin September 1, 1995, or later. Headquartered in College Station, and including 10 coastal Marine Advisory Service offices, the TAMU Sea Grant College Program employs a staff of 30 with a total budget of approximately $2.1 million.

Applicants must have a Ph.D. or equivalent experience, and at least eight (8) years of experience in administration or management of marine programs. Consideration of applications will begin April 15, 1995, and will continue until position is filled.

Send applications, including curriculum vitae and three references, to: **Dr. Robert D. Brown, Sea Grant Search Committee Chairman, Department of Wildlife and Fisheries Sciences, 210 Nagle Hall, Texas A&M University, College Station, TX 77843-2258. Telephone: 409-845-1261.**

Texas A&M University is an Affirmative Action/Equal Opportunity Employer and welcomes applications from qualified women and minority candidates.

WAYNE STATE UNIVERSITY
FACULTY POSITION
Drug Delivery/Drug Transport Technology and Pulmonary Inflammation Research
College of Pharmacy and Allied Health Professions

The Department of Pharmaceutical Sciences is seeking candidates for a **TENURE-TRACK POSITION** available immediately in Drug Delivery/Drug Transport Technology with focus on molecular and biochemical aspects of drug delivery and transport systems. A **NON-TENURE-TRACK FACULTY** position is also available for research on extracellular matrix in lungs. Candidates for both positions will be expected to establish a funded research program. Applicants should possess a Ph.D. and/or M.D. degree in pharmacology, pharmaceutical sciences, immunology or related disciplines and have postdoctoral experience. Rank and salary commensurate with experience. Qualified candidates should send a curriculum vitae and the names and addresses of three references to: **Fusao Hirata, M.D., Ph.D., Interim Chair, Department of Pharmaceutical Sciences, College of Pharmacy and Allied Health Professions, 528 Shapero Hall, Detroit, MI 48202.** *Wayne State University is an Equal Opportunity/Affirmative Action Employer. Minorities and women are encouraged to apply. Wayne State University-People working together to provide quality service. All buildings, structures and vehicles at Wayne State University are smoke-free.*

The Kellogg Eye Center and the Center for Ultrafast Optical Science at the University of Michigan is seeking an accomplished individual, with Ph.D. or equivalent, for a **RESEARCH** or **TENURE-TRACK POSITION** to participate in establishing an Ultrafast Biomedical Laboratory. The candidate shall have documented credentials with demonstrated accomplishments in the field of ultrafast optical science. Responsibilities of this position will include assembly, operation, and use of femtosecond lasers for medical and biologically based experiments. Ideally the candidate shall have a background in physics and biology with very strong and recognized abilities in ultrafast optics, laser matter interactions, and medical applications of ultrafast lasers. In addition the candidate shall be expected to represent this technology to the financial and investment community and be capable of transferring the results of research into the biomedical business arena. Send résumé and background information to: **Paul R. Lichter, M.D., Professor and Chairman, Department of Ophthalmology, W. K. Kellogg Eye Center, University of Michigan, 1000 Wall Street, Ann Arbor, MI 48105.** *The University of Michigan is an Equal Opportunity Employer.*

Department of Psychiatry, University of Pennsylvania, has two **FACULTY POSITIONS** available for program in neurobiology and behavior. Positions are at either the junior or senior level depending on candidates' qualifications. Candidates must be M.D., Ph.D. with training in genetics and experience in endocrinology, molecular pharmacology and neuroanatomy. Please send letter of intent and curriculum vitae to: **Peter C. Whybrow, M.D., Chairman, Department of Psychiatry, University of Pennsylvania, 305 Blockley Hall, 418 Guardian Drive, Philadelphia, PA 19104-6021.** *Equal Opportunity/Affirmative Action Employer.*

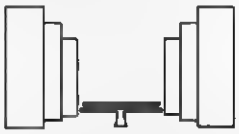

THE SALK INSTITUTE FOR BIOLOGICAL STUDIES

Postdoctoral Research Associate

Position available in an ongoing project studying cell cycle control in the fission yeast *Schizosaccharomyces pombe*, with particular focus on START and the initiation of DNA replication. The project uses classical and molecular genetics, cell biology and biochemical techniques to identify and characterize the regulatory genes involved in the G1/S phase transition.

A Ph.D. in Molecular Biology or related field and relevant experience in molecular biology required. Experience with cell biology or yeast genetic techniques would be helpful.

Send curriculum vitae, brief research summary, and the names of three references to: **Dr. Susan L. Forsburg, Molecular Biology and Virology Laboratory, The Salk Institute for Biological Studies, 10010 N. Torrey Pines Road, La Jolla, CA 92037.** EOE/AA.

POSTDOCTORAL FELLOWSHIP

Human Genome Center

The Human Genome Center at the Lawrence Berkeley Laboratory is a multi-disciplinary program focused on large-scale sequencing and analysis of the human genome. Postdoctoral positions are available in the areas of the development of new instrumentation, informational tools, and biological approaches related to accelerating the process of mapping, map assembly, sequencing, sequence assembly, and sequence analysis. Individuals are needed to work in all aspects of the program, particularly in projects involving cross-disciplinary interactions. Recent Ph.D. in molecular biology, engineering, physics, statistics, computer sciences, or related field is required.

Send curriculum vitae (6 copies) and names and addresses of three references, to: **The Human Genome Center, c/o Lawrence Berkeley Laboratory, Staffing Office, Box #JSCI3245, One Cyclotron Road, Bldg. 938A, Berkeley, CA 94720.** We are an equal opportunity employer.

LAWRENCE BERKELEY LABORATORY
UNIVERSITY OF CALIFORNIA
Department of Energy

POSTDOCTORAL OPPORTUNITIES

The Genentech Postdoctoral Program consists of more than 50 Fellows and is a vibrant and intensive environment for advanced scientific training. Postdoctoral Fellows conduct basic research in the areas of our scientific interests, publish in scientific journals, attend and present work at scientific conferences and maintain close ties with the academic community. Several positions are available for outstanding candidates in the fields of:

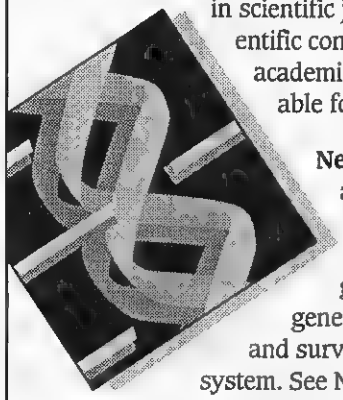

Neurobiology: A position is available in the area of developmental neurobiology. The successful candidate will utilize advanced molecular, cellular, and genetic approaches to identify and study genes that control commitment differentiation and survival of neurons in the central nervous system. See Nature 363, 266 (1993); Science 266, 1062 (1994); Neuron 113, 1245 (1994); PNAS 91, 3304 (1994); Cell 80, 95 (1995); Nature 373, 339 (1995). Send your resume to Dr. Arnon Rosenthal, Department of Neuroscience.

Molecular Biology: A position is available to study cytokine receptor signal transduction and participate in the identification of novel receptors and ligands with potential therapeutic interest. Experience in hematopoiesis and/or signal transduction is an advantage. See Nature 369, 533 (1994) and Science 265, 1445 (1994). Send your resume to Dr. Frederic de Sauvage, Department of Molecular Biology.

Molecular Biology: A position is available to study receptors and GTP-binding proteins and to identify novel genes that regulate essential cell functions. The successful candidate will have a background in molecular and cell biology, biochemistry and genetics. See Cell 56, 487 (1989); Nature 340, 146 (1989); PNAS 88, 10535 (1991); Nature 360, 161 (1992); JBC 268, 26059 (1993); JI 152, 1347 (1994). Send your resume to Dr. Avi Ashkenazi, Department of Molecular Biology.

Genentech offers an excellent salary and benefits package which includes child care resources, free health club membership and fully paid medical, dental and vision coverage. Please send your resume to the appropriate investigator at Genentech, Inc., Human Resources, 460 Point San Bruno Blvd., South San Francisco, CA 94080. We actively support and promote affirmative action and equal employment opportunity. Women and minorities are encouraged to apply.

Genentech, Inc.

TENURE-TRACK FACULTY RESEARCH POSITIONS MOLECULAR AND CELLULAR PATHOLOGY

The Department of Pathology, University of Alabama at Birmingham, is seeking individuals for positions at the faculty level who are interested in joining an active and growing group of investigators in basic research and graduate training. Applicants should have a Ph.D. or M.D. degree and are expected to develop independently funded research programs. Special consideration will be given to individuals with experience in cellular and molecular biology, signal transduction, a desire to interact with other investigators and a willingness to participate in graduate and postdoctoral training. Level of appointment will be determined by qualifications. Please send a detailed curriculum vitae including description of research, recent reprints and names of three references to: **Thomas M. Lincoln, Ph.D., Acting Director, Division of Molecular and Cellular Pathology, Department of Pathology, University of Alabama at Birmingham, 1670 University Boulevard, Birmingham, AL 35294-0019.** *University of Alabama at Birmingham is an Affirmative Action/Equal Opportunity Employer and welcomes applications from women and minorities.*

DEPARTMENT OF NUTRITION CASE WESTERN RESERVE UNIVERSITY

We seek a **FACULTY** member to conduct basic and clinical investigations in nutritional biochemistry and metabolism. We are particularly interested in (i) the intra- and inter-organ metabolism of nutrients, (ii) the use of stable isotope techniques for investigating these processes, and (iii) the design and testing of synthetic nutrients. The appointee will develop independent research programs and participate in the teaching and training of graduate and postgraduate students. Send curriculum vitae, representative reprints, outline of research program and names of three persons we could contact as references by May 1, 1995, to: **Dr. Henri Brunengraber, Chair, Department of Nutrition, Case Western Reserve University, Cleveland, OH 44106.** *Case Western Reserve University is an Equal Opportunity Employer and encourages applications from minorities and women.*

BIOLOGY LABORATORY INSTRUCTORS

Ohio University Department of Biological Sciences invites applications for seven full-time, permanent laboratory **INSTRUCTOR** positions for the following laboratory courses: principles of physiology series, introductory zoology series, human anatomy, human physiology, exercise physiology, anatomy and histology, and comparative vertebrate anatomy. The normal teaching load is 20 contact hours per week. Preference will be given to individuals who can teach in several of these areas. A minimum of a Master's degree in a biological science, a strong commitment to an undergraduate teaching career, excellent teaching skills, a broad knowledge of the field, and a demonstrated commitment and ability to integrate the latest educational technologies are required. The Department has 50 tenure-track faculty members, teaches 1,600 undergraduate, 80 graduate, and 250 professional students. The positions begin September 1, 1995, at a minimum nine-month salary of $26,000 plus benefits. Send curriculum vitae, college transcripts, a statement of teaching experience and philosophy, and three letters of recommendation by April 1, 1995, to: **Biology Instructor Search, J. Witkowski, Department of Biological Sciences, Ohio University, Athens, OH 45701.**

Ohio University is an Equal Opportunity/Affirmative Action Employer and women and minorities are encouraged to apply.

POSTDOCTORAL POSITION in molecular parasitology available immediately to study kinetoplast DNA replication genes and proteins in the trypanosomatid *Crithidia fasciculata*. Areas of research in our laboratory include 1) cloning and analysis of genes required for kinetoplast DNA replication, 2) cell cycle control of the expression of DNA replication genes, and 3) identification and characterization of proteins involved in the organization and condensation of kinetoplast DNA. (See **Pasion et al.,** *J. Cell Sci.,* **107**:3515-3520, 1994; **Xu and Ray,** *PNAS,* **90**:1786-1789, 1993; **Melendy et al.,** *CELL,* **55**:1083-1088, 1988.) Requires a strong background in Molecular Biology or Biochemistry with experience in recombinant DNA and protein methods. Interested applicants should send their résumé including reprints and names and telephone numbers of three references to: **Dr. Dan S. Ray, Molecular Biology Institute, UCLA, Los Angeles, CA 90095-1570.**

POSTDOCTORAL/RESEARCH FACULTY Theoretical, Computational, and Experimental Chemistry and Physics

We are looking for exceptionally able (1) theoretical/computational chemists or physicists with a strong background in quantum or classical dynamics, intense light-matter interactions, quantum control of chemical dynamics, or related areas, (2) experimentalists, particularly with a background in one or more of the following: ultrafast lasers, atomic and molecular beams, laser generated X-rays, charged particle beams, or X-ray physics. Current research interests in our group include (1) theoretical and experimental quantum control of chemical dynamics with femtosecond lasers, (2) development of multi-terawatt femtosecond lasers and their application to high field chemistry and physics, (3) ultrafast, short wavelength electron and X-ray diffraction as applied to imaging molecular quantum dynamics. For a description of current group activities and personnel see our World Wide Web site, **http://www-wilson.ucsd.edu/** or send Email with no text to **wilsjob@ucsd.edu**. To apply, please send a curriculum vitae to: **Prof. Kent R. Wilson, Department of Chemistry 0339, University of California, San Diego, La Jolla, CA 92093-0339.** *Affirmative Action/Equal Opportunity Employer.*

POSTDOCTORAL POSITION MOLECULAR RADIOBIOLOGIST

POSTDOCTORAL POSITION available July 1, 1995, in the Radiobiology Laboratory of the Johns Hopkins Oncology Center. The applicant should have a background in cellular and molecular biology with an interest in the cellular response to ionizing radiation. This is a starting faculty position at the Instructor or Assistant Professor level with three years of initial support. Send curriculum vitae and names of three references to:

Moody D. Wharam, Jr., M.D.
Professor
Oncology, Radiological Sciences, Neurosurgery, and Pediatrics
Director
Division of Radiation Oncology
The Johns Hopkins Oncology Center
600 North Wolfe Street
Baltimore, MD 21287-8922

The Johns Hopkins University School of Medicine is an Equal Opportunity Employer.

POSTDOCTORAL POSITION available immediately to participate in NIH-funded Program Project Grant on the role of lipid mediators in lung injury. The research bridges molecular biology/biochemistry to pathogenesis of inflammation in diseases including asthma and ARDS. This position is focused on regulation of phospholipases A_2, and is an interdepartmental project combining senior faculty of the Departments of Medicine and Biochemistry. Experience in molecular biology and lipid chemistry would be important. Send curriculum vitae and names and telephone numbers of three references to: **Dr. David A. Bass, Pulmonary and Critical Care Medicine, Bowman Gray School of Medicine of Wake Forest University, Medical Center Boulevard, Winston-Salem, NC 27157-1054. FAX: 910-716-7277.** *An Affirmative Action/Equal Opportunity Employer.*

POSTDOCTORAL POSITION available for three years to study electrophysiology of cancer cells, cardiac myocytes and cloned human cardiac potasium channels. Experience of voltage clamp methods essential, with interest in molecular biology. Opportunities to interact with a number of different investigators and groups. Please send curriculum vitae and names of two references to: **Dr. David Fedida, Department of Physiology, Queen's University, Kingston, Ontario K7L 3N6 Canada. Telephone: 613-545-2799; FAX: 613-545-6880.** *In accordance with Canadian immigration requirements, priority will be given to Canadian citizens and permanent residents.*

POSTDOCTORAL POSITIONS available immediately to study the molecular/biochemical mechanisms of retinoic acid-regulated cell growth/differentiation in myeloid cells and drug resistance in breast tumor cells. Candidates with background in molecular biology/biochemistry, interested in pursuing career in the area of cancer biology should send résumé and the names and addresses of three references to: **Kapil Mehta, Ph.D., Department of Clinical Investigation, Box 60, University of Texas M.D. Anderson Cancer Center, Houston, TX 77030. Telephone: 713-792-2649; FAX: 713-796-1731.**

POSTDOCTORAL POSITION HIV RESEARCH

POSTDOCTORAL POSITION available immediately to study cytokine and cytokine antagonist control of HIV replication and immune response. The *in vitro* research is oriented toward designing therapeutic approaches for *in vivo* use. A Ph.D. or M.D. degree is required and a strong background in HIV research or molecular biology is highly desirable. Send curriculum vitae and names of three references to: **Paul Skolnik, M.D., Division of Infectious Diseases, Tufts University-New England Medical Center, 750 Washington Street, NEMCH 67, Boston, MA 02111. FAX: 617-636-3216; Email: paul.skolnik@es.nemc.org.** *New England Medical Center is an Equal Opportunity/Affirmative Action Employer. Women and minorities are encouraged to apply.*

Full-time **POSTDOCTORAL POSITION** available immediately to study molecular mechanism of tumorigensis, involving tumor suppressor genes and oncogenes. Competitive salary depends on experience. Please send curriculum vitae with names and telephone numbers of three references to:

Anne T'Ang, Ph.D.,
Assistant Professor of Pathology/Ophthalmology
University of Southern California
Division of Ophthalmology
Childrens Hospital Los Angeles
4650 Sunset Boulevard, Mailstop No. 94
Los Angeles, CA 90027

USC/Childrens Hospital Los Angeles is an Affirmative Action/Equal Opportunity Employer.

POSTDOCTORAL ASSOCIATE

Available for Ph.D., M.D. or M.D./Ph.D. with interest in the application of molecular approaches to address questions in appetite, regulation of food intake and peripheral metabolism. Initial experiments in animals but opportunities exist for progression to human experimentation. Proficiency in protein chemistry, RNA/DNA techniques, PCR and electrophoresis required. Please send curriculum vitae and names and complete addresses of three references to: **Richard Galbraith, M.D., Ph.D., The University of Vermont, 795 Baird, The College of Medicine, Burlington, VT 05401.** *The University of Vermont is an Affirmative Action/Equal Opportunity Employer.*

POSTDOCTORAL POSITION, USDA, Agricultural Research Service (ARS), National Animal Disease Center, Ames, Iowa. The candidate will investigate expression of heat shock proteins by the host cell and bacterium after infection with *Mycobacterium paratuberculosis*. Evaluation of these proteins as potential antigens for activation of lymphocyte populations will also be expected. Candidate will be part of a team consisting of an immunologist and a pathologist. Applicants must have a Ph.D. degree. Minimal of 24 month appointment; salary is commensurate with experience ($35,578 to $42,641 per annum). Send curriculum vitae or an application and names of three references to: **Dr. Judith R. Stabel, USDA, ARS, National Animal Disease Center, P.O. Box 70, Ames, IA 50010. Telephone: 515-239-8304.** Applications in response to this advertisement should be marked 5N029. Applications will be accepted until the position is filled. *USDA/ARS is an Equal Opportunity Employer.*

POSTDOCTORAL POSITIONS—One available immediately to study the role of the helix-loop-helix proto-oncogene *TAL1/SCL* in avian vascular development. Other position available July 1, 1995, supported by NIH training grant to study the role of *TAL1/SCL* in leukemogenesis. Candidates should have experience in cellular and/or molecular biology. Previous experience in developmental biology desirable. Send curriculum vitae and names of three references to: **Dr. Stephen J. Brandt, Division of Hematology, Room C-3101 Medical Center North, Vanderbilt University Medical Center, Nashville, TN 37232. FAX: 615-343-4589.** *An Affirmative Action/Equal Opportunity Employer.*

POSTDOCTORAL POSITION available to characterize mutants isolated from a genetic screen on metal-regulated gene expression. The NIH-funded research requires background in yeast genetics and molecular biology. Send curriculum vitae and three letters of reference to: **Dr. Dennis R. Winge, University of Utah Health Sciences Center, Salt Lake City, UT 84132.**

The University of Utah is an Equal Opportunity Employer.

National Institutes of Health / National Institute of Allergy and Infectious Diseases
Division of Acquired Immunodeficiency Syndrome

BRANCH CHIEF

Clinical Development Branch, Vaccine and Prevention Research Program

Location: Bethesda, MD

The Division of AIDS, NIAID/NIH is seeking a Branch Chief for its newly established Clinical Development Branch. This individual is responsible for the overall scientific leadership and management of Phase I and II clinical trials of candidate AIDS vaccines. Currently, the Branch supports the AIDS Vaccine Evaluation Group (AVEG) at six clinical sites, a Statistical and Coordinating Center Contract, and two Immunology Laboratory Contracts. The Division plans and directs a national and international extramural research program into the causes, diagnosis, prevention and treatment of HIV and its associated opportunistic infections.

Desirable qualifications include an M.D. and/or Ph.D. degree, extensive postgraduate research experience, demonstrated ability to direct a biomedical research effort, broad knowledge of the basic and clinical research aspects of vaccine testing and vaccine clinical trials and an understanding of the policies, procedures, and mechanisms used within the Institute and DHHS for accomplishing research through extramural activities. U.S. citizenship is required.

This is a GS-15 Civil Service position. A recruitment or relocation bonus of up to 25% of base pay may be available. Physicians may be eligible for a Physician's Comparability Allowance of up to $20,000 per year.

Selection for this position will be based solely on merit with no discrimination for non-merit reasons such as race, color, religion, gender, national origin, disability, age, or sexual orientation.

For additional information on the position listed, please contact Ms. Janice Cordell, Assistant to the Associate Director, Vaccine and Prevention Research Program, DAIDS at: 301-402-5535. ***Applicants should submit a curriculum vitae by April 3, 1995 to:***

Kristie Daniel, NIAID Personnel Office, Room 7A-20
9000 Rockville Pike, Bethesda, MD 20892
Merit Promotion Vacancy Announcement #95-020

Nutritional Biochemist (Project Leader)

ROSS PRODUCTS DIVISION

Ross Products Division, a division of Abbott Laboratories and the leading manufacturer of pediatric and medical nutritional products, has two excellent opportunities for experienced professionals with Ph.D.s in Nutritional Biochemistry or a related field.

Position #1 - Research expertise in the fields of metabolism and biochemistry of cells and tissues is desired. A general comprehension of physiology is helpful.

Position #2 - Research expertise in the fields of diabetes and cell signaling is desired. A general comprehension of integrative metabolism is helpful.

These persons will provide technical leadership on current projects as well as participation in new product concept development for disease specific areas. The selected candidates will be assigned projects with a high degree of technical responsibility, be expected to establish research internally and externally in support of projects and work with outside experts and sister divisions. These individuals will be independent contributors to team oriented endeavors. Strong communication skills are necessary.

Ross Products Division, headquartered in Columbus, Ohio, offers an excellent compensation and benefits program in a smoke-free environment. For confidential consideration, please direct your CV to: **ROSS PRODUCTS DIVISION, 625 Cleveland Avenue, Columbus, OH 43215. Attn: Staff Recruiter.** Ross is an Equal Opportunity Employer.

ABBOTT LABORATORIES
ROSS PRODUCTS DIVISION

Ph.D. PROTEIN BIOCHEMIST

DowElanco, a leading company in the development of innovative products for crop production, has an immediate opening for a Ph.D. Protein Biochemist in the Biotechnology and Plant Genetics Department. The Department is part of DowElanco Discovery Research effort which is located in a new state-of-the-art research center in Indianapolis, Indiana.

As part of an interdisciplinary team, this individual will be responsible for the isolation and characterization of proteins from diverse sources, for use in programs focused on the development of transgenic plants and microbial products. The successful candidate will have a strong background in protein biochemistry and enzymology with experience in the optimization of bacterial systems for production of proteins or metabolites. An excellent understanding of Streptomyces (or Actinomycetales) metabolic biochemistry and regulation is desirable. Excellent communication skills and a high level of self motivation are essential.

To learn how to advance your career while enhancing the agricultural environment, send a resume by April 15, 1995 to: Kathy McIntyre, Dept. YDBM-1, DowElanco, 9330 Zionsville Road, Indianapolis, IN 46268-1054. An Equal Opportunity Employer.

DowElanco

POSITIONS OPEN

PITTSBURGH TRANSPLANTATION INSTITUTE

A **POSTDOCTORAL FELLOWSHIP** is available for studies concerning the regulation of antigen-presenting cell (APC) function (see e.g., *J. Exp. Med.*, 178:1823, 1994) and the role of donor-derived APCs in transplantation tolerance. Candidates should have a Ph.D. in immunology and/or molecular biology relevant to transplantation science and up to two years of postdoctoral experience. Please submit curriculum vitae and provide three references to: **Angus W. Thomson, D.Sc., Research Professor, Pittsburgh Transplantation Institute, W1544 Biomedical Science Tower, University of Pittsburgh Medical Center, 200 Lothrop Street, Pittsburgh, PA 15213 USA. FAX: 412-624-1172.**

POSTDOCTORAL FELLOW. Position available spring 1995 to conduct research on the role of macrophages in atherosclerosis using molecular biological and transgenic mouse techniques. Experience in molecular biology necessary. Send curriculum vitae and references to: **Dr. I. Tabas, Department of Medicine, Columbia University, New York, NY 10032.** *Columbia University is an Equal Opportunity/Affirmative Action Employer.*

POSTDOCTORAL POSITION in Neuroscience. NIH-funded position available immediately to study the electrophysiological properties of vestibular sensory neurons in chick brain slices and/or immunocytochemical studies on vestibular central synapses. Candidate should have experience in voltage clamp, pharmacology, and/or immunocytochemistry. Please send curriculum vitae, statement of research interests and three references to: **Dr. Kenna D. Peusner, Department of Anatomy and Neuroscience Program, George Washington University School of Medicine, 2300 I Street, N.W., Washington, DC 20037.** *The George Washington University is an Equal Opportunity Employer.*

A **POSTDOCTORAL POSITION** is available to clone and characterize the developmentally regulated genes in sweetpotato. A Ph.D. in molecular biology, plant science or related discipline with research experience in differential display PCR, DNA sequencing, vector construction and *in situ* hybridization required. Send résumé and three letters of reference to: **Dr. C. S. Prakash, Tuskegee University, School of Agriculture, Tuskegee, AL 36088. FAX: 334-727-8067.** *U.S. citizens only. Minorities and women are strongly encouraged to apply.*

POSTDOCTORAL FELLOWSHIPS

The College of Medicine and the H. Lee Moffitt Cancer Center and Research Institute at the University of South Florida has **POSTDOCTORAL/RESEARCH ASSOCIATE** positions available in a stimulating academic environment that includes excellent laboratory and clinical facilities. Investigators providing mentorship include **Julie Djeu, Ph.D., Jie Wu, Ph.D., W. J. Pledger, Ph.D., and Timothy Yeatman, M.D.**

The individuals sought should hold a M.D. or Ph.D. and have a demonstrated interest in cancer related research with training in molecular biology and/or cellular biology. Research areas include: signal transduction, regulation of growth and differentiation, processes of metastasis, and mechanisms of action of cytokines and growth factors.

Send current curriculum vitae and a brief statement of major academic interests to: **W. J. Pledger, Ph.D., Associate Center Director for Basic Research, Office of Faculty Recruitment, Moffitt Cancer Center, 12902 Magnolia Drive, Tampa, FL 33612.** Applicants who need a reasonable accommodation in order to participate in the selection process must notify **Jody Swanson** in the Office of Faculty Recruitment, **813-975-7894**, five days in advance. Applications must be postmarked by deadline of April 20, 1995.

Moffitt Cancer Center is an Equal Opportunity Employer. The University of South Florida is an Equal Opportunity/Equal Access/Affirmative Action Employer.

Immediate opening for **POSTDOCTORAL FELLOW/RESEARCH ASSOCIATE.** Candidate should have a Ph.D. in a biologically relevant discipline, training and experience in immunoassays, and technical writing ability. Candidate would interface with clinical studies. Competitive salary and fringe benefits. Send letter of interest, curriculum vitae, and official transcript to: **Dr. David J. Baylink, Distinguished Professor of Medicine, Loma Linda University, J. L. Pettis VAH (151), 11201 Benton Street, Loma Linda, CA 92357.**

POSITIONS OPEN

POSTDOCTORAL RESEARCH ASSOCIATE NEUROSCIENCE

A **POSTDOCTORATE** or **RESEARCH ASSOCIATE** position is available in the Neuroscience Program at the Loeb Resource Institute of the Ottawa Civic Hospital, a University of Ottawa affiliate, to participate in peer-reviewed and funded studies of neurotransmitter and peptide receptors, ligand- and voltage-activated conductances and second messenger mechanisms in mammalian CNS neurons controlling autonomic and pituitary function. The Program comprises nine PIs with expertise in molecular and cellular neurobiology applied to exocytosis, membrane trafficking, signal transduction, gene regulation, ion channel function, post-ischemic neuronal function and survival. Requires: M.D. and/or Ph.D. degree; minimum of four years of postdoctorate experience with electrophysiology and neuropharmacology in slice and/or explant preparations; demonstrated ability and productivity (authorship on peer-reviewed publications) with current, voltage- and patch clamp techniques, data analysis and anatomical marking methods. Position is tenable for a minimum of three years, and involves teaching and lab supervision. Salary and benefits commensurate with experience. In accordance with Canadian immigration regulations, this advertisement is directed first, but not solely, to Canadian citizens and permanent residents.

Forward or FAX **(613-761-5360)** curriculum vitae with addresses of three references and a statement of goals/interests/experience by March 31, 1995, to: **Dr. Leo Renaud, Director, Neurology/Neurosciences, Ottawa Civic Hospital and Loeb Research Institute, 1053 Carling Avenue, Ottawa, Ontario, K1Y 4E9 Canada.**

POSTDOCTORAL FELLOW CELL REGULATION
University of Texas Southwestern Medical Center at Dallas

An exciting new area in cell regulation research is emerging. Evidence is accumulating that two plasma membrane domains that are specialized for endocytosis (clathrin coated pits and caveolae) are sites where hormonal and mechanical signals are modulated. Our laboratory has mounted a major research effort to study the role of these membrane domains in compartmentalized signal transduction.

POSTDOCTORAL POSITIONS are now available for individuals who want to receive training in this exciting new research area. If you have either a Ph.D. or M.D. and have experience in molecular and cell biology, please apply. Send curriculum vitae and three letters of recommendation to:

Dr. Richard G. W. Anderson
Department of Cell Biology and Neuroscience
University of Texas Southwestern Medical Center at Dallas
Dallas, TX 75235-9039

An Equal Opportunity Employer

POSTDOCTORAL FELLOWSHIP

Position available in cellular and molecular neurobiology for a Ph.D. or M.D./Ph.D. Research projects involve transgenic and gene targeting strategies to generate animal models of human neurodegenerative diseases, including Alzheimer's disease, ALS, and spinal muscular atrophy. Studies of the mechanisms of neuronal injury and cell death are integral to our program. A strong background in cellular and molecular biology and familiarity with neurobiology are desirable. Send curriculum vitae and references to: **Donald L. Price, M.D., Neuropathology Laboratory, The Johns Hopkins University School of Medicine, 558 Ross Research Building, 720 Rutland Avenue, Baltimore, MD 21205-2196.** *Please, U.S. citizens or permanent residents only (because of funding limitations). An Equal Opportunity Employer; women and minorities are encouraged to apply.*

POSTDOCTORAL POSITIONS in Adhesion Receptor Research: Positions available immediately to study (1) integrin mediated signal transduction (with **R. L. Juliano**)—background in mammalian molecular biological techniques essential; or (2) sickle cell adhesion to ECM (with **L. Parise**)—background in protein biochemistry essential. Applicants should send curriculum vitae and names of two references to: **Brenda Rosen, Department of Pharmacology, University of North Carolina-Chapel Hill, Chapel Hill, NC 27599-7365. FAX: 919-966-5640.** *An Equal Opportunity/Affirmative Action Employer.*

POSITIONS OPEN

POSTDOCTORAL/RESEARCH ASSOCIATE to study CNS remyelination. *In vivo* and *in vitro* cellular and molecular techniques will be integrated to identify signals mediating proliferation and migration of remyelinating cells in experimentally demyelinated mice. Send curriculum vitae, a summary of research interests/experience, and names and telephone numbers of at least three references to: **Dr. R. C. Armstrong, Department of Anatomy and Cell Biology, Uniformed Services University of the Health Sciences, 4301 Jones Bridge Road, Bethesda, MD 20814-4799.** This is a civilian research position within the medical school.

Affirmative Action/Equal Opportunity Employer.

POSTDOCTORAL TRAINEES, Neuroscience. Research with **Drs. Eric Simon** (opioid receptors), **Eric Stone** (catecholamines and stress) or **Ken Carr** (opioids and motivated behavior). Start April 1 to September 1, 1995. Contact: **Dr. Carr, Millhauser Lab, NYU Medical Center, 550 First Avenue, New York, NY 10016.** *U.S. citizenship or permanent residency required. An Affirmative Action/Equal Opportunity Employer.*

IMMUNOLOGY AND HEMATOLOGY/BMT

City of Hope, a world-renowned cancer treatment and research center has the following opportunities.

Immunology: Position for a **POSTDOCTORAL RESEARCH FELLOW** with experience in tissue culture, molecular biology and immunology techniques. Experience with neutrophils and cellular biochemistry is desired. Ph.D. or M.D. required. Please reference position KF.

Hematology/BMT. Position for a Doctoral-level **SCIENTIST** to participate in the development of a subunit/peptide vaccine against CMV in the transplantation setting. The program is supported by a five-year NIH grant. Requires extensive background in cellular immunology with expertise in protein chemistry or molecular biology. Please reference position DD.

Send résumé to: **Human Resources, City of Hope and Beckman Research Institute, 1500 East Duarte Road, Duarte, CA 91010-3000. FAX: 818-301-8448.** For consideration, position reference must be identified. *Equal Opportunity Employer.*

NMR SPECTROSCOPY

The Cardiovascular Institute at Columbia University seeks applicants with an M.D. or Ph.D. and one to two years of postdoctoral experience in NMR spectroscopy. Additional expertise in MR imaging is desirable. Our current interests are in pursuing multi-nuclear imaging and spectroscopy of the cardiovascular system including proton, sodium and phosphorus on 3T and 5T whole-body NMR systems. This is primarily a **RESEARCH POSITION** with no clinical responsibilities. Please send curriculum vitae, a reprint of a key publication and the names of two references to: **Dr. Jose Katz, Division of Cardiology, College of Physicians and Surgeons, Columbia University, 630 West 168th Street, New York, NY 10032.** *Columbia University is an Affirmative Action/Equal Opportunity Employer.*

LABORATORY SUPERVISOR

A position is available to participate in the NHLBI-sponsored Mammalian Genotyping Service in the laboratory of Dr. James Weber. The goal of this project is to provide high quality, cost-effective and automated genotyping of DNA polymorphisms to support genetic studies aimed at identifying genes responsible for cardiovascular, lung and blood diseases. The successful candidate will lead a team of about five technicians and computer specialists. A doctorate degree and research experience in human molecular genetics are required. Completion of a postdoctoral fellowship is desired. Competitive salary and benefits are offered. Interested applicants should send curriculum vitae and three reference letters to: **Human Resources, Employment Generalist, Marshfield Clinic, 1000 North Oak Avenue, Marshfield, WI 54449.** *The Marshfield Clinic is an Equal Opportunity Employer, Minority/Female/Disabled/Veterans.*

ELECTROPHORESIS RESEARCHERS

Established manufacturer seeks help with development efforts for an electrophoresis product. Individuals must own or have direct access to an IEF device (Phast®, Multiphor®, ICE® System, etc.) and prior experience in electrophoresis. Incentives provided for rapid data generation. Please send a brief description of your electrophoresis capabilities to: **RHD, P.O. Box 2555, Acton, MA 01720.**

Tenure Track Position

HUMAN AND ANIMAL GENETICS & MOLECULAR GENETICS OF DRUG ABUSE

George R. Uhl, M.D., Ph.D.

Tenure track position available to lead a research program that will extend and complement ongoing research in the Genetics and Molecular Genetics of Drug Abuse. Candidates should have experience in genetics and molecular genetics, with preference given to expertise in human genetics of nonMendelizing disorders. Support by senior fellows, technical staff, extensive laboratory and animal space for up to six years. The candidate will be evaluated for tenure within a period not to exceed six years. If you hold a doctoral degree(s) and would like to be considered for the position, please send a cover letter, a curriculum vitae with bibliography, statement of research interests and goals (not to exceed two pages), and three letters of recommendation to: **G.R. Uhl, M.D., Ph.D., Molecular Neurobiology Branch, Division of Intramural Research, National Institute on Drug Abuse, National Institutes of Health, Box 5180, Baltimore, Maryland 21224.** Competitive salary levels with full federal benefits - an equal opportunity employer. Candidates must be U.S. citizens or permanent residents.

EARLE. A CHILES RESEARCH INSTITUTE
PORTLAND, OREGON

The Earle A. Chiles Research Institute, located at Providence Portland Medical Center and a member of the Oregon Cancer Center, is a not-for-profit, academic organization committed to translational research in biological cancer therapy. Research programs, under the direction of **Bernard A. Fox** and **Deric D. Schoof**, include basic human and animal tumor immunobiology, tumor vaccine development, clinical immunotherapy and gene therapy. Applications are being accepted for the following positions:

- *POSTDOCTORAL FELLOWSHIP IN CANCER IMMUNOLOGY* (2 positions available)
  Applicants must have a Ph.D. or M.D. degree with experience in cell culture, animal tumor models or molecular and cell biology.
- *GRADUATE TRAINING PROGRAM IN TUMOR IMMUNOLOGY*
  Applications are invited for a program of study leading to a Ph.D. from the Department of Molecular Microbiology and Immunology at Oregon Health Sciences University.

Salary is commensurate with experience. Please send curriculum vitae and the names of three references to: Research Staff Committee, Earle A. Chiles Research Institute, Providence Medical Center, 4805 NE Glisan Street, Portland, OR 97213, email: kalezm@ohsu.edu. *An equal opportunity/ affirmative action employer.*

Imagine The Possibilities

At Berlex, we've built our reputation on FDA-approved product successes and a proven track record in the pharmaceutical industry. Currently, we are seeking Senior Scientists/Scientists to contribute to our Oncology research projects in the beautiful San Francisco Bay Area.

ONCOLOGY
SENIOR SCIENTISTS/SCIENTISTS

In Vitro/In Vivo Tumor Models

You will develop in vitro and in vivo tumor models, conduct therapy studies and support antitumor drug discovery programs as part of our new Oncology Research team. You will need a Ph.D. in cell/tumor biology or pharmacology and some post-doctoral training, preferably working with the prostrate, along with 2-5 years' industry experience in tumor biology and drug discovery. Dept. B95-009.

Tumor Biology

Calling on your skills and extensive experience in cell and molecular biology (culture of normal and neoplastic cells as well as the elucidation of autocrine and paracrine signalling pathways), you will design assay systems to help identify novel targets and characterize promising compounds for antitumor drug discovery. You will need a Ph.D. in cell biology, molecular biology or biochemistry supported by post-doctoral experience to include 2-5 years' experience in tumor biology and drug discovery in industry. Dept. B95-008.

As a US subsidiary of an international Fortune 500 company, Berlex is proud to offer competitive salaries and a generous benefits package. To apply, send your CV/resume, indicating the Dept. number corresponding with the position of your interest to: BERLEX, HUMAN RESOURCES EMPLOYMENT, 15049 SAN PABLO AVE., RICHMOND, CA 94804-0099. Principals only, please. EOE.

BERLEX

THE BEST IS YET TO COME

Postdoctoral Training in Cancer Biology
Massey Cancer Center
Medical College of Virginia-Richmond, VA

Postdoctoral training opportunities are available at the Massey Cancer Center encompassing faculty in the Departments of Microbiology/Immunology, Pharmacology, and Medicine.

Signal Transduction and Genetic Control of Apoptosis

This program focuses on the molecular and signal transduction events that regulate drug-induced apoptosis in human leukemia cells. The goal is to elucidate the role of protein kinase C and other signaling pathways in apoptotic events, as well as the contribution of oncogenes such as bc1-2, c-jun, and p21 to this process. Training is within the context of a collaborating group of faculty in the Developmental Therapeutics and Growth Regulation Programs of the Massey Cancer Center.

Molecular Pharmacology of Anti-neoplastic Agents

This program provides trainees with perspectives and laboratory skills to explore the development of anti-cancer drugs, and their biochemical modulations and chemical modifications. There is special focus on new generation antimetabolites and DNA damaging agents. Training is supported by a collaborating group of faculty with expertise in pharmacology, biochemistry, molecular biology and biophysics. Trainees are introduced to concepts in structural biology and computer modelling to prepare them for modern drug development strategies.

The Biology of Follicular Dendritic Cells

Follicular dendritic cells are the long-lived lymphoid cells that retain antigen elements and are a critical factor in immune cell memory. This project will focus on the role of follicular dendritic cells in cell growth and differentiation in a variety of lymphoma models. The Department of Microbiology/Immunology is an internationally recognized center for studies on the biology of follicular dendritic cells.

Molecular Aspects of Oncogenesis

This project will focus on the development of a novel approach to investigate the mechanisms controlling oncogene translocations. This work will be undertaken as a collaboration between laboratories working on regulation of oncogene expression and isotype switch recombination.

Massey is an NCI designated center with an established NCI funded postdoctoral training program. There is extensive faculty and trainee collaboration and utilization of center core laboratory facilities for antibody, oligonucleotide and protein production, DNA sequencing and FACS services. There is a track record of successful trainee placement in positions in academics, government and research units of the pharmaceutical industry. Trainees participate in the development of grants as part of the training experience and have had an excellent record of peer-reviewed funding.

Molecular and Genetic Mechanisms of Prostate Cancer Progression

Studies will focus on differential gene expression, as well as cytogenetic and molecular marker analysis, in both surgical specimens and novel laboratory models of prostate tumor invasion and metastasis. Opportunity for training in interdisciplinary prostate cancer research program. Experience in genetics, molecular biology, or cell biology preferred.

Starting stipend is $25,000/yr. Applicants should submit a curriculum vitae along with the names and addresses of three references and a statement of their research background and interests to **Dr. I. David Goldman, Director, Massey Cancer Center, Medical College of Virginia, MCV P.O. Box 980230, Richmond, VA 23298-0230.** *US citizenship or permanent residence status is required. MCV/VCU is an equal opportunity employer. Women and minorities are encouraged to apply.*

The Women, Gender, and Science Question:

What do research on the history of women and science and research on science and gender have to do with each other?

May 12-14, 1995

University of Minnesota
St. Paul, Minnesota

For further information:
phone Susan Potratz
(612) 625-5886,
fax (612)626-1632
or email
sburke@mail.cee.umn.edu

The University of Minnesota is an equal opportunity educator and employer.

UNIVERSITY
OF MINNESOTA

DEAN OF THE MEDICAL SCHOOL
UNIVERSITY OF WISCONSIN-MADISON

The University of Wisconsin-Madison is the original University of Wisconsin, and is one of the largest land-grant Universities in the United States. There are approximately 2,500 faculty, 4,000 professional and administrative staff, 8,000 classified employees and 40,000 undergraduate, graduate and professsional students at the institution.

The Dean of the Medical School serves as the chief academic and executive officer of the school with responsibility for staffing, budget, curriculum, student academic affairs, and space. The school is a component of the Health Sciences, which includes the Schools of Nursing and Pharmacy as well as University Hospital and is housed almost entirely on the Madison campus. The Medical School is composed of approximately 600 medical students, 500 graduate students, and 200 postdoctoral trainees. The Dean leads a faculty of approximately 750 and a professional staff of over 1,000 located in Madison and a network of educational programs throughout the state. In addition to the MD degree, the school offers master's and doctoral degrees in the fields of anatomy, biomolecular chemistry, history of medicine, medical genetics, medical microbiology, medical physics, neurophysiology, oncology, pathology, pharmacology, physiology, preventive medicine and radiobiology. The school sponsors over 500 house staff in residency and fellowship training in all medical fields, using the University Hospital in Madison and community teaching hospitals throughout the state. The Medical School is responsible for the programs in training Physician Assistants and Medical Technologists and provides instruction for numerous undergraduates in the Schools of Pharmacy, Nursing, Education, and in the Colleges of Letters and Science, Agricultural and Life Sciences, and Engineering.

The major qualifications for this position include a successful record of academic achievement and administrative leadership in medical education including internal management skills and the creative advocacy of private support; accomplishments that meet standards for a tenured appointment at the rank of full professor in the University of Wisconsin-Madison faculty; a commitment to enhance excellence in medical, graduate student, and residency education in research, public service and outreach activities; and the ability to articulate the vision and needs of the school to diverse constituencies includes potential private donors, legislators and various government officials. The Dean must also have a commitment to encouraging interdisciplinary collaboration among members of the faculty within the school as well as within the larger community of scholars at other schools and colleges within the university. The Dean should have a commitment as well to exploring collaborative opportunities that exist in partnerships with health care providers, state agencies, and other educational programs within the state. **Under Wisconsin Statutes, the names of nominees and applicants who explicitly request confidentiality will not be made public, although the university is required to release the names of the finalists, who will be interviewed by the UW-Madison Chancellor.**

The position is available July 1, 1995.

All applications and nominations must be received by Monday, April 17, 1995.

Submit applications and nominations to:

John J. Frey (Chair)
Search and Screen Committee
University of Wisconsin-Madison
129 Bascom Hall
500 Lincoln Drive
Madison, Wisconsin 53706
Telephone: (608)262-9337
Fax: (608)265-5728

The University of Wisconsin is an Equal Opportunity Affirmative Action Employer

IMMUNOLOGIST

The Department of Biology at the University of Northern Iowa invites applications for a tenure-track assistant professor position effective August 1995. The individual will have primary responsibility for an upper division course in immunology and also teach in other areas. The department expects effectiveness in both teaching and research. The applicant's research program should invite participation by master's and undergraduate students. Ph.D. in a biological science is required. Teaching and postdoctoral research experience are preferred.

Screening of applications will begin April 1, 1995 and continue until the position is filled . The department encourages applications from minority persons, women, Vietnam era veterans, and disabled persons. Please send a curriculum vitae, transcripts, statement of interests and goals in both teaching and research, and three letters of recommendation to:

Dr. Darrell Wiens
Chair, Search Committee
Department of Biology
University of Northern Iowa
Cedar Falls, IA 50614-0421
Fax: (319) 273-7125

THE UNIVERSITY OF NORTHERN IOWA IS AN EQUAL OPPORTUNITY EDUCATOR AND EMPLOYER.

National Institutes of Health / Public Health Service / Department of Health and Human Services

ASSOCIATE DIRECTOR FOR SCIENCE AND TECHNOLOGY TRANSFER POLICY

The National Institutes of Health (NIH) invites applications for the position of Associate Director for Science and Technology Transfer Policy, Office of the Director. This is a Civil Service position in the Senior Executive Service (SES), with a base salary ranging from the ES-1 to ES-6 pay level per annum (currently $97,991 to $122,040 including locality pay). Recruitment and relocation bonuses may be applicable for candidates. A one year probationary period must be served by the individual selected if not currently or previously in the career Senior Executive Service.

The Associate Director for Science and Technology Transfer Policy is the principal NIH official responsible for advising the Director, NIH, on agency wide biomedical and behavioral science policy and technology transfer policy. This position also serves as principal advisor to the Assistant Secretary for Health on technology transfer policy. The advice provided pertains primarily to issues generated by the interface between science and the public at large, which includes responsibilities for assessing the biomedical and behavioral research and technology transfer programs to target areas suitable for new policy initiatives and to determine which mechanisms are best suited for effective and efficient policy development. This position also advises the Director, NIH, and senior NIH staff on all aspects of technology transfer policy, including policy related to technology management, licensing and marketing activities, and patent administration and prosecution activities. In addition, this position serves as the focal point for the NIH for coordinating the development, management, and oversight of strategic program plans associated with the NIH mission, which includes planning and conducting a comprehensive program of policy development, program evaluation, and economic and resource analyses. The incumbent of this position also manages the Recombinant DNA Advisory Committee and develops and implements NIH policies and procedures for the safe conduct of recombinant DNA studies.

Applicants should submit either a curriculum vitae, an Optional Application for Federal Employment (OF-612), or any other written format (including an SF-171 or resume); a bibliography; and a written statement addressing the mandatory and desirable qualification factors for this position. The vacancy announcement with mandatory/desirable qualifications requirements can be obtained by calling (301) 496-3365. Application materials must be sent to the following address:

National Institutes of Health
Building 31, Room 2A25
31 CENTER DR MSC 2425
BETHESDA MD 20892-2425
Attn: Sharon Porter

Applications must be postmarked no later than April 12, 1995.

Selection for this position will be based solely on merit, with no discrimination for nonmerit reasons such as race, color, religion, gender, national origin, political affiliation, marital status, disability, age, sexual orientation or membership or nonmembership in an employee organization.

NIH is an Equal Opportunity Employer

NEW.....NEUROSCIENCE

THE EJLB FOUNDATION SCHOLAR RESEARCH PROGRAMME

The EJLB Foundation announces that it will award each year up to six (6) grants for research projects in all areas of neuroscience that pertain directly or indirectly to schizophrenia and mental disease.

Eligibility for such grants is restricted to young scientists who are pursuing an independent research career and have given evidence of having significant potential. It is also a requirement that these scientists have earned an MD and/or a Ph.D. degree, have completed their post-graduate training and been admitted, after June 15, 1990, as faculty members of a leading university or an affiliated non-profit research centre, in Canada or elsewhere in the world.

Each grant totals CAN$300,000, is disbursed over three (3) years and is non-renewable.

The next closing date for receipt of letters of intent is June 15, 1995.

Full details and letter of intent forms may be obtained from The EJLB Foundation, 1350 Sherbrooke Street West, Suite 1050, Montréal, Québec, H3B 1J1. Fax (*for inquiries only* 514-843-4080).

The Life Sciences Division at Lawrence Berkeley Laboratory is currently seeking the following:

SENIOR or STAFF SCIENTIST

DNA Repair

Seeking a Senior or Junior Investigator to work on the molecular and cell biology of DNA repair mechanisms in higher eukaryotic cells. A senior scientist must have a nationally and internationally established track record in the field and an active and well funded research program. A staff scientist may have a less established track record with a funded research program. We seek candidates who can effectively interact with the LBL Human Genome Center, as well as molecular and cell biologists whose interests include radiation biology, structural, genetic and enzymatic aspects of DNA damage and repair, genomic stability, molecular cytogenetics, and control of cell proliferation, differentiation, carcinogenesis and tumor suppression. The Laboratory will provide well equipped Laboratory space, the possibility of up to two years of start up funds, after which the program is expected to be self-supporting. Job #JSCI3248

STAFF SCIENTIST

Chromatin/Nuclear Structure

Seeking a Junior or mid career investigator working in the area of chromatin and nuclear structure, particularly as it relates to the control of gene expression. Must have an established track record and a funded research program. We seek candidates who can effectively interact with molecular and cell biologists in the Division whose interests include the control of cell proliferation, differentiation and replicative senescence, carcinogenesis and tumor suppression, genomic stability and DNA repair, and molecular cytogenetics. LBL will provide well-equipped laboratory space and a comprehensive fringe benefits package. Job #JSCI3247

LBL is adjacent to the University of California, (UC) Berkeley campus. Investigators will have the opportunity to interact closely with faculty at both UC Berkeley and UC San Francisco. Please send a curriculum vitae; a list of publications (complete for last three years); a list of current and pending funding; a brief (one page or less) summary of the research program and future directions; and the names, addresses, and telephone numbers of three references by April 14, 1995 to: **Chair, LSD Search Committee, c/o Lawrence Berkeley Laboratory, Staffing Office, One Cyclotron Road, Bldg. 938A, Berkeley, CA 94720.** Please indicate Job #. We are an equal opportunity employer.

LAWRENCE BERKELEY LABORATORY
UNIVERSITY OF CALIFORNIA
Department of Energy

The Jackson Laboratory

PRE- DOCTORAL AND POST-DOCTORAL TRAINING PROGRAMS

RESEARCH PROGRAMS

Genome Organization
Developmental Biology
Metabolic Diseases
Neurobiology
Genetics of Complex Traits
Cancer Genetics
Immunology/Hematology
Bioinformatics

The Jackson Laboratory: a unique research environment with unparalleled mouse resources.

Letters of inquiry should include: curriculum vitae, statement of research interests, list of publications, and names of three references. (Predoctoral programs are in conjunction with the University of Maine and Yale University.)

To apply or request further information, contact: Phyllis Mobraaten, Box 65, The Jackson Laboratory, 600 Main Street, Bar Harbor, ME 04609 Phone: 207-288-3371, ext 1376; FAX 207-288-5079; e-mail: pam@aretha.jax.org **EE/AA Employer**

ADVANCES IN MOLECULAR GENETICS

Fundamental Strategies and Methods in Gene Hunting and Molecular Characterization

A new, international recombinant DNA course with a focus on the fundamental strategies and methods in gene hunting and molecular characterization will be held June 19 – June 30, 1995. The intensive three-credit course featuring lectures, lab work and student presentations will be conducted at the BioPharmaceutical Technology Center Institute (BTCI) in Madison, Wisconsin.

The program is designed as a model partnership between the educational and business communities, enabling students to design strategies and practice techniques for the isolation, characterization and manipulation of genes, including library construction and screening, vector design and gene cloning, mutagenesis, sequencing, gene amplification and gene expression.

Course instructors include: Prof. Richard Burgess (UW-Madison), Dr. Don Court (National Cancer Institute), Prof. Alik Honigman (Hebrew University), Prof. Haim Rosen (Hebrew University) and Dr. Keith Wood (Promega Corporation).

BioPharmaceutical Technology Center Institute

Co-sponsored by

BioPharmaceutical Technology Center Institute (BTCI)
University of Wisconsin Biotechnology Center (UWBC)
University of Wisconsin-Madison Department of Oncology
with support from Promega Corporation

For more information contact:

Dr. Karin Borgh, Executive Director, BTCI
5445 East Cheryl Parkway, Madison, WI, 53711
Telephone 608/273-9737 or FAX 608/273-6992
E-MAIL: KBORGH@PROMEGA.COM

SangStat Medical Corporation is a biopharmaceutical company developing novel therapeutic and monitoring products to improve the outcome of organ transplantation. To expand our research capabilities, we are looking for highly motivated individuals to fill the following position:

Post-doctoral Scientist

An exceptional opportunity to work on the development of novel immunomodulatory compounds based on peptides derived from the heavy chain of MHC class I molecules. Some of these peptides prolong allograft survival in mice and rats in a non-allele restricted manner. In vitro these peptides inhibit several cell-mediated immune responses. Despite their effectiveness in in vitro and in vivo models, the mechanism of action of these peptides is still unclear. The successful candidate with experience in cellular and molecular immunology will work in a small team to elucidate the mechanism of action.

We offer an energetic environment in the San Francisco Bay Area and an opportunity for research in a rapidly changing field. Competitive salary benefits. EEO employer. Write or Fax your resume to V.P. of Research at:

SangStat Medical Corporation
The Transplant Company™

1505-B Adams Drive
Menlo Park, CA 94025
Telephone: 415.328.0300
Facsimile: 415.328.8892

Graduate Program in Molecular & Cellular Biology The University of Illinois at Chicago College of Medicine

The Molecular & Cellular Biology Training Program provides interdisciplinary training. Over 40 faculty members from different departments participate in the program. Students can choose from many possible areas of research, including:

- Cell Growth & Differentiation
- Cell Structure
- Developmental Biology
- DNA Structure & Function
- Gene Regulation
- Immunology
- Molecular Biology of Cancer
- Molecular Endocrinology
- Protein Structure & Function
- Signal Transduction

Principal Participating Departments:

- Anatomy & Cell Biology
- Biochemistry
- Genetics
- Microbiology & Immunology
- Pharmacology
- Physiology & Biophysics

Stipends of $14,000 are available to all doctoral students in the form of tuition-free fellowships. Interested candidates are encouraged to seek application and information from:

MCBTP
c/o Heidi Hamm
Dept. of Physiology and Biophysics
835 S. Wolcott M/C 901
Chicago, IL 60612-7342

Research Positions
Molecular Neurobiology of Drug Abuse

George R. Uhl, M.D., Ph.D.

Fellow and senior fellow positions are available to pursue the molecular neurobiology and genetics of drug abuse. Candidates should have expertise in molecular biology and/or molecular genetics, with preference given to experience in neuropharmacology. Ongoing work examines the structure and function of the dopamine transporter/cocaine receptor, μ opiate receptor/heroin receptor, genes regulated by abused drugs, and genes important for interindividual differences in substance abuse vulnerability in animal models and humans. If you hold a doctoral degree(s) and would like to be considered for a position, please send a cover letter, curriculum vitae with bibliography, statement of research interests and goals (not to exceed two pages), and three letters of recommendation to:

G.R. Uhl, M.D., Ph.D.
Molecular Neurobiology Branch
Division of Intramural Research
National Institute on Drug Abuse
National Institutes of Health, Box 5180
Baltimore, Maryland 21224

Competitive salary levels will full federal benefits - an equal opportunity employer. Candidates must be U.S. citizens or permanent residents.

BIOANALYTICAL OR BIOPHYSICAL CHEMISTRY Ph.D. SCIENTIST

Analytical Research & Specifications Development

The Upjohn Company, is seeking a scientist for a challenging position in drug development, with an emphasis on analytical methods development and chemical characterization of new drug candidates, including peptides and proteins.

The successful candidate will conduct independent research to define and measure important quality characteristics of drug entities and formulations. Responsibilities will include the development of analytical methods for major and minor components, elucidation of chemical degradation pathways and kinetics, characterization of critical chemical and physical properties, and development of specifications for regulatory submissions. You will communicate and collaborate with scientists in other areas through multidisciplinary project teams, and contribute to the development and/or application of new technology through independent research. Growth of scientific expertise and reputation through external presentations and publications encouraged.

A Ph.D. degree in Analytical Biochemistry, Biophysical Chemistry, or a related discipline is required. Training in protein and peptide characterization is desirable. Experience in molecular biology, immunology, glycosylation chemistry and/or related areas is a plus.

In addition to an excellent salary and benefits package, Upjohn Laboratories offers a stimulating, multi-disciplinary research environment at our modern facilities located in Kalamazoo, a southwestern Michigan community located midway between Detroit and Chicago. This region provides an outstanding mix of cultural and recreational pursuits and a reasonable housing cost market. For confidential consideration please send your C.V. with list of publications to: **The Upjohn Company, Corporate Recruiting, Ad #254, 7000 Portage Road, Kalamazoo, Michigan 49001.** We are an equal opportunity employer with a commitment to workplace diversity.

Upjohn

DISCOVER SUGEN:

A LEADER IN SIGNAL TRANSDUCTION RESEARCH

SUGEN, Inc. is a dynamic biopharmaceutical company focused on the discovery and development of drugs for the treatment of cancer and diabetes. We currently have the following vacancies at our San Francisco Bay Area facility.

Neurobiology

Director: This key scientist will take overall responsibility for the Neurobiology Program at SUGEN, which currently consists of three research teams. The position demands several years' postdoctoral experience in neurobiology, as well as proven leadership skills. Experience in electrophysiology an advantage.

Protein Tyrosine Phosphatases

Group Leader: You will be prepared with a Ph.D. as well as several years of postdoctoral experience in the area of protein tyrosine phosphatases. You will lead a group studying the regulation and function of this diverse group of enzymes, particularly in regard to their involvement in clinical disease.

Immunology

Group Leader: This group will focus on immunosuppression and inflammation. The position requires a Ph.D. and several years of experience in immunological research. Experience in signal transduction pathways essential.

Gene Expression

Group Leader: For this Ph.D.-level position, we seek someone experienced in vector construction and eukaryotic and prokaryotic expression systems.

Signal Transduction

We also have openings for Ph.D. scientists with experience in signal transduction research to join a number of the new and existing groups in our Research Division.

To reply to one of the positions above, please note position of interest and send *c.v.*, along with the names, addresses and telephone/fax numbers of three references, to: SUGEN, Inc., Attn: Dorian Rinella, 515 Galveston Drive, Redwood City, CA 94063. Informal inquiries for Group Leader and Director positions only should be addressed via FAX to Sara A. Courtneidge, Ph.D., at (415) 306-7613. Competitive salary and benefits, including stock options, support these positions. Equal Opportunity Employer.

SUGEN, Inc.

INDEPENDENT, TENURE TRACK STAFF POSITION AT NIH

The Laboratory of Biochemistry, National Cancer Institute, National Institutes of Health seeks to appoint a junior scientist to initiate an independent, tenure track program of basic research. Applications are invited from candidates with demonstrated potential for creative research in the biological sciences. The Laboratory of Biochemistry is composed of 14 research groups that study diverse problems in bacteria, yeast, fly, and animal cells, employing techniques of classical and molecular genetics, protein chemistry, biochemistry, and cell biology.

To apply, please send a curriculum vitae, bibliography, brief statement of research interests, and three letters of recommendation to:

Dr. Carl Wu, Chair, Search Committee
Laboratory of Biochemistry
NIH/National Cancer Institute
Bldg. 37, Room 4E28
9000 Rockville Pike
Bethesda, MD 20892-4255

NIH/NCI is an Equal Opportunity Employer

ARE YOU AN INNOVATIVE SCIENTIST?

If so, the Gene Therapy Business Unit of Baxter Healthcare Corporation is the place for you. Having conducted some of today's most innovative and important research, Baxter continues to pioneer the future of health care products. Currently, we have two outstanding opportunities for experienced Scientists to join us in our northwest suburban Chicago location.

GENE THERAPY

You will design viral vectors for *in vivo* gene therapy and molecular devices for transgene regulation. This will involve collaboration with other scientists, and leading a research team. Other duties include maintaining familiarity with new technologies through literature searches, as well as organizing research data and writing patents, manuscripts and reports.

We require a Ph.D in Molecular Biology, Virology, or Biochemistry, along with 3-5 years of post-doctoral experience in gene expression and viral vector development. We also require a solid background in virology, immunology, molecular biology, and biochemistry. Preferred candidates will be currently participating in a leading research lab.

We provide a highly professional environment conducive to career development, as well as a competitive compensation and benefits program. Please send resume with salary history to: Baxter **Healthcare Corporation, Human Resources, Dept. GT95104, Route 120 & Wilson Rd., WG2-3S, Round Lake, IL 60073.** An Equal Opportunity Employer.

Baxter

Technical Service Chemist

Sigma Chemical Company currently has a position in the Technical Service Department of the Research Division. This is an opportunity for someone with a Ph. D. degree in Biochemistry or an M.S. degree with extensive experience in biochemical techniques to be presented a diversity of challenges.

The ideal candidate will have Postdoctoral or industrial experience in isolating and characterizing proteins. A broad background in teaching, purification, synthesis, analytical and detection techniques would be advantageous. Responsibilities include gathering and interpreting technical information, telephone and FAX interactions with our research customers worldwide, and the documentation and resolution of technical problems. Candidate MUST possess excellent verbal and written communication and customer relations skills.

Take advantage of this excellent opportunity with a rapidly-growing company offering competitive compensation and benefits, including a 401(k) plan. To apply, send resume and cover letter, including salary history to: SIGMA CHEMICAL COMPANY; Attn: Human Resources; Position T.S./N.V. 3050 Spruce Street; St. Louis, MO 63103.

SIGMA CHEMICAL COMPANY
P.O. BOX 14508, ST. LOUIS, MO 63178 USA

An Equal Opportunity Employer

The Molecular Therapeutics Program at Duke University has expanded the program for developmental and clinical trials in novel gene and cellular based therapeutics for human cancers and viral infections. We are seeking qualified individuals as research scientists and postdoctoral fellows in the following areas:

Cellular Immunology

Experienced cellular immunologists form an integral component of a cellular and gene based therapeutics program. Extensive experience in T cell activation, cloning, in vitro expansion, and phenotypic and functional assessment of human and murine T cells required.

Molecular Biology

We seek experienced molecular biologists to join a gene therapy program involved in anti-tumor and anti-viral strategies for clinical use. Extensive experience in cloning, vector construction, in vitro expression, RT-PCR required.

Cellular Biology

We seek experienced cell biologists to develop and implement human gene therapy trials involving tumor cell culture, in vitro gene transfer into tumor cells, and in vitro and in vivo assessment of gene transfer and gene expression.

Contact Dr. Eli Gilboa at Box 2601, Medical Sciences Research Building, Room 401, Duke University Medical Center, Durham, NC, USA 27710 or FAX (919) 681-7970.

Duke University is An Equal Opportunity/ Affirmative Action Employer

Program Directors
Division of Elementary, Secondary, and Informal Education
National Science Foundation

The National Science Foundation's (NSF's) Division of Elementary, Secondary, and Informal Education (ESIE) is seeking qualified applicants for Program Director positions in its Teacher Enhancement, Instructional Materials Development, and Young Scholars Programs. Openings are available commencing in Summer/Fall 1995 for a period of one-to-two-years. Positions may be filled as a Temporary employee or through the Visiting Scientist (VS) or Intergovernmental Personnel Act (IPA). Applicants must hold a Ph.D. plus have six plus more years of equivalent experience in research and/or education related to science, mathematics, or technology, or have related experience in referenced areas. Positions are open in the following areas:

- Elementary Science
- Elementary Mathematics
- Technological Education.

The salary range is from $51,557 to 94,953 per annum; locality pay adjustments are included for VS/IPA appointments. Applicants must submit a resume, current salary,, and up to three letters of recommendation by March 15, 1995 to the NSF, **ATTN: NINA BEARD, DIVISION OF HUMAN RESOURCE MANAGEMENT, SUITE 315, 4201 WILSON BLVD., ARLINGTON, VA 22230.** For general information, or information about the appointing authorities, call Ms. Beard at (703) 306-1185 (X3026). For information about the Division and its Programs, contact Ms. Jean Vanski, Deputy Division Director, ESIE, at (703) 306-1620. Hearing-impaired individuals should call TDD 703-306-0189. Qualified individuals who are women, ethnic/ racial minorities, and/or persons with disabilities are strongly encouraged to apply. NSF is an equal opportunity employer committed to employing a highly qualified staff that reflects the diversity of our nation.

The National Institutes of Health
National Center for Human Genome Research

The intramural program of the National Center for Human Genome Research (NCHGR), the National Institutes of Health (NIH) in Bethesda, Maryland, is now in operation. Scientists with a unique range of expertise and interests have been recruited to focus on the identification, localization, diagnosis, and treatment of human genetic disease.

We are now actively recruiting a tenure-track scientist in the field of

HUMAN AND MURINE GENOMICS

for a position within the Laboratory of Genetic Disease Research. The successful applicant will be provided with the space and resources needed to pursue an independent research program in mapping, isolating, and characterizing genes involved in human and/or murine genetic disease.

Candidates must have a Ph.D. and/or M.D. as well as advanced training in genome science: demonstrable expertise in genetic and physical mapping and positional cloning in humans or mice.

Competitive salary and benefit packages are available. Please forward curriculum vitae and three references to:

Robert L. Nussbaum, M.D.
Chief, Laboratory of Genetic Disease Research
NIH/NCHGR
Building 49, Room 4A72
49 Convent Drive MSC 4470
Bethesda, MD 20892-4470

Closing Date: April 1, 1995

NIH is an Equal Opportunity Employer

The *Extracellular Matrix* in Invasion, Metastasis, and Angiogenesis

Friday, March 10, 1995

MAYER AUDITORIUM
University of Southern California Health Sciences Campus

Program

Welcome
PETER A. JONES, PHD
University of Southern California

Introduction
YVES A. DE CLERCK, MD
University of Southern California

ERKKI RUOSLAHTI, MD
La Jolla Cancer Research Foundation
Integrins as Signaling Molecules in Cell Proliferation, Migration and Apoptosis

DAVID A. CHERESH, PHD
The Scripps Research Institute
Role of Integrin $\alpha_v\beta_3$ in Angiogenesis of Human Tumors

LYNN M. MATRISIAN, PHD
Vanderbilt University
Metalloproteinases in Tumor Progression

BONNIE F. SLOANE, PHD
Wayne State University
Cathepsins in Cellular Invasion

JAMES P. QUIGLEY, PHD
State University of New York at Stony Brook
The Plasminogen Activator System in Tumor Invasion and Metastasis

YVES A. DE CLERCK, MD
University of Southern California
Tissue Inhibitors of Metalloproteinases in Tumor Invasion and Metastasis

ZENA WERB, PHD
University of California San Francisco
Proteolytic Degradation of the Extracellular Matrix During Physiological Invasion

DANIEL B. RIFKIN, PHD
New York University Medical Center
Interplay Between Growth Factors, Matrix and Proteases in Angiogenesis

HELENE SAGE, PHD
University of Washington
Positive and Negative Regulators of Angiogenesis: Sparc and Angiostatin

Symposium organized by USC/Amgen Inc.
No registration fee · Information: (213) 764-0816

CELLULAR & MOLECULAR CANCER RESEARCH

The College of Medicine and the H. Lee Moffitt Cancer & Research Institute at the University of South Florida are seeking applications from Assistant, Associate and Full Professor level individuals to participate in the Cancer Center Research Programs under a stimulating academic environment that includes excellent laboratory and clinical facilities. Research programs include Immunology, Cancer Cell Biology, Molecular Oncology and Cancer Genetics. Academic rank and salary will be commensurate with experience and qualifications. These positions will be assigned to a specific, mutually agreed upon department within the College of Medicine with the possibility of tenure.

Successful individuals must hold an M.D. or Ph.D. with a minimum of 2 years post doctoral training. Individuals at the rank of Associate Professor must have a demonstrated potential for extramural funding. Individuals for Full Professor must have a proven track record of independent research, leadership ability and training backed by publications and extramural funding.

Send current curriculum vitae and a brief statement of major academic interests to W.J. Pledger, Ph.D., Associate Center Director for Basic Research, Office of Faculty Recruitment, Moffitt Cancer Center, 12902 Magnolia Drive, Tampa, Florida 33612. Applicants who need a reasonable accommodation in order to participate in the selection process must notify Jody Swanson in the Office of Faculty Recruitment, (813) 975-7894, five days in advance. Applications must be postmarked by deadline of April 20, 1995.

The H. Lee Moffitt Cancer Center & Research Institute is a free standing Cancer Center located adjacent to the Health Sciences Center on the Tampa campus of the University of South Florida. In addition to a 162-bed full service cancer treatment facility, the Center has research laboratory space in four buildings including over 50,000 square feet of dedicated laboratory and support space in a new Cancer Research Center slated to open in June 1995.

H. LEE MOFFITT CANCER CENTER
& RESEARCH INSTITUTE
University of South Florida College of Medicine

Moffitt Cancer Center is an Equal Opportunity Employer.
The University of South Florida is an
EO/Equal Access/Affirmative Action Employer.

Help Deliver A New Era In Pharmaceuticals

Since 1888, Abbott has been at the forefront of discovery in the health care industry. In 1993, we committed $881 million to R&D to answer some of today's most important scientific questions. As we continue our work, our Pharmaceutical Products Division has the following outstanding opportunity available.

SENIOR RESEARCH SCIENTIST/RESEARCH INVESTIGATOR

You will be responsible for high capacity screening with emphasis in the identification of agents for treatment in the Neuroscience disease area.

We require a PhD in Biochemistry, Pharmacology, or Molecular Biology as well as 3+ years of postdoctoral experience. We also require experience in high capacity screening, automation of bioassay, neuroscience drug discovery, and biochemical/ pharmacological characterization of new agents.

Abbott provides an excellent salary and benefits package, including profit sharing and a stock retirement plan. We are located in an attractive suburban area, approximately 30 miles north of Chicago. For confidential consideration, please send your resume with salary history to: **Alison Burke, D-583, AP6B, Job #NB73857, Abbott Laboratories, 100 Abbott Park Rd., Abbott Park, IL 60064.** Abbott is an Affirmative Action/Smoke-Free Employer.

ABBOTT LABORATORIES

Quality Health Care Worldwide Since 1888

Experience The Abbott Edge.

LeukoSite is a growing Biopharmaceutical Company focused on the process of tissue-specific leukocyte trafficking and the discovery of novel therapies for inflammatory and autoimmune diseases. Founded by Tim Springer of Harvard Medical School, an outstanding team of scientists has been assembled to lead the Company's research and discovery program.

LEUKOSITE INC.

DIRECTOR, MOLECULAR BIOLOGY

Applications are sought for a senior management position as Director of Molecular Biology. Through extensive publications in peer reviewed journals, applicants will have established a national reputation in their chosen field. Candidates should have broad experience in a range of techniques including cloning and gene expression. Respondents should have a strong interest or experience in the field of inflammation, a hands-on approach, and a commitment to an integrated and team oriented approach to drug discovery. Prior industry experience would be advantageous.

Respondents should submit their complete CV and the names of three references to: Personnel Director, LeukoSite, Inc., 215 First St., Cambridge, MA 02142. An Equal Opportunity Employer.

Greenville Hospital System
Clemson University

DISTINGUISHED PROFESSORSHIP IN BIOLOGICAL SCIENCES

The Greenville Hospital System/ Clemson University Biomedical Cooperative invites applications for a tenured Distinguished Professorship in the area of Cell and Developmental Biology with special competence in molecular techniques. The successful candidate must have a Ph.D., an outstanding research and teaching record, a strong history of grant support, and be able to work in both a medical and academic setting. S/he will be expected to collaborate with hospital-based clinicians, develop a graduate program in medically related research, and teach undergraduates. Applications must be received by April 21, 1995. Send letter of application, curriculum vita, a brief description of research plans and the names of five references to: Dr. J. David Gangemi, Director, GHS/CU Biomedical Cooperative, 445 Brackett Hall, Clemson University, Clemson, SC 29634-1912.

GHS/CU is an Equal Opportunity/ADA/ Affirmative Action Employer and encourages applications from minorities and women.

Attention Non-U.S . Advertisers!

SCIENCE announces the 1995 pounds sterling rate card! Advertisers not based in the United States may choose to pay in U.S. dollars or pounds sterling.

SCIENCE continues its surge in the global marketplace, meeting the needs of advertisers! We are proud of our 71% growth in the non-U.S. market since 1991!

Contact your advertising representative for more information:

In the U.S., call Janis Crowley at (212) 496-7704, or fax to (202) 682-0816.
In Europe, call Gordon Clark at (44) 0223 302067, or fax to (44) 0223 302068.
In Japan, call Mashy Yoshikowa at (81) 3 3235-5961, or fax to (81) 3 3235-5852.
In Australia, call Keith Sandell at (61) 02 922 2977, or fax to (61) 02 922 1100.

SCIENCE

Sultan Qaboos-University- Sultanate of Oman
Department of Environmental Science,
College of Sciences

Sultan Qaboos University, the National University of the Sultanate of Oman, urgently invites applications and nominations for the post of Professor and Head of the Department of Environmental Science in the College of Science.

The basic requirements for eligibility are: (1) Ph.D. in Environmental Science, (2) a minimum of ten years teaching and research experience in a recognized university, of least two years of which must have been spent as a full professor.

It is planned to start a separate Environmental Science Department from September 1995 and the Head of Department is expected to lead the establishment of the department. The first offering will be an Msc in Environmental Science, further details of which are available on request.

Apart from a very attractive tax free base salary depending upon qualifications and experience, the University offers free furnished accommodation, two years renewable employment contract with end of service gratuity, annual leave with return first class air tickets, a contribution towards the school fees of two dependent children below 18 studying in the Sultanate of Oman, free medical treatment in Government Hospitals.

Interested candidates are requested to submit their full C.V., along with copies of academic and experience certificates, quoting our Ref: ADV/SCI/02/95. to:

The Director, Personnel Affairs,
Sultan Qaboos University,
P.O. Box 50, Al-Khod - 123,
Sultanate of Oman

KAROLINSKA INSTITUTET
Department of Bioscience at Novum
Center for Structural Biochemistry

Research assistant/ Postdoctoral fellow
NMR spectroscopy in biology

The position is available within the Unit for NMR Spectroscopy with placement at the Center for Structural Biochemistry (CSB) within the Department of Bioscience. CSB is situated at the South Campus of the Karolinska Institutet encompassing the NOVUM Research Park in Huddinge, about 20 km south of the center of Stockholm. The CSB has a staff of about 40 researchers and includes units for X-ray crystallography, molecular modelling, electron microscopy and NMR spectroscopy. The NOVUM Research Park provides an excellent environment with over 400 researchers within various biomedical disciplines.

The research within the Unit for NMR Spectroscopy includes structural and biophysical studies of biomolecules. The research presently concerns nuclear receptors, other steroid-binding proteins, ribosomal proteins and DNA-binding proteins from archaebacteria. The NMR unit is equipped with a Varian Unity 500 MHz NMR spectrometer with all necessary hardware and extensive computing resources.

The applicant should have a solid background in NMR spectroscopy and biomolecular NMR. A second condition is that applicants should have experience in either physical and biophysical chemistry or protein expression and protein biochemistry. The position is available for four years with an initial limitation of one or two years.

For further information contact Dr. Torleif Härd (email th@csb.ki.se) (questions regarding qualifications etc.) or Ingwar Lennerfors (administrative questions) +46-8 608 92 33.

Applications should be sent to Karolinska Institutet, Department of Bioscience at Novum, S-141 57 HUDDINGE, SWEDEN together with CV, relevant publications, a short description of research interests and two recommendation letters. Please quote reference no 53021/4 and note that we want your application in 1 original and 1 copy.

Closing date: March 31, 1995

LECTURER IN AQUATIC ECOPHYSIOLOGY

Required by Department of Biological Sciences from September 1995. Candidates should have active research interests in the field of Aquatic Ecophysiology. The appointee will complement the research of existing Departmental strengths in this area. Salary on Lecturer scales either Grade A £14,756 - £19,326 p.a. or Grade B £20,133 - £25,735 p.a.

Information from Personnel, University of Exeter, Exeter EX4 4QJ; (01392) 263100 or e.mail Personnel@exeter.ac.uk, quoting reference no.3962. Closing date: 3 April 1995.

Promoting Excellence In Education & Research

Equal Opportunities Employer

UNIVERSITY of EXETER

UNIVERSITY OF MANCHESTER
SCHOOL OF BIOLOGICAL SCIENCES

Two New Lectureships

Following our recent success in recruiting to a number of new lectureships, the School of Biological Sciences now seeks to appoint outstanding individuals to two further posts, recently created to support our continuing programme of development.

LECTURESHIP IN ANIMAL BIOLOGY Ref: 62/95

This post aims to strengthen our existing research into animal biology at the whole-animal level by using genetic, molecular, endocrinological or cellular-based techniques. We therefore seek applicants from any biological discipline (physiology, pharmacology, anatomy, developmental biology, zoology etc) with an interest in environmental physiology, reproductive biology, or animal behaviour using either invertebrate or vertebrate model systems. The successful candidate will establish a vigorous research programme and contribute to undergraduate and postgraduate teaching.

Contact: Professor M J Emes tel: 0161 275 3899, fax: 0161 275 3954,
E-Mail MEmes@fs2.scg.man. ac.uk

LECTURESHIP IN MICROBIOLOGY Ref: 63/95

Applications are invited from any area of bacteriology but individuals with an interest in researching molecular aspects of bacterial pathogenesis are particularly welcome. The successful candidate will be expected to develop an independent research group, encouraged to establish collaborative research projects and contribute to undergraduate and postgraduate teaching.

Contact: Professor Tony Trinci tel: 0161 275 3893, fax: 0161 275 5656,
E-Mail Tony.Trinci@ man.ac.uk

Salary in the range £14,756 - £25,735 per annum. For application forms, further particulars and an information pack covering all of the posts in this new development, prospective applicants should contact The Director of Personnel, Academic Staffing Office, The University of Manchester, Manchester M13 9PL, tel: 0161 275 2028, fax: 0161 273 5306. Quote the reference given above. Enquiries by E-Mail to the Dean's Secretary: SLong@fs2.scg.man.ac.uk Informal enquiries concerning individual posts should be made to the contact persons listed above who will be happy to discuss the opportunities in more detail and to arrange for informal visits, etc. Closing date for applications 31st March 1995. As an Equal Opportunities Employer, the University welcomes applications from suitably qualified people from all sections of the community regardless of race, religion, gender or disability.

POSITIVE ABOUT DISABLED PEOPLE

Promoting quality teaching and research.

Leicester University

Department of Biochemistry

POSTDOCTORAL RESEARCH

Control of Gene Expression by RNA Splicing

Applications are invited to join research into the selection of alternative splice sites in mammalian pre-mRNA. This will involve cross-linking, affinity purification and a number of techniques in molecular biology. The position is funded by the European Commission and is part of a collaboration with colleagues elsewhere in Europe.

The position is available for up to two years. The salary would be on the R&A IA, II or III scales (£13,941 - £30,533 pa). A PhD and a good first degree are required, with expertise in protein biochemistry or molecular biology. Applicants should be nationals of the EU or states participating in the Human Capital and Mobility Programme but not of the UK.

Applications (including a CV and the names of two referees) should be sent as soon as possible to **Dr Ian Eperon, Department of Biochemistry, University of Leicester, University Road, Leicester LE1 7RH, UK.** Informal enquiries are welcome and should be made to **Dr Eperon (Tel: (44) 116 252 3482; Fax: (44) 116 252 3369; e-mail, eci@leicester.ac.uk).**

Towards equal opportunities

Promoting excellence in University teaching and research

JCU

PROFESSOR OF ZOOLOGY

Townsville

Applications are invited for the Chair in Zoology which has become vacant following the appointment of Professor R E Jones as Deputy Vice-Chancellor (Science and Engineering). The appointee will also be Head of the Department of Zoology.

Applicants must have an international reputation for excellence in a field of Zoology and be able to provide academic leadership that maintains and enhances the existing strengths of the Department. The appointee will be required to contribute to both undergraduate and postgraduate teaching. In this regard applications should include a teaching portfolio.

The Department has 23 full-time academic staff and over 60 postgraduate research students. Research and teaching are focussed on whole animal biology with an emphasis on population and community ecology, wildlife and conservation biology, ecophysiology and animal behaviour, and systematics and evolution. In addition applied programs in aquaculture and entomology/pest management are offered.

As a joint member of the School of Biological Sciences the Department has close research and teaching links with the Departments of Marine Biology and Botany and Tropical Agriculture and is a member of the Cooperative Research Centres for Tropical Rainforest Ecology, Aquaculture and Tropical Savannas. The Department received over 3.6 million dollars in external research funding in the period 1992 -1994. The location of the University and its field stations present outstanding opportunities for research in tropical terrestrial, freshwater and marine environments.

Tenure: The position is available on a permanent basis.

Salary: Academic Level E - A$80176 a year.

Further information may be obtained from the Recruitment Officer, Human Resources Division, James Cook University of North Queensland, Townsville Q 4811 Australia. Phone 61 77 81 4880; Fax 61 77 81 5644. Applications close on 28 April 1995. Quote JI95028.

Equal Opportunity in Employment is University Policy

The University has a "Smoke-Free Working Environment" Policy

JAMES COOK UNIVERSITY
OF NORTH QUEENSLAND

THE HONG KONG UNIVERSITY OF SCIENCE AND TECHNOLOGY

SCHOOL OF SCIENCE

seeks candidates for

HEAD OF DEPARTMENT OF BIOCHEMISTRY

The Hong Kong University of Science and Technology (HKUST) was incorporated in April 1988, and opened in October 1991, as a technological university dedicated to the advancement of learning and scholarship, with special emphasis on research, postgraduate education, and close collaboration with industry and business. Enrolment is expected to grow to 7,000 (FTE) by 1996-97, and possibly to higher levels further on. The School of Science which comprises five departments: Biochemistry, Biology, Chemistry, Mathematics, and Physics enrols about one quarter of the University's undergraduate and postgraduate students.

HEAD, DEPARTMENT OF BIOCHEMISTRY

The Department of Biochemistry has comprehensive teaching and research programmes in both basic and applied aspects of biochemistry. It offers the following academic degrees: Bachelor of Science, Master of Science, Master of Philosophy and Doctor of Philosophy. It also maintains a close relationship with the Biotechnology Research Institute. There are 16 faculty members specializing in (1) Genetic Engineering and Protein Design, (2) Immunochemistry, (3) Neurochemistry, and (4) Plant and Medicinal Biochemistry. By 1997 the faculty strength will grow to 21.

Qualifications and Experience

Applications/nominations are invited from well-qualified and accomplished scientists for the post of Head of the Department of Biochemistry. In addition to extensive teaching and research experience, the successful candidate must have demonstrated leadership qualities necessary to lead and manage the Department.

Salary and Conditions of Service

Salary will be very competitive. Generous fringe benefits including medical and dental benefits, annual leave and children's education allowances are provided; housing benefit is provided at a charge of 7.5% of salary. Air passages are also provided where applicable; and a gratuity of 25% of the total basic salary drawn will be payable where applicable.

Application/Nomination Procedures

Applications/nominations together with a detailed curriculum vitae and the names and addresses/fax numbers of at least three and up to five referees should be sent to the **Director of Personnel, The Hong Kong University of Science and Technology, Clearwater Bay, Kowloon, Hong Kong (Fax No.: (852) 2358-0700) before 15 April 1995. Please quote Ref. BICH.HD on your application/ nomination. The search will continue until a suitable appointment is made.**

Université de Montréal
Faculté de médecine

MEMBRANE TRANSPORT

The **Département de physiologie**, Faculté de médecine, Université de Montréal seeks applicants for a position at the level of assistant professor. **Functions:** The successful applicant will become member of the Membrane Transport Research Group of the Université de Montréal and is expected to join ongoing projects involving measurements of transport systems on membrane vesicles, and/or vesicle fusion onto planar lipid bilayer. The selected candidate must develop a strong independent research program and compete successfully for funding from agencies such as the Medical Research Council of Canada or the Fonds de la recherche en santé du Québec. Duties also include a minimum of teaching in physiology (less than 20% of time) and graduate student supervision. **Requirements:** Suitable candidates must have a minimum of three years of postdoctoral training and have a proven record of excellence in the field of molecular biology of membrane transport systems with a special focus on the structure-function relationship of P-glycoproteins. Knowledge of the French language is an asset. **Starting date:** Fall 1995. Applicants must send their curriculum vitae, a synopsis of research interest and three letters of reference, **before April 15th 1995 to:** Dr. Rémy Sauvé, Département de physiologie, Faculté de médecine, Université de Montréal, C.P. 6128, succursale Centre-ville, Montréal (Québec), H3C 3J7, CANADA. In accordance with Canadian immigration requirements, priority will be given to Canadian citizens and permanent residents of Canada. The University is committed to equal employment opportunity for women.

(0529)

POSITIONS OPEN

A non-profit educational institution located in northeastern Ohio is seeking an **ENGINEER II.** The candidate will be responsible for technical aspects of research and technical aspects of clinical management e.g., computer programming, systems analysis, statistical analysis, control mechanisms and electrical systems interfacing in the Pediatric Intensive Care Unit. He/She will assist investigators and clinicians with computer interfacing and on-line data acquisition from various types of mechanical ventilators and bedside cardiorespiratory monitors as well as design new equipment for cardiovascular and respiratory monitoring to meet specific research needs. The candidate will have direct contact with critically ill infants and children and must maintain a professional demeanor around patients and their families as well as strict confidentiality concerning patient's medical records. He/She will also be required to work on several clinical research projects including pulmonary mechanics and weaning mechanical ventilation using various types of clinically used mechanical ventilators (e.g., Siemens Servo 900C, NewPort Wave E200, and VIP Bird ventilators), pulmonary function equipment and indirect calorimetry in the Pediatric Intensive Care Unit. The minimum requirements for the job are a B.S. in biomedical engineering with two years of experience in the job described above. Alternatively the candidate will have an M.S. in biomedical engineering; no experience required, but will qualify with specific education in pulmonary physiology, pulmonary mechanics and mechanical ventilation. The salary will be $36,600 per year. Monday through Friday 8:30 a.m. to 5:00 p.m. (37½ hours per week). Send two cover letters and résumés with names, telephone numbers, and addresses of three (3) recent professional or academic references who can confirm experience or education requirements (No Calls) to: **T. Do, J.O. No. 00434, Ohio Bureau of Employment Services, P.O. Box 1618, Columbus, OH 43216.** *An Affirmative Action/Equal Employment Opportunity Employer.*

SYMPOSIUM

You are invited to attend a **SYMPOSIUM** on "The Relation of Periodontal Infections to Systemic Diseases," May 20, 1995, in Buffalo, New York. Experts will discuss risk factors for periodontal disease, such as smoking, diabetes, altered phagocyte function, stress, distress, coping behaviors, and osteopenia. The effects of periodontal disease as increasing the risk for poor diabetic control, adverse pregnancy outcomes, and respiratory and cardiovascular diseases will also be discussed. Contact: **Dr. Robert Genco, State University of New York at Buffalo. Telephone: 716-829-2854 or FAX: 716-829-2387.**

COURSES AND TRAINING

METHODS IN COMPUTATIONAL NEUROSCIENCE

July 30–August 26, 1995. This is an intensive, lecture/laboratory course that addresses issues relevant to computational neuroscience: the study of how the biophysical and biochemical properties of neurons and synapses, together with the architecture of neural circuits, produce animal behavior. The program of the course consists of two daily lectures, presented by a faculty of 30 established investigators, computer simulation tutorial projects, and an individualized modeling project. The course is designed for advanced graduate students, postdoctoral fellows, and faculty members who have trained in a variety of disciplines, including neurobiology, physics, electrical engineering, computer science, and psychology. Enrollment is limited to 23 participants. Directors: **David Kleinfeld and David W. Tank,** Biological Computation Research Department, AT&T Bell Laboratories, Murray Hill, NJ.

Tuition: $1,500 (room and board available at no additional charge). Limited financial aid is available.

Application Deadline: April 12, 1995.

For information and application forms contact: **Admissions Coordinator, Marine Biological Laboratory, Woods Hole, MA 02543. Telephone: 508-289-7401; Internet: admissions@mbl.edu; World Wide Web: http://www.mbl.edu.**

COURSES AND TRAINING

MECHANISMS OF NEURAL DISEASE: GRADUATE AND FELLOWSHIP TRAINING

Opportunities for research training at the graduate and postgraduate level in an NIH-sponsored training program "Molecular Mechanisms of Neurological Diseases," are available at the Cornell University Graduate School of Medical Science. Applicants may contact **John A. Wagner,** the director of the graduate program and the training grant, or any of the participating faculty for additional information about specific opportunities. Participating faculty include **Drs. Michael Caudy, Moses Chao, Robert Duvoisin, Henry Furneaux, Sam Gandy, Gary Gibson, Steve Goldman, Bernice Grafstein, Charles Inturrisi, Tong Joh, Peter MacLeish, Teresa Milner, Gavril Pasternak, Virginia Pickel, Fred Plum, Jerome Posner,** and **Donald Reis. Cornell University Graduate School of Medical Science, 1300 York Avenue, New York, NY 10021.** *Cornell University Medical College is an Affirmative Action/Equal Opportunity Employer.*

ANNOUNCEMENTS

American Institute for Cancer Research

American Institute for Cancer Research

ANNUAL RESEARCH CONFERENCE

"Dietary Phytochemicals in Cancer Prevention and Treatment"

August 31 and September 1, 1995
Washington, DC

For more information please call the **AICR Research Department** at **202-328-7744** or **1-800-843-8114** or **Email: jcohn@capcon.net**

THE SIXTH INTERNATIONAL MEETING ON CHEMICAL SENSORS
July 22—25, 1996
National Institute of Standards and Technology
Gaithersburg, Maryland 20899

The meeting will be held at the National Institute of Standards and Technology in Gaithersburg, Maryland located just outside of Washington, DC, USA. The scientific program will include plenary presentations, and oral and poster presentations of contributed papers. Oral and poster sessions will be devoted to various areas including: sensing principles and mechanisms; new materials development; novel approaches to sensing, acoustic sensors, electrochemical sensors, ion selective electrodes, optical devices, biosensors, gas sensors, humidity sensors, environmental monitoring, process control sensing, sensor fabrication technology, and signal processing. The official language of the meeting will be English. Contributed papers will be published.

For further information call or write: **Howard H. Weetall, National Institute of Standards and Technology, 222/A353, Gaithersburg, MD 20899 USA. Telephone: 301-975-2628; FAX: 301-330-3447; Email: weetall@micf.nist.gov.**

MARKETPLACE

Polyclonal Antisera

THE HIGHEST QUALITY AT THE LOWEST PRICE
—PLUS—
SPECIAL INTRODUCTORY DISCOUNTS

CALL FOR A FREE CATALOG
800-454-6790
FAX (619) 454-7851

La Jolla Diagnostics
A division of
PATHFINDER HOLDING CORPORATION
800 Silverado
La Jolla CA., 92037

Circle No. 59 on Readers' Service Card

MARKETPLACE

Custom Polyclonal Antibodies
BEST PRICES • BEST ANIMALS
ANIMAL PHARM SERVICES
(800)808-0550

Circle No. 88 on Readers' Service Card

enzymes **CATALOG AVAILABLE!**
• CELL ISOLATION / CULTURE
• MOLECULAR BIOLOGY
• PROTEIN RESEARCH
QUALITY • VALUE • SERVICE
AACR BOOTH #621
enzymes 1994-95 biochemicals
worthington
Ph: 800-445-9603 • Fax: 800-368-3108
Halls Mill Road • Freehold, NJ • 07728

Circle No. 30 on Readers' Service Card

JETstar Mini, Midi, Maxi
Plasmid Purification
GENOMED Inc. – simply the BEST!
800–436–6548 fax: 919–870–9352

Circle No. 75 on Readers' Service Card

EVERYTHING YOU NEED FOR PROTEIN CRYSTAL GROWTH
Crystallization research products for proteins, peptides & nucleic acids
FREE CATALOG
(800) 452-3899
Fax (909) 784-2215
Internet XTALROX@AOL.COM
HAMPTON RESEARCH

Circle No. 4 on Readers' Service Card

The premium antibody for phosphotyrosine detection is available from the laboratory where it originated, for the low price of

PY20 from **TRANSDUCTION LABORATORIES**
1-800-227-4063
only **$100/mg!**

Quality Antibodies for Signal Transduction Research

Circle No. 43 on Readers' Service Card

custom custom custom

Marketplace ads continued from page 1561

MARKETPLACE

CUSTOM ANTIBODIES TO PEPTIDES & PROTEINS
Purification, Conjugation and ELISA Titration Available
HTI BIO-PRODUCTS, INC.
1 (800) 481-9737 OR (619) 788-9691 Fax (619) 788-9694

Circle No. 38 on Readers' Service Card

ROCKLAND
Immunochemicals for Research
Antibodies to ENZYMES
Anti-apoLIPOPROTEINS
Antibodies to COLLAGENS
800-656-ROCK Fax 610-367-7825

Circle No. 27 on Readers' Service Card

The Complete Oligonucleotide Company
KEYSTONE
Introducing
MiniScale Oligos
$1.75 per base
No set-up fee.
Minimum order 30 oligonucleotides.

Keystone Laboratories, Inc.
961 Hamilton Avenue Menlo Park, CA 94025
tel 800-788-4DNA fax 800-786-4DNA
e-mail keydna@keydna.com
VISA, Mastercard, American Express.

Circle No. 16 on Readers' Service Card

CUSTOM DNA SYNTHESIS
PURE & SIMPLE
- Price as low as $2.19 per base plus set up
+
- Superb Technical Support
+
- Impeccable Quality
+
- World's Fastest Service

MIDLAND
THE UNDISPUTED #1
CUSTOM DNA SYNTHESIS SERVICE
THE MIDLAND CERTIFIED REAGENT COMPANY
3112-A West Cuthbert Avenue
Midland, Texas 79701
Phone 1-800-247-8766 FAX 915-694-2387

Circle No. 8 on Readers' Service Card

DNA | PEPTIDES
- $1.75/base • Column Purified • No setup fee
- $20/residue • 15-40 mg in 5 days • No setup fee

GENEMED BIOTECHNOLOGIES
1 (800) 344-5337 • Fax (415) 952-9540

Circle No. 77 on Readers' Service Card

$195 CUSTOM PEPTIDES
•15 - 30 mg •8 - 20 residues
•Mass Spec. Provided
•Quantity discounts available
CHIRON MIMOTOPES PEPTIDE SYSTEMS
North America:
Tel: 1-800-338-4965
Fax: 1-800-654-5592
CM 0945

Circle No. 9 on Readers' Service Card

Custom **PEPTIDES**
$20/RES. (worldwide service) (Discount for 1st order)
No setup charge, free HPLC/A.A. analysis
PEPTIDE ANTIBODY: $250/RABBIT
UNBEATABLY: NO CHARGE IF NO ANTIBODY PRODUCTION
PEPTIDE LIBRARY: FROM $150/LIBRARY
TANA LAB., LC. 1-800-400-0070(Tel) 1-713-663-7163(Fax)

Circle No. 31 on Readers' Service Card

QED
Monoclonal Antibodies are just the Beginning...
Monoclonal Antibody Products
Hybridoma Development
CDR Sequencing/Modeling
(800) 929-2114 FAX (619) 451-0105
A business unit of ImmunoPharmaceutics, Inc.

Circle No. 54 on Readers' Service Card

Activated For Protein Modification
PEGs
Shearwater Polymers, Inc.
(800) 457–1806
(205) 533–4805 (fax)

Circle No. 2 on Readers' Service Card

Human Microvascular Cells
Complete Cell System
NOW ONLY $350
NEW DEFINED ANIMAL ENDOTHELIAL CELL SYSTEMS:
Porcine Aortic Endothelial Cell System
Bovine Aortic Endothelial Cell System
cell systems
800-697-1211

Circle No. 58 on Readers' Service Card

World leader in Synthetic DNA and Peptides
Custom **DNA**
• NO SETUP charge • NO minimum order
$1.99 base
• Column Purified
• 10.0 OD's (~330 µg)
• Gel Picture Q. C.
• Synthesis Report
• 24 hour SHIPPING
Custom **PEPTIDES**
! FREE MASS SPEC !
• NO SETUP charge • Free HPLC Tracing
$20.00* /res.
• 15-40 mgs
• 8 - 30 residues
* desalted • Shipped in 5 days
! Antipeptide Antibodies production services, & more !
Since 1984, serving you with quality products
BIO-SYNTHESIS
1-800-227-0627 Fax: 214-420-0442

Circle No. 7 on Readers' Service Card

FREE DEMO DISK
Software for Combinatorial Mutagenesis and Directed Evolution of Proteins
KAIROS SCIENTIFIC, INC.
CyberDope™
10^6 times better than random
FAX: (408) 362-1200
E-Mail: cyberdope@aol.com

Circle No. 10 on Readers' Service Card

ONLY DNA
No frills, Just good DNA at very low prices
$1.60 per base
• No set-up fee • 48 hour turnaround
• 50 nanomole synthesis
1-800-359-5794 email onlydna@wln.com

Circle No. 39 on Readers' Service Card

ANTIBODIES
Conjugates
Secondary
Custom
Aj Antibodies Inc.
Price below competitors.
Call
1-800-824-8540
Fax: (916) 758-6307

Circle No. 1 on Readers' Service Card

Custom DNA
Purified & Delivered in 48 hours
$5.00 per base • Purified
Guaranteed minimum 100µg
Research Genetics, Inc.
1-800-533-4363

Circle No. 12 on Readers' Service Card

GENERELEASER

PCR* READY DNA IN 5 MINUTES

1993
R&D
100
WINNER

BLOOD

ANIMAL TISSUE

PLANTS

BACTERIA

VIRUSES

SAMPLE TYPES

PCR

DNA

RT-PCR

RNA

* FIVE MINUTE PROTOCOL

* MULTIPLE ASSAYS

* KITS NOW AVAILABLE

IN ADDITION TO THE STOCK GENERELEASER REAGENT, KITS FOR DNA AND RNA PREPARATION FROM MOUSE TAILS, WHOLE TISSUES, YEASTS, PLANTS, AND PARAFFIN EMBEDDED TISSUES ARE AVAILABLE COMPLETE WITH PROTOCOLS, MICROWAVE RACK, DISPOSABLE PESTLES AND TUBES FOR 50 ASSAYS.

CALL NOW FOR ONE OF THE MOST COST EFFECTIVE, INNOVATIVE SAMPLE PREPS AVAILABLE

BioVentures, Inc.

Phone 800-235-8938 FAX 615-896-4837

AUSTRALIA: *Integrated Sciences Pty. Ltd.* (02) 436-2611 **AUSTRIA**: *Vienna Lab* (1) 740-40-190 **BELGIUM**: *Eurogentec* (41) 66 01 50 **CANADA**: *General Synthesis & Diagnostics* (416) 978-8805 & *Kara-Tech* (604) 264-8844 **CHINA**: *Jingmei Biotech* 364-273 & *T.W.C. BioSearch International* (852) 699-6208 **CZECH REPUBLIC**: *BioVendor sro* (49) 69-6772127 **FRANCE**: *ATGC Biotechnologie* (1) 43 04 21 00 & *Eurogentec* (41) 66 01 50 **GERMANY**: *Angewandte Gentechnologie Systeme mbH* (6221) 831023 & *Eurogentec* (41) 66 01 50 & *Syrinx-Vertriebsges mbH* (69) 359686 or (6221) 161720 **ISRAEL**: *Talron* (8) 472563 **ITALY**: *Polymed srl* (55) 8071285 **JAPAN**: *Funakoshi* (3) 5684-1622 **KUWAIT**: *Boushahri Medtech* 5729000 **THE NETHERLANDS**: Eurogentec (41) 66 01 50 **NEW ZEALAND**: *Integrated Sciences Pty. Ltd.* (02) 436-2611 **SOUTH AFRICA**: *Whitehead Scientific* (21) 981-1560 **SPAIN**: *Bio-Synthesis* (1) 352-63-99 & *C.E. Durviz sl* (6) 347-6409 **TAIWAN**: *Pro-Tech* (2) 3810844 **UNITED KINGDOM**: *Cambio* 223-66500

*PCR IS COVERED BY PATENTS OWNED BY HOFFMANN-LA ROCHE

Circle No. 14 on Readers' Service Card

Quantikine™ Immunoassays

Precise, Accurate and Highly Reproducible...

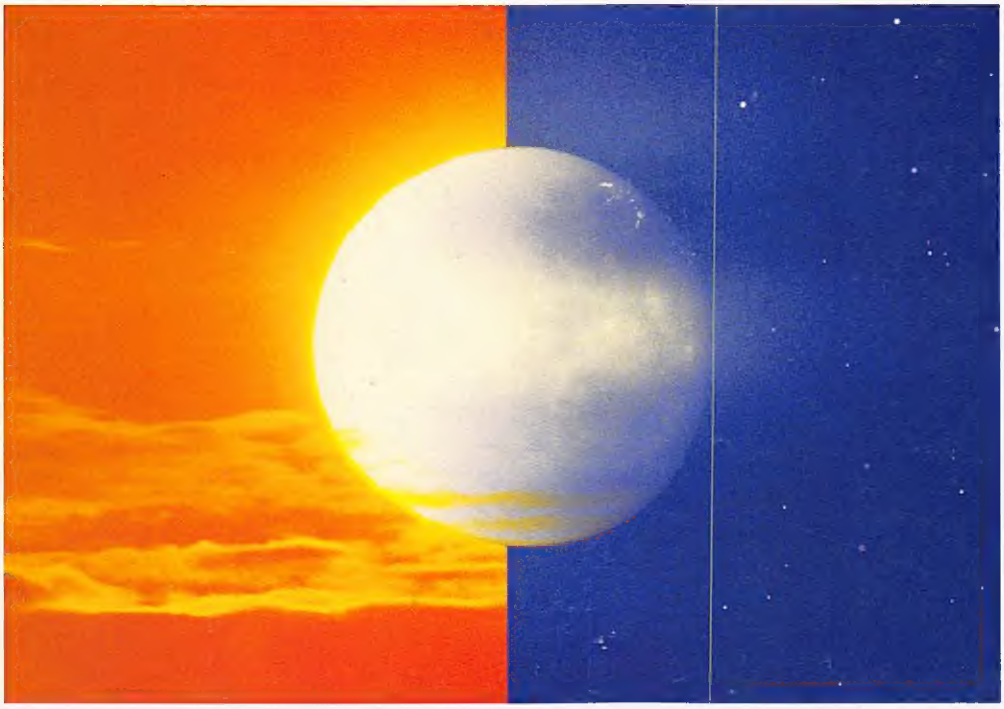

...as sure as night follows day.

The components of R&D Systems' Quantikine Immunoassays are engineered to provide outstanding performance:

- Precision
- Sensitivity
- Accuracy
- Specificity

More than 45 different immunoassays available for the measurement of cytokines and cytokine receptors.

Typical IL-6 Standard Curve

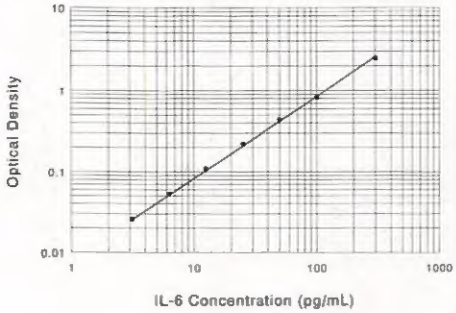

Quantikine

- human IL-1α
- human IL-1β
- human IL-1ra
- human IL-2
- *NEW* human IL-2 sRα
- human IL-3
- human IL-4
- human IL-5
- human IL-6
- human IL-6 sR
- human IL-7
- human IL-8
- *NEW* human IL-10
- human IL-11
- human IL-12
- human ANG
- human EGF
- human FGF basic
- human G-CSF
- human GM-CSF
- human GROα
- *NEW* human IFN-γ
- human LIF
- human M-CSF
- *NEW* human MCP-1
- human MIP-1α
- *NEW* human MIP-1β
- human OSM
- human PDGF-AB
- human RANTES
- human SCF
- human SLPI
- human sTNF RI
- human sTNF RII
- human TfR
- human TGF-β1
- human TGF-β2
- human TNF-α
- human TNF-β
- *NEW* human VEGF

Quantikine HS

- human IL-1β
- human IL-3
- human IL-6
- human IL-7
- human FGF basic
- human TNF-α

Quantikine IVD™

- human Epo

RESEARCH AND DIAGNOSTICS

R&D SYSTEMS

1-800-343-7475

FOR RESEARCH USE ONLY. NOT FOR USE IN DIAGNOSTIC OR THERAPEUTIC PROCEDURES.

U.S.A. and Canada
R&D Systems, Inc.
614 McKinley Place NE
Minneapolis MN 55413, USA.
Tel: 612 379-2956
Fax: 612 379-6580

Europe
R&D Systems Europe Ltd.
4-10 The Quadrant, Barton Lane
Abingdon, OX14 3YS, UK.
Tel: +44 (0)1235 531074
Fax: +44 (0)1235 533420

Japan
Funakoshi Co., Ltd.
9-7, Hongo 2-Chrome
Bunkyo-ku, Tokyo 113, Japan
Tel: +81 (03) 56841622
Fax: +81 (03) 56841633

Circle No. 49 on Readers' Service Card